Marginal Deformations and Open String Field Theory

by

Matheson Edward Longton

B.Sc., The University of Victoria, 2004
M.Sc., The University of British Columbia, 2007

A THESIS SUBMITTED IN PARTIAL FULFILLMENT OF
THE REQUIREMENTS FOR THE DEGREE OF

DOCTOR OF PHILOSOPHY

in

The Faculty of Graduate and Postdoctoral Studies

(Physics)

THE UNIVERSITY OF BRITISH COLUMBIA

(Vancouver)

August 2015

© Matheson Edward Longton 2015

Abstract

The study of solutions to open string field theory remains very much a work in progress, even for the bosonic string. In this dissertation I consider in detail two of these solutions involving marginal deformations of the original boundary conformal field theory. The first is a previously unknown solution in which two D-branes are translated before tachyon condensation occurs. This solution is studied in the level truncation scheme, in a sector which is larger than the universal subspace, but still less than the whole string Fock space due to several symmetries of the theory which take on a different content in the presence of two D-branes. This solution brings us a step closer to a full understanding of the relationship between the magnitude of a marginal deformation in BCFT and the strength of the corresponding marginal operator in OSFT. The other solution I study was first written down formally by Kiermaier and Okawa, and involves the renormalization of an exactly marginal operator. I consider the same solution with a more general renormalization scheme and find a set of sufficient restrictions for the solution's validity. While this proceeds much as in the original work on this solution, I find some freedom in the solution as well as additional algebraic structure for renormalization schemes. I also present a collection of procedures written in Maple which define and manipulate wedge states with insertions, as well as computing correlation functions for such states provided that all inserted operators are sufficiently simple. Using this code I am able to calculate the tachyon profile of this solution for the time-symmetric rolling tachyon at 6th order in λ and describe its properties in comparison to previously known rolling tachyon profiles. I find the same unwanted oscillations that were seen in previous work on the time-asymmetric rolling tachyon.

Preface

The research and calculations in this dissertation were carried out by Matheson Longton under the supervision of Dr. Joanna Karczmarek. While Dr. Karczmarek often provided direction and conceptual assistance, nearly all of the work and writing is my own. With the exception of numerical integration routines noted in section 5.3.7, all digital computations described were performed by programs I wrote, primarily in the Maple language.

Versions of chapters 3 and 4 have been published in the Journal of High Energy Physics as [1] and [2] respectively. These papers were based on the work I have done for this dissertation, and were cowritten starting from drafts of these chapters rather than the other way around. The work of chapter 3 was also presented at the conference String Field Theory and Related Aspects V, which took place in Jerusalem in 2012.

A paper containing much of chapter 5 has appeared on the arXiv [3] and has now been accepted for publication by the Journal of High Energy Physics. Appendix A has also appeared on the arXiv as [4], but was never intended for peer reviewed publication.

Table of Contents

List of Tables

List of Figures

List of Programs

Glossary

Acronyms

bcc : A "boundary condition changing" operator implements a change in conformal boundary conditions. A pair of bcc operators is commonly used to change the boundary condition on a finite segment of the boundary.

BCFT : Boundary Conformal Field Theory is a CFT on a surface with a boundary. The boundary conditions imposed there must also be conformal.

BRST : Named for Becchi, Rouet, Stora, and Tyutin, the BRST operator, Q_B, is used to define the physical states of string theory.

CFT : Conformal Field Theory.

OPE : The Operator Product Expansion. A pair of operators can be expanded as $\phi_i(0)\phi_j(z) = \sum_k C_{ij}^k(z)\phi_k(0)$ provided there are no other operators closer to the pair than each other.

OSFT : Open String Field Theory.

SFT : String Field Theory. Since we will be focused on open strings this will be used interchangeably with OSFT.

Notation

$: \; :$ Normal ordering as defined in Polchinski's book [6]. This sorts raising and lowering operators, or equivalently removes singular parts of expressions with operator insertions.

$\overset{\circ}{\circ}\ \overset{\circ}{\circ}_g$ Normal ordering using a specified subtraction, g. Occasionally g will be omitted, in which case the subtraction is $\frac{1}{(s_1-s_2)^2}$. Defined in section 4.3.2.

$[x, y]\,,\ \{x, y\}$ The commutator and anti-commutator.

$[\ldots]_r$ Renormalization of operators by a generic renormalization scheme assumed to satisfy certain assumptions.

$[\ldots]_G$ Renormalization of operators by a "big G" scheme which regulates distances between operators and then subtracts counterterms which depend on the regulator.

$[\ldots]_g$	Renormalization of operators by a "little g" scheme which subtracts off regulator-independent functions which are to be integrated over the same (possibly regulated) domain as the operators they renormalize.
$\circ$	Function composition operator.
$\dagger$	Hermitian conjugation, also sometimes referred to as *h.c.*.
$\ddagger$	This conjugation is used to define the reality condition for a string field $\Psi = \Psi^\ddagger$, which ensures that the action will be real-valued. It is defined by $A^\ddagger = \text{bpz}^{-1}\, A^\dagger$. Unlike bpz and hermitian conjugation, this conjugation does not exchange bra and ket states.
$\langle\ ,\ \rangle$	While this is treated like an inner product for string field theory, it is really a symplectic bilinear form. It is used in the action to get a real number from a pair of string fields.
$\langle\ldots\rangle_S$	This is the CFT expectation value defined on the Riemann surface S. Often the surface S will be W_n, the wedge state of circumference $n+1$.
$*$	The star-product of string field theory glues two worldsheets together, allowing for string interactions.
$\lfloor\ \rfloor$	Floor operator. The notation $\lfloor n/2 \rfloor$ will often appear in the limit of sums, when the sum is over the number of pairs of operators to contract.
α'	The fundamental scale of the theory is determined by this constant with dimension length squared. The target space length scale is $\sqrt{\alpha'}$. We will use the convention $\alpha' = 1$ except where it is helpful to include it explicitly.
$\alpha_n,\ b_n,\ c_n$	Raising and lowering operators for the matter and ghost sectors of the theory. α_n are matter operators, b_n are anti-ghost operators, and c_n are ghost operators. The operator α_0 is neither a creation or annihilation operator, as the vacuum is an eigenvector.
$\beta_n^{(j)}$	Coefficients of the rolling tachyon profile. The tachyon profile of the rolling tachyon is defined by the series $T(t) = 2\sum_{n=0}^{\infty}\sum_{j=0}^{\lfloor n/2\rfloor} \lambda^n \beta_n^{(j)} \cosh\left((n-2j)t\right)$.
bpz	The bpz operator is defined by $\text{bpz}(z) = -\frac{1}{z}$, and has the effect of exchanging the "in" and "out" states of a string.
$c(t)$	The ghost operator, which is commonly inserted on the boundary of a worldsheet. The c_n operators are its modes.
$\hat{d}$	The physical distance separating two D-branes in chapter 3. $d = \frac{\hat{d}}{\pi\sqrt{2\alpha'}}$ defines simple units for this distance.
$\Gamma_\epsilon^{a,b}(x,y,\ldots)$	The region (a,b) minus any places where two or more of the coordinates $(x,y,\ldots)$ are within ϵ of each other. This regulates the region (a,b) so that divergences due to operator collisions do not occur.

$h.c.$	Hermitian conjugation, also referred to with †.
L_n	Virasoro raising and lowering operators. These are modes of the energy-momentum tensor in some sector, which is normally indicated by a superscript.
λ	Commonly used to parameterize the strength of a marginal deformation. Specifically, in chapters 4 and 5 the marginal deformation V will always appear in the combination λV.
Ω	The twist operator which reverses the orientation of the string, $\sigma \to \pi - \sigma$.
Q_B	The BRST operator $Q_B = \frac{1}{2\pi i} \oint \left(dz\, j_b + d\tilde{z}\, \tilde{j}_B \right)$, where $j_B = cT^m + :bc\partial c: + \frac{3}{2}\partial^2 c$ and T^m is the matter part of the energy tensor.
$V(t)$	Commonly used to refer to a marginal operator which is inserted on the boundary of a worldsheet. Throughout most of chapters 4 and 5 this will have the self-OPE $V(0)V(t) \sim \frac{1}{t^2}$.
$V(a,b)$	The marginal operator $V(t)$ integrated between a and b: $V(a,b)^n = \int_a^b d^n t \prod_{i=1}^n V(t_i)$.
X_a	The coefficient of the marginal term representing translation for the solution of chapter 3 on separated D-branes.

Chapter 1

Introduction

The most basic objects in string theory are strings. These can be closed strings (loops) or open strings (with ends), but in either case the worldsheet interpretation of string theory forms a conformal field theory, or CFT. These are two dimensional CFT's, as they describe dynamics within the two dimensions of a string: length and time. In the case of closed strings, the CFT can be taken on the plane $\mathbb{R}^2$, but for open strings the endpoints create a boundary for the space. The boundary conditions placed on the string at its endpoints must be conformal, resulting in a boundary conformal field theory, or BCFT. While for some time these boundary conditions were viewed as nothing more than that, in [7] it was recognized that they could also be thought of in terms of D-branes. D-branes are objects which the ends of strings are "attached" to, and they can have varying size, shape, dimension, energy, and even other properties such as charge. In this picture, the tachyon in the spectrum of the bosonic open string can be explained as corresponding to the instability of the D-brane it is attached to. This is where open string field theory is useful: while a given string theory only studies the strings allowed by a given D-brane configuration, a single string field theory can describe many different D-brane configurations.

Classical solutions of open string field theory, or OSFT, describe the different conformal boundary conditions available for a given conformal field theory. Since in the language of string theory these boundary conditions are the D-brane configurations, finding these classical solutions is an important tool for understanding D-branes. If we have such a solution we know that an associated D-brane configuration is allowed, and we can easily find its energy. In principle the structure of OSFT can also tell us about the configuration's stability and any moduli. Time-dependent solutions can even teach us about D-brane dynamics. Unfortunately, the known solutions to OSFT only begin to scratch the surface of the entire space of D-brane configurations. While recent developments describe a procedure for constructing a solution from a desired boundary condition, the solutions which have been explicitly written down and studied are a very small subset of all allowed D-brane configurations.

In the first part of this dissertation, we find a new solution using the level truncation approximation scheme. One solution which is well known describes the decay of an existing space-filling D-brane. When N of these D-branes are present, the solution for D-brane decay gains an $SU(N)$ symmetry, so linear combinations of the D-branes can decay. The solution representing D-brane decay also exists when the initial D-brane is not space-filling, and in this case we can still gain an $SU(N)$ symmetry by duplicating the initial D-brane. In the case of D-branes with non-zero codimension, however, we can break this symmetry by placing the D-branes at different spatial locations. A non-trivial linear combination of D-branes cannot decay if the D-branes are not in the same place, because the result — half a D-brane in one place, and half somewhere else — would not be a valid D-brane configuration. We will examine the set of solutions to the approximate theory in the case where the initial configuration is two D-branes separated by a known distance which will parameterize our set of solutions.

Another solution of OSFT which should exist describes marginal deformations of the initial BCFT. While such solutions have been constructed analytically in a number of cases, they do not exist as solutions in the level truncated approximate theory. The truncation raises the marginal direction in the string field space, and only points which are local extrema will be solutions to the approximate theory. In practice this means that only the trivial solution survives from the marginal set. One such marginal deformation is the massless string mode perpendicular to a D-brane which is not space-filling. This marginal deformation causes translation of the D-brane, and it is the one we study in the first part of this document.

We have seen that when two D-branes are initially separated either one can decay, but linear combinations can only decay when they are coincident. In this case, the enhanced symmetry at the point where the two D-branes coincide allows for the solution with a marginal deformation and a decay to survive level truncation. Although level truncation breaks a continuous set of solutions to a few discrete ones, by searching for an $SU(2)$ of solutions to the full theory we know that the level truncated action should have some extrema on that set, and solutions will survive. We find such a solution and study its properties, parameterized by the initial separation of the D-branes.

We take the first step towards a map between the OSFT marginal parameter and the physical impact of the marginal deformation without performing CFT calculations. Previous maps have involved calculating a quantity in OSFT for a marginal solution and comparing the same quantity to a marginally deformed CFT, but we attempt to do this directly. We have taken the first steps but require a better understanding of the field redefinition which takes place when OSFT is reexpanded about one of its solutions. Even without the full mapping between the OSFT marginal vev and the physical translation, however, we do find evidence that there is a maximum physical translation that can be achieved through marginal solutions. While it has long been known that there is a maximum value of the marginal vev in level truncated OSFT, this maximum physical effect is unexpected and casts doubt on earlier explanations of the maximum vev, in which the value of the marginal parameter was bounded but the corresponding deformation of the BCFT was not.

In the second part of this dissertation we examine a previously known formal solution for a class of marginal deformations. These marginal deformations are the more difficult case, in which the OPE of two copies of the associated operator is singular: $V(0)V(t) \sim \frac{1}{t^2} + O(1)$. The specific marginal deformation we are interested in is the so-called "rolling tachyon", which localizes a D-brane in the time direction. There are two different versions of the rolling tachyon. The simpler version has regular self-OPE and is not our focus. That rolling tachyon solution represents an unstable D-brane which exists in the infinite past and then decays at a finite time. Our focus will be on the time-symmetric rolling tachyon which exists only for an interval of time, decaying in the past and future. The marginal operator associated with such a decay is $V(t) = \sqrt{2}\cosh\left(\frac{X^0(t)}{\alpha'}\right)$.

First we examine the mathematical framework necessary for that solution in detail. We search for the most general renormalization scheme we can apply to properly cancel the singularities arising from the OPE and satisfy the assumptions necessary for a formal solution. We consider two different approaches to constructing general renormalization schemes, which we call the "big G" and "little g" schemes. We rigorously prove that the trivially exponentiated version of the little g scheme gives a two parameter family of finite operators satisfying all of the necessary assumptions. The big G scheme fails to give finite operators when naively

exponentiated, but it offers an attractive framework for the construction of the most general renormalization scheme allowed at any finite order. We also briefly examine the renormalization scheme originally proposed for this solution and show that it is nearly identical to our little g scheme. It is clear that there are at least two free parameters in the renormalization, and likely infinitely many, so we ask what this implies for uniqueness of the solution. The free parameters we have identified correspond to rescalings of the renormalized operators. Because of the way the renormalized operators appear in the solution, such a rescaling changes the solution and we expect that it corresponds to gauge transformations, but this is not proven.

Returning our focus from general marginal deformations with singular self-OPE to the case of the rolling tachyon, I have written a computer program to explicitly construct this solution at any order in the marginal deformation parameter λ. The program also computes arbitrary tachyon correlation functions in the conformal frame we are using. As a result, in addition to the formal solution the program can also produce the tachyon profile in the form of unevaluated integrals. At moderate order in λ these integrals require numerical evaluation using 3rd party integration routines. In addition to the tachyon profile of the solution, the program can also compute the equation of motion and take its correlation function with any other string field built from insertions of tachyon modes. Testing that such quantities vanish gives us evidence that the formal solution does satisfy the equation of motion when explicitly constructed and renormalized. The Maple procedures are designed to be flexible enough to manipulate many wedge states, and can be used to find correlation functions for other wedge states involving only the c ghosts and simple marginal operators. Adding more operators, however, should be fairly straightforward provided the correlators with each other and with the operators already considered can be written down in a closed form.

Examining the tachyon profile, we find that for small λ the solution looks very much like two copies of the simple exponential rolling tachyon. In particular, the coefficients which control the behaviour for small λ show the same asymptotic behaviour as the exponential rolling tachyon solutions. When λ is increased, however, the rest of the coefficients must be included and the free parameters in the renormalization scheme come into play. The tachyon profile is not a gauge independent quantity so the fact that it depends on the parameters tells us very little, aside from the fact that the solution really is affected by those rescalings. Whether they are genuine gauge transformations is not known. It is known that the period of the tachyon field's oscillations is gauge dependent, so it is interesting that that period changes quite suddenly as λ is increased to the point where all of the coefficients are important. This suggests that a change in marginal parameter λ for the time-symmetric rolling tachyon has a similar effect to a change of gauge in the time-asymmetric case. Finally, the presence of an approximately constant period for small λ tells us that the coefficients responsible for that part of the tachyon profile are a convergent series for any appropriate λ. Including additional coefficients is most naturally done by considering "rows" with constant momentum deficit. While there is not a great deal of data, it suggests that each row converges, but there is no suggestion yet that the sum of rows is a convergent series. In the small λ limit, we show that only one row of coefficients contributes to the tachyon profile, so there is no sum of rows. If this sum does not converge for large λ it raises the interesting possibility that marginal deformations really do have a maximum strength, as has been found in level truncation studies including our work on separated D-branes.

This document is structured as follows. Chapter 2 discusses some of the work that has

previously been done in string field theory, and describes the approaches that we will use. Chapter 3 finds the level truncated solution representing a combination of translation and decay for separated D-branes, and discusses the properties of that solution and difficulties involved in writing down a precise correspondence between the marginal parameter X_a and the translation distance $\hat{d}$. The work on formal solutions for marginal deformations with singular self-OPE is split over chapters 4 and 5. Chapter 4 expands on the work of Kiermaier and Okawa by describing in detail the construction and properties of a renormalization scheme compatible with a solution of OSFT, and chapter 5 deals with the numerical calculations using the renormalization scheme we find. Appendix A contains the level truncated action used for separated D-branes in chapter 3. Appendix B details the actual Maple program used to construct the rolling tachyon solution and its tachyon profile, and gives sample C++ code for numerically evaluating the resulting integrals.

Chapter 2

Background

An obvious question in the study of boundary conformal field theories is exactly which boundary conditions preserve the conformal symmetry. We refer to the collection of all CFT's with all such boundary conditions for each as the BCFT landscape. We will only be interested in two-dimensional BCFT's, since these are equivalent to string theories. In this context the boundary conditions are identified with the D-brane configuration on which the open strings are allowed to propagate. A background independent study of the BCFT landscape is therefore an important tool in the study of D-branes and their dynamics.

The landscape of boundary conformal field theories contains all possible D-brane configurations of string theory, so we use string field theory to study it. Open string field theory is an interacting theory of off-shell open strings, with closed strings appearing only in loop diagrams. It can be formulated using any BCFT as a starting point, and classical solutions of the equation of motion describe new BCFTs which the theory can in principle be re-expanded about. The energy of a solution is the energy of the new D-brane configuration relative to the initial one, and the cohomology of the modified BRST operator for a solution describes the physical excitations of strings allowed on the configuration. While it is not at all clear that all BCFTs should exist as possible solutions, every D-brane configuration for the starting string theory should. In this context, OSFT is background independent. It may also be that there are exotic solutions corresponding to D-branes for string theories with different field content, for example finding an open superstring theory beginning with only bosonic strings. Such solutions, if they exist, have not yet been found. The most well known solutions represent either the decay of a D-brane or a marginal deformation of the boundary conditions. We will focus primarily on the latter.

2.1 String Theory

We begin by describing the first quantized bosonic string theory. Once we have done that we can construct OSFT by replacing each string mode with a classical field. Quantizing those fields will result in a quantum string field theory, but that subject is well beyond the scope of this dissertation.

A common parameterization of the open string has endpoints at $\Re w = 0, \pi$ and time running in the imaginary direction, where w is the worldsheet coordinate. A more useful parameterization is $z = e^{-iw}$ which has the string endpoints on the real axis, with time running radially outward from the origin. The field content of bosonic string theory is a matter field for each dimension of the target space and two anticommuting Fadeev-Popov ghost fields which are introduced in gauge-fixing to the conformal gauge. All of these fields live in the two-dimensional

space of the worldsheet. The action is

$$S = \frac{1}{2\pi\alpha'} \int d^2z \; \partial X^\mu \bar{\partial} X_\mu + \frac{1}{\pi} \int d^2z \; b\bar{\partial} c \; . \tag{2.1}$$

Our convention will be to set the constant $\alpha' = 1$, and we will only write it where it is useful for explicitly dimensionful quantities. If we take Neumann boundary conditions at the endpoints of the string ($\Im z = 0$), the solution to this system has the following mode expansion

$$X^\mu(z, \bar{z}) = x_0^\mu - i\alpha' p^\mu \ln(z\bar{z}) + i\sqrt{\frac{\alpha'}{2}} \sum_{n \neq 0} \frac{\alpha_n^\mu}{n} \left(z^{-n} + \bar{z}^{-n} \right) \tag{2.2}$$

and

$$b(z) = \sum_n b_n z^{-n-2}, \quad c(z) = \sum_n c_n z^{-n+1}. \tag{2.3}$$

The modes α_{-n}^μ with $n \geq 1$, b_{-n} with $n \geq 2$, and c_{-n} with $n \geq -1$ are raising operators, while α_0^μ is a constant proportional to p^μ. All of the other modes are lowering operators, and annihilate the vacuum. The commutation relations are

$$[\alpha_m^\mu, \alpha_n^\nu] = m\delta_{m+n,0}\eta^{\mu,\nu} \; , \quad \{b_m, c_n\} = \delta_{m+n,0} \; , \quad \{b_m, b_n\} = \{c_m, c_n\} = 0 \; . \tag{2.4}$$

In addition, the holomorphic energy-momentum tensor $T(z)$ has a Laurent expansion in terms of the Virasoro operators

$$T(z) = \sum_{m=-\infty}^{\infty} \frac{L_m}{z^{m+2}} \; , \tag{2.5}$$

where the Virasoro operators L_m obey the Virasoro algebra

$$\left[L_m^{\text{total}}, L_n^{\text{total}} \right] = (m-n) L_{m+n}^{\text{total}} + \frac{c}{12}(m^3 - m)\delta_{m+n,0} \; . \tag{2.6}$$

The central charge of the theory is set to $c = 0$ by choosing the matter content appropriately. Specifically, for the bosonic string we can accomplish this by insisting on having $D = 26$ for our target space. The anti-holomorphic part of the energy-momentum tensor has its own Virasoro modes with an identical algebra, but since we are working with open strings, our Riemann surface will always have a boundary and the boundary conditions mean that $T(z)$ and its anti-holomorphic partner $\tilde{T}(\bar{z})$ are not independent quantities. In terms of the fundamental matter oscillators, the matter Virasoro modes are

$$L_n = \begin{cases} \sum_{m=0}^{\infty} \alpha_{-m}^\mu \alpha_{\mu m}, & m = 0 \\ \frac{1}{2} \sum_{m=-\infty}^{\infty} \alpha_{n-m}^\mu \alpha_{\mu m}, & m \neq 0 \; , \end{cases} \tag{2.7}$$

and the Virasoro operators in the ghost sector are

$$L_n^{(g)} = \sum_{m=-\infty}^{\infty} (2n - m) : b_m c_{n-m} : -\delta_{n,0} \; , \tag{2.8}$$

where : : represents the standard normal ordering.

The vacuum state $|0;0\rangle$ with zero momentum is $SL(2,\mathbb{R})$ invariant, meaning in the state operator correspondence it is mapped to the identity operator in the upper half plane. This vacuum is related to those in the notation of Polchinski [6] by

$$c_1 |0;k^\mu\rangle = |k^\mu\rangle_m \otimes |\downarrow\rangle , \tag{2.9}$$

where $|k^\mu\rangle_m$ is the matter vacuum with momentum k^μ and $|\downarrow\rangle$ is one of the two ghost vacua.

The number of states in this theory is too large as we have not yet done anything to remove null states and those with negative norm. This is done by identifying physical states as the cohomology of the BRST operator. The BRST operator has the form

$$Q_B = \sum_n c_n L_{-n} + \sum_{n,m} \frac{m-n}{2} : c_m c_n b_{-m-n} : -c_0 \ . \tag{2.10}$$

Physical states are those satisfying $Q_B |\phi\rangle = 0$, but the nilpotency of Q_B means that states of the form $Q_B |\chi\rangle$ are null (orthogonal to all physical states including itself) as well as being physical. The null states are identified with zero and removed from the spectrum. The lightest physical state is the tachyon $c_1 |0;k\rangle$ with mass given by $m^2 = -\frac{1}{\alpha'}$, and the first excited state $\alpha^\mu_{-1} c_1 |0;k^\nu\rangle$ is massless. An infinite tower of more massive states is created by acting on the tachyonic state with matter oscillators α^μ_{-n} and certain combinations of the ghost oscillators b_{-n} and c_{-n}.

The state-operator correspondence allows us to view this theory in a different way. Instead of operators such as α^μ_n, c_n, b_n, and L_n acting on states such as the vacuum $|0;k^\mu\rangle$, we can view it as the local operators $X^\mu(z,\bar{z})$, $c(z)$, $b(z)$, and the energy-momentum tensor $T(z)$ inserted in a Riemann surface. The canonical choice of Riemann surface is the infinite strip with $0 \leq \Re w \leq \pi$ for an open string, as the string's spatial coordinate is defined to run from 0 to π while the worldsheet time coordinate is clearly unbounded. This is a conformal field theory, however, and as such we have the conformal transformations available to us. Local conformal transformations are the holomorphic coordinate transformations $z' = f(z)$. The conformal transformation $z = e^{-iw}$ maps the infinite strip to the upper half plane $\Im z \geq 0$, which is in many cases the simplest Riemann surface to consider for open strings. Slices of constant worldsheet time are mapped to semicircular curves of constant radius, with the time increasing radially outward. The string endpoints lie on the boundary $\Im z = 0$, and the infinite past is mapped to the point $z = 0$. When changing conformal frames any correlation functions in the new frame are given by

$$\langle \phi_1(z'_1,\bar{z}'_1) \dots \phi_n(z'_n,\bar{z}'_n) \rangle = \prod_{i=1}^{n} \left(\frac{dz'}{dz}\right)^{-h_i}_{z'=z'_i} \left(\frac{d\bar{z}'}{d\bar{z}}\right)^{-\bar{h}_i}_{\bar{z}'=\bar{z}'_i} \langle \phi_1(z_1,\bar{z}_1) \dots \phi_n(z_n,\bar{z}_n) \rangle \ . \tag{2.11}$$

The exponents h_i and $\bar{h}_i$ here are called the conformal weights of the operators ϕ_i and define how the operators transform under conformal mappings. The conformal weights can also be defined in terms of an operator's scaling dimension and spin [6][8]. An n-point function will be computed by inserting operators at n distinct locations on the Riemann surface. Incoming or outgoing open string states correspond to operators inserted on the boundary, and closed string states correspond to operators inserted in the bulk. For the open strings we will be studying, we must specify the locations of exactly three operator insertions in order to fix the three moduli of the disc.

2.2 String Field Theory

While there were several attempts to formulate an off-shell theory of strings, it was Witten's model [9] that succeeded in providing the foundations of OSFT. His theory is based on a $\mathbb{Z}_2$ graded algebra satisfying several axioms.

$$\deg(a*b) = \deg(a) + \deg(b), \quad Q(a*b) = (Q(a))*b + (-1)^a a * Q(b), \quad Q^2 = 0 \tag{2.12}$$

The nilpotent derivation Q turns out to be the BRST operator. The resulting theory is based on a δ-function interaction of half-strings. It has a non-commutative star product that glues the right half ($\sigma > \frac{\pi}{2}$) of one string to the left half ($\sigma < \frac{\pi}{2}$) of the other, effectively joining two open-string worldsheets together. The $*$-product provides the interactions, but we still need a map from the space of string fields to the complex numbers in order to construct an action. The integration operation is introduced for this purpose. It glues the two halves of a string to each other, also using a δ-function glue. Although actual calculations are not performed this way, for the matter sector these operations are defined in [10] as

$$\int \Psi \stackrel{\text{def}}{=} \int \prod_{0\le\sigma\le\pi} dX^\mu(\sigma) \prod_{0\le\tau\le\frac{\pi}{2}} \delta\left[X^\mu(\tau) - X^\mu(\pi-\tau)\right] \Psi\left[X^\mu(\tau)\right], \tag{2.13a}$$

$$\begin{aligned}(\Psi * \Phi)\left[Z^\mu(\tau)\right] \stackrel{\text{def}}{=} \int \prod_{0\le\tilde\tau\le\frac{\pi}{2}} dY^\mu(\tilde\tau) dX^\mu(\pi-\tilde\tau) \times \\ \prod_{\frac{\pi}{2}\le\tau\le\pi} \delta\left[X^\mu(\tau) - Y^\mu(\pi-\tau)\right] \Psi\left[X^\mu(\tau)\right] \Phi\left[Y^\mu(\tau)\right],\end{aligned} \tag{2.13b}$$

where

$$Z^\mu(\tau) = X^\mu(\tau) \text{ for } 0 \le \tau \le \frac{\pi}{2}, \quad \text{and} \quad Z^\mu(\tau) = Y^\mu(\tau) \text{ for } \frac{\pi}{2} \le \tau \le \pi. \tag{2.13c}$$

Given this, the action is

$$S = -\frac{1}{2}\int \Psi * Q\Psi - \frac{g}{3}\int \Psi * \Psi * \Psi \ , \tag{2.14}$$

where g is a coupling constant and Q is the BRST operator. The first term is a kinetic term which reproduces the free string theory spectrum due to its use of the same BRST operator, while the second term introduces cubic interactions. Since a single string field is made up of all possible string modes at all different momenta, the interaction mixes all of these infinitely many fields. This action is valid even for string fields which are not on the mass shell.

Because the action is cubic, it does have the problem that the action is unbounded both above and below. Quantum mechanically it is not a sound theory to study, but the classical theory still has perfectly valid solutions at the action's critical points. Superstring field theory does not have this problem, so quantum superstring field theory should be a well defined thing to study, but at present classical solutions are not fully understood. The cubic bosonic theory is therefore a useful thing to study since many solutions have a similar structure, but are simpler in the bosonic case. It is suggested in [11] that it may be possible to add higher order terms to the action, but such terms would also appear as a violation of the associativity of the star-product.

The ghost number of a string field can be defined as the number of c ghosts minus the number of b antighosts acting on the vacuum. With this convention, the $\int$ operation vanishes unless the ghost number of its argument is 3. For string fields of definite ghost number, this means that the action is only non-zero for ghost number one. All physical string fields such as the tachyon and massless vector have ghost number 1, while some toy models involve string fields of ghost number 0 for simplicity. The action (2.14) has a large gauge symmetry

$$\delta\Psi = Q\Lambda + \Psi * \Lambda - \Lambda * \Psi \ , \tag{2.15}$$

where Λ is any string field of ghost number 0. Since the BRST operator Q increases a string field's ghost number by 1, and ghost number is also additive under the $*$-product, the ghost number is preserved under such transformations provided that the string field Ψ has ghost number 1 and the gauge field Λ has ghost number 0.

The simplest way to think of the string field is as a sum over all possible open string states.

$$\Psi = \int d^{26}p \prod_{\mu} \sum_{I_\mu,J,K} \phi_{I_\mu,J,K}(p)\, \alpha^{\mu}_{I} b_J c_K \,|0;p\rangle \tag{2.16}$$

Here the upper case indices I, J, K represent multiple oscillator indices for products of operators, so that a random example of a term in the sum would be

$$\phi_{(-2,-1),(-2),(0,1)}(p)\, \alpha^{25}_{-2}\alpha^{25}_{-1} b_{-2}c_0c_1 \,|0;p\rangle \ .$$

Each state in the open string Fock space comes with a spacetime field as its coefficient, but in most practical situations we are only interested in translationally invariant solutions. In this case the coefficient fields $\phi(p)$ are only non-zero for $p = 0$ and can be treated as simple constant coefficients. The action (2.14) then has the form of a cubic polynomial in the infinitely many coefficients.

Let us now turn to some common notation and computational tools used when the string field is expressed in the open string Fock space. The integration operator and triple star product used in the cubic term of the action are written as

$$\int A * B = \langle A, B\rangle \,, \quad \langle A, B * C\rangle = \langle A, B, C\rangle \,. \tag{2.17}$$

Absorbing a factor of the coupling constant into the string field, $\Phi = g\Psi$, the action becomes

$$S = -\frac{1}{g^2}\left(\frac{1}{2}\langle\Psi, Q\Psi\rangle + \frac{1}{3}\langle\Psi,\Psi,\Psi\rangle\right). \tag{2.18}$$

The $*$-product of two string fields is not at all simple to write down in the basis (2.16). Fortunately, Gross and Jevicky [12] found a state in the product of three SFT Hilbert spaces such that

$$|\Phi * \Psi\rangle_3 = \langle\Phi|_1 \langle\Psi|_2 |V_3\rangle \,. \tag{2.19}$$

Specifically, the cubic term in the action is easily written in terms of this 3-vertex.

$$\langle\Psi,\Psi,\Psi\rangle = \langle V_3| \,|\Psi\rangle_1 \,|\Psi\rangle_2 \,|\Psi\rangle_3 \tag{2.20}$$

Switching from ket states to bra states is done using bpz conjugation: $\langle\Psi| = \text{bpz}\,|\Psi\rangle$. In the Fock space basis this is similar to hermitian conjugation with additional sign factors. It is described in more detail in section 3.1.1 and the bpz conjugates of simple states are given in equation (3.9). The action's kinetic term is most easily calculated directly in terms of oscillators.

$$\langle\Psi|\, Q\, |\Psi\rangle \tag{2.21}$$

The calculation of both terms in the action is explained in detail in section 3.1.

Using the state-operator correspondence, we can also represent the string field without referring to oscillator modes. In this form, a string field can be defined by its inner product with an arbitrary test state. Any open string state can be expressed as an operator inserted at the origin in the upper half plane. For example, we might define a string field A by

$$\langle\phi, A\rangle = \langle f_1 \circ \phi(0) f_2 \circ \mathcal{O}_A(0)\rangle_S \tag{2.22}$$

where f_1 and f_2 are conformal maps from the upper half disc to disjoint regions making up the Riemann surface S, and $\mathcal{O}_\mathcal{A}$ is the operator corresponding to the state $|A\rangle$. We will often relax the assumption made here that the string field is expressed as a single operator inserted at the origin of the upper half plane, and permit any number of operators inserted anywhere in the portion of S associated with the image of the upper half disc under the function f_2, or equivalently, the portion of S which is the image of $|z| > 1$ under f_1. The region $f_1(|z| < 1)$ is sometimes referred to as the conformal patch and is reserved for the test state representing the asymptotic future. We often think of the string field A as being the Riemann surface S with operator insertions, but to be precise we should remember that it is really still a Fock space state defined by its correlation function with an arbitrary test state $|\phi\rangle$. Since the CFT correlation function must saturate the ghosts in order to produce non-zero results, a physical string field A requires a test state ϕ with ghost number 2. The test operator producing information about the tachyon component of a string field is $c\partial c$.

Since OSFT can be formulated for any open string boundary conditions and solutions represent D-brane configurations, there must be a new formulation of OSFT for every solution. Taking the original OSFT action and expanding it about the string field Ψ gives an action with the same form except that the BRST operator is modified as

$$Q_\Psi \phi = Q_0 \phi + \Psi * \phi - (-1)^{(\Psi)(\phi)} \phi * \Psi \ . \tag{2.23}$$

Q_0 is the BRST operator for the initial reference BCFT (corresponding to the solution $\Psi = 0$) and ϕ is any string field. The sign factor in the last term uses the standard notation that when a string field appears in the exponent of -1 it is taken to mean the ghost number of that string field. This way the new terms in (2.23) combine to make a commutator for physical string fields, but in general can be either a commutator or an anti-commutator. This is a significant amount of background independence, as only the field content is still defined in terms of the first reference BCFT. Schnabl has referred to this as being "half-way" to background independence [13].

A surge of interest in OSFT began in 1999 when Sen predicted an explanation for the tachyon in the spectrum of the bosonic open string and suggested that his conjectures could be best tested in string field theory [14]. He suggested that any D-brane system with a tachyon in its spectrum can decay to the vacuum with no D-branes. He claimed that at this point in

the space of string fields, the negative value of the tachyon potential exactly cancels the initial tension of the D-branes, indicating the true vacuum with 0 energy. He also provided some evidence that there would be no dynamical degrees of freedom at that vacuum. This was a necessary result in order to explain the absence of the brane-antibrane system's $U(1)$ gauge field from the true vacuum. The existence of solutions to OSFT representing certain other D-brane configurations was also considered, with the discussion focusing on the fact that these configurations should also be unstable to decaying to the same tachyon vacuum. In time, these conjectures were rewritten and presented in their best known form [10].

1. The tachyon potential has a locally stable minimum, whose energy density $\mathcal{E}$, measured with respect to that of the unstable critical point, is equal to minus the tension of the D25-brane:
$$\mathcal{E} = -T_{25}.$$

2. Lower dimension D-branes are solitonic solutions of the string theory on the background of a D25-brane.

3. The locally stable vacuum of the system is the closed string vacuum. In this vacuum the D25-brane is absent and no conventional open string excitations exist.

These conjectures imply that the open string with purely Neumann boundary conditions actually lives on a space-filling D25-brane. The tachyon in the string spectrum is associated with the instability of this D-brane.

2.2.1 Level Truncation

Early attempts to find the tachyon vacuum solution of OSFT used the oscillator basis for the string field. The first challenge in solving the equations of motion in this approach is the infinite number of fields. A suitable approximation scheme is needed to reduce the problem to a finite number of variables. The level truncation scheme sorts the states in the string field (2.16) according to their L_0 eigenvalue [15]. It was initially used only for translationally independent solutions so that the level essentially counted the indices on all of the oscillators acting on the vacuum, but the method was later extended to include the whole L_0 eigenvalue so that solutions with $p \neq 0$ could be considered [16]. The difference between a term's eigenvalue and that of the zero momentum tachyon is called the level, and only terms in the string field with level up to a fixed value are included. With a string field truncated to level L, it is sometimes helpful to also truncate the action (which has level $3L$) to a lower level M. Of course M must still be at least $2L$ in order to include the kinetic term for each field. Solutions to a level truncated system are approximate solutions to the full OSFT equations of motion, with the approximation typically improving as L is increased.

A number of solutions are known in level truncated OSFT, but the first is the solution representing the tachyon vacuum. Sen and Zwiebach first found this solution for low levels [17], and that was followed by calculations at higher levels [18]. The string field Sen and Zwiebach used at level 2 had the form of (2.16) with constant coefficients:

$$|T\rangle = t\, c_1 |0\rangle + u\, c_{-1} |0\rangle + v \frac{1}{\sqrt{13}} L_{-2} c_1 |0\rangle \ . \tag{2.24}$$

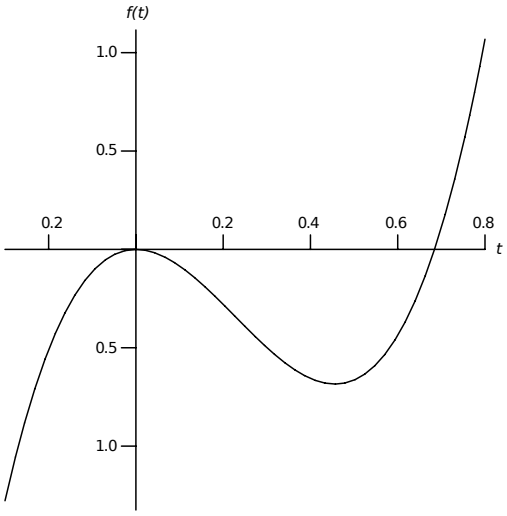

Figure 2.1: The potential at level 0 as a function of the tachyon zero mode t.

This makes several simplifying assumptions about which fields to include. First is the obvious choice of a spatially uniform solution, so that the infinite tower of momentum modes for each string field can be dropped, keeping only the 0 momentum states based on $|0\rangle \stackrel{\text{def}}{=} |0;0\rangle$. Next they imposed Siegel gauge, which is $b_0 |T\rangle = 0$. This gauge choice is imposed level by level, and it can be shown that this gauge choice is valid locally at $|T\rangle = 0$ for every level except level 1, where the necessary gauge transformations become singular. If any level 1 terms are to be dropped from the string field, we must find a different justification. Fortunately, in this case the twist symmetry of the theory allows us to consider only terms with even level. The twist symmetry reverses the parameterization of the worldsheet space coordinate $\sigma \to \pi - \sigma$. Of the zero-momentum fields with Neumann boundary conditions that we are considering, all of the odd level fields change sign under this symmetry while the even level ones do not. The action is invariant under twist, so any twist-odd fields can only appear in pairs, and their equations of motion will never be sourced by twist-even fields. It is consistent to set all twist-odd fields to 0, reducing the space of solutions which will be found, but in no way invalidating the solutions which remain. Since the tachyon vacuum solution is in the twist-even subspace, imposing this symmetry on the string field will greatly simplify calculations.

The energy of any solution will depend on the entire string field, but it is often useful to consider it as a function of only the tachyon vev t in $tc_1 |0\rangle$. This is achieved by using the equations of motion to eliminate all of the fields except for the tachyon. This is not a unique procedure since there are many different solutions, but for any given solution we can see a profile which will have critical points at values of t which correspond to solutions on the branch under consideration. Often the energy is rescaled to units where the tension of the initial D-brane is 1, and this is typically referred to as $f(t)$. The simplest (level 0) tachyon potential $V(t)$ has the form of a cubic polynomial shown in figure 2.1. For the tachyon vacuum solution this profile remains qualitatively the same when higher level fields are included. The trivial solution is at

$t = 0$ and the tachyon vacuum solution appears at $t \approx 0.456$ in this approximation. We also notice that the potential is unbounded below for negative values of t. The physical interpretation of this region is unknown, but there are no classical solutions in that region, corresponding to no D-brane configurations. The energy of the tachyon vacuum solution was found to converge quite quickly to the correct value of negative the D-brane tension. At level 0 it reaches $\approx 68\%$ of this energy, while by level 4 it is already $\approx 95\%$. It does pass the predicted asymptotic value of the energy at level 14, but extrapolations show it turning around and approaching the correct energy from the other side [18]. The spectrum of physical open strings about the tachyon vacuum is expected to be empty, but verifying this with an approximate solution is a difficult task. The modified BRST operator for the theory expanded about a solution obviously has to depend on that solution, as seen in (2.23). By using an approximate solution we will get an operator that is not the correct BRST operator. Additionally, by truncating the string field, we have broken gauge invariance, so Q_Ψ will not be nilpotent. Such an approximate BRST operator will not have the correct cohomology. Attempts were made, however, such as by Giusto and Imbimbo [19][20], to show that the tachyon vacuum has no physical excitations. There the "modified kinetic operator" $\tilde{L}_0 = \{Q_\Psi, b_0\}$ is examined, with Q_Ψ the BRST operator for the theory expanded about the tachyon vacuum solution. At each ghost number n they search for momenta where $\det \tilde{L}_0^{(n)} = 0$. Their assumption is that closely grouped zeros are the result of a single degenerate zero being broken up by the level truncation approximation, and they consider such a group as a single zero for the purposes of finding the cohomology of the BRST operator Q_Ψ. They found that the cohomology is indeed empty at ghost number one, up to the limits imposed by level truncation. At other ghost numbers, however, the cohomology they found was non-trivial. Since physical states all have ghost number 1, it is not at all clear what these states represent.

While the vacuum solution confirms two of Sen's conjectures, there is still the matter of lower dimensional D-branes appearing as solitons. In the framework of OSFT, lower dimension D-branes are solutions. The so-called "lump solutions" were studied by Moeller, Sen and Zwiebach [16] for codimension 1. They are approximately zero where the D-brane is localized, and take values approaching the tachyon vacuum far from the lump. This requires infinitely many momentum modes, and is studied with a compactified direction so that the spectrum is discrete and can be level truncated to a finite number of modes at any given level. The string field analogous to (2.24) now has the form

$$|T\rangle = \frac{1}{2}\sum_{n=0}^{\cdots} \left(t_n c_1 + u_n c_{-1} + v_n c_1 L^X_{-2} + w_n L'_{-2} + z_n c_1 L^X_{-1} L^X_{-1}\right)\left(\left|0; \frac{n}{R}\right\rangle + \left|0; \frac{-n}{R}\right\rangle\right) \quad . \quad (2.25)$$

The vacuum state $\left|0; \frac{n}{R}\right\rangle$ is the n-th momentum mode in the compact direction. In the non-compact directions the solution remains translationally invariant, so the momentum only has one non-zero component. Here L^X_n are the Virasoro operators in the "lump" direction in which the D-brane is to be localized, while L'_n are the matter Virasoro operators in all of the other directions. In principle the sum in (2.25) runs to ∞, but in the level truncated calculation performed, it is noted that the level (L_0 eigenvalue) receives a contribution $\frac{n^2}{R^2}$ from the momentum, so that at any fixed level the number of modes to consider is finite. In fact, the number of modes to consider decreases for terms which have a higher level at $p = 0$. By examining the solution for a D-$(p-1)$ brane at different levels and radii, they found that the

solution appears to converge quite quickly to a lump which is independent of the compactified radius, so long as that radius is large enough that the lowest non-zero momentum tachyon has a negative "kinetic" energy (the quadratic term in the action). For smaller radii they did not find any solutions. While such solutions may well exist, this is an example of the phenomenon that string field theory has a great deal of trouble finding solutions with higher energy than the initial CFT ground state.

The third class of known solutions is those representing a marginal deformation of the initial BCFT. In level truncated SFT these solutions are found by turning on a marginal conformal primary operator by hand and allowing it to excite other fields through the interaction term. Without including all of the infinitely many interactions, the resulting collection of fields will not have the same energy as the exact string field, though it should be closer for higher levels. Since level truncation breaks the marginality of such operators at the non-linear level, the result is not actually a solution at all. For example, a flat one-parameter family of solutions in the full theory is broken to a collection of string fields with nearly-flat potential, and the equations of motion drive solutions back to the extremum of the family. Sen and Zwiebach [21] studied such solutions with a Wilson line marginal deformation by ignoring the equation of motion for the marginal field and imposing the rest. This way a single marginal parameter results in a one-parameter family of string fields containing a single solution: the string field 0 at vanishing marginal parameter. Since the action is close to flat, this family does represent string fields which are almost solutions, and as the level of truncation was increased the action becomes flatter.

Perhaps unexpectedly, Sen and Zwiebach found that these marginal string fields only remain real for a finite range of the marginal parameter. In addition to becoming flatter when the level was increased, the action evaluated at the "solutions" of [21] remained real for progressively larger ranges of the marginal parameter. The expectation from BCFT, however, is that marginal deformations by a Wilson line should exist for any vev of the Wilson line. Several possibilities have been suggested. Since level truncation does give increasing values of the maximum marginal parameter with increased level, it is possible that the maximum increases without bound at infinite level. The values of the maximum at finite level, however, do not increase very fast and lead us to be skeptical of this possibility. In [21] it was suggested that the finite marginal parameter in SFT might correspond to an infinite marginal vev in the CFT. An elaboration of this idea [22] claims that the map from the SFT parameter to the CFT one is double valued. In a toy model, once the SFT parameter reaches its maximum it begins to decrease on a different solution branch while the CFT parameter continues to increase. In chapter 3 we will find evidence that the maximum SFT parameter does correspond to a finite CFT parameter, and we will not see another solution branch corresponding to any higher value of the CFT marginal parameter at the level which we do our calculations. Which explanation is correct, if any, presently remains unknown.

More recently, a level truncated solution with positive energy was found [23] by constructing a string field theory from the BCFT of the Ising model. This model simplified calculations by reducing the number of conformal primaries, and that work was able to find solutions representing all expected boundary conditions. What is unexpected is that the solution representing the higher energy D-brane was found using the lower energy D-brane as the starting BCFT. Interestingly, that solution was complex until level 14 fields were considered, at which point it suddenly became real and remained that way at higher levels. While it may be unlikely, this

does present us with another possible explanation for the lack of marginal solutions beyond a critical value of the deformation strength. They could be there as complex solutions waiting for high level calculations to reveal them.

The issue of matching a marginal SFT parameter to the corresponding CFT parameter was also examined in [24] for a different marginal deformation. While this is not directly applicable, it is a good representative of the type of comparison that is typically attempted. A physical quantity, in this case the energy momentum tensor, is calculated on both sides and the correspondence is found by setting the two to be equal. We will take an alternative approach to relating the marginal parameter to its physical effect. Rather than studying level truncated string fields which are close to being solutions of the equations of motion, we will examine ones which are solutions to all of the level truncated equations of motion, but involve a D-brane decay in addition to the marginal deformation. This is possible because we use a pair of D-branes. When two D-branes are coincident there is a continuous family of allowed decays, since the action gains an $SU(2)$ symmetry. Separating the D-branes breaks the symmetry, and in principle a marginal deformation to restore the coincidence of the D-branes will also restore the symmetry. In practice, however, level truncation prevents us from completely restoring the symmetry (see section 3.2.6). This is why we want to have a continuous set of solutions. Despite the hypothetical set of exact solutions being raised to have different values of the action, there must still be some critical points in the set where the action has a maximum or a minimum, and these will appear as solutions even in the level truncated model. We will try to then compare the marginal parameter of the surviving solutions to the physical displacement which we can adjust as a parameter of the theory. We will not claim a definitive correspondence, as there is a contribution from the decay part of the solution, but the problem is reduced to understanding this contribution.

2.2.2 Analytic Solutions

Going beyond level truncation, there are known analytical solutions to SFT. These are often defined using the test state method for representing the string field, as in (2.22). Alternatively, they are sometimes expressed as operators acting on known string fields such as the $*$-product identity. This form of solution will simplify the theory provided the Riemann surface is chosen so that the star product is easy to implement. The simplest choice is to take the conformal map $z \propto \arctan\xi$ of the upper half plane. This gives a semi-infinite cylinder called a wedge state, with the boundary remaining on the real axis. This conformal frame is shown in figure 2.2b. A wedge state can be easily broken into any number of disjoint parts by changing the scaling of the conformal map so that the $|z| < 1$ portion of the upper half plane gets mapped to a vertical strip of any desired width, and then translating those strips along the real axis. What is important about this frame is that the star product acts by cutting open two cylinders and glueing them together to make a new cylinder with (typically) larger circumference. In the process, a part of each string field's conformal patch is removed, so that only one conformal patch, or "future" worth of Riemann surface remains. A wedge state with circumference $n+1$ is denoted $\mathcal{W}_n$, and the star product acts on such states as $\mathcal{W}_m * \mathcal{W}_n = \mathcal{W}_{m+n}$. The wedge state $\mathcal{W}_0$ with circumference 1, for example, is an identity string field, since it glues in to any string field exactly the width that is removed. Wedge states with insertions consist of such cylinders with operators inserted outside the conformal patch, often on the boundary.

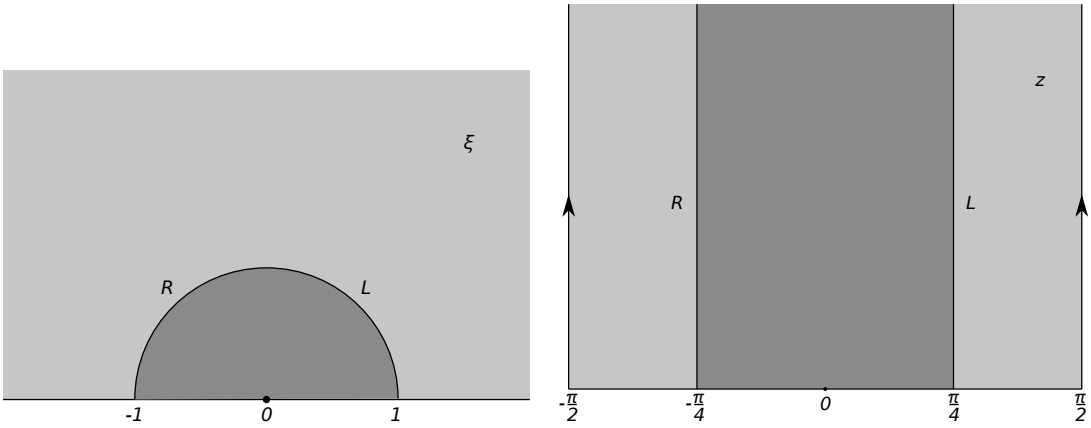

(a) (b)

Figure 2.2: The Riemann surfaces used in the two common conformal frames of the upper half plane (a) and the wedge (b). In each frame the infinite past is located at 0 and the $\tau = 0$ line on the open string worldsheet is drawn separating two shades of grey. The two conformal frames are related by $z = \tan^{-1}\xi$. The coordinate ξ here is z in (2.2), since z is conventionally used for the final coordinate being considered.

The first analytical solution to SFT was found by Schnabl [25], and was constructed using wedge states with insertions. The solution contains two pieces.

$$\Psi = \lim_{N\to\infty}\left(\psi_N - \sum_{n=0}^{\infty}\partial_n\psi_n\right) \tag{2.26}$$

where the string field ψ_n is a Riemann surface with insertions which are defined for this conformal frame using straightforward notation. The c ghost field in the conformal frame of the wedge is $\tilde{c}$, and the zero modes of the b ghost and virasoro operators in this conformal frame are $\mathcal{B}_0$ and $\mathcal{L}_0$ respectively.

$$\psi_n = \frac{2}{\pi^2}e^{-\frac{n}{2}(\mathcal{L}_0+\mathcal{L}_0^\dagger)}\left[\left(\mathcal{B}_0+\mathcal{B}_0^\dagger\right)\tilde{c}\left(-\frac{\pi}{4}n\right)\tilde{c}\left(\frac{\pi}{4}n\right)+\frac{\pi}{2}\left(\tilde{c}\left(-\frac{\pi}{4}n\right)+\tilde{c}\left(\frac{\pi}{4}n\right)\right)\right]|0\rangle \tag{2.27}$$

The vacuum here is the Riemann surface for the conformal transformation $z = \arctan\xi$: the wedge state of circumference π with no insertions. Curiously, the first term does not contribute to any of the coefficients in the standard level truncated basis. In that basis it appears to be 0, but it is required in order for the string field to be a solution.

Remarkably, this term is responsible for all of the physical content of the solution, as explained by Erler and Maccaferri [26]. Given any two solutions Ψ and Φ of OSFT, they suggested a method for splitting Ψ into two parts:

$$\Psi = \Phi_1(\epsilon) + \psi_{12}(\epsilon)\ . \tag{2.28}$$

This requires a "left gauge transformation" $(Q+\Phi)U = U\Psi$ which can always be constructed as

$$U = Qb + \Phi b + b\Psi\ , \tag{2.29}$$

for any string field b with ghost number -1. The first part

$$\Phi_1(\epsilon) = \frac{1}{U+\epsilon}\left(Q+\Phi\right)\left(U+\epsilon\right) \tag{2.30}$$

is a gauge transformation of Φ with finite gauge parameter $U+\epsilon$. The second term

$$\psi_{12}(\epsilon) = \frac{\epsilon}{U+\epsilon}\left(\Psi-\Phi\right) \tag{2.31}$$

is simply the remainder in (2.28). In the limit as $\epsilon \to 0$, two things can happen. If the string field U is invertible then it defines a gauge transformation relating Ψ and Φ, and the remainder term $\psi_{12}(\epsilon)$ goes to zero. If the two are not gauge equivalent then the operator in the remainder is called the "boundary condition changing projector" and is denoted $X^\infty = \lim_{\epsilon\to 0}\frac{\epsilon}{U+\epsilon}$. As far as I am aware, there is no proof that the gauge parameter defined by (2.29) will give a vanishing boundary condition changing projector if two solutions are gauge equivalent, but since $\Phi_1(\epsilon)$ is a valid gauge transformation for all finite ϵ if two solutions differ then X^∞ will capture the physical distinction between the two.

In the case of Schnabl's solution for the tachyon vacuum (2.26), the "phantom" term $\lim_{N\to\infty}\psi_N$ plays a role which is very similar to the boundary condition changing projector. The way the solution is written, the second term is not a solution by itself, so it cannot have the form of ψ_{12} in (2.28). It was shown in [26] that the phantom term in Schnabl's solution is $X^\infty\Psi$ rather than $X^\infty(\Psi-\Phi)$. The splitting of the solution is still into a part with all of the physical content and a part which is gauge equivalent to the perturbative vacuum. What is unusual in the case of Schnabl's solution is that the phantom term is 0 when expanded in the level truncation basis (2.16). While this seems to suggest that the phantom term is 0 and that Schnabl's solution is gauge equivalent to the perturbative vacuum, this is not the case, and $\lim_{N\to\infty}\psi_N$ contains important non-perturbative information about the solution.

The resolution to the seemingly vanishing phantom term most likely lies in the fact pointed out by Ellwood [27] that the vector space of the string field does not have a norm. The operation $\langle A, B\rangle$ in OSFT is sometimes referred to as an inner product, but it is correctly identified as a symplectic bilinear form [11]. This is because the operation $\langle A, B\rangle$ lacks the positivity condition of an inner product, that $\langle x, x\rangle \geq 0$ with the bound saturated only for $x = 0$. For the bilinear form itself this is trivial since two copies of a physical string field will not saturate the ghosts and we will always find 0. Even if we were to consider non-physical ghost numbers, by definition the bilinear form has the property that $\langle x, y\rangle = -\langle y, x\rangle$, so any string field at all will have zero norm if we tried to use this as the inner product. A more reasonable choice to define a norm would be the kinetic term of the action $\langle x, Qx\rangle$, but for terms in the string field such as $c_{-1}\left|0\right\rangle$ we find a kinetic term which is negative. The possibility $\langle x, c_0 x\rangle$ has similar problems. Without a norm on the vector space, we cannot say if two string fields are equal or close to one another. In many cases the coefficients in the level truncation basis provide a good indication of a string field, but there is no guarantee that they give an accurate representation, especially since we can never calculate all of the infinitely many coefficients appearing in that basis.

Schnabl's analytic solution was initially shown to have energy of -1 in units of the D-brane tension, cancelling the energy of the D-brane that the starting CFT lived on, but the other two Sen conjectures were not immediately verified. The third conjecture, that the cohomology at the tachyon vacuum is empty so that there are no physical open string degrees of freedom

without a D-brane, was verified by Schnabl and Ellwood [28]. This is done by first proving the lemma that Q has no cohomology if and only if there exists a string field A such that $QA = I$ with I the identity string field. The task of proving that Q_Ψ has vanishing cohomology becomes a matter of finding such a string field A satisfying $Q_\Psi A = I$. This was accomplished with the string field $A = \frac{1}{\mathcal{L}_0}\mathcal{B}_0 I$.

Once the first solution was written down, a few variants on it appeared. One in particular generalized the same approach as in [25] for conformal frames which are "special projectors" [29]. A projector of the star product is a string field P such that $P * P = P$. As the circumference of a wedge state with no insertions is taken to infinity we can see that it becomes a projector, since the star product with itself gives another cylinder with twice the already infinite circumference. This limit is known as the "sliver" frame. Wedge states can be constructed by acting on the identity string field with exponentials of the Virasoro zero-mode together with its hermitian conjugate, $\mathcal{L}_0 + \mathcal{L}_0^\dagger$. The sliver state is called a "special projector" because the commutator of $\mathcal{L}_0$ with its bpz conjugate $\mathrm{bpz}\,\mathcal{L}_0$ satisfies $[\mathcal{L}_0, \mathrm{bpz}\,\mathcal{L}_0] = s\,(\mathcal{L}_0 + \mathrm{bpz}\,\mathcal{L}_0)$ as well as some regularity conditions. Using instead the zero-modes from the conformal frame of a different special projector yields alternative sets of states with algebraic properties similar to the wedge states, and Schnabl's solution will still exist with all operators from the sliver frame replaced by their counterparts in the new frame, because all of the necessary algebraic structure is reproduced in the new frame.

A simpler form of the solution was found several years later [30]. This uses the so-called KBc subalgebra generated by the three string fields K, B, and c which are defined by acting on the identity wedge state with simple operators.

$$K = \frac{\pi}{2}(L_1 + L_{-1})_L\,|I\rangle\,, \quad B = \frac{\pi}{2}(b_1 + b_{-1})_L\,|I\rangle\,, \quad c = \frac{1}{\pi}c(1)\,|I\rangle \tag{2.32}$$

The subscript $_L$ indicates the part of the operator acting on the left half of the string. This can be obtained by integrating the charges over the right half of the unit circle, from $-i$ to i. These string fields satisfy

$$[K, B] = 0, \quad \{B, c\} = 1, \quad B^2 = c^2 = 0, \tag{2.33}$$

$$Q_B K = 0, \quad Q_B B = K, \quad Q_B c = cKc. \tag{2.34}$$

Further details of the KBc subalgebra can be found in a number of places, for example [31] or [32]. Two different solutions, both gauge equivalent to each other and to the original tachyon vacuum solution, can be written down.

$$\Psi = c\,(1 + K)\,Bc\frac{1}{1+K} \tag{2.35}$$

$$\Psi = \frac{1}{\sqrt{1+K}}c\,(1 + K)\,Bc\frac{1}{\sqrt{1+K}} \tag{2.36}$$

Both forms satisfy the equations of motion, and the second form satisfies the reality condition on the string field which guarantees that the action will be real valued.

Since the tachyon vacuum, another class of analytic solution has been found, corresponding to marginal deformations. These solutions are generally written as a taylor series in the marginal parameter λ, but the string field can be written down explicitly at each order. If the marginal

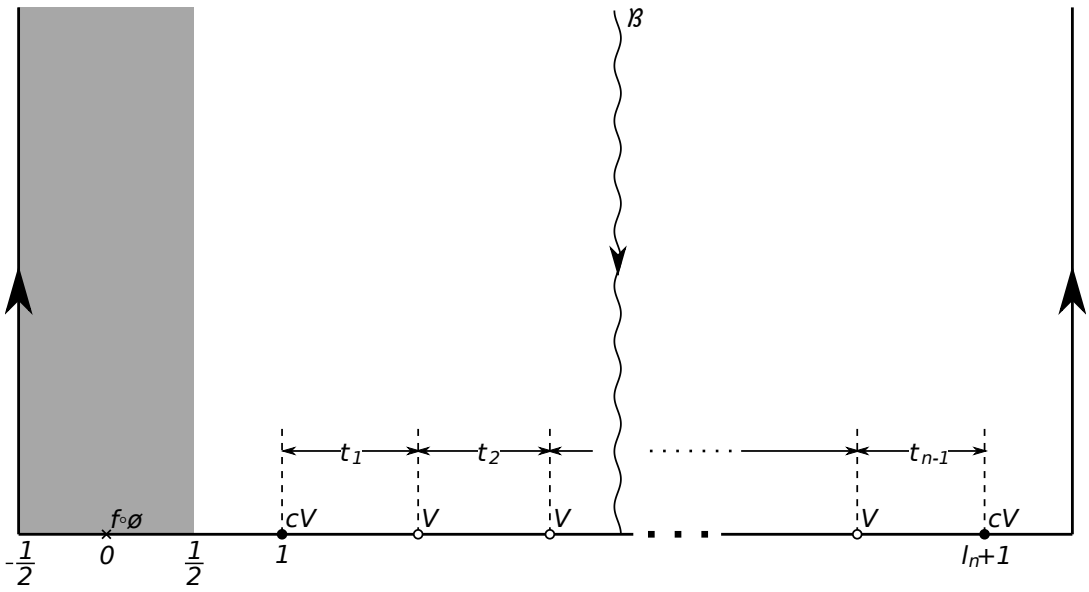

Figure 2.3: The λ^n term for the marginal solution of [5] for a marginal operator $V(t)$ with regular self-OPE. The ghost part drawn has fewer insertions than in (2.37) because the anticommutator $\{\mathcal{B}, c\} = 1$ can be used to simplify it.

deformation is regular, that is if its OPE with itself is regular, then solutions are quite well known [33][5][34]. These solutions take the form of wedge states with insertions of the marginal operator along the boundary, along with a few ghost insertions. The positions of the marginal insertions are mostly integrated over regions which depend on the specific solution, since the three moduli of the disc tell us that only one marginal operator should be inserted at a fixed location, as the other two moduli are fixed by the ghost number 2 test state in (2.22). The solution of [5] is given as $\Psi = \sum_{n=1}^{\infty} \lambda^n \Psi^{(n)}$ where

$$\left\langle \phi, \Psi^{(n)} \right\rangle = \int_0^1 dt_1 \ldots \int_0^1 dt_{n-1} \left\langle f \circ \phi(0) cV(1) \prod_{i=1}^{n-1} \left(\mathcal{B} cV(1 + \sum_{j=1}^{i} t_j) \right) \right\rangle_{\mathcal{W}_{1+\sum_{j=1}^{n-1} t_j}} . \quad (2.37)$$

This solution can be seen in figure 2.3. The operator $\mathcal{B} = \int \frac{dz}{2\pi i} b(z)$ here does not have a fixed insertion location, as it only matters which ghost operators it is between.

One example of a marginal deformation with regular self-OPE is the exponential or time-asymmetric rolling tachyon. Solutions involving this deformation represent placing a D-brane in the infinite past and letting it decay at a finite time. This is intended to show the dynamics of D-brane decay. The tachyon profile $T(t)$ is the coefficient field of the tachyon in the level truncation expansion, and for uniform decay it is only a function of time. The tachyon profile was calculated for two analytical solutions in [5] and [34], as well as for level truncation in [35]. In each case the tachyon profile shows oscillations with exponentially growing amplitude beginning when the D-brane decays and continuing without bound. This is in contrast to the expectation that the late time limit of the tachyon profile should be the tachyon vev of the tachyon vacuum solution. A few possible explanations have been suggested. In [35] it was

argued that a time-dependent field redefinition could be used to make the time dependence of rolling tachyon solution a simple exponential, matching the BCFT result for the corresponding marginal operator. In [27] this idea was reinterpreted as meaning that a time-dependent gauge transformation of the rolling tachyon solution could be used to give a solution with the expected time dependence. That same work claimed that the late time limit of the rolling tachyon solution is in fact Schnabl's solution, despite the numerical evidence of the tachyon profile.

If the marginal deformation has a singular self-OPE, then a detailed renormalization scheme is required in order to prevent divergences from the places where integrated insertions collide with fixed insertions or with each other. Such a renormalization scheme is constructed in [36]. This will be covered in detail and expanded on in chapter 4. An alternate approach was laid out in [37], in which solutions are considered which are formally gauge equivalent to the perturbative vacuum, but with a gauge parameter outside the Hilbert space. In [38], the regular-OPE solution of [34] was extended to operators with singular OPE. This approach used integrals away from the boundary of the worldsheet to find finite solutions which are equivalent to several previously found solutions in different limits. Recently, another new approach was suggested in which a Wilson line in the time direction is used to cancel the divergence of singular operators in the matter direction [39]. This approach does not apply to the case of the rolling tachyon because it requires that the time direction is left unused and free to soften the divergences. It also uses boundary condition changing operators, rather than the bare marginal operators which the solution of [36] was constructed from. However, given a boundary condition changing operator which is trivial in the time direction, this approach apparently produces solutions for any new boundary condition, not only marginally deformed ones. We will not be investigating solutions of this type. We will further investigate the singular marginal deformations by finding explicit numerical results for the tachyon profile in the renormalized approach. This will involve careful examination of the renormalization scheme used, and a re-evaluation of the freedom involved in doing so. We find that the renormalization must be chosen very carefully to guarantee that the sufficient conditions for a solution are met, but that at least two free parameters remain. The renormalization scheme cannot be further restricted by structural properties of the string field, or by numerical evidence, and we believe the remaining freedom may represent residual gauge transformations of the solution.

Simply constructing string fields which satisfy the equations of motion does not mean very much if nothing is known about what the solutions represent, so gauge invariant quantities are of particular interest. The simplest gauge invariant quantity is the energy of a solution, which is easily calculated. For a second test, however, the most clearcut quantity to consider is the boundary state. This is a state in the closed string Fock space which describes the D-brane in the sense that all amplitudes for closed strings interacting with the D-brane are given by overlaps with the boundary state. The task of calculating the boundary state was first accomplished in [40], and more recently a different approach was taken in [41]. The first method of computing the boundary state gives an exact closed string state as the result of inserting multiple copies of the OSFT solution around the boundary of a disc. In practice this is transformed to the sliver frame so that glueing in multiple copies of the solution is only a matter of considering larger cylinders with more insertions on the boundary. The second method writes the boundary state in a basis of Ishibashi states. For each bulk conformal primary operator V_α, the associated

Ishibashi state is the closed string state $\|V_\alpha\rangle\rangle$ satisfying

$$(L_n - \bar{L}_{-n}) \, \|V_\alpha\rangle\rangle = 0 \ . \tag{2.38}$$

In this basis it is shown that the coefficient of each basis state can be simply calculated from the string field in terms of BCFT amplitudes. Using this approach, the overlap of the boundary state $|B_\Psi\rangle$ corresponding to a string field solution Ψ with any closed string insertion $\mathcal{V}_{cl}$ is given by

$$\langle \mathcal{V}_{cl}| \, c_0^- \, |B_\Psi\rangle = -4\pi i \, \langle I| \, \mathcal{V}_{cl}(i) \, |\Psi - \Psi_{\rm TV}\rangle \ . \tag{2.39}$$

This method has the advantage that it can be applied to level truncated solutions as well as analytic solutions. The disadvantage is that there are in principle infinitely many Ishibashi coefficients to compute in order to find the whole boundary state. In practice there may be only a finite number which are non-zero or are of interest, so the approach is still effective. While the first approach, [40], was used to calculate the boundary state for Schnabl's tachyon vacuum solution and a few regular marginal deformation solutions, the other approach, [41], has been applied to many recent solutions. Originally, it was applied to an analytical tachyon vacuum solution and the numerical lump solution of [16]. After that, it was used to suggest that for level truncated marginal solutions with a periodic marginal direction the marginal parameter covers one fundamental domain [42]. Another level truncated solution representing change of boundary conditions for the Ising model also included a discussion of boundary states [23]. The recent analytical solutions of [38, 39] also include calculations of the boundary state for marginal deformation and tachyon vacuum solutions respectively. I am not familiar with any cases where the boundary state calculated from an OSFT solution does not agree with the predictions of BCFT, so it appears to be a remarkably robust tool for the study of the physical interpretation and properties of solutions to string field theory. In the case of this work the boundary state could be helpful for identifying the physical meaning of new solutions and determining which related solutions are gauge-equivalent, but calculation of the boundary state for the solutions we study here will be left for future work.

Chapter 3

Separated D-branes

Although string field theory is in principle a background independent theory, it still requires an initial choice of BCFT to determine its field content. In the majority of studies, the initial BCFT is chosen to be a single D-brane, often a space-filling one so that the full rotational symmetry is preserved. In the event that multiple D-branes are considered, the initial BCFT is almost always just the product of the single D-brane theory with a suitable gauge group, so that the theory describes a collection of identical D-branes. In this chapter we consider a situation where the starting locations of the D-branes are different so that the initial BCFT is more complicated, since the off-diagonal sector consists of strings that are stretched between the two D-branes and have a different spectrum than the diagonal sector.

One of the outstanding problems in OSFT is regarding solutions for marginal deformations. As a simple example, consider a single D-brane which is not space-filling. One marginal deformation is the translation of this D-brane, and we would expect that we could position this D-brane anywhere leading to an unbounded deformation. In string field theory, such configurations would correspond to a continuous set of solutions with a marginal parameter. In level truncation studies, however, this marginal parameter always has an upper bound which does not appear to grow fast enough as the level is increased, leading to speculation that only a finite range of marginal deformations are allowed. While several attempts have been made to explain this [21][22][24], here we will use the separated D-brane system to gain a new perspective on the problem by using the initial separation as a reference distance.

We will see that we are genuinely unable to find solutions corresponding to large D-brane translations, and that this seems unlikely to change with the inclusion of more terms in the string field. We will also use this reference distance to move one step closer to an alternative calculation of the relationship between the marginal parameter in OSFT and the marginal deformation of the BCFT. Previous methods have all compared quantities calculated in string field theory to those calculated in the BCFT, but we are able to rephrase the problem entirely in terms of OSFT calculations. The solution described here is the first step in this comparison, and I will leave the analysis of necessary field redefinitions about a marginal solution to future work.

The work presented in this chapter has been published in the Journal of High Energy Physics [1] and presented at the conference String Field Theory and Related Aspects V, which took place in 2012.

3.1 Preliminaries

Following a procedure similar to that of [17], we begin by defining the states in the expansion of the string field

$$|\Phi\rangle = (t_{ij}c_1 + x_{ij}\alpha_{-1}c_1 + h_{ij}c_0 + \ldots)\,|ij\rangle\,. \tag{3.1}$$

We are considering N parallel D-branes, so the state $|ij\rangle$ is the unexcited string beginning on brane i and ending on j. The sum over brane indices is implied. The matter oscillator α_{-1} belongs to the CFT transverse to the branes. In principle we should have $x_\mu \alpha^\mu_{-1}$, but we assume that all of the oscillators parallel to the brane are unexcited as we will discuss later. Of course there is an infinite set of higher level states such as $\alpha_{-2}|ij\rangle$, but to begin we will truncate the expansion here, at level (1,3). This means that the string field is truncated at level 1 and the action is truncated at level 3. Level is determined by the L_0 eigenvalue, counting from the tachyon at level 0.

The embedding function for the coordinates tangent to the branes are the standard string expansion with Neumann boundary conditions in (2.2). The transverse embedding functions have Dirichlet boundary conditions and are

$$X^\mu_{\rm D} = \hat{d}^\mu_i + i\frac{\hat{d}^\mu_j - \hat{d}^\mu_i}{2\pi}\ln\frac{z}{\bar{z}} + i\sqrt{\frac{\alpha'}{2}}\sum_{n\neq 0}\frac{\alpha^\mu_n}{n}\left(\frac{1}{z^n} - \frac{1}{\bar{z}^n}\right) \tag{3.2}$$

and we find the positions of the branes are $\hat{d}_i$. For the special case of codimension one branes this is only the mode expansion for X^{25}, so we can drop the target space index. The zero-modes are

$$\alpha^{25}_0|ij\rangle = -\frac{\hat{d}_j - \hat{d}_i}{\sqrt{2\alpha'}\pi}|ij\rangle \stackrel{\rm def}{=} (d_i - d_j)|ij\rangle\,. \tag{3.3}$$

Ignoring momentum parallel to the branes, the matter virasoro zero-mode is

$$L_0|ij\rangle = \frac{1}{2}\alpha^\mu_0\alpha_{0\mu}|ij\rangle = \frac{1}{2}(d_j - d_i)^2|ij\rangle \stackrel{\rm def}{=} \frac{1}{2}d^2_{ij}|ij\rangle \tag{3.4}$$

By definition $d_{ii} = 0$, and for two branes we can always set $d_1 = 0$ and $d_2 \stackrel{\rm def}{=} d$.

We will only need to focus on terms in the string field with zero-momentum. For these modes, the potential of the string field is proportional to the action (2.18). If we divide out the mass of the D-brane, essentially a choice of units, the potential is

$$\mathcal{V} = 2\pi^2\left(\frac{1}{2}\langle\Phi|\,Q_B\,|\Phi\rangle + \frac{1}{3}\langle\Phi,\Phi,\Phi\rangle\right)\,. \tag{3.5}$$

Technically, since we are working in a non-compact space, the D-brane mass is infinite, but we can still think of this as the limit of the potential as the spacetime volume goes to infinity. Alternatively, we could calculate the potential energy density and work in units where the D-brane energy density is 1, and we would find the same form.

3.1.1 Symmetries and the String Field

The string field is constructed by acting on the vacuum $c_1|ij\rangle$ with both matter and ghost creation operators. We can group these operators into CFT^X, CFT$'$, and CFT^g representing the X^{25} matter sector, the $X^{\mu\neq 25}$ sector, and the ghost sector respectively. For our purposes we only need the subspace with ghost number one. Of course there are as many ways to act on a state with the composite operators L^X_{-n}, L'_{-n}, and $(L_g)_{-n}$ as with the simple oscillators α_{-n}, b_{-n}, and c_{-n} while preserving ghost number, so the Virasoro basis is equally valid as long

as all states are linearly independent. As discussed in [16][8], this is the case provided there are no null states. When we find a null state we must replace it, and its descendants, with the conformal family descended from another primary state.

At level 1 we find that $L'_{-1}c_1\left|ij\right\rangle$ is a null state, so we must instead include the primary states $\alpha^\mu_{-1}c_1\left|ij\right\rangle$. While $L^X_{-1}c_1\left|ij\right\rangle$ is not technically a null state for a stretched string vacuum, $L^X_{-1}c_1\left|ii\right\rangle$ is, and in any case it is a simple rescaling of $\alpha^{25}_{-1}c_1\left|ij\right\rangle$ so we will use that state in both cases to avoid having to consider different states in the different sectors. There are no other null states at the levels we will consider. The states α^μ_{-1} with $\mu \neq 25$ can be dropped due to rotational invariance. All matter oscillators in the brane-parallel directions must come in pairs with their spacetime indices contracted. Any term with an odd number of matter oscillators in these directions can be ruled out, which means we can drop the extra conformal primary $\alpha'_{-1}c_1\left|0\right\rangle$ and its descendants in these directions.

The String Field Theory action is invariant under the twist operator Ω as discussed in [10]. Twist is defined by reversing the parameterization of the worldsheet space coordinate, $\sigma \to \pi - \sigma$. Typically Ω acts on individual states as $(-1)^{L_0+1}$, with every odd-level state also being twist odd. Since the action is twist-even we can never have a single twist-odd state appearing coupled to twist-even states, so those states' equations of motion are trivially satisfied by setting all twist-odd states to zero. This is the justification used to drop the odd-level states from the string field in analyses of D-brane decay. With Dirichlet boundary conditions, however, the twist eigenvalue of the operator X^μ also changes sign so that every matter oscillator α_n contributes an extra sign to the twist eigenvalue. In addition we have the added complication that the vacuum for stretched strings is not a twist eigenvalue. For a single D-brane the vacuum $\left|0\right\rangle$ is twist-odd, but with multiple branes $\Omega(\left|ij\right\rangle) = -\left|ji\right\rangle$, so we can construct twist-even and twist-odd vacua as

$$\left|ij\right\rangle_e = \frac{1}{2}(\left|ij\right\rangle - \left|ji\right\rangle), \quad \left|ij\right\rangle_o = \frac{1}{2}(\left|ij\right\rangle + \left|ji\right\rangle). \tag{3.6}$$

Instead of simply acting on the twist-odd vacuum with a twist-odd collection of operators, we must now also consider the possibility of acting on the twist-even vacuum with twist-even operators.

We can drop any terms from the string field that are odd under $(-1)^{L_0+n_\alpha}\Omega_{\text{vac}}$ where n_α is the number of α^{25}_n matter oscillators with dirichlet boundary conditions. While any operator content can create a twist-even state by applying it to the correct choice of vacuum, this will restrict each state to have either a symmetric or anti-symmetric coefficient matrix.

The string field can now be written down, and at level 3 it is

$$\begin{aligned}\left|\Phi\right\rangle = \big(&t_{ij}c_1 + h_{ij}c_0 + u_{ij}c_{-1} + v_{ij}L'_{-2}c_1 + w_{ij}L^X_{-2}c_1 + o_{ij}(b_{-2}c_{-1}c_1 - 2c_{-2}) \\ &+ \tilde{o}_{ij}(b_{-2}c_{-1}c_1 + 2c_{-2}) + p_{ij}L'_{-3}c_1 + q_{ij}L^X_{-3}c_1 + \ldots\big)\left|ij\right\rangle \\ + \big(&x_{ij}c_1 + f_{ij}L^X_{-1}c_1 + r_{ij}c_{-1} + s_{ij}L'_{-2}c_1 + y_{ij}L^X_{-2}c_1 + z_{ij}L^X_{-1}L^X_{-1}c_1 + \ldots\big)\,\alpha^X_{-1}\left|ij\right\rangle.\end{aligned} \tag{3.7}$$

In order to be twist-even the fields t, x, u, v, w, r, s, y, and z are symmetric matrices, while h, f, o, $\tilde{o}$, p, and q are anti-symmetric.

When dealing with the twist-even subspace on a single D-brane the coefficient of each state is a single real number (or real-valued function). Little discussion is given to this point, as real numbers seem a natural choice. Now that the coefficients are matrix-valued we must decide how to correctly generalize this. In [11] it was shown that in order to guarantee the reality of the

action we must impose the condition that the string field be invariant under the composition of hermitian conjugation and inverse bpz conjugation.

$$|\Phi\rangle = \text{bpz}^{-1} \circ h.c. \, |\Phi\rangle = |\Phi\rangle^{\ddagger} \tag{3.8}$$

As in [36], we denote this combined conjugation by $(\ )^{\ddagger}$. For a generic single state constructed from the ghost number one vacuum by applying operators α_{-n} and L_{-n}, we know that hermitian conjugation simply switches the order of operators and the sign of each index. Bpz conjugation has a similar effect, but introduces a sign factor.

$$\text{bpz}^{-1} \langle 0| = |0\rangle \,, \quad \text{bpz}^{-1} \, L_n = (-1)^n L_{-n}, \quad \text{bpz}^{-1} \, \phi_n = (-1)^{n+h} \phi_{-n} \tag{3.9}$$

for any primary field ϕ with conformal dimension h. For composite operators, we multiply their bpz conjugates in the reverse order, but with an additional sign factor when there are multiple ghosts. This additional factor depends on the number of fermionic operators as $(-1)^{n_f(n_f-1)/2}$. Since we are looking at ghost number one, this is equivalent to including an extra (-1) with every b ghost. When we work out the action of $\text{bpz}^{-1} \circ h.c.$ on any term, we can find the same sign as the twist eigenvalue, ignoring the possibility of the twist-even vacuum. If the twist-even vacuum is used then the sign factor from this conjugation is opposite the twist eigenvalue. We can now say that for any state built on the twist-odd vacuum

$$a_{ij} \, |\phi; ij\rangle = (a_{ij} \, |\phi; ij\rangle)^{\ddagger} = \text{bpz}^{-1}(a_{ij}^{\dagger} \, \langle \phi; ij|) = a_{ij}^{\dagger} \Omega_{\phi} \, |\phi; ij\rangle \tag{3.10}$$

will guarantee the reality of the action, where Ω_{ϕ} represents the twist eigenvalue of the state $|\phi; ij\rangle$. This gives the result

$$a_{ij} = \Omega_{\phi} a_{ij}^{\dagger}. \tag{3.11}$$

For states built on the twist-even vacuum we similarly find

$$a_{ij} = -\Omega_{\phi} a_{ij}^{\dagger}. \tag{3.12}$$

Since all the states we are considering are twist-even, these conditions reduce to requiring the coefficient matrices, which are already either symmetric or anti-symmetric, to be real-valued. If we were to examine states with odd twist eigenvalues then we would need to assign them imaginary coefficient matrices. However, since those terms must always appear quadratically in the action, making their coefficient matrices real would introduce a factor of -1 multiplying all such terms, and the action would remain real.

The term $h_{ij} c_0 \, |ij\rangle$ is a special case. Level truncation calculations are typically done in Siegel gauge, which is defined by setting $b_0 \, |\Phi\rangle = 0$. This removes a number of terms including h_{ij}, but the standard proof that Siegel gauge states are complete and distinct fails for level 1 states because the eigenvalue of L_0 is 0. Since Siegel gauge can be imposed level by level, this is not a problem for studies of tachyon condensation, where level 1 states are dropped completely. While the standard proof fails this does not mean that Siegel gauge is necessarily invalid. In any case, the matrix h_{ij} has already been reduced to a real anti-symmetric matrix by the reality condition and twist symmetry. With the diagonal part of the matrix removed we can once again impose Siegel gauge on the off-diagonal parts as long as the initial D-brane separation is non-zero. Separating the D-branes gives L_0 a non-zero contribution and rescues the proof of Siegel

gauge's validity. Even if we take $d = 0$ we can still use the exchange symmetry described next to ensure that h_{ij} is consistently 0, but if we were to study solutions involving the twist-odd sector then we should include h and Siegel gauge would be violated at level 1.

Once we restrict our attention to the case of two D-branes we will find another simple symmetry related to exchanging the two D-branes. Consider any single cubic term in the action and define the function f by

$$f(d_{ij}, d_{jk}, d_{ki}) A_{ij} B_{jk} C_{ki} \stackrel{\text{def}}{=} A_{ij} B_{jk} C_{ki} \langle {}_i\mathcal{A}_j, {}_j\mathcal{B}_k, {}_k\mathcal{C}_i \rangle \ . \tag{3.13}$$

Because all brane indices are summed, terms will appear in pairs like

$$f(0, d_{12}, d_{21}) A_{11} B_{12} C_{21} + f(0, d_{21}, d_{12}) A_{22} B_{21} C_{12}. \tag{3.14}$$

It is straightforward to see that for operators $\mathcal{A}$, $\mathcal{B}$, and $\mathcal{C}$ with a definite number of matter oscillators in the dirichlet direction, the function f will transform under $d \to -d$ in the same way as the product of the three operators does under $X^{25} \to -X^{25}$, picking up a factor of $(-1)^{n_\alpha}$. Now (3.14) will take the form

$$\begin{aligned} f(0, d_{12}, d_{21}) A_{11} B_{12} C_{21} + f(0, -d_{12}, -d_{21}) A_{22} B_{21} C_{12} & \\ = f(0, d_{12}, d_{21}) \left(A_{11} B_{12} C_{21} + (-1)^{n_\alpha} A_{22} B_{21} C_{12} \right) & \end{aligned} \tag{3.15}$$

This part of the action is invariant under taking $X^{25} \to -X^{25}$ and swapping the D-brane indices. Terms in the action which take place entirely on a single D-brane trivially satisfy the same symmetry, as does the quadratic part of the action. We can then consistently restrict ourselves to string fields which are even under this operation. There are solutions which are not, such as the solution where one D-brane decays and the other does not, but it happens that the solution we are interested in is exchange-even so we can focus on that part of the string field. Choosing a parameterization of the matrices

$$A_{ij} = \begin{pmatrix} A_s - A_a & a_s + a_a \\ a_s - a_a & A_s + A_a \end{pmatrix} \tag{3.16}$$

we see that if the operator $\mathcal{A}$ has an even number of dirichlet matter oscillators then we can consistently set $A_a = \alpha_a = 0$. If, on the other hand, n_α is odd then we can set $A_s = \alpha_s = 0$. Because we will begin our solution by exciting only twist-even and exchange-even fields at level 0 we can restrict all higher levels to the same subspace. The most dramatic consequence of this is to completely drop the fields h, o, $\tilde{o}$, p, and q because they have an even n_α but are already restricted to have real anti-symmetric matrices through the twist symmetry and reality condition.

Alternate basis

We have chosen to write the string field up to level 3 as the two primary fields $c_1 |ij\rangle$ and $\alpha_{-1} c_1 |ij\rangle$ and their virasoro descendants, but we could have chosen an alternate form. It can be useful to see the string field written in terms of the basic matter and ghost oscillators. In

this basis we have

$$\begin{aligned}|\Phi\rangle = \Big(&t_{ij}c_1 + h_{ij}c_0 + x_{ij}\alpha_0^{25}c_1 + u_{ij}c_{-1} + \tilde{v}_{ij}\alpha_{-1}\cdot\alpha_{-1}c_1 + \tilde{w}_{ij}\alpha_{-1}^{25}\alpha_{-1}^{25}c_1 + \tilde{f}_{ij}\alpha_{-2}^{25}c_1 \\ &+ o_{ij}(b_{-2}c_{-1}c_1 - 2c_{-2}) + \tilde{o}_{ij}(b_{-2}c_{-1}c_1 + 2c_{-2}) + p_{ij}\alpha_{-1}\cdot\alpha_{-2}c_1 + \tilde{q}_{ij}\alpha_{-1}^{25}\alpha_{-2}^{25}c_1 \\ &+ r_{ij}\alpha_{-1}^{25}c_{-1} + \tilde{s}_{ij}\alpha_{-1}\cdot\alpha_{-1}\alpha_{-1}^{25}c_1 + \tilde{y}_{ij}\alpha_{-1}^{25}\alpha_{-1}^{25}\alpha_{-1}^{25}c_1 + \tilde{z}_{ij}\alpha_{-3}^{25}c_1 + \ldots\Big)|ij\rangle\,. \end{aligned} \tag{3.17}$$

The terms were defined this way so that the new coefficients denoted with tildes have the same properties under twist and exchange symmetries as their partners in (3.7). The fields and their coefficients are related to the ones in (3.7). Defining states such as $t_{ij}c_1|ij\rangle = t_{ij}|t\rangle$ for notational convenience, we can state the relationships between the states themselves as

$$\begin{aligned} |v\rangle = \frac{1}{2}|\tilde{v}\rangle\,, \quad |s\rangle = \frac{1}{2}|\tilde{s}\rangle\,, \quad |w\rangle = \frac{1}{2}|\tilde{w}\rangle + \alpha_0|\tilde{f}\rangle, \quad |f\rangle = |\tilde{f}\rangle + \alpha_0|\tilde{w}\rangle \\ |q\rangle = |\tilde{q}\rangle + \alpha_0|\tilde{z}\rangle\,, \quad |y\rangle = \frac{1}{2}|\tilde{y}\rangle + |\tilde{z}\rangle + \alpha_0|\tilde{q}\rangle\,, \quad |z\rangle = 2|\tilde{z}\rangle + 3\alpha_0|\tilde{q}\rangle + \alpha_0\alpha_0|\tilde{y}\rangle\,. \end{aligned} \tag{3.18}$$

With this transformation known, it is simple to go from solutions in one basis to another using the relationships between the coefficients. Let $\phi_I|\phi_I\rangle$ be an arbitrary state and its coefficient (with brane indices suppressed), then for every change of states $|\phi_I\rangle = C_{IJ}\left|\tilde{\phi}_J\right\rangle$ the coefficients are related by $\tilde{\phi}_J = \phi_I C_{IJ}$.

This change of variables becomes singular at specific separations. While we can still formally work in the virasoro basis, we must bear in mind that it is only complete almost everywhere. Off-diagonal components of the fields w and f are linearly dependent when the matter zero-mode has eigenvalue $\alpha_0 = \frac{1}{\sqrt{2}}$, and the fields q, y, and z contain a linearly dependent part at both $\alpha_0 = \frac{1}{\sqrt{2}}$ and $\alpha_0 = \sqrt{2}$.

3.1.2 The Potential

With the initial brane configuration and string field defined, we can work out the string field theory potential. The solutions we are looking for will be the critical points. For calculations, the potential of (3.5) can be written using the 3-string vertex defined by

$$\langle\Psi_1, \Psi_2, \Psi_3\rangle = \langle\Psi_1|\Psi_2 * \Psi_3\rangle = \langle V_3|\left|\Psi_1^{(1)}\right\rangle\left|\Psi_2^{(2)}\right\rangle\left|\Psi_3^{(3)}\right\rangle. \tag{3.19}$$

This vertex can be written as

$$\langle V_3| = \frac{3^4\sqrt{3}}{2^6}\sum_{i,j,k}\langle ij|\langle jk|\langle ki|\, c_{-1}^{(1)}c_{-1}^{(2)}c_{-1}^{(3)}c_0^{(1)}c_0^{(2)}c_0^{(3)}e^{\Xi}\,, \tag{3.20a}$$

$$\Xi = \sum_{r,s}\sum_{m,n=0}^{\infty}\left(\frac{1}{2}\alpha_m^{(r)\mu}N_{mn}^{rs}\alpha_{n,\mu}^{(s)} + c_m^{(r)}X_{mn}^{rs}b_n^{(s)}\right)\,, \tag{3.20b}$$

where the coefficients N_{mn}^{rs} and X_{mn}^{rs} are known. The first few coefficients are given by table 3.1 and it will be useful to define $\hat{N}_{mn}^{rs} = N_{mn}^{rs} + N_{nm}^{sr}$. The creation and annihilation operators here have an extra upper index indicating which oscillator vacuum they act on. The Neumann coefficients N_{mn}^{rs} were derived in [12] with a minor correction to the matter coefficients appearing

m	n	N^{rr}_{mn}	$N^{r(r+1)}_{mn}$	$N^{r(r-1)}_{mn}$
0	0	$\ln 4\sqrt{3}/9$	0	0
0	1	0	$-2\sqrt{3}/9$	$2\sqrt{3}/9$
1	0	0	$2\sqrt{3}/9$	$-2\sqrt{3}/9$
0	2	$-2/27$	$1/27$	$1/27$
1	1	$-5/27$	$16/27$	$16/27$
2	0	$-2/27$	$1/27$	$1/27$
0	3	0	$22\sqrt{3}/729$	$-22\sqrt{3}/729$
1	2	0	$32\sqrt{3}/243$	$-32\sqrt{3}/243$
2	1	0	$-32\sqrt{3}/243$	$32\sqrt{3}/243$
3	0	0	$-22\sqrt{3}/729$	$22\sqrt{3}/729$

m	n	X^{rr}_{mn}	$X^{r(r+1)}_{mn}$	$X^{r(r-1)}_{mn}$
0	0	0	0	0
0	1	0	0	0
1	0	0	$4\sqrt{3}/9$	$-4\sqrt{3}/9$
0	2	0	0	0
1	1	$11/27$	$8/27$	$8/27$
2	0	$16/27$	$-8/27$	$-8/27$
0	3	0	0	0
1	2	0	$40\sqrt{3}/243$	$-40\sqrt{3}/243$
2	1	0	$-80\sqrt{3}/243$	$80\sqrt{3}/243$
3	0	0	$-68\sqrt{3}/243$	$68\sqrt{3}/243$

Table 3.1: The first few Neumann coefficients appearing in (3.20b).

in [43]. The conventions introduced in (3.20b) are the same ones appearing in [44], though I have included the zero-modes which did not appear there. The ghost coefficients $X^{rs}_{0n} = 0$ for $m = 0$ are included here only for clarity, as those terms are typically omitted from the definition of Ξ.

In order to calculate the cubic terms in (3.5) we use the Baker-Haussdorf formula

$$e^X Y = \left(Y + [X,Y] + \frac{1}{2}[X,[X,Y]] + \dots \right) e^X \tag{3.21}$$

which allows us to commute the exponential e^{Ξ} past each of the operators in our string field and get a new set of operators in its place. The triple product can then be computed using straight-forward commutator algebra. A number of useful commutation relations are given in (3.22).

$$\left[\alpha^{(r),\mu}_m, \alpha^{(s),\nu}_n\right] = m\delta_{m+n}\delta^{r,s}\delta^{\mu,\nu} \tag{3.22a}$$

$$\left\{c^{(r)}_m, b^{(s)}_n\right\} = \delta_{m+n}\delta^{r,s} \tag{3.22b}$$

$$\left[\alpha^{(r),\mu}_m, L^{(s)}_n\right] = m\alpha^{(r),\mu}_{m+n}\delta^{r,s} \tag{3.22c}$$

$$\left[(L_g)^{(r)}_m, b^{(s)}_n\right] = (m-n)b_{m+n}\delta^{r,s} \tag{3.22d}$$

$$\left[(L_g)^{(r)}_m, c^{(s)}_n\right] = -(2m+n)c_{m+n}\delta^{r,s} \tag{3.22e}$$

$$\left[\Xi, \alpha^{(q),\mu}_{-k}\right] = \frac{k}{2}\sum_{m=0}^{\infty} \tilde{N}^{rq}_{mk}\alpha^{(r),\mu}_m \tag{3.22f}$$

$$\left[\Xi, L^{(q)}_{-k}\right] = \sum_{m,n=0}^{\infty} \frac{m}{4}\tilde{N}^{qr}_{mn}\left\{\alpha^{(r)}_{n,\mu}, \alpha^{(q),\mu}_{m-k}\right\} \tag{3.22g}$$

$$\left[\Xi, \left[\Xi, L^{(q)}_{-k}\right]\right] = \frac{1}{4}\sum_{i,j,m,n=0}^{\infty} in\tilde{N}^{rq}_{mn}\tilde{N}^{qs}_{ij}\alpha^{(r),\mu}_m\alpha^{(s)}_{j,\mu}\delta_{n+i-k} \tag{3.22h}$$

$$\left[\Xi, c_{-k}^{(q)}\right] = \sum_{m=0}^{\infty} X_{mk}^{rq} c_m^{(r)} \tag{3.22i}$$

$$\left[\Xi, b_{-k}^{(q)}\right] = -\sum_{n=0}^{\infty} X_{kn}^{qs} b_n^{(s)} \tag{3.22j}$$

$$\left[\Xi, (L_g)_{-k}^{(q)}\right] = \sum_{m,n=0}^{\infty} (2k+m) X_{mn}^{qs} c_{m-k}^{(q)} b_n^{(s)} - \sum_{m,n=0}^{\infty} (n+k) X_{mn}^{rq} c_m^{(r)} b_{n-k}^{(q)} \tag{3.22k}$$

$$\begin{aligned}\left[\Xi, \left[\Xi, (L_g)_{-k}^{(q)}\right]\right] = &- \sum_{i,j,m,n=0}^{\infty} (j+k) X_{mn}^{qs} X_{ij}^{tq} c_i^{(t)} b_n^{(s)} \delta_{m+j-k} \\ &- \sum_{i,j,m,n=0}^{\infty} (2k+i) X_{mn}^{rq} X_{ij}^{qt} c_m^{(r)} b_j^{(t)} \delta_{n+i-k}\end{aligned} \tag{3.22l}$$

$$\left[\Xi, \left[\Xi, \left[\Xi, L_{-k}^{(q)}\right]\right]\right] = \left[\Xi, \left[\Xi, \left[\Xi, (L_g)_{-k}^{(q)}\right]\right]\right] = 0 \tag{3.22m}$$

The operator $L^{(r)}$ refers to the matter part of the Virasoro operator on the r-th string vacuum, and the ghost part of the Virasoro operator is $(L_g)^{(r)}$. The results shown include the entire matter Virasoro operators $L_n^{(r)} = (L')_n^{(r)} + (L^X)_n^{(r)}$, so for commutators involving only a part of that, the spacetime indices behave as expected. For example, $\left[\alpha_m^{(r),25}, (L')_n^{(s)}\right] = 0$ and $\left[\Xi, (L^X)_{-k}^{(q)}\right] = \sum_{m,n=0}^{\infty} \frac{m}{4} \tilde{N}_{mn}^{qs} \left\{\alpha_n^{(s),25}, \alpha_{m-k}^{(q),25}\right\}$. It is useful to note that since the right hand side of $\left[\Xi, \left[\Xi, L_{-k}^{(q)}\right]\right]$ is summed over non-negative integers we can use the fact that $mn\delta_{m+n-2} = \delta_{m-1}\delta_{n-1}$ to simplify the case where $k = 2$. As an example, we can now show that

$$e^{\Xi} L_{-2}^{(q)} = \left(L_{-2}^{(q)} + \frac{m}{4} \tilde{N}_{mn}^{qr} (\alpha_n^{(r)\mu} \alpha_{m-2,\mu}^{(q)} + \alpha_{m-2}^{(q)\mu} \alpha_{n,\mu}^{(r)}) + \frac{1}{8} \tilde{N}_{m1}^{rq} \tilde{N}_{1j}^{qs} \alpha_m^{(r)\mu} \alpha_{j,\mu}^{(s)}\right) e^{\Xi}. \tag{3.23}$$

Once Ξ is all the way to the right, all of its operators except for the zero-modes will annihilate the vacuum. Using the zero-mode Neumann coefficients we find

$$e^{\Xi} |0\rangle^{(1)} |0\rangle^{(2)} |0\rangle^{(3)} = \left(\frac{4}{3\sqrt{3}}\right)^{\frac{1}{2}((\alpha_0^{(1)})^2 + (\alpha_0^{(2)})^2 + (\alpha_0^{(3)})^2)} |0\rangle^{(1)} |0\rangle^{(2)} |0\rangle^{(3)}. \tag{3.24}$$

Throughout this we have assumed the rule (3.22b) despite the fact that for $r \neq s$ the operators act in different sectors. It could be argued that since $c_m^{(r)}$ acts only on the r-sector, it is bosonic in the s-sector and the commutator should be zero rather than the anti-commutator. This, however, would only amount to some extra sign factors, which can be checked against known results found by other methods. The use of anti-commutators with our form of the 3-vertex gives a result for the coefficient of u^3 which matches the coefficient in [17], which appears to have been calculated directly from the disc amplitude. We chose the u^3 term to consider because if we were to change the sign on X_{mn}^{rs} with $r \neq s$ we would not get the same result.

If one of the three fields is different than the others then there are three ways to order them. Since the triple product $\langle \mathcal{A}, \mathcal{B}, \mathcal{C} \rangle$ is invariant under cyclic permutations of fields with ghost number one, though, we only need to calculate it in one order and then multiply the end result by 3. If all three are different then there are six ways to order the fields. Again we can use

cyclicity of the triple product to reduce the problem to two distinct orders, and then multiply each by 3. The twist operator will tell us how the two distinct orderings are related to each other. We know from [10] that

$$\langle \mathcal{A}, \mathcal{B} \rangle = \langle \Omega(\mathcal{A}), \Omega(\mathcal{B}) \rangle \tag{3.25a}$$

$$\Omega(\mathcal{A} * \mathcal{B}) = \Omega(\mathcal{B}) * \Omega(\mathcal{A}) \tag{3.25b}$$

for string fields with ghost number one. From this we can easily see that the reverse ordering is

$$\langle \mathcal{C}, \mathcal{B}, \mathcal{A} \rangle = \langle \Omega(\mathcal{A}), \Omega(\mathcal{B}), \Omega(\mathcal{C}) \rangle \,. \tag{3.26}$$

For the twist-even fields we are considering this results in 6 times the coefficient for one ordering of the fields. In more generality, we can still use this result as long as we remember to include the necessary signs and exchange the D-brane indices as Ω acts on each string field.

In order to check the vertex, we can use it to compute several couplings that are already known. Since most work neglects the zero-modes we have to use [16], which contains a detailed action for states with non-zero momentum. Because they use states which are eigenvalues of $|p|$ rather than the signed momentum, we must take care to include all the necessary combinatorics. We should then be able to match their couplings. As an example, we will examine their coupling for $t_0 t_1 v_1$.[1] We begin by using our 3-vertex to find the cubic term for two copies of the field t and one field that we call w. We then choose $\alpha_0^{(1)} = 0$ and $\alpha_0^{(2)} = -\alpha_0^{(3)} = \frac{\sqrt{2}}{R}$ to match the zero-modes to the momenta $|p| = \frac{1}{R}$. To avoid complications due to conventions, we use the value of α_0 for which the L_0 eigenvalue matches the contribution of the momentum to the level in that work. There are two ways to pick which state has positive momentum; we could have swapped $\alpha_0^{(2)}$ and $\alpha_0^{(3)}$, so we pick up a combinatoric factor of 2, but each of the cosines appearing with t_1 and v_1 has a factor of $\frac{1}{2}$ when expressed in terms of the necessary exponentials, contributing an additional $\frac{1}{4}$. The three fields in question are all distinct, so there is a factor of 6 for the number of ways to order them. The cubic term in the action has a factor of $\frac{1}{3}$ in front which we must also remember to include. We then find exactly the same result as in [16]:

$$\left(-\frac{3\sqrt{3}}{8R^2} - \frac{15\sqrt{3}}{128} \right) \left(\frac{4}{3\sqrt{3}} \right)^{\frac{2}{R^2}} .$$

The couplings for $t_0 t_1 v_1$, $t_1 t_2 v_1$, $t_0 v_1 v_1$, $t_1 v_0 v_1$, and $t_1 w_0 v_1$ have all been checked this way.

Finally, we need to be concerned with the boundary conditions. The Neumann coefficients, N_{mn}^{rs} and X_{mn}^{rs} were derived for Neumann boundary conditions, and since we are starting with D-branes that have codimension 1, we will also need to consider the vertex for Dirichlet boundary conditions. Fortunately, T-duality guarantees that the vertex is identical. With Neumann boundary conditions, the radius of a compact direction only appears through the allowed values of α_0. We can contract the radius to 0 while holding $\alpha_0 = -d$ constant by giving the gauge field the value $A_{25;2,2} = \frac{-\hat{d}}{2\pi\alpha'} = \frac{-d}{\sqrt{2\alpha'}}$, $A_{25;ij} = 0$ otherwise, equivalent to $\theta_2 = \frac{R\hat{d}}{\alpha'}$. When we then T-dualize to get a non-compact Dirichlet theory we will have the same value of α_0 we wanted, and the same mass spectrum. Because the 3-vertex can be defined by the 3-point function in (3.19) and the amplitude is the same with Neumann or Dirichlet boundary conditions by T-duality, the 3-vertex will have the same form and the same coefficients in either case.

[1] While several of the states we will use are also in [16], only t and u will be labeled the same.

The quadratic term in (3.5) is much easier to compute. The only sums in this term appear due to the BRST operator

$$Q_B = c_n L_{-n} + \frac{m-n}{2} : c_m c_n b_{-m-n} : -c_0. \tag{3.27}$$

The other thing we need in order to calculate $\langle\Phi| Q_B |\Phi\rangle$ is the bra state. Conjugation is done using the bpz conjugate which we already defined in (3.9).

The quadratic terms are verified similarly to the cubic ones. For the coefficient of $v_1 v_1$ we have a factor of $\frac{2}{4}$ from the two cosines and the number of ways to make the momentum vanish. Letting $\alpha_0 = \frac{\sqrt{2}}{R}$ and including the $\frac{1}{2}$ from the action we find that the coefficient is

$$\frac{1}{8} + \frac{9}{8R^2} + \frac{1}{R^4}$$

in perfect agreement again. The coefficients of $t_0 t_0$, $t_1 t_1$, $t_2 t_2$, $u_0 u_0$, $u_1 u_1$, $v_0 v_0$, $v_1 v_1$, $w_0 w_0$, $w_1 w_1$, and $v_1 z_1$ have all been checked. The coefficient for $z_1 z_1$ requires an additional detail. While $v_1 z_1$ can be easily matched by multiplying an extra α_0 into the quadratic term to match the normalization difference between our f and their z, when we calculate quadratic terms with z on the left we must remember to multiply our coefficient of f by $\mathrm{bpz}(\alpha_0) = -\alpha_0$. With this additional overall sign, we agree with [16].

The potential of (3.5) can be evaluated, and at level $(1,3)$ it is

$$\begin{aligned}\mathcal{V} = 2\pi^2 \Bigg[& \frac{1}{2}\left((-1 + \frac{\Delta_{ij}}{2}) t_{ij} t_{ji} + \frac{\Delta_{ij}}{2} x_{ij} x_{ji} - 2 h_{ij} h_{ji} \right) \\ & + \frac{3^3\sqrt{3}}{2^6}\Bigg(t_{ij} t_{jk} t_{ki} + \frac{3}{2}\tilde{N}^{r3}_{01}\alpha^r_0 t_{ij} t_{jk} x_{ki} + \frac{3}{2}(\tilde{N}^{32}_{11} + \frac{1}{2}\tilde{N}^{r2}_{01}\tilde{N}^{s3}_{01}\alpha^r_0\alpha^s_0) t_{ij} x_{jk} x_{ki} \\ & + \frac{1}{4}(\tilde{N}^{12}_{11}\tilde{N}^{3r}_{10}\alpha^r_0 + \tilde{N}^{23}_{11}\tilde{N}^{1r}_{10}\alpha^r_0 + \tilde{N}^{31}_{11}\tilde{N}^{2r}_{10}\alpha^r_0 + \frac{1}{2}\tilde{N}^{r1}_{01}\tilde{N}^{s2}_{01}\tilde{N}^{t3}_{01}\alpha^r_0\alpha^s_0\alpha^t_0) x_{ij} x_{jk} x_{ki} \\ & + \frac{16}{9} t_{ij} h_{jk} h_{ki} + \frac{8}{9}\tilde{N}^{r3}_{01}\alpha^r_0 h_{ij} h_{jk} x_{ki} \Bigg) \left(\frac{4}{3\sqrt{3}}\right)^{\frac{1}{2}(\Delta_{ij}+\Delta_{jk}+\Delta_{ki})} \Bigg] \end{aligned} \tag{3.28}$$

Here the states have already been removed by taking the inner product with the vertex, so the α^r_0 should be taken to mean the eigenvalue of α_0 against the r-th vacuum in the 3-string state $|ij\rangle |jk\rangle |ki\rangle$. For example, $\alpha^{(2)}_0 = d_j - d_k$. A full listing of the higher level couplings used in this work is given in appendix A.

3.2 Solutions

Now once again restricting our attention to $N = 2$ branes, we can use the twist and exchange symmetries to simplify the potential. First we will define the coefficient matrices such as t_{ij} appearing in the string field expansion (3.1).

$$t_{ij} = \begin{pmatrix} T_s - T_a & \tau e^{i\theta_t} \\ \tau e^{-i\theta_t} & T_s + T_a \end{pmatrix} = \begin{pmatrix} T_s & \tau \\ \tau & T_s \end{pmatrix}, \quad x_{ij} = \begin{pmatrix} X_s - X_a & \chi e^{i\theta_x} \\ \chi e^{-i\theta_x} & X_s + X_a \end{pmatrix} = \begin{pmatrix} -X_a & 0 \\ 0 & X_a \end{pmatrix} \tag{3.29}$$

$T_s = \frac{t_{11}+t_{22}}{2}$ and $T_a = \frac{t_{22}-t_{11}}{2}$ are the symmetric and anti-symmetric parts of the diagonal. A complete list of terms which are even under both twist and exchange symmetries is now relatively short at this level.

$$\begin{gathered} t_{ij} = \begin{pmatrix} T_s & \tau \\ \tau & T_s \end{pmatrix}, \quad x_{ij} = \begin{pmatrix} -X_a & 0 \\ 0 & X_a \end{pmatrix}, \quad u_{ij} = \begin{pmatrix} U_s & \upsilon \\ \upsilon & U_s \end{pmatrix} \\ v_{ij} = \begin{pmatrix} V_s & \nu \\ \nu & V_s \end{pmatrix}, \quad w_{ij} = \begin{pmatrix} W_s & \omega \\ \omega & W_s \end{pmatrix}, \quad f_{ij} = \begin{pmatrix} 0 & \phi \\ -\phi & 0 \end{pmatrix} \\ r_{ij} = \begin{pmatrix} -R_a & 0 \\ 0 & R_a \end{pmatrix}, \quad s_{ij} = \begin{pmatrix} -S_a & 0 \\ 0 & S_a \end{pmatrix}, \quad y_{ij} = \begin{pmatrix} -Y_a & 0 \\ 0 & Y_a \end{pmatrix}, \quad z_{ij} = \begin{pmatrix} -Z_a & 0 \\ 0 & Z_a \end{pmatrix} \end{gathered} \tag{3.30}$$

3.2.1 Level 0 Calculation

As a first approximation, we will include only the lowest level states in the string field expansion. Setting x_{ij} and all higher level terms to zero and keeping only t_{ij} we can write down the truncated potential.

$$\mathcal{V} = 2\pi^2 \left[-T_s^2 - T_a^2 + (-1 + \frac{d^2}{2})\tau^2 + \frac{27\sqrt{3}}{32} \left(T_s^3 + 3T_s T_a^2 + 3 \left(\frac{4}{3\sqrt{3}} \right)^{d^2} T_s \tau^2 \right) \right] \tag{3.31}$$

This polynomial has 5 critical points. The trivial point $T_s = T_a = \tau = 0$ corresponds to the perturbative vacuum where neither D-brane has decayed. There are three other diagonal solutions with $T_s = \pm T_a = \frac{T_0}{2}$ and $T_a = 0, T_s = T_0$, where T_0 is the tachyon value decaying a single D-brane at level 0. These represent solutions where one or both D-branes have decayed separately. These four solutions are all expected, since the presence of another brane does not affect a brane's ability to decay. This is the diagonal subset of the solutions found in [28].

There is a fifth solution, shown in figure 3.1, in which there is an off-diagonal tachyon $\tau \neq 0$. In the zero separation limit, it is the solution where a symmetric linear combination of the two branes has decayed; an $SU(2)$ rotation of the solution where one of the branes decays. As the D-brane separation is increased the solution goes to zero at $d = \sqrt{2}$. This solution is only valid for $d \leq \sqrt{2}$, as for larger separations it becomes complex and violates the condition that the matrix t_{ij} must be hermitian. We can explore the physical interpretation of this solution at higher levels.

3.2.2 Level 1 Calculation

Now that we have an approximation to the tachyon sector of the solutions we are looking for, we can begin including more terms in the string field (3.7). The transverse scalars x_{ij} will be of key interest, which is why we have explicitly included them in section 3.1. With the explicit parameterization of the matrices t_{ij} and x_{ij} given in (3.29) as well as the Neumann coefficients

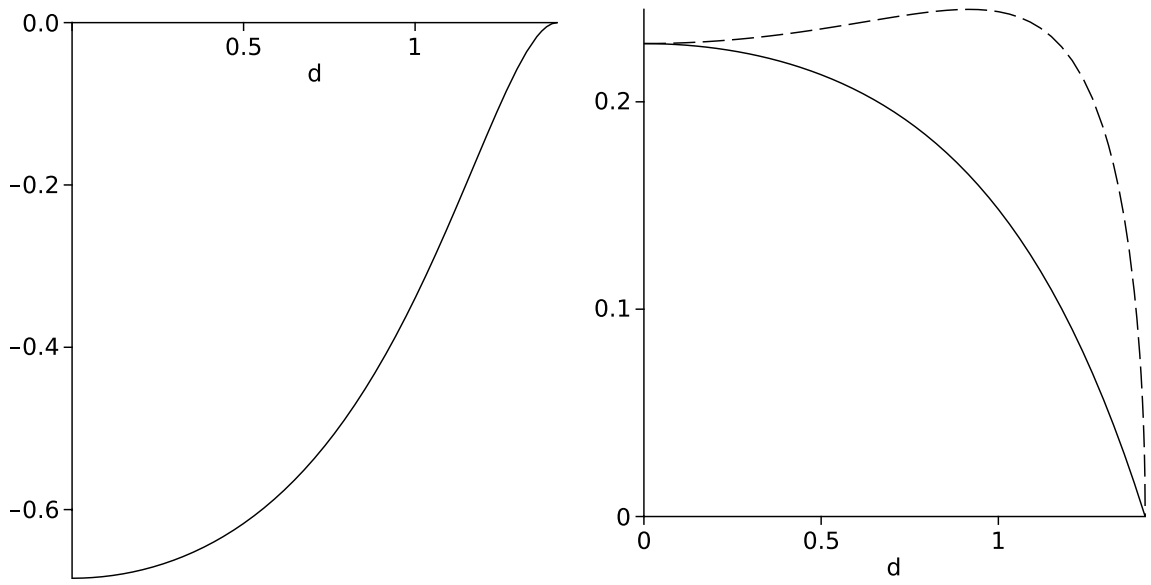

(a) (b)

Figure 3.1: The level 0 solution for separated D-branes which decays a non-trivial linear combination of two D-branes. The energy is shown in (a) and the non-zero components T_s (solid line) and τ (dashed line) of t_{ij} are in (b).

N^{rs}_{mn}, we can rewrite the full level 1 potential of (3.28) as

$$\begin{aligned}\mathcal{V} = 2\pi^2 \Bigg[& -T_s^2 - T_a^2 + (-1 + \frac{d^2}{2})\tau^2 + \frac{d^2}{2}\chi^2 + 2\gamma^2 \\ & + \frac{27\sqrt{3}}{32}T_s^3 + \frac{81\sqrt{3}}{32}T_s T_a^2 + \frac{3\sqrt{3}}{2}T_s(X_s^2 + X_a^2) + 3\sqrt{3}T_a X_s X_a \\ & + \left(\frac{4}{3\sqrt{3}}\right)^{d^2} \left(\frac{81\sqrt{3}}{32}T_s\tau^2 + \frac{27}{8}dX_a\tau^2 - \frac{27}{8}dT_a\tau\chi - \frac{3\sqrt{3}}{2}T_s\gamma^2 \right. \\ & \left. +3\sqrt{3}(1 - \frac{d^2}{2})X_s\tau\chi + \frac{3\sqrt{3}}{2}(1 + \frac{d^2}{4})T_s\chi^2 + \frac{d^3}{2}X_a\chi^2 - 2dX_a\gamma^2 \right) \Bigg] \end{aligned} \quad (3.32)$$

Here we find the first example of an unexpected quadratic term. The tachyon's mass is clearly -1 with an additional $\frac{d^2}{2}$ if it's stretched, and the level 1 vector has a mass of $0 + \frac{d_{ij}^2}{2}$ which makes perfect sense. The ghost term γ corresponding to the off-diagonal part of h_{ij}, however, has mass 2 and does not change at all when stretched. We will see at level 2 that the second ghost term, $c_{-1}|0\rangle$, is actually tachyonic, despite being at level 2. It even becomes more tachyonic as the string is stretched. Fortunately, this is a ghost mode, so in all likelihood it is one of the non-normalizable modes that are not present in the cohomology.

As discussed in section 3.1.1 we do not need to consider the entire set of 6 fields. Using the twist and exchange symmetries, only T_s, τ, and X_a are excited with the off-diagonal level

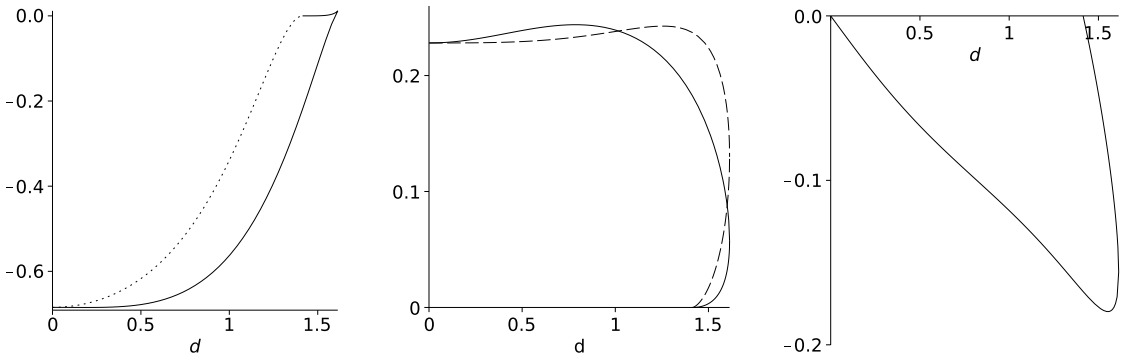

(a) (b) (c)

Figure 3.2: The level 1 solution for separated D-branes which decays a non-trivial linear combination of two D-branes. The energy (a) with the level 0 energy dotted for comparison, the tachyon matrix (b) T_s (solid) and τ (dashed), and the transverse scalar X_a (c).

0 solution as our starting point, so we can remove all of the other variables, and get a model for the effective potential of this solution.

$$\mathcal{V} = 2\pi^2 \left[-T_s^2 + (\frac{d^2}{2} - 1)\tau^2 + \frac{27\sqrt{3}}{32} T_s^3 + \frac{3\sqrt{3}}{2} T_s X_a^2 + \left(\frac{4}{3\sqrt{3}}\right)^{d^2} \left(\frac{81\sqrt{3}}{32} T_s \tau^2 + \frac{27}{8} d X_a \tau^2 \right) \right] \tag{3.33}$$

This system is now simple enough that it can be solved exactly. Apart from the obvious cases where either nothing happens or both branes decay, one solution is found. The physical branches of this solution are shown in figure 3.2.

Since the field responsible for transverse fluctuations of a brane is α_{-1}, the X_a field gives a constant positive shift to the position of brane 2, and a negative shift to brane 1, representing the first term in their separation. The negative value of X_a on this solution means that the two branes have moved closer together. The correct sign can be easily verified by noting that an increase to the value of X_a in (3.33) contributes a positive τ^2 term. An increased effective tachyon mass corresponds to increasing the brane separation felt by the tachyon.

There is every reason to expect that there are analytical solutions to string field theory consisting of a marginal deformation followed by a Schnabl type decay. In fact an analytic solution of this form was found for a single D-brane shortly after this work was published [45]. Since we know from [28] that any appropriate linear combination of two branes can decay as long as they are coincident, any such linear combination of separated branes should be able to decay as long as they first move to become coincident. We believe that the solution we have found is one of these. That only one specific linear combination of the branes has been found to decay like this is no surprise, since the $SU(2)$ symmetry of two D-branes was broken by separating them. In principle we expect this symmetry to be restored after the translation, but since level-truncated solutions are approximate the symmetry has not been restored here.

In the limit as $d \to 0$ we see that X_a goes to 0 as well, since the branes do not need to move when they are already coincident. In fact, for small d the solution behaves as $X_a = -\frac{4}{27} d + O\left(d^3\right)$, which is linear in the physical starting separation of the branes. To see if

the magnitude is reasonable, we can find the value of X_a for which the $SU(2)$ symmetry of the tachyon is restored. We accomplish this by equating the eigenvalues of the Hessian matrix for the three tachyon fields and solving. What we find is that $\chi = 0$ and, remarkably, $X_a = -\frac{4}{27}d + O(d^3)$. Because of the severe level truncation approximation, we only expect this to hold for small separations. x_{ij} is the leading term contributing to a translation, as shown in [21]. Infinitely many other fields will contribute at higher orders in separation, and indeed the $O(d^3)$ terms in the two calculations of X_a above do not even have the same sign.

At $d > \sqrt{2}$ this off-diagonal solution becomes double-valued, and the two branches meet and cease to exist for $d \gtrsim 1.61$. It is easy to see that $d = \sqrt{2}$ is the point where the stretched tachyon becomes massless. While there is no proof that the level truncation scheme is a consistent approximation, we can understand that the more massive modes tend to be less important contributions to a solution. This was refined in [16] where they pointed out that the level-truncation scheme should use the entire L_0 eigenvalue, including the zero-modes. What this means for us is that for $d \geq \sqrt{2}$ we should be including the diagonal fields before off-diagonal fields from one level previous. While at level 1 this would not make a difference to our solution since χ is already 0, we should bear in mind that our solutions are not necessarily valid for large d. For larger distances we should still be able to translate D-branes, but we don't know if such solutions can be found from a level-truncated system.

We should note that the reality condition on the string field is a sufficient condition to guarantee the reality of the action, but not a *necessary* condition. In fact, when the level 0 solution becomes complex the potential remains real for all separations. At level 1, however, the potential has an imaginary part that grows polynomially for separations above the critical distance $d_{\max} \approx 1.61$. As a result we will consider the reality condition on the string field rather than the reality of the action when discussing the range of separations for which our solution remains valid.

Direction of translation by T-dual method

I have claimed that the negative sign of x_{ij} indicates that the branes move towards each other because of the effect it has on the mass of the stretched tachyon. We can also check that the negative sign of X_a opposes the initial separation by considering the T-dual picture. The position $\hat{d}_i$ is dual to $-2\pi\alpha' A_{25}^{ii}$ where A_{25}^{ii} is the gauge flux on the i-th D-brane. The action with this charge is

$$S = \frac{1}{2\pi\alpha'} \int_M dz d\bar{z} \partial X_\mu \bar{\partial} X^\mu + i \int_{\partial M} A_\mu dX^\mu. \tag{3.34}$$

A shift in the position of a D-brane by ϵ is a shift $A_{25}^{ii} \to A_{25}^{ii} - \frac{\epsilon}{2\pi\alpha'}$, and under this perturbation the action changes as

$$e^{-S} = e^{-S_0} \left(1 + \frac{i\epsilon}{2\pi\alpha'} \int_{\partial M} \partial X^{25} dz + O(\epsilon^2) \right) \tag{3.35}$$

On the other hand, the state $x_{ij}\alpha_{-1}^{25} c_1 |ij\rangle$ corresponds to inserting the operators $\sqrt{\frac{2}{\alpha'}} i x_{ij} \partial X^{25}(0) c(0)$ at the origin on the upper half plane. For any operator we can write

$$|\mathcal{A}\rangle = \int DX_i e^{-S[X_i]} \mathcal{A}(0) \tag{3.36}$$

so we can see that for a translation of a single D-brane, we get

$$x\alpha_{-1}^{25}c_1\left|0\right\rangle = ix\sqrt{\frac{2}{\alpha'}}\int DX_i e^{-S[X_i]}\partial X^{25}(0). \tag{3.37}$$

Splitting the solution into a classical piece X_{cl} and a perturbation X' so that $DX_i = DX'$, (3.37) becomes

$$= ix\sqrt{\frac{2}{\alpha'}}e^{-S[X_{cl}]}\left(\partial X_{cl}^{25}(0)\int DX' e^{-S[X']} + \int DX' e^{-S[X']}\partial X'^{25}(0)\right) \tag{3.38}$$

$$= ix\sqrt{\frac{2}{\alpha'}}e^{-S[X_{cl}]}\partial X_{cl}^{25}(0)\int DX' e^{-S[X']} \tag{3.39}$$

$$= ix\sqrt{\frac{2}{\alpha'}}\partial X_{cl}^{25}(0)\int DX_i e^{-S[X_i]} \tag{3.40}$$

where the second term in (3.38) vanished because the integrand is odd. The sign of the operator insertion associated with a positive constant times the state $\alpha_{-1}^{25}c_1\left|0\right\rangle$ is clearly the same as the sign associated with the operator insertions from a gauge field which induces a positive shift in D-brane position in the T-dual picture. This is confirmation that when we find a solution with $X_a < 0$ the D-branes have moved towards each other.

3.2.3 Level 3

We will now include all of the fields listed in (3.30). The full potential used can be found in appendix A, and must then be simplified by dropping all fields which are not even under both twist and exchange symmetries. Beyond level 1 we can only get numerical solutions for the critical points of the potential, but we can do this for any initial separation d. We have plotted each field in figures 3.3-3.5.

The t_{ij} and x_{ij} fields look similar to what we found at level 1. In fact, as seen in figure 3.6, the X_a field has very nearly the same slope at $d = 0$ as it did before. The additional terms all go to 0 at $d = \sqrt{2}$ just as the string field has at all lower levels. This appears to be related to the fact that $d = \sqrt{2}$ is a special point where the tachyon is exactly massless, and that is not affected by level. The maximum separation before solutions become complex is now $d \approx 1.92$, which is another increase beyond previous levels, but not a very large change. In physical units, this separation is $\hat{d} \approx 8.55\sqrt{\alpha'}$.

3.2.4 Discussion

The level 3 slope of X_a at small separations is now $X_a \approx -0.1745d$, which is slightly steeper than the -0.1481 that we found at level 1. It is tempting to relate this to the marginal vev required to translate a D-brane a distance $\frac{d}{2}$. The translation induced by small values of the marginal field would then be

$$x\alpha_{-1}\left|0\right\rangle \to d \approx 2.866x, \quad \hat{d} \approx 12.73\sqrt{\alpha'}x, \tag{3.41}$$

but this is not the whole story. We will consider a hypothetical exact solution Ψ corresponding to the combination of translation and off-diagonal decay that we are studying. The solution

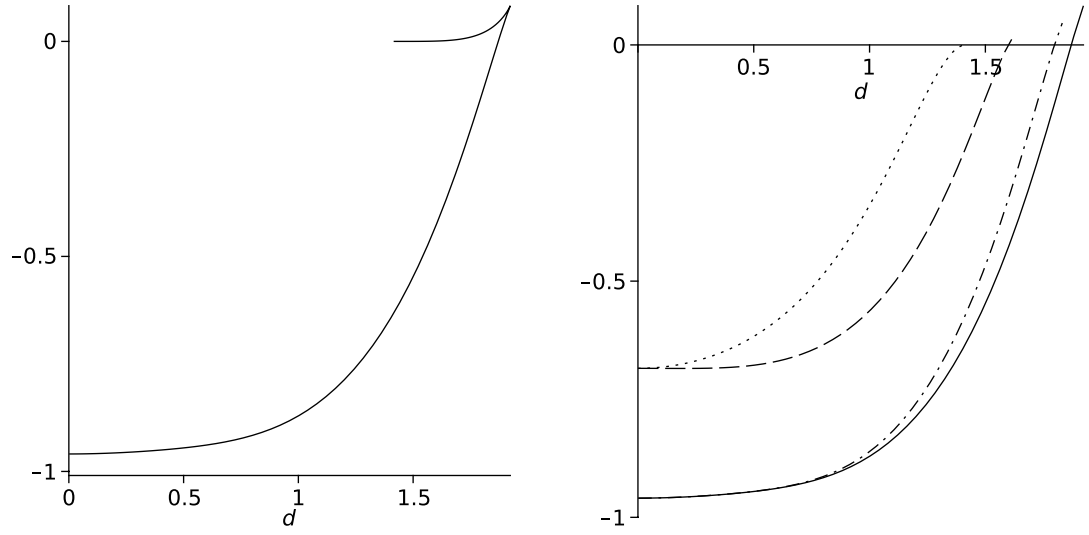

(a) (b)

Figure 3.3: The potential of the off-diagonal solution at (a) level 3 and (b) levels 0 through 3 with the second branch omitted.

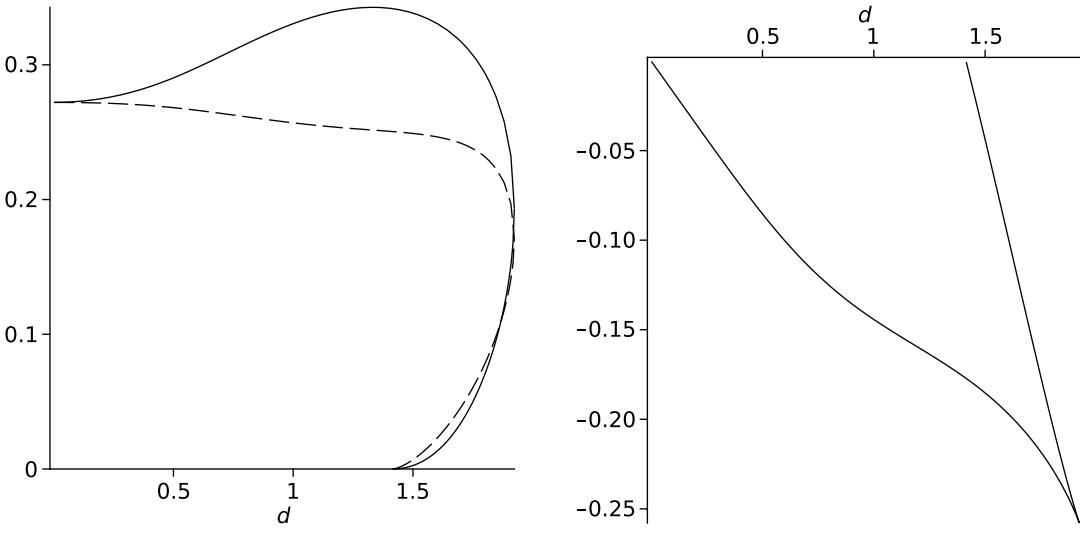

(a) (b)

Figure 3.4: The tachyon and marginal fields of the off-diagonal solution plotted at level 3 over the allowed range of separations, d. In (a) we see the tachyons T_s (solid) and τ (dashed), while in (b) we have the field X_a.

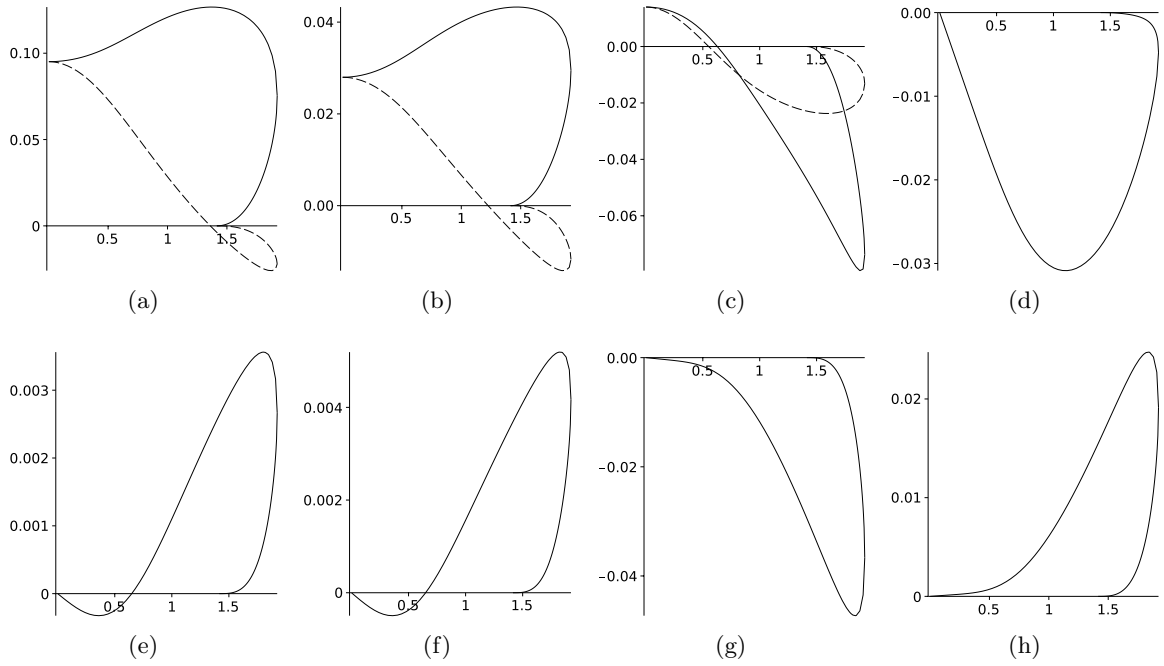

Figure 3.5: The remaining components of the off-diagonal solution at level (3,9) plotted over the allowed range of separations, d. When two fields are plotted together, the solid line is the diagonal component, while the dashed line is off-diagonal. (a) U_s and υ, (b) V_s and ν, (c) $\tilde{W}_s$ and $\tilde{\omega}$, (d) $\tilde{\phi}$, (e) R_a, (f) S_a, (g) Y_a, and (h) Z_a as defined in (3.30). The matrices w_{ij} and f_{ij} were replaced by their alternate forms defined in (3.18) to avoid singularities. All other component fields are 0 at level 3.

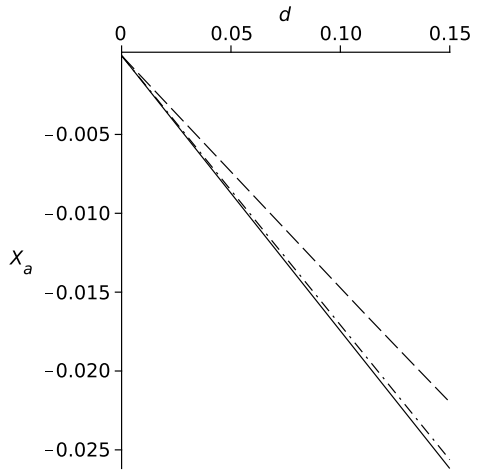

Figure 3.6: The slope of the field X_a for small separations. Level 3 is the solid line, with lower levels having shallower slopes.

should then be split into a part $\bar{\Psi}$ which is a solution for the translation leaving the D-branes coincident, and a part Ψ' which represents the decay, but is not a solution about the perturbative vacuum by itself. Each component of the string field can then be split in the same way, so that we will write the marginal component of the string field as $X_a = \bar{X}_a + X'_a$. We will label all other fields as $\phi_I = \bar{\phi}_I + \phi'_I$ with I an index. Since $\bar{\Psi}$ is a solution to the full OSFT, we can expand the theory about that point and must find the same action we would expect for two coincident D-branes, up to a field redefinition. We will write this field redefinition as

$$\tilde{X}_a = c_{XX} X'_a + \sum_I c_{XI} \phi'_I, \tag{3.42}$$

$$\tilde{\phi}_I = c_{IX} X'_a + \sum_J c_{IJ} \phi'_j, \tag{3.43}$$

where $\tilde{X}_a$ is the marginal field belonging to the new theory expanded about $\bar{\Psi}$. The action will have the form of the action on coincident D-branes, but in terms of the redefined fields:

$$S_d(\bar{X}_a + X'_a, \bar{\phi}_I + \phi'_I) = S_{d=0}(\tilde{X}_a, \tilde{\phi}_I) \ . \tag{3.44}$$

Since this off-diagonal decay of the coincident D-branes is an $SU(2)$ rotation of a single brane decay, it will not involve the marginal field, so $\tilde{X}_a = 0$.

It is clear that the action S_d has terms like $\bar{X}_a X'_a \phi'_I$ arising, for example, from the $T_s X_a X_a$ term in the action of (3.33). Since for small separations we know $\bar{X}_a \propto d$, the action has terms like $d X'_a \phi'_I$. We then infer that for small separations

$$c_{XX} \to 1, \quad c_{XI} \sim d \to 0 \tag{3.45}$$

$$c_{IX} \to 0, \quad c_{IJ} \to \delta_{IJ} \ . \tag{3.46}$$

The redefined marginal field $\tilde{X}_a = 0$ together with our ansatz for the field redefinition then gives us that for small separations

$$X'_a \approx -\sum_I c_{XI} \phi'_I \approx -\sum_I c_{XI} \tilde{\phi}_I \ . \tag{3.47}$$

But for D-brane decay many of the fields $\tilde{\phi}_I$ such as the tachyon are non-zero, so $X'_a \propto d$. Unless there is a cancellation, which we have no reason to expect, this correction to $\bar{X}_a$ is the same order of magnitude as $\bar{X}_a$ itself. What we have accomplished is to remove any BCFT calculations from the question of relating the two parameters. Using this method, the problem has been reduced to one entirely within OSFT, to find the precise field redefinition. Finding the redefinition, however, is beyond the scope of this work.

We have interpreted the solution as an off-diagonal D-brane decay after a translation makes the two branes coincident, so we expect that as the level of approximation increases the interpretation should be approximately valid for a larger range of separation d. From figure 3.3b we can see that as each even level lowers the energy exactly as happens with a single D-brane decay, both odd levels flatten out the preceding level somewhat. While it is surprising that the level 1 curve is so flat, we can understand that it is flatter than the higher level curves shown. In [21], they studied the behaviour of the potential near the single D-brane vacuum as a marginal parameter was turned on, and they found that the leading quadratic term did not

decrease monotonically as the level was increased. Instead the largest single increase in that quadratic term came from level 1 to level 2, which may explain why we saw a similar increase in our solution.

For $d = 0$ we see that the entire string field takes the value $\frac{1}{2}\left(\begin{smallmatrix}1&1\\1&1\end{smallmatrix}\right)\Phi_0$. It remains the same symmetric SU(2) rotation of the string field Φ_0 which describes the decay of a single D-brane. All of the fields which are descended from the primary state $\alpha_{-1}^{25}c_1\left|0\right\rangle$ go to 0 as $d \to 0$, since no translation is needed when the D-branes are initially coincident. We might also think that the two tachyon curves in figure 3.4a should remain together longer as the level increases, but this is not true. The approximate string field responsible for translating a D-brane without any decay does include a tachyonic component. For our situation where we move both D-branes equally in opposite directions, exciting X_a, the tachyon in question is T_s and the off-diagonal term is not excited at all. This explains the separation between the two curves in each of the plots for the tachyon t_{ij}, as well as u_{ij}, v_{ij}, and w_{ij} as the separation is increased and a translation becomes necessary.

There is one new feature at level 3 which did not appear at level 1. The change of variables described in (3.18) is singular at $d = \frac{1}{\sqrt{2}}$, and so we find a pole in the fields ω and ϕ at that point. In the alternate basis, however, the fields $\tilde{\omega}$ and $\tilde{\phi}$ defined in (3.17) remain finite as d approaches the singularity. We do not see any singularity in the level 3 fields r_{ij}, s_{ij}, y_{ij}, and z_{ij} because their off-diagonal components are protected by exchange symmetry, and the diagonal parts have $\alpha_0 = 0$ so that the transformation has no singularities there.

While the correspondence between the marginal parameter and the physical translation remains unknown, the physical translation of the solution is known exactly in this case. That the maximum translation remains finite is troubling. There is no reason why the translation of a D-brane should be limited, but this and all previous marginal solutions have found a maximum value of the deformation parameter. In previous cases there was still the possibility that the physical translation was unbounded, either by a singular correspondence between the marginal parameter and its physical effect, or through a second branch of the solution with decreasing marginal parameter but increasing effect as was found in a toy model [22]. In our case, however, we know exactly what the physical translation distance is, and we already see a second branch which does not have a larger displacement. It seems unlikely that either of these hypotheses could apply based on our solution. If D-brane translations are to be unbounded then we must hope that the small increases in the maximum with each level do not shrink too quickly and form a divergent series. One last possibility comes from recent work [23] where a level truncated solution underwent a sudden change from complex to real at level 14. Perhaps certain levels could have similar behaviour in our system and cause the solution to exist for a much larger range of D-brane separations. It is not known how this problem is resolved.

We have not done anything with the second branch of the solution, which begins at $d = \sqrt{2}$. The relatively flat energy of this branch suggests that it represents a truly marginal deformation, and if it is a pure translation then we could use the slope of that branch to directly determine a relationship. Unfortunately we do not know the physical interpretation of this branch, so we cannot be sure that it is only a translation, or if it is how far the D-branes move.

It is worth mentioning that the boundary state was calculated for a level-truncated marginal solution in [42], and that method should be applicable here too. We know that the first branch of our solution represents a single D24-brane at the origin, so we would expect that the boundary state constructed by the method of [41] should reflect this. It would be interesting to see if the

Level	$\bar{X}_a$	$X_a^{(0)}$	$\bar{a}_s$	$\bar{t}_1/\sqrt{2}$	$t_1^{(0)}/\sqrt{2}$
1	-0.1798	-0.1557	0.2963	0.296	0.286
2	-0.2464	-0.2431	0.3214	0.321	0.309
3	-0.2579	-0.2579	0.3301	0.330	0.316

Table 3.2: Values of maximum marginal parameters taken from four different cases and various levels. $\bar{X}_a$ is taken from this work, $\bar{a}_s$ from [21], and $\bar{t}_1$ from [24]. For the situations where it was considered, we have also included the value of the marginal parameter which has the greatest physical effect, $X_a^{(0)}$ and $t_1^{(0)}$. The values from [24] are estimated from plots.

boundary state for the second branch corresponds to two D-branes at the origin, as we would expect from the energy of the solution and the sign of X_a. We also do not know precisely what happens near the maximum separation, but as we expect higher level terms to play a larger role for such separations a boundary state based on an approximate solution is not likely to give accurate results. While a calculation of the boundary state would not give results independent of CFT (the boundary state must be compared to known CFT results), it is a powerful gauge-independent tool for determining physical properties of a SFT solution.

3.2.5 Comparison to Previous Solutions

We can also examine the extremum of the X_a field at the three levels where it was computed. At levels 1 and 2 we can see that the largest X_a is actually reached before the two branches meet. At level 3 we see what appears to be a cusp, though it may actually be the beginnings of a loop, based on one data point for the branch starting at $d = \sqrt{2}$ having an X_a value which is slightly below the value at the other branch at that point. The extremum values themselves are comparable to the maximum value of the marginal parameter found in [21] before their two branches also meet and become complex. The difference between our methods is that they are turning on a gauge field by itself, T-dual to translating a single D-brane without any decay, while in our system the translation will combine with the off-diagonal decay which allows us to get a true level truncated solution without dropping one equation of motion. While our values of X_a are smaller than their $\bar{a}_s$, they are on the same order of magnitude, and are growing faster as the level increases, going from 60% at level 1 to nearly 78% at level 3. Numerical values are listed in table 3.2.

Another marginal deformation that has been studied numerically is the lump solution at marginal radius [24]. Sen examined a very similar question to ours, attempting to match the strength of the marginal parameter to the physical effect of that parameter on the CFT. In that work, the energy-momentum tensor was used to link the two. Despite the fact that the marginal deformation studied was different, the two should be dual to each other with the rescaling

$$\lambda = t_1 \leftrightarrow \sqrt{2} a_s \tag{3.48}$$

where a_s is defined in [21] and is equivalent to our x on a single D-brane, and the parameters on the left hand side of the duality are defined in [24]. In this way we were able to extend table 3.2 to include the value of the marginal parameter with the greatest physical effect. The rate of growth with level is similar in both cases, and since the t_1 marginal deformation is understood

to be periodic with period 1, this suggests that our marginal deformation remains valid only for a finite range of the marginal parameter even at arbitrarily high level. We also notice that the value of the marginal parameter corresponding to the peak physical effect on the CFT side is quite close to the maximum value of the parameter in all cases. In [24] it was speculated that as the level increased the greatest effect $t_1^{(0)}$ might coincide with the maximum of the parameter $\bar{t}_1$, which is actually occurring at a much lower level in our solution than in that work. However, there is some suggestion that in our case the two points may begin moving apart again.

We can also use this relationship between the two marginal deformations to estimate a value for the slope (3.41). For this we will assume the exact result proposed in [24], that as the truncation level becomes large the lump marginal deformation causes the dimension of the initial D-brane to reduce by one at precisely $t_1 = \frac{1}{2}$. From [46] we see that this marginal deformation is also dual to turning on a periodic gauge field on a circle of radius 1, and that the value of the marginal parameter which reduces the D-brane dimension is exactly half the period. This corresponds to a translation half way around the circumference of the circle, a distance π. We also assume that the translation is a linear function of the marginal parameter. It is this assumption of linearity that we cannot justify, and which means our comparison will be rough at best. With all of this in mind, we can now say that

$$\hat{d} = \pi \longleftrightarrow t_1 = \frac{1}{2} \longleftrightarrow a_s = \frac{1}{2\sqrt{2}} \tag{3.49}$$

$$a_s \alpha_{-1} |0\rangle \to \hat{d} = 2\sqrt{2}\pi a_s \approx 8.89 a_s. \tag{3.50}$$

This slope is the same order of magnitude as the one we found from our off-diagonal solution combining a translation and a decay. In fact as we increased the level we saw our slope heading in that direction, though we certainly do not expect perfect agreement at infinite level because we had to assume a linear relationship between translation and marginal parameter in order to extrapolate this slope from only two known positions on the circle, and because we have seen that the presence of a D-brane decay will alter the slope of the marginal parameter in the combined solution studied here.

3.2.6 Restoration of $SU(2)$ Symmetry

Here we will attempt an alternate method of relating the marginal parameter to the physical displacement of the D-branes. Without a D-brane decay, the marginal parameter is directly related to the displacement, so we can consider other properties of the theory besides off-diagonal decays which are special for coincident D-branes. An obvious choice is to look for the $SU(2)$ symmetry of the theory, which is only present for coincident branes.

We consider the $SU(2)$ symmetry of a system of D-branes to be restored if the effective quadratic terms of the potential for our fields can be written as $C_I \phi^I_{ij} \phi^I_{ji}$ with some mass C_I. Taking the tachyon as an example, the mass would be $-\pi^2$ and the quadratic term in the action would be $-\pi^2 t_{ij} t_{ji}$. This means that the eigenvalues of the second derivative matrix over the coordinates T_s, T_a, and τ must all be equal. Allowing for field redefinitions, we search for the more general condition that the second derivative eigenvalues come in degenerate sets of 3. We hope that near such a degenerate point the masses of the fields would also show the same splitting for stretched strings as we find with initially separated D-branes.

In [21] Sen and Zwiebach found marginal "solutions" by dropping the one equation of motion for the field that we call x. This gave them a one parameter family of string fields which represent the marginal deformation of a D-brane. Due to level truncation, their string field was not exactly marginal, but was a good approximation for small values of the parameter. Taking the same approach, we can adjust the parameter to try to restore the SU(2) symmetry which was broken by beginning with separated D-branes. With only one parameter we find it impossible to restore the degeneracy for more than one cluster of fields.

We will plot the eigenvalues of the second derivative matrix expanded about such string fields which are approximately marginal and approximately solutions to the level truncated theory. In this case we have two parameters to adjust. We want to pick some value of the initial separation and see if there is some value of the marginal parameter which restores the degeneracy of the eigenvalue triplets. Focusing on the sextuplet of figure 3.7a formed by the mixing of the tachyon and the level 2 ghost u_{ij}, which have the same mass on coincident D-branes, we see three eigenvalues which are mostly unaffected by the marginal parameter, as well as three eigenvalues which clearly are affected. The parabola opening upwards makes good physical sense, as it has a minimum at $X_a \approx -0.022$, which we can interpret as the symmetry-restored point where the D-branes are once again coincident. As the marginal parameter moves away from this point the stretched string becomes heavier. This point would correspond to $X_a \approx -0.44d$ which is significantly steeper than the relationship at level 1, $X_a^{(1)} = -\frac{4}{27}d$. Since this is only the minimum of one eigenvalue it does not necessarily represent a restored SU(2) symmetry. The stretched u ghost does become lighter as the D-branes separate, so a downward-opening parabola is not unexpected, but this is a double eigenvalue with its maximum at $X_a = 0$, which does not agree with either our expectation that a non-zero marginal parameter is required to restore the symmetry and coincidence of the D-branes, or our expectation that only the stretched u mode should become more tachyonic as the D-branes are separated.

We can also examine the other sets of eigenvalues which we hope to be degenerate. For these fields the masses on a single D-brane tend not to be degenerate, so when we consider two D-branes we need to look at sets of three eigenvalues unlike the tachyon case where the u_{ij} field's degeneracy with t_{ij} meant that we had to consider a set of six eigenvalues. What happens in most cases is that two of the eigenvalues, corresponding to the diagonal fields, will be degenerate and relatively flat, while the off-diagonal eigenvalue is quadratic in the marginal parameter. We would hope to see an extremum that coincides with the diagonal values, all located near the same value of the marginal parameter. Instead we see extrema beyond the diagonal, so that the two sets of eigenvalues cross twice as in figure 3.7b, and while most of the extrema are located at $X_a = 0$, some are not. Some sets of fields have no flat eigenvalue, either similar to figure 3.7a without the constant modes, or having two parabolas opening in the same direction.

This suggests that the level-truncated approach of [21] does not give accurate results even for small separations. Note that while we focus on the matrix of second derivatives, in level truncation, the first derivatives of the potential do not all vanish, since the equation of motion for X_a is not satisfied. This effect decreases with increased truncation level. The computation used twist-even fields only. The approximate solution is also exchange-even, and we included all twist-even (both exchange-even and exchange-odd) fields in the computation of the second derivative matrix. Unfortunately, the features we were looking for do not seem to be unambiguously visible at level (3,9). Apparently, the cubic couplings to higher level fields with non-zero vev

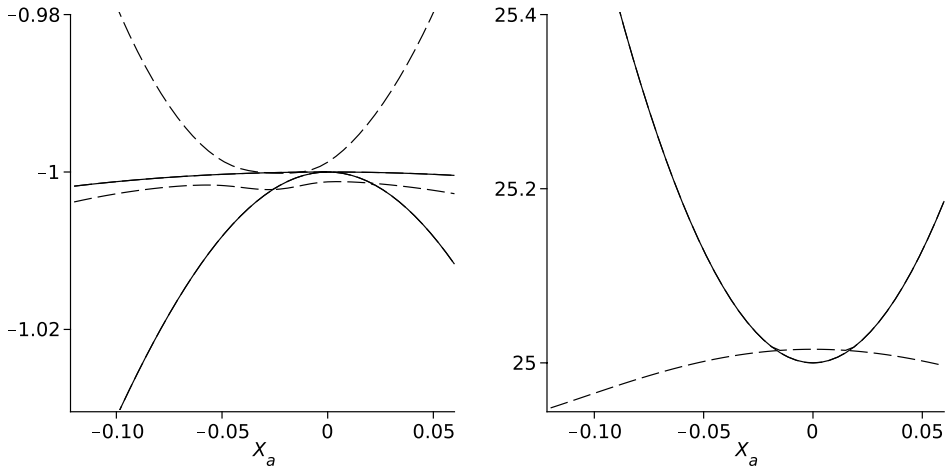

(a) (b)

Figure 3.7: Masses of several particles in an effective theory expanded about a marginal string field. Several eigenvalues of $\partial_{\phi^{(i)}}\partial_{\phi^{(j)}}\mathcal{V}$ are plotted over the marginal parameter X_a and with an initial separation of $d = 0.05$. The six eigenvalues in (a) have eigenvectors consisting primarily of the components of t_{ij} and u_{ij}, while the three in (b) are primarily associated with s_{ij}. Single eigenvalues are dashed lines, while degenerate pairs are solid.

contribute nontrivially to the masses of the lower modes when the D-branes are translated. It would be interesting to see whether this can be improved at higher levels.

Chapter 4

Renormalized Marginal Operators

In this chapter we will study the solution of [36] which represents a marginal deformation of the conformal boundary condition in the initial BCFT. What sets this solution apart from earlier marginal solutions in OSFT is that it still holds when the marginal operator V which generates the deformation has a singular self-OPE, $V(0)V(t) \sim \frac{1}{t^2}$. This is done by using a renormalization scheme for integrated operators, which must satisfy six assumptions in order for the solution to satisfy the equation of motion. When this particular solution was first presented in [36], a model renormalization scheme was included to demonstrate the process. Our purpose is to examine the space of possible renormalization schemes compatible with the conditions required for a real SFT solution.

Recently, an alternative method was given for constructing finite solutions to OSFT from operators with singular OPE [39]. This solution, however, does not apply to our main focus, the rolling tachyon, because it requires that the boundary condition changing operator σ acts as the identity in the time direction. For the rolling tachyon, the time direction is the only matter field which is affected by the boundary condition changing operator. Even in cases where the time direction is untouched, the solution of [39] may not always be useful. It is based on the boundary condition changing operator relating the desired solution to some known reference solution, and this may not always be available. It may still be possible to use without knowing what that boundary condition changing operator is, as long as some of their properties and three-point functions are known, but the method we will study does not require the bcc operators at all.

The simplest renormalization scheme replaces every pair of marginal operators which can collide with a counterterm which properly cancels the divergence, and then sums over all possible pairwise replacements. The OPE completely determines the singular part of the counterterm, but we can also ask whether the counterterm should have a finite part and if so what it should be. For a pairwise counterterm, the six assumptions will restrict the finite part to an arbitrary linear function of the length of boundary over which the operators are integrated. Considering more general schemes, we allow for higher order counterterms beyond simple pairwise subtractions. At each order in the marginal operator we will find new counterterms which can be added. The singular part of each counterterm is once again determined by the OPE and the counterterms at lower order, but the finite parts will each have some amount of freedom. This gives us an infinite dimensional space of renormalization schemes which satisfy four of the six assumptions. If we restrict this space to renormalization schemes which are linear, it may be a useful starting point for future studies of renormalized marginal boundary operators.

The two assumptions which are not immediately satisfied by the space we have outlined are also the most physically meaningful. The BRST conditions (4.5a) and (4.5b) represent the conformality of the new boundary conditions corresponding to the OSFT solution. If they do not hold then deforming the initial BCFT with a marginal operator renormalized in this way will no longer give conformal boundary conditions. Unfortunately, the sheer size of the

space of renormalization schemes makes a thorough examination of which schemes preserve conformality of the boundary beyond our reach. Instead we consider the "little g" scheme which closely resembles the model used in [36]. This choice is made because the integrands which appear in the little g scheme are more clearly finite than what we see in more general approaches. As a result, we will actually prove that the BRST conditions hold for this scheme at all orders in the marginal parameter.

This examination of the space of renormalization schemes is really just a starting point, as there are many unanswered questions which remain. Most obviously, is it possible to prove finiteness and the BRST conditions for some larger subset of general renormalization schemes. There is no reason to expect that only one renormalization scheme will satisfy the BRST conditions, so there is a question of uniqueness. If we have two equally valid renormalization schemes which are supposed to represent the same marginal boundary deformation, are they related to each other by a nontrivial rescaling of the marginal parameter, or do they somehow represent different deformations? Since the little g scheme is actually a two-parameter family of valid renormalization schemes, we have infinitely many such schemes. We expect that they are related by gauge transformations, but this will not be proven.

Another unanswered question pertains to the conformal properties of boundary condition changing operators. For many boundary conditions, the boundary condition changing operator is a conformal primary operator, and so it must behave in a given way when acted upon by the BRST operator, but when we explicitly construct this for the little g scheme, there is an extra term which behaves differently. It may be that this gives an additional constraint on the counterterm, requiring such extra terms to vanish. Since solutions to OSFT correspond to BCFT's, however, we would expect such a constraint to appear without needing to consider the BCFT side, for example as a violation of the equation of motion, but we have not seen any evidence that the OSFT solution fails with the counterterm considered. Perhaps such renormalization schemes correspond to non-primary boundary condition changing operators.

This chapter is structured as follows. In section 4.1 we begin by briefly reviewing the solution of [36]. We then construct the most general renormalization scheme for two marginal operators in section 4.2. Because the problem is simpler at this order, we will thoroughly examine the properties of this scheme. Moving to higher orders in section 4.3, we use a third order example to see how the addition of extra counterterms is allowed at each order. We then have to restrict ourselves to the little g scheme in order to get useful results which hold at all orders. In section 4.3.8 we describe a simple method for defining general linear renormalization schemes, and then give some evidence that the little g scheme can be described this way. Finally, in section 4.4 we will describe a few unanswered questions regarding the structure of general renormalization schemes.

A version of the work presented in this chapter has been published in the Journal of High Energy Physics [2].

4.1 Setup

Many analytical solutions to string field theory are constructed as wedge states with insertions, as in (2.22). For the case of solutions representing marginal deformations of the starting boundary CFT, the operators inserted on the boundary are generally the marginal operator in question as well as some ghosts. While several such marginal solutions have been studied,

[5][33][34], they have been limited to marginal deformations with regular self-OPE. The case of singular self-OPE was examined in [36] in a more formal setting. Here we will review the solution of [36]. More recently, an alternative solution has been proposed [38]. In that solution the singular OPE of the marginal operators is handled by performing extra integrals into the bulk of the worldsheet to soften the divergences until a finite result is achieved. The solution of [37] also deals with singular marginal deformations, but its focus was on the photon marginal deformation. It is likely that the same approach could be used for the rolling tachyon, but we will not be examining this more closely. It has also been suggested [32] that that solution is most likely equivalent to the one we study.

A few pieces of notation must be taken care of. The marginal operator is $V(t)$, and is taken to have self-OPE

$$V(t)V(0) \sim \frac{1}{t^2} + O(1) \tag{4.1}$$

with no $\frac{1}{t}$ term. In CFT a deformed boundary condition on the interval (a, b) is achieved by inserting an exponential of the marginal operator integrated between a and b, defined in terms of a Taylor series in the deformation parameter λ:

$$e^{\lambda V(a,b)} = \sum_{n=0}^{\infty} \frac{\lambda^n}{n!} V(a,b)^n \ , \tag{4.2}$$

where

$$V(a,b)^n = \left(\int_a^b dt V(t) \right)^n = \int_{(a,b)^n} d^n t \ V(t_1) \dots V(t_n) \ . \tag{4.3}$$

Since $V(t)$ has a singular self-OPE, the above expressions need to be regulated. We will denote the regulated (or renormalized) operators by enclosing them with $[\quad]_r$. The string field is defined in terms of its inner product with an arbitrary test state ϕ. Such a definition would typically appear as

$$\langle \phi, \Lambda \rangle = \langle f \circ \phi(0) \dots \rangle_{W_n} \, . \tag{4.4}$$

In this example the ellipsis represents the operator content to be inserted in order to define the string field Λ, and W_n is the wedge state (of circumference $n+1$) on which the inner product is to be taken. This example simplifies the typical case in which a string field theory solution is the superposition of such states defined on wedges with many different circumferences. For our purposes the function f will always be $f(\xi) = \frac{2}{\pi} \arctan \xi$ which maps the upper half plane to the wedge state W_1. $f \circ \phi(0)$ is the conformal transformation of the operator $\phi(t)$ corresponding to the state ϕ, inserted at 0.

The formal solution of [36] depends on six assumptions which must be satisfied by the renormalization procedure. If these conditions are satisfied, the formal solution constructed in [36] will satisfy the SFT equations of motion and be real; however, different renormalization schemes can possibly lead to different SFT solutions. These conditions are basically physical conditions which ensure that when $[e^{\lambda V(a,b)}]_r$ is inserted on the boundary, the effect is a conformal change

of boundary conditions on the interval (a, b), and nothing else. The conditions are

$$Q_B \left[e^{\lambda V(a,b)}\right]_r = \left[e^{\lambda V(a,b)} O_R(b)\right]_r - \left[O_L(a) e^{\lambda V(a,b)}\right]_r \ , \tag{4.5a}$$

$$Q_B \left[O_L(a) e^{\lambda V(a,b)}\right]_r = - \left[O_L(a) e^{\lambda V(a,b)} O_R(b)\right]_r \ , \tag{4.5b}$$

$$\left[\dots e^{\lambda V(a,c)} \dots\right]_r = \left[\dots e^{\lambda V(a,b)} e^{\lambda V(b,c)} \dots\right]_r \ , \tag{4.5c}$$

$$\left[\dots e^{\lambda_1 V(a,b)} e^{\lambda_2 V(c,d)} \dots\right]_r = \left[\dots e^{\lambda_1 V(a,b)}\right]_r \left[e^{\lambda_2 V(c,d)} \dots\right]_r , \ b < c \ , \tag{4.5d}$$

$$\left[e^{\lambda V(a,b)}\right]_r \text{ and } \left[O_L(a) e^{\lambda V(a,b)}\right]_r \text{ do not depend on the circumference of the wedge} \ , \tag{4.5e}$$

$$\left[e^{\lambda \int_a^b dt V(t)}\right]_r = \left[e^{\lambda \int_a^b dt V(a+b-t)}\right]_r \ . \tag{4.5f}$$

The first two conditions ensure that the resulting boundary condition is conformal. The first condition defines two local (unintegrated) operators O_L and O_R, which play an important role in the solution. The first condition, (4.5a) requires the existence and finiteness of the renormalized operators $\left[O_L(a) e^{\lambda V(a,b)}\right]_r$ and $\left[e^{\lambda V(a,b)} O_R(b)\right]_r$, implying that the OPE of the marginal operator V with $O_{L,R}$ is not so singular that it cannot be renormalized within the scheme we choose. The second of these two assumptions, (4.5b) expresses the fact that Q_B is anti-commuting. The third condition, (4.5c) ensures that changing the boundary condition on the interval (a, b) and (b, c) using the same deformation parameter should be the same as changing the boundary condition on the interval (a, c). In other words, renormalization should not spoil factorization of exponentials. This condition was called the "replacement condition" in [36] to differentiate it from the factorization condition (4.5d). We will continue to use this term. The factorization condition guarantees that the insertion $[e^{\lambda V(a,b)}]_r$ does not modify the boundary conditions away from the interval (a, b). In particular, it requires that when products of operators that are inserted away from each other are renormalized, it is sufficient to renormalize each term separately. In other words, the renormalized operator factorizes for operators with disjoint support. Next, (4.5e) is a kind of locality condition: the assumption that the subtractions involved in renormalizing operators depend only on the operators in question, and not on the size of the wedge state on which they are inserted. Finally, in order to obtain a real solution it is important not to violate the reflection symmetry of the operators, (4.5f). In addition to these explicitly stated conditions, a very natural condition of translation invariance was also implied in [36]. Counterterms may depend on the operator being renormalized as well as its properties such as the size and shape of the region the operator is integrated over, but should not depend on the location of the operator.

At this point, it is relevant to ask what classes of operators we need to provide a renormalization scheme for. Clearly, we need to be able to renormalize exponentials and their products. This is done order by order, so operators such as $V(a, b)^n$ must be renormalizable. Further, the action of the BRST operator Q_B on $V(a, b)$ ($Q_B V(t) = \frac{\partial}{\partial t}(cV(t))$) immediately implies that $O_L(a) = \lambda c V(a) + O(\lambda^2)$ and $O_R(b) = \lambda c V(b) + O(\lambda^2)$. Thus, we must be able to at least write down such operators as $\left[V(a) e^{\lambda V(a,b)}\right]_r$. In fact, we will see that this is sufficient: we need to renormalize products of exponentials of integrated operators with possible insertions of a single unintegrated V on either the left, or the right, or both. These operators also arise naturally when derivatives are taken, for example: $\frac{\partial}{\partial a}\left[e^{\lambda V(a,b)}\right]_r$.

Once we have decided on the renormalization scheme for $\left[e^{\lambda V(a,b)}\right]_r$, derivative operators such as $Q_B\left[e^{\lambda V(a,b)}\right]_r$ and $\frac{\partial}{\partial a}\left[e^{\lambda V(a,b)}\right]_r$ will be fixed. The choice of renormalization scheme for such operators as $\left[V(a)e^{\lambda V(a,b)}\right]_r$ can influence the explicit form of operators $O_{R,L}$ and the existence of natural properties such as

$$\frac{\partial}{\partial a}\left[e^{\lambda V(a,b)}\right]_r \stackrel{?}{=} -\left[V(a)e^{\lambda V(a,b)}\right]_r , \tag{4.6}$$

but it does not change $Q_B\left[e^{\lambda V(a,b)}\right]_r$ or $\frac{\partial}{\partial a}\left[e^{\lambda V(a,b)}\right]_r$ themselves. In other words, our choice of renormalization scheme for operators with unintegrated insertions will not affect the SFT solution. However, it does affect the linearity of the renormalization scheme (for example, property (4.6)). The implications of both this and the replacement condition for linearity will be discussed in section 4.2.3, and a general procedure for constructing a fully linear renormalization scheme order by order will be discussed in section 4.3.8.

With these assumptions on the renormalization scheme, a solution for regular marginal operators can be generalized to operators with singular self-OPE. The solution is

$$\Psi = \frac{1}{\sqrt{U}}A_L\frac{1}{\sqrt{U}} + \frac{1}{\sqrt{U}}Q_B\sqrt{U}, \tag{4.7}$$

where the wedge states U and A_L need to be defined.

$$U \equiv 1 + \sum_{n=1}^{\infty}\lambda^n U^{(n)}, \quad A_L \equiv \sum_{n=1}^{\infty}\lambda^n A_L^{(n)} \tag{4.8a}$$

where 1 is the $*$-product identity and the wedge states in the λ-expansion are given by

$$\left\langle \phi, U^{(n)}\right\rangle = \left\langle f\circ\phi\left[V^{(n)}(1,n)\right]_r\right\rangle_{W_n}, \tag{4.8b}$$

$$\left\langle \phi, A_L^{(n)}\right\rangle = \sum_{l=0}^{n}\left\langle f\circ\phi\left[O_L^{(l)}(1)V^{(n-l)}(1,n)\right]_r\right\rangle_{W_n}, \tag{4.8c}$$

$$\left\langle \phi, A_R^{(n)}\right\rangle = \sum_{l=0}^{n}\left\langle f\circ\phi\left[V^{(n-l)}(1,n)O_R^{(l)}(n)\right]_r\right\rangle_{W_n}. \tag{4.8d}$$

We should notice that with this definition $U^{(1)} = 0$. The operator $O_{L/R}^{(l)}$ is the l-th coefficient when $O_{L/R}$ is expanded in powers of λ. In practice, we will show that

$$O_L(t) = \lambda cV(t) - \frac{1}{2}\lambda^2\partial c(t) + \lambda^2 C_1 c(t), \quad O_R(t) = \lambda cV(t) + \frac{1}{2}\lambda^2\partial c(t) + \lambda^2 C_1 c(t) \tag{4.9}$$

so only $O_L^{(1)}$ and $O_L^{(2)}$ are non-zero. This is explained in section 4.2.5 and generalizes the argument of [36] which found the same form but with $C_1 = 0$. Since everything has been defined in terms of series in λ, we define powers of string fields using the appropriate power series, with the star product implied whenever string fields are multiplied. For example

$$U^{-1} = 1 - \sum_{n=1}^{\infty}\lambda^n U^{(n)} + \left(\sum_{n=1}^{\infty}\lambda^n U^{(n)}\right) * \left(\sum_{n=1}^{\infty}\lambda^n U^{(n)}\right) - \dots \tag{4.10}$$

$$= 1 - \lambda U^{(1)} + \lambda^2\left(U^{(1)} * U^{(1)} - U^{(2)}\right) - \dots . \tag{4.11}$$

The solution Ψ is a gauge transformation of the simpler solution

$$\Psi_L = A_L U^{-1}, \tag{4.12}$$

which is a solution that does not satisfy the reality condition already mentioned in chapter 3 guaranteeing reality of the string field theory action: $\Psi = \text{bpz} \circ h.c. \Psi = \Psi^\ddagger$. Ψ_L will not be the focus of our study, but it is much simpler to show that this form is a solution to the equation of motion.

Using (4.8b), (4.5a), and (4.8c) it is straightforward to show that $Q_B U = A_R - A_L$. We can then compute

$$\begin{aligned} Q_B \Psi_L &= Q_B (A_L * U^{-1}) && \text{(4.13a)} \\ &= (Q_B A_L) * U^{-1} + A_L * U^{-1} * (Q_B U) * U^{-1} && \text{(4.13b)} \\ &= (Q_B A_L + A_L * U^{-1} * A_R) * U^{-1} - \Psi_L * \Psi_L && \text{(4.13c)} \end{aligned}$$

so the problem of showing that the equation of motion is satisfied is reduced to the problem of showing that $Q_B A_L + A_L * U^{-1} * A_R = 0$. This is accomplished by using (4.5b) to write $Q_B A_L$ in terms of operators inserted on a wedge state, then showing the structural equivalence of the two terms by applying (4.5c) and (4.5d). This is the topic of appendix A of [36], and we will not repeat the details here.

While the purpose of this chapter is to give a detailed construction of renormalized operators suitable for use in the solution (4.7), we will also study the general structure of allowed operators along the way. The operators we use will generalize the example renormalization scheme provided by Kiermaier and Okawa in [36]. The formal approach they used for describing the singularity structure of well regulated operator collisions (for example in equation (4.35)) can be used to explicitly define a general renormalization scheme for quadratic operators, as we will demonstrate in section 4.2. When renormalizing products of more than two operators, however, this approach breaks down and we must resort to a less general approach in order to prove the assumptions (4.5). This is the primary concern of section 4.3.

4.2 Quadratic Operators

The renormalization of operators discussed above is necessary whenever two operators with singular OPE become arbitrarily close to one another. As we mentioned previously, the OPE is assumed to be $V(0)V(t) \sim \frac{1}{t^2}$, but the finite part of the OPE can contain operators other than the identity. In order for a relatively simple renormalization scheme to be possible, we require that any divergences which appear when a marginal operator V approaches this OPE are not too bad. More precisely, we require the finiteness condition which is equation (4.10) of [36]. This condition can be restated as requiring that

$$\circ \prod_i V(t_i) \circ = \exp\left(-\frac{1}{2} \int ds_1 ds_2 \; \frac{1}{(s_1 - s_2)^2} \frac{\delta}{\delta V(s_1)} \frac{\delta}{\delta V(s_2)} \right) \prod_i V(t_i) \tag{4.14}$$

remains finite even when more than two of the coordinates t_i collide simultaneously. This is a condition on the marginal operator V and will not hold for all marginal operators.

Since the solution (4.7) is given order by order in λ, the renormalized exponentiated integrated operators such as $\left[e^{\lambda V(a,b)}\right]_r$ should be interpreted as a series, and the renormalization of powers of integrated operators is what we will need to define, rather than the exponentials. To start with, we will see what counterterms are compatible with renormalizing two operators. Even at this order the structure of renormalized operators differs from the regular case in a number of ways.

We have seen that there are two ways for operators to collide in this solution: they can both be integrated with overlapping regions, or one can be fixed at the end of an integration region. The latter case is simpler so we will start there. Setting any other operator insertions aside, the singularity we are studying appears in

$$\int_{a+\epsilon}^{b} dt \, \langle V(a)V(t)\rangle_{W_n} = \frac{1}{\epsilon} - \frac{\pi}{n+1}\cot\left(\frac{\pi}{n+1}(b-a)\right) + O(\epsilon)\,, \tag{4.15}$$

where $n+1$ is the circumference of the wedge state's boundary. The renormalized operator $[V(a)V(a,b)]_r$ can now be written as

$$[V(a)V(a,b)]_G = \lim_{\epsilon\to 0}\left[\int_{a+\epsilon}^{b} dt \; V(a)V(t) - G^L_{ab}\right] \,, \tag{4.16}$$

where the counterterm G^L_{ab} is implicitly a function of ϵ. The subscript G on the renormalization bracket indicates this approach to subtracting off counterterms which are given as functions G of epsilon. Requiring finiteness means that the singular part must be the integral of the OPE, but the finite part is not constrained by this, so

$$G^L_{ab} = \frac{1}{\epsilon} + O(\epsilon^0) \,. \tag{4.17}$$

This cancels the divergence in (4.15). Similarly, we have

$$G^R_{ab} = \frac{1}{\epsilon} + O(\epsilon^0) \,. \tag{4.18}$$

Next we will define the renormalization of the doubly integrated operator

$$\int_a^{b-\epsilon} dt_1 \int_{t_1+\epsilon}^{b} dt_2 \, \langle V(t_1)V(t_2)\rangle_{W_n} = \frac{b-a}{\epsilon} + \ln\epsilon - 1 + \ln\left(\frac{\pi}{(n+1)\sin\left(\frac{b-a}{n+1}\pi\right)}\right) + O(\epsilon). \tag{4.19}$$

For this operator we have the form

$$\left[V(a,b)^2\right]_G = 2\lim_{\epsilon\to 0}\left[\int_a^{b-\epsilon} dt_1 \int_{t_1+\epsilon}^{b} dt_2 V(t_1)V(t_2) - G^D_{ab}\right] \,, \tag{4.20}$$

where the counterterm is

$$G^D_{ab} = \frac{b-a}{\epsilon} + \ln\epsilon + O(\epsilon^0) \,. \tag{4.21}$$

The factor of 2 in (4.20) is due to the fact that the operators have been written in a specific order. Instead of including integrals with $t_2 < t_1$, we used the indistinguishability of the operators and doubled the result.

Although it never appears in the solution of the form (4.7), we will need an additional renormalized operator in order to prove the assumptions. When two integrated operators collide only at a shared edge, we get the operator

$$[V(a,b)V(b,c)]_G = \lim_{\epsilon\to 0}\left[\int_a^b dt_1 \int_{b\vee(t_1+\epsilon)}^c dt_2 V(t_1)V(t_2) - G^E_{abc}\right] . \tag{4.22}$$

Here the notation $b \vee (t_1 + \epsilon)$ represents the minimum of b and $t_1 + \epsilon$. In this case the only divergence is logarithmic, and we get

$$G^E_{abc} = -\ln\epsilon + O(\epsilon^0) . \tag{4.23}$$

4.2.1 The "Little g" Scheme

While the renormalization scheme we have just described is extremely useful at this order, when more than two operators need to be renormalized, it is often useful to take a different approach. While the "little g" scheme is not as useful at quadratic order, it is perfectly valid, so we will introduce it here.

The critical problem which the "big G" scheme, $[\ldots]_G$, has is that the operators are integrated and the counterterm is not. At higher orders this will mean that a renormalized operator is the sum of terms with different numbers of integrals over different regions, which makes some proofs intractable, and causes many other issues including for the finiteness of the scheme. Even setting aside the analytical proofs, when performing numerical calculations the renormalization scheme described so far is extremely cumbersome. The integrals over various regulated regions must be evaluated repeatedly as the regulator ϵ approaches 0. Since each integral can generally not be performed analytically and requires a numerical algorithm, this would be an extremely time consuming process. In addition, since the limit only exists once all of the counterterms are included, each integral itself will diverge as $\epsilon \to 0$, and the results will most likely not be trustworthy due to large roundoff errors.

The solution is to combine the counterterms into the integrand. We want functions $g^D(t_1,t_2)$, $g^L(a,t)$, and $g^E(t_1,t_2)$ which once integrated over the correct ϵ-regulated regions will give the counterterms G^D_{ab}, G^L_{ab}, and G^E_{abc} respectively. This can be accomplished by

$$g^D_{ab}(t_1,t_2) = \frac{1}{(t_1-t_2)^2} + \frac{2}{(b-a)^2}\left(1+\ln(b-a)+\ldots\right) , \tag{4.24a}$$

$$g^L_{ab}(t_1,t_2) = \frac{1}{(t_1-t_2)^2} + \frac{1}{(b-a)^2} + \frac{\ldots}{b-a} , \tag{4.24b}$$

$$g^E_{abc}(t_1,t_2) = \frac{1}{(t_1-t_2)^2} + \frac{1}{(c-b)(b-a)}\left(1+\ln\left(\frac{(c-b)(b-a)}{c-a}\right)+\ldots\right) , \tag{4.24c}$$

where the ellipsis in each right hand side is the finite part of the corresponding counterterm G. These functions have no more dependence on ϵ; it has been shifted to the region over which they are integrated. Additionally, we did not have to choose the functions we did. Any function with the same integral over the appropriate regulated regions will produce an equivalent renormalization scheme. In particular the constant terms appearing in each of these functions could have been any function of t_1 and t_2 with the same integral, but we have chosen constant

values purely for simplicity. This will be examined in more detail in section 4.3.3. The left counterterm $g^L_{ab}(t_1, t_2)$ is nearly always used with one insertion at a since that is the endpoint of the interval. In this case we should feel free to use the shorthand

$$g^L_{ab}(t) \stackrel{\text{def}}{=} g^L_{ab}(a, t) \ . \tag{4.25}$$

Now if we define the renormalization by

$$\left[V(a,b)^2\right]_g = 2 \lim_{\epsilon\to 0} \int_a^{b-\epsilon} dt_1 \int_{t_1+\epsilon}^{b} dt_2 \left(V(t_1)V(t_2) - g^D_{ab}(t_1,t_2)\right) \ , \tag{4.26a}$$

$$\left[V(a)V(a,b)\right]_g = \lim_{\epsilon\to 0} \int_{a+\epsilon}^{b} dt \left(V(a)V(t) - g^L_{ab}(t)\right) \ , \tag{4.26b}$$

$$\left[V(a,b)V(b,c)\right]_g = \lim_{\epsilon\to 0} \int_a^{b} dt_1 \int_{b\vee(t_1+\epsilon)}^{c} dt_2 \left(V(t_1)V(t_2) - g^E_{abc}(t_1,t_2)\right) \ , \tag{4.26c}$$

then this renormalization scheme is identical to the "big G" scheme when renormalizing these quadratic operators. The finiteness of these integrals stems from the fact that the integrands are now completely finite. Whenever two operators approach each other, the counterterm has a singular term which cancels the divergence and gives a finite quantity. This is apparent from the finiteness condition (4.14) which we impose on the marginal operator V.

4.2.2 Small Integrated Operators

Here we will take a moment to briefly discuss one unusual feature of our renormalization scheme, demonstrating that it may not be viable for all wedge states. It naively seems reasonable to expect that a fully renormalized integrated operator over a set of measure 0 would be 0 itself. Specifically, we will look at the equation

$$\lim_{b\to a} \left[V(a,b)^2\right]_r = 0 \tag{4.27}$$

and see if it can be satisfied.

The OPE for exponential operators on the boundary gives us the form we will be considering.

$$:V(t_1)::V(t_2): = \frac{1}{(t_1-t_2)^2} + O\left((t_1-t_2)^0\right) \tag{4.28}$$

The operator (4.27) is then

$$\begin{aligned}
\frac{1}{2}\lim_{b\to a}\left[V(a,b)^2\right]_G &= \lim_{b\to a}\lim_{\epsilon\to 0}\left[\int_a^{b-\epsilon} dt_1 \int_{t_1+\epsilon}^{b} dt_2 \left(\frac{1}{(t_1-t_2)^2} + O\left((t_1-t_2)^0\right)\right)\right. \\
&\qquad \left. -\frac{b-a}{\epsilon} - \ln\epsilon + \ldots\right] && \text{(4.29a)} \\
&= -1 + \lim_{b\to a}\left[-\ln(b-a) + \int_a^{b-\epsilon} dt_1 \int_{t_1+\epsilon}^{b} dt_2 \ O\left((t_1-t_2)^0\right) + \ldots\right] && \text{(4.29b)} \\
&= -1 - \lim_{b\to a}\ln(b-a) \ . && \text{(4.29c)}
\end{aligned}$$

We see that the operator has a finite piece which could be cancelled by making a specific choice of the finite piece of G^D_{ab} similar to [36]. But there is also a divergent part which cannot be cancelled without the finite piece having $\ln(b-a)$ and this would conflict with the assumptions (4.5). Integrating over a smaller region has caused this operator to diverge, and we cannot consistently set it to 0 despite our intuition. We will also see the necessity of this divergence when we compute the derivative of a renormalized operator in section 4.2.3. The logarithmic divergence of $\left[V(a-\Delta,a)^2\right]_G$ provides the counterterm that makes $V(a)V(a,b)$ finite. The structure of the renormalization scheme satisfying the replacement condition (4.5c) forces us to accept a divergence for some integrated operators in order for others to remain finite.

What this has shown us is that some operators must be handled with care despite being renormalized, if we wish to see finite results. Fortunately, the solution (4.7) is built entirely out of operators with integer domains, so it is safe from this kind of divergence. This does remain a concern for the possible future construction of renormalized solutions on wedge states of continuous circumference, as in [34].

4.2.3 Linearity

The replacement condition (4.5c) as stated is trivially satisfied because $e^{\lambda V(a,c)} = e^{\lambda V(a,b)} e^{\lambda V(b,c)}$ holds for the bare operators. The implied condition, however, is for us to take the assumption at each order in λ and bring the combinatoric sum outside of the renormalization.

$$\frac{\lambda^n}{n!}\left[V(a,c)^n\right]_r = \sum_{j=0}^{n} \frac{\lambda^n}{j!(n-j)!}\left[V(a,b)^j V(b,c)^{n-j}\right]_r \tag{4.30}$$

Repeated application of this means that operators of the form

$$V(a_1)V^{n_1}(a_1,b_1)\ldots V^{n_k}(a_k,b_k)V(b_k) \tag{4.31}$$

satisfy linearity provided $a_1 < b_1 < a_2 < \ldots < b_k$ so that the intervals are of finite length and do not overlap. The replacement condition also does not provide linearity if the fixed operators $V(a_1)$ and $V(b_k)$ are not inserted at the same place in each term of the sum. A stronger condition is needed if we want full linearity, including the ability to perform derivatives and integrals either before or after renormalization with equal results.[2] We will return to this once we have examined the consequences of the replacement condition alone.

Beginning with (4.5c) we will examine its consequences. The singular parts of G^L_{ab}, G^D_{ab} and G^E_{abc} are already known, so we will focus primarily on the finite parts. Imposing the obvious requirement of translation invariance we will take the ansatz

$$G^L_{ab} = \frac{1}{\epsilon} + C^L_{b-a}\ , \tag{4.32a}$$

$$G^D_{ab} = \frac{b-a}{\epsilon} + \ln\epsilon + C^D_{b-a}\ , \tag{4.32b}$$

$$G^E_{abc} = -\ln\epsilon + C^E_{c-b,b-a}\ , \tag{4.32c}$$

[2]Integration only commutes with renormalization if both sides are well defined and finite. For an example where this does not work see the discussion of (4.73).

where the functions $C^{L/D/E}$ have no more ϵ-dependence. This means that our renormalization scheme is

$$[V(a)V(a,b)]_G = \lim_{\epsilon\to 0}\left[\int_{a+\epsilon}^{b} dt\ V(a)V(t) - \frac{1}{\epsilon} - C^L_{b-a}\right]\ , \tag{4.33a}$$

$$\left[V(a,b)^2\right]_G = 2\lim_{\epsilon\to 0}\left[\int_{a}^{b-\epsilon} dt_1 \int_{t_1+\epsilon}^{b} dt_2\ V(t_1)V(t_2) - \frac{b-a}{\epsilon} - \ln\epsilon - C^D_{b-a}\right]\ , \tag{4.33b}$$

$$[V(a,b)V(b,c)]_G = \lim_{\epsilon\to 0}\left[\int_{a}^{b} dt_1 \int_{b\vee(t_1+\epsilon)}^{c} dt_2\ V(t_1)V(t_2) + \ln\epsilon - C^E_{c-b,b-a}\right]\ . \tag{4.33c}$$

We now take (4.5c) and (4.5d) and explore some restrictions which we can impose on the counterterms. The first quantity we see is

$$[V(a,c)]_r = [V(a,b)]_r + [V(b,c)]_r\,, \tag{4.34}$$

which is trivial as there is no renormalization involved. If we insert a fixed operator at a, however, we find our first condition.

$$[V(a)V(a,c)]_G = [V(a)V(a,b)]_G + [V(a)]_G\,[V(b,c)]_G \tag{4.35a}$$

$$\begin{aligned}\int_{a+\epsilon}^{c} dtV(a)V(t) - \frac{1}{\epsilon} - C^L_{c-a} = \int_{a+\epsilon}^{b} dtV(a)V(t) - \frac{1}{\epsilon} - C^L_{b-a} \\ + \int_{b}^{c} dtV(a)V(t)\end{aligned} \tag{4.35b}$$

$$C^L_{c-a} = C^L_{b-a} \stackrel{\text{def}}{=} C^L \tag{4.35c}$$

The finite part of the counterterm for collision of an integrated operator with a fixed operator is in fact constant, and does not depend on the size of the integration region. In addition to linearity, this result involved the assumption that there are no counterterms for the renormalization of operators which do not meet. If we had allowed a finite part in the renormalization of $[V(a)V(b,c)]_G$ even though it is not necessary, we could not say anything about the constant C^L. Fortunately, neglecting counterterms for any two operators which do not collide is clearly equivalent to the assumption (4.5d), so this is not only permitted, but required.

This property is more general than just the case $[V(a)V(a,b)]_r$. If we insert an arbitrary local operator $\mathcal{O}_A$ to the left of an integrated operator we get the same result.

$$\left[\mathcal{O}_A(a)\int_a^c dt\mathcal{O}_B(t)\right]_r = \left[\mathcal{O}_A(a)\int_a^b dt\mathcal{O}_B(t)\right]_r + \left[\mathcal{O}_A(a)\int_b^c dt\mathcal{O}_B(t)\right]_r \tag{4.36a}$$

$$= \left[\mathcal{O}_A(a)\int_a^b dt\mathcal{O}_B(t)\right]_r + \mathcal{O}_A(a)\left[\int_b^c dt\mathcal{O}_B(t)\right]_r \tag{4.36b}$$

$$\mathcal{O}_A(a)\int_{a+\epsilon}^{c} dt\mathcal{O}_B(t) - G^{(AB)}_{ac} = \mathcal{O}_A(a)\int_{a+\epsilon}^{b} dt\mathcal{O}_B(t) - G^{(AB)}_{ab} + \mathcal{O}_A(a)\int_b^c dt\mathcal{O}_B(t) \tag{4.36c}$$

$$G^{(AB)}_{ac} = G^{(AB)}_{ab} \stackrel{\text{def}}{=} G^{(AB)} \tag{4.36d}$$

Using only the linearity of the renormalization and a generalization of assumption (4.5d) to the operators being considered, we have shown that the counterterm for one fixed and one

integrated operator must always be independent of the limits of integration. Using exactly the same reasoning as the above two arguments, we apply linearity and factorization to the renormalized operator

$$[V(a,b)V(b,d)]_r = [V(a,b)V(b,c)]_r + V(a,b)V(c,d) \ . \tag{4.37}$$

This tells us that the counterterm for integrated operators colliding at an edge is also independent of the integration ranges:

$$C^E_{c-b,b-a} = C^E \ . \tag{4.38}$$

We will rarely discuss the right handed counterterm G^R because it is normally identical to G^L. The same argument applies that we used for C^L, and we know that $C^R_{b-a} = C^R$ is a constant. Strictly speaking, the condition (4.5c) does not imply any relationship between C^L and C^R, but stronger linearity conditions such as (4.6) do. Even without the strong linearity condition, a natural extension of the reflection condition (4.5f) would imply equality of the two constants. If we require that $\left[\int_a^b dt_2 V(t_1)V(t_2)V(t_3)|_{t_1=a,t_3=b}\right]_r$ is invariant under the reflection operation $t_i \to b+a-t_i$, then we get

$$V(a)V(a+\epsilon,b-\epsilon)V(b) - G^R V(a) - G^L V(b) = V(a)V(a+\epsilon,b-\epsilon)V(b) - G^R V(b) - G^L V(a) \tag{4.39}$$

and immediately have $G^R = G^L$ which implies $C^R = C^L$. This equation is not required, however. In fact, because the solution is built out of the wedge state U and $A_{L/R}$ (which can be obtained by acting on U with Q_B), it cannot have any dependence on the constants $C^{L/R}$ which don't appear in U. We will see an explicit C^L dependence later on, but this is only introduced to cancel the implicit dependence from the renormalization of the operators in A_L. Since C^L and C_R play no part in the solution, we should not expect any constraints on them. The constraints imposed by (4.6) come about because that condition gives the renormalization scheme a linear structure that goes beyond what is necessary for a solution.

Next we will examine the replacement condition (4.5c) for two integrated operators:

$$\left[V(a,c)^2\right]_r = \left[V(a,b)^2\right]_r + \left[V(b,c)^2\right]_r + 2\left[V(a,b)V(b,c)\right]_r . \tag{4.40}$$

Our restriction on C^D_{b-a} can now be calculated.

$$[V(a,b)V(b,c)]_G = \frac{1}{2}\left[V(a,c)^2\right]_G - \frac{1}{2}\left[V(a,b)^2\right]_G - \frac{1}{2}\left[V(b,c)^2\right]_G \tag{4.41a}$$

$$\begin{aligned}\int_a^b dt_1 \int_{b\vee(t_1+\epsilon)}^c dt_2 \left(V(t_1)V(t_2)\right) + \ln\epsilon - C^E \\ = \left(\int_a^{c-\epsilon} dt_1 \int_{t_1+\epsilon}^c dt_2 - \int_a^{b-\epsilon} dt_1 \int_{t_1+\epsilon}^b dt_2 - \int_b^{c-\epsilon} dt_1 \int_{t_1+\epsilon}^c dt_2\right)\left(V(t_1)V(t_2)\right) \\ - \frac{c-a+b-c+a-b}{\epsilon} + \ln\epsilon - C^D_{c-a} + C^D_{b-a} + C^D_{c-b}\end{aligned} \tag{4.41b}$$

$$C^D_{c-a} - C^D_{c-b} - C^D_{b-a} - C^E = 0 \tag{4.41c}$$

In order to satisfy this, the finite renormalization terms must be $C^D(\Delta t) = C_0 + C_1\Delta t$, and $C^E = -C_0$. Together with C^L and C^R this leaves us with four free parameters which are not fixed. In chapter 5 we will reduce the number by one by fixing $C^R = C^L$ and consider the three remaining parameters to be free when we numerically check the validity of the solution and examine the tachyon profile.

A stronger linearity condition

This is all that the weak version of linearity can tell us about the counterterms. Strong linearity, however, gives us one additional restriction. We would naturally expect that the derivative of a renormalized operator might behave in the same way as an unrenormalized operator. By this I mean that we could choose to require that

$$\partial_a \left[V(a,b)^2\right]_r \stackrel{?}{=} -2\left[V(a)V(a,b)\right]_r \tag{4.42}$$

and consequently the related condition

$$\int_a^b dt\,[V(t)V(t,c)]_r \stackrel{?}{=} \left[\int_a^b dt\; V(t)V(t,c)\right]_r . \tag{4.43}$$

This will also be relevant when we examine the boundary condition changing operator in section 4.4.2. The integral condition is simpler to study, so we write

$$\left[\int_a^b dt_1 \int_{t_1}^c dt_2\; V(t_1)V(t_2)\right]_G = \int_a^b dt_1 \left[\int_{t_1}^c dt_2\; V(t_1)V(t_2)\right]_G \tag{4.44a}$$

$$= \lim_{\epsilon\to 0}\int_a^b dt_1 \left(\int_{t_1+\epsilon}^c dt_2\; V(t_1)V(t_2) - \frac{1}{\epsilon} - C^L\right) \tag{4.44b}$$

$$= \lim_{\epsilon\to 0}\left(\left(\int_a^{b-\epsilon} dt_1 \int_{t_1+\epsilon}^b dt_2 + \int_a^b dt_1 \int_{b\vee(t_1+\epsilon)}^c dt_2\right) V(t_1)V(t_2) - \frac{b-a}{\epsilon} - (b-a)C^L\right) . \tag{4.44c}$$

But we can also split the integral before renormalizing it, and write

$$\left[\int_a^b dt_1 \int_{t_1}^c dt_2\; V(t_1)V(t_2)\right]_G = \left[\frac{1}{2}V(a,b)^2 + V(a,b)V(b,c)\right]_G \tag{4.44d}$$

$$= \lim_{\epsilon\to 0}\left(\int_a^{b-\epsilon} dt_1 \int_{t_1+\epsilon}^b dt_2 V(t_1)V(t_2) - \frac{b-a}{\epsilon} - \ln\epsilon - C^D_{b-a} + \int_a^b dt_1 \int_{b\vee(t_1+\epsilon)}^c dt_2 V(t_1)V(t_2) + \ln\epsilon - C^E\right) . \tag{4.44e}$$

The singularities and ϵ-regulated operators cancel – as they must for a consistent theory – and we find

$$C^D_{b-a} = -C^E + (b-a)C^L . \tag{4.45}$$

This has the same effect as the replacement condition but with an added constraint on C^L:

$$C^D_\Delta = C_0 + \Delta C_1 \ , \qquad C^E = -C_0 \ , \qquad C^L = C_1 \ . \tag{4.46}$$

Because a similar calculation gives $C^R = C_1$, the strong linearity condition also enforces the extra reflection condition $C^R = C^L$ which is convenient.

While the derivative must give the same condition, we will need the result later, so we derive it here. Consider the expression $\partial_a \left[V(a,b)^2\right]_r$ using the definition of a derivative.

$$\partial_a \left[V(a,b)^2\right]_G = \lim_{\Delta\to 0} \frac{[V(a,b)^2]_G - [V(a-\Delta,b)^2]_G}{\Delta} \tag{4.47a}$$

$$= -\lim_{\Delta\to 0} \frac{[V(a-\Delta,a)^2]_G + 2[V(a-\Delta,a)V(a,b)]_G}{\Delta} \tag{4.47b}$$

We saw in section 4.2.2 that when the renormalized product of two marginal operators is integrated over a small region the result diverges as

$$\lim_{b\to a} \frac{1}{2} \left[V(a,b)^2\right]_G = -1 - C_0 - (b-a)C_1 - \lim_{b\to a} \ln(b-a) \ . \tag{4.48}$$

We have included the C_1 term which vanishes because the overall $\frac{1}{\Delta}$ will allow us to keep it. The next corrections, however, are $O((b-a)^2)$ and can be safely dropped. We will use this result to get

$$\partial_a \left[V(a,b)^2\right]_G = 2 \lim_{\Delta\to 0} \lim_{\epsilon\to 0} \frac{-\left(V(a-\Delta,a)V(a,b)\right)_\epsilon - \ln\epsilon + \ln\Delta + 1 + C_1\Delta}{\Delta} \ . \tag{4.49}$$

Here we make the observation that

$$\begin{aligned}&\left(V(a-\Delta,a)V(a,b)\right)_\epsilon + \ln\epsilon - \ln\Delta - 1 \\ &\quad = \int_0^\epsilon dz \left(\int_{a-z+\epsilon}^b dt\ V(a-z)V(t) - \frac{1}{\epsilon}\right) + \int_\epsilon^\Delta dz \left(\int_a^b dt\ V(a-z)V(t) - \frac{1}{z}\right) \ .\end{aligned} \tag{4.50}$$

The first term is small:

$$\int_0^\epsilon dz \left(\int_{a-z+\epsilon}^b dt\ V(a-z)V(t) - \frac{1}{\epsilon}\right) = \epsilon \left(\int_{a+\epsilon}^b dt\ V(a)V(t) - \frac{1}{\epsilon}\right) + O(\epsilon^2) \ . \tag{4.51}$$

Without the factor of ϵ in front, the $\epsilon \to 0$ limit would give the renormalized operator $[V(a)V(a,b)]_r$, so this quantity must go to zero in that limit despite the $\frac{1}{\epsilon}$ term. Since the ϵ-dependence came from the renormalized operators inside the $\Delta \to 0$ limit, the ϵ limit must be taken first, so this operator vanishes despite the $\frac{1}{\Delta}$ factor appearing in (4.49). The other term is

$$\int_\epsilon^\Delta dz \left(\int_a^b dt\ V(a-z)V(t) - \frac{1}{z}\right) = \int_0^\Delta dz \left(\int_a^b dt\ V(a-z)V(t) - \frac{1}{z}\right) + O(\epsilon) \tag{4.52a}$$

$$= \Delta \lim_{z\to 0} \left(\int_a^b dt\ V(a-z)V(t) - \frac{1}{z}\right) + O(\epsilon) + O(\Delta^2) \tag{4.52b}$$

$$= \Delta \left[V(a)V(a,b)\right]_G + \Delta C^L \ . \tag{4.52c}$$

So by applying (4.50), we get that

$$\partial_a \left[V(a,b)^2\right]_G = -2 \lim_{\Delta\to 0} \left(\frac{1}{\Delta} \left(\Delta \left[V(a)V(a,b)\right]_G + \Delta(C^L - C_1) + O(\Delta^2) \right) \right) \tag{4.53a}$$

$$= -2 \left[V(a)V(a,b)\right]_G + 2\left(C_1 - C^L\right) \ . \tag{4.53b}$$

Of course from (4.47a), if we are to require linearity to the extent that the limit $\Delta \to 0$ commutes with renormalization along with the sum of two terms, then we would have

$$\partial_a \left[V(a,b)^2\right]_r = \left[\lim_{\Delta\to 0} \frac{V(a,b)^2 - V(a-\Delta,b)^2}{\Delta} \right]_r \tag{4.54a}$$

$$= \left[\partial_a V(a,b)^2\right]_r \tag{4.54b}$$

$$= -2 \left[V(a)V(a,b)\right]_r \ . \tag{4.54c}$$

So we once again see that strong linearity requires $C^L = C_1$.

We have found a condition on the counterterms that gives linearity for any operators we have considered so far at quadratic order, but we would still like to prove that the full linearity condition holds for all operators, given the condition $C^L = C_1$. To prove linearity, we can construct a linear operator which acts on the singular operators to produce the renormalized ones. This will be done as the composition of two linear operators: one to produce the counterterms, and the other to properly regulate the integrals with ϵ separations. The two linear operators will not commute with each other, so we must apply the one to produce counterterms first. The operator

$$\begin{aligned} L = &\int dxdy\ \delta(x-y) G^L \frac{\delta}{\delta V(x)} \frac{\delta}{\delta V(y)} \\ &+ \frac{1}{2} \lim_{\Delta\to 0} \int dxdy\ \left(\delta'(x-y+\Delta) - \delta'(x-y-\Delta)\right) G^E \frac{\delta}{\delta V(x)} \frac{\delta}{\delta V(y)} \end{aligned} \tag{4.55}$$

replaces a pair of operators which can collide with the appropriate counterterm. We will refer to the first term as L_1 and the second as L_2. Taking the δ function to be the limit of symmetric peaks at zero so that $\int_0^\infty \delta(x)dx = \frac{1}{2}$, the following are straightforward to show.

$$L_1\left(V(a)V(a,b)\right) = 2\int_a^b dx\ G^L \delta(x-a) = G^L \tag{4.56a}$$

$$L_2\left(V(a)V(a,b)\right) = \int_a^b dx\ G^E \left(\delta'(x-a+\Delta) - \delta'(x-a-\Delta)\right) = 0 \tag{4.56b}$$

$$L_1\left(V(a,b)V(b,c)\right) = 2\int_a^b dx \int_b^c dy\ \delta(x-y) G^L = 0 \tag{4.56c}$$

$$L_2\left(V(a,b)V(b,c)\right) = \int_a^b dx \int_b^c dy \left(\delta'(x-y+\Delta) - \delta'(x-y-\Delta)\right) G^E = G^E \tag{4.56d}$$

$$L_1\left(V(a,b)^2\right) = 2\int_a^b dx\ G^L = 2(b-a)G^L \tag{4.56e}$$

$$L_2\left(V(a,b)^2\right) = \int_a^b dx \int_a^b dy \left(\delta'(x-y+\Delta) - \delta'(x-y-\Delta)\right) G^E = -2G^E \tag{4.56f}$$

From the definitions of the counterterms, we know that $G^D_{ab} = -G^E + (b-a)G^L$, so the operator L correctly produces the counterterms for each operator being considered. In the event that the two operators never meet, the δ functions will ensure that no counterterms are added, and the factorization property (4.5d) will hold. To add in the appropriate counterterms for any operator consisting of two (or less) marginal operators, we apply $1 - L$. This proves that the inclusion of these counterterms is a linear operation.

The full renormalization procedure must ϵ-regulate the operator insertions as well as including the counterterms. We will define this order by order for all orders, so that we can use the notation throughout the rest of this chapter. We apply different linear operators depending on the number of V operators that are inserted. Let $\mathcal{A}$ be the most general operator with n insertions of V, $\mathcal{A} = \int_M V(t_1) \dots V(t_n)$ where M is some measure on $\mathbb{R}^n$. For example, $V(a)V(a,b)^2$ is associated with a uniform measure on $\{a\} \times (a,b) \times (a,b)$ (where $\{a\}$ is a point and (a,b) is an interval). When adding two such operators, we simply add the corresponding measures. The map $\mathcal{A} \to (\mathcal{A})_\epsilon$ acts on the measure $M(\mathcal{A})$ associated with $\mathcal{A}$ by setting it to zero for any point $(t_1, \dots, t_n)$ such that $|t_i - t_j| < \epsilon$ and leaving it unchanged otherwise. Denote this map by U_ϵ so that $U_\epsilon\left(M(\mathcal{A})\right) = M\left((\mathcal{A})_\epsilon\right)$. Since the action of the map U_ϵ on any given point within a measure depends only on the coordinates of that point, we have that $U_\epsilon(M(\mathcal{A}) + M(\tilde{\mathcal{A}})) = U_\epsilon(M(\mathcal{A})) + U_\epsilon(M(\tilde{\mathcal{A}}))$. $\mathcal{A} \to (\mathcal{A})_\epsilon$ is a linear map for any operator, which together with the existence of the linear operator L shows that renormalization defined by

$$[\mathcal{A}]_r = \left((1-L)\mathcal{A}\right)_\epsilon \tag{4.57}$$

is a linear map.

Now let us consider the operator $\left[V(a,b)^2\right]_G$ again. We already know from the definition that this is $\left(V(a,b)^2\right)_\epsilon - 2G^D_{ab}$, but we can also write it as

$$\left[V(a,b)^2\right]_G = \left[\int_a^b dt \left(\int_a^t ds + \int_t^b ds\right) V(t)V(s)\right]_G . \tag{4.58a}$$

If we are to assume full linearity then we get

$$= \int_a^b dt \left([V(a,t)V(t)]_G + [V(t)V(t,b)]_G\right) \tag{4.58b}$$

$$= \lim_{\epsilon\to 0} \int_a^b dt \left(\left(V(a,t)V(t)\right)_\epsilon + \left(V(t)V(t,b)\right)_\epsilon - G^R - G^L\right) \tag{4.58c}$$

$$= \lim_{\epsilon\to 0} \left[\left(V(a,b)^2\right)_\epsilon - (b-a)\left(G^R + G^L\right)\right] . \tag{4.58d}$$

This has only produced part of the necessary counterterm, as $\ln\epsilon$ and C_0 are both absent from $G^{L/R}$. This suggests that a fully linear renormalization scheme is impossible, but the existence of the linear operators L and U_ϵ tells us otherwise. The answer is that when L acts on the

operators there is an extra term.

$$L\,V(t)V(t,b) = \int_t^b dx\ \left(2G^L\delta(x-t) + \lim_{\Delta\to 0^+} G^E\left(\delta'(x-t+\Delta) - \delta'(x-t-\Delta)\right)\right) V(t)V(t,b) \tag{4.59a}$$

$$= \left(G^L + G^E \lim_{\Delta\to 0^+} \left(\delta(b-t+\Delta) - \delta(b-t-\Delta)\right)\right) V(t)V(t,b) \tag{4.59b}$$

$$= \left(G^L - G^E \lim_{\Delta\to 0^+} \delta(b-t-\Delta)\right) V(t)V(t,b) \tag{4.59c}$$

The last term vanishes when t is fixed (as in $V(a)V(a,b)$), but not when t is allowed to approach b continuously. Infinite sums and infinitesimal regions are some of the differences between the replacement condition and the stronger linearity we have been discussing, and this is an example of that. To get a fully linear renormalization scheme the left counterterm should really be

$$G^L_{ab} = \frac{1}{\epsilon} + C_1 + (\ln\epsilon + C_0) \lim_{\Delta\to 0^+} \delta(b-a-\Delta)\ . \tag{4.60}$$

4.2.4 Assumptions (4.5d), (4.5e), and (4.5f)

We did not discuss the factorization condition (4.5d) in much detail in the last section, but we did effectively prove that it holds for the renormalization scheme discussed. The δ functions appearing in every term of the operator L in (4.55) mean that there are no counterterms for operators which do not meet at a point.

The assumption (4.5e) is trivial in our construction, since at no point in the renormalization of the integrated operators have we considered the wedge state on which they are embedded. By constructing the counterterms using the local OPE rather than the two-point functions, we have avoided any difficulties that this assumption may have caused.

For the sixth assumption we will ask ourselves the same question we asked about linearity: what does this condition really mean and what do we really require? The construction of the simple solution (4.12) does not require a reflection condition at all. It is only when we wish to impose the reality condition that we need the renormalized operators to preserve the bare operators' twist symmetry in a particular way. Looking at page 29 of [36], we see that the precise condition required is

$$U^\ddagger = U, \qquad A_L^\ddagger = A_R, \qquad A_R^\ddagger = A_L\ . \tag{4.61}$$

As before, the operator ‡ represents the composition of inverse bpz conjugation and hermitian conjugation, which has the effect of reversing the orientation of all operators inserted in the worldsheet.

For the string field U this is quite simple, as only the fully integrated operator $[V(a,b)^n]_r$ appears. By the definition, (4.33), the counterterms are constant in terms of the integration variables. We must also consider the region of integration used for $(V(a,b)^n)_\epsilon$, to ensure that it is invariant under the reflection. This amounts to the understanding that we can parameterize the region in a number of equivalent ways. For example,

$$\int_a^{b-(n-1)\epsilon} dt_1 \ldots \int_{t_{n-1}+\epsilon}^b dt_n \prod_{i=1}^n V(t_i) = \int_{a+(n-1)\epsilon}^b dt_n \ldots \int_a^{t_2-\epsilon} dt_1 \prod_{i=1}^n V(t_i)\ . \tag{4.62}$$

The two regions are identical, as are many other similar parameterizations. If we perform the change of variables $t_i \to a + b - t_{n-i+1}$ on the right hand side we get

$$\int_a^{b-(n-1)\epsilon} dt_1 \dots \int_{t_{n-1}+\epsilon}^{b} dt_n \prod_{i=1}^{n} V(a+b-t_i) \ , \tag{4.63}$$

which is precisely the effect of (4.5f) acting on the original integrated operator. In the last step we changed the order in which the operators are written in order to make our equation look like that of (4.5f), but since thy are bosonic operators we are free to do so. That the counterterms are also invariant under taking $t_i \to a+b-t_i$ and then being rearranged is trivial since they are not functions of the coordinates t_i at all. The reparameterization of the integrals in (4.62) was the important step, but it is an identity for the subsets of $\mathbb{R}^n$ in question, and would actually hold for any integrand.

When we consider the other condition, $A_L^\ddagger = A_R$, we must now consider what happens when fixed operators are inserted at the endpoints. With the argument that U is symmetric in mind, the only thing left to show is that the operators inserted at the endpoints, $O_{L/R}$ are mapped to each other by twist. This is guaranteed by the BRST operator having the property

$$(Q_B U)^\ddagger = -(-1)^U Q_B U^\ddagger \ , \tag{4.64}$$

which since U is even means that $A_R - A_L$ is odd under this conjugation. Now

$$A_L^\ddagger - A_R^\ddagger = A_R - A_L \tag{4.65a}$$

naturally leads us to the conclusion

$$A_L^\ddagger = A_R \ , \quad A_R^\ddagger = A_L \ . \tag{4.65b}$$

This can also be viewed as a statement about the transformation property of $O_{L/R}$, but that approach would require consideration of each term separately.

4.2.5 Assumptions (4.5a) and (4.5b)

These two assumptions are easily proven at second order in λ. Here we will review the proof of each at the lowest nontrivial order and discuss problems which can occur at higher orders as they arise. We will also see what happens when we attempt an alternate form of the proof, and resolve the apparent inconsistencies that arise. Throughout this section we will omit writing the limit $\epsilon \to 0$, and it should be inferred.

Recall that the first assumption is

$$Q_B \left[e^{\lambda V(a,b)} \right]_r = \left[e^{\lambda V(a,b)} O_R(b) \right]_r - \left[O_L(a) e^{\lambda V(a,b)} \right]_r \ . \tag{4.5a}$$

At second order this statement reads as

$$\frac{1}{2} Q_B \left[V(a,b)^2 \right]_G = \sum_{n=0}^{2} \frac{1}{(2-n)!} \left(\left[V(a,b)^{2-n} O_R^{(n)}(b) \right]_G - \left[O_L^{(n)}(a) V(a,b)^{(2-n)} \right]_G \right) \tag{4.66}$$

where $O_{L/R} = \sum_n \lambda^n O^{(n)}_{L/R}$ is a local operator to be determined. Since the counterterm is not an operator, it vanishes when acted on by Q_B. The behaviour of the primitive operators when acted on by the BRST charge is not difficult to determine by integrating the BRST current on a contour about the operator in question. The results we will need are

$$\begin{aligned} Q_B V(t) &= \partial_t(cV(t)) \ , \qquad Q_B(cV(t)) = 0 \ , \\ Q_B c(t) &= c\partial c(t) \ , \qquad Q_B \partial c(t) = c\partial^2 c(t) \ . \end{aligned} \tag{4.67}$$

Using the first of these and the definition of the renormalization scheme, we can start working out the left hand side of (4.66) explicitly.

$$\frac{1}{2} Q_B \left[V(a,b)^2\right]_G = \frac{1}{2} Q_B \left(V(a,b)^2\right)_\epsilon \tag{4.68a}$$

$$= Q_B \int_a^{b-\epsilon} dt_1 \int_{t_1+\epsilon}^{b} dt_2 V(t_1)V(t_2) \tag{4.68b}$$

$$= \int_a^{b-\epsilon} dt_1 \int_{t_1+\epsilon}^{b} dt_2 \left(\partial_{t_1} cV(t_1)V(t_2) + V(t_1)\partial_{t_2} cV(t_2)\right) \tag{4.68c}$$

The next step is to integrate by parts:

$$\frac{1}{2} Q_B \left[V(a,b)^2\right]_G = \int_a^{b-\epsilon} dt \ V(t)\left(cV(b) - cV(t+\epsilon)\right) + \int_{a+\epsilon}^{b} dt \left(cV(t-\epsilon) - cV(a)\right) V(t) \tag{4.69a}$$

$$= V(a,b-\epsilon)cV(b) - cV(a)V(a+\epsilon,b) + \int_{a+\epsilon}^{b} dt \left(cV(t-\epsilon)V(t) - V(t-\epsilon)cV(t)\right) \tag{4.69b}$$

$$= V(a,b-\epsilon)cV(b) - cV(a)V(a+\epsilon,b) + \int_{a+\epsilon}^{b} dt \ V(t-\epsilon)V(t)\left(c(t-\epsilon) - c(t)\right) \ . \tag{4.69c}$$

In the remaining integral we notice that the ghost factor is $O(\epsilon)$ and will suppress an finite contributions from the matter part. Now when we rewrite the matter factor using the OPE, we only need to keep the relatively simple divergent term.

$$\int_{a+\epsilon}^{b} dt \ V(t-\epsilon)V(t)\left(c(t-\epsilon) - c(t)\right) = \int_{a+\epsilon}^{b} dt \ \frac{1}{\epsilon^2}\left(-\epsilon\partial c(t) + \frac{\epsilon^2}{2}\partial^2 c(t)\right) \tag{4.70a}$$

$$= -\frac{1}{\epsilon}\left(c(b) - c(a+\epsilon)\right) + \frac{1}{2}\left(\partial c(b) - \partial c(a)\right) \tag{4.70b}$$

$$= -\frac{1}{\epsilon}\left(c(b) - c(a)\right) + \frac{\epsilon\partial c(a)}{\epsilon} + \frac{1}{2}\left(\partial c(b) - \partial c(a)\right) \tag{4.70c}$$

$$\frac{1}{2} Q_B \left[V(a,b)^2\right]_G = V(a,b-\epsilon)cV(b) - \frac{c(b)}{\epsilon} + \frac{1}{2}\partial c(b) - cV(a)V(a+\epsilon,b) + \frac{c(a)}{\epsilon} + \frac{1}{2}\partial c(a) \tag{4.71a}$$

$$= \left[V(a,b)cV(b)\right]_G + C^R c(b) + \frac{1}{2}\partial c(b) - \left[cV(a)V(a,b)\right]_G - C^L c(a) + \frac{1}{2}\partial c(a) \tag{4.71b}$$

This has the form of (4.66) where

$$O_R(b) = \lambda cV(b) + \frac{\lambda^2}{2}\partial c(b) + \lambda^2 C^R c(b) \ , \quad O_L(a) = \lambda cV(a) - \frac{\lambda^2}{2}\partial c(a) + \lambda^2 C^L c(a) \ . \quad (4.72)$$

The operators $O_{L/R}$ have an explicit dependence on $C^{L/R}$, but this only serves to cancel the dependence of the renormalization scheme so that the full operators $\left[e^{\lambda V(a,b)} O_R(b)\right]_G$ and $\left[O_L(a) e^{\lambda V(a,b)}\right]_G$ are independent of $C^{L/R}$. This has to be the case because in the left hand side of (4.5a) neither of Q_B or $\left[e^{\lambda V(a,b)}\right]_G$ has or introduces any dependence on those parameters. It is because of this cancellation that the reflection condition (4.5f) does not impose any restrictions on $C^{L/R}$.

There is another approach which looks very simple but has a subtle difficulty. This approach involves a less well-regulated expression which produces a part of the correct result without any counterterms or higher order pieces of $O_{L/R}$. To demonstrate, we will again consider the second order calculation. We proceed as before to

$$\frac{1}{2} Q_B \left[V(a,b)^2\right]_G = \int_a^b dt \left(V(a, t-\epsilon)\partial(cV(t)) + \partial(cV(t))V(t+\epsilon, b)\right) \quad (4.73a)$$

$$= \int_a^b dt \left(V(a,b)\partial(cV(t))\right)_\epsilon \ . \quad (4.73b)$$

Now the ϵ-bracket is a linear operator so we would normally expect it to commute with the integral, and we would get

$$\frac{1}{2} Q_B \left[V(a,b)^2\right]_G = \left(V(a,b) \int_a^b dt \ \partial(cV(t))\right)_\epsilon \quad (4.73c)$$

$$= \left(V(a,b)(cV(b) - cV(a))\right)_\epsilon \ . \quad (4.73d)$$

This has the correct first term, but no counterterms or ∂c terms. Where has this approach failed? While the linearity of the ϵ-bracket implies that we should be able to bring the integral over t inside, in practice this does not work. We have assumed that by thinking of the integral as the limit of Riemann sums, the linearity of the ϵ-bracket justifies bringing the integral inside, but this is not always the case. An integral such as $\int \frac{dt}{t^3}$ is not finite itself and integrating by parts ignores the singularity by using a principal value prescription in order to avoid getting an undefined result. More accurately, this means introducing a small regulator to protect the singularity. When the ϵ-bracket is taken first, there is no singularity in the integrand because ϵ serves the role of regulator. When the integral is performed first, we must have two regulators, and the direction of the limit in this two-dimensional plane has changed. It is this direction of the limit which prevents principal value integrals from commuting with the ϵ-bracket.

Taking the form of $O_{L/R}$ found from the calculation above, the final assumption to prove at quadratic order, (4.5b), is

$$Q_B \left([cV(a)V(a,b)]_G - \frac{1}{2}\partial c(a) + C^L c(a) \right) = -cV(a)cV(b) \ . \quad (4.74)$$

This is relatively straightforward to show. We begin by expanding the left hand side, and then

apply (4.67).

$$\begin{aligned} Q_B &\left([cV(a)V(a,b)]_G - \frac{1}{2}\partial c(a) + C^L c(a) \right) \\ &= Q_B \left(cV(a) \int_{a+\epsilon}^{b} dt V(t) - c(a) G^L_{ab} - \frac{1}{2}\partial c(a) + C^L c(a) \right) \\ &= -cV(a)\left(cV(b) - cV(a+\epsilon)\right) - \frac{c\partial c(a)}{\epsilon} - C^L c\partial c(a) - \frac{1}{2} c\partial^2 c(a) + C^L c\partial c(a) \end{aligned} \tag{4.75}$$

As we did for the first BRST condition, we write $V(a)V(a+\epsilon) = \frac{1}{\epsilon^2} + O(\epsilon^0)$ and we now also write $c(a)c(a+\epsilon) = \epsilon c\partial c(a) + \frac{1}{2}\epsilon^2 c\partial^2 c$. Several terms cancel and we end up with

$$Q_B \left([cV(a)V(a,b)]_G - \frac{1}{2}\partial c(a) + C^L c(a) \right) = -cV(a)cV(b) \tag{4.76}$$

Thus, the second BRST condition is satisfied at this order.

4.3 Renormalizing Higher Order Operators

When only two operators needed to be renormalized, the big G and little g schemes provided identical results. At higher orders, however, the two approaches naturally extend in different ways. We will carefully examine and compare these two schemes at third and fourth order, and find that the big G scheme is incorrect at higher orders. Focusing on the little g scheme, we will prove that it satisfies all of the assumptions (4.5) at any order. This proceeds similarly to [36], but I will include all of the technical details necessary for more rigorous proofs.

While we do not know whether the BRST conditions can be proven for other renormalization schemes, it seems likely that there is still some freedom to choose differing schemes. We will briefly consider this question beginning with full linearity as a starting point. Considering linearity first gives a relatively straightforward path to writing down a general renormalization scheme order by order which is compatible with all of the assumptions except for the BRST conditions. Those two assumptions, however, look extremely difficult with this approach, so we will not pursue it any farther here.

4.3.1 Third Order Operators

Before we plunge into a computation at all orders, we will consider an extension of the big G scheme to third order, i.e. the renormalization of a product of three Vs.

At this order, we define a regularized operator involving a single cubic integrated operator by following the same regularization pattern as we did for the quadratic operator:

$$\left[V(a,b)^3\right]_G = \lim_{\epsilon\to 0} \left[\left(V(a,b)^3\right)_\epsilon - 6 G^{(3),D}_{ab} V(a,b) \right] , \tag{4.77}$$

where

$$G^{(3),D}_{ab} = \frac{b-a}{\epsilon} + \ln\epsilon + C^{(3),D}_{b,a} . \tag{4.78}$$

The extra superscript $^{(3)}$ indicates that these are the counterterms at third order. We also define a regularized operator involving two integrated operators:

$$\big[V(a,b)^2V(b,c)\big]_G = \lim_{\epsilon\to 0}\Big[\big(V(a,b)^2V(b,c)\big)_\epsilon - 2G^{(3),DE}_{abc}V(b,c) - 2G^{(3),E}_{abc}V(a,b)\Big] \ , \tag{4.79}$$

and three operators:

$$[V(a,b)V(b,c)V(c,d)]_G = \lim_{\epsilon\to 0}\Big[(V(a,b)V(b,c)V(c,d))_\epsilon - G^{(3),EE}_{abcd}V(a,b) - G^{(3),EE}_{abcd}V(c,d)\Big] \ , \tag{4.80}$$

where

$$G^{(3),E}_{abc} = -\ln\epsilon + C^{(3),E}_{abc} \ , \tag{4.81a}$$

$$G^{(3),DE}_{abc} = \frac{b-a}{\epsilon} + \ln\epsilon + C^{(3),DE}_{abc} \ , \tag{4.81b}$$

$$G^{(3),EE}_{abcd} = -\ln\epsilon + C^{(3),EE}_{abcd} \ . \tag{4.81c}$$

Notice that we have four new and potentially different finite constants. Using translation invariance together with the factorization and replacement conditions in a way similar to that presented in the quadratic case, we can show that

$$C^{(3),E}_{abc} = -C_0 \tag{4.82a}$$

$$C^{(3),EE}_{abce} = -C_0 \tag{4.82b}$$

$$C^{(3),D}_{ab} = (b-a)C_1 + C^{(3)}_0 \tag{4.82c}$$

$$C^{(3),DE}_{abc} = (b-a)C_1 + C_0 \ , \tag{4.82d}$$

where the constants C_0 and C_1 are necessarily the same as the ones used at quadratic order but $C^{(3)}_0$ is a new independent constant. One can check, by examining all combinations, that the replacement condition at third order is satisfied for any value of this constant.

We also need to define renormalized operators involving fixed insertions at the endpoints. Using factorization and replacement conditions, these can be constrained to

$$[V(a)V(a,b)^2]_G = \lim_{\epsilon\to 0}\Big[(V(a)V(a,b)^2)_\epsilon - 2V(a)G^{(3),DL}_{ab} - 2V(a,b)G^{(3),L}_{ab}\Big] \tag{4.83a}$$

$$[V(a)V(a,b)V(b)]_G = \lim_{\epsilon\to 0}\Big[(V(a)V(a,b)V(b))_\epsilon - V(a)G^{(3),RL}_{ab} - V(b)G^{(3),LR}_{ab}\Big] \tag{4.83b}$$

$$[V(a)V(a,b)V(b,c)]_G = \lim_{\epsilon\to 0}\Big[(V(a)V(a,b)V(b,c))_\epsilon - V(a)G^{(3),EL}_{abc} - V(b,c)G^{(3),LE}_{abc}\Big] \ , \tag{4.83c}$$

where

$$G^{(3),DL}_{ab} = \frac{b-a}{\epsilon} + \ln\epsilon + C^{(3),DL}_0 + (b-a)C_1 \ , \tag{4.84a}$$

$$G^{(3),L}_{ab} = \frac{1}{\epsilon} + C^L \ , \tag{4.84b}$$

$$G^{(3),RL}_{ab} = \frac{1}{\epsilon} + C^R \ , \tag{4.84c}$$

$$G^{(3),LR}_{ab} = \frac{1}{\epsilon} + C^L \ , \tag{4.84d}$$

$$G^{(3),EL}_{abc} = -\ln\epsilon - C_0 \ , \tag{4.84e}$$

$$G^{(3),LE}_{abc} = \frac{1}{\epsilon} + C^L \ . \tag{4.84f}$$

There are two new constants: $C_0^{(3),DL}$ and its partner, $C_0^{(3),DR}$, along with $C_0^{(3)}$ from (4.82). Just like C^L and C^R, however, the constants $C_0^{(3),DL}$ and $C_0^{(3),DR}$ cannot change the SFT solution and can only affect the form of the BRST insertions O_L and O_R. Only $C_0^{(3)}$ and the quadratic order constants C_0 and C_1 have a physical effect on the solution.

It is clear that if we were to continue our order-by-order approach to renormalization, we would find new free parameters. However, at quartic and higher orders, this approach in unwieldy: it is hard to write down the most general renormalized operator that is demonstratively finite. To study renormalization to all orders, we will no longer try to study the space of all renormalizations and instead focus on a particular renormalization scheme. The scheme we chose will have C_0 and C_1 as free parameters, however we will not add new constants at every order. We will return to the question of classifying all renormalization schemes in sections 4.3.8 and 4.4.1.

4.3.2 Extension to All Orders

The big G scheme with strong linearity was defined in (4.57), and we would naturally want to extend this by exponentiating it. We would define the scheme by

$$[A]_G \stackrel{\text{def}}{=} \lim_{\epsilon\to 0} \left(e^{-L}A\right)_\epsilon \ . \tag{4.85}$$

The simplest exponentiation using the same L as in (4.55) would correspond at third order to $C_0^{(3)} = C_0^{(3),DL} = C_0^{(3),DR} = C_0$ and $C^L = C^R = C_1$ as before. In practice this would mean

$$[V(a,b)^n]_G = \lim_{\epsilon\to 0} \sum_{k=0}^{\lfloor n/2\rfloor} \frac{(-1)^k n!}{k!(n-2k)!} \left(G^D_{ab}\right)^k \left(V(a,b)^{n-2k}\right)_\epsilon \ . \tag{4.86}$$

The little g scheme, on the other hand, does not have as simple an exponential form, but the idea is the same. Since we were not focused on the little g scheme at quadratic order, we should

restate the exact form of the counterterms we use:

$$g^D_{ab}(t_1,t_2) = \frac{1}{(t_1-t_2)^2} + \frac{2}{(b-a)^2}\left(1+\ln(b-a)+C_0+(b-a)C_1\right) \ , \tag{4.87a}$$

$$g^L_{ab}(t_1,t_2) = \frac{1}{(t_1-t_2)^2} + \frac{1}{(b-a)^2} + \frac{C^L}{b-a} \ , \tag{4.87b}$$

$$g^E_{abc}(t_1,t_2) = \frac{1}{(t_1-t_2)^2} - \frac{1}{(c-b)(b-a)}\left(1+\ln\left(\frac{(c-b)(b-a)}{c-a}\right)+C_0\right) \ . \tag{4.87c}$$

We require that for every pair of marginal operators which can meet, we subtract off a counterterm defined with the appropriate range. For example,

$$[(V(a,b))^n]_g = \lim_{\epsilon\to 0}\int_{\Gamma^{a,b}_\epsilon} d^n t \sum_{\sigma\in S_n}\sum_{k=0}^{\lfloor n/2\rfloor}\frac{(-1)^k}{2^k k!(n-2k)!}\prod_{i=1}^{k} g^D_{ab}(t_{\sigma(i)},t_{\sigma(i+k)})\prod_{j=2k+1}^{n} V(t_{\sigma(j)}) \ . \tag{4.88}$$

We define $\Gamma^{a,b}_\epsilon(t_1,\ldots,t_n)$ to be the region $(a,b)^n$ minus the places where any two coordinates are within ϵ of each other. This is the same region used in the definition of $(V(a,b)^n)_\epsilon$ but now the counterterms are included in the integral. We will often suppress the coordinate list of Γ^{ab}_ϵ when it is unambiguously implied by the coordinates being integrated over. From this form of $[V(a,b)^n]_g$ there are two directions we can go. Since the region we integrate over is symmetric we can remove the sum over the symmetric group to get the slightly more compact form

$$[(V(a,b))^n]_g = \lim_{\epsilon\to 0}\int_{\Gamma^{a,b}_\epsilon} d^n t \sum_{0\le k\le \frac{n}{2}}\frac{(-1)^k n!}{2^k k!(n-2k)!}\prod_{i=1}^{k} g^D_{ab}(t_i,t_{i+k})\prod_{j=2k+1}^{n} V(t_j) \ . \tag{4.89}$$

An alternative viewpoint is to write the integrand of (4.88) as a "normal ordered" operator which subtracts a counterterm for every pair of operators:

$$\overset{\circ}{\underset{\circ}{\prod_i}} V(t_i) \overset{\circ}{\underset{\circ g}{}} \overset{\text{def}}{=} \exp\left(-\frac{1}{2}\int ds_1 ds_2\, g(s_1,s_2)\frac{\delta}{\delta V(s_1)}\frac{\delta}{\delta V(s_2)}\right)\prod_i V(t_i) \tag{4.90}$$

The subscript g on the normal ordering is our notation to indicate what counterterms to subtract. When we normal order more complicated products including things like fixed marginal operators at an endpoint, the normal ordering $\overset{\circ}{\underset{\circ}{\ldots}}\overset{\circ}{\underset{\circ g}{}}$ should be interpreted as meaning to subtract whichever g counterterm, g^D, $g^{L/R}$, or g^E is appropriate to the region the operators will eventually be integrated over. So, for example, in the context of

$$[V(a)V(a,b)^2]_g = \int_a^b dt_1 dt_2 \overset{\circ}{\underset{\circ}{}} V(a)V(t_1)V(t_2)\overset{\circ}{\underset{\circ g}{}} \ , \tag{4.91a}$$

our notation $\overset{\circ}{\underset{\circ}{}}\ \overset{\circ}{\underset{\circ g}{}}$ indicates

$$\overset{\circ}{\underset{\circ}{}} V(a)V(t_1)V(t_2)\overset{\circ}{\underset{\circ g}{}} = V(a)V(t_1)V(t_2) - V(a)g^D_{ab}(t_1,t_2) - g^L_{ab}(t_1)V(t_2) - g^L_{ab}(t_2)V(t_1) \ . \tag{4.91b}$$

It is useful to notice that all of the little g counterterms have the same divergent part, $\frac{1}{(t_1-t_2)^2}$. This is the same function used in the finiteness condition (4.14), so we can represent the little g normal ordering as

$$\overset{\circ}{\underset{\circ}{\prod}} V(t_i) \overset{\circ}{\underset{\circ g}{}} = \overset{\circ}{\underset{\circ}{}} \exp\left(\int dr_1 dr_2 \,(\text{finite terms}) \frac{\delta}{\delta V(r_1)} \frac{\delta}{\delta V(r_1)}\right) \prod_i V(t_i) \overset{\circ}{\underset{\circ \frac{1}{(s_1-s_2)^2}}{}} \tag{4.92}$$

which is clearly still finite as long as (4.14) holds. This demonstrates how using one counterterm or another, or even different counterterms within a single normal ordered operator as is the case when both g^D and g^L are needed, will always result in a finite operator as long as all of the counterterms have the same singular term $\frac{1}{(s_1-s_2)^2}$. Since the normal ordering gives finite operators for any choice of coordinates, we can now remove the holes in the integral and write (4.88) as

$$[V(a,b)^n]_g = \int_a^b d^n t \overset{\circ}{\underset{\circ}{\prod_{i=1}^n}} V(t_i) \overset{\circ}{\underset{\circ g}{}} \,. \tag{4.93}$$

It is possible to write the renormalization scheme in an exponential form as well:

$$\left[e^{\lambda V(a,b)}\right]_g = \sum_{n=0}^{\infty} \frac{\lambda^n}{n!} \int_a^b d^n t \overset{\circ}{\underset{\circ}{\prod_{i=1}^n}} V(t_i) \overset{\circ}{\underset{\circ g}{}} \tag{4.94a}$$

$$= \sum_{n=0}^{\infty} \int_a^b d^n t \overset{\circ}{\underset{\circ}{}} e^{\lambda V} \overset{\circ}{\underset{\circ g}{}} \,. \tag{4.94b}$$

The notation in the second line is similar to that commonly used, for example, for the Chern-Simons action on a D-brane: under an n-dimensional integral, we include all the terms from the Taylor expansion of the integrand that have the right number of variables to saturate the integral. It is easy to see that this is the same definition as that in equation (4.88).

As long as the integrand is fully normal ordered, the limit $\epsilon \to 0$ can be used to simplify the integration region to $(a,b)^n$ and the little g scheme seems to exponentiate quite cleanly. Once we start separating terms and examining the structure in detail, however, the regulated region $\Gamma_\epsilon^{a,b}(t_1,\ldots,t_n)$ is highly nontrivial instead of being the product of lower dimensional regions. One drawback of this is that linearity is not so clear for this scheme. By subtracting off counterterms which depend on the region of integration in a non-trivial way, and specifying that we only subtract off counterterms if the operators can meet, we make it unfeasible to write down a linear operator like L for this scheme. We might ask whether the two schemes are still identical, as they were at quadratic order, but it can be shown that they are not. The critical difference between the big G and little g schemes is illustrated by considering

$$(2G_{ab}^D)^k \int_{\Gamma_\epsilon^{a,b}} dt_1 \ldots dt_i \prod_{j=1}^i V(t_j) \tag{4.95a}$$

$$= \int_{\Gamma_\epsilon^{a,b}(t_1,\ldots,t_i)\times\Gamma_\epsilon^{a,b}(s_1,s_2)\times\ldots\times\Gamma_\epsilon^{a,b}(s_{2k-1},s_{2k})} dt_1 \ldots dt_i \, ds_1 \ldots ds_{2k} \prod_{j=1}^i V(t_j) \prod_{j=1}^k g_{ab}^D(s_{2j-1},s_{2j}) \tag{4.95b}$$

$$\neq \int_{\Gamma_\epsilon^{a,b}} dt_1 \dots dt_i \, ds_1 \dots ds_{2k} \prod_{j=1}^{i} V(t_j) \prod_{j=1}^{k} g_{ab}^D(s_{2j-1}, s_{2j}) \ . \tag{4.95c}$$

If $n = 2k + i$ then the first line is a term in $[V(a,b)^n]_G$ and the third line is the corresponding term in $[V(a,b)^n]_g$. We might try to argue that since the integrand has no singularity where one of the s_j approaches a t_j or an s_j belonging to another counterterm, the difference vanishes as $\epsilon \to 0$ and the difference between the integration regions shrinks. The flaw in this reasoning is that when, for example, s_1 is within 2ϵ of some t, then the integrand does become large for $|s_2 - t| < \epsilon$, which is one of the small regions of difference between the two integrals. As a concrete example, it can be shown that for any finite function f,

$$\lim_{\epsilon\to 0} \left(\int_a^b dt \int_{\Gamma_\epsilon^{a,b}} ds_1 ds_2 - \int_{\Gamma_\epsilon^{a,b}} dt \, ds_1 ds_2 \right) f(t) g(s_1, s_2) = (6 + 2\ln 2) \int_a^b dt \ f(t) \ . \tag{4.96}$$

This leads to a more severe issue. By comparing the big G and little g schemes at fourth order, we can show that they are not both finite. From the form (4.89) we know that

$$\frac{1}{24} \left[V(a,b)^4\right]_g = \lim_{\epsilon\to 0} \int_{\Gamma_\epsilon^{ab}} d^4t \left(\frac{1}{24} \prod_{i=1}^{4} V(t_i) - \frac{1}{4} V(t_1)V(t_2) g_{ab}^D(t_3,t_4) + \frac{1}{8} g_{ab}^D(t_1,t_2) g_{ab}^D(t_3,t_4) \right) \ . \tag{4.97a}$$

For the last two terms we can add and subtract the same thing integrated over the factorized regions used by the big G scheme:

$$\begin{aligned} = \lim_{\epsilon\to 0} \Bigg[& \frac{1}{24} \left(V(a,b)^4\right)_\epsilon - \frac{1}{2} G_{ab}^D \left(V(a,b)^2\right)_\epsilon + \frac{1}{2} \left(G_{ab}^D\right)^2 \\ & + \frac{1}{4} \left(\int_{\Gamma_\epsilon^{ab}} d^2t \int_{\Gamma_\epsilon^{ab}} d^2s - \int_{\Gamma_\epsilon^{ab}} d^2t \, d^2s \right) V(t_1)V(t_2) g_{ab}^D(s_1,s_2) \\ & - \frac{1}{8} \left(\int_{\Gamma_\epsilon^{ab}} d^2t \int_{\Gamma_\epsilon^{ab}} d^2s - \int_{\Gamma_\epsilon^{ab}} d^2t \, d^2s \right) g_{ab}^D(t_1,t_2) g_{ab}^D(s_1,s_2) \Bigg] \end{aligned} \tag{4.97b}$$

$$\begin{aligned} = & \frac{1}{24} \left[V(a,b)^4\right]_G \\ & + \frac{1}{4} \lim_{\epsilon\to 0} \left(\int_{\Gamma_\epsilon^{ab}} d^2t \int_{\Gamma_\epsilon^{ab}} d^2s - \int_{\Gamma_\epsilon^{ab}} d^2t \, d^2s \right) \left(V(t_1)V(t_2) - g_{ab}^D(t_1,t_2) \right) g_{ab}^D(s_1,s_2) \\ & + \frac{1}{8} \lim_{\epsilon\to 0} \left(\int_{\Gamma_\epsilon^{ab}} d^2t \int_{\Gamma_\epsilon^{ab}} d^2s - \int_{\Gamma_\epsilon^{ab}} d^2t \, d^2s \right) g_{ab}^D(t_1,t_2) g_{ab}^D(s_1,s_2) \ . \end{aligned} \tag{4.97c}$$

We know that the two schemes are not the same beyond second order, so the appearance of terms representing the difference is expected. The term with the integral of $(V(t_1)V(t_2) - g_{ab}^D(t_1,t_2)) g_{ab}^D(s_1,s_2)$ is the equivalent of (4.96) at fourth order. It is the integral over a small region of a divergent quantity giving a finite result, times the integral of the finite function

$V(t_1)V(t_2) - g^D_{ab}(t_1, t_2)$. The last term, however, integrates two divergent quantities over this region, and is itself infinite.

$$\left(\int_{\Gamma^{ab}_\epsilon} d^2t \int_{\Gamma^{ab}_\epsilon} d^2s - \int_{\Gamma^{ab}_\epsilon} d^2t d^2s\right) g^D_{ab}(t_1, t_2) g^D_{ab}(s_1, s_2) = 4\left(\frac{4}{3} + 4\ln 2 + \frac{5}{3}\ln 3\right)\frac{(b-a)}{\epsilon} + O(\ln\epsilon) \tag{4.98}$$

This proves that the two schemes are not only different, but cannot both be finite at fourth order. We have already shown that the little g scheme is finite by demonstrating that the integrand is finite. This confirms that the big G scheme must not properly renormalize all operators, so the trivial exponentiation of the quadratic renormalization scheme is not correct.

To see exactly where the big G scheme has failed, consider the operator $V(a,b)^n$. Each term with k counterterms in the corresponding renormalized operator $[V(a,b)^n]_G$ represents the collision of $2k$ marginal operators, and subtracts k powers of the divergence for two colliding operators. If each pair of operators which are colliding were integrated over the full range $(a,b)^2$ the counterterm would be correct, but the small differences due to avoiding the other operators will give rise to subleading divergences. For $k = 1$ the worst divergence is $O(\epsilon^{-1})$ so the subleading terms are finite, but for $k \geq 2$ these subleading divergences need to be cancelled. This is what the big G scheme fails to do. By integrating counterterms over the same regions as the colliding operators, the little g scheme naturally produces the correct subleading divergences at each k without having to explicitly write them down, or even know what they are.

4.3.3 Alternative Little g Schemes

Now we will consider a renormalization scheme with a different counterterm, $\tilde{g}^D_{ab}(t_1, t_2) = g^D_{ab}(t_1, t_2) + \Delta_{ab}(t_1, t_2)$. The difference Δ_{ab} is assumed to be a finite function of t_1 and t_2. If the divergent parts of g and $\tilde{g}$ do not agree then $\tilde{g}$ will not properly renormalize simple quadratic operators unless the extra divergences in $\tilde{g}$ integrate to a finite contribution, but we will not consider this case.

The new renormalized operator is

$$\frac{[V(a,b)^n]_{\tilde{g}}}{n!} \stackrel{\text{def}}{=} \int_a^b d^nt \sum_{\sigma\in S_n} \sum_{0\leq k\leq \frac{n}{2}} \frac{(-1)^k}{2^k k!(n-2k)!} \prod_{i=1}^{k} \tilde{g}^D_{ab}(t_{\sigma(2i-1)}, t_{\sigma(2i)}) \prod_{j=2k+1}^{n} V(t_{\sigma(j)}) \tag{4.99a}$$

$$\begin{aligned} &= \int_a^b d^nt \sum_{\sigma\in S_n} \sum_{0\leq k\leq \frac{n}{2}} \frac{(-1)^k}{2^k k!(n-2k)!} \\ &\quad \times \sum_{m=0}^{k} \binom{k}{m} \prod_{l=1}^{m} \Delta^D_{ab}(t_{\sigma(2l-1)}, t_{\sigma(2l)}) \prod_{i=m+1}^{k} g^D_{ab}(t_{\sigma(2i-1)}, t_{\sigma(2i)}) \prod_{j=2k+1}^{n} V(t_{\sigma(j)}) \end{aligned} \tag{4.99b}$$

$$\begin{aligned} &= \int_a^b d^nt \sum_{\sigma\in S_n} \sum_{0\leq m\leq \frac{n}{2}} \prod_{l=1}^{m} \frac{(-1)^m}{2^m m!} \Delta^D_{ab}(t_{\sigma(2l-1)}, t_{\sigma(2l)}) \\ &\quad \times \sum_{m\leq k\leq \frac{n}{2}} \frac{(-1)^{k-m}}{2^{k-m}(k-m)!(n-2k)!} \prod_{i=m+1}^{k} g^D_{ab}(t_{\sigma(2i-1)}, t_{\sigma(2i)}) \prod_{j=2k+1}^{n} V(t_{\sigma(j)}) \end{aligned} \tag{4.99c}$$

$$= \int_a^b d^n t \sum_{0\le m\le \frac{n}{2}} \frac{(-1)^m}{2^m m!} \prod_{l=1}^{m} \Delta^D_{ab}(t_{2l-1}, t_{2l}) \times \sum_{\sigma\in S_{n-m}} \sum_{m\le k\le \frac{n}{2}} \frac{(-1)^{k-m}}{2^{k-m}(k-m)!(n-2k)!} \prod_{i=m+1}^{k} g^D_{ab}(t_{\sigma(2i-1)}, t_{\sigma(2i)}) \prod_{j=2k+1}^{n} V(t_{\sigma(j)}) \tag{4.99d}$$

$$= \sum_{0\le m\le \frac{n}{2}} \frac{(-1)^m}{2^m m!} \prod_{l=1}^{m} \int_a^b dt_{2l-1} dt_{2l} \Delta^D_{ab}(t_{2l-1}, t_{2l}) \int_a^b dt_{m+1} \dots dt_n \sum_{\sigma\in S_{n-m}} \sum_{m\le k\le \frac{n}{2}} \frac{(-1)^{k-m}}{2^{k-m}(k-m)!(n-2k)!} \prod_{i=m+1}^{k} g^D_{ab}(t_{\sigma(2i-1)}, t_{\sigma(2i)}) \prod_{j=2k+1}^{n} V(t_{\sigma(j)}) \tag{4.99e}$$

$$= \sum_{0\le m\le \frac{n}{2}} \frac{1}{m!} \left(-\frac{1}{2}\int_a^b d^2 s \Delta^D_{ab}(s_1, s_2)\right)^m \times \int_a^b d^{n-2m} t \sum_{\sigma\in S_{n-m}} \sum_{0\le k\le \frac{n}{2}-m} \frac{(-1)^k}{2^k (k)!(n-2m-2k)!} \times \prod_{i=1}^{k} g^D_{ab}(t_{\sigma(2i-1)}, t_{\sigma(2i)}) \prod_{j=2k+1}^{n-2m} V(t_{\sigma(j)}) \tag{4.99f}$$

$$= \sum_{0\le m\le \frac{n}{2}} \frac{1}{m!(n-2m)!} \left(-\frac{1}{2}\int_a^b d^2 s \Delta^D_{ab}(s_1, s_2)\right)^m [V(a,b)^{n-2m}]_g \ . \tag{4.99g}$$

While the exponential form would automatically make the combinatorial factors 'work out', using this form makes it easier to ensure that the integrand stays finite at every step, a crucial part of the proof. This result implies, in particular, that if $\int_a^b d^2 s \Delta^D_{ab}(s_1, s_2) = 0$, then the operator renormalized using $\tilde{g}^D_{ab}$ is the same as that renormalized using g^D_{ab}. However, if $\int_a^b d^2 s \Delta^D_{ab}(s_1, s_2) \neq 0$, then the new operator is different, but the difference exponentiates as

$$\left[e^{\lambda V(a,b)}\right]_{\tilde{g}} = e^{-\frac{1}{2}\lambda^2 \int_a^b d^2 s \Delta^D_{ab}(s_1,s_2)} \left[e^{\lambda V(a,b)}\right]_g \ . \tag{4.100}$$

Extending this idea to include a fixed operator at the endpoint is not too difficult. It is best done as a two step process, where only one counterterm is altered in each step. We define $\tilde{g}^L_{ab}(s_1, s_2) = g^L_{ab}(s_1, s_2) + \Delta^L_{ab}(s_1, s_2)$. After a small calculation, we find the expected result

$$\left[V(a)e^{\lambda V(a,b)}\right]_{\tilde{g}} = e^{-\frac{1}{2}\lambda^2 \int_a^b d^2 s \, \Delta^D_{ab}(s_1,s_2)} \left[\left(V(a) - \lambda \int_a^b ds \, \Delta^L_{ab}(a,s)\right) e^{\lambda V(a,b)}\right]_g \ . \tag{4.101}$$

We will not have any need for an alternative edge counterterm $\tilde{g}^E_{abc}$, so it is not included here.

4.3.4 Assumptions (4.5c), (4.5d), (4.5e), and (4.5f)

We have mentioned that linearity is more difficult to show for the little g scheme than for the trivial (but divergent) exponentiation of the big G scheme. While an argument for the

likelihood of strong linearity will be given in section 4.3.8, it remains beyond proof for now. We can, however, prove that weak linearity (4.5c) holds at all orders.

Using the finiteness of the "normal ordered" operators, we extend the definition of the little g scheme to multiple integrated operators:

$$\left[\prod_{i=1}^{p} e^{\lambda_i V(a_i,a_{i+1})}\right]_g = \sum_{k_1=0}^{\infty}\cdots\sum_{k_p=0}^{\infty}\prod_{i=1}^{p}\int_{a_i}^{a_{i+1}} d^{k_i}t \; {}^{\circ}_{\circ}\prod_{i=1}^{p} e^{\lambda_i V_{a_i,a_{i+1}}}{}^{\circ}_{\circ g} \tag{4.102a}$$

$$= \sum_{k_1=0}^{\infty}\cdots\sum_{k_p=0}^{\infty}\prod_{i=1}^{p}\int_{a_i}^{a_{i+1}} d^{k_i}t \left(\prod_{i=1}^{p} e^{-\frac{1}{2}\lambda_i^2 g^D_{a_i,a_{i+1}}}\prod_{i=1}^{p-1} e^{-\frac{1}{2}\lambda_i\lambda_{i+1} g^E_{a_i,a_{i+1},a_{i+2}}}\prod_{i=1}^{p} e^{\lambda_i V_{a_i,a_{i+1}}}\right) . \tag{4.102b}$$

Here the operators $V_{a_i,a_{i+1}}$ are interpreted as vanishing outside of their natural domain (a_i, a_{i+1}). The normal ordering here will insert both $g^D_{a_i,a_{i+1}}$ and $g^E_{a_i,a_{i+1},a_{i+2}}$ counterterms depending on the operators being replaced, and those functions should also be defined to vanish outside of their natural domains. Instead of taking the operators and functions to vanish when appropriate, we could have said that when we taylor expand the exponentials each operator can only be located at one of the coordinates integrated between the correct endpoints. These two approaches are obviously equivalent. The factor of $\frac{1}{2}$ appearing with $g^E_{a_i,a_{i+1},a_{i+2}}$ is due to the fact that we must consider $\vec{t}$ in the region $(a_{i+1}, a_{i+2}) \times (a_i, a_{i+1})$ in addition to the region $(a_i, a_{i+1}) \times (a_{i+1}, a_{i+2})$ which was used to relate $g^E_{a_i,a_{i+1},a_{i+2}}$ to G^E, just as the $\frac{1}{2}$ appearing with $g^D_{a_i,a_{i+1}}$ must also make up for the fact that we consider $t_2 < t_1$.

For our study of the replacement condition we will only need to use two integrated operators, and the ellipses representing operators inserted at the endpoints are not important for the proof. We will focus on

$$\left[e^{\lambda V(a,b)} e^{\lambda V(b,c)}\right]_g = \sum_{i=0}^{\infty}\sum_{j=0}^{\infty}\int_a^b d^i t \int_b^c d^j t \; {}^{\circ}_{\circ} e^{\lambda V}{}^{\circ}_{\circ g} \ . \tag{4.103}$$

Now we will define an alternative little g scheme, as in the previous section. We choose

$$\tilde{g}^D_{ac}(t_1,t_2) = \begin{cases} g^D_{ab}(t_1,t_2) \ , & a < t_1, t_2 < b \\ g^D_{bc}(t_1,t_2) \ , & b < t_1, t_2 < c \\ g^E_{abc}(t_1,t_2) \ , & a < t_1 < b < t_2 < c, \text{ or } a < t_2 < b < t_1 < c \ . \end{cases} \tag{4.104}$$

This is chosen so that the statement $\left[e^{\lambda V(a,b)} e^{\lambda V(b,c)}\right]_g = \left[e^{\lambda V(a,c)}\right]_{\tilde{g}}$ is trivial. The replacement condition holds as long as $\tilde{g}$ and g are equivalent renormalization schemes, and from the previous section, we know that two little g schemes are equivalent as long as the difference $\Delta^D_{ac} = \tilde{g}^D_{ac} - g^D_{ac}$ vanishes when integrated. Since this is only two-dimensional integration, up to corrections which vanish as $\epsilon \to 0$, we have

$$\frac{1}{2}\int_{\Gamma_\epsilon^{a,c}} d^2t \left(\tilde{g}^D_{ac}(t_1,t_2) - g^D_{ac}(t_1,t_2)\right) = G^D_{ab} + G^D_{bc} + G^E - G^D_{ac} \ . \tag{4.105}$$

The divergent parts have to and do cancel, because both the g and $\tilde{g}$ schemes use the same divergent part of the counterterms. This is why we are justified in freely swapping the domain of

integration between $(a,c)^2$ used in (4.100) and the $\Gamma_\epsilon^{a,c}$ shown here. We included the divergent part of the counterterms simply to demonstrate that this is the same condition we found at quadratic order. As a result the replacement condition (4.5c) holds for the little g scheme at all orders with the same conditions that we found at quadratic order.

The factorization property (4.5d) is imposed by the fact that we defined the little g scheme to include counterterms only for pairs of operators which are integrated over domains which intersect at at least one point. By defining it this way, factorization is trivial. The locality and reflection properties (4.5e) and (4.5f) can be shown using exactly the same arguments as we used at quadratic order. The g counterterms are still independent of any global properties of the Riemann surface in which they are inserted, and while not completely independent of the insertion coordinates, they depend only on $(t_2 - t_1)^2$. The fact that this dependence is even and translationally invariant means that reflection will still go through without any problems.

4.3.5 Comparison to Kiermaier and Okawa

The renormalization scheme used by Kiermaier and Okawa [36] is nearly equivalent to the little g scheme. We will construct an alternative little g scheme which is equal to ours up to $O(\epsilon)$ corrections, and which is also equal to the renormalization scheme of [36] for all operators which appear explicitly in the solution Ψ.

The renormalization of the operator $\left[V(a,b)^2\right]_r$ is performed using pair-wise subtractions, as we did, but consists of two stages. The first stage gives a finite operator which does *not* obey all of the assumptions (4.5). This operator is denoted by normal ordering.

$$\overset{\circ}{\circ} V(t_1)V(t_2) \overset{\circ}{\circ}_{\mathcal{G}} = V(t_1)V(t_2) - \mathcal{G}_m(t_1,t_2) \tag{4.106}$$

where

$$\mathcal{G}_m(t_1,t_2) = \langle V(t_1)V(t_2)\rangle_{W_m} = \frac{\pi^2}{(m+1)^2 \sin^2\left(\frac{\pi(t_2-t_1)}{m+1}\right)} \tag{4.107}$$

is the two-point function in the matter BCFT. The two point function depends on the global properties of the Riemann surface, and in this case is defined to use the semi-infinite cylinder W_m, which has circumference $m+1$. The wedge index m is only given a fixed value once the full wedge state has been built and the correlation function is taken – it is not a fixed value for the renormalization of a given wedge state. This presents the first obvious problem for such a renormalization scheme: the counterterms are not local and violate (4.5e). This will be solved by the second step in the renormalization process, but first we must define the normal ordering of integrated operators.

Unlike the normal ordering we have defined, when acting on integrated operators they define this operation to include an ϵ-regularization as well. In practice we can define this by applying the ϵ-regularization and a limit in all cases, and similarly to equation (4.9) of [36] define [3]

$$\overset{\circ}{\circ} \prod_i V(t_i) \overset{\circ}{\circ}_{\mathcal{G}} \overset{\text{def}}{=} \lim_{\epsilon\to 0} \exp\left(-\frac{1}{2}\int dt_1 dt_2\, \mathcal{G}_m(t_1,t_2)\frac{\delta}{\delta V(t_1)}\frac{\delta}{\delta V(t_2)}\right)\left(\prod_i V(t_i)\right)_\epsilon . \tag{4.108}$$

[3] This is only valid for integrated operators and fixed operators with finite separation. In the case of $\overset{\circ}{\circ} V(t)^n \overset{\circ}{\circ}_{\mathcal{G}}$ as in equation (4.10) of [36], this definition fails, but we will not need to consider this case.

Applying this to operators which actually appear in the solution, we have

$$\begin{aligned}\overset{\circ}{\circ} V(a,b)^2 \overset{\circ}{\circ}_{\mathcal{G}} = &\lim_{\epsilon\to 0}\int_a^{b-\epsilon} dt_1 \int_{t_1+\epsilon}^{b} dt_2 \left(V(t_1)V(t_2) - \mathcal{G}_m(t_1,t_2)\right) \\ &+ \lim_{\epsilon\to 0}\int_{a+\epsilon}^{b} dt_1 \int_a^{t_1-\epsilon} dt_2 \left(V(t_1)V(t_2) - \mathcal{G}_m(t_1,t_2)\right)\end{aligned} \tag{4.109a}$$

and

$$\overset{\circ}{\circ} V(a)V(a,b) \overset{\circ}{\circ}_{\mathcal{G}} = \lim_{\epsilon\to 0}\int_{a+\epsilon}^{b} dt \left(V(a)V(t) - \mathcal{G}_m(a,t)\right) \ . \tag{4.109b}$$

The renormalization of higher powers of operators as defined by (4.108) looks exactly as expected, subtracting off the two-point function for every pair of operators.

$$\overset{\circ}{\circ}(V(a,b))^n \overset{\circ}{\circ}_{\mathcal{G}} = \lim_{\epsilon\to 0}\int_{\Gamma_\epsilon^{a,b}} d^n t \sum_{0\le k\le \frac{n}{2}} \frac{(-1)^k n!}{2^k k!(n-2k)!} \prod_{i=1}^{k} \mathcal{G}_m(t_i,t_{i+k}) \prod_{j=2k+1}^{n} V(t_j) \tag{4.110}$$

Now that we have defined the normal ordering which gives a finite version of each integrated operator in question, we need to repair the locality condition (4.5e). Kiermaier and Okawa accomplished this by adding back in the finite part of the two-point function for each counterterm. This is designed to cancel the m-dependence of the propagator. The finite pieces which are used are

$$\left\langle V(a,b)^2 \right\rangle_r = \ln\left(\frac{\pi^2}{(m+1)^2 \sin^2\left(\frac{\pi(b-a)}{m+1}\right)}\right) = \ln \mathcal{G}_m(a,b) \ , \tag{4.111a}$$

$$\left\langle V(a)V(a,b) \right\rangle_r = -\frac{\pi}{m+1}\cot\left(\frac{\pi(b-a)}{m+1}\right) \ . \tag{4.111b}$$

At quadratic order, the finished renormalized operators are

$$\left[(V(a,b))^2\right]_{\mathcal{G}} = \overset{\circ}{\circ}(V(a,b))^2 \overset{\circ}{\circ}_{\mathcal{G}} + \left\langle V(a,b)^2 \right\rangle_r \ , \tag{4.112a}$$

$$\left[V(a)V(a,b)\right]_{\mathcal{G}} = \overset{\circ}{\circ} V(a)V(a,b) \overset{\circ}{\circ}_{\mathcal{G}} + \left\langle V(a)V(a,b) \right\rangle_r \ . \tag{4.112b}$$

More useful for our purposes is the extension of this to all orders.

$$\left[e^{\lambda V(a,b)}\right]_{\mathcal{G}} = e^{\frac{1}{2}\lambda^2 \left\langle V(,b)^2 \right\rangle_r} \overset{\circ}{\circ} e^{\lambda V(a,b)} \overset{\circ}{\circ}_{\mathcal{G}} \ , \tag{4.113a}$$

$$\left[V(a)e^{\lambda V(a,b)}\right]_{\mathcal{G}} = e^{\frac{1}{2}\lambda^2 \left\langle V(,b)^2 \right\rangle_r} \overset{\circ}{\circ} \left(V(a) + \lambda \left\langle V(a)V(a,b) \right\rangle_r\right) e^{\lambda V(a,b)} \overset{\circ}{\circ}_{\mathcal{G}} \ . \tag{4.113b}$$

At first glance, this may look quite different from the little g scheme, but by noticing the result of section 4.3.3 we can combine the finite term $\left\langle V(a,b)^2 \right\rangle_r$, which acts like $\int d^2s \Delta_{ab}^D(s_1,s_2)$, with the counterterm containing the divergence $\mathcal{G}_m$ to get an alternate form of this renormalization scheme which involves only one step. We need to decide what function we should use to

get $\langle V(a,b)^2 \rangle_r$ once we integrate it. Fortunately, we notice that in [36] this function is defined by equation (4.38):

$$\langle V(a,b)^2 \rangle_r \stackrel{\text{def}}{=} 2 \lim_{\epsilon \to 0} \left(\int_a^{b-\epsilon} dt_1 \int_{t_1+\epsilon}^{b} dt_2 \; \mathcal{G}_m(t_1,t_2) - \frac{b-a-\epsilon}{\epsilon} - \ln \epsilon \right) . \tag{4.114}$$

Half of the needed function is already supplied by $\mathcal{G}_m$. The rest can be easily found by integrating our function g^D_{ab} with the appropriate choice of constants, $C_0 = -1$ and $C_1 = 0$. The little g scheme which is equivalent to the renormalization scheme of [36] uses the counterterm

$$\hat{g}^D_{ab}(t_1,t_2) = \mathcal{G}_m(t_1,t_2) - \left(\mathcal{G}_m(t_1,t_2) - g^D_{ab}(t_1,t_2)\big|_{C_0=-1,C_1=0} \right) \tag{4.115a}$$

$$= g^D_{ab}(t_1,t_2)\big|_{C_0=-1,C_1=0} \; . \tag{4.115b}$$

Of course for the renormalization scheme of [36] to be completely equivalent to this $\hat{g}$ scheme, they must be equivalent for more operators than just $\left[e^{\lambda V(a,b)}\right]_{\hat{g}}$. The calculation for $\left[V(a)e^{\lambda V(a,b)}\right]_{\hat{g}}$ goes through exactly like the doubly integrated case and gives

$$\hat{g}^L_{ab}(a,t) = g^L_{ab}(a,t)\big|_{C^L=0} \; . \tag{4.116}$$

Together with the always-similar right handed operator, this shows equivalence for all operators which appear explicitly in the solution. The remaining operator we are interested in is actually treated slightly differently in [36]. The ϵ-bracket used in [36] for the edge collision operator $[V(a,b)V(b,c)]_{\mathcal{G}}$ is not the linear one we have been using. Instead they used

$$(V(a,b)V(b,c))^{\text{KO}}_{\epsilon} = \int_a^{b-\frac{\epsilon}{2}} dt_1 \int_{b+\frac{\epsilon}{2}}^{c} dt_2 \, V(t_1)V(t_2) \; . \tag{4.117}$$

The difference between this and our ϵ-bracket is illustrated in figure 4.1. The finite term associated with this operator is

$$\langle V(a,b)V(b,c) \rangle_r \stackrel{\text{def}}{=} \lim_{\epsilon \to 0} \left(\int_a^{b-\frac{\epsilon}{2}} dt_1 \int_{b+\frac{\epsilon}{2}}^{c} dt_2 \, \mathcal{G}(t_1,t_2) + \ln \epsilon \right) , \tag{4.118}$$

which makes the total counterterm subtracted for that operator equivalent to

$$\hat{g}^E_{abc}(t_1,t_2) = g^E_{abc}(t_1,t_2)\big|_{C_0=-1} \; . \tag{4.119}$$

The choice of C_0 exactly replaces the missing contribution from integrating $\frac{1}{(t_2-t_1)^2}$ over the subregion where one of the coordinates is within $\frac{\epsilon}{2}$ of b.

Whether or not this renormalization scheme satisfies replacement or even linearity at higher orders is not a simple question. The ϵ-bracket is not linear because it sets the measure to zero for coordinates like $(\frac{b+a}{2}, b)$ when the operator being renormalized is $V(a,b)V(b,c)$ but leaves the measure intact at the same location for $V(a,b)V(b)$. This lack of linearity for this operator suggests that the renormalization scheme built on it should fail to be linear as well, and with the replacement condition being closely related to linearity it must be re-evaluated as well. If we were to treat this as a big G scheme, subtracting off fixed counterterms from integrated

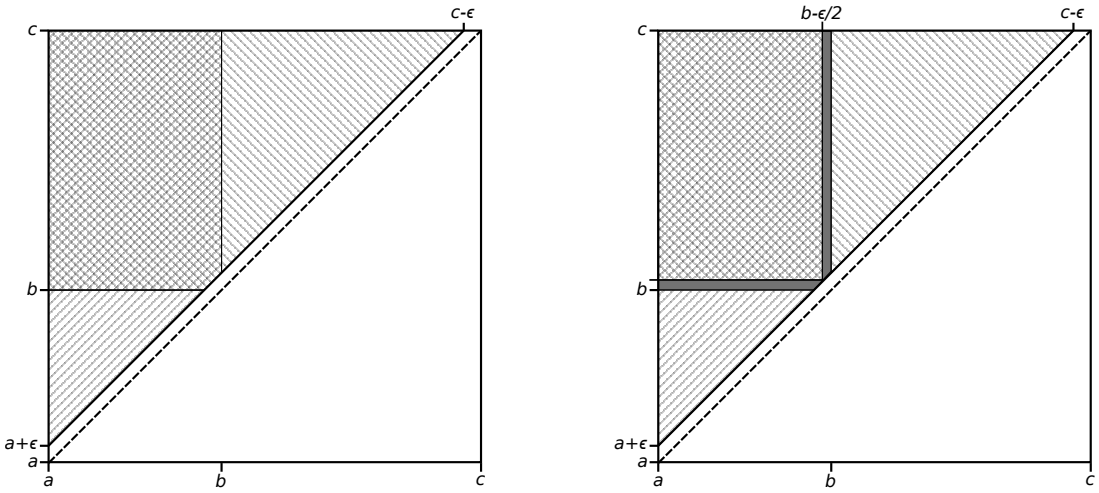

Figure 4.1: Comparison of the two choices of integration region used for the renormalization of the integrated operators $\big(V(a,b)^2\big)_\epsilon$ and $\big(V(b,c)^2\big)_\epsilon$ (diagonal hatching), and $\big(V(a,b)V(b,c)\big)_\epsilon$ (cross-hatched): (a) using our prescription for the renormalizations. (b) using the prescription of [36]. The difference is the grey strips, which are not covered using the latter choice. The dashed line indicates the singularity due to colliding operators.

operators, then in addition to finiteness failing as we know it must, the replacement condition would fail as well. The non-linear ϵ-bracket would cause operators to exponentiate differently from counterterms and the form of C^D_{ab} would have to be different at each order to make up for it. On the other hand, as long as we insist on using a little $\hat{g}$ scheme to define the renormalization, the fully symmetrized form of the renormalized integrand remains finite as the limit $\epsilon \to 0$ is taken, so this combination of operators and counterterms does not care about alterations of the region of integration which are $O(\epsilon)$. This means that the renormalization scheme of [36] most likely satisfies replacement, and perhaps even strong linearity (when $C^L = C^R = C_1$) as a result of this insensitivity to holes. We will not dwell on proving this, however, as we have already proven the replacement condition for our little g scheme with the linear ϵ-bracket.

Because our scheme is so similar to the Kiermaier and Okawa scheme, it is not surprising that in the next sections when we prove the BRST assumptions (4.5a) and (4.5b) we will take an approach very similar to the one they used. None of the steps they used to prove those two conditions are wrong, but a few will need more justification than was originally given. Specifically, the first BRST condition requires the lemma (4.132), and the second BRST condition requires that we take great care to ensure that integrands are finite whenever small changes are made to the integration region. We must also be clear about why the first BRST condition can be safely applied without corrections even when multiplied by divergent factors or other operators close to the integration region. These technical details, while they do not change the structure of how we approach the proof, are certainly not trivial and will each be explained as they are encountered.

4.3.6 Proof of the First BRST Condition (4.5a)

Because the little g scheme is very similar to the example renormalization scheme from Kiermaier and Okawa in [36], we will follow the proof of (4.5a) there quite closely. The renormalized operator we start with this time is, as in (4.89),

$$\frac{1}{n!}\left[(V(a,b))^n\right]_g = \int_{\Gamma_\epsilon^{a,b}} dt_1 \dots dt_n \sum_{k=0}^{\lfloor n/2 \rfloor} \frac{(-1)^k}{2^k k!(n-2k)!} \prod_{i=1}^{k} g_{ab}^D(t_i, t_{i+k}) \prod_{j=2k+1}^{n} V(t_j) \ . \tag{4.120}$$

As in section 4.2.5, we will omit the limit $\epsilon \to 0$ throughout this and the next section (where we prove the second BRST condition). Because the counterterm g_{ab}^D appears very frequently, as long as there is no ambiguity we will also drop the indices and simply refer to it as g for this section and the next only.

We wish to show that

$$\frac{1}{n!} Q_B \left[V(a,b)^n\right]_g = \sum_{l=1}^{2} \frac{1}{(n-l)!} \left(\left[V(a,b)^{n-l} O_R^{(l)}(b) \right]_g - \left[O_L^{(l)}(a) V(a,b)^{n-l} \right]_g \right) \ . \tag{4.121}$$

To begin with we use the well known action of the BRST operator on the marginal deformation (4.67).

$$\frac{1}{n!} Q_B \left[V(a,b)^n\right]_g = Q_B \left(\sum_{k=0}^{\lfloor n/2 \rfloor} \frac{(-1)^k}{2^k k!(n-2k)!} \int_{\Gamma_\epsilon^{a,b}} d^n t \left(\prod_{i=1}^{k} g(t_i, t_{i+k}) \right) \left(\prod_{j=2k+1}^{n} V(t_j) \right) \right) \tag{4.122a}$$

$$= \sum_{k=0}^{\lfloor \frac{n-1}{2} \rfloor} \frac{(-1)^k}{2^k k!(n-2k-1)!} \int_{\Gamma_\epsilon^{a,b}} d^n t \left(\prod_{i=1}^{k} g(t_i, t_{i+k}) \right) \left(\prod_{j=2k+1}^{n-1} V(t_j) \right) \partial_{t_n} \left(c V(t_n) \right) \tag{4.122b}$$

$$= \sum_{k=0}^{\lfloor n/2 \rfloor} \frac{(-1)^k}{2^k k!(n-2k)!} \int_{\Gamma_\epsilon^{a,b}} d^n t \ \partial_{t_n} \left((n-2k) \prod_{i=1}^{k} g(t_i, t_{i+k}) \prod_{j=2k+1}^{n} V(t_j) c(t_n) \right) \tag{4.122c}$$

In the last line we have simply noticed that a term with $k = n/2$ vanishes, so we can include it in the sum if n is even. We can now add and subtract the following quantity:

$$\sum_{k=1}^{\lfloor n/2 \rfloor} \frac{(-1)^k}{2^k k!(n-2k)!} \int_{\Gamma_\epsilon^{a,b}} d^n t \ \partial_{t_n} \left(2k \prod_{j=1}^{n-2k} V(t_j) \prod_{i=n-2k+1}^{n-k} g(t_i, t_{i+k}) c(t_n) \right) \tag{4.123a}$$

$$= \sum_{k=0}^{\lfloor n/2 \rfloor - 1} \frac{(-1)^{k+1}}{2^{k+1}(k+1)!(n-2k-2)!} \times \int_{\Gamma_\epsilon^{a,b}} d^n t \ \partial_{t_n} \left(2(k+1) \prod_{j=1}^{n-2k-2} V(t_j) \prod_{i=n-2k-1}^{n-k-1} g(t_i, t_{i+k+1}) c(t_n) \right) \tag{4.123b}$$

$$= - \sum_{k=0}^{\lfloor n/2 \rfloor - 1} \frac{(-1)^k}{2^k k!(n-2k-2)!} \int_{\Gamma_\epsilon^{a,b}} d^n t \ \partial_{t_n} \left(\prod_{i=1}^{k} g(t_i, t_{i+k}) \prod_{j=2k+1}^{n-2} V(t_j) g(t_{n-1}, t_n) c(t_n) \right) \tag{4.123c}$$

In the first two lines, (4.123a) and (4.123b), the $V(t_j)$ insertions are listed before the $g(t_i, t_{i+k})$ factors, but since the integration region is symmetric we can relabel any index except for t_n. As long as the number of factors of each type is the same and the combinatorics match up, the expressions are equal. In this instance, we can go from (4.123b) to (4.123c) by relabelling the indices as in table 4.1. Now we take (4.122c) and we add (4.123a) and subtract (4.123c). This

V				g							
t_1	t_2		t_{n-2k-2}	t_{n-2k-1}		t_{n-k-2}	t_{n-k-1}	t_{n-k}		t_{n-1}	t_n
$\downarrow$	$\downarrow$	$\cdots$	$\downarrow$	$\downarrow$	$\cdots$	$\downarrow$	$\downarrow$	$\downarrow$	$\cdots$	$\downarrow$	$\downarrow$
t_{2k+1}	t_{2k+2}		t_{n-2}	t_1		t_k	t_{n-1}	t_{k+1}		t_{2k}	t_n

Table 4.1: How to relabel the integration variables in going from (4.123b) to (4.123c).

gives us

$$\begin{aligned}\frac{1}{n!}Q_B\left[V(a,b)^n\right]_g = &\sum_{k=0}^{\lfloor n/2\rfloor}\frac{(-1)^k}{2^k k!(n-2k)!}\int_{\Gamma_\epsilon^{a,b}} d^n t\ \partial_{t_n}\\ &\left((n-2k)\prod_{i=1}^{k} g(t_i,t_{i+k})\prod_{j=2k+1}^{n} V(t_j)c(t_n) + 2k\prod_{j=1}^{n-2k} V(t_j)\prod_{i=n-2k+1}^{n-k} g(t_i,t_{i+k})c(t_n)\right)\\ &+\sum_{k=0}^{\lfloor n/2\rfloor-1}\frac{(-1)^k}{2^k k!(n-2k-2)!}\int_{\Gamma_\epsilon^{a,b}} d^n t\ \partial_{t_n}\left(\prod_{i=1}^{k} g(t_i,t_{i+k})\prod_{j=2k+1}^{n-2} V(t_j)g(t_{n-1},t_n)c(t_n)\right).\end{aligned} \tag{4.124}$$

We will consider the two integrals separately, defining $\mathcal{A}$ and $\mathcal{B}$ for convenience.

$$\begin{aligned}\mathcal{A} \stackrel{\text{def}}{=} &\int_{\Gamma_\epsilon^{a,b}} d^n t\sum_{k=0}^{\lfloor n/2\rfloor}\frac{(-1)^k}{2^k k!(n-2k)!}\\ &\partial_{t_n}\left((n-2k)\prod_{i=1}^{k} g(t_i,t_{i+k})\prod_{j=2k+1}^{n} V(t_j)c(t_n) + 2k\prod_{j=1}^{n-2k} V(t_j)\prod_{i=n-2k+1}^{n-k} g(t_i,t_{i+k})c(t_n)\right)\end{aligned} \tag{4.125a}$$

$$\mathcal{B} \stackrel{\text{def}}{=} \sum_{k=0}^{\lfloor n/2\rfloor-1}\frac{(-1)^k}{2^k k!(n-2k-2)!}\int_{\Gamma_\epsilon^{a,b}} d^n t\ \partial_{t_n}\left(\prod_{i=1}^{k} g(t_i,t_{i+k})\prod_{j=2k+1}^{n-2} V(t_j)g(t_{n-1},t_n)c(t_n)\right) \tag{4.125b}$$

By splitting the expression into $\mathcal{A}$ and $\mathcal{B}$, we have given a precise implementation of the idea

$$\left[V(a,b)^n\right]_r \leftrightarrow \left[V(a,b)^{n-1}\right]_r V(a,b) - (n-1)\left[V(a,b)^{n-2}\right]_r G^D_{ab}\ . \tag{4.126}$$

We have taken a quantity with $n-1$ renormalized insertions and one insertion not renormalized (inserted at t_n), and broken it into $\mathcal{A}$ with n renormalized operators, and $\mathcal{B}$ with $n-2$ of them and an extra counterterm. Put another way, the BRST operator acts like a derivative hitting

only the marginal operators and not the counterterms. By using (4.126) we can write this as a derivative hitting the entire expression regardless of whether the coordinate has an operator or a counterterm, plus a term where the derivative only hits the counterterm. It is this trick that allows us to proceed.

While this has given us a longer expression, it is advantageous because we can make the integrand of $\mathcal{A}$ finite and do the integral over t_n. If we symmetrize all of the dummy coordinates other than t_n, we get an integrand

$$\partial_{t_n}\left(c(t_n)\frac{1}{(n-1)!}\sum_{\sigma\in S_n}\sum_{k=0}^{\lfloor n/2\rfloor}\frac{(-1)^k}{2^k k!(n-2k)!}\prod_{i=1}^{k}g(t_{\sigma(i)},t_{\sigma(i+k)})\prod_{j=2k+1}^{n}V(t_{\sigma(j)})\right)$$
$$=\frac{1}{(n-1)!}\partial_{t_n}\left(c(t_n)\overset{\circ}{_\circ}\prod_{i=1}^{n}V(t_i)\overset{\circ}{_{\circ g}}\right) \quad (4.127)$$

which is manifestly finite. In this form, it is safe to change the integration region to $(a,b)^n$ and perform the trivial integral over t_n using the fundamental theorem of calculus. We can then change the region of integration to $\Gamma_\epsilon^{a+\epsilon,b-\epsilon}(t_1,\ldots,t_{n-1})$ and use the still-symmetric region of integration to reorder the coordinate labels again and get the simpler expression

$$\mathcal{A}=\int_{\Gamma_\epsilon^{a+\epsilon,b-\epsilon}}d^{n-1}t\sum_{k=0}^{\lfloor n/2\rfloor}\frac{(-1)^k}{2^k k!(n-2k)!}$$
$$\left((n-2k)\prod_{i=1}^{k}g(t_i,t_{i+k})\prod_{j=2k+1}^{n-1}V(t_j)(cV(b)-cV(a))\right.$$
$$\left.+2k\prod_{j=1}^{n-2k}V(t_j)\prod_{i=2-2k+1}^{n-k-1}g(t_i,t_{i+k})\left(g_{ab}^D(t_{n-k},b)c(b)-g_{ab}^D(t_{n-k},a)c(a)\right)\right) . \quad (4.128)$$

This has localized t_n at the boundary, turning $\left[V(a,b)^{n-1}\int_a^b dt_n\partial_{t_n}cV(t_n)\right]_r$ into something similar to $\left[V(a,b)^{n-1}(cV(b)-cV(a))\right]_r$. The reason that the derivative does not do exactly this is that when t_n appears in a counterterm it gives $c(a)g_{ab}^D(a,t_i)$, whereas in order to get the correctly renormalized operator with a fixed insertion we need $c(a)g_{ab}^L(a,t_i)$. Correcting for this, we can write that

$$\mathcal{A}=\frac{1}{(n-1)!}\left[V(a,b)^{n-1}(cV(b)-cV(a))\right]_g$$
$$+\frac{1}{(n-2)!}\left[V(a,b)^{n-2}\right]_g\left(c(b)\int_a^b dt(g_{ab}^R(t,b)-g_{ab}^D(t,b))-c(a)\int_a^b dt(g_{ab}^L(a,t)-g_{ab}^D(a,t))\right) . \quad (4.129)$$

While it is not normally correct to write a fully renormalized operator times a counterterm, as in the second line here, in this case it is allowed because the counterterms' divergent parts cancel so that everything is finite and independent of ϵ. The limit does not prevent us from

treating the two factors independently. From the definitions in (4.87) we know that

$$g^L_{ab}(x,y) - g^D_{ab}(x,y) = \frac{1}{(b-a)^2} + \frac{C^L}{b-a} + \frac{2}{(b-a)^2}\left(1 + \ln(b-a) + C_0 + (b-a)C_1\right) \quad (4.130a)$$

$$= \frac{1}{(b-a)^2} + \frac{C^L}{b-a} + f^D_{ab} \ . \quad (4.130b)$$

where $f^D_{ab} \stackrel{\text{def}}{=} \frac{2}{(b-a)^2}(1 + \ln(b-a) + C_0 + (b-a)C_1)$ is the constant part of g^D_{ab}. Then

$$\mathcal{A} = \frac{1}{(n-1)!}\left[V(a,b)^{n-1}(cV(b) - cV(a))\right]_g + \frac{1}{(n-2)!}\left[V(a,b)^{n-2}\right]_g \left(\frac{c(b)-c(a)}{b-a} + c(b)C^R - c(a)C^L - (c(b)-c(a))(b-a)f^D_{ab}\right) \ . \quad (4.131)$$

Returning now to the other integral, $\mathcal{B}$ in (4.125), we notice that the integrand diverges whenever t_{n-1} and t_n approach each other, but not when these two variables approach any of the others. This alone is not enough to factorize the region of integration, but with (4.126) in mind we notice that the rest of the integrand (including the sum and combinatoric factors) is what we would see for $\left[V(a,b)^{n-2}\right]_g$, so there are no divergences due to t_i approaching any point for $i < n-1$. We can show, as a lemma, that

$$\int_{\Gamma^{a,b}_\epsilon} d^n t \int_{\Gamma^{a,b}_\epsilon} d^2 s \ f(\vec{t})\, \partial_{s_2}\left(g^D_{ab}(s_1,s_2)c(s_2)\right) = \int_{\Gamma^{a,b}_\epsilon} d^n t \ d^2 s \ f(\vec{t})\, \partial_{s_2}\left(g^D_{ab}(s_1,s_2)c(s_2)\right) \quad (4.132)$$

for any function $f(\vec{t})$ which is finite on $(a,b)^n$. The difference of the two regions can be written in terms of three other regions.

$$\left(\int_{\Gamma^{a,b}_\epsilon} d^n t \int_{\Gamma^{a,b}_\epsilon} d^2 s - \int_{\Gamma^{a,b}_\epsilon} d^n t \ d^2 s\right) f(\vec{t})\, \partial_{s_2}\left(g^D_{ab}(s_1,s_2)c(s_2)\right)$$
$$= \sum_{i=1}^n \int_{\Gamma^{a,b}_\epsilon} d^2 s \left(\int_{\Gamma^{a,b}_\epsilon \cap |t_i - s_1| < \epsilon} d^n t + \int_{\Gamma^{a,b}_\epsilon \cap |t_i - s_2| < \epsilon} d^n t\right) f(\vec{t})\, \partial_{s_2}\left(g^D_{ab}(s_1,s_2)c(s_2)\right)$$
$$- \sum_{i=1}^n \int_{\Gamma^{a,b}_\epsilon} d^2 s \int_{\Gamma^{a,b}_\epsilon \cap |t_i - s_1| < \epsilon \cap |t_i - s_2| < \epsilon} d^n t \ f(\vec{t})\, \partial_{s_2}\left(g^D_{ab}(s_1,s_2)c(s_2)\right) \quad (4.133)$$

The first and second lines of the right hand side both vanish independently, so we will compute them separately, starting with the first line.

Because the function f is finite and is integrated over a region with area of order ϵ, we notice that each of those integrals over $\vec{t}$ is ϵ times a finite function of one of the two remaining coordinates. Specifically, by defining

$$F(s) = \frac{1}{\epsilon}\sum_{i=1}^n \int_{\Gamma^{a,b}_\epsilon \cap |t_i - s| < \epsilon} d^n t \ f(\vec{t}) \ , \quad (4.134)$$

the first line of (4.133) is

$$\epsilon \int_{\Gamma_\epsilon^{a,b}} d^2s \; \partial_{s_2} \left(g_{ab}^D(s_1,s_2) c(s_2) \right) \left(F(s_1) + F(s_2) \right) \; . \tag{4.135a}$$

We will not need to know the precise form of $F(s)$ so long as it and its derivative are finite. With the full expression having an ϵ factor out front from the small area of the t_i integral, we know that the finite part of g_{ab}^D will not play any role, and we only need to consider the singular term. Integrating by parts, we have

$$\begin{aligned} \epsilon \int_a^{b-\epsilon} ds \left(\frac{c(b)F(s) + c(b)F(b)}{(b-s)^2} - \frac{c(s+\epsilon)F(s) - c(s+\epsilon)F(s+\epsilon)}{\epsilon^2} \right) \\ + \epsilon \int_{a+\epsilon}^{b} \left(\frac{c(s-\epsilon)F(s) + c(s-\epsilon)F(s-\epsilon)}{\epsilon^2} - \frac{c(a)F(s) + c(a)F(a)}{(s-a)^2} \right) \\ - \epsilon \left(\int_a^{b-\epsilon} ds_1 \int_{s_1+\epsilon}^{b} ds_2 + \int_{a+\epsilon}^{b} ds_1 \int_a^{s_1-\epsilon} ds_2 \right) \frac{c(s_2)F'(s_2)}{(s_2-s_1)^2} \; . \end{aligned} \tag{4.135b}$$

The integrals with $\frac{1}{(b-s)^2}$ and $\frac{1}{(s-a)^2}$ can be done explicitly by taylor expanding $F(s)$ about the appropriate endpoint. The integrals with $\frac{1}{\epsilon^2}$ can be put over a common region by shifting the coordinate s in one of them. For the double integrals, we will taylor expand the numerator about s_1 in order to perform the s_2 integral.

$$\begin{aligned} 2cF(b) - 2cF(a) + \int_{a+\epsilon}^{b} ds \frac{\left(c(s-\epsilon) - c(s) \right) \left(F(s-\epsilon) + F(s) \right)}{\epsilon} \\ - \epsilon \left(\int_a^{b-\epsilon} ds_1 \int_{s_1+\epsilon}^{b} ds_2 + \int_{a+\epsilon}^{b} ds_1 \int_a^{s_1-\epsilon} ds_2 \right) \left(\frac{cF'(s_1)}{(s_2-s_1)^2} + \frac{\partial(cF')(s_1)}{s_2-s_1} + \dots \right) \end{aligned} \tag{4.135c}$$

Evaluating this further, we get

$$\begin{aligned} 2cF(b) - 2cF(a) - 2\int_a^b ds \; \partial c(s) F(s) - \epsilon \int_a^{b-\epsilon} ds \left(\frac{cF'(s)}{\epsilon} - \frac{cF'(s)}{b-s} \right) \\ - \epsilon \int_{a+\epsilon}^{b} ds \left(\frac{cF'(s)}{\epsilon} - \frac{cF'(s)}{s-a} \right) \end{aligned} \tag{4.135d}$$

$$= 2cF(b) - 2cF(a) - 2\int_a^b ds \; \partial c(s) F(s) - 2\int_a^b ds \; cF'(s) + O(\epsilon \ln \epsilon) \tag{4.135e}$$

$$= 2cF(b) - 2cF(a) - 2\int_a^b ds \; \partial_s \left(cF(s) \right) + O(\epsilon \ln \epsilon) \tag{4.135f}$$

which goes to zero in the $\epsilon \to 0$ limit.

Turning now to the last line in (4.133), where t_i is close to both s_1 and s_2, we define

$$F_2(s_1,s_2) = \frac{1}{\epsilon} \sum_{j=1}^{n} \int_{\Gamma_\epsilon^{a,b} \cap |t_i - s_1| < \epsilon \cap |t_i - s_2| < \epsilon} d^n t \; f(\vec{t}), \quad F_3(s_1,s_2) = F_2(s_1,s_2) c(s_2) \; . \tag{4.136}$$

Both of these functions are finite for the same reasons as $F(s)$ above: they are finite operators integrated over a region with area proportional to ϵ, and then divided by ϵ. The term we wish to evaluate is

$$\epsilon\left(\int_{a+2\epsilon}^{b} ds_1 \int_{s_1-2\epsilon}^{s_1-\epsilon} ds_2 + \int_{a}^{b-2\epsilon} ds_1 \int_{s_1+\epsilon}^{s_1+2\epsilon} ds_2 + \int_{a+\epsilon}^{a+2\epsilon} ds_1 \int_{a}^{s_1-\epsilon} ds_2 + \int_{b-2\epsilon}^{b-\epsilon} ds_1 \int_{s_1+\epsilon}^{b} ds_2\right) F_2(s_1,s_2)\partial_{s_2}\left(g^D_{ab}(s_1,s_2)c(s_2)\right) \quad . \tag{4.137a}$$

As with the other term, we will integrate this by parts.

$$\begin{aligned}
&\epsilon\int_{a+2\epsilon}^{b} ds\left(\frac{F_3(s,s-\epsilon)}{\epsilon^2} - \frac{F_3(s,s-2\epsilon)}{4\epsilon^2}\right) + \epsilon\int_{a}^{b-2\epsilon} ds\left(\frac{F_3(s,s+2\epsilon)}{4\epsilon^2} - \frac{F_3(s,s+\epsilon)}{\epsilon^2}\right)\\
&\quad + \epsilon\int_{a+\epsilon}^{a+2\epsilon} ds\left(\frac{F_3(s,s-\epsilon)}{\epsilon^2} - \frac{F_3(s,a)}{(s-a)^2}\right) + \epsilon\int_{b-2\epsilon}^{b-\epsilon} ds\left(\frac{F_3(s,b)}{(b-s)^2} - \frac{F_3(s,s+\epsilon)}{\epsilon^2}\right)\\
&-\epsilon\left(\int_{a+2\epsilon}^{b} ds_1\int_{s_1-2\epsilon}^{s_1-\epsilon} ds_2 + \int_{a}^{b-2\epsilon} ds_1\int_{s_1+\epsilon}^{s_1+2\epsilon} + \int_{a+\epsilon}^{a+2\epsilon} ds_1\int_{a}^{s_1-\epsilon} ds_2 + \int_{b-2\epsilon}^{b-\epsilon} ds_1\int_{s_1+\epsilon}^{b} ds_2\right)\\
&\qquad\qquad \frac{\partial_{s_2}(F_2(s_1,s_2))c(s_2)}{(s_2-s_1)^2}
\end{aligned} \tag{4.137b}$$

For the terms with a $\frac{1}{\epsilon^2}$ we will gather like denominators, shifting the integration variable when necessary to match intervals. For the other single integrals, the functions $F_3(s,a)$ and $F_3(s,b)$ can be taylor expanded about the endpoints a and b and only the first term will contribute, with the rest of the taylor series giving at most terms of order $O(\epsilon\ln\epsilon)$. For the double integrals, we will also taylor expand $\partial_{s_2}F_2(s_1,s_2)c(s_2)$ in s_2 about $s_2=s_1$ and again only the first term will contribute. In addition, the last two double integrals will not contribute at all because the s_1 integrals there provide extra suppression.

$$\begin{aligned}
&\int_{a+2\epsilon}^{b} ds\frac{F_3(s-2\epsilon,s)-F_3(s,s-2\epsilon)}{4\epsilon} + \int_{a+\epsilon}^{b} ds\frac{F_3(s,s-\epsilon)-F_3(s-\epsilon,s)}{\epsilon}\\
&\qquad + \epsilon F_3(b,b)\int_{b-2\epsilon}^{b-\epsilon}\frac{ds}{(b-s)^2} + \epsilon F_3(a,a)\int_{a+\epsilon}^{a+2\epsilon}\frac{ds}{(s-a)^2}\\
&\qquad -\epsilon\left(\int_{a+2\epsilon}^{b} ds_1\int_{s_1-2\epsilon}^{s_1-\epsilon} ds_2 + \int_{a}^{b-2\epsilon} ds_1\int_{s_1+\epsilon}^{s_1+2\epsilon} ds_2\right)\frac{\partial_2(F_2(s_1,s_1))c(s_1)}{(s_1-s_2)^2}
\end{aligned} \tag{4.137c}$$

Here $\partial_2 F_2$ is the derivative with respect to the second parameter, and ∂_1 will be with respect to the first. Now we taylor expand the numerators on the first line and evaluate an integral for everything else.

$$\frac{1}{2}\int_a^b ds\,(\partial_1-\partial_2)\,F_3(s,s) \;+\; \frac{F_3(b,b)-F_3(a,a)}{2} \;-\; \left(\int_{a+2\epsilon}^{b} ds + \int_{a}^{b-2\epsilon} ds\right)\frac{\partial_2 F_2(s,s)c(s)}{2} \tag{4.137d}$$

In order to remove the middle term, we would like to change $(\partial_1-\partial_2)$ to $-(\partial_1+\partial_2)=-\partial_s$ in

the first term, which we can do by adding an extra ∂_1 piece.

$$-\frac{1}{2}\int_a^b ds\ \partial_s F_3(s,s) + \frac{F_3(b,b)-F_3(a,a)}{2} + \int_a^b ds\ \partial_1 F_3(s,s) - \int_a^b ds\ \partial_2 F_2(s,s)c(s) \quad (4.137e)$$

$$= \int_a^b ds\,(\partial_1 F_2(s,s) - \partial_2 F_2(s,s))\,c(s) \quad (4.137f)$$

Now we look back at the definition of $F_2(s_1,s_2)$ and see that it is a symmetric function of its two parameters, so that the two derivatives are equal when acting on the line $s_1 = s_2$. We thus have zero for all of (4.133).

We can now finally evaluate $\mathcal{B}$. This lemma tells us that the domain of integration is equivalent to $\Gamma_\epsilon^{a,b}(t_1,\ldots,t_{n-2}) \times \Gamma_\epsilon^{a,b}(t_{n-1},t_n)$ and we evaluate the integrals with respect to t_{n-1} and t_n. The expression in question was

$$\mathcal{B} = \sum_{k=0}^{\lfloor n/2\rfloor-1} \frac{(-1)^k}{2^k k!(n-2k-2)!}\int_{\Gamma_\epsilon^{a,b}} d^n t\ \partial_{t_n}\left(\prod_{i=1}^{k} g(t_i,t_{i+k}) \prod_{j=2k+1}^{n-2} V(t_j) g(t_{n-1},t_n)c(t_n)\right) \quad (4.138a)$$

$$= \sum_{k=0}^{\lfloor n/2\rfloor-1} \frac{(-1)^k}{2^k k!(n-2k-2)!}\left(\int_{\Gamma_\epsilon^{a,b}} d^{n-2}t \prod_{i=0}^{k} g(t_i,t_{i+k}) \prod_{j=2k+1}^{n-2} V(t_j)\right) \quad (4.138b)$$
$$\times \left(\int_a^{b-\epsilon} dt_1 \int_{t_1+\epsilon}^{b} dt_2 + \int_{a+\epsilon}^{b} dt_1 \int_a^{t_1-\epsilon} dt_2\right)\partial_{t_2}\left(g(t_1,t_2)c(t_2)\right)$$

$$= \frac{\left[V(a,b)^{n-2}\right]_g}{(n-2)!}\left(\int_a^{b-\epsilon} dt\left(\frac{c(b)}{(t-b)^2} - \frac{c(t+\epsilon)}{\epsilon^2}\right) + \int_{a+\epsilon}^{b}\left(\frac{c(t-\epsilon)}{\epsilon^2} - \frac{c(a)}{(t-a)^2}\right)\right. \quad (4.138c)$$
$$\left. + \int_a^b dt\,(c(b) - c(t+\epsilon) + c(t-\epsilon) - c(a))\,f_{ab}^D\right)$$

$$= \frac{\left[V(a,b)^{n-2}\right]_g}{(n-2)!}\left(\frac{c(b)-c(a)}{\epsilon} + \frac{c(a)-c(b)}{b-a} + \int_a^{b-\epsilon} dt \frac{c(t)-c(t+\epsilon)}{\epsilon^2}\right. \quad (4.138d)$$
$$\left. + (c(b)-c(a))(b-a)f_{ab}^D\right)$$

$$= \frac{\left[V(a,b)^{n-2}\right]_g}{(n-2)!}\left(\frac{c(b)-c(a)}{\epsilon} + \frac{c(a)-c(b)}{b-a} - \frac{c(b-\epsilon)}{\epsilon} - \frac{\partial c(b)}{2} + \frac{c(a)}{\epsilon} + \frac{\partial c(a)}{2}\right. \quad (4.138e)$$
$$\left. + (c(b)-c(a))(b-a)f_{ab}^D\right)$$

$$= \frac{\left[V(a,b)^{n-2}\right]_g}{(n-2)!}\left(\frac{c(a)-c(b)}{b-a} + \frac{\partial c(b)}{2} + \frac{\partial c(a)}{2} + (c(b)-c(a))(b-a)f_{ab}^D\right)\ . \quad (4.138f)$$

Putting the pieces back together, we get

$$\begin{aligned}\mathcal{A}+\mathcal{B} = &\frac{1}{(n-1)!}\left[V(a,b)^{n-1}(cV(b)-cV(a))\right]_g \\ &+\frac{\left[V(a,b)^{n-2}\right]_g}{(n-2)!}\left(\frac{c(b)-c(a)}{b-a}+c(b)C^R-c(a)C^L-(c(b)-c(a))(b-a)f^D_{ab}\right) \\ &+\frac{\left[V(a,b)^{n-2}\right]_g}{(n-2)!}\left(\frac{c(a)-c(b)}{b-a}+\frac{\partial c(b)}{2}+\frac{\partial c(a)}{2}+(c(b)-c(a))(b-a)f^D_{ab}\right) \qquad (4.139a)\end{aligned}$$

$$\begin{aligned}= &\frac{\left[V(a,b)^{n-1}cV(b)\right]_g}{(n-1)!}+\frac{\left[V(a,b)^{n-2}\right]_g}{(n-2)!}\left(\frac{\partial c(b)}{2}+C^Rc(b)\right) \\ &-\frac{\left[cV(a)V(a,b)^{n-1}\right]_g}{(n-1)!}+\left(\frac{\partial c(a)}{2}-C^Lc(a)\right)\frac{\left[V(a,b)^{n-2}\right]_g}{(n-2)!}\ . \qquad (4.139b)\end{aligned}$$

If we take (4.139b) and multiply it by λ^n and then sum over n, we arrive at the precise form we wanted.

$$Q_B\left[e^{\lambda V(a,b)}\right]_g=\left[e^{\lambda V(a,b)}O_R(b)\right]_g-\left[O_L(a)e^{\lambda V(a,b)}\right]_g \qquad (4.140)$$

where

$$O_L(a)=\lambda cV(a)+\lambda^2C^Lc(a)-\frac{\lambda^2}{2}\partial c(a),\quad O_R(b)=\lambda cV(b)+\lambda^2C^Rc(b)+\frac{\lambda^2}{2}\partial c(b)\ . \qquad (4.141)$$

The first BRST condition is satisfied for the little g scheme without any higher order corrections to $O_{L/R}$.

4.3.7 Proof of the Second BRST Condition (4.5b)

To prove the second BRST condition, we want to evaluate

$$\frac{Q_B}{(n-1)!}\left[cV(a)V(a,b)^{n-1}\right]_g-\frac{Q_B}{(n-2)!}\frac{1}{2}\partial c(a)\left[V(a,b)^{n-2}\right]_g\ . \qquad (4.142)$$

We have left off the C^L term in O_L because we know that the constants C^L and C^R are pure gauge in that they never appear in the solution. We are free to make the choice to set them all to zero, which we will do throughout this section in order to simplify the calculation.

Let's take a moment to discuss some notation we will be using to simplify this section. We have previously defined the little g scheme by

$$[V(a,b)^n]_g=\int_a^b d^nt\ {}^{\circ}_{\circ}\prod_{i=1}^n V(t_i)\,{}^{\circ}_{\circ g}\ , \qquad (4.143)$$

but for a given interval (a,b) we could have chosen to write it as

$$[V(a,b)^n]_{g^D_{ab}}=\int_a^b d^nt\ {}^{\circ}_{\circ}\prod_{i=1}^n V(t_i)\,{}^{\circ}_{\circ g^D_{ab}}\ . \qquad (4.144)$$

This notation will allow us to use a counterterm g^D_{ab} whose parameters do not match the region of integration of V exactly. For example

$$[V(a+\epsilon,b)^n]_{g^D_{ab}} = \int_{a+\epsilon}^b d^n t \; \overset{\circ}{\underset{\circ}{\prod_{i=1}^n}} V(t_i) \overset{\circ}{\underset{\circ g^D_{ab}}{}} \; . \tag{4.145}$$

Further, since the counterterms g^D and $g^{L/R}$ will need to be modified independently, we will use a notation $[\;\cdot\;]_{g^D_{ab},g^{L/R}_{ab}}$ to list the appropriate counterterms and, when necessary, their parameters.

Using the first BRST condition, is it straightforward to show that the second term in (4.142) is

$$\begin{aligned} -\frac{Q_B}{(n-2)!}\frac{1}{2}\partial c(a)\left[V(a,b)^{n-2}\right]_g &= -\frac{1}{(n-2)!}\frac{c\partial^2 c(a)}{2}\left[V(a,b)^{n-2}\right]_g \\ &+ \frac{1}{(n-3)!}\frac{\partial c(a)}{2}\left[V(a,b)^{n-3}cV(b)\right]_g + \frac{1}{(n-3)!}\frac{c\partial c(a)}{2}\left[V(a)V(a,b)^{n-3)}\right]_g \\ &+ \frac{1}{(n-4)!}\frac{\partial c(a)}{2}\left[V(a,b)^{n-4}\right]_g\frac{\partial c(b)}{2} \; . \end{aligned} \tag{4.146}$$

In order to compute the other term, however, we will need to know how the first BRST condition works for alternative little g schemes. Recalling the general rules for alternative schemes, (4.100) and (4.101), we write

$$Q_B\left[e^{\lambda V(a,b)}\right]_{\tilde g} = e^{-\frac{\lambda^2}{2}\int_a^b d^2s\,\Delta^D_{ab}(s_1,s_2)} Q_B\left[e^{\lambda V(a,b)}\right]_g \tag{4.147a}$$

$$= e^{-\frac{\lambda^2}{2}\int_a^b d^2s\,\Delta^D_{ab}(s_1,s_2)}\left(\left[e^{\lambda V(a,b)}O_R(b)\right]_{g^D,g^R} - \left[O_L(a)e^{\lambda V(a,b)}\right]_{g^D,g^L}\right) \tag{4.147b}$$

$$= \left[e^{\lambda V(a,b)}O_R(b)\right]_{\tilde g^D,g^R} - \left[O_L(a)e^{\lambda V(a,b)}\right]_{\tilde g^D,g^L} \; . \tag{4.147c}$$

Since $O_{L/R}$ are defined for the standard little g scheme, they have the simple form of (4.141). To shift the counterterms from $g^{L/R}_{ab}$ to $\tilde g^{L/R}_{ab} = g^{L/R}_{ab} + \Delta^{R/L}_{ab}$ we must use equation (4.101):

$$\begin{aligned} &= \left[e^{\lambda V(a,b)}\left(O_R(b) + \lambda^2\int_a^b dt\,\Delta^R_{ab}(t,b)\right)\right]_{\tilde g^D,\tilde g^R} \\ &\qquad - \left[\left(O_L(a) + \lambda^2\int_a^b dt\,\Delta^L_{ab}(a,t)\right)e^{\lambda V(a,b)}\right]_{\tilde g^D,\tilde g^L} \end{aligned} \tag{4.147d}$$

$$\begin{aligned} &= \left[e^{\lambda V(a,b)}O_R(b)\right]_{\tilde g} - \left[O_L(a)e^{\lambda V(a,b)}\right]_{\tilde g} \\ &\qquad + \lambda^2\int_a^b dt\left(\Delta^R_{ab}(t,b) - \Delta^L_{ab}(a,t)\right)\left[e^{\lambda V(a,b)}\right]_{\tilde g} \; . \end{aligned} \tag{4.147e}$$

The BRST condition has the same form and the same operators $O_{L/R}$ provided that the left and right differences $\Delta^{L/R}_{ab}$ are equal, or at least have the same integral. The specific alternative

scheme we are interested in is the one where the counterterms are too big for the region of integration by a small constant amount, ϵ. Since we are taking $C^{L/R} = 0$ in this section, in this case $\Delta^R_{ab}(t_1, t_2) = \Delta^L_{ab}(t_1, t_2) = \frac{1}{(b-a+\epsilon)^2} - \frac{1}{(b-a)^2}$ so the first BRST condition goes through without any additional terms.

With the preliminaries out of the way, the main part of the proof of (4.5b) consists of calculating the first term in (4.142).

$$\frac{Q_B}{(n-1)!}\left[cV(a)V(a,b)^{n-1}\right]_g = \frac{Q_B}{(n-1)!}\int_a^b d^{n-1}t \overset{\circ}{_\circ} cV(a)\prod_{i=1}^{n-1} V(t_i) \overset{\circ}{_{\circ g}} \tag{4.148a}$$

At this point, we introduce a small parameter ϵ which is implicitly taken to zero. Since the integrand is finite, we can modify the integration region. We make an ϵ-sized modification to the integration region at a to examine the divergence there and write

$$= \frac{Q_B}{(n-1)!}\int_{a+\epsilon}^b d^{n-1}t \left(cV(a) \overset{\circ}{_\circ}\prod_{i=1}^{n-1} V(t_i) \overset{\circ}{_{\circ g^D_{ab}}} -(n-1)c(a)g^L_{ab}(a,t_1) \overset{\circ}{_\circ}\prod_{i=2}^{n-1} V(t_i) \overset{\circ}{_{\circ g^D_{ab}}} \right) ,$$

(4.148b)

where the counterterms used in the normal ordering no longer match the integration region due to the ϵ regulator. The lack of holes for the bulk of the integrated operators means we can rewrite those as renormalized integrated operators, where the implicit regulator should be taken to zero before ϵ. Also using the fact that $Q_B(cV) = 0$, we find

$$\begin{aligned} = &-\frac{cV(a)}{(n-1)!}Q_B\left[V(a+\epsilon,b)^{n-1}\right]_{g_{ab}} + \frac{c(a)}{(n-2)!}\int_{a+\epsilon}^b dt\, g^L_{ab}(a,t)\, Q_B\left[V(a+\epsilon,b)^{n-2}\right]_{g_{ab}} \\ &- \frac{c\partial c(a)}{(n-2)!}\int_{a+\epsilon}^b dt\, g^L_{ab}(a,t)\, \left[V(a+\epsilon,b)^{n-2}\right]_{g_{ab}} . \end{aligned} \tag{4.148c}$$

The BRST operator can now act on these renormalized operators using (4.147e) since the ϵ-regulator is holding the unintegrated insertion 'away', resulting in

$$\begin{aligned}
&= -\frac{cV(a)}{(n-2)!}\left(\left[V(a+\epsilon,b)^{n-2}cV(b)\right]_{g_{ab}} - \left[cV(a+\epsilon)V(a+\epsilon,b)^{n-2}\right]_{g_{ab}}\right) \\
&\quad - \frac{cV(a)}{(n-3)!}\left[V(a+\epsilon,b)^{n-3}\right]_{g_{ab}}\left(\frac{1}{2}\partial c(b) + \frac{1}{2}\partial c(a)\right) \\
&\quad + \frac{c(a)}{(n-3)!}\int_{a+\epsilon}^{b} dt\, g^L_{ab}(a,t)\left(\left[V(a+\epsilon,b)^{n-3}cV(b)\right]_{g_{ab}} - \left[cV(a+\epsilon)V(a+\epsilon,b)^{n-3}\right]_{g_{ab}}\right) \\
&\quad + \frac{c(a)}{(n-4)!}\int_{a+\epsilon}^{b} dt\, g^L_{ab}(a,t)\ \left[V(a+\epsilon,b)^{n-4}\right]_{g_{ab}}\left(\frac{1}{2}\partial c(b) + \frac{1}{2}\partial c(a)\right) \\
&\quad - \frac{c\partial c(a)}{(n-2)!}\int_{a+\epsilon}^{b} dt\, g^L_{ab}(a,t)\ \left[V(a+\epsilon,b)^{n-2}\right]_{g_{ab}}\ .
\end{aligned} \tag{4.148d}$$

Rearranging and recombining some of the integrands into finite combinations, and in one place using the fact that $\int_{a+\epsilon}^{b} dt\ g^L_{ab}(t) = \epsilon^{-1} + O(\epsilon)$, we get

$$\begin{aligned}
&= -\frac{1}{(n-2)!}\int_{a+\epsilon}^{b} d^{n-2}t\, \overset{\circ}{\underset{\circ}{}}cV(a)\prod_{i=1}^{n-2}V(t_i)cV(b)\overset{\circ}{\underset{\circ}{}}_{g_{ab}} \\
&\quad - \frac{1}{(n-3)!}\int_{a+\epsilon}^{b} d^{n-3}t\, \overset{\circ}{\underset{\circ}{}}cV(a)\prod_{i=1}^{n-3}V(t_i)\overset{\circ}{\underset{\circ}{}}_{g_{ab}}\frac{1}{2}\partial c(b) \\
&\quad - \frac{1}{(n-3)!}\int_{a+\epsilon}^{b} d^{n-3}t\, \frac{1}{2}c\partial c(a)\overset{\circ}{\underset{\circ}{}}V(a)\prod_{i=1}^{n-3}V(t_i)\overset{\circ}{\underset{\circ}{}}_{g_{ab}} \\
&\quad + \frac{1}{(n-2)!}\int_{a+\epsilon}^{b} d^{n-2}t\left(cV(a)\overset{\circ}{\underset{\circ}{}}cV(a+\epsilon)\prod_{i=1}^{n-2}V(t_i)\overset{\circ}{\underset{\circ}{}}_{g_{ab}} - \frac{c\partial c(a)}{\epsilon}\overset{\circ}{\underset{\circ}{}}\prod_{i=1}^{n-2}V(t_i)\overset{\circ}{\underset{\circ}{}}_{g_{ab}}\right. \\
&\qquad\qquad \left. -(n-2)c(a)g^L_{ab}(a,t_1)\overset{\circ}{\underset{\circ}{}}cV(a+\epsilon)\prod_{i=2}^{n-2}V(t_i)\overset{\circ}{\underset{\circ}{}}_{g_{ab}}\right)\ .
\end{aligned} \tag{4.148e}$$

Now that we have some finite integrands, we can once again heal the hole at the left endpoint.

$$\begin{aligned}
&= -\frac{1}{(n-2)!}\left[cV(a)V(a,b)^{n-2}cV(b)\right]_g - \frac{1}{(n-3)!}\left[cV(a)V(a,b)^{n-3}\right]_g\frac{1}{2}\partial c(b) \\
&\quad - \frac{c\partial c(a)}{2(n-3)!}\left[V(a)V(a,b)^{n-3}\right]_g + \frac{c\partial^2 c(a)}{2(n-2)!}\left[V(a,b)^{n-2}\right]_g
\end{aligned} \tag{4.148f}$$

In the last term of (4.148e) we have used the expansion

$$\overset{\circ}{\circ} cV(a)cV(a+\epsilon)V(a+\epsilon,b)^{n-2} \overset{\circ}{\circ}_{g_{ab}} = O(\epsilon) \tag{4.149a}$$

$$= cV(a) \overset{\circ}{\circ} cV(a+\epsilon)V(a+\epsilon,b)^{n-2} \overset{\circ}{\circ}_{g_{ab}} - \frac{c(a)c(a+\epsilon)}{\epsilon^2} \overset{\circ}{\circ} V(a+\epsilon,b)^{n-2} \overset{\circ}{\circ}_{g_{ab}} - (n-2)c(a) \int_{a+\epsilon}^{b} dt\, g_{ab}^{L}(a,t) \overset{\circ}{\circ} cV(a+\epsilon,b)V(a+\epsilon,b)^{n-3} \overset{\circ}{\circ}_{g_{ab}} \tag{4.149b}$$

$$= cV(a) \overset{\circ}{\circ} cV(a+\epsilon)V(a+\epsilon,b)^{n-2} \overset{\circ}{\circ}_{g_{ab}} - \frac{c\partial c(a)}{\epsilon} \overset{\circ}{\circ} V(a+\epsilon,b)^{n-2} \overset{\circ}{\circ}_{g_{ab}} - \frac{1}{2} c\partial^2 c(a) \overset{\circ}{\circ} V(a+\epsilon,b)^{n-2} \overset{\circ}{\circ}_{g_{ab}} - (n-2)c(a) \int_{a+\epsilon}^{b} dt\, g_{ab}^{L}(a,t) \overset{\circ}{\circ} cV(a+\epsilon,b)V(a+\epsilon,b)^{n-3} \overset{\circ}{\circ}_{g_{ab}} \tag{4.149c}$$

to replace the parentheses in (4.148e) with $\frac{c\partial^2 c(a)}{2} \overset{\circ}{\circ} \prod_{i=1}^{n-2} V(t_i) \overset{\circ}{\circ}_{g_{ab}}$. This requires defining $\overset{\circ}{\circ} V(a)V(a+\epsilon)\dots \overset{\circ}{\circ}_{g_{ab}}$, which should technically not have any counterterm for the two fixed operators since they do not meet, but it is clear that including a $\frac{1}{(t_1-t_2)^2}$ counterterm for those two operators gives a normal ordered operator which is finite as $\epsilon \to 0$. It is also clear that which finite part we choose for that counterterm is irrelevant since the ghost factor will suppress it anyways.

It is also worth mentioning that we can use explicit third order calculations to show that any of these steps is correct at the order where the number of operators is manageable. Specifically, I have checked that at third order (4.148c) and (4.148d) both match the expected result

$$\frac{1}{2} Q_B \left[cV(a)V(a,b)^2 \right]_g = -\left[cV(a)V(a,b)cV(b) \right]_g - \frac{1}{2} cV(a)\partial c(b) + \frac{1}{2} c\partial^2 c(a)V(a,b) - \frac{1}{2} c\partial cV(a)\,. \tag{4.150}$$

Finally we add the two pieces (4.148f) and (4.146) together to see

$$\frac{Q_B}{(n-1)!} \left[cV(a)V(a,b)^{n-1} \right]_g - \frac{Q_B}{(n-2)!} \frac{1}{2} \partial c(a) \left[V(a,b)^{n-2} \right]_g \tag{4.151a}$$

$$= -\frac{1}{(n-2)!} \left[cV(a)V(a,b)^{n-2}cV(b) \right]_g - \frac{1}{(n-3)!} \left[cV(a)V(a,b)^{n-3} \right]_g \frac{1}{2} \partial c(b) - \frac{c\partial c(a)}{2(n-3)!} \left[V(a)V(a,b)^{n-3} \right]_g + \frac{c\partial^2 c(a)}{2(n-2)!} \left[V(a,b)^{n-2} \right]_g - \frac{c\partial^2 c(a)}{2(n-2)!} \left[V(a,b)^{n-2} \right]_g + \frac{1}{(n-3)!} \frac{1}{2} \partial c(a) \left[V(a,b)^{n-3} cV(b) \right]_g + \frac{c\partial c(a)}{2(n-3)!} \left[V(a)V(a,b)^{n-3} \right]_g + \frac{1}{(n-4)!} \frac{1}{2} \partial c(a) \left[V(a,b)^{n-4} \right]_g \frac{1}{2} \partial c(b) \tag{4.151b}$$

$$= -\frac{1}{(n-2)!} \left[cV(a)V(a,b)^{n-2}cV(b) \right]_g - \frac{1}{(n-3)!} \left[cV(a)V(a,b)^{n-3} \right]_g \frac{1}{2} \partial c(b) + \frac{1}{(n-3)!} \frac{1}{2} \partial c(a) \left[V(a,b)^{n-3} cV(b) \right]_g + \frac{1}{(n-4)!} \frac{1}{2} \partial c(a) \left[V(a,b)^{n-4} \right]_g \frac{1}{2} \partial c(b)\,. \tag{4.151c}$$

Multiplying by λ^n and summing this over n gives

$$Q_B\left[\left(\lambda cV(a)-\frac{\lambda^2}{2}\partial c(a)\right)e^{\lambda V(a,b)}\right]_g = -\left[\left(\lambda cV(a)-\frac{\lambda^2}{2}\partial c(a)\right)e^{\lambda V(a,b)}\left(\lambda cV(b)+\frac{\lambda^2}{2}\partial c(b)\right)\right]_g . \quad (4.152)$$

This proves that the assumption (4.5b) holds for the little g scheme at all orders.

4.3.8 Linear Renormalization

For quadratic operators we were able to define a fully linear renormalization scheme by making a specific choice for the constants $C^L = C^R = C_1$. Since C^L and C^R do not affect the solution in any way, this was like a gauge choice. Unfortunately, we saw that this big G scheme was insufficient to get finiteness at fourth order and higher. The method we used to construct a linear renormalization scheme is not particularly well suited to products of many operators, but we can still sketch how it works and show that at least for third order the little g scheme with the same choice of constants $C^L = C^R = C_1$ can be defined in terms of linear operators.

We begin with a straightforward and general extension of the quadratic result to higher orders, and define a renormalization scheme by

$$[O(t_1,\dots,t_n)]_r \stackrel{\text{def}}{=} \lim_{\epsilon\to 0}\left(e^{-L_r}\left(O(t_1,\dots,t_n)\right)\right)_\epsilon . \quad (4.153)$$

We know from section 4.2.3 that the simplest (but not finite) big G scheme can be found by choosing

$$L_G = \int dxdy\ \delta(x-y)G^L\frac{\delta}{\delta V(x)}\frac{\delta}{\delta V(y)} + \frac{1}{2}\lim_{\Delta\to 0}\int dxdy\ \left(\delta'(x-y+\Delta)-\delta'(x-y-\Delta)\right)G^E\frac{\delta}{\delta V(x)}\frac{\delta}{\delta V(y)} . \quad (4.154)$$

Since we have already thoroughly examined the allowed renormalization schemes at quadratic order, we know that the action of L_r on any two marginal operators $V(t_1)V(t_2)$ must match L_G. An appropriate choice of ansatz is then

$$L_r = \sum_{n=2}^{\infty}\int d^nx\ \mathcal{L}_n^r(x_1,\dots,x_n)\prod_{i=1}^{n}\frac{\delta}{\delta V(x_i)} , \quad (4.155)$$

with

$$\mathcal{L}_2^r(x,y) = \mathcal{L}_2^G(x,y) = G^L\delta(x-y)+\frac{1}{2}\lim_{\Delta\to 0}G^E\left(\delta'(x-y+\Delta)-\delta'(x-y-\Delta)\right) . \quad (4.156)$$

The higher order counterterms $\mathcal{L}_n^r$ with $n>2$ are not determined, giving us a huge space of possible counterterms to consider. This is not unexpected, and is how this approach generates new constants such as the $C_0^{(3)}$ and $C_o^{(3),DL}$ that we saw in section 4.3.1. Obviously the space of all functions $\mathcal{L}_n^r$ is much larger than the free parameters which are allowed at each order, but

this can be reduced somewhat by the assumptions (4.5). The assumptions give restrictions on the functions, but at arbitrary order the space will remain too large for us to fully examine.

The first restriction we can find, which follows trivially from the factorization condition (4.5d), is the need for δ-functions to put all of the operators being replaced at a single point. A coefficient, $\mathcal{L}$, which does not include some sort of δ-function would be non-zero even for operators which never meet, and violate the factorization condition.

Since operators are renormalized pairwise, we expect only counterterms in which the number of surviving operators is the same as the number we started with mod 2. At third order, the obvious candidates are

$$\mathcal{L}_3^r(x,y,z) = A^{(3)}V(x)\delta(x-y)\delta(x-z) + B^{(3)}V(x)\delta(x-y)\delta(y-z) \ . \tag{4.157}$$

Other permutations of the coordinates are redundant because the integrals in (4.155) symmetrize the result. At this point we might ask why we are not considering slightly more general counterterms, such as the second line in (4.55), which contains derivatives of the δ function. We know from the explicit third order calculations of section 4.3.1 that the only free parameters we expect at third order are $C_0^{(3)}$, $C_0^{(3),DL}$, and $C_0^{(3),DR}$, and just as linearity enforced $C^L = C^R$ at quadratic order, we expect $C_0^{(3),DL} = C_0^{(3),DR}$, so there should not be more than the two counterterms we already have in $A^{(3)}$ and $B^{(3)}$. A simple example of a counterterm we have not included is $\mathcal{L}_3' = V(x)\delta(x-y)\left(\delta'(y-z+\Delta) - \delta'(y-z-\Delta)\right)$ which when applied to the operator $V(a,b)^3$ adds a fixed marginal operator at each endpoint, $V(a)+V(b)$. This is unwanted because it will not satisfy the BRST conditions.

Using the calculations of section 4.3.8 and comparing those results to the generic third order renormalization scheme of section 4.3.1, we can show that the cubic linear operator of (4.157) gives rise to

$$C_0^{(3)} = C_0 + A^{(3)} + B^{(3)}, \quad C_0^{(3),DL} = C_0^{(3),DR} = C_0 + A^{(3)} + \frac{7}{8}B^{(3)} \ . \tag{4.158}$$

What we have discussed so far at third order is only a shift in the finite part of the big G scheme's counterterms at third order. We saw from (4.97) that there are subleading divergences at fourth order which are not cancelled by the quadratic counterterms of the big G scheme. As a result, we will require an additional counterterm at fourth order. While explicitly performing fourth order calculations can be quite difficult, the form of the difference between the big G and little g schemes suggests that we need a counterterm like

$$\mathcal{L}_4^r(x_1,x_2,x_3,x_4) \sim \frac{1}{\epsilon}\delta(x_1-x_2)\delta(x_2-x_3)\delta(x_3-x_4) + O(\ln\epsilon) \ . \tag{4.159}$$

With this approach, we could in principle write down the most general finite scheme at quartic order that satisfies conditions (4.5c) and (4.5d). Then, we would need to check that the BRST conditions do not impose any extra restriction on the free parameters. This would allow us to discover whether there are any free parameters at quartic order that affect the SFT solution in a nontrivial way, without analyzing all possible restrictions due to the replacement condition at this order. It is, of course, extremely likely that such free parameters do exist.

Linearity of the little g scheme

The little g scheme was not defined as in (4.153), so we would like to show that it is in that space of linear renormalization schemes. Although we do not have a proof that this is the case, we will find the exact form of L up to third order. Because we have exhaustively studied renormalization schemes at quadratic order, we know that linearity is only possible when $C^L = C^R = C_1$, and we must impose this condition on the constants of the little g scheme as well. Taking (4.157) as our starting point, we define a new third order renormalization scheme using

$$\mathcal{L}_3^{\tilde{g}}(x,y,z) = A^{(3)}V(x)\delta(x-y)\delta(x-z) + B^{(3)}V(x)\delta(x-y)\delta(y-z) \ . \tag{4.160}$$

We then find constants $A^{(3)}$ and $B^{(3)}$ such that $[\ldots]_{\tilde{g}} = [\ldots]_g$ at third order. We do this by evaluating the distinct operators $\left[V(a,b)^3\right]_r$, $\left[V(a)V(a,b)^2\right]_r$, and $\left[V(a,b)V(b,c)^2\right]_r$ using both renormalization schemes. For the first of these operators, it is obvious that

$$\int dxdydz\ \mathcal{L}_3^{\tilde{g}}(x,y,z)\frac{\delta}{\delta V(x)}\frac{\delta}{\delta V(y)}\frac{\delta}{\delta V(z)}V(a,b)^3 = 6\left(A^{(3)}+B^{(3)}\right)\int_a^b dt\ V(t) \ , \tag{4.161}$$

and then

$$\begin{aligned}&\left[V(a,b)^3\right]_{\tilde{g}} = \\ &\lim_{\epsilon\to 0}\left[\left(V(a,b)^3\right)_\epsilon - 3\left(\int_a^b dt\int_{\Gamma_\epsilon^{a,b}(s_1,s_2)} d^2s\ V(t)g_{ab}^D(s_1,s_2) + 2\left(A^{(3)}+B^{(3)}\right)\int_a^b dt\ V(t)\right)\right] \ .\end{aligned} \tag{4.162}$$

By comparing this to (4.96), we must choose $A^{(3)} + B^{(3)} = -3 - \ln 2$ in order to get the little g scheme. A full derivation of (4.96), as well as similar formulae for other regions, is not very instructive. The important step is simply to write down an explicit form of the region to integrate over, corresponding to the difference of the two integrals on the left hand side. The most common case is that of (4.96), so here we will include that region:

$$\begin{aligned}&\left(\int_a^b dt\int_{\Gamma_\epsilon^{a,b}} ds_1ds_2 - \int_{\Gamma_\epsilon^{a,b}} dtds_1ds_2\right)f(t,s_1,s_2) \\ &= \Bigg[\int_{a+2\epsilon}^{b-\epsilon} dt\int_{t-\epsilon}^{t+\epsilon} ds_1\int_a^{s_1-\epsilon} ds_2 + \int_{a+\epsilon}^{b-2\epsilon} dt\int_{t-\epsilon}^{t+\epsilon} ds_1\int_{s_1+\epsilon}^{b} ds_2 - \int_{a+2\epsilon}^{b-2\epsilon} dt\int_{t-\epsilon}^{t} ds_1\int_{s_1+\epsilon}^{t+\epsilon} ds_2 \\ &\qquad + \int_{a+\epsilon}^{a+2\epsilon} dt\int_a^{t-\epsilon} ds_1\int_{s_1+\epsilon}^{t+\epsilon} ds_2 + \int_{b-2\epsilon}^{b-\epsilon} dt\int_{t+\epsilon}^{b} ds_1\int_{t-\epsilon}^{s_1-\epsilon} ds_2 \\ &\quad + \int_a^{a+\epsilon} dt\int_a^{t+\epsilon} ds_1\int_{s_1+\epsilon}^{b} ds_2 + \int_{b-\epsilon}^{b} dt\int_{t-\epsilon}^{b} ds_1\int_a^{s_1-\epsilon} ds_2 + s_1 \leftrightarrow s_2\Bigg] f(t,s_1,s_2) \ .\end{aligned} \tag{4.163}$$

This holds for any function $f(t,s_1,s_2)$, but we often have a symmetric function of s_1 and s_2, in which case we can trade the exchanged indices $s_1 \leftrightarrow s_2$ for an overall factor of 2. (4.96) is derived by explicitly performing all of the integrals over s_1 and s_2 in this formula, and then series expanding in ϵ.

For the second operator we wish to check, $\left[V(a)V(a,b)^2\right]_{\tilde{g}}$, it is important that we distinguish the two terms in (4.160) because

$$\int_a^b dxdz\ V(x)\delta(x-a)\delta(x-z) = \frac{3}{8}V(a)\ , \tag{4.164a}$$

$$\int_a^b dxdz\ V(x)\delta(x-a)\delta(a-z) = \frac{1}{4}V(a)\ . \tag{4.164b}$$

With this in mind, the extra counterterms for this operator are given by

$$\begin{aligned}\int dxdydz\ \mathcal{L}_3^{\tilde{g}}(x,y,z)&\frac{\delta}{\delta V(x)}\frac{\delta}{\delta V(y)}\frac{\delta}{\delta V(z)}\left(V(a)V(a,b)^2\right)\\ &= A^{(3)}\left(2\int_a^b dydz\ V(a)\delta(a-y)\delta(a-z) + 4\int_a^b dxdz\ V(x)\delta(x-a)\delta(x-z)\right)\\ &\quad + B^{(3)}\left(2\int_a^b dydz\ V(a)\delta(a-y)\delta(y-z) + 4\int_a^b dxdz\ V(x)\delta(x-a)\delta(a-z)\right)\end{aligned} \tag{4.165a}$$

$$= \left(2A^{(3)} + \frac{7}{4}B^{(3)}\right)V(a)\ . \tag{4.165b}$$

This represents the difference between the $\tilde{g}$ scheme and the big G scheme. We compare this to the little g scheme by explicitly finding the difference between the g and G schemes for this operator. It is

$$\begin{aligned}\lim_{\epsilon\to 0}\Bigg[2\left(\int_{\Gamma_\epsilon^{a+\epsilon,b}} dtds - \int_a^b dt\int_{a+\epsilon}^b ds\right)g_{ab}^L(a,s)V(t)\\ + \left(\int_{\Gamma_\epsilon^{a+\epsilon,b}} d^2s - \int_{\Gamma_\epsilon^{ab}} d^2s\right)g_{ab}^D(s_1,s_2)V(a)\Bigg] = -2\left(3+\ln 2\right)V(a)\ .\end{aligned} \tag{4.166}$$

This tells us that $2A^{(3)} + \frac{7}{4}B^{(3)} = -2(3+\ln 2)$, which together with $A^{(3)} + B^{(3)} = -(3+\ln 2)$ means that in order for the $\tilde{g}$ and g schemes to match we must choose

$$A^{(3)} = -(3+\ln 2), \quad B^{(3)} = 0\ . \tag{4.167}$$

The final condition to check, that $\left[V(a,b)V(b,c)^2\right]_{\tilde{g}}$ matches the corresponding operator from the little g scheme, proceeds similarly. This time the delta functions are on regions which can only touch at a point, so the correction to the pairwise renormalization is

$$\int_a^b dxdydz\ \mathcal{L}_3^{\tilde{g}}(x,y,z)\frac{\delta}{\delta V(x)}\frac{\delta}{\delta V(y)}\frac{\delta}{\delta V(z)}\left(V(a,b)V(b,c)^2\right) = 0\ . \tag{4.168}$$

For the schemes to be equivalent we need to show that the corresponding little g calculation is

$$\begin{aligned}\lim_{\epsilon\to 0}\Bigg[&\left(\int_a^b dt\int_{\Gamma_\epsilon^{bc}(s_1,s_2)} d^2s - \int_a^b dt\int_{\Gamma_\epsilon^{b\vee(t+\epsilon),c}(s_1,s_2)} d^2s\right)V(t)g_{bc}^D(s_1,s_2)\\ &+2\left(\int_a^b ds_1\int_b^c dt\int_{b\vee(s_1+\epsilon)}^c ds_2 - \int_a^b ds_1\int_{\Gamma_\epsilon^{b\vee(s_1+\epsilon),c}(t,s_2)} ds_2dt\right)V(t)g_{abc}^E(s_1,s_2)\Bigg] = 0\ .\end{aligned} \tag{4.169}$$

For the first term, we can see that the region in the s_1, s_2 plane can be non-zero only when $b - \epsilon < t < b$. This further suppresses what would otherwise be a finite correction, and we find zero. The second term requires some calculation to verify, but the largest surviving correction there is $O(\epsilon \ln \epsilon)$.

At third order we needed only the one term

$$\mathcal{L}_3^g(x, y, z) = -(3 + \ln 2)V(x)\delta(x - y)\delta(x - z) \tag{4.170}$$

to correct the big G scheme and make it equivalent to the little g scheme. In the notation of section 4.3.1 the little g scheme has

$$C_0^{(3)} = C_0^{(3),DL} = C_0^{(3),DR} = C_0 - (3 + \ln 2) \ . \tag{4.171}$$

At higher orders we know that the big G scheme is not finite so there will be additional counterterms carrying the subleading divergences, and we expect additional finite contributions at each order. At any given order, however, there are many possible counterterms to add, so I expect that there will always be enough degrees of freedom to represent the little g scheme as a linear operator. We will leave any attempts to prove this for future work.

4.4 Discussion

There are a number of open questions regarding the choice of renormalization schemes and their properties. Here we briefly look at what we know and do not know about them.

4.4.1 Uniqueness

The little g scheme alone has two free parameters which alter the way operators are renormalized. The space of allowed linear renormalization schemes, while still not fully understood, looks much larger, and the space of renormalization schemes satisfying the replacement condition (4.5c) instead of full linearity is larger still. In contrast, the solutions built from these renormalized operators represent BCFT's in which the conformal boundary condition has been deformed in the same way. The BCFT is parameterized by only one parameter, λ, so we are left to wonder what the other renormalization parameters do.

We have already noticed that some of the extra parameters do not appear in the solution. This is the case for C^L and C^R, as well as $C_0^{(3),DL}$, $C_0^{(3),DR}$ and any other left- or right-constants. The solution is built from the wedge states U and A_L which only contain the fully integrated operator $[V(a,b)^n]_r$ and the operator $[O_L(a)V(a,b)^n]_r$ which is derived from the BRST transformation of the fully integrated one. Only constants which appear in the fully integrated operator will be in the solution. Constants such as C^L which naively appear in O_L must cancel against the same constant in $[cV(a)V(a,b)^n]_r$. This does not deal with the constants appearing in the fully integrated operator, however. By third order we already have C_0, C_1, and $C_0^{(3)}$ which must be understood. Using the little g scheme as an example, we will start with a renormalization scheme that chooses $C_0 = C_1 = 0$ and call it $[\ldots]_{g_0}$. Then the result (4.100) tells us that these parameters are simply a rescaling of the renormalized operator

$$\left[e^{\lambda V(a,b)}\right]_g = e^{-\lambda^2(C_0+(b-a)C_1)} \left[e^{\lambda V(a,b)}\right]_{g_0} \ . \tag{4.172}$$

To see whether this rescaling changes the solution, consider the definition (4.8b) of the wedge state U which the solution is primarily constructed from. While it may appear that C_0 gives a simple rescaling of U, the interval on which V is integrated is different at each order: $b-a = n-1$. Including a λ-dependent rescaling factor, the width of the integration interval will no longer match the number of marginal insertions, and the final expression for U will be changed. We leave the question of whether SFT solutions given by different values of C_1 and C_0 are related by a gauge transformations to future work, and offer only one more observation: introducing a nonzero C_1 is the same as replacing $V(t)$ with $V(t) - \lambda C_1$. It is worth mentioning that the C_1 dependence of the derivative in (4.53b) can be found from this rescaling. Clearly

$$\partial_a \left(e^{-\lambda^2(C_0+(b-a)C_1)} \left[e^{\lambda V(a,b)} \right]_{g_0} \right) = e^{-\lambda^2(C_0+(b-a)C_1)} \partial_a \left[e^{\lambda V(a,b)} \right]_{g_0} + \lambda^2 C_1 \left[e^{\lambda V(a,b)} \right]_g \quad (4.173)$$

produces the C_1 term in (4.53b), but the C^L dependence must still be found separately in order to make the result independent of that constant.

Leaving now the confines of the renormalization scheme defined in section 4.3, we can ask whether changing $C_0^{(3)}$ changes the SFT solution. It is easy to see that generalizing the rescaling in equation (4.172) to include higher order terms, as in

$$\left[e^{\lambda V(a,b)} \right]_{\tilde{g}} = e^{-(C_0\lambda^2+C_0^{(4)}\lambda^4+\ldots)-(C_1\lambda^2+C_1^{(4)}\lambda^4+\ldots)(b-a)} \left[e^{\lambda V(a,b)} \right]_{g_0} , \quad (4.174)$$

does not result in a change of $C_0^{(3)}$ from the value it has in the scheme of section 4.3, $C_0^{(3)} = -(3+\ln 2) + C_0$. There is, however, another simple change in the renormalization schemes which does affect $C_0^{(3)}$: a renormalization of the perturbation parameter λ. Specifically, we can take

$$\left[e^{\lambda V(a,b)} \right]_{\tilde{g}} = \left[e^{(\lambda+6\Delta C_0^{(3)}\lambda^3+\ldots)V(a,b)} \right]_g , \quad (4.175)$$

where $\Delta C_0^{(3)} = C_0^{(3)} + (3+\ln 2) - C_0$. The conclusion is then that changing $C_0^{(3)}$ away from $-(3+\ln 2) + C_0$ does affect the SFT solution, but in a benign and easy to understand way: by reparameterizing the deformation flow. This observation also explains why there is no independent parameter $C_1^{(3)}$.

4.4.2 Boundary Condition Changing Operators

We might assume (as has been the focus of recent work [39]) that the point where the boundary condition is changed behaves as if a boundary condition changing operator σ was inserted there. Specifically, a BCFT with $\sigma_L(a)\sigma_R(b)$ inserted on the boundary has a new boundary condition between a and b and the original boundary condition elsewhere. In our case this is implemented using

$$\sigma_L(a)\sigma_R(b) = \left[e^{\lambda V(a,b)} \right]_r \quad (4.176)$$

without having to know an explicit form of the local operators $\sigma_{L/R}$. As a result we know that

$$Q_B \left(\sigma_L(a)\sigma_R(b) \right) = \left[e^{\lambda V(a,b)} O_R(b) \right]_r - \left[O_L(a) e^{\lambda V(a,b)} \right]_r , \quad (4.177)$$

but for any conformal primary operator ϕ_h with conformal weight h, we would expect that [47]

$$Q_B\phi_h(t) = c(t)\partial_t\phi_h(t) + h\left(\partial c(t)\right)\phi_h(t) \ . \tag{4.178}$$

These two results suggest that

$$\left[O_L(a)e^{\lambda V(a,b)}\right]_r = -c(a)\partial_a\left[e^{\lambda V(a,b)}\right]_r - h(\lambda)\partial c(a)\left[e^{\lambda V(a,b)}\right]_r \ . \tag{4.179}$$

We saw in (4.53b) how the derivative acts on quadratic operators, so expanding (4.179) at order λ^2 we see

$$\begin{aligned}&[cV(a)V(a,b)]_r - \frac{1}{2}\partial c(a) + C^L c(a) \\ &\qquad = [cV(a)V(a,b)]_r - (C_1 - C^L)c(a) - \sum_{l=0}^{2}\frac{1}{(2-l)!}h^{(l)}\partial c(a)\left[V(a,b)^{2-l}\right]_r \ ,\end{aligned} \tag{4.180}$$

where $h^{(l)}$ are the taylor coefficients of the conformal weight $h(\lambda)$. This equation is only satisfied if $h(\lambda) = \frac{\lambda^2}{2}$ and $C_1 = 0$. C_1 was a free parameter in the construction of a SFT solution, and can still take any value, but this suggests that the boundary condition changing operator corresponding to the new boundary condition is only primary if the operators are renormalized with $C_1 = 0$.

As usual, at higher orders there is still more to consider, but in this case there may not be any further restrictions. At third order, using the ansatzes of section 4.3.1 it is straightforward to show that

$$\partial_a\left[V(a,b)^3\right]_r = -3\left[V(a)V(a,b)^2\right]_r + 6V(a,b)\left(C_1 - C^L\right) + 6V(a)\left(C_0^{(3)} - C_0^{(3),DL}\right) \ . \tag{4.181}$$

The first BRST condition, (4.5a), can also be worked out at third order while including the extra constants $C_0^{(3)}$, $C_0^{(3),DL}$, and $C_0^{(3),DR}$. This results in slightly altered operators at the endpoints.

$$O_L(a) = \lambda cV(a) - \frac{1}{2}\lambda^2\partial c(a) + \lambda^2 C^L c(a) + \lambda^3\left(C_0^{(3),DL} - C_0^{(3)}\right)cV(a) + O(\lambda^4) \tag{4.182a}$$

$$O_R(b) = \lambda cV(b) + \frac{1}{2}\lambda^2\partial c(b) + \lambda^2 C^R c(b) + \lambda^3\left(C_0^{(3),DR} - C_0^{(3)}\right)cV(b) + O(\lambda^4) \tag{4.182b}$$

This has the same extra terms as the derivative, so the condition $C_1 = 0$ is still enough to give a primary boundary condition changing operator with conformal weight $h(\lambda) = \frac{\lambda^2}{2}$.

In many works, when arbitrary boundary condition changing operators are considered, it is assumed for simplicity that they are primary. Here we see a case where the boundary conditions related to generic renormalization require non-primary bcc operators. It is surprising that a change to the renormalization scheme, which we expect to correspond to a gauge transformation or reparameterization of λ, can have such an impact on the associated bcc operator. We saw in section 4.4.1 that the C_1 dependence of the derivative comes from rescaling the exponential operator. In this context it is natural that $C_0^{(3)}$ should not affect the primarity of the bcc operator since that rescaling is simply a reparameterization of λ, while the other constants are a more complicated rescaling. This represents a possible topic of further investigation.

We know that the BRST operator is similar to a derivative and a c ghost when acting on the marginal operator $V(a, b)$, so it should not be surprising that the additional terms at higher orders are the same as those appearing in the derivative. If this relationship holds at all orders it could greatly simplify the calculation of $O_{L/R}$ at arbitrary order, but any proof of such a claim would likely entail the calculation of corrections to $O_{L/R}$ for arbitrary counterterms anyways. Alternatively, similarities between Q_B and the derivative might lead to a better understanding of how to prove the BRST conditions. This remains an open question.

Chapter 5

Rolling Tachyon

Now that we have examined the algebraic structure of renormalized integrated marginal operators, we will apply this knowledge to a specific case: the rolling tachyon. This is particularly instructive due to the existence of previously studied and related solutions with regular self-OPE. We can use our renormalization scheme to examine how the presence of renormalized operators affects the solution.

We will begin this chapter by summarizing our results and their relation to the literature. This is followed by the details of the tachyon profile and a discussion of the results. We then proceed to discuss how the calculations were performed. This begins in sections 5.3.1-5.3.6 with an explanation of the computer program written to construct the solution algebraically. In section 5.3.7 we discuss how numerical integration was performed, and how floating point roundoff errors due to the counterterms were handled. In this section we also examine the equation of motion and the action in order to check the validity of our results and see how accurate the numerical process is and whether the results converge as the precision of the numerical process is increased.

Most of this chapter has been posted on the arXiv [3] and has recently been accepted for publication by the Journal of High Energy Physics.

5.1 Rolling Tachyon Introduction and Conclusions

As we have seen, in a boundary CFT the boundary condition can be deformed on any section of the boundary by exponentiating a marginal operator integrated along it, as in

$$e^{\lambda \int dt\, V(t)} \ . \tag{5.1}$$

The marginal parameter λ controls the strength of the deformation. In Open String Field Theory, allowed D-brane configurations are in one to one correspondence with classical solutions. The rolling tachyon is the time-dependent solution which corresponds to a decaying D-brane. There are two rolling tachyon solutions obtained by different marginal deformations of the D-brane CFT. The simpler case, the exponential rolling tachyon, involves the marginal operator $V(t) = e^{X^0(t)}$ and represents a D-brane which exists in the infinite past and then decays at a finite time. This case has been studied using level truncation methods [35, 48] as well as analytically [5, 33, 34], and is relatively simple because the OPE of the marginal operator with itself is finite. The more difficult case uses the time-symmetric marginal operator $V = \sqrt{2}\cosh(X^0)$, which has the singular self-OPE $V(0)V(x) \sim \frac{1}{x^2}$. This rolling tachyon corresponds to placing a D-brane at $t = 0$ and letting it decay at both $t = -\infty$ and $t = +\infty$. Notice that this t is time and not the worldsheet boundary coordinate frequently referred to in chapter 4.

In SFT, the tachyon profile is the tachyon component of the string field as a function of time. Higher level modes are, of course, part of the solution Ψ, but are not calculated. In the

symmetric case, the tachyon profile has the form

$$T(t) = 2\sum_{n=1}^{\infty}\sum_{j=0}^{\lfloor n/2\rfloor} \lambda^n \beta_n^{(j)} \cosh((n-2j)t) \ , \tag{5.2}$$

where $\beta_n^{(j)}$ are coefficients which can be calculated numerically and $\lfloor n/2\rfloor$ is the greatest integer less than or equal to $n/2$, so that $n-2j \geq 0$. In this notation the deformation strength λ is taken to be negative for physical solutions [5]. In the exponential case, λ controls the time at which the D-brane decays, while for the time-symmetric case it determines the lifetime of the D-brane, with longer lifetimes corresponding to λ closer to zero.

In BCFT studies of D-brane decay such as [49, 50] it was noticed that the point $\lambda_{\text{BCFT}} = \frac{1}{2\sqrt{2}}$ should exhibit some kind of special behaviour with this normalization for V. The recent work of [51] tells us that the parameter λ here is equivalent to the BCFT parameter for small λ (up to the sign, which is a matter of convention), but that the precise relationship for stronger deformations is in fact gauge-dependent. They also found that λ_{SFT} in string field theory has a maximum which occurs close to, but not in general at, the critical value of the BCFT parameter. This does not represent any limitation on λ_{BCFT}, as the relationship is not one-to-one, and it does not necessarily limit our λ parameter either, as the relationship between it and λ_{SFT} of [51] will also have higher order corrections. In any event, since the solution we study is written as a taylor series about $\lambda = 0$, we should not expect such features at large λ to be evident.

In the regular OPE case, instead of the double sum and time-symmetric cosh functions, energy conservation tells us that there is only a single sum of exponentials involving coefficients with $\beta_n^{(0)}$:

$$T_{\text{reg}}(t) = \sum_{n=1}^{\infty} \lambda^n \beta_n^{(0)} e^{nt} \ . \tag{5.3}$$

While the $\beta_n^{(j)}$ are in general gauge-dependent, for one choice of gauge it was proven that the sum in the regular OPE case converges for all λ, with the asymptotic behaviour $\beta_n^{(0)} \sim e^{-\gamma n^2}$ [34]. Numerical data suggests that this is true in other gauges as well, as shown in figure 5.3b. The trouble with this is that the tachyon profile itself exhibits wild oscillations which grow exponentially in magnitude, while the vacuum without any D-branes is a well defined and finite point in string field space. How these two very different looking string fields are reconciled has been the source of much speculation (see, for example, [27]). Both that work and the calculation of the boundary state in [40, 41] indicate that these wild oscillations are not physical. The boundary state appears to asymptotically approach the tachyon vacuum despite the component fields taking values which are very different. This may imply that there is a time-dependent gauge transformation relating the rolling tachyon solution to one where the string field smoothly interpolates the perturbative and tachyon vacuum states. It has also been suggested that the energy of the D-brane should be radiated away in the form of closed strings, and the wild oscillations come from attempting to describe closed string physics using only open strings. Our results confirm that the tachyon profile has the same growing oscillatory behaviour in the time-symmetric case, and do not appear to exclude any of the current hypotheses.

When studying the marginal operator $V = \sqrt{2}\cosh(X^0)$ leading to the time-symmetric rolling tachyon, we must be careful to avoid singularities arising from the operator's OPE.

Analytic solutions for marginal deformations require the insertion of many copies of the marginal operator with separations that are integrated over, and there will be divergences when two operators approach each other. Fortunately there are several solutions which are intended to handle this issue [36, 37, 38, 39]. The most recent work, by Erler and Maccaferri, does not apply to solutions which have a non-trivial time direction, so we cannot use it for the rolling tachyon. Fuchs, Kroyter and Potting's solution was designed with the photon marginal deformation in mind, but it is possible that it could describe the rolling tachyon as well. The solution of [38] is a generalization of [34] to operators with singular OPE, and it could be applied to the rolling tachyon. In fact it has been suggested that this solution could give the tachyon profile in the form (5.9), which would help settle the convergence issue.

Our focus, however, will be on the work of Kiermaier and Okawa. They proposed the general construction dependent on the existence of a suitable renormalization scheme [36], which we investigated and refined in chapter 4. We found a general renormalization scheme satisfying the necessary conditions and showed that it has at least two free parameters, suggesting that the tachyon profile could have free parameters as well. Here we will perform the first explicit numerical calculations for the time-symmetric rolling tachyon solution, and we will show that the tachyon profile is a finite function which does in fact depend on the free parameters.

When we implement the solution Ψ of [36] with our renormalization scheme we can find the tachyon profile for the symmetric rolling tachyon. This involves algebraically constructing the wedge states with insertions corresponding to the solution, taking expectation values, and then performing the required integrals numerically. Here this is done up to 6th order in λ. It will have the form (5.2), where now the function is symmetric in t and all the $\beta_n^{(j)}$ are non-zero. The marginal operator $\sqrt{2}\cosh(X^0)$ contains the operators $e^{\pm X^0}$ with both signs, and the coefficients $\beta_n^{(j)}$ correspond to terms with $n-j$ factors of one of the two operators and j factors of the other. Since renormalization has the effect of adding counterterms for collisions of operators with opposite sign, the $j=0$ coefficients involve no counterterms and behave very similarly to exponential solutions. These show the same $\beta_n^{(0)} \sim e^{-\gamma n^2}$ asymptotic behaviour, implying that the sum $\sum_{n=1}^{\infty} \lambda^n \beta_n^{(0)} \cosh(nt)$ converges absolutely for all λ. For $|\lambda| \ll 1$, as is the case when the D-brane survives for a long time, the $j>0$ coefficients are suppressed due to extra factors of λ. This results in a decay process which looks very much like the regular case, as the decay is well separated from the "anti-decay" by the D-brane's lifetime. Once this lifetime is long enough, further shrinking λ even has the same effect on the decay time as it would with the exponential rolling tachyon, simply shifting the time of the decay.

For the $\beta_n^{(j)}$ coefficients with $j>0$, each coefficient is calculated using a number of counterterms determined by j. The counterterms in turn are functions of the two parameters of the renormalization scheme, C_0 and C_1. The bulk coefficients are therefore polynomial functions of C_0 and C_1. Because these coefficients are not constants, patterns such as the asymptotic behaviour for $j=0$ could depend on the choice of C_0 and C_1. Considering only the $j=1$ coefficients, with $C_0 = C_1 = 0$ they are quite a good fit to $\beta_n^{(1)} \sim e^{-\gamma_1 (n-2)^3}$. In fact there is no choice of those constants for which the exponential quadratic behaviour $\beta_n^{(1)} \sim e^{-\gamma_1 (n-2)^2}$ fits as closely. This suggests that the sum $\sum_{n=2}^{\infty} \lambda^n \beta_n^{(1)} \cosh((n-2)t)$ also converges, but there may still be some choices of C_0 and C_1 for which this is not the case, or for which the radius of convergence in λ is finite. For example, choosing the constants so that $\beta_n^{(1)}$ are a best fit to the exponential cubic behaviour results in $\beta_n^{(2)}$ which are increasing, at least for the three

coefficients we can calculate with $j = 2$.

So how does the inclusion of all the $\beta_n^{(j)}$ coefficients affect the shape of the tachyon profile? We show that for $|\lambda| \ll 1$ these coefficients are negligible, but as the D-brane lifetime is decreased there comes a point where more coefficients must be considered. Some terms cease to dominate for any range of time, and the number of oscillations actually decreases. The missing oscillation means that the effective "period" is significantly decreased. What this means physically is not clear, since the period is a gauge dependent quantity related to the coefficient γ in the exponent of the asymptotic behaviour. The tachyon profile for small λ is very similar to that of [5], while for larger λ it has some features similar to the tachyon profile of [34], so perhaps the solution is interpolating between regular-OPE solutions in different gauges as the marginal deformation strength is changed. Understanding this phenomenon is left for future work.

While here we will only calculate the tachyon profile, it would be interesting in the future to study the boundary state using the approach of [41]. Previous work on the boundary state for time-asymmetric rolling tachyon solutions suggests that it is the same as predicted by BCFT, and our results suggest that we can expect that that would hold true for the time-symmetric rolling tachyon at weak deformation parameter as well. For larger λ, however, it would be very interesting to see if the renormalization parameters really are gauge, or if they affect the boundary state. In particular, C_1 controls whether the boundary condition changing operator is a conformal primary, and it is not at all clear what physical effect that will have.

5.2 The Tachyon Profile

The solution of [36] presents a promising framework for construction of a time-symmetric rolling tachyon solution, but it was not applied to any specific marginal deformation. Taking that approach and inserting the marginal deformation $V = \sqrt{2}\cosh(X^0)$ we are able to numerically compute the tachyon profile up to 6th order in the deformation parameter λ. Since the tachyon profile has previously been calculated for several exponential rolling tachyon solutions, we can compare our results in order to determine what qualitative differences appear in the time-symmetric case. It is also useful to have explicit numerical evidence that the renormalization scheme we found in chapter 4 is effective and the solution remains finite despite the singular OPE that the marginal operator has with itself.

The solution takes the form of a wedge state with insertions on the boundary. While one insertion will always be at a fixed location, the rest are integrated. The renormalization procedure replaces pairs of operators with appropriate counterterms under the integral. Each operator V contains two terms carrying ± 1 unit of "momentum" in the time direction, but the counterterms are functions and carry no momentum. In (5.2) the coefficient $\beta_n^{(j)}$ clearly contains the part of the tachyon profile with n factors of λ and $k = n - 2j$ units of this momentum, so it follows that the coefficients $\beta_n^{(0)}$ contain no counterterms. This is as it should be since operators $e^{\pm X^0}$ with the same sign have a regular OPE; the singular OPE of the $\cosh(X^0)$ marginal operator comes entirely from the collision of exponentials with opposite sign. The index j, which counts the momentum deficit, also has the effect of counting the maximum number of counterterm factors. For the coefficients $\beta_n^{(j)}$, table 5.1 shows their values as calculated by the `Cuhre` algorithm, and with the exception of two terms we will use those coefficients. For technical reasons explained in section 5.3.7, the two terms marked with asterisks will use values

found by the `Suave` algorithm instead, and those are shown in table 5.2. Occasionally we will want to think of the tachyon profile in terms of these timelike momentum modes, and write

$$T(t) = \sum_{k=0}^{\infty} 2\cosh(kt) \sum_{n=k}^{\infty} \lambda^n \beta_n^{\left(\frac{n-k}{2}\right)} \ . \tag{5.4}$$

This form is equivalent to (5.2) as long as we define $\beta_n^{(j)}$ to vanish for non-integer j, as well as for $n = j = 0$.

The tachyon profile for several different solutions with regular OPE has been calculated before. It has the simpler form of $T(t) = \sum_{n=0}^{\infty} \lambda^n \beta_n \sqrt{2}^n e^{nt}$ where the coefficients $\beta_n \stackrel{\text{def}}{=} \beta_n^{(0)}$ are only non-zero for maximal momenta. In table 5.3 we compare the coefficients for those solutions to the ones we have found. We have changed the normalization of their coefficients by $2^{-\frac{n}{2}}$ for better comparison with our coefficients, due to the relative normalizations of the marginal operators e^{X^0} and $\sqrt{2}\cosh(X^0)$. Our coefficients show very similar falloff to [5] as n is increased, though we do not expect exact agreement between any of the sets of coefficients because the tachyon profile is a gauge dependent quantity. We believe that each of these lists is related to the others by such gauge transformations, but constructing them is beyond the scope of this work.

As in [5], we take λ to be negative in order to study physical solutions. With this assumption, the tachyon profile (5.2) can be rewritten as

$$T(t) = \sum_{n=1}^{\infty} \sum_{j=0}^{\lfloor n/2 \rfloor} (-1)^n \beta_n^{(j)} \left(e^{n(\ln|\lambda|+t)-2jt} + e^{n(\ln|\lambda|-t)+2jt} \right) \ , \tag{5.5}$$

where in practice the sum over n only runs up to some cutoff N where the coefficients can be computed. When only the $j = 0$ coefficients and the first term in parentheses are considered, as in the regular OPE case, we can clearly see that a change of $\ln|\lambda|$ will only shift the time of the D-brane decay. For the singular case, however, the tachyon profile will have a different shape depending on the strength of the marginal deformation, controlled by $\ln|\lambda|$. The renormalization scheme also contains the constants C_0 and C_1, which will appear nontrivially in $\beta_n^{(j)}$ with $j > 0$.

5.2.1 Small λ

We begin our analysis with the case $|\lambda| \ll 1$, where only the coefficients $\beta_n^{(0)}$ need to be considered. Following the notation of [5, 34], we will refer to these coefficients as $\beta_n \stackrel{\text{def}}{=} \beta_n^{(0)}$. We will focus on (5.5), which receives significant contributions from the first term in parentheses when $t > 0$ and from the second term when $t < 0$. Knowing that $T(t)$ is an even function, we will assume $t > 0$ and not need to consider the second term. Since we are considering $-1 \ll \lambda < 0$, each term in the sum of (5.5) will be suppressed by the exponential until t is large compared to $-\ln|\lambda|$. For a large fixed t, terms with $j > 0$ will be small relative to others, so only the $j = 0$ coefficients need to be considered. Since this is the case, the tachyon profile does not depend on the renormalization constants C_0 and C_1 at all. This had to be the case since there is no renormalization when all of the marginal operators have momentum in the same direction. We can then unambiguously plot the tachyon profile for small $|\lambda|$. In figure 5.1 we

n	j	$\beta_n^{(j)}$
1	**0**	$\frac{1}{\sqrt{2}}$
2	1	$(-1.29904\ldots \pm 3\cdot 10^{-11}) + (0 \pm 1\cdot 10^{-14})C^L$
2	**0**	$(0.0760297\ldots \pm 8\cdot 10^{-16})$
3	1	$(-1.30572 \pm 4.3\cdot 10^{-5}) - (0.707107\ldots \pm 3\cdot 10^{-14})C_1 - (0 \pm 2\cdot 10^{-4})C^L$
3	**0**	$(9.150 \pm 0.019)\cdot 10^{-4}$
4	2	$(0.655579 \pm 6\cdot 10^{-6}) + (0 \pm 3\cdot 10^{-4})C^L + (3.2858 \pm 0.0021)C_1 + (4.9 \pm 7.8)\cdot 10^{-15}C^LC_1$ $+(0 \pm 1\cdot 10^{-3})C_0 + (0 \pm 1\cdot 10^{-14})C^LC_0$
4	1	$-(0.4488 \pm 0.0031) + (0 \pm 8\cdot 10^{-4})C^L - (0.2349 \pm 0.0023)C_1 + (1.4 \pm 0.7)\cdot 10^{-7}C_0$
4	**0**	$(1.17222 \pm 0.00013)\cdot 10^{-6}$
5	2	$(0.723 \pm 0.011) + (0 \pm 1\cdot 10^{-3})C^L + (4.387 \pm 0.041)C_1 + (0 \pm 0.02)C^LC_1 + (3.53553\ldots \pm 7\cdot 10^{-15})C_1^2$ $+(0 \pm 6\cdot 10^{-3})C_0 + (0 \pm 0.01)C^LC_0$
5	1	$(-0.01221 \pm 1.2\cdot 10^{-4}) + (0 \pm 2\cdot 10^{-5})C^L - (5.86 \pm 0.34)\cdot 10^{-3}C_1 - (1.27 \pm 0.61)\cdot 10^{-4}C_0$
5	**0**	$(1.598 \pm 0.007)\cdot 10^{-10}$
6	3	$(-0.3 \pm 0.4)^* + (0 \pm 3\cdot 10^{-3})C^L - (2.572 \pm 0.026)C_1 + (0.3 \pm 1.2)\cdot 10^{-3}C^LC_1 - (23.9401 \pm 0.0013)C_1^2$ $+(1.5 \pm 3.1)\cdot 10^{-14}C^LC_1^2 + (0.0955 \pm 0.0030)C_0 + (0 \pm 5\cdot 10^{-3})C^LC_0 - (0.135 \pm 0.015)C_0C_1$ $-(1.2 \pm 3.9)\cdot 10^{-14}C^LC_0C_1 + (5.8 \pm 1.5)\cdot 10^{-6}C_0^2$
6	2	$(0.4991 \pm 0.0050) + (0.4 \pm 1.3)\cdot 10^{-5}C^L + (1.912 \pm 0.019)C_1 + (0.8 \pm 4.1)\cdot 10^{-3}C^LC_1 + (1.715 \pm 0.024)C_1^2$ $+(1.879 \pm 0.025)\cdot 10^{-2}C_0 + (0 \pm 2\cdot 10^{-3})C^LC_0 + (4.77 \pm 0.38)\cdot 10^{-2}C_0C_1 - (2.37 \pm 0.09)\cdot 10^{-7}C_0^2$
6	1	$(-2.686 \pm 0.027)\cdot 10^{-5} - (1.6 \pm 5.9)\cdot 10^{-8}C^L - (9.1 \pm 2.2)\cdot 10^{-6}C_1 - (7.3 \pm 0.7)\cdot 10^{-7}C_0$
6	**0**	$(2.18 \pm 0.04)\cdot 10^{-15}$ *

Table 5.1: Deterministic results for the non-zero coefficients $\beta_n^{(j)}$ of the tachyon profile for the cosh rolling tachyon with singular self-OPE. Results are calculated with the `Cuhre` and `QAG` algorithms. The constant C^L is part of the renormalization scheme, but it can not influence the solution, so we safely set it to zero in our analysis. C^L was included in these numerical results only to demonstrate that it does not contribute to the solution at all.

* These two coefficients found using the Cuhre algorithm appear to be unreliable, so the corresponding Suave results in table 5.2 will be used for analysis instead.

n	j	$\beta_n^{(j)}$
1	**0**	$\frac{1}{\sqrt{2}}$
2	1	$-(1.2985 \pm 0.0003) - (4.134 \pm 0.007) \cdot 10^{-6} C^L$
2	**0**	$(7.61 \pm 0.07) \cdot 10^{-2}$
3	1	$-(1.301 \pm 0.005) - (0.001 \pm 0.010) C^L - (0.707107\ldots \pm 7 \cdot 10^{-18}) C_1$
3	**0**	$(8.99 \pm 0.09) \cdot 10^{-4}$
4	2	$(0.659 \pm 0.007) + (0.2 \pm 2.6) \cdot 10^{-3} C^L + (3.288 \pm 0.003) C_1 + (0 \pm 1 \cdot 10^{-17}) C_1 C^L + (0.5 \pm 3.4) \cdot 10^{-3} C_0$ $+(0 \pm 5 \cdot 10^{-9}) C_0 C^L$
4	1	$-(0.449 \pm 0.004) - (0.1 \pm 1.4) \cdot 10^{-3} C^L - (0.235 \pm 0.002) C_1 + (1.39 \pm 0.07) \cdot 10^{-4} C_0$
4	**0**	$(1.163 \pm 0.002) \cdot 10^{-6}$
5	2	$(0.722 \pm 0.012) + (1.3 \pm 1.3) \cdot 10^{-3} C^L + (4.38 \pm 0.04) C_1 + (0.014 \pm 0.034) C_1 C^L + (3.53553\ldots \pm 3 \cdot 10^{-8}) C_1^2$ $+(0.1 \pm 6.5) \cdot 10^{-3} C_0 - (0.3 \pm 1.3) \cdot 10^{-2} C_0 C^L$
5	1	$-(1.21 \pm 0.01) \cdot 10^{-2} + (2.2 \pm 1.1) \cdot 10^{-5} C^L - (5.81 \pm 0.06) \cdot 10^{-3} C_1 - (1.17 \pm 0.01) \cdot 10^{-4} C_0$
5	**0**	$(1.27 \pm 0.01) \cdot 10^{-10}$
6	3	$-(0.307 \pm 0.004) - (1.6 \pm 2.9) \cdot 10^{-3} C^L - (2.55 \pm 0.05) C_1 + (0.5 \pm 3.6) \cdot 10^{-2} C_1 C^L - (23.943 \pm 0.008) C_1^2$ $+(0 \pm 1 \cdot 10^{-17}) C_1^2 C^L + (9.5 \pm 0.5) \cdot 10^{-2} C_0 - (8.0 \pm 6.6) \cdot 10^{-3} C_0 C^L - (0.12 \pm 0.02) C_0 C_1$ $+(0 \pm 1 \cdot 10^{-17}) C_0 C_1 C^L + (5.0 \pm 4.4) \cdot 10^{-5} C_0^2$
6	2	$(0.497 \pm 0.005) - (2.1 \pm 1.1) \cdot 10^{-4} C^L + (1.92 \pm 0.02) C_1 - (1.7 \pm 2.6) \cdot 10^{-3} C_1 C^L + (1.718 \pm 0.013) C_1^2$ $+(1.774 \pm 0.014) \cdot 10^{-2} C_0 - (1.2 \pm 2.3) \cdot 10^{-3} C_0 C^L + (4.71 \pm 0.05) \cdot 10^{-2} C_0 C_1 - (1.156 \pm 0.016) \cdot 10^{-4} C_0^2$
6	1	$-(2.54 \pm 0.02) \cdot 10^{-5} - (3.5 \pm 0.3) \cdot 10^{-8} C^L - (1.222 \pm 0.012) \cdot 10^{-5} C_1 - (7.618 \pm 0.014) \cdot 10^{-7} C_0$
6	**0**	$(2.3 \pm 0.3) \cdot 10^{-15}$

Table 5.2: `Suave` results for the non-zero coefficients $\beta_n^{(j)}$ of the tachyon profile for the cosh rolling tachyon with singular self-OPE. These Monte Carlo results are shown for comparison with the deterministic results of table 5.1.

	[5]	[34]	[35]	Ψ here
n	β_n			
1	$\frac{1}{\sqrt{2}}$	$\frac{1}{\sqrt{2}}$	$\frac{1}{\sqrt{2}}$	$\frac{1}{\sqrt{2}}$
2	0.0760295	0.290	0.0760297	0.0760297
3	$7.59312 \cdot 10^{-4}$	0.0506	$7.732 \cdot 10^{-4}$	$9.149 \cdot 10^{-4}$
4	$6.54812 \cdot 10^{-7}$	$4.18 \cdot 10^{-3}$	$9.8145 \cdot 10^{-7}$	$1.173 \cdot 10^{-6}$
5	$4.93424 \cdot 10^{-11}$	$1.54 \cdot 10^{-4}$	$8.734 \cdot 10^{-11}$	$1.275 \cdot 10^{-10}$
6	$3.50136 \cdot 10^{-16}$	$2.45 \cdot 10^{-6}$	$7.903 \cdot 10^{-13}$	$2.26 \cdot 10^{-15}$
7	$2.41180 \cdot 10^{-22}$	$1.64 \cdot 10^{-8}$		

Table 5.3: Comparison of rolling tachyon profile for three previously calculated solutions with regular self-OPE. Calculated from the solutions of [5], [34], and [35]. The $n = k$ coefficients for our calculations based on [36] are included for comparison.

see $\ln|T(t)|$ for $\ln|\lambda| = -4$. Each "peak" represents the range of t for which $T(t)$ is dominated by a specific exponential in the sum. For different values of $|\lambda|$ the shape of the oscillating part of the tachyon profile remains unchanged, and the whole half-plot shifts horizontally, with the size of the plateau in the middle changing as expected.

The size of the plateau which describes the time when the D-brane exists can be estimated by the time of the first zero of the tachyon profile. This time is plotted in figure 5.2a, and is linear for the region where $|\lambda| \ll 1$ is valid. The slope is -1 as it had to be from (5.5) when t is significantly larger than 0. We can also examine the "period" of the oscillations. The oscillations result from each exponential overtaking the one before, so we can calculate an estimate of their spacing by setting adjacent terms to be equal.

$$\beta_n e^{n(\ln|\lambda|+t_n)} = \beta_{n+1} e^{(n+1)(\ln|\lambda|+t_n)} \tag{5.6a}$$

$$t_n = -\ln|\lambda| + \ln\left(\frac{\beta_n}{\beta_{n+1}}\right) \tag{5.6b}$$

$$\Delta t_n = \ln\left(\frac{(\beta_n)^2}{\beta_{n-1}\beta_{n+1}}\right) \tag{5.6c}$$

While there is no reason to expect this a priori, let us suppose that Δt is a constant. In this case we have

$$\frac{\beta_{n+1}}{\beta_n} = e^{-\Delta t}\frac{\beta_n}{\beta_{n-1}} \ , \tag{5.7a}$$

which is a recursion relation with the solution

$$\beta_n \propto \rho^n e^{-\frac{n^2}{2}\Delta t} \ . \tag{5.7b}$$

The factor ρ^n can always be removed by taking $\beta_n^{(j)} \to \frac{\beta_n^{(j)}}{\rho^n}$ and simultaneously $\lambda \to \lambda\rho$, which does not alter the tachyon profile. In one particular solution for the rolling tachyon with regular OPE, Kiermaier, Okawa, and Soler [34] found that their solution's coefficients had the asymptotic behaviour

$$\beta_n \sim e^{-\gamma n^2 + O(n\ln n)} \ , \tag{5.8}$$

and in [33] it was shown that a solution equivalent to the one in [5] has coefficients which closely fit $b_n \sim e^{-\gamma n^2}$ without significant corrections. We have just shown that this same recurring

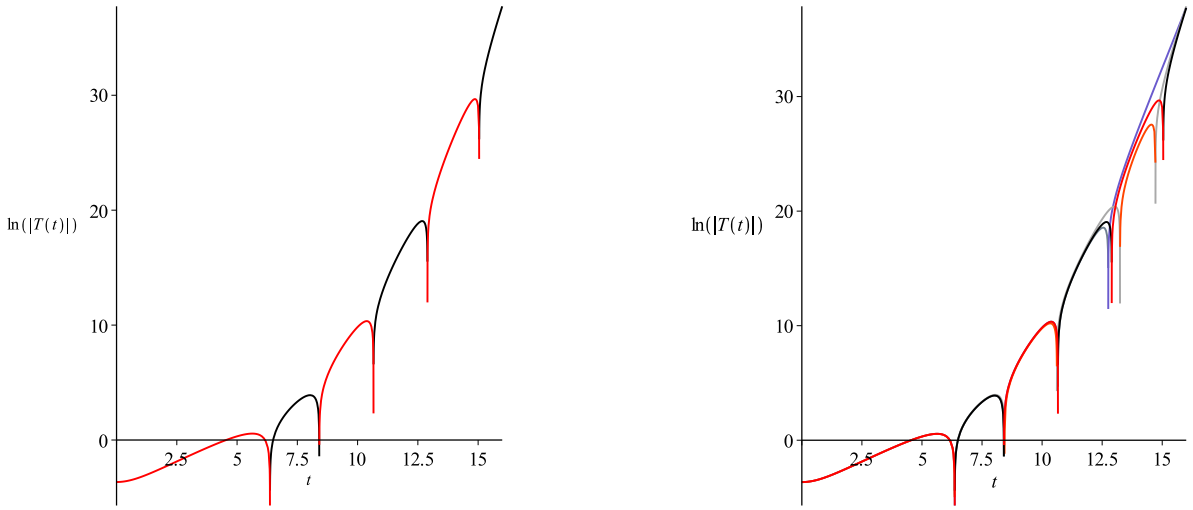

Figure 5.1: The tachyon profile $T(t)$ with only the $j = 0$ coefficients considered. This is plotted for $\ln|\lambda| = -4$, where the approximation is valid. a) Black is for positive values of $T(t)$ and red is for negative values. b) The tachyon profile with all `Suave` coefficients from table 5.2 is also shown in orange and grey, and where the `Cuhre`-only results deviate is indicated with a blue line. We can see that the `Suave` results are qualitatively equivalent to the ones we use.

pattern can be derived from the assumption of exponentially growing oscillations with constant period. In figure 5.3 we see the best fit lines for our $j = 0$ coefficients, as well as those of several other known solutions, to the form $\beta_n \sim e^{-\gamma n^2}$. This was only predicted to be a fit for one solution at large n, but we see good agreement in all cases, even with n never rising past 6 or 7 for any of the solutions considered. In figure 5.3a the fit is to the deterministic results of table 5.1 for $n \leq 5$ and the `Suave` result for $n = 6$, but the `Suave` results with smaller n are shown as the red points for reference. It is curious that the coefficients fall so close to the $e^{-\gamma n^2}$ lines without any correction, even such as choosing $\rho \neq 1$ in (5.7b). While this trend was derived in our case from a constant period of oscillation, if it holds at higher n it guarantees that the edge coefficients are a convergent series. The fact that all of the solutions appear to behave similarly suggests that they are also all convergent.

5.2.2 Large λ

Once we loosen the $|\lambda| \ll 1$ restriction, we must consider all of the coefficients $\beta_n^{(j)}$ and search for patterns there. Due to the small number of coefficients, and particularly the small number of rows with constant j, it is not possible to get a good understanding of any patterns or asymptotics for these coefficients, but we can speculate as to possible trends. The first thing we notice from table 5.1 is that the sign of the coefficients appears to alternate as $(-1)^{\frac{j}{2}}$. This is not strictly true even for the coefficients we have calculated, however, as choosing non-zero C_0 and especially C_1 will alter many of the coefficients and can affect their sign. With only a small number of the coefficients known, we do not know whether the large n asymptotics are

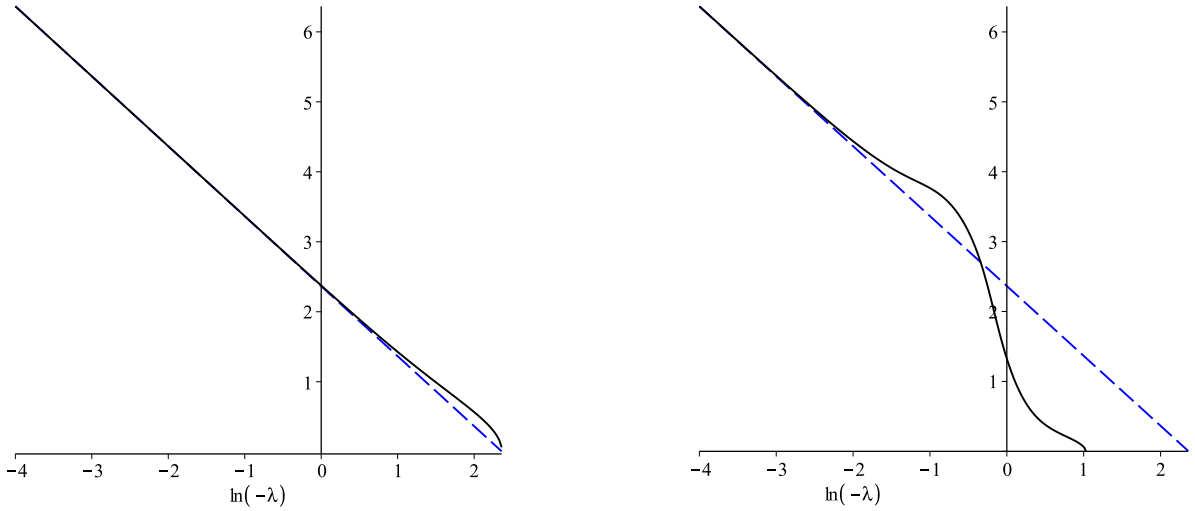

Figure 5.2: The time of the first zero of the rolling tachyon profile as a function of $\ln|\lambda|$. An approximation to the asymptotic behaviour is shown as a dashed line. a) Only the $\beta_n^{(0)}$ coefficients are considered, so the plot is not valid for large $|\lambda|$. b) The whole tachyon profile is considered with coefficients from the fit of figure 5.4a.

fixed or can be changed by a choice of the two free parameters. We can, however, attempt to force a few patterns and see which appear more naturally.

As a first choice we pick $C_0 = C_1 = 0$ and notice that the $j = 1$ coefficients appear to be a good fit to $\beta_n^{(1)} \sim e^{-\gamma_1 k^3}$ with $k = n - 2j$, which is shown in figure 5.4a. While this can be made to fit even better by a choice of renormalization constants, this would lead to some of $\beta_n^{(2)}$ being less than zero or to that row having increasing magnitudes. On the other hand, if we attempt to pick renormalization constants which are a fit to $\beta_n^{(1)} \sim e^{\gamma_1 k^2}$, as shown in figure 5.4c, we do not find as good a fit. The same is true of $\beta_n^{(1)} \sim e^{\gamma_1 n^2}$ using n instead of k in the exponent. It appears that the $j = 1$ coefficients have a tendency towards the cubic exponential decay, while for $j = 2$ we lack enough points to reach any conclusions. The red points in figure 5.4 again represent the `Suave` coefficients, and we see that $\beta_n^{(2)}$ have significantly different values once the renormalization constants are changed, but a look at table 5.2 suggests that this is mainly due to large errors in the `Suave` coefficients, so it is unlikely that the deterministic plots would change significantly if more sample points were used.

While five points is not a lot of data, the $\beta_n^{(1)}$ coefficients suggest that each row with constant j may eventually be a convergent series for at least some choice of renormalization constants. Showing that the full tachyon profile converges when these rows are added together, however, remains impossible until much higher order calculations can be performed. In particular, the large dependence of coefficients such as $\beta_6^{(3)}$ on C_1 is troubling since it suggests that if that constant is of order 1 then the sequence $\beta_n^{\left(\frac{n-k}{2}\right)}$ with constant k could have increasing magnitudes.

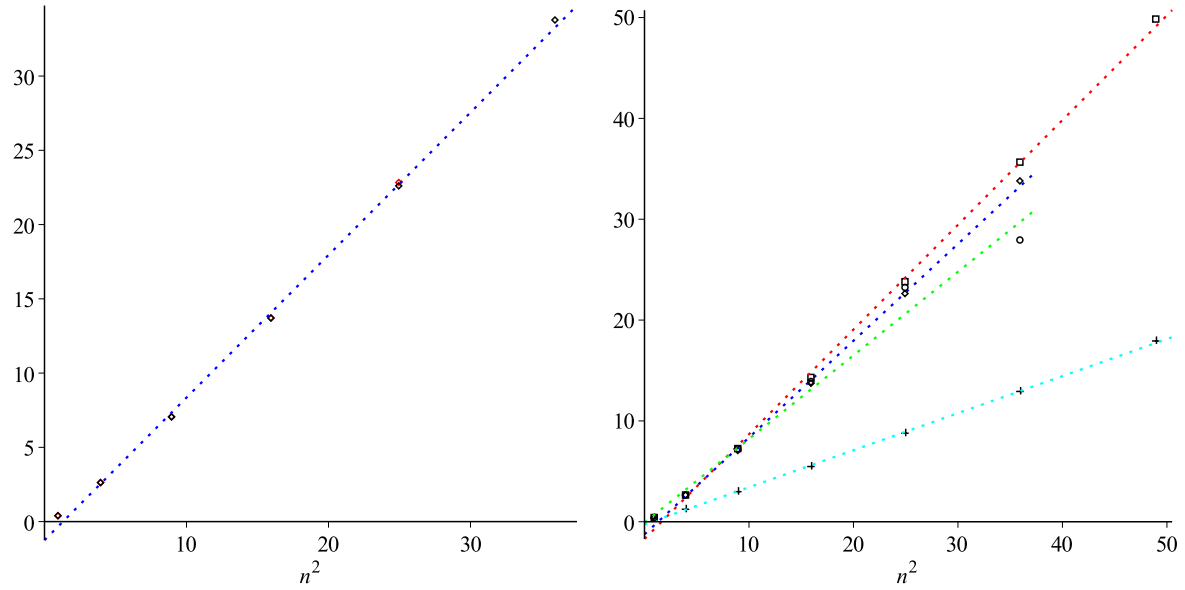

(a) (b)

Figure 5.3: The falloff of the $j = 0$ coefficients of the rolling tachyon profile shown as $-\ln \beta_n^{(0)}$ versus n^2. A linear graph indicates that $\beta_n \propto e^{-\gamma n^2}$ holds, with γ given by the slope. The best linear fit is also shown. a) The solution shown here, with slope 0.9599. Red points are `Suave` values. b) Our solution as well as the other three presented in table 5.3. Square points are for [5], crosses are for [34], and circles for [35].

Thinking of (5.4) as

$$T(t) = 2\sum_{k=0}^{\infty} \beta_{\text{eff}}^{(k)}(\lambda)\, \cosh(kt)\ , \tag{5.9}$$

the effective coefficients $\beta_{\text{eff}}^{(k)}(\lambda)$ would then be defined by series which do not converge for non-zero renormalization constants. Looking at table 5.1, even with vanishing renormalization constants, the magnitudes of the terms β_{2j}^{j} do not drop off very fast. We know that for small λ the series is convergent, but this suggests that the radius of convergence in λ may be finite. This could support either the claim of [22, 51] that there is a second branch with decreasing marginal parameter, or our result from chapter 3 that the marginal deformation simply has an unexpectedly finite maximum. Either case would be worth further investigation.

Now that we have seen what the bulk coefficients look like, we can begin examining the tachyon profile for larger values of $|\lambda|$. Of course as we do this we must be aware that we are missing all coefficients $\beta_n^{(j)}$ with $n \geq 7$, and as we increase the strength of the marginal deformation those coefficients will begin to play a larger role, but we can still get a qualitative idea of the impact of the bulk coefficients on the tachyon profile. Since none of the optimized fits in figure 5.4 were significantly better than simply setting the renormalization constants to zero, we will choose that from now on. Other reasonable choices will not give results that are qualitatively different. For large negative λ we see a tachyon profile in figure 5.5 with fewer

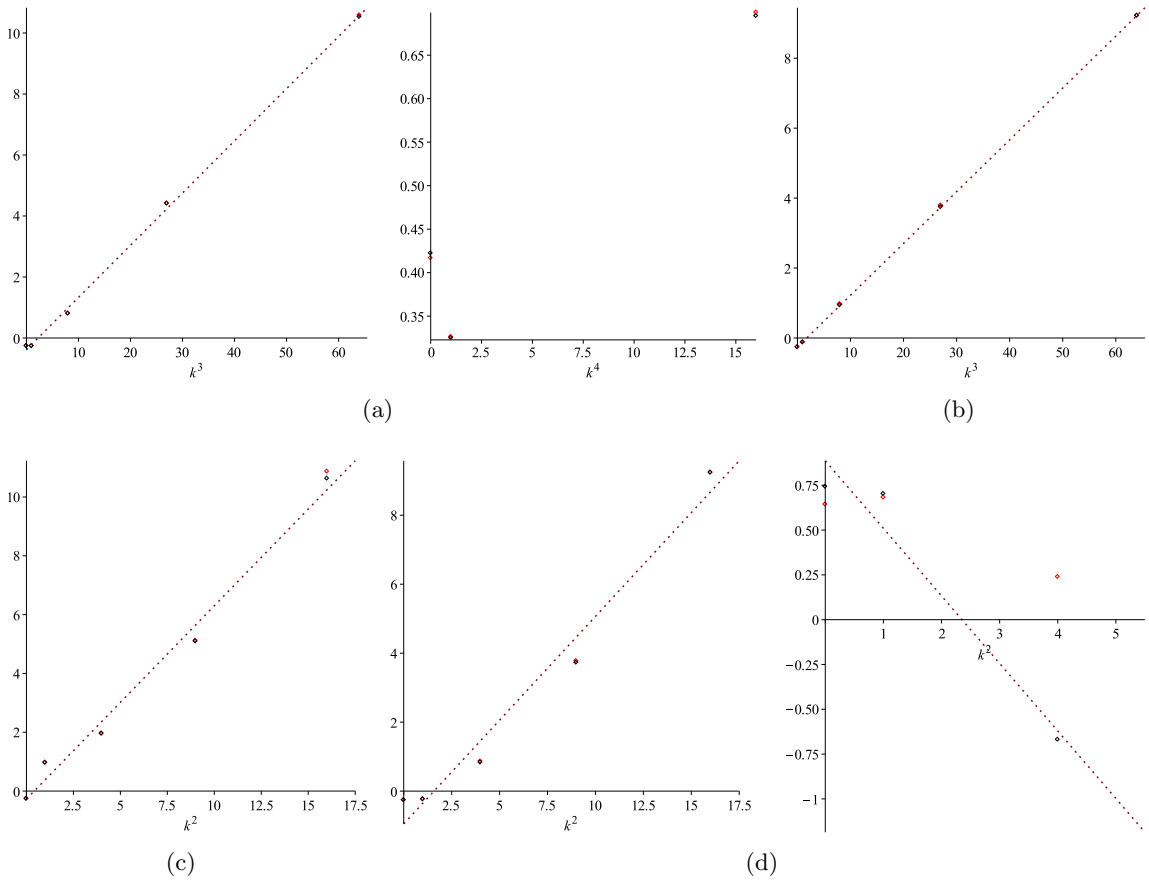

Figure 5.4: Several attempts to determine a trend for the $j > 0$ coefficients in the rolling tachyon profile. $\ln|\beta_n^{(j)}|$ is plotted vs. functions of $k = n - 2j$ with several different choices for C_0 and C_1. Black points are `Cuhre` values while red points are from the `Suave` algorithm. In a) we set $C_0 = C_1 = 0$ and plot $j = 1$ coefficients on the left and $j = 2$ on the right. The $j = 1$ coefficients with C_0 and C_1 optimized for the best linear fit appear in b), and c) attempts the same linear fit assuming a k^2 horizontal axis rather than k^3. d) attempts a linear fit to both the $j = 1$ and $j = 2$ sets of coefficients assuming a k^2 horizontal axis, with $j = 1$ coefficients on the left and $j = 2$ on the right.

oscillations than we had with just the edge coefficients from figure 5.1. As $|\lambda|$ decreases, the additional oscillation appears at $\ln|\lambda| \approx -1.948$. Once $\ln|\lambda| \lesssim -2.5$ the profile has stabilized and the plateau continues growing as $|\lambda|$ shrinks, just as we know it should from our discussion of the tachyon profile for small $|\lambda|$. The disappearance of this oscillation for large $|\lambda|$ is because the $j > 0$ coefficients cannot be neglected in this region, and they change the effective coefficients in (5.9).

The behaviour we see for these large values of $|\lambda|$ is not unprecedented; in [34] the tachyon profile had coefficients (seen in table 5.3) which did not decrease as quickly as other time-asymmetric solutions. Taking the asymptotic ansatz $\beta \sim e^{-\gamma n^2}$ and decreasing γ beyond a critical value causes some oscillations to vanish, which is what happens in [34] where some of the exponentials did not dominate for any range of time. As λ is increased for our solution, the effective coefficients in (5.9) change in a way that causes an oscillation to disappear. If we keep increasing λ beyond this point, some of the coefficients will even change sign, but once the tachyon profile has stabilized with the missing oscillation it does not change significantly. For λ this large, however, we should not trust our results since coefficients with higher n will have larger contributions.

Aside from the obvious, that the singular OPE case is a symmetric function where the D-brane exists for a limited time while with regular OPE it exists until it decays at a finite time, the qualitative difference between the tachyon profiles seems to be that the period and number of oscillations can change this way. Because the strong deformation tachyon profile we have found is similar to the profile of [34], it suggests that changing the strength of the marginal deformation in the time-symmetric case is much like changing gauge in the time-asymmetric case. If the late time behaviour is equivalent to the tachyon vacuum under a time-dependent gauge transformation, as has been hypothesized [35], then in this case the gauge transformation should depend on both time and the marginal parameter in a non-trivial way. That our solution appears qualitatively like time-asymmetric ones for both weak and strong deformation parameter suggests that such gauge transformations remain a valid explanation of the oscillations in the time-symmetric case, although we are not aware of any examples of gauges where coefficients have negative sign, so there may be a limit to the range of λ where this approach is valid.

5.3 Technical Details

It takes a surprising amount of Maple and C++ code to fully construct the solution Ψ for a marginal deformation with singular self-OPE and then evaluate the integrals corresponding to its tachyon profile. This section describes what steps are necessary and why, as well as some of the limitations that remain. Despite the limitations, this ends up being general enough to calculate more than just the tachyon profile of the solution, so the action and equation of motion are also considered. This section gives a rough description of the program used, with a focus on what it is and is not able to do. To see precisely how these steps are accomplished, appendix B contains the full commented code used. We then study a few tests of the validity of the program by using it to calculate known quantities.

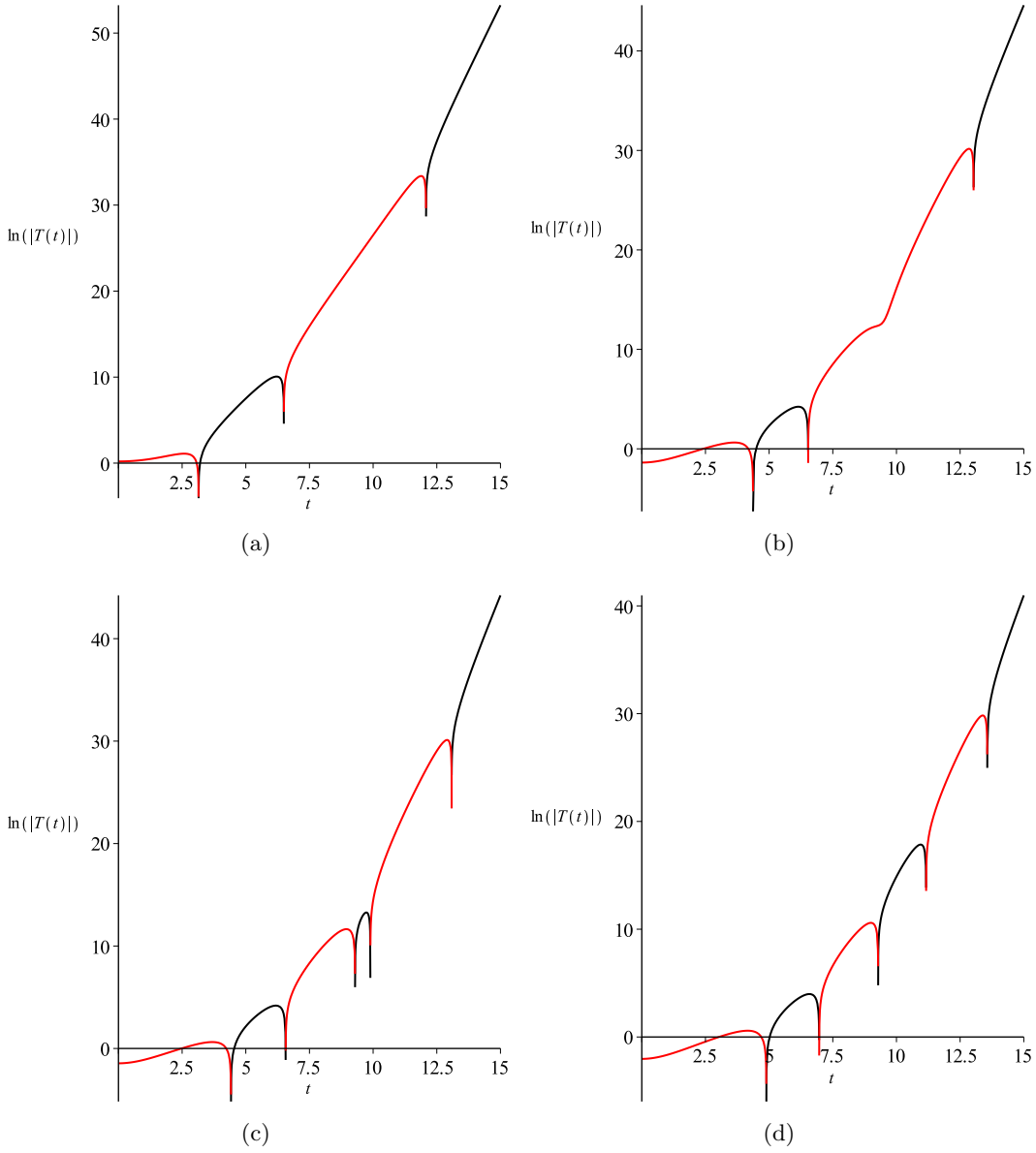

Figure 5.5: The tachyon profile of the time-symmetric rolling tachyon solution. We plot the log of the tachyon profile at a) $\ln|\lambda| = -0.5$, b) $\ln|\lambda| = -1.92$, c) $\ln|\lambda| = -1.98$, and d) $\ln|\lambda| = -2.5$. Positive values represented by black, negative values by red. The renormalization constants C_0 and C_1 are both set to zero.

5.3.1 Conventions

The first step in writing a program to perform calculations on wedge states with operator insertions is to decide how the mathematical objects will be represented. Maple has datatypes for mathematical expressions, but in our case we need more. A wedge state is a semi-infinite cylinder with a given circumference, and operators are inserted at varying locations which for our purposes will always be on the boundary. We define the `wedge` datatype as a three-part list containing the width of the wedge, a set of variables with their (possibly integrated) positions in the wedge, and finally the list of operators to insert, along with any constants. When we add wedges, we do not want a wedge with circumference equal to the sum of the two wedges' circumferences any more than we would want one with the arithmetic sum of two sets attempting to describe the insertion locations. In order to avoid this, all wedge sums should be written using the inert operator `&+` to avoid Maple's default behaviour of adding lists element by element. `&+` is treated as a binary operator and can be used infix, but has no evaluation rules and will be left alone by Maple's simplification routines.

When we eventually perform calculations, we will have to truncate to a finite number of marginal operator insertions, or equivalently a finite order in the marginal parameter λ. As the order increases, the number of terms will increase very quickly, and if we are not careful the execution time for simple operations such as the star product will become a problem. To help with this, we will define an alternative form of the wedge state datatype. This is called `wpoly` and has the same first two items as the `wedge` type, but the third term representing the operators to insert is replaced with a list representing the taylor series of those operators in λ. When only a given order in λ is desired, parts of this list which give results at too high an order can be skipped. We then define a few more labels for determining the type of an object for conditional processing: `wsing` evaluates to either of `wedge` or `wpoly`, `wsum` is a sum of `wsing` types added using `&+`, and `wtype` evaluates to either of `wsing` or `wsum` and so covers all wedge state types.

Multiplication in Maple is naturally commutative, so keeping track of ghosts requires some extra thought. I have chosen to represent the ghost *operators* using the *functions* `c(t)` and `dc(t)` which are undefined and will never be evaluated. For most situations the order of ghost insertions is defined by their ordering along the boundary. `c(1)*c(2)` means $c(1)c(2)$, and so does `c(2)*c(1)`, while to get $c(2)c(1)$ we would need to write `-c(1)*c(2)`. A problem arises, however, when two ghosts are coincident, as in $c\partial c(t)$. In this case I chose to break the tie lexicographically using the name of the insertion location. This means that $c\partial c(0)$ must be represented by something like `c(t[1])*dc(t[2])` where the insertions will only be set to 0 once the expectation value has been taken and there are no more ghost operators in the expression. Because of this, two ghosts should never be inserted using the same coordinate, and care must be taken when creating wedge states to guarantee that the sign is correct for the ghost insertions given.

5.3.2 Basic Functions

With our datatypes defined, we can now move on to begin writing routines to manipulate them. The most obvious operation we will perform on wedge states is the star product, which we will do with a function called `star`. This takes two or more wedge states or sums of wedge states and multiplies them from left to right. The danger in this is apparent when we consider an

example like $A * A$, where both copies of the wedge state A would have their insertions at the same locations. In addition to shifting all insertions in the second wedge state to the right by the circumference of the first wedge state, we must ensure that the name of the coordinate used to label those locations is unique. For this, I wrote a subroutine called `newvar`, which renames variables to prevent conflicts. The `star` function must be careful to call this on the coordinates in the second wedge state in lexicographic order so that the ordering is preserved and the ghost factors will not inadvertently change sign. Our star product can take an additional named parameter, `LAMBDA_MAX`, which will truncate the resulting string field to the given power of λ. This is especially efficient when all wedge states to be multiplied are given in the `wpoly` form.

At times it can also be very useful to be able to simplify expressions involving inert sums of wedge states. For example, in a long sum many terms can become zero when acted on by the BRST operator or truncated to a given order of λ, so the function `plus0` will identify vanishing wedge states and remove them. This function will also flatten sums, effectively removing extra parentheses in what is an associative operation. When the operator content of a wedge state can be expanded, there is `wexpand` to do this and make each term its own wedge state, and the function `wcombine` attempts to perform the inverse operation. As with addition, multiplication of a wedge state by a scalar should not be done with the standard Maple multiplication operator because that would multiply each item of the list that represents the wedge state. Instead, there is `ctimesw` to multiply the operator content of a wedge state by any expression and leave the rest of the wedge unchanged. Finally, when we want to examine only one component of the taylor series in λ, there is `pickoff` to return the taylor coefficient wedge state of its input at a given order. Of course `pickoff` is extremely simple for `wpoly` types.

All of the basic operations we have seen in this section apply equally to all wedge datatypes. There are alternative cases for the `wedge` and `wpoly` types, and they properly distribute over the inert addition `&+`.

5.3.3 Known Wedge States

We now turn our attention away from the basic operations defined on wedge states, and towards the computation of the specific solution found in [36] and reviewed in chapter 4. The first wedge states which are defined are zero and the star product identity, each coming in both `wedge` and `wpoly` versions. The solution is built from the string fields A_L and U, as well as the powers $U^{\frac{1}{2}}$ and $U^{-\frac{1}{2}}$. Each of these string fields is in turn defined as a sum of wedge states with insertions.

So far we have talked about manipulating wedge states with insertions, but we have not discussed what those insertions are. The renormalized integrated operators we found in chapter 4 are complicated constructions which will each need to be created before they can be used in numerical calculations. The operators we will need are $[V(a,b)^n]_r$, $\left[V(a)V(a,b)^{n-1}\right]_r$, $\left[V(a,b)^{n-1}V(b)\right]_r$, and $\left[V(a)V(a,b)^{n-2}V(b)\right]_r$. Because the action of the BRST operator on all but the last of these is well understood from the assumptions (4.5a) and (4.5b), expanding them in terms of bare marginal operators and counterterms too early would be a mistake. Instead we will make use of inert functions, as we did with addition, and name these renormalized operators `V_ren`, `V_L_ren`, `V_R_ren`, and `V_LR_ren` respectively. Each of these should be given five parameters, representing the total number of marginal insertions, n, the left and right endpoints, a and b, a list of the variable names where the marginal operators are to be inserted, and a name used for the total circumference of the wedge state the operator is inserted on. The last

parameter is never used when the operators are defined by our little g renormalization scheme, but the sample scheme of [36] which is discussed in section 4.3.5 requires it, so we will include that parameter for backward compatibility. Once all operations which are simpler on the total renormalized operators have been performed, the inert functions representing them can be replaced with active ones that use bare insertions of the marginal operator and counterterms. The active functions are named `V_r`, `V_Left`, `V_Right`, and `V_LR`.

The active functions representing renormalized operators insert counterterms using the little g scheme, which depend on the insertion coordinates. They are inserted for every pair of coordinates, as in $\overset{\circ}{\circ}\prod V(t_i)\overset{\circ}{\circ_g}$, with the fully symmetrized integrand being finite at all coordinates, as described in (4.88) of section 4.3.2. The counterterms to be inserted are the functions `G_r`, `G_Left`, and `G_Right`. The capitalization of the counterterms in the code goes back to the use of the two-point function in [36], but the functions they represent are the correct little g scheme terms. Finiteness of the integrand is important for numerical calculations. If we were to try something like a big G scheme where the integrals of the marginal operators are regulated by ϵ and the counterterms are explicit functions of ϵ, actual integration would be extremely difficult. First we would have to implement the regulated integration regions, which are not simple at all, and then we would have to perform the integrals many times so that the limit in ϵ could be taken numerically. This is not practical, so instead we guarantee that the integrands are always finite and then integrate over unregulated regions once. The minor disadvantage of this approach is that we cannot integrate terms in the result separately, since they may have cancelling singularities. The more serious related problem occurs when the divergent terms being added to give a finite integrand have differing rounding errors. This will be considered in more detail in section 5.3.7.

Once renormalized integrated operators are defined, we can begin using them to make string fields. The string field U is given order by order as a wedge state with n fully integrated operators inserted between 1 and n. The 0th order of U is defined to be the star product identity, and this means that functions of U can be defined in terms of Taylor series of the function about 1. The first order term in U vanishes because it consists of a single (non-renormalized) operator integrated over a vanishing region. The function `Utail` returns the string field $U-1$ for use in these Taylor expansions. Specifically, we need `Uinv`, `Usqrt`, and `Uinvsqrt`, which return the string fields U^{-1}, $U^{\frac{1}{2}}$, and $U^{-\frac{1}{2}}$ in the `wpoly` type. Finally, we also define the functions A_L and A_R to give the corresponding string fields in `wpoly` form. It is worth mentioning that since the wedge states used for both U and $A_{L/R}$ have different circumferences at each order in λ, each order must be its own wedge state and the lists representing the Taylor series of the operator insertions will each have only one non-zero element.

The solutions `Psi_L_real`, `Psi_R_real`, `Psi_L`, and `Psi_R` all have simple definitions in terms of the string fields defined so far. As in [36], they are

$$\Psi = \frac{1}{\sqrt{U}}A_L\frac{1}{\sqrt{U}} + \frac{1}{\sqrt{U}}Q_B\sqrt{U} \ , \tag{5.10a}$$

$$= \frac{1}{\sqrt{U}}A_R\frac{1}{\sqrt{U}} + \sqrt{U}Q_B\frac{1}{\sqrt{U}} \ , \tag{5.10b}$$

$$\Psi_L = A_L\frac{1}{U} \ , \tag{5.10c}$$

$$\Psi_R = \frac{1}{U}A_R \ . \tag{5.10d}$$

The real solutions Ψ in the first two lines are equal, while Ψ_L and Ψ_R are related to Ψ by gauge transformations. Having several forms of the solution is useful for debugging, since we can compare calculations. The number of terms in each of these forms of the solution grows very rapidly as the order in λ is increased, but it is still possible to do 6th order calculations in a very reasonable amount of time.

The last string field we will need is the conformal patch. When we define string fields in terms of wedge states with insertions, what we are really saying is that the string field Φ is such that its overlap with an arbitrary test state is the same as the expectation value of the operator corresponding to the test state ϕ inserted on the corresponding wedge state. See also the discussion of (2.22). The test state we will be using is quite simple, having ghost number two and no matter content except for an amount of momentum in the time direction. The operator corresponding to this test state is, up to the conformal factor going from the upper half plane to Schnabl frame,

$$\phi(0) = \partial c(0) c(0) e^{kX^0(0)} \ . \tag{5.11}$$

We implement this by defining a wedge state with width 0 and the appropriate operator content, so that when it is multiplied by a wedge state the result has all of the operators needed for the expectation value in question, all inserted in the correct positions. The zero width is so that this conformal patch does not alter the circumference of the resulting wedge state.

5.3.4 The BRST Operator

In the construction of the solution Ψ, the BRST operator is not terribly complicated. This is because it only acts on $U^{\pm\frac{1}{2}}$ which has ghost number zero and no fixed operators. In this case only an implementation of the first BRST condition (4.5a) is needed. Acting separately on each term in a sum of wedge states, `Q_B` goes through any product of renormalized operators and replaces each one with the sum of terms representing the right hand side of

$$\begin{aligned}\frac{1}{n!} Q_B \left[V(a,b)^n\right]_g = \frac{1}{(n-1)!} \left[V(a,b)^{n-1} cV(b)\right]_g - \frac{1}{(n-1)!} \left[cV(a)V(a,b)^{n-1}\right]_g \\ + \frac{1}{(n-2)!} \left(O_R^{(2)}(b) - O_L^{(2)}(a)\right) \left[V(a,b)^{n-2}\right]_g\end{aligned} \tag{5.12a}$$

where

$$O_R^{(2)}(b) = \frac{1}{2}\partial c(b) + C^L c(b) \ , \quad O_L^{(2)}(a) = -\frac{1}{2}\partial c(a) + C^L c(a) \ . \tag{5.12b}$$

As we have already mentioned, in this chapter we assume that $C^R = C^L$, but do not neglect that constant.

While this is all we need in order to construct the solution, if we wish to test the equation of motion we will need to implement the second BRST condition (4.5b). This raises a number of additional issues for a clear definition of Q_B. One obvious difficulty is in the fact that Q_B is a graded derivation satisfying $Q_B(A*B) = (Q_B A)*B + (-1)^{G_A} A*(Q_B B)$. For wedge states with insertions of operators such as $\left[cV(a)V(a,b)^{n_1}\right]_g \left[V(c,d)^{n_2}\right]_g$ we want to have Q_B act on the first renormalized operator as a whole without picking up a sign change from acting on operators to the right of a ghost until it gets to the second renormalized operator. This is an issue whenever the fixed operator does not appear in the last renormalized group. To do this, for the purposes of determining sign we view integrated operators as being inserted at their left

endpoint, and ghosts as being inserted slightly to the right of where they actually are. Then by considering the action of Q_B on all operators from left to right and changing sign whenever we pass a ghost, the signs will be correct.

The other problem with applying the BRST operator to operators of ghost number one comes from the fact that we are treating the matter and ghost parts separately, whereas in section 4.3.6 we had to consider them together so that the ghosts could properly soften some of the divergences. What we will do is assume that Q_B only acts on renormalized operators with one fixed insertion in the form $\left[cV(a)V(a,b)^{n-1}\right]_g$ or the right handed version; there is always a c ghost included with the fixed insertion. We then take the result

$$\begin{aligned} Q_B \left(\left[cV(a)V^{(n-1)}(a,b)\right]_g - \frac{1}{2}\left[\partial c(a)V^{(n-2)}(a,b)\right]_g \right) &= -\left[cV(a)V^{(n-2)}(a,b)cV(b)\right]_g \\ -\frac{1}{2}\left[cV(a)V^{(n-3)}\partial c(b)\right]_g + \frac{1}{2}\left[\partial c(a)V^{(n-3)}(a,b)cV(b)\right]_g &+ \frac{1}{4}\left[\partial c(a)V^{(n-4)}(a,b)\partial c(b)\right]_g \end{aligned} \tag{5.13}$$

and rearrange it to get

$$\begin{aligned} Q_B \left[V(a)V^{(n-1)}(a,b)\right]_r \overset{\text{eff}}{=} &-\left[V(a)V^{(n-2)}(a,b)V(b)\right]_r c(b) - \left[V(a)V^{(n-3)}(a,b)\right]_r O_R^{(2)}(b) \\ &- \frac{1}{c(a)}O_L^{(2)}(a)\left[V^{(n-3)}(a,b)V(b)\right]_r c(b) - \frac{1}{c(a)}O_L^{(2)}(a)\left[V^{(n-4)}(a,b)\right]_r O_R^{(2)}(b) \\ &- \frac{1}{c(a)}O_L^{(2)}(a)\left[V^{(n-3)}(a,b)V(b)\right]_r c(b) - \frac{1}{c(a)}O_L^{(2)}(a)\left[V^{(n-4)}(a,b)\right]_r O_R^{(2)}(b) \\ &- O_L^{(2)}(a)\left[V(a)V^{(n-3)}(a,b)\right]_r - \frac{1}{c(a)}(O_L^2(a))^2\left[V^{(n-4)}(a,b)\right]_r . \end{aligned} \tag{5.14}$$

The notation used here is $\left[V^{(n)}(a,b)\right]_r \overset{\text{def}}{=} \frac{1}{n!}\left[V(a,b)^n\right]_r$, which is standard in [36] and is convenient for writing renormalized operators which have an exponential form. The right handed version of this is

$$\begin{aligned} Q_B \left[V^{(n-1)}(a,b)V(b)\right]_g = &-c(a)\left[V(a)V^{(n-2)}(a,b)V(b)\right]_g - O_L^{(2)}(a)\left[V^{(n-2)}(a,b)V(b)\right]_g \\ &- \left[V^{(n-4)}(a,b)\right]_g O_R^{(2)}(b)O_R^{(2)}(b)\frac{1}{c(b)} - \left[V^{(n-3)}(a,b)V(b)\right]_g O_R^{(2)}(b) . \end{aligned} \tag{5.15}$$

Obviously these cannot be used if they are not multiplied by $c(a)$. We have also assumed that Q_B does not act on the ghosts. In reality this is not true, but as long as ghosts appear only in the specific combinations of $O_{L/R}$ produced by (4.5a) we can pretend that Q_B only acts on the matter sector and combine the ghost part into those results. That is the approach taken here, and while it is definitely a hack from the point of view of all allowed renormalized operators, it is enough to produce correct results for the string fields we are interested in, namely those used in the solution Ψ, as well as the equation of motion and the action evaluated on the solution Ψ.

The BRST code which replaces one operator with another is quite dense so I will explain one term in detail. The term $-\frac{1}{c(a)}O_L^{(2)}(a)\left[V^{(n-3)}(a,b)V(b)\right]c(b)$ coming from the third and fifth terms in (5.14) will be our example.

```
877     grandterm[i]:=grassign*subsop(1=op(1,grand[i])-2,4=[op(3..op(1,
            grand[i])-1,op(4,grand[i])),op(4,grand[i])[2]],V_R_ren(op(
            grand[i]))):
878     outw:=outw &+ [expr[1],remove(has,remainv,op(4,grand[i])[op(1,
            grand[i])]) union map((x->lhs(x)=op(2,rhs(x))),removev)
            ,`*`(-2,OL2(op(4,grand[i])[1]),c(op(4,grand[i])[2]),op(remove(
            has,grandterm,c(op(4,grand[i])[1]))))]:
```

The first line alters the call to the inert function representing a renormalized integrated operator. The maple function `subsop` performs substitutions which replace the operands of its argument. In this case the first operand of `V_L_ren` is reduced by 2 since there are two fewer insertions of the marginal operator, and the fourth operand is changed from $[t_1, \ldots, t_n]$ to $[t_3, \ldots, t_{n-1}, t_2]$. The operator itself is then changed from `V_L_ren` to `V_R_ren` without any further changes to its arguments. In the second line we see the construction of the wedge state to be added to the output. In the coordinate selection part, the integrated t_2 coordinate is replaced with $t_2 = b$ by removing it and then taking the union with the removed coordinate evaluated at its right endpoint. Finally, the product `` `*`(...) `` gives the operators inserted along the boundary. The initial 2 comes from the sum of the third and fifth terms in (5.14), and then the ghost operators $O_L^{(2)}$ and c are inserted at the left and right hand endpoints respectively. The remainder of the operators are inserted at the end, with the exception of `c(t[1])`, which is removed from the product.

5.3.5 Expectation Values

The string fields we are interested in are defined by having the same overlap with an arbitrary test state as a given collection of wedge states with insertions. We have now described everything needed to produce those wedge states with insertions, and include an insertion for a useful class of test states. This leaves us with the question of how to find those CFT expectation values. This will be done in two steps, with the algebraic work to produce integrands done in Maple, and the numerical integration done in C++.

The algebraic portion of the correlation functions is found with the function `corr`. The first step is to replace all of the inert renormalized operators with active ones and then `wexpand` the result so that each wedge state contains a single product of operators and functions. Next we go through the operator content and collect each type of operator. Obviously, it is not possible to handle every operator which exists in the CFT, but the only ones we need for our purposes are $e^{kX^0(t)}$, $c(t)$, and $\partial c(t)$. If we want to see how other marginal deformations compare, the deformation ∂X has the same self-OPE as the rolling tachyon $\sqrt{2}\cosh X^0$, so we also allow this operator in addition to the previous three. In the matter sector this is implemented by going to the upper half plane where we have

$$\begin{aligned}\left\langle \prod_{i=1}^{n} e^{ik_i\cdot X(t_i)} \prod_{j=1}^{m} \partial_{s_j} X^{\mu_j}(s_j) \right\rangle &= \lim_{\alpha\to 0} \left\langle \left(\prod_{i=1}^{n} e^{ik_i\cdot X(t_i)}\right) \left(\prod_{j=1}^{m} \frac{\partial_{s_j}}{\alpha} e^{\alpha X^{\mu_j}(s_j)}\right) e^{-\alpha\sum_{j=1}^{m} X^{\mu_j}(u)} \right\rangle \\ &= \lim_{\alpha\to 0} \prod_{j=1}^{m} \frac{\partial_{s_j}}{\alpha} \prod_{i<i'} (t_i - t_{i'})^{2\alpha' k_i\cdot k_{i'}} \prod_{i,j} (t_i - s_j)^{-2i\alpha'\alpha k_i^{\mu_j}} \prod_{j<j'} (s_j - s_{j'})^{-2\alpha'\alpha^2\delta_{\mu_j}^{\mu_{j'}}} \quad . \end{aligned} \tag{5.16}$$

The ghost sector is easily represented in Schnabl frame, where we can use the result from equation (D.11) of [25],

$$\langle c(x)c(y)c(z)\rangle_{W_{\pi-1}} = \sin(x-y)\sin(x-z)\sin(y-z)\ . \tag{5.17}$$

The matter sector result is only valid when $\sum_{i=1}^{n} k_i = 0$ so that momentum is conserved, and the ghost factor will be zero unless the ghost number is three. Both of these restrictions are checked for, and zero is returned if either one is not satisfied.

So far, the correlators have been done on the operator content without using the second element of the `wedge` datatype which says where the insertions really are. Now the list of coordinates is separated into those which are integrated and those which are fixed. For each integrated coordinate, the expectation value is wrapped in Maple's inert integration function, `Int`, so that excessive execution time is not wasted trying to evaluate the integrals at this stage. For each fixed insertion, an attempt is made to substitute the insertion location for the variable name. This may fail if, for example, diametrically opposed insertions on the wedge state cause a divergence which is cancelled by the conformal factors. If direct substitution fails, a limit is used instead, and if that still cannot be evaluated for whatever reason an inert limit function is used. Fortunately, the solution is well enough behaved that the inert limit should never be needed.

5.3.6 Handling and Exporting Integrands

As a result of the `corr` function, we now have a long sum of integrals, many of them multi-integrals. Each integral represents one product of matter exponential and ghost operators appearing in the quantity being evaluated. As we have mentioned, these integrals are unregulated because we are using the little g scheme which has finite integrands. At this point, however, many of the integrands are still divergent because a single product of (unrenormalized) operators is naturally divergent in this setup. Only when all of the terms associated with a renormalized operator are added together do we have a finite integrand. Since the integrals are unregulated we have to add the integrands before we can integrate. Some numerical integration routines require that the region of integration is the unit hypercube, $(0,1)^n$. Of course it is a simple matter to rescale functions at the time of integration, but by making the change of variables at this point, the process of adding integrands is simplified. Instead of searching through all of the terms to identify which ones have matching integration domains, the function `to_cube` rescales every integrand to be integrated from 0 to 1, and then simply adds all terms which are integrated over the same dimension. This gives sums with even more terms than we needed for finiteness, and would only be an issue if we were interested in finding the values of specific terms separately.

In order to perform the integrals using C++ routines, we need to output the integrands that we have produced so far to a file. A single file containing a hundred integrands as C++ functions would require a great deal of work to incorporate into a working program, so we include code to keep track of what should be done to each of those functions, and even what output to print with descriptions of each term. The function `tacconst` is set up to do all of this. First it constructs the solution at a given order in λ, and optionally the action and equation of motion. Next it finds the tachyon profile of the solution, and if the equation of motion was computed the overlap of that with several ghost number one test states, as unevaluated integrals.

Now each of those quantities is still a function of the renormalization constants C_0, C_1, and C^L, but because of the structure of the renormalization scheme, they are actually polynomial functions, so by differentiating we can separate the integrals into Taylor coefficients. Now by treating each of these Taylor coefficients as a separate integral to be computed, the integrands are entirely floating point functions which can be evaluated and integrated numerically. A line is then written to a file to call a C++ function called `CubeInt` on each of these integrands, since that is what we will call the function to integrate over the unit hypercube. After that, `printf` statements are written to the file which will output a few characters describing what quantity is being given, followed by the reconstructed Taylor series for that quantity with the Taylor coefficient integrals replaced by their floating point results. Finally, each of the integrand functions is written to the file. This is done at the end because they can often make up many megabytes of text, and it is easier to separate them into a header file if they are all together.

5.3.7 Numerical Integration

The integration is handled by off-the-shelf C++ routines. The CUBA library appears to be a good choice in most cases [52].[4] It is a collection of four algorithms for multi-dimensional numerical integration, three of which use pseudo-random sampling while the fourth is a deterministic algorithm. Since we are working at sixth order in λ and the solution has ghost number one (corresponding to the number of fixed moduli), there are never more than five integrated coordinates in a given integral. While Monte Carlo algorithms do scale better as the dimension rises, in five or less dimensions it appears that the deterministic algorithm, `Cuhre`, is slightly more efficient. As we will see, `Cuhre` is also more reliable in most cases. Unfortunately, it only integrates functions of more than one variable, so in the one-dimensional case we use the `QAG` routine from the GNU scientific library.[5] Each of the routines in the CUBA and GNU libraries provides its own error estimate, and the CUBA library routines also provide a chi-square estimate of the probability that the error is sufficient.

A single quantity to be calculated numerically, such as an individual term in the tachyon profile of table 5.1 or in one of the consistency checks of tables 5.6 and 5.7, generally consists of a small number of integrals. Each integral contains all of the terms in the solution which are integrated over a given number of coordinates, or equivalently all of the terms with the same number of integrated operators. Most quantities are the sum of two integrals, but a few are only a single integral, and quantities in the action can consist of more than two.

Convergence

In order to get as much data as possible, the collection of integrals we look at here will include all of the ones used in calculating the tachyon profile as well as the action and several components of the equation of motion. The action and equation of motion will be discussed as checks of consistence later in this section.

It is difficult to study convergence of the one-dimensional integrals due to the fact that the `QAG` algorithm does not report the number of samples used. We can, however, take several full sets of data for these integrals and compare the different calculations of the same integrals. We

[4] The CUBA library is distributed from `http://www.feynarts.de/cuba/`.
[5] The GNU scientific library is found at `https://www.gnu.org/software/gsl/`.

find that they all agree with each other well within the error estimates. The only troubling one-dimensional case is that of a constant integrand. This can be seen in the kinetic energy of the solution at fourth order in λ, which is the particularly simple quantity $\int_0^1 dt\ \frac{3}{2} - \frac{3}{2}$. The integration algorithm performs operations on the constant causing tiny roundoff errors which, when the constant value is subtracted, causes the result to differ from zero. This would not be a problem except that error analysis in numerical integration is based on variation of the integrand, and as such gives an estimated error which is extremely small. While in principle error estimates should account for the roundoffs inherent in their algorithm, in practice this does not seem to be the case. The error estimate becomes small enough that the reported result can actually be incorrect, and even unstable with respect to changing the desired accuracy. Most integrands worth using a numerical algorithm to integrate undoubtedly vary enough that this is not normally an issue. This is the only instance of such a problem that we encounter, but since the integral is trivial we do not need to rely on numerical integration for its value.

We now turn our attention to the `Cuhre` algorithm, so we will only be considering integrals over two or more dimensions. The first question we will ask here is whether the error bars reported by the integration algorithms are sufficient. Because we do not know the correct results for most of the integrals, we evaluate each integral with at least three different choices for the sample size, N. Making the assumption that the calculation with the largest N is "correct", we can compare the difference between each computed integral and the most accurate one to the error estimate reported by that integral. This is shown in figure 5.6a, where blue points have sufficient error bars and green points are within twice the error bars. The few red points are the outliers which differ from their largest N partners by more than twice their error estimates. In a moment we will compare every computed integral with other calculations of the same integral, so the red points here will also have greater than 2σ difference in that comparison. Many of these points come from the same integrals, so there are actually not very many integrals which will need to be examined in detail. Our choice to prefer the `Cuhre` algorithm over the adaptive Monte Carlo algorithm `Suave` is justified by figure 5.6b, where we see that the `Suave` algorithm is as likely as not to underestimate the error. In its defence, `Suave` frequently reports a 100% χ^2 estimate that the reported error is insufficient, but this is not particularly helpful in finding accurate values.

The `Suave` algorithm can still be useful for comparison, however. Its error bars are not helpful, but if the same quantity computed in `Cuhre` and `Suave` differs by more than a few percent it is worth closer examination. This is how the two terms marked with asterisks in table 5.1 were identified. The integrals responsible for the troublesome behaviour of these two quantities are plotted in figures 5.7a and 5.7b. There were some other terms which were flagged by this test, but they converged reasonably well once the sample size was increased sufficiently.

With many integrals each calculated for several different values of N, we have a sizeable collection of data to examine. Among the 848 `Cuhre` integrals, there is only one instance of the error estimate increasing as the sample size was increased, so we can safely say that the reported error bars decrease monotonically as $N \to \infty$. We can then examine the quantity $\frac{|x_i - x_j|}{\sqrt{\Delta x_i^2 + \Delta x_j^2}}$ for every pair of calculations of the same integral. We find that 88% of pairs are within σ of each other, while 94% are within 2σ. Those which disagree by more than 2σ can be studied individually, since they correspond to only 15 different integrals. Of those, four only disagree due to a single computation each with very low N (about 500 samples) that has a 50%

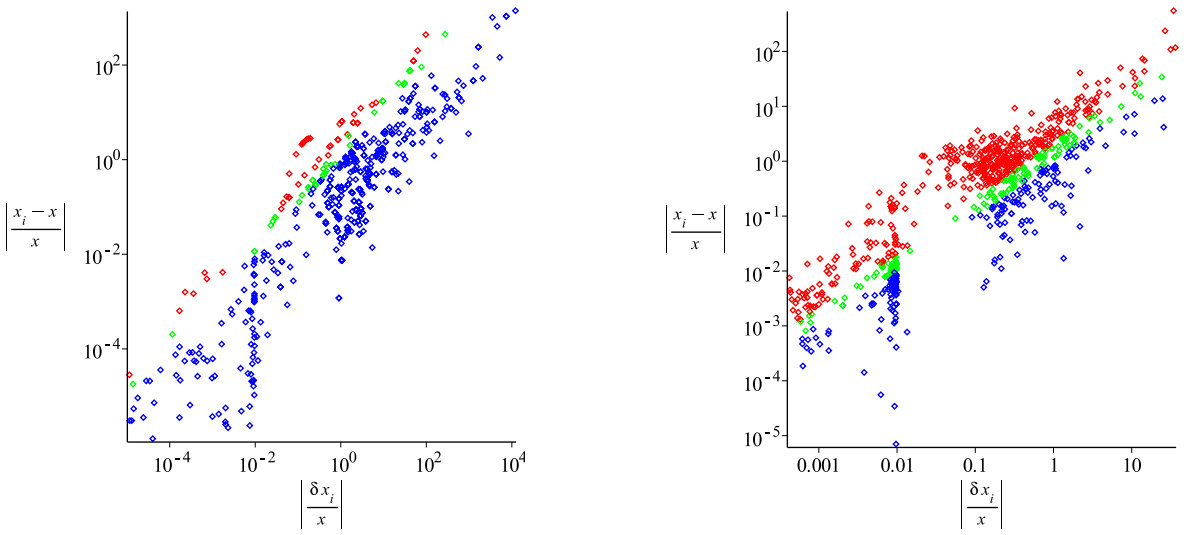

Figure 5.6: Plots showing the reliability of error estimates. The vertical axis is the difference of two calculations relative to the more precise of the two, and the horizontal axis is the relative error reported by the numerical integration. The `Cuhre` algorithm results are shown in a) and `Suave` results are in b). Points with differences greater than twice the reported errors are red, those with differences between one and two times the error are green, and those with error estimates large enough to cover their difference from the "best" value are blue.

χ^2 chance of being incorrect. One of the remaining 11 integrals is also the one responsible for the tachyon profile coefficient $\beta_6^{(0)}$, so adding in the integral responsible for the other flagged term in table 5.1 we have 12 integrals to examine. These are plotted with various values of N in figures 5.7 and 5.8. The values and their error bars are shown in blue, and when appropriate to the scale of the plot the corresponding `Suave` results are also shown in green.

The first two plots represent the parts of the tachyon profile for which we used the `Suave` results. In figure 5.7a the problem is not that the results are inconsistent, but that the errors are so large that the results are meaningless. It looks likely that as N is increased the results will continue to converge to something quite close to the `Suave` result. For the other integral, figure 5.7b shows that as N is made extremely large we finally find something like the much more consistent `Suave` results. The slope, however, does not yet appear to be significantly slowing down, so we cannot be sure that it is convergent. The rest of the plots in figures 5.7c-5.7e show the other integrals that contribute to the tachyon profile and have more than a 2σ variation between points. They all show signs that once N is sufficiently large they converge quite well. Only for smaller N do the error estimates appear to be insufficient.

Moving on to integrals which contribute to consistency checks, in figure 5.8 we see that the majority are fine. Only 5.8c does not appear to converge. As with the examples shown in figure 5.7, this may well be linear until some critical N where it begins to converge. In addition, while only the quantities composed of small sums of these integrals are supposed to vanish, in many cases each of the integrals will vanish independently. These seven examples all become closer

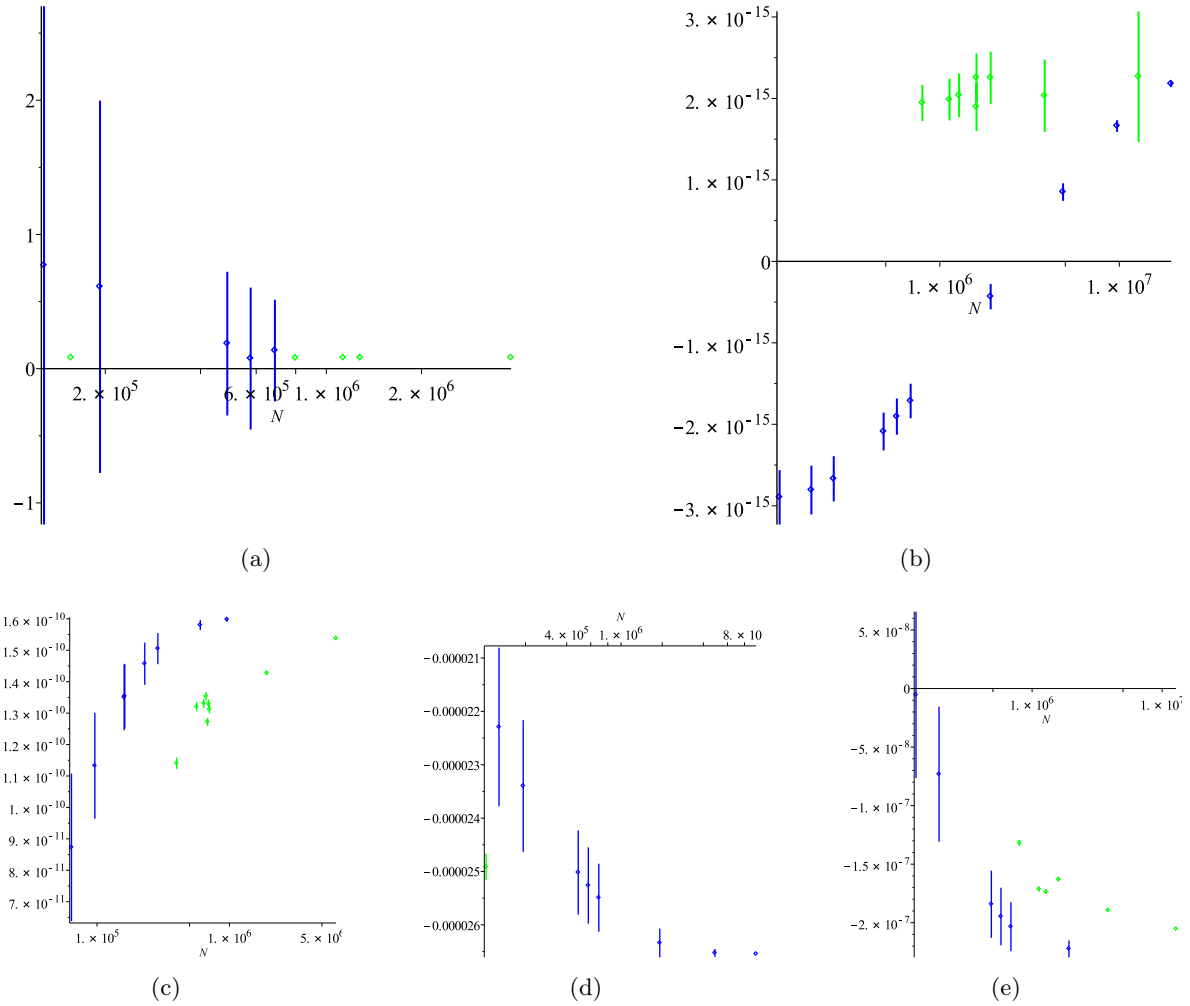

Figure 5.7: Several integrals from the tachyon profile calculated with different values of N. The error bars are those reported by the `Cuhre` algorithm. When the `Suave` algorithm gives results which fit on the same scale they are included as the green data.

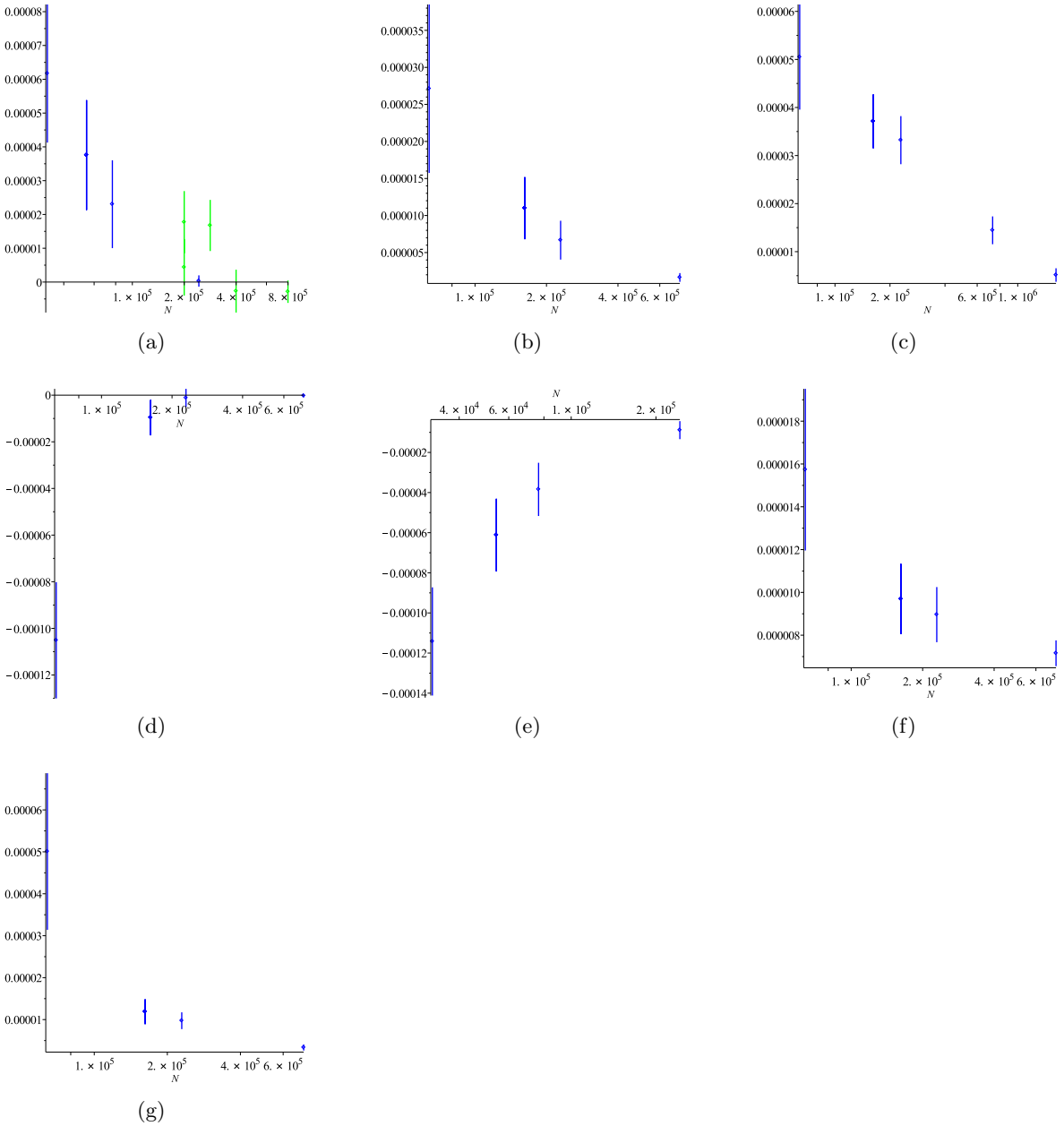

Figure 5.8: Several integrals from the consistency checks calculated with different value of N. The error bars are those reported by the `Cuhre` algorithm. When the `Suave` algorithm gives results which fit on the same scale they are included as the green data.

to vanishing as N is increased, and only 5.8f is not getting very close to zero. Convergence of these results does not appear to be very much of an issue, and I expect that if we continued to increase N by another factor of ten they would all continue to approach zero.

Roundoff errors

Each integrand may contain a number of terms which are divergent either on the boundary of the region, $t_i \in \{a, b\}$, or on a diagonal, $t_i = t_j$. While the renormalization is designed specifically so that these divergences will cancel, individual terms evaluated near these regions can be very large. Because we are limited to the double precision floating point datatype, each term has a relative precision of approximately 10^{-16}. Any time an individual term is more than 10^{16} times the theoretical value of the integrand evaluated at the same point, the machine uncertainty coming from that term can dominate the result. We would hope that since this only happens for a small subset of the points sampled the effect will be negligible as the number of points increases, but this is not the case. If we take a random sample of N points, as is done for Monte Carlo integration, we would expect the closest point to a given boundary (or other codimension 1 subspace) to be $\sim \frac{1}{N}$ away. Individual terms, however, often have a $\frac{1}{t^2}$ divergence from the OPE of the marginal operator, which would lead to $\sim N^2$ divergence for the closest point. This grows faster than the denominator, N, so the roundoff error in the resulting integral should increase linearly with the number of points. The deterministic case is actually worse because some points are intentionally chosen near or even right on the boundary. To combat this, whenever a sample point is close to a boundary or a diagonal, we can replace it with a nearby point giving a decent approximation to the integrand. The integrand function is effectively replaced by one where the value is held constant on small strips. While this means that a perfect integration with no uncertainty would give an incorrect result, the errors introduced this way are less problematic than the roundoff errors when we sample many points without any regulation.

When we discussed the differences between the big G and little g renormalization schemes, I mentioned that the lack of a regulator was an advantage of the little g scheme. Here we have introduced another regulator, so we naturally ask why this is not a problem. The regulator in the big G scheme was required by the theory in that scheme, and we wanted the limit as it approached zero. This regulator is to prevent roundoff error, which is the unavoidable result of using a floating point datatype. Since we are regulating the integration region anyway, we might ask why (aside from issues regarding finiteness at higher orders) we did not use the big G scheme. By using the little g scheme, the integrand is independent of the regulator, which simplifies the integration process. There is not a different integrand for each value of the regulator, and instead of a limit, we only use a small value of the regulator, namely $3 \cdot 10^{-4}$, for which the integrands always evaluate with negligible errors. The choice of regulator for these roundoff errors is arbitrary, but we can estimate the error we have introduced by using the same regulator to replace the value of the integrand with zero near boundaries and diagonals. Fortunately, the differences are minor compared with the statistical errors which are accounted for by the algorithms' reported uncertainties.

Consistency checks

Since the programs to construct wedge states with insertions and produce and evaluate integrals corresponding to the tachyon profile are quite complicated, it is worth using them to evaluate some known quantities. We will see that the numerical integration process gives results which are consistent with expectations the majority of the time, despite the presence of counterterms and the uncertain nature of numerical integration. An obvious choice for a quantity which we know is the equation of motion, which should vanish. The equation of motion, however, has ghost number two, which means that its expectation value by itself will trivially vanish because the ghosts are not saturated. In order to test that $Q_B\Psi + \Psi * \Psi$ vanishes we test that its overlaps with various other string fields all vanish. Because the equation of motion is stronger than just requiring that the equation of motion annihilates all states and actually tells us that it should vanish exactly, as long as the string field is constructed properly these correlation functions should work out to zero whether they themselves were computed correctly or not. In order to test that a non-trivial result also gives the correct answer, we look to the action. Because this is an exactly marginal solution, we expect the energy to vanish, and because the energy is proportional to the action, the action should vanish as well. The action has ghost number three and does not need any additional test states inserted. That this also vanishes is our first strong test that non-trivial expectation values are computed successfully. A summary of these test calculations and their results using the deterministic algorithms is found in tables 5.6 and 5.7 at the end of this section, and all of them are expected to vanish. The majority of the results are consistent with zero, but a few exceptions require detailed examination. These six examples are in table 5.4, which restates their values using the deterministic algorithms and then includes the corresponding results with Monte Carlo calculations and with deterministic calculations using a vanishing integrand near borders and diagonals where cancelling singularities may occur.

The values in tables 5.6 and 5.7 all use a border with width $\epsilon = 3 \cdot 10^{-4}$. When the integrand is sampled within ϵ of a boundary or a diagonal, the closest point on the edge of this strip is used instead. In the last column of table 5.4, when the integrand was sampled at points within these strips, zero was returned instead. The difference between these results gives an estimate of how important the regulated region is to the final result of the integral, and we can see that in most cases it is small compared to the error estimates.

Looking at table 5.4, the first two quantities, $\langle ce^{X^{(0)}}, \mathrm{EOM}^{(3)} \rangle$ and $\langle \Psi^{(1)}, \mathrm{EOM}^{(3)} \rangle$, have very similar behaviours because the second integrand is $\sqrt{2}$ times the first. They are one dimensional integrals, so we can do them analytically and find that the results are exactly zero. The integrands for these two are increasing as they approach each of the boundaries, which would suggest that the discrepancy comes from the regulated region, but the results with 0 inserted near the boundaries are identical. In fact, the `QAG` algorithm always seems to give identical results with either choice of regulation near the boundaries, suggesting that that it does not pick points too close to the limits of integration. If we redo these integrals requesting much higher accuracy, however, we find results which are less precise but consistent with zero. Perhaps requesting a higher accuracy causes the algorithm to notice the cusp where the regulated strips at the boundary are, and that increases the error estimate. The kinetic energy at fourth order is a peculiar case of rounding errors, and it was already discussed in the context of convergence. None of the integration algorithms is correct all of the time, and we should not expect them to be, but `QAG` is problematic because it gives less control over the

Quantity	`Cuhre`/`QAG`	`Suave`	`Cuhre`/`QAG` with 0
$\langle ce^{X^{(0)}}, \mathrm{EOM}^{(3)}\rangle$	$(-6.1 \pm 0.6) \cdot 10^{-11}$	$(4.1 \pm 0.4) \cdot 10^{-4}$	$(-6.1 \pm 0.6) \cdot 10^{-11}$
$\langle \Psi^{(1)}, \mathrm{EOM}^{(3)}\rangle$	$(-8.5 \pm 0.8) \cdot 10^{-11}$	$(6.1 \pm 0.7) \cdot 10^{-4}$	$(-8.5 \pm 0.8) \cdot 10^{-11}$
$\langle \Psi, Q_B\Psi\rangle^{(4)}$	$(-8.7 \pm 1.2) \cdot 10^{-10}$	$(-1.5 \pm 1.3) \cdot 10^{-2}$	$(-8.7 \pm 1.2) \cdot 10^{-10}$
$\frac{\partial}{\partial C^L}\langle ce^{3X^0}, \mathrm{EOM}^{(5)}\rangle$	$(6.2 \pm 2.1) \cdot 10^{-5}$	$(-0.3 \pm 1.1) \cdot 10^{-6}$	$(-0.4 \pm 1.3) \cdot 10^{-4}$
$\frac{\partial}{\partial C_0}\langle c, \mathrm{EOM}^{(6)}\rangle$	$(-2.2 \pm 0.5) \cdot 10^{-4}$	$(8.7 \pm 7.8) \cdot 10^{-4}$	$(0.1 \pm 2.1) \cdot 10^{-2}$
$\frac{\partial}{\partial C_1}\langle \Psi^{(3)}, \mathrm{EOM}^{(3)}\rangle$	$(-3.0 \pm 0.2) \cdot 10^{-8}$	$(-5.1 \pm 0.7) \cdot 10^{-4}$	$(0.8 \pm 1.7) \cdot 10^{-3}$

Table 5.4: Numerical results for consistency checks which require further analysis. Among the results which are expected to vanish, these six have deterministic results which do not. They are given using the standard deterministic algorithms `Cuhre` and `QAG`, using the adaptive Monte Carlo algorithm `Suave`, and using the deterministic algorithms with the integrand replaced with 0 on the regulated strips near potential singularities instead of using the value of the integrand at a safe nearby point.

sample size and does not report the total number of points it uses. We cannot show these results with different sample sizes, as we do for other quantities of interest. Because these are one-dimensional integrals, however, we can expect that the majority of them will be computed very accurately.

For the other three quantities, the integrals are multidimensional so we can evaluate them using the `Cuhre` algorithm with several different sample sizes and see if they become closer to zero. This is shown in table 5.5. The first two of these both have error estimates that decrease as the sample size is increased, and values that decrease even faster. For the first, we see agreement once the sample size is large enough, and for the second we can suspect that the result will continue to tend towards zero. The most important integrals in these two quantities were shown in figures 5.8a and 5.8d respectively, where we can see the convergence to 0 as N is increased. In the case of the final quantity, however, the result clearly does not vanish. If we change the thickness of the regulating border, however, it causes a significant fluctuation, and for extremely thin borders both the result and the uncertainty become much larger. This suggests that it is a genuine case of the border region having a significant impact. Unfortunately, the only way to resolve this issue would be to use higher precision floating point datatypes.

Algorithm	Quantity	Result	Dimensions and Sample Sizes			
`Cuhre`	$\frac{\partial}{\partial C^L}\langle ce^{3X^0}, \mathrm{EOM}^{(5)}\rangle$	$(6.2 \pm 2.1) \cdot 10^{-5}$ $(3.7 \pm 1.6) \cdot 10^{-5}$ $(2.3 \pm 1.3) \cdot 10^{-5}$ $(0.2 \pm 1.7) \cdot 10^{-6}$	2	16055 18005 25545 81055	3	32131 54229 76581 243205
`Cuhre`	$\frac{\partial}{\partial C_0}\langle c, \mathrm{EOM}^{(6)}\rangle$	$(-2.2 \pm 0.5) \cdot 10^{-4}$ $(-7.1 \pm 2.6) \cdot 10^{-5}$ $(-4.0 \pm 1.7) \cdot 10^{-5}$ $(-9.1 \pm 5.2) \cdot 10^{-6}$	3	32131 54229 76581 243205	4	64107 162027 229347 729045
`Cuhre`	$\frac{\partial}{\partial C_1}\langle \Psi^{(3)}, \mathrm{EOM}^{(3)}\rangle$	$(-2.96 \pm 0.19) \cdot 10^{-8}$ $(-2.99 \pm 0.13) \cdot 10^{-8}$ $(-2.99 \pm 0.11) \cdot 10^{-8}$ $(-3.01 \pm 0.06) \cdot 10^{-8}$	3	32131 54229 76581 243205		

Table 5.5: Three of the consistency checks in table 5.4 are shown with different sample sizes. The first two are computed as the sum of two integrals with different dimensions, while the third is a single integral. We expect to see results which tend towards zero as the sample size is increased.

$\langle c, \mathrm{EOM}^{(2)} \rangle$	0
$\langle ce^{2X^0}, \mathrm{EOM}^{(2)} \rangle$	0
$\langle ce^{X^0}, \mathrm{EOM}^{(3)} \rangle$	$-(6.1 \pm 0.6) \cdot 10^{-11}$
$\langle ce^{3X^0}, \mathrm{EOM}^{(3)} \rangle$	$0 \pm 1.1 \cdot 10^{-16}$
$\langle c, \mathrm{EOM}^{(4)} \rangle$	$-(0.6 \pm 1.9) \cdot 10^{-6} - (0.8 \pm 1.3) \cdot 10^{-6} C^L$
$\langle ce^{2X^0}, \mathrm{EOM}^{(4)} \rangle$	$(1.7 \pm 2.5) \cdot 10^{-6} + (9.2 \pm 9.7) \cdot 10^{-7} C^L$
$\langle ce^{4X^0}, \mathrm{EOM}^{(4)} \rangle$	$(2.8 \pm 8.7) \cdot 10^{-11}$
$\langle ce^{X^0}, \mathrm{EOM}^{(5)} \rangle$	$(1.8 \pm 2.5) \cdot 10^{-5} - (1.3 \pm 1.8) \cdot 10^{-5} C^L - (0.2 \pm 3.2) \cdot 10^{-4} (C^L)^2 + (2.1 \pm 2.0) \cdot 10^{-5} C_1 + (0.6 \pm 2.3) \cdot 10^{-5} C_0$
$\langle ce^{3X^0}, \mathrm{EOM}^{(5)} \rangle$	$(0.2 \pm 2.3) \cdot 10^{-5} + (6.2 \pm 2.1) \cdot 10^{-5} C^L - (0.3 \pm 2.7) \cdot 10^{-5} C_1 - (0.7 \pm 6.6) \cdot 10^{-6} C_0$
$\langle ce^{5X^0}, \mathrm{EOM}^{(5)} \rangle$	$(0.2 \pm 3.8) \cdot 10^{-11}$
$\langle c, \mathrm{EOM}^{(6)} \rangle$	$-(0.8 \pm 2.0) \cdot 10^{-3} + (0.7 \pm 1.9) \cdot 10^{-4} C^L - (1.6 \pm 5.4) \cdot 10^{-5} (C^L)^2 - (1.8 \pm 2.3) \cdot 10^{-4} C_1 + (0.2 \pm 7.1) \cdot 10^{-3} C^L C_1 - (2.2 \pm 0.5) \cdot 10^{-4} C_0 + (1.9 \pm 6.5) \cdot 10^{-5} C_0 C^L$
$\langle ce^{2X^0}, \mathrm{EOM}^{(6)} \rangle$	$-(0.1 \pm 1.3) \cdot 10^{-3} + (0.7 \pm 3.7) \cdot 10^{-4} C^L + (0.2 \pm 1.9) \cdot 10^{-3} (C^L)^2 + (0.1 \pm 2.1) \cdot 10^{-3} C_1 + (0 \pm 1.5 \cdot 10^{-2}) C^L C_1 + (0.9 \pm 5.1) \cdot 10^{-4} C_0 - (0.1 \pm 2.9) \cdot 10^{-3} C^L C_0$
$\langle ce^{4X^0}, \mathrm{EOM}^{(6)} \rangle$	$0 \pm 1.1 \cdot 10^{-5} + (1.4 \pm 1.0) \cdot 10^{-6} C^L - (0.2 \pm 5.9) \cdot 10^{-6} C_1 + (0.4 \pm 8.9) \cdot 10^{-7} C_0$
$\langle ce^{6X^0}, \mathrm{EOM}^{(6)} \rangle$	$-(0.6 \pm 1.3) \cdot 10^{-14}$
$\langle \Psi^{(1)}, \mathrm{EOM}^{(2)} \rangle$	0
$\langle \Psi^{(2)}, \mathrm{EOM}^{(2)} \rangle$	0
$\langle \Psi^{(3)}, \mathrm{EOM}^{(2)} \rangle$	0
$\langle \Psi^{(4)}, \mathrm{EOM}^{(2)} \rangle$	0
$\langle \Psi^{(5)}, \mathrm{EOM}^{(2)} \rangle$	0
$\langle \Psi^{(1)}, \mathrm{EOM}^{(3)} \rangle$	$-(8.5 \pm 0.8) \cdot 10^{-11}$
$\langle \Psi^{(2)}, \mathrm{EOM}^{(3)} \rangle$	0
$\langle \Psi^{(3)}, \mathrm{EOM}^{(3)} \rangle$	$-(0.5 \pm 1.3) \cdot 10^{-5} - (0.1 \pm 3.4) \cdot 10^{-6} C^L - (3.0 \pm 0.2) \cdot 10^{-8} C_1$
$\langle \Psi^{(4)}, \mathrm{EOM}^{(3)} \rangle$	0
$\langle \Psi^{(1)}, \mathrm{EOM}^{(4)} \rangle$	0
$\langle \Psi^{(2)}, \mathrm{EOM}^{(4)} \rangle$	$-(0.3 \pm 2.4) \cdot 10^{-3} + (2.3 \pm 5.2) \cdot 10^{-5} C^L - (0.2 \pm 1.8) \cdot 10^{-5} (C^L)^2$
$\langle \Psi^{(3)}, \mathrm{EOM}^{(4)} \rangle$	0
$\langle \Psi^{(1)}, \mathrm{EOM}^{(5)} \rangle$	$(2.4 \pm 3.9) \cdot 10^{-5} - (1.9 \pm 2.5) \cdot 10^{-5} C^L - (0.3 \pm 4.5) \cdot 10^{-4} (C^L)^2 + (3.0 \pm 2.8) \cdot 10^{-5} C_1 + (0.8 \pm 3.2) \cdot 10^{-5} C_0$
$\langle \Psi^{(2)}, \mathrm{EOM}^{(5)} \rangle$	0
$\langle \Psi^{(1)}, \mathrm{EOM}^{(6)} \rangle$	0

Table 5.6: Deterministic tests of the equation of motion for the rolling tachyon. Superscripts represent the order in λ of each quantity. `Cuhre`/`QAG` results shown.

$\langle\Psi, Q_B\Psi\rangle^{(2)}$	0
$\langle\Psi, \Psi * \Psi\rangle^{(2)}$	0
$\langle\Psi, Q_B\Psi\rangle^{(3)}$	0
$\langle\Psi, \Psi * \Psi\rangle^{(3)}$	0
$\langle\Psi, Q_B\Psi\rangle^{(4)}$	$-(8.7 \pm 1.2) \cdot 10^{-10} + (0 \pm 4.2 \cdot 10^{-14})C^L$
$\langle\Psi, \Psi * \Psi\rangle^{(4)}$	0
$\langle\Psi, Q_B\Psi\rangle^{(5)}$	0
$\langle\Psi, \Psi * \Psi\rangle^{(5)}$	0
$\langle\Psi, Q_B\Psi\rangle^{(6)}$	$(0.02 \pm 0.30) + (0 \pm 3.5 \cdot 10^{-2})C^L + (0 \pm 0.11)(C^L)^2 + (0.5 \pm 9.6) \cdot 10^{-13}(C^L)^3 + (0 \pm 6.7 \cdot 10^{-2})C_1 - (0.1 \pm 2.3) \cdot 10^{-13}C^L C_1 + (0 \pm 1.1 \cdot 10^{-2})C_0 + (0.1 \pm 1.5) \cdot 10^{-14}C^L C_0$
$\langle\Psi, \Psi * \Psi\rangle^{(6)}$	0

Table 5.7: Deterministic evaluation of the action for the rolling tachyon. Kinetic and cubic terms are found separately as a consistency check. Superscripts represent the order in λ. `Cuhre/QAG` results shown.

Chapter 6

Summary

This thesis consisted of three main projects. All three involved solutions to string field theory with marginal deformations of the initial D-brane configuration, and two also had connections to the tachyon condensation that represents D-brane decay. We saw both the level truncation and analytical approaches to string field theory. While there are still unanswered questions, progress has been made on each of these topics.

In chapter 3 we saw a new solution to level truncated string field theory. Building on known solutions involving tachyon condensation and marginal deformations, this solution combined those two phenomenon. The result is a solution where a pair of separated D-branes move to become coincident and then a linear combination of the two decays. A combination of tachyon decay after a marginal deformation has since been studied analytically in [45], finding that the energy is independent of the marginal deformation without examining any limitations on the presumably unbounded analytical marginal deformation, but at the time the system examined here had only been seen in the context of separated brane-antibrane decay [53]. That system lacked the enhanced symmetry when the D-branes are coincident, but otherwise had very similar results.

We saw that the part of the string field primarily responsible for D-brane translation is approximately a linear function of the separation as long as that separation is small. Unfortunately, we are also able to show that a field redefinition mixes the terms, so that this linear relationship is not by itself the correspondence between the marginal parameter and its physical effect. We also saw that both the parameter and the physical deformation have finite maximum values. This is in conflict with the natural expectation that translation of a D-brane should be unbounded, but in agreement with all previous level-truncated results on marginal deformations. In fact, we found evidence that contradicts early explanations for this maximum which involved either a singular correspondence or a second branch of the solution, since in our case it is the physical translation distance that is known and bounded.

In chapter 4 we focused on the work of Kiermaier and Okawa [36]. For a class of marginal deformations with the OPE $V(0)V(t) \sim \frac{1}{t^2}$ they showed that it is possible to define a solution using renormalized marginal operators. That work also provides an example of a renormalization scheme which is compatible with the sufficient conditions for their solution. Here I have carefully studied those conditions and proven that they are all satisfied for a slightly more general family of renormalization schemes with two parameters. This also filled some gaps in the original proofs. Considering the most general case, we saw that there are likely to be infinitely many free parameters, but for our proofs we only included two. We hope that this freedom is connected to gauge transformations, but that remains unproven. After studying two different approaches to renormalizing the marginal operators, we saw that they are not equivalent beyond quadratic order, and that the more natural approach at quadratic order needs subleading corrections in order to remain finite beyond cubic order.

One well known example of a marginal deformation is the rolling tachyon. Physically it corresponds to the time-dependent process of D-brane decay. The time-asymmetric rolling tachyon has been studied extensively, and no further calculations were necessary here. The time-symmetric case, however, was not previously studied due to the fact that it has a singular self-OPE of precisely the form that Kiermaier and Okawa's solution was intended to renormalize. In practice, the solution is difficult to construct, but we found in chapter 5 that it can be done up to 6th order in λ by combining symbolic algebra and numerical integration programs. Such a calculation to explicitly construct component fields of a renormalized marginal solution had not previously been attempted. In this way we found that the tachyon profile for small λ is qualitatively no different from what we would find if we took the tachyon profile of the time-asymmetric case and symmetrized it. Unlike that simple case, however, when we increased λ we found that the shape of the profile can change in ways that appear similar to gauge transformations.

We found that the two free parameters we allowed in the renormalization scheme play no part for small λ, but that they do affect the tachyon profile for larger λ. The part of the tachyon profile responsible for the small λ behaviour is also quite clearly a convergent series for all times, but it is not at all clear that the rest of the tachyon profile still converges when λ is increased. This is especially true since the renormalization parameters could in principle take any value. Whether the tachyon profile is finite for all λ and what consequences this has for the topic of maximum marginal deformations remains an open question.

Bibliography

[1] J. L. Karczmarek and M. Longton, *SFT on separated D-branes and D-brane translation*, *JHEP* **1208** (2012) 057, [arXiv:1203.3805].

[2] J. L. Karczmarek and M. Longton, *Renormalization schemes for SFT solutions*, *JHEP* **1504** (2015) 007, [arXiv:1412.3466].

[3] M. Longton, *Time-Symmetric Rolling Tachyon Profile*, arXiv:1505.0080.

[4] M. Longton, *SFT Action for Separated D-branes*, arXiv:1203.4615.

[5] M. Kiermaier, Y. Okawa, L. Rastelli, and B. Zwiebach, *Analytic solutions for marginal deformations in open string field theory*, *JHEP* **01** (2008) 028, [hep-th/0701249].

[6] J. Polchinski, *String theory. Vol. 1: An introduction to the bosonic string*, . Cambridge, UK: Univ. Pr. (1998) 402 p.

[7] J. Dai, R. Leigh, and J. Polchinski, *New Connections Between String Theories*, *Mod.Phys.Lett.* **A4** (1989) 2073–2083.

[8] P. Di Francesco, P. Mathieu, and D. Senechal, *Conformal field theory*, . New York, USA: Springer (1997) 890 p.

[9] E. Witten, *Noncommutative Geometry and String Field Theory*, *Nucl.Phys.* **B268** (1986) 253.

[10] W. Taylor and B. Zwiebach, *D-branes, tachyons, and string field theory*, hep-th/0311017.

[11] M. R. Gaberdiel and B. Zwiebach, *Tensor constructions of open string theories I: Foundations*, *Nucl. Phys.* **B505** (1997) 569–624, [hep-th/9705038].

[12] D. J. Gross and A. Jevicki, *Operator Formulation of Interacting String Field Theory. 2*, *Nucl. Phys.* **B287** (1987) 225.

[13] M. Schnabl, *Algebraic solutions in Open String Field Theory - A Lightning Review*, arXiv:1004.4858.

[14] A. Sen, *Universality of the tachyon potential*, *JHEP* **9912** (1999) 027, [hep-th/9911116].

[15] V. A. Kostelecky and S. Samuel, *On a Nonperturbative Vacuum for the Open Bosonic String*, *Nucl.Phys.* **B336** (1990) 263.

[16] N. Moeller, A. Sen, and B. Zwiebach, *D-branes as tachyon lumps in string field theory*, *JHEP* **08** (2000) 039, [hep-th/0005036].

[17] A. Sen and B. Zwiebach, *Tachyon condensation in string field theory*, *JHEP* **03** (2000) 002, [hep-th/9912249].

[18] D. Gaiotto and L. Rastelli, *Experimental string field theory*, *JHEP* **08** (2003) 048, [hep-th/0211012].

[19] S. Giusto and C. Imbimbo, *Physical states at the tachyonic vacuum of open string field theory*, *Nucl.Phys.* **B677** (2004) 52–86, [hep-th/0309164].

[20] C. Imbimbo, *The Spectrum of open string field theory at the stable tachyonic vacuum*, *Nucl.Phys.* **B770** (2007) 155–178, [hep-th/0611343].

[21] A. Sen and B. Zwiebach, *Large marginal deformations in string field theory*, *JHEP* **10** (2000) 009, [hep-th/0007153].

[22] B. Zwiebach, *A Solvable toy model for tachyon condensation in string field theory*, *JHEP* **0009** (2000) 028, [hep-th/0008227].

[23] M. Kudrna, M. Rapcak, and M. Schnabl, *Ising model conformal boundary conditions from open string field theory*, arXiv:1401.7980.

[24] A. Sen, *Energy momentum tensor and marginal deformations in open string field theory*, *JHEP* **08** (2004) 034, [hep-th/0403200].

[25] M. Schnabl, *Analytic solution for tachyon condensation in open string field theory*, *Adv. Theor. Math. Phys.* **10** (2006) 433–501, [hep-th/0511286].

[26] T. Erler and C. Maccaferri, *The Phantom Term in Open String Field Theory*, *JHEP* **1206** (2012) 084, [arXiv:1201.5122].

[27] I. Ellwood, *Rolling to the tachyon vacuum in string field theory*, *JHEP* **0712** (2007) 028, [arXiv:0705.0013].

[28] I. Ellwood and M. Schnabl, *Proof of vanishing cohomology at the tachyon vacuum*, *JHEP* **02** (2007) 096, [hep-th/0606142].

[29] Y. Okawa, L. Rastelli, and B. Zwiebach, *Analytic Solutions for Tachyon Condensation with General Projectors*, hep-th/0611110.

[30] T. Erler and M. Schnabl, *A Simple Analytic Solution for Tachyon Condensation*, *JHEP* **10** (2009) 066, [arXiv:0906.0979].

[31] T. Erler, *Split String Formalism and the Closed String Vacuum*, *JHEP* **0705** (2007) 083, [hep-th/0611200].

[32] E. Fuchs and M. Kroyter, *Analytical Solutions of Open String Field Theory*, *Phys.Rept.* **502** (2011) 89–149, [arXiv:0807.4722].

[33] M. Schnabl, *Comments on marginal deformations in open string field theory*, *Phys. Lett.* **B654** (2007) 194–199, [hep-th/0701248].

[34] M. Kiermaier, Y. Okawa, and P. Soler, *Solutions from boundary condition changing operators in open string field theory*, *JHEP* **03** (2011) 122, [arXiv:1009.6185].

[35] E. Coletti, I. Sigalov, and W. Taylor, *Taming the tachyon in cubic string field theory*, *JHEP* **0508** (2005) 104, [hep-th/0505031].

[36] M. Kiermaier and Y. Okawa, *Exact marginality in open string field theory: a general framework*, *JHEP* **11** (2009) 041, [arXiv:0707.4472].

[37] E. Fuchs, M. Kroyter, and R. Potting, *Marginal deformations in string field theory*, *JHEP* **0709** (2007) 101, [arXiv:0704.2222].

[38] C. Maccaferri, *A simple solution for marginal deformations in open string field theory*, arXiv:1402.3546.

[39] T. Erler and C. Maccaferri, *String Field Theory Solution for Any Open String Background*, *JHEP* **1410** (2014) 029, [arXiv:1406.3021].

[40] M. Kiermaier, Y. Okawa, and B. Zwiebach, *The boundary state from open string fields*, arXiv:0810.1737.

[41] M. Kudrna, C. Maccaferri, and M. Schnabl, *Boundary State from Ellwood Invariants*, *JHEP* **1307** (2013) 033, [arXiv:1207.4785].

[42] M. Kudrna, T. Masuda, Y. Okawa, M. Schnabl, and K. Yoshida, *Gauge-invariant observables and marginal deformations in open string field theory*, *JHEP* **01** (2013) 103, [arXiv:1207.3335].

[43] L. Rastelli, A. Sen, and B. Zwiebach, *Classical solutions in string field theory around the tachyon vacuum*, *Adv. Theor. Math. Phys.* **5** (2002) 393–428, [hep-th/0102112].

[44] W. Taylor, *D-brane effective field theory from string field theory*, *Nucl. Phys.* **B585** (2000) 171–192, [hep-th/0001201].

[45] S. Inatomi, I. Kishimoto, and T. Takahashi, *Tachyon Vacuum of Bosonic Open String Field Theory in Marginally Deformed Backgrounds*, *PTEP* **2013** (2013) 023B02, [arXiv:1209.4712].

[46] A. Sen, *Descent relations among bosonic D-branes*, *Int. J. Mod. Phys.* **A14** (1999) 4061–4078, [hep-th/9902105].

[47] M. Kiermaier and Y. Okawa, *General marginal deformations in open superstring field theory*, *JHEP* **0911** (2009) 042, [arXiv:0708.3394].

[48] T. Erler, *Level truncation and rolling the tachyon in the lightcone basis for open string field theory*, hep-th/0409179.

[49] A. Sen, *Rolling tachyon*, *JHEP* **0204** (2002) 048, [hep-th/0203211].

[50] D. Gaiotto, N. Itzhaki, and L. Rastelli, *Closed strings as imaginary D-branes*, *Nucl.Phys.* **B688** (2004) 70–100, [hep-th/0304192].

[51] C. Maccaferri and M. Schnabl, *Large BCFT moduli in open string field theory*, arXiv:1506.0372.

[52] T. Hahn, *CUBA: A Library for multidimensional numerical integration*, *Comput.Phys.Commun.* **168** (2005) 78–95, [hep-ph/0404043].

[53] A. Bagchi and A. Sen, *Tachyon Condensation on Separated Brane-Antibrane System*, *JHEP* **05** (2008) 010, [arXiv:0801.3498].

Appendix A

Action For Separated D-branes

This appendix contains the details necessary to easily reproduce the action used in chapter 3. A version of this apears on the arXiv as [4]. That work was intended as supplementary material to [1], and is not intended for publication in a peer reviewed journal.

A.1 Level (3,9) Potential

In level-truncated studies of string field theory, the string field is expanded in a basis of conformal primaries and their descendants and then truncated at some eigenvalue of the virasoro zero-mode operator. In this note we present the potential, proportional to the action, for all terms in the string field up to level 3. Our intended theory is a collection of D-24 branes whose transverse directions are all aligned, but which are not necessarily coincident. The choice of D24-branes means that there should be one direction which is singled out, and this is the main assumption we have made on our string field. Any system of bosonic D-branes with a rotational symmetry in 25 of the 26 dimensions should be described at level 3 by this potential. The string field we use will then be equivalent to (3.7) studied in chapter 3:

$$\begin{aligned}|\Phi\rangle = \sum_d \big(&t_d c_1 + h_d c_0 + u_d c_{-1} + v_d L'_{-2} c_1 + w_d L^{25}_{-2} c_1 + o_d(b_{-2}c_{-1}c_1 - 2c_{-2}) \\ &+ \tilde{o}_d(b_{-2}c_{-1}c_1 + 2c_{-2}) + p_d L'_{-3} c_1 + q_d L^{25}_{-3} c_1 + \ldots\big)\,|0;d\rangle \\ + \sum_d \big(&x_d c_1 + f_d L^{25}_{-1} c_1 + r_d c_{-1} + s_d L'_{-2} c_1 + y_d L^{25}_{-2} c_1 + z_d L^{25}_{-1} L^{25}_{-1} c_1 + \ldots\big)\,\alpha^{25}_{-1}\,|0;d\rangle \ . \end{aligned} \quad \text{(A.1)}$$

where $L^X_n = L^{25}_n$ are the virasoro operators in the transverse direction, and L'_n contain the sum over the other 25 directions of matter oscillators. The ghost CFT is handled explicitly in terms of b_n and c_n operators.

Unlike in (3.7), in this case the vacuum states and the coefficients are not labeled with D-brane indices. They are labeled only by d, the eigenvalue of α^{25}_0. The vacuum is defined by $\alpha^{25}_0\,|0;d\rangle = d\,|0;d\rangle$, and $\alpha^{\mu\neq 25}_0\,|0;d\rangle = 0$. This does not uniquely determine the vacuum state, as there are many different ways to achieve a given zero-mode, but once a physical situation is chosen the appropriate values can be inserted for d. In our case this meant replacing the sum over d with a sum over brane indices and the eigenvalue with the separation. Since the action is more general than the case we have considered the coefficients given here are in as general a form as possible. While the case of non-zero α_0 eigenvalues in the rotationally symmetric directions has not been considered, the twist-odd states have been. The action in this appendix does contain all of the necessary couplings to include twist-odd states in the string field.

With the string field defined, we can move on to writing down the action. The quadratic term is a function of the zero-mode eigenvalue d, assuming that the vacuum states have been

put into a basis which is orthogonal. For every set of three fields there is a cubic term which is a function of the three zero-modes of the strings. For the study of separated D-branes or non-zero momentum states these zero-modes must sum to 0, but we will leave them unconstrained. The action can be written as

$$S = -\frac{1}{2}\sum_{l,m}\sum_{d} A_{lm}(d)\phi_d^{(l)\dagger}\phi_d^{(m)} - \sum_{l,m,n}\sum_{d_1,d_2,d_3} B_{lmn}(d_1,d_2,d_3)\left(\frac{4}{3\sqrt{3}}\right)^{\frac{1}{2}(d_1^2+d_2^2+d_3^2)}\phi_{d_1}^{(l)}\phi_{d_2}^{(m)}\phi_{d_3}^{(n)}, \tag{A.2}$$

where l, m, and n run over the set of all fields we are considering. The cubic interaction term is normally written with a factor of $\frac{1}{3}$, but I will define the coefficients B_{lmn} to include it. This action is equivalent to the potential of (3.5) after rescaling to the appropriate units $\mathcal{V} = -2\pi^2 S$. The purpose of this appendix is then to explicitly list the coefficient functions A_{lm} and B_{lmn} for the first few levels. The quadratic coefficients $A_{lm}(d)$ are presented in table A.2, and the cubic coefficients $B_{lmn}(d_1,d_2,d_3)$ are in table A.3.

For our special case of separated D-branes, where the vacuum states are represented by Chan-Paton factors, the cubic terms use $d_1 = d_i - d_j$, $d_2 = d_j - d_k$, $d_3 = d_k - d_i$, and the field associated with such a state has the appropriate indices such as $\phi_{d_1}^{(t)} = t_{ij}$. For example, the potential for only the fields t_{ij} and x_{ij} would contain the terms

$$S = -\frac{1}{2}\left(A_{tt}t_{ij}t_{ji} + A_{xx}x_{ij}x_{ji}\right) - \left(B_{ttt}t_{ij}t_{jk}t_{ki} + 3B_{ttx}t_{ij}t_{jk}x_{ki} + 3B_{txx}t_{ij}x_{jk}x_{ki} + B_{xxx}x_{ij}x_{jk}x_{ki}\right) \tag{A.3}$$

where the separation parameters of the coefficients were omitted for brevity. The other orderings of fields, such as $B_{txt}t_{ij}x_{jk}t_{ki}$, are equivalent to the ones shown once the D-brane indices are summed over, which is why the factors of 3 appear.

There are in principle as many as six orderings for the cubic interaction of each set of three fields, but we have shown in section 3.1.2 using the twist operator that we only need to calculate one of them. Similarly we know from the properties of the inner product and the hermicity of Q_B that $A_{lm} = \pm A_{ml}$. Specifically, we know that

$$A_{lm}(d)\phi_d^{(l)\dagger}\phi_d^{(m)} = A_{ml}(d)\phi_d^{(m)\dagger}\phi_d^{(l)} \ , \tag{A.4a}$$

$$B_{lmn}(d_1,d_2,d_3) = B_{mnl}(d_2,d_3,d_1) = B_{nlm}(d_3,d_1,d_2) \ , \tag{A.4b}$$

$$B_{lmn}(d_1,d_2,d_3) = -\Omega_l\Omega_m\Omega_n B_{nml}(-d_3,-d_2,-d_1) \ , \tag{A.4c}$$

where Ω_l is the twist eigenvalue of the operator associated with the state $\left|\phi^{(l)}\right\rangle$. Since the quadratic reordering rule involves the behaviour of the coefficient field under hermitian conjugation and not just the masses A_{lm}, table A.2 includes both orderings for the few non-zero off-diagonal quadratic terms.

The separation parameters d_1, d_2, and d_3 in (A.2) are the eigenvalues of the operators α_0^{25} acting on the vacua of the three string fields, so this allows our coefficients B_{lmn} to be useful in describing other situations, such as lump solutions. The same coefficients can be used with a different choice of parameters. This is also true of the quadratic terms A_{lm}. The first terms $A_{lm}(0)$ and $B_{lmn}(0,0,0)$ were given in [21] and an action including terms with non-zero momentum was given in [16], so for comparison a brief dictionary of fields is given in table A.1. The couplings A_{lm} and B_{lmn} found here can then be used to reproduce the action in either of those works up to level (3,9). An example of such a calculation was given in section 3.1.2.

Here	t	x	h	u	v	w	f	o	p	q	r	s	y	z
[21]	t	a_s	NA	u	w	v	NA	NA	NA	NA	s	r	$\bar{r}$	y
[16]	t	NA	NA	u	w	v	z^*	NA	NA	NA	NA	NA	NA	NA

Table A.1: A comparison of our field definitions to those used in two other works on level truncated solutions.

*There is a d-dependent difference in normalization for this field.

$l\,m$	$A_{lm}(d)$
$t\ t$	$1/2\,d^2 - 1$
$x\ x$	$1/2\,d^2$
$h\ h$	-2
$u\ u$	$-1 - 1/2\,d^2$
$v\ v$	$\frac{25}{2} + \frac{25}{4}\,d^2$
$w\,w$	$1/4\,(4\,d^2+1)(d^2+2)$
$w\ f$	$3/2\,d(d^2+2)$
$f\ w$	$-3/2\,d(d^2+2)$
$f\ f$	$-(d^2+2)(d^2+1)$
$o\ o$	$8 + 2\,d^2$
$\tilde{o}\ \tilde{o}$	$-8 - 2\,d^2$
$p\ p$	$-100 - 25\,d^2$
$q\ q$	$-1/2\,(3\,d^2+2)(4+d^2)$
$q\ y$	$-5/2\,d(4+d^2)$
$y\ q$	$5/2\,d(4+d^2)$
$q\ z$	$-6\,d(4+d^2)$
$z\ q$	$6\,d(4+d^2)$
$r\ r$	$-2 - 1/2\,d^2$
$s\ s$	$\frac{25}{4}\,d^2 + 25$
$y\ y$	$1/4\,(4+d^2)(4\,d^2+9)$
$y\ z$	$3/2\,(3\,d^2+2)(4+d^2)$
$z\ y$	$3/2\,(3\,d^2+2)(4+d^2)$
$z\ z$	$3\,(4+d^2)(d^2+2)(d^2+1)$

Table A.2: The quadratic coefficients for the fields in the action up to level 3. Off-diagonal terms which are not shown are all 0.

$l\,m\,n$	$B_{lmn}(d_1, d_2, d_3)$
$t\ t\ t$	$\frac{27}{64}\sqrt{3}$
$t\ t\ x$	$\frac{9}{32}\,d_1 - \frac{9}{32}\,d_2$
$t\ t\ h$	0
$t\ t\ u$	$\frac{11}{64}\sqrt{3}$
$t\ t\ v$	$-\frac{125}{128}\sqrt{3}$
$t\ t\ w$	$\frac{1}{128}\sqrt{3}(4\,{d_1}^2 - 8\,d_1d_2 + 4\,{d_2}^2 + 4\,d_3d_1 + 4\,d_3d_2 - 8\,{d_3}^2 - 5)$
$t\ t\ f$	$\frac{1}{64}\sqrt{3}(2\,d_2 + 4\,d_3{d_1}^2 - 8\,d_3d_2d_1 + 4\,d_3{d_2}^2 - 9\,d_3 + 2\,d_1)$
$t\ t\ o$	0
$t\ t\ \tilde{o}$	0
$t\ t\ p$	0
$t\ t\ q$	$\frac{1}{96}\,(d_1 - d_2)(2\,d_1 - 15\,d_3 + 2\,d_2)$
$t\ t\ r$	$\frac{11}{96}\,d_1 - \frac{11}{96}\,d_2$
$t\ t\ s$	$-\frac{125}{192}\,d_1 + \frac{125}{192}\,d_2$
$t\ t\ y$	$\frac{1}{192}\,(d_1 - d_2)(4\,{d_1}^2 + 4\,d_3d_1 - 8\,d_1d_2 - 37 - 8\,{d_3}^2 + 4\,{d_2}^2 + 4\,d_3d_2)$
$t\ t\ z$	$\frac{1}{96}\,(d_1 - d_2)(4\,{d_3}^2{d_1}^2 - 8\,{d_3}^2d_2d_1 + 6\,d_3d_1 - 22 - 27\,{d_3}^2 + 4\,{d_3}^2{d_2}^2 + 6\,d_3d_2)$
$t\ x\ x$	$-1/16\,\sqrt{3}(-4 - d_1d_2 + {d_1}^2 - d_3d_1 + d_3d_2)$
$t\ x\ h$	0
$t\ x\ u$	$-\frac{11}{96}\,d_1 + \frac{11}{96}\,d_3$
$t\ x\ v$	$\frac{125}{192}\,d_1 - \frac{125}{192}\,d_3$
$t\ x\ w$	$-1/48\,{d_1}^3 - 1/6\,d_2 - 1/16\,d_3d_2d_1 - 1/24\,{d_3}^3 + 1/48\,{d_3}^2d_2 + 1/48\,d_3{d_2}^2 + 1/24\,{d_1}^2d_2 + 1/16\,{d_3}^2d_1 + \frac{37}{192}\,d_1 + \frac{59}{192}\,d_3 - 1/48\,d_1{d_2}^2$
$t\ x\ f$	$-1/24\,d_3{d_1}^3 - 1/12\,{d_3}^2d_2d_1 - 1/24\,d_3d_1{d_2}^2 - 1/48\,d_1d_2 + 1/24\,{d_3}^2{d_2}^2 - \frac{5}{16}\,d_3d_2 + 1/24\,{d_3}^2{d_1}^2 - 1/48\,{d_1}^2 - \frac{3}{32}\,{d_3}^2 + \frac{43}{96}\,d_3d_1 + 1/12\,d_3d_2{d_1}^2 + 1/3$
$t\ x\ o$	0
$t\ x\ \tilde{o}$	0
$t\ x\ p$	0
$t\ x\ q$	$-\frac{1}{432}\,\sqrt{3}(-17\,d_3{d_1}^2 + 15\,d_3d_2d_1 - 15\,{d_3}^2d_2 + 28\,d_3 + 2\,{d_1}^3 + 15\,{d_3}^2d_1 + 2\,d_3{d_2}^2 - 2\,d_1{d_2}^2 + 24\,d_2 - 40\,d_1)$
$t\ x\ r$	$-\frac{11}{432}\,\sqrt{3}(-4 - d_1d_2 + {d_1}^2 - d_3d_1 + d_3d_2)$
$t\ x\ s$	$\frac{125}{864}\sqrt{3}(-4 - d_1d_2 + {d_1}^2 - d_3d_1 + d_3d_2)$
$t\ x\ y$	$-\frac{1}{864}\,\sqrt{3}(-4\,d_1{d_2}^3 + 84 - 8\,{d_3}^3d_2 + 8\,{d_3}^3d_1 + 133\,d_1d_2 + 8\,{d_3}^2d_2d_1 + 12\,{d_1}^2{d_2}^2 - 12\,{d_3}^2{d_1}^2 - 12\,d_2{d_1}^3 + 4\,{d_3}^2{d_2}^2 + 4\,{d_1}^4 + 4\,d_3{d_2}^3 + 32\,{d_3}^2 - 85\,{d_1}^2 - 48\,{d_2}^2 + 12\,d_3d_2{d_1}^2 - 43\,d_3d_1 + 11\,d_3d_2 - 16\,d_3d_1{d_2}^2)$
$t\ x\ z$	$-\frac{1}{432}\,\sqrt{3}(-4\,{d_3}^3{d_1}^3 + 24 + 12\,{d_3}^3d_2{d_1}^2 - 27\,{d_3}^3d_2 + 27\,{d_3}^3d_1 + 22\,d_1d_2 + 123\,{d_3}^2d_2d_1 - 81\,{d_3}^2{d_1}^2 - 42\,{d_3}^2{d_2}^2 - 4\,{d_3}^2{d_2}^3d_1 + 108\,{d_3}^2 - 22\,{d_1}^2 - 12\,{d_3}^3{d_2}^2d_1 + 4\,{d_3}^3{d_2}^3 - 98\,d_3d_1 + 50\,d_3d_2 + 4\,{d_3}^2{d_1}^4 + 6\,d_3{d_1}^3 - 6\,d_3d_1{d_2}^2 - 12\,{d_3}^2d_2{d_1}^3 + 12\,{d_1}^2{d_2}^2{d_3}^2)$
$t\ h\ h$	$1/4\,\sqrt{3}$
$t\ h\ u$	$1/6$
$t\ h\ v$	0
$t\ h\ w$	0
$t\ h\ f$	0
$t\ h\ o$	$-2/9\,\sqrt{3}$
$t\ h\ \tilde{o}$	$\frac{4}{27}\,\sqrt{3}$
$t\ h\ p$	0
$t\ h\ q$	0
$t\ h\ r$	$1/27\,\sqrt{3}(d_1 - d_2)$
$t\ h\ s$	0
$t\ h\ y$	0
$t\ h\ z$	0
$t\ u\ u$	$\frac{19}{576}\,\sqrt{3}$
$t\ u\ v$	$-\frac{1375}{3456}\,\sqrt{3}$
$t\ u\ w$	$\frac{11}{3456}\,\sqrt{3}(4\,{d_1}^2 - 8\,d_1d_2 + 4\,{d_2}^2 + 4\,d_3d_1 + 4\,d_3d_2 - 8\,{d_3}^2 - 5)$
$t\ u\ f$	$\frac{11}{1728}\,\sqrt{3}(2\,d_2 + 4\,d_3{d_1}^2 - 8\,d_3d_2d_1 + 4\,d_3{d_2}^2 - 9\,d_3 + 2\,d_1)$

Table A.3: The cubic couplings for all of the fields in the action up to level 3.

$l\,m\,n$	$B_{lmn}(d_1, d_2, d_3)$
$t\ u\ o$	$\frac{20}{81}$
$t\ u\ \tilde{o}$	0
$t\ u\ p$	0
$t\ u\ q$	$\frac{11}{2592}\,(d_1 - d_2)(2\,d_1 - 15\,d_3 + 2\,d_2)$
$t\ u\ r$	$\frac{19}{864}\,d_1 - \frac{19}{864}\,d_2$
$t\ u\ s$	$-\frac{1375}{5184}\,d_1 + \frac{1375}{5184}\,d_2$
$t\ u\ y$	$\frac{11}{5184}\,(d_1 - d_2)(4\,{d_1}^2 + 4\,d_3 d_1 - 8\,d_1 d_2 - 37 - 8\,{d_3}^2 + 4\,{d_2}^2 + 4\,d_3 d_2)$
$t\ u\ z$	$\frac{11}{2592}\,(d_1 - d_2)(4\,{d_3}^2{d_1}^2 - 8\,{d_3}^2 d_2 d_1 + 6\,d_3 d_1 - 22 - 27\,{d_3}^2 + 4\,{d_3}^2{d_2}^2 + 6\,d_3 d_2)$
$t\ v\ v$	$\frac{9475}{2304}\,\sqrt{3}$
$t\ v\ w$	$-\frac{125}{6912}\,\sqrt{3}(4\,{d_1}^2 - 8\,d_1 d_2 + 4\,{d_2}^2 + 4\,d_3 d_1 + 4\,d_3 d_2 - 8\,{d_3}^2 - 5)$
$t\ v\ f$	$-\frac{125}{3456}\,\sqrt{3}(2\,d_2 + 4\,d_3{d_1}^2 - 8\,d_3 d_2 d_1 + 4\,d_3{d_2}^2 - 9\,d_3 + 2\,d_1)$
$t\ v\ o$	0
$t\ v\ \tilde{o}$	0
$t\ v\ p$	$\frac{400}{81}$
$t\ v\ q$	$-\frac{125}{5184}\,(d_1 - d_2)(2\,d_1 - 15\,d_3 + 2\,d_2)$
$t\ v\ r$	$-\frac{1375}{5184}\,d_1 + \frac{1375}{5184}\,d_2$
$t\ v\ s$	$\frac{9475}{3456}\,d_1 - \frac{9475}{3456}\,d_2$
$t\ v\ y$	$-\frac{125}{10368}\,(d_1 - d_2)(4\,{d_1}^2 + 4\,d_3 d_1 - 8\,d_1 d_2 - 37 - 8\,{d_3}^2 + 4\,{d_2}^2 + 4\,d_3 d_2)$
$t\ v\ z$	$-\frac{125}{5184}\,(d_1 - d_2)(4\,{d_3}^2{d_1}^2 - 8\,{d_3}^2 d_2 d_1 + 6\,d_3 d_1 - 22 - 27\,{d_3}^2 + 4\,{d_3}^2{d_2}^2 + 6\,d_3 d_2)$
$t\ w\ w$	$\frac{1}{6912}\,\sqrt{3}(80\,d_1{d_2}^3 + 537 - 16\,{d_3}^3 d_2 + 80\,{d_3}^3 d_1 - 236\,d_1 d_2 - 80\,{d_3}^2 d_2 d_1 - 48\,{d_1}^2{d_2}^2 - 48\,{d_3}^2{d_1}^2 - 16\,d_2{d_1}^3 + 96\,{d_3}^2{d_2}^2 + 16\,{d_1}^4 - 16\,d_3{d_2}^3 + 532\,{d_3}^2 - 296\,{d_1}^2 + 532\,{d_2}^2 + 112\,d_3 d_2{d_1}^2 - 32\,{d_2}^4 - 32\,{d_3}^4 - 236\,d_3 d_1 - 3368\,d_3 d_2 - 16\,d_3{d_1}^3 - 80\,d_3 d_1{d_2}^2)$
$t\ w\ f$	$\frac{1}{3456}\,\sqrt{3}(-32\,{d_3}^3 d_2 d_1 - 48\,d_3{d_2}^2{d_1}^2 + 80\,d_3{d_2}^3 d_1 - 16\,d_3 d_2{d_1}^3 + 80\,{d_3}^2 d_2{d_1}^2 - 64\,{d_3}^2 d_1{d_2}^2 - 260\,d_3 d_2 d_1 + 572\,d_3{d_2}^2 - 284\,{d_3}^2 d_2 - 16\,{d_2}^3 - 328\,d_3{d_1}^2 - 266\,d_1 - 1546\,d_2 + 8\,{d_1}^3 + 16\,{d_3}^3{d_2}^2 + 16\,{d_3}^3{d_1}^2 + 336\,{d_3}^2 d_1 - 8\,d_1{d_2}^2 + 16\,{d_1}^2 d_2 + 16\,{d_3}^2{d_2}^3 - 32\,{d_3}^2{d_1}^3 - 32\,d_3{d_2}^4 + 16\,d_3{d_1}^4 - 36\,{d_3}^3 + 813\,d_3)$
$t\ w\ o$	0
$t\ w\ \tilde{o}$	0
$t\ w\ p$	0
$t\ w\ q$	$\frac{1}{648}\,d_2{d_1}^3 - \frac{55}{864}\,{d_1}^2 + \frac{709}{2592}\,{d_2}^2 - \frac{7}{162}\,{d_3}^2 + \frac{5}{432}\,{d_3}^3 d_2 + \frac{49}{1296}\,d_3 d_1{d_2}^2 + \frac{619}{5184}\,d_3 d_1 - \frac{2891}{5184}\,d_3 d_2 + \frac{2}{81}\,{d_3}^2{d_1}^2 - \frac{19}{1296}\,d_3{d_1}^3 - \frac{23}{81}\,d_1 d_2 + \frac{13}{1296}\,{d_3}^2{d_2}^2 - \frac{5}{432}\,{d_3}^3 d_1 - \frac{1}{216}\,{d_1}^2{d_2}^2 + \frac{1}{648}\,d_3 d_2{d_1}^2 - \frac{5}{144}\,{d_3}^2 d_2 d_1 + \frac{1}{324}\,{d_2}^4 + \frac{1}{648}\,{d_1}^4 - \frac{1}{648}\,d_1{d_2}^3 - \frac{2}{81}\,d_3{d_2}^3 + \frac{16}{81}$
$t\ w\ r$	$-\frac{11}{648}\,d_3{d_1}^2 + \frac{11}{1296}\,{d_1}^3 - \frac{11}{432}\,d_1{d_2}^2 + \frac{11}{432}\,d_3 d_2 d_1 - \frac{407}{5184}\,d_1 - \frac{11}{1296}\,{d_3}^2 d_2 + \frac{11}{648}\,{d_2}^3 + \frac{11}{162}\,d_3 + \frac{11}{1296}\,{d_3}^2 d_1 - \frac{649}{5184}\,d_2 - \frac{11}{1296}\,d_3{d_2}^2$
$t\ w\ s$	$\frac{4625}{10368}\,d_1 + \frac{7375}{10368}\,d_2 - \frac{125}{324}\,d_3 - \frac{125}{864}\,d_3 d_2 d_1 - \frac{125}{2592}\,{d_3}^2 d_1 + \frac{125}{2592}\,{d_3}^2 d_2 + \frac{125}{2592}\,d_3{d_2}^2 + \frac{125}{1296}\,d_3{d_1}^2 + \frac{125}{864}\,d_1{d_2}^2 - \frac{125}{2592}\,{d_1}^3 - \frac{125}{1296}\,{d_2}^3$
$t\ w\ y$	$-\frac{1}{108}\,{d_3}^3 d_2 d_1 - \frac{1}{54}\,d_3{d_2}^2{d_1}^2 + \frac{1}{162}\,d_3{d_2}^3 d_1 + \frac{1}{81}\,d_3 d_2{d_1}^3 - \frac{1}{324}\,{d_3}^2 d_2{d_1}^2 + \frac{11}{648}\,{d_3}^2 d_1{d_2}^2 - \frac{1039}{2592}\,d_3 d_2 d_1 + \frac{421}{1296}\,d_3{d_2}^2 + \frac{59}{2592}\,{d_3}^2 d_2 - \frac{29}{288}\,{d_2}^3 + \frac{5}{2592}\,d_3{d_1}^2 + \frac{2393}{10368}\,d_1 - \frac{6521}{10368}\,d_2 - \frac{23}{432}\,{d_1}^3 + \frac{1}{648}\,{d_3}^3{d_2}^2 + \frac{5}{648}\,{d_3}^3{d_1}^2 + \frac{197}{2592}\,{d_3}^2 d_1 + \frac{4}{27}\,d_1{d_2}^2 + \frac{5}{864}\,{d_1}^2 d_2 - \frac{1}{108}\,{d_3}^2{d_2}^3 - \frac{1}{216}\,{d_3}^2{d_1}^3 + \frac{1}{648}\,d_3{d_2}^4 - \frac{1}{648}\,d_3{d_1}^4 + \frac{1}{81}\,{d_1}^2{d_2}^3 - \frac{7}{648}\,d_1{d_2}^4 - \frac{1}{324}\,{d_1}^4 d_2 - \frac{1}{324}\,{d_2}^2{d_1}^3 - \frac{1}{324}\,{d_3}^4 d_1 + \frac{1}{324}\,{d_3}^4 d_2 - \frac{2}{81}\,{d_3}^3 + \frac{43}{324}\,d_3 + \frac{1}{324}\,{d_2}^5 + \frac{1}{648}\,{d_1}^5$
$t\ w\ z$	$-\frac{91}{432}\,{d_3}^3 d_2 d_1 - \frac{1}{72}\,d_3{d_2}^2{d_1}^2 - \frac{1}{216}\,d_3{d_2}^3 d_1 + \frac{1}{216}\,d_3 d_2{d_1}^3 + \frac{7}{432}\,{d_3}^2 d_2{d_1}^2 + \frac{61}{216}\,{d_3}^2 d_1{d_2}^2 - \frac{1}{162}\,{d_3}^2{d_1}^4 d_2 - \frac{7}{324}\,{d_3}^2 d_1{d_2}^4 + \frac{1}{108}\,{d_3}^4{d_2}^2 d_1 + \frac{7}{324}\,{d_3}^3 d_2{d_1}^3 + \frac{2}{81}\,{d_3}^2{d_2}^3{d_1}^2 - \frac{1}{162}\,{d_3}^2{d_2}^2{d_1}^3 + \frac{1}{324}\,{d_3}^2{d_1}^5 - \frac{1}{324}\,{d_3}^3{d_2}^4 - \frac{1}{324}\,{d_3}^4{d_2}^3 - \frac{1}{162}\,{d_3}^3{d_1}^4 - \frac{65}{72}\,d_3 d_2 d_1 + \frac{1}{162}\,{d_3}^2{d_2}^5 + \frac{1}{324}\,{d_3}^4{d_1}^3 + \frac{2171}{2592}\,d_3{d_2}^2 - \frac{431}{5184}\,{d_3}^2 d_2 - \frac{11}{324}\,{d_2}^3 - \frac{407}{2592}\,d_3{d_1}^2 + \frac{151}{2592}\,d_1 - \frac{2935}{2592}\,d_2 - \frac{11}{648}\,{d_1}^3 + \frac{13}{144}\,{d_3}^3{d_2}^2 + \frac{13}{108}\,{d_3}^3{d_1}^2 + \frac{3407}{5184}\,{d_3}^2 d_1 + \frac{11}{216}\,d_1{d_2}^2 - \frac{247}{1296}\,{d_3}^2{d_2}^3 - \frac{35}{324}\,{d_3}^2{d_1}^3 + \frac{1}{108}\,d_3{d_2}^4 + \frac{1}{216}\,d_3{d_1}^4 - 1/48\,{d_3}^4 d_1 + 1/48\,{d_3}^4 d_2 - 1/6\,{d_3}^3 + 5/9\,d_3 + \frac{5}{324}\,{d_3}^3{d_2}^3 d_1 - \frac{1}{108}\,{d_3}^4 d_2{d_1}^2 - 1/36\,{d_3}^3{d_2}^2{d_1}^2$
$t\ f\ f$	$\frac{1}{1728}\,\sqrt{3}(-768 + 320\,{d_3}^2 d_2 d_1 - 32\,{d_3}^2 d_2{d_1}^3 - 32\,d_3{d_2}^2{d_1}^3 + 16\,d_3{d_2}^3{d_1}^2 - 18\,{d_2}^2 + 64\,{d_1}^2{d_2}^2{d_3}^2 - 32\,{d_3}^3{d_2}^2 d_1 + 16\,{d_3}^3 d_2{d_1}^2 + 16\,d_3 d_2{d_1}^4 - 32\,{d_3}^2{d_2}^3 d_1 - 360\,d_3 d_2{d_1}^2 + 1109\,d_3 d_2 + 4\,{d_1}^2 + 320\,d_3 d_1{d_2}^2 - 36\,{d_3}^3 d_2 - 270\,d_1 d_2 - 18\,{d_3}^2 - 270\,d_3 d_1 + 8\,{d_3}^2{d_1}^2 - 36\,d_3{d_2}^3 - 240\,{d_3}^2{d_2}^2 + 8\,{d_1}^2{d_2}^2 + 8\,d_2{d_1}^3 + 8\,d_3{d_1}^3 + 16\,{d_3}^3{d_2}^3)$
$t\ f\ o$	0
$t\ f\ \tilde{o}$	0
$t\ f\ p$	0

Table A.3: The cubic couplings for all of the fields in the action up to level 3 (continued).

$l\,m\,n$	$B_{lmn}(d_1, d_2, d_3)$
$t\ f\ q$	$-\frac{26}{81}\,d_1 + 2/3\,d_2 - \frac{41}{81}\,d_3 + \frac{5}{216}\,d_3{d_2}^2{d_1}^2 + \frac{709}{2592}\,d_3d_2d_1 + \frac{1}{162}\,d_3{d_2}^3d_1 - \frac{1}{324}\,{d_3}^2{d_2}^3 - \frac{1}{324}\,{d_1}^2{d_2}^3 + \frac{5}{216}\,{d_3}^3{d_2}^2 - \frac{5}{216}\,{d_3}^3d_2d_1 - \frac{19}{648}\,d_3d_2{d_1}^3 - \frac{5}{432}\,{d_3}^2d_1 - \frac{97}{1296}\,{d_3}^2d_2 - \frac{331}{2592}\,d_3{d_2}^2 - \frac{13}{1296}\,d_3{d_1}^2 + \frac{47}{648}\,d_1{d_2}^2 + \frac{1}{648}\,{d_1}^3 + \frac{1}{324}\,{d_1}^4d_2 - \frac{169}{1296}\,{d_1}^2d_2 + \frac{4}{81}\,{d_3}^2d_2{d_1}^2 + \frac{1}{144}\,{d_2}^3 - \frac{5}{108}\,{d_3}^2d_1{d_2}^2$
$t\ f\ r$	$\frac{11}{648}\,d_2{d_1}^3 - \frac{11}{648}\,{d_1}^2{d_2}^2 - \frac{11}{648}\,{d_3}^2{d_2}^2 + \frac{11}{288}\,{d_2}^2 + \frac{11}{324}\,d_3d_1{d_2}^2 + \frac{11}{1296}\,{d_1}^2 - \frac{11}{324}\,d_3d_2{d_1}^2 - \frac{11}{81} - \frac{473}{2592}\,d_1d_2 + \frac{55}{432}\,d_3d_2 + \frac{11}{648}\,{d_3}^2d_2d_1 + \frac{11}{1296}\,d_3d_1$
$t\ f\ s$	$-\frac{125}{1296}\,d_2{d_1}^3 - \frac{125}{2592}\,{d_1}^2 - \frac{125}{576}\,{d_2}^2 - \frac{125}{648}\,d_3d_1{d_2}^2 - \frac{125}{2592}\,d_3d_1 - \frac{625}{864}\,d_3d_2 + \frac{5375}{5184}\,d_1d_2 + \frac{125}{1296}\,{d_3}^2{d_2}^2 + \frac{125}{1296}\,{d_1}^2{d_2}^2 + \frac{125}{648}\,d_3d_2{d_1}^2 - \frac{125}{1296}\,{d_3}^2d_2d_1 + \frac{125}{162}$
$t\ f\ y$	$\frac{209}{1296}\,{d_3}^2d_2d_1 - \frac{1}{162}\,{d_3}^4d_2d_1 + \frac{1}{162}\,d_3d_1{d_2}^4 - \frac{1}{108}\,{d_3}^2d_2{d_1}^3 + \frac{1}{54}\,d_3{d_2}^2{d_1}^3 - \frac{7}{324}\,d_3{d_2}^3{d_1}^2 - \frac{25}{54} - \frac{751}{1728}\,{d_2}^2 - \frac{1}{324}\,{d_1}^2{d_2}^2{d_3}^2 - \frac{1}{81}\,{d_3}^3{d_2}^2d_1 + \frac{5}{324}\,{d_3}^3d_2{d_1}^2 - \frac{1}{324}\,d_3d_2{d_1}^4 + \frac{5}{324}\,{d_3}^2{d_2}^3d_1 - \frac{5}{1296}\,d_3d_2{d_1}^2 + \frac{1429}{2592}\,d_3d_2 - \frac{229}{2592}\,{d_1}^2 + \frac{1}{324}\,d_2{d_1}^5 + \frac{1}{162}\,{d_3}^4{d_2}^2 - \frac{125}{1296}\,d_1{d_2}^3 - \frac{83}{648}\,d_3d_1{d_2}^2 - \frac{1}{324}\,{d_3}^3d_1 + \frac{1}{144}\,{d_2}^4 + \frac{1}{648}\,{d_1}^4 + \frac{1}{108}\,{d_2}^3{d_1}^3 - \frac{1}{324}\,{d_3}^2{d_2}^4 - \frac{1}{108}\,{d_1}^4{d_2}^2 - \frac{1}{324}\,{d_1}^2{d_2}^4 - \frac{5}{108}\,{d_3}^3d_2 + \frac{3383}{5184}\,d_1d_2 + \frac{4}{81}\,{d_3}^2 - \frac{869}{2592}\,d_3d_1 - \frac{1}{648}\,{d_3}^2{d_1}^2 + \frac{103}{1296}\,d_3{d_2}^3 - \frac{79}{1296}\,{d_3}^2{d_2}^2 + \frac{131}{648}\,{d_1}^2{d_2}^2 - \frac{37}{324}\,d_2{d_1}^3 + \frac{1}{324}\,d_3{d_1}^3 - \frac{1}{324}\,{d_3}^3{d_2}^3$
$t\ f\ z$	$\frac{4337}{2592}\,{d_3}^2d_2d_1 - 1/24\,{d_3}^4d_2d_1 - \frac{25}{108}\,{d_3}^2d_2{d_1}^3 - \frac{1}{108}\,d_3{d_2}^3{d_1}^2 + \frac{1}{54}\,{d_3}^2{d_2}^3{d_1}^3 - \frac{1}{54}\,{d_3}^4{d_2}^2{d_1}^2 + \frac{1}{81}\,{d_3}^3{d_2}^4d_1 + \frac{1}{54}\,{d_3}^4{d_2}^3d_1 + 1/27\,{d_3}^3{d_2}^2{d_1}^3 - 1/27\,{d_3}^3{d_2}^3{d_1}^2 + \frac{1}{162}\,{d_3}^4d_2{d_1}^3 + \frac{1}{162}\,{d_3}^2d_2{d_1}^5 - \frac{1}{162}\,{d_3}^2{d_2}^4{d_1}^2 - \frac{1}{81}\,{d_3}^3d_2{d_1}^4 - \frac{1}{54}\,{d_3}^2{d_1}^4{d_2}^2 - \frac{11}{144}\,{d_2}^2 + \frac{7}{18}\,{d_1}^2{d_2}^2{d_3}^2 - \frac{10}{27}\,{d_3}^3{d_2}^2d_1 + \frac{25}{108}\,{d_3}^3d_2{d_1}^2 + \frac{1}{108}\,d_3d_2{d_1}^4 - \frac{113}{648}\,{d_3}^2{d_2}^3d_1 - \frac{10}{9} - \frac{419}{1296}\,d_3d_2{d_1}^2 + \frac{1259}{648}\,d_3d_2 - \frac{11}{648}\,{d_1}^2 + 1/24\,{d_3}^4{d_2}^2 + \frac{97}{648}\,d_3d_1{d_2}^2 - 1/48\,{d_3}^3d_1 + \frac{1}{72}\,{d_3}^2{d_2}^4 - \frac{5}{16}\,{d_3}^3d_2 + \frac{217}{1296}\,d_1d_2 + 1/3\,{d_3}^2 - \frac{635}{648}\,d_3d_1 - \frac{71}{432}\,{d_3}^2{d_1}^2 - \frac{1}{162}\,{d_3}^4{d_2}^4 + 1/48\,d_3{d_2}^3 - \frac{2663}{2592}\,{d_3}^2{d_2}^2 + \frac{11}{324}\,{d_1}^2{d_2}^2 - \frac{11}{324}\,d_2{d_1}^3 + \frac{1}{216}\,d_3{d_1}^3 + \frac{11}{81}\,{d_3}^3{d_2}^3 + \frac{1}{324}\,{d_3}^2{d_1}^4 + \frac{1}{324}\,{d_3}^3{d_1}^3$
$t\ o\ o$	$\frac{368}{729}\,\sqrt{3}$
$t\ o\ \tilde{o}$	0
$t\ o\ p$	0
$t\ o\ q$	0
$t\ o\ r$	$-\frac{40}{729}\,\sqrt{3}(d_1 - d_2)$
$t\ o\ s$	0
$t\ o\ y$	0
$t\ o\ z$	0
$t\ \tilde{o}\ \tilde{o}$	$\frac{32}{729}\,\sqrt{3}$
$t\ \tilde{o}\ p$	0
$t\ \tilde{o}\ q$	0
$t\ \tilde{o}\ r$	0
$t\ \tilde{o}\ s$	0
$t\ \tilde{o}\ y$	0
$t\ \tilde{o}\ z$	0
$t\ p\ p$	$-\frac{6400}{729}\,\sqrt{3}$
$t\ p\ q$	0
$t\ p\ r$	0
$t\ p\ s$	$-\frac{800}{729}\,\sqrt{3}(d_1 - d_2)$
$t\ p\ y$	0
$t\ p\ z$	0
$t\ q\ q$	$-\frac{1}{11664}\,\sqrt{3}(30\,d_1{d_2}^3 + 4096 - 30\,{d_3}^3d_2 + 30\,{d_3}^3d_1 - 504\,d_1d_2 - 225\,{d_3}^2d_2d_1 - 4\,{d_1}^2{d_2}^2 - 4\,{d_3}^2{d_1}^2 - 30\,d_2{d_1}^3 + 229\,{d_3}^2{d_2}^2 + 4\,{d_1}^4 - 30\,d_3{d_2}^3 + 1368\,{d_3}^2 - 912\,{d_1}^2 + 1368\,{d_2}^2 + 285\,d_3d_2{d_1}^2 - 504\,d_3d_1 - 8532\,d_3d_2 - 30\,d_3{d_1}^3 - 225\,d_3d_1{d_2}^2)$
$t\ q\ r$	$-\frac{11}{11664}\,\sqrt{3}(28\,d_2 + 15\,d_3d_2d_1 + 2\,{d_1}^3 - 15\,d_3{d_2}^2 + 24\,d_3 - 17\,{d_1}^2d_2 + 2\,{d_3}^2d_2 - 2\,{d_3}^2d_1 - 40\,d_1 + 15\,d_1{d_2}^2)$
$t\ q\ s$	$\frac{125}{23328}\,\sqrt{3}(28\,d_2 + 15\,d_3d_2d_1 + 2\,{d_1}^3 - 15\,d_3{d_2}^2 + 24\,d_3 - 17\,{d_1}^2d_2 + 2\,{d_3}^2d_2 - 2\,{d_3}^2d_1 - 40\,d_1 + 15\,d_1{d_2}^2)$
$t\ q\ y$	$-\frac{1}{23328}\,\sqrt{3}(-2139\,d_3d_2d_1 + 3579\,d_3{d_2}^2 - 120\,{d_3}^3d_2d_1 - 554\,{d_1}^3 - 1707\,d_1{d_2}^2 + 1898\,{d_3}^2d_1 - 1610\,{d_3}^2d_2 + 1925\,{d_1}^2d_2 - 144\,{d_3}^2d_1{d_2}^2 + 240\,d_3{d_2}^3d_1 + 128\,{d_3}^3{d_2}^2 - 8\,{d_3}^3{d_1}^2 - 1536\,d_3{d_1}^2 - 52\,{d_3}^2{d_2}^3 - 24\,{d_3}^2{d_1}^3 - 188\,{d_1}^2{d_2}^3 + 336\,{d_2}^3 + 840\,d_1 - 19020\,d_2 + 220\,{d_3}^2d_2{d_1}^2 + 60\,d_1{d_2}^4 + 204\,{d_2}^2{d_1}^3 + 16\,{d_3}^4d_1 - 16\,{d_3}^4d_2 - 60\,d_3{d_2}^4 + 8\,d_3{d_1}^4 - 84\,{d_1}^4d_2 - 188\,d_3{d_2}^2{d_1}^2 + 10760\,d_3 + 8\,{d_1}^5 - 192\,{d_3}^3)$

Table A.3: The cubic couplings for all of the fields in the action up to level 3 (continued).

$l\,m\,n$	$B_{lmn}(d_1,d_2,d_3)$
$t\ q\ z$	$-\frac{1}{11664}\sqrt{3}(-1842\,d_3d_2d_1 - 90\,d_3d_2{d_1}^3 - 84\,{d_3}^2{d_1}^4d_2 + 60\,{d_3}^2d_1{d_2}^4 - 24\,{d_3}^4{d_2}^2d_1 + 60\,{d_3}^3d_2{d_1}^3 - 188\,{d_3}^2{d_2}^3{d_1}^2 + 204\,{d_3}^2{d_2}^2{d_1}^3 + 180\,{d_3}^3{d_2}^3d_1 + 24\,{d_3}^4d_2{d_1}^2 - 180\,{d_3}^3{d_2}^2{d_1}^2 + 4434\,d_3{d_2}^2 - 981\,{d_3}^3d_2d_1 - 44\,{d_1}^3 - 330\,d_1{d_2}^2 + 6452\,{d_3}^2d_1 - 5840\,{d_3}^2d_2 + 374\,{d_1}^2d_2 - 1557\,{d_3}^2d_1{d_2}^2 - 8\,{d_3}^4{d_1}^3 + 90\,d_3{d_2}^3d_1 + 705\,{d_3}^3{d_2}^2 + 276\,{d_3}^3{d_1}^2 - 2736\,d_3{d_1}^2 + 246\,{d_3}^2{d_2}^3 - 534\,{d_3}^2{d_1}^3 - 2832\,d_1 - 15528\,d_2 + 1845\,{d_3}^2d_2{d_1}^2 + 54\,{d_3}^4d_1 - 54\,{d_3}^4d_2 + 12\,d_3{d_1}^4 - 12\,d_3{d_2}^2{d_1}^2 - 60\,{d_3}^3{d_2}^4 + 8\,{d_3}^4{d_2}^3 + 8\,{d_3}^2{d_1}^5 + 15216\,d_3 - 648\,{d_3}^3)$
$t\ r\ r$	$-\frac{19}{3888}\sqrt{3}(-4 - d_1d_2 + {d_1}^2 - d_3d_1 + d_3d_2)$
$t\ r\ s$	$\frac{1375}{23328}\sqrt{3}(-4 - d_1d_2 + {d_1}^2 - d_3d_1 + d_3d_2)$
$t\ r\ y$	$-\frac{11}{23328}\sqrt{3}(-4\,d_1{d_2}^3 + 84 - 8\,{d_3}^3d_2 + 8\,{d_3}^3d_1 + 133\,d_1d_2 + 8\,{d_3}^2d_2d_1 + 12\,{d_1}^2{d_2}^2 - 12\,{d_3}^2{d_1}^2 - 12\,d_2{d_1}^3 + 4\,{d_3}^2{d_2}^2 + 4\,{d_1}^4 + 4\,d_3{d_2}^3 + 32\,{d_3}^2 - 85\,{d_1}^2 - 48\,{d_2}^2 + 12\,d_3d_2{d_1}^2 - 43\,d_3d_1 + 11\,d_3d_2 - 16\,d_3d_1{d_2}^2)$
$t\ r\ z$	$-\frac{11}{11664}\sqrt{3}(-4\,{d_3}^3{d_1}^3 + 24 + 12\,{d_3}^3d_2{d_1}^2 - 27\,{d_3}^3d_2 + 27\,{d_3}^3d_1 + 22\,d_1d_2 + 123\,{d_3}^2d_2d_1 - 81\,{d_3}^2{d_1}^2 - 42\,{d_3}^2{d_2}^2 - 4\,{d_3}^2{d_2}^3d_1 + 108\,{d_3}^2 - 22\,{d_1}^2 - 12\,{d_3}^3{d_2}^2d_1 + 4\,{d_3}^3{d_2}^3 - 98\,d_3d_1 + 50\,d_3d_2 + 4\,{d_3}^2{d_1}^4 + 6\,d_3{d_1}^3 - 6\,d_3d_1{d_2}^2 - 12\,{d_3}^2{d_2}d_1^3 + 12\,{d_1}^2{d_2}^2{d_3}^2)$
$t\ s\ s$	$-\frac{9475}{15552}\sqrt{3}(-4 - d_1d_2 + {d_1}^2 - d_3d_1 + d_3d_2)$
$t\ s\ y$	$\frac{125}{46656}\sqrt{3}(-4\,d_1{d_2}^3 + 84 - 8\,{d_3}^3d_2 + 8\,{d_3}^3d_1 + 133\,d_1d_2 + 8\,{d_3}^2d_2d_1 + 12\,{d_1}^2{d_2}^2 - 12\,{d_3}^2{d_1}^2 - 12\,d_2{d_1}^3 + 4\,{d_3}^2{d_2}^2 + 4\,{d_1}^4 + 4\,d_3{d_2}^3 + 32\,{d_3}^2 - 85\,{d_1}^2 - 48\,{d_2}^2 + 12\,d_3d_2{d_1}^2 - 43\,d_3d_1 + 11\,d_3d_2 - 16\,d_3d_1{d_2}^2)$
$t\ s\ z$	$\frac{125}{23328}\sqrt{3}(-4\,{d_3}^3{d_1}^3 + 24 + 12\,{d_3}^3d_2{d_1}^2 - 27\,{d_3}^3d_2 + 27\,{d_3}^3d_1 + 22\,d_1d_2 + 123\,{d_3}^2d_2d_1 - 81\,{d_3}^2{d_1}^2 - 42\,{d_3}^2{d_2}^2 - 4\,{d_3}^2{d_2}^3d_1 + 108\,{d_3}^2 - 22\,{d_1}^2 - 12\,{d_3}^3{d_2}^2d_1 + 4\,{d_3}^3{d_2}^3 - 98\,d_3d_1 + 50\,d_3d_2 + 4\,{d_3}^2{d_1}^4 + 6\,d_3{d_1}^3 - 6\,d_3d_1{d_2}^2 - 12\,{d_3}^2{d_2}d_1^3 + 12\,{d_1}^2{d_2}^2{d_3}^2)$
$t\ y\ y$	$-\frac{1}{46656}\sqrt{3}(-38628 + 3944\,{d_3}^2d_2d_1 - 5688\,d_3d_2{d_1}^2 + 128\,{d_3}^4d_2d_1 + 160\,d_3d_2{d_1}^4 + 128\,d_3d_1{d_2}^4 - 160\,d_3{d_2}^2{d_1}^3 - 64\,d_3{d_2}^3{d_1}^2 - 5808\,{d_2}^2 + 368\,{d_1}^2{d_2}^2{d_3}^2 - 160\,{d_3}^2d_2{d_1}^3 - 160\,{d_3}^3{d_2}^2d_1 - 160\,{d_3}^2{d_2}^3d_1 - 64\,{d_3}^3d_2{d_1}^2 + 32633\,d_3d_2 + 96\,{d_3}^3{d_2}^3 + 7993\,{d_1}^2 - 1876\,d_1{d_2}^3 + 636\,d_2{d_1}^3 + 1728\,{d_1}^2{d_2}^2 + 3944\,d_3d_1{d_2}^2 - 1876\,{d_3}^3d_1 + 340\,d_3{d_2}^3 + 340\,{d_3}^3d_2 - 6313\,d_1d_2 + 384\,{d_2}^4 + 16\,{d_1}^6 + 384\,{d_3}^4 - 5808\,{d_3}^2 - 32\,{d_3}^2{d_1}^4 - 6313\,d_3d_1 + 1728\,{d_3}^2{d_1}^2 - 32\,{d_1}^4{d_2}^2 - 32\,d_3{d_1}^5 + 32\,{d_3}^5d_1 - 112\,{d_1}^2{d_2}^4 - 16\,{d_3}^2{d_2}^4 - 32\,{d_3}^5d_2 - 32\,d_2{d_1}^5 - 3752\,{d_3}^2{d_2}^2 - 872\,{d_1}^4 - 16\,{d_3}^4{d_2}^2 + 636\,d_3{d_1}^3 + 128\,{d_3}^3{d_1}^3 + 32\,d_1{d_2}^5 - 32\,d_3{d_2}^5 - 112\,{d_3}^4{d_1}^2 + 128\,{d_2}^3{d_1}^3)$
$t\ y\ z$	$-\frac{1}{23328}\sqrt{3}(-31224 + 3817\,{d_3}^2d_2d_1 - 4872\,d_3d_2{d_1}^2 + 1584\,{d_3}^4d_2d_1 + 24\,d_3d_2{d_1}^4 + 48\,d_3d_1{d_2}^4 - 72\,d_3{d_2}^2{d_1}^3 - 24\,d_3{d_2}^3{d_1}^2 - 192\,{d_2}^2 + 128\,{d_3}^2{d_2}^3{d_1}^3 + 192\,{d_3}^4{d_2}^2{d_1}^2 + 96\,{d_3}^3{d_2}^4d_1 - 96\,{d_3}^4{d_2}^3d_1 - 112\,{d_3}^3{d_2}^2{d_1}^3 - 48\,{d_3}^3{d_2}^3{d_1}^2 - 160\,{d_3}^4d_2{d_1}^3 - 32\,{d_3}^2d_2{d_1}^5 - 112\,{d_3}^2{d_2}^4{d_1}^2 - 48\,{d_3}^5{d_2}^2d_1 + 144\,{d_3}^3d_2{d_1}^4 + 32\,{d_3}^2{d_2}^5d_1 - 32\,{d_3}^2{d_1}^4{d_2}^2 + 1728\,{d_1}^2{d_2}^2{d_3}^2 + 636\,{d_3}^2d_2{d_1}^3 + 156\,{d_3}^3{d_2}^2d_1 - 1796\,{d_3}^2{d_2}^3d_1 - 2520\,{d_3}^3d_2{d_1}^2 + 48\,{d_3}^5d_2{d_1}^2 + 38950\,d_3d_2 + 668\,{d_3}^3{d_2}^3 + 1102\,{d_1}^2 - 176\,d_1{d_2}^3 + 264\,{d_1}^2{d_2}^2 + 5518\,d_3d_1{d_2}^2 - 9551\,{d_3}^3d_1 - 400\,d_3{d_2}^3 + 5087\,{d_3}^3d_2 - 16\,{d_3}^5{d_1}^3 - 6478\,d_1d_2 + 1296\,{d_3}^4 - 17340\,{d_3}^2 - 904\,{d_3}^2{d_1}^4 + 1130\,d_3d_1 + 10749\,{d_3}^2{d_1}^2 + 24\,d_3{d_1}^5 + 108\,{d_3}^5d_1 + 336\,{d_3}^2{d_2}^4 - 108\,{d_3}^5d_2 - 10246\,{d_3}^2{d_2}^2 - 88\,{d_1}^4 - 660\,{d_3}^4{d_2}^2 - 1398\,d_3{d_1}^3 + 1696\,{d_3}^3{d_1}^3 + 16\,{d_3}^5{d_2}^3 - 48\,{d_3}^3{d_1}^5 - 32\,{d_3}^3{d_2}^5 + 16\,{d_3}^4{d_2}^4 + 48\,{d_3}^4{d_1}^4 + 16\,{d_3}^2{d_1}^6 - 924\,{d_3}^4{d_1}^2)$
$t\ z\ z$	$-\frac{1}{11664}\sqrt{3}(-30864 + 18186\,{d_3}^2d_2d_1 - 8208\,d_3d_2{d_1}^2 + 144\,{d_3}^3{d_2}^3{d_1}^4 + 48\,{d_3}^5{d_2}^3{d_1}^2 - 16\,{d_3}^2{d_2}^5{d_1}^3 - 144\,{d_3}^4{d_2}^3{d_1}^3 + 16\,{d_3}^2{d_2}^2{d_1}^6 - 48\,{d_3}^3{d_2}^2{d_1}^5 + 48\,{d_3}^4{d_2}^2{d_1}^4 - 16\,{d_3}^5{d_2}^2{d_1}^3 + 48\,{d_3}^3{d_2}^5{d_1}^2 - 48\,{d_3}^4{d_2}^5d_1 + 144\,{d_3}^4{d_2}^4{d_1}^2 - 48\,{d_3}^2{d_2}^3{d_1}^5 + 48\,{d_3}^2{d_2}^4{d_1}^4 - 48\,{d_3}^5{d_2}^4d_1 - 144\,{d_3}^3{d_2}^4{d_1}^3 - 24\,d_3{d_2}^4{d_1}^3 + 24\,d_3{d_2}^2{d_1}^5 + 162\,{d_3}^4d_2d_1 + 36\,d_3d_2{d_1}^4 + 162\,d_3d_1{d_2}^4 - 1338\,d_3{d_2}^2{d_1}^3 + 564\,d_3{d_2}^3{d_1}^2 - 648\,{d_2}^2 + 1656\,{d_3}^2{d_2}^3{d_1}^3 - 852\,{d_3}^4{d_2}^2{d_1}^2 + 1404\,{d_3}^3{d_2}^4d_1 + 1404\,{d_3}^4{d_2}^3d_1 + 1656\,{d_3}^3{d_2}^2{d_1}^3 - 2952\,{d_3}^3{d_2}^3{d_1}^2 - 24\,{d_3}^4d_2{d_1}^3 + 24\,{d_3}^2d_2{d_1}^5 - 852\,{d_3}^2{d_2}^4{d_1}^2 + 108\,{d_3}^5{d_2}^2d_1 + 108\,{d_3}^2{d_2}^5d_1 - 936\,{d_3}^2{d_1}^4{d_2}^2 + 13485\,{d_1}^2{d_2}^2{d_3}^2 - 1338\,{d_3}^2d_2{d_1}^3 - 10745\,{d_3}^3{d_2}^2d_1 - 10745\,{d_3}^2{d_2}^3d_1 + 564\,{d_3}^3d_2{d_1}^2 + 54916\,d_3d_2 + 6925\,{d_3}^3{d_2}^3 + 484\,{d_1}^2 - 594\,d_1{d_2}^3 - 132\,d_2{d_1}^3 + 1014\,{d_1}^2{d_2}^2 + 18186\,d_3d_1{d_2}^2 - 594\,{d_3}^3d_1 - 1350\,d_3{d_2}^3 + 16\,{d_3}^5{d_2}^5 - 1350\,{d_3}^3d_2 - 8980\,d_1d_2 - 648\,{d_3}^2 - 88\,{d_3}^2{d_1}^4 - 8980\,d_3d_1 + 1014\,{d_3}^2{d_1}^2 - 88\,{d_1}^4{d_2}^2 + 1134\,{d_3}^2{d_2}^4 - 33084\,{d_3}^2{d_2}^2 + 1134\,{d_3}^4{d_2}^2 - 132\,d_3{d_1}^3 + 88\,{d_3}^3{d_1}^3 - 108\,{d_3}^5{d_2}^3 - 108\,{d_3}^3{d_2}^5 - 528\,{d_3}^4{d_2}^4 + 88\,{d_3}^3{d_1}^3)$
$x\ x\ x$	$-1/24\,(d_2 - d_3)(d_1 - d_3)(d_1 - d_2)$
$x\ x\ h$	0
$x\ x\ u$	$-\frac{11}{432}\sqrt{3}(-4 + d_1d_2 + {d_3}^2 - d_3d_1 - d_3d_2)$
$x\ x\ v$	$\frac{125}{864}\sqrt{3}(-4 + d_1d_2 + {d_3}^2 - d_3d_1 - d_3d_2)$
$x\ x\ w$	$-\frac{1}{864}\sqrt{3}(4\,d_1{d_2}^3 - 108 + 12\,{d_3}^3d_2 + 12\,{d_3}^3d_1 - 37\,d_1d_2 - 24\,{d_3}^2d_2d_1 - 8\,{d_1}^2{d_2}^2 + 4\,d_2{d_1}^3 - 4\,d_3{d_2}^3 + 155\,{d_3}^2 + 16\,{d_1}^2 + 16\,{d_2}^2 + 8\,d_3d_2{d_1}^2 - 8\,{d_3}^4 - 75\,d_3d_1 - 75\,d_3d_2 - 4\,d_3{d_1}^3 + 8\,d_3d_1{d_2}^2)$

Table A.3: The cubic couplings for all of the fields in the action up to level 3 (continued).

$l\,m\,n$	$B_{lmn}(d_1,d_2,d_3)$
$x\,x\,f$	$-\frac{1}{432}\sqrt{3}(4\,{d_3}^3{d_1}^2-40\,d_2+14\,d_3{d_1}^2-45\,d_3d_2d_1-4\,{d_3}^2{d_2}^3-8\,{d_3}^3d_2d_1+14\,d_3{d_2}^2+4\,d_3d_2{d_1}^3-28\,d_3-4\,{d_3}^2{d_1}^3+2\,{d_1}^2d_2+11\,{d_3}^2d_2+11\,{d_3}^2d_1+4\,d_3{d_2}^3d_1+4\,{d_3}^2d_1{d_2}^2+4\,{d_3}^2d_2{d_1}^2-8\,d_3{d_2}^2{d_1}^2-40\,d_1+2\,d_1{d_2}^2+4\,{d_3}^3{d_2}^2-9\,{d_3}^3)$
$x\,x\,o$	0
$x\,x\,\tilde{o}$	0
$x\,x\,p$	0
$x\,x\,q$	$-\frac{1}{648}(d_1-d_2)(2\,{d_1}^2d_2-2\,d_3{d_1}^2+17\,{d_3}^2d_1-19\,d_3d_2d_1-32\,d_1+2\,d_1{d_2}^2-2\,d_3{d_2}^2+96\,d_3-15\,{d_3}^3+17\,{d_3}^2d_2-32\,d_2)$
$x\,x\,r$	$-\frac{11}{648}(d_2-d_3)(d_1-d_3)(d_1-d_2)$
$x\,x\,s$	$\frac{125}{1296}(d_2-d_3)(d_1-d_3)(d_1-d_2)$
$x\,x\,y$	$-\frac{1}{1296}(d_1-d_2)(4\,d_2{d_1}^3-4\,d_3{d_1}^3-8\,{d_1}^2{d_2}^2+8\,d_3d_2{d_1}^2+32\,{d_1}^2+4\,d_1{d_2}^3+12\,{d_3}^3d_1-27\,d_3d_1-101\,d_1d_2-24\,{d_3}^2d_2d_1+8\,d_3d_1{d_2}^2-320+91\,{d_3}^2-8\,{d_3}^4-4\,d_3{d_2}^3+32\,{d_2}^2+12\,{d_3}^3d_2-27\,d_3d_2)$
$x\,x\,z$	$-\frac{1}{648}(d_1-d_2)(4\,{d_3}^2d_2{d_1}^3-4\,{d_3}^3{d_1}^3+26\,{d_3}^2{d_1}^2+4\,{d_3}^4{d_1}^2+6\,d_3d_2{d_1}^2+4\,{d_3}^3d_2{d_1}^2-8\,{d_1}^2{d_2}^2{d_3}^2+4\,{d_3}^2{d_2}^3d_1-74\,d_3d_1-8\,{d_3}^4d_2d_1-103\,{d_3}^2d_2d_1-22\,d_1d_2+33\,{d_3}^3d_1+6\,d_3d_1{d_2}^2+4\,{d_3}^3{d_2}^2d_1+33\,{d_3}^3d_2+4\,{d_3}^4{d_2}^2-74\,d_3d_2-214\,{d_3}^2+64+26\,{d_3}^2{d_2}^2-27\,{d_3}^4-4\,{d_3}^3{d_2}^3)$
$x\,h\,h$	$1/6\,d_2-1/6\,d_3$
$x\,h\,u$	$1/27\sqrt{3}(d_2-d_3)$
$x\,h\,v$	0
$x\,h\,w$	0
$x\,h\,f$	0
$x\,h\,o$	$-\frac{4}{27}\,d_2+\frac{4}{27}\,d_3$
$x\,h\,\tilde{o}$	$\frac{8}{81}\,d_2-\frac{8}{81}\,d_3$
$x\,h\,p$	0
$x\,h\,q$	0
$x\,h\,r$	$\frac{2}{81}\,d_1d_2-\frac{2}{81}\,{d_2}^2-\frac{2}{81}\,d_3d_1+\frac{2}{81}\,d_3d_2+\frac{8}{81}$
$x\,h\,s$	0
$x\,h\,y$	0
$x\,h\,z$	0
$x\,u\,u$	$\frac{19}{864}\,d_2-\frac{19}{864}\,d_3$
$x\,u\,v$	$-\frac{1375}{5184}\,d_2+\frac{1375}{5184}\,d_3$
$x\,u\,w$	$-\frac{11}{432}\,{d_3}^2d_2+\frac{11}{1296}\,{d_1}^2d_2+\frac{11}{1296}\,{d_2}^3+\frac{11}{162}\,d_1-\frac{11}{1296}\,{d_3}^2d_1-\frac{11}{648}\,d_1{d_2}^2+\frac{11}{432}\,d_3d_2d_1-\frac{11}{1296}\,d_3{d_1}^2-\frac{407}{5184}\,d_2-\frac{649}{5184}\,d_3+\frac{11}{648}\,{d_3}^3$
$x\,u\,f$	$\frac{11}{648}\,d_3d_2{d_1}^2+\frac{11}{1296}\,{d_2}^2+\frac{11}{324}\,{d_3}^2d_2d_1+\frac{55}{432}\,d_3d_1+\frac{11}{1296}\,d_1d_2+\frac{11}{648}\,d_3{d_2}^3-\frac{11}{324}\,d_3d_1{d_2}^2-\frac{473}{2592}\,d_3d_2-\frac{11}{648}\,{d_3}^2{d_1}^2-\frac{11}{648}\,{d_3}^2{d_2}^2+\frac{11}{288}\,{d_3}^2-\frac{11}{81}$
$x\,u\,o$	$\frac{40}{729}\sqrt{3}(d_2-d_3)$
$x\,u\,\tilde{o}$	0
$x\,u\,p$	0
$x\,u\,q$	$\frac{11}{11664}\sqrt{3}(17\,d_3{d_2}^2-15\,{d_3}^2d_2-2\,{d_2}^3-15\,d_3d_2d_1+15\,{d_3}^2d_1-2\,d_3{d_1}^2-24\,d_1+40\,d_2-28\,d_3+2\,{d_1}^2d_2)$
$x\,u\,r$	$\frac{19}{3888}\sqrt{3}(4+d_1d_2-{d_2}^2-d_3d_1+d_3d_2)$
$x\,u\,s$	$-\frac{1375}{23328}\sqrt{3}(4+d_1d_2-{d_2}^2-d_3d_1+d_3d_2)$
$x\,u\,y$	$\frac{11}{23328}\sqrt{3}(12\,d_1{d_2}^3-84-8\,{d_3}^3d_2+8\,{d_3}^3d_1-133\,d_1d_2-8\,{d_3}^2d_2d_1-12\,{d_1}^2{d_2}^2-4\,{d_3}^2{d_1}^2+4\,d_2{d_1}^3+12\,{d_3}^2{d_2}^2-32\,{d_3}^2+48\,{d_1}^2+85\,{d_2}^2+16\,d_3d_2{d_1}^2-4\,{d_2}^4-11\,d_3d_1+43\,d_3d_2-4\,d_3{d_1}^3-12\,d_3d_1{d_2}^2)$
$x\,u\,z$	$\frac{11}{11664}\sqrt{3}(-4\,{d_3}^3{d_1}^3-24+12\,{d_3}^3d_2d_1^2-27\,{d_3}^3d_2+27\,{d_3}^3d_1-22\,d_1d_2-123\,{d_3}^2d_2d_1+42\,{d_3}^2{d_1}^2+81\,{d_3}^2{d_2}^2+12\,{d_3}^2{d_2}^3d_1-6\,d_3{d_2}^3-108\,{d_3}^2+22\,{d_2}^2+6\,d_3d_2{d_1}^2-12\,{d_3}^3{d_2}^2d_1+4\,{d_3}^3{d_2}^3-4\,{d_3}^2{d_2}^4-50\,d_3d_1+98\,d_3d_2+4\,{d_3}^2d_2{d_1}^3-12\,{d_1}^2{d_2}^2{d_3}^2)$
$x\,v\,v$	$\frac{9475}{3456}\,d_2-\frac{9475}{3456}\,d_3$
$x\,v\,w$	$-\frac{125}{324}\,d_1+\frac{4625}{10368}\,d_2+\frac{7375}{10368}\,d_3-\frac{125}{864}\,d_3d_2d_1+\frac{125}{2592}\,{d_3}^2d_1+\frac{125}{864}\,{d_3}^2d_2+\frac{125}{2592}\,d_3{d_1}^2+\frac{125}{1296}\,d_1{d_2}^2-\frac{125}{2592}\,{d_1}^2d_2-\frac{125}{1296}\,{d_3}^3-\frac{125}{2592}\,{d_2}^3$
$x\,v\,f$	$-\frac{125}{2592}\,{d_2}^2-\frac{125}{576}\,{d_3}^2+\frac{125}{648}\,d_3d_1{d_2}^2-\frac{625}{864}\,d_3d_1+\frac{5375}{5184}\,d_3d_2+\frac{125}{1296}\,{d_3}^2{d_1}^2-\frac{125}{2592}\,d_1d_2+\frac{125}{1296}\,{d_3}^2{d_2}^2-\frac{125}{1296}\,d_3d_2{d_1}^2-\frac{125}{648}\,{d_3}^2d_2d_1+\frac{125}{162}-\frac{125}{1296}\,d_3{d_2}^3$
$x\,v\,o$	0
$x\,v\,\tilde{o}$	0

Table A.3: The cubic couplings for all of the fields in the action up to level 3 (continued).

$l\,m\,n$	$B_{lmn}(d_1,d_2,d_3)$
$x\,v\,p$	$\frac{800}{729}\sqrt{3}(d_2-d_3)$
$x\,v\,q$	$-\frac{125}{23328}\sqrt{3}(17\,d_3{d_2}^2-15\,{d_3}^2d_2-2\,{d_2}^3-15\,d_3d_2d_1+15\,{d_3}^2d_1-2\,d_3{d_1}^2-24\,d_1+40\,d_2-28\,d_3+2\,{d_1}^2d_2)$
$x\,v\,r$	$-\frac{1375}{23328}\sqrt{3}(4+d_1d_2-{d_2}^2-d_3d_1+d_3d_2)$
$x\,v\,s$	$\frac{9475}{15552}\sqrt{3}(4+d_1d_2-{d_2}^2-d_3d_1+d_3d_2)$
$x\,v\,y$	$-\frac{125}{46656}\sqrt{3}(12\,d_1{d_2}^3-84-8\,{d_3}^3d_2+8\,{d_3}^3d_1-133\,d_1d_2-8\,{d_3}^2d_2d_1-12\,{d_1}^2{d_2}^2-4\,{d_3}^2{d_1}^2+4\,d_2{d_1}^3+12\,{d_3}^2{d_2}^2-32\,{d_3}^2+48\,{d_1}^2+85\,{d_2}^2+16\,d_3d_2{d_1}^2-4\,{d_2}^4-11\,d_3d_1+43\,d_3d_2-4\,d_3{d_1}^3-12\,d_3d_1{d_2}^2)$
$x\,v\,z$	$-\frac{125}{23328}\sqrt{3}(-4\,{d_3}^3{d_1}^3-24+12\,{d_3}^3d_2{d_1}^2-27\,{d_3}^3d_2+27\,{d_3}^3d_1-22\,d_1d_2-123\,{d_3}^2d_2d_1+42\,{d_3}^2{d_1}^2+81\,{d_3}^2{d_2}^2+12\,{d_3}^2{d_2}^3d_1-6\,d_3{d_2}^3-108\,{d_3}^2+22\,{d_2}^2+6\,d_3d_2{d_1}^2-12\,{d_3}^3{d_2}^2d_1+4\,{d_3}^3{d_2}^3-4\,{d_3}^2{d_2}^4-50\,d_3d_1+98\,d_3d_2+4\,{d_3}^2d_2{d_1}^3-12\,{d_1}^2{d_2}^2{d_3}^2)$
$x\,w\,w$	$\frac{1}{10368}\,(d_2-d_3)(-32\,{d_2}^4+80\,d_1{d_2}^3-16\,d_3{d_2}^3-80\,d_3d_1{d_2}^2-48\,{d_1}^2{d_2}^2+96\,{d_3}^2{d_2}^2+1044\,{d_2}^2-16\,d_2{d_1}^3+112\,d_3d_2{d_1}^2-2088\,d_3d_2-16\,{d_3}^3d_2-1260\,d_1d_2-80\,{d_3}^2d_2d_1+1044\,{d_3}^2+80\,{d_3}^3d_1+16\,{d_1}^4-2695-48\,{d_3}^2{d_1}^2+216\,{d_1}^2-32\,{d_3}^4-16\,d_3{d_1}^3-1260\,d_3d_1)$
$x\,w\,f$	$-\frac{319}{1296}\,d_3d_1{d_2}^2+\frac{7}{216}\,d_3d_2{d_1}^2+\frac{181}{1296}\,{d_3}^2d_2d_1-1/27\,{d_1}^2+\frac{2}{81}\,{d_1}^2{d_2}^2{d_3}^2-\frac{1}{324}\,{d_3}^2d_2{d_1}^3-\frac{205}{5184}\,{d_3}^2+\frac{1}{162}\,{d_3}^3{d_2}^2d_1-1/36\,{d_3}^2{d_2}^3d_1-\frac{1}{81}\,{d_3}^3d_2{d_1}^2+\frac{1}{162}\,{d_3}^4d_2d_1+\frac{1}{324}\,d_3d_2{d_1}^4+\frac{5}{324}\,d_3d_1{d_2}^4-\frac{1}{324}\,d_3{d_2}^2{d_1}^3-\frac{1}{108}\,d_3{d_2}^3{d_1}^2-\frac{1}{648}\,d_3{d_1}^3-\frac{581}{2592}\,{d_2}^2-\frac{1}{324}\,{d_2}^4-\frac{107}{648}\,{d_3}^2{d_2}^2+\frac{25}{648}\,{d_3}^2{d_1}^2+\frac{37}{162}+\frac{1}{648}\,d_2{d_1}^3-\frac{1193}{5184}\,d_3d_2+\frac{1}{324}\,{d_1}^2{d_2}^2-\frac{13}{324}\,{d_3}^3d_1+\frac{5}{216}\,{d_3}^3d_2+\frac{1}{108}\,{d_3}^2{d_2}^4-\frac{1}{648}\,d_1{d_2}^3+\frac{1}{162}\,{d_3}^3{d_1}^3+\frac{275}{1296}\,d_3{d_2}^3-\frac{55}{864}\,d_1d_2+\frac{1}{144}\,{d_3}^4+\frac{119}{864}\,d_3d_1-\frac{1}{324}\,{d_3}^4{d_2}^2-\frac{1}{324}\,{d_3}^2{d_1}^4-\frac{1}{162}\,d_3{d_2}^5-\frac{1}{324}\,{d_3}^4{d_1}^2$
$x\,w\,o$	0
$x\,w\,\tilde{o}$	0
$x\,w\,p$	0
$x\,w\,q$	$\frac{1}{23328}\sqrt{3}(120\,{d_3}^3d_2d_1+32\,d_3{d_2}^2{d_1}^2+123\,d_3d_2d_1+204\,d_3{d_2}^3d_1-84\,d_3d_2{d_1}^3+120\,{d_3}^2d_2{d_1}^2-376\,{d_3}^2d_1{d_2}^2+970\,{d_2}^3-160\,{d_1}^3+180\,{d_3}^2{d_2}^3+3195\,{d_3}^2d_2-3029\,d_3{d_2}^2+1400\,d_1-4040\,d_2-128\,{d_3}^3{d_1}^2-971\,{d_3}^2d_1+954\,d_3{d_1}^2-1056\,d_1{d_2}^2-138\,{d_1}^2d_2+76\,{d_3}^2{d_1}^3-24\,{d_1}^2{d_2}^3-8\,d_1{d_2}^4+8\,{d_1}^4d_2+8\,{d_2}^2{d_1}^3+60\,{d_3}^4d_1-144\,d_3{d_2}^4-8\,d_3{d_1}^4+8\,{d_3}^3{d_2}^2+16\,{d_2}^5-1780\,d_3+112\,{d_3}^3-60\,{d_3}^4d_2)$
$x\,w\,r$	$\frac{11}{23328}\sqrt{3}(-12\,d_1{d_2}^3+108+4\,{d_3}^3d_2-4\,{d_3}^3d_1+75\,d_1d_2-8\,{d_3}^2d_2d_1+8\,{d_3}^2{d_1}^2+4\,d_2{d_1}^3-12\,d_3{d_2}^3-16\,{d_3}^2-16\,{d_1}^2-155\,{d_2}^2-8\,d_3d_2{d_1}^2+8\,{d_2}^4+37\,d_3d_1+75\,d_3d_2-4\,d_3{d_1}^3+24\,d_3d_1{d_2}^2)$
$x\,w\,s$	$-\frac{125}{46656}\sqrt{3}(-12\,d_1{d_2}^3+108+4\,{d_3}^3d_2-4\,{d_3}^3d_1+75\,d_1d_2-8\,{d_3}^2d_2d_1+8\,{d_3}^2{d_1}^2+4\,d_2{d_1}^3-12\,d_3{d_2}^3-16\,{d_3}^2-16\,{d_1}^2-155\,{d_2}^2-8\,d_3d_2{d_1}^2+8\,{d_2}^4+37\,d_3d_1+75\,d_3d_2-4\,d_3{d_1}^3+24\,d_3d_1{d_2}^2)$
$x\,w\,y$	$\frac{1}{46656}\sqrt{3}(3876-5244\,d_3d_1{d_2}^2+920\,d_3d_2{d_1}^2+2832\,{d_3}^2d_2d_1+64\,{d_3}^4d_2d_1+160\,{d_1}^2{d_2}^2{d_3}^2-272\,{d_3}^3{d_2}^2d_1+112\,{d_3}^3d_2{d_1}^2+16\,d_3d_2{d_1}^4+176\,d_3d_1{d_2}^4+112\,{d_3}^2{d_2}^3d_1-176\,{d_3}^2d_2{d_1}^3+160\,d_3{d_2}^2{d_1}^3-320\,d_3{d_2}^3{d_1}^2+32\,{d_2}^6-24\,d_3{d_1}^3-104\,d_2{d_1}^3+3580\,d_3{d_2}^3-7159\,d_1d_2-44\,{d_3}^3d_2-980\,{d_3}^3d_1+2967\,d_3d_1-1684\,{d_2}^4-928\,{d_1}^2-4455\,d_3d_2-2576\,{d_3}^2+812\,{d_3}^2{d_1}^2+128\,{d_3}^4-32\,{d_1}^4{d_2}^2+16\,{d_3}^4{d_2}^2-16\,d_3{d_1}^5+32\,{d_3}^5d_1+128\,{d_1}^2{d_2}^4-112\,{d_3}^2{d_2}^4-32\,{d_3}^5d_2+16\,d_2{d_1}^5-112\,d_1{d_2}^5+16\,{d_3}^2{d_1}^4-80\,{d_3}^4{d_1}^2+112\,{d_3}^3{d_2}^3+3392\,d_1{d_2}^3+64\,{d_1}^4-1980\,{d_3}^2{d_2}^2-16\,d_3{d_2}^5+48\,{d_3}^3{d_1}^3-1668\,{d_1}^2{d_2}^2-32\,{d_2}^3{d_1}^3+3959\,{d_2}^2)$
$x\,w\,z$	$\frac{1}{23328}\sqrt{3}(-648-3696\,d_3d_1{d_2}^2-238\,d_3d_2{d_1}^2-1849\,{d_3}^2d_2d_1-32\,{d_3}^2{d_2}^3{d_1}^3+96\,{d_3}^4{d_2}^2{d_1}^2+192\,{d_3}^3{d_2}^4d_1-32\,{d_3}^4{d_2}^3d_1+144\,{d_3}^3{d_2}^2{d_1}^3-272\,{d_3}^3{d_2}^3{d_1}^2-96\,{d_3}^4d_2{d_1}^3+16\,{d_3}^2d_2{d_1}^5+128\,{d_3}^2{d_2}^4{d_1}^2-48\,{d_3}^5{d_2}^2d_1-112\,{d_3}^2{d_2}^5d_1-32\,{d_3}^2{d_1}^4{d_2}^2+48\,{d_3}^5d_2{d_1}^2+600\,{d_3}^4d_2d_1-1572\,{d_1}^2{d_2}^2{d_3}^2-2940\,{d_3}^3{d_2}^2d_1+1116\,{d_3}^3d_2{d_1}^2+24\,d_3d_2{d_1}^4-24\,d_3d_1{d_2}^4+3344\,{d_3}^2{d_2}^3d_1-136\,{d_3}^2d_2{d_1}^3+24\,d_3{d_2}^2{d_1}^3-72\,d_3{d_2}^3{d_1}^2-392\,d_3{d_1}^3-88\,d_2{d_1}^3+3174\,d_3{d_2}^3-1906\,d_1d_2-2593\,{d_3}^3d_2-623\,{d_3}^3d_1+3386\,d_3d_1-176\,{d_2}^4+608\,{d_1}^2-5834\,d_3d_2+252\,{d_3}^2+238\,{d_3}^2{d_1}^2+432\,{d_3}^4-168\,{d_3}^4{d_2}^2+108\,{d_3}^5d_1-1676\,{d_3}^2{d_2}^4-108\,{d_3}^5d_2+40\,{d_3}^2{d_1}^4-432\,{d_3}^4{d_1}^2+1520\,{d_3}^3{d_2}^3+264\,d_1{d_2}^3+5547\,{d_3}^2{d_2}^2-16\,{d_3}^5{d_1}^3+16\,{d_3}^5{d_2}^3-16\,{d_3}^3{d_1}^5-48\,{d_3}^3{d_2}^5+32\,{d_3}^4{d_1}^4+32\,{d_3}^2{d_2}^6+48\,d_3{d_2}^5+304\,{d_3}^3{d_1}^3-4270\,{d_2}^2)$
$x\,f\,f$	$\frac{1}{2592}\,(d_2-d_3)(608+192\,d_3d_1{d_2}^2-232\,d_3d_2{d_1}^2+192\,{d_3}^2d_2d_1+64\,{d_1}^2{d_2}^2{d_3}^2-32\,{d_3}^3{d_2}^2d_1+16\,{d_3}^3d_2{d_1}^2+16\,d_3d_2{d_1}^4-32\,{d_3}^2{d_2}^3d_1-32\,{d_3}^2d_2{d_1}^3-32\,d_3{d_2}^2{d_1}^3+16\,d_3{d_2}^3{d_1}^2+8\,d_3{d_1}^3+8\,d_2{d_1}^3-36\,d_3{d_2}^3-334\,d_1d_2-36\,{d_3}^3d_2-334\,d_3d_1-188\,{d_1}^2+565\,d_3d_2-18\,{d_3}^2+8\,{d_3}^2{d_1}^2+8\,{d_1}^2{d_2}^2+16\,{d_3}^3{d_2}^3-112\,{d_3}^2{d_2}^2-18\,{d_2}^2)$
$x\,f\,o$	0
$x\,f\,\tilde{o}$	0
$x\,f\,p$	0

Table A.3: The cubic couplings for all of the fields in the action up to level 3 (continued).

$l\,m\,n$	$B_{lmn}(d_1,d_2,d_3)$
$x\ f\ q$	$\frac{1}{11664}\sqrt{3}(-2048-279\,d_3d_1{d_2}^2+936\,d_3d_2{d_1}^2-1091\,{d_3}^2d_2d_1+60\,{d_3}^4d_2d_1+68\,{d_1}^2{d_2}^2{d_3}^2+60\,{d_3}^3{d_2}^2d_1-128\,{d_3}^3d_2{d_1}^2-8\,d_3d_2{d_1}^4+16\,d_3d_1{d_2}^4-136\,{d_3}^2{d_2}^3d_1+76\,{d_3}^2d_2{d_1}^3-76\,d_3{d_2}^2{d_1}^3+68\,d_3{d_2}^3{d_1}^2-4\,d_3{d_1}^3-156\,d_2{d_1}^3-413\,d_3{d_2}^3+744\,d_1d_2+82\,{d_3}^3d_2+30\,{d_3}^3d_1+248\,d_3d_1+18\,{d_2}^4+16\,{d_1}^2-3124\,d_3d_2+1256\,{d_3}^2+26\,{d_3}^2{d_1}^2-178\,{d_1}^2{d_2}^2-60\,{d_3}^4{d_2}^2-8\,{d_3}^2{d_2}^4+68\,{d_3}^3{d_2}^3+252\,d_1{d_2}^3+777\,{d_3}^2{d_2}^2+8\,{d_1}^4{d_2}^2-8\,{d_1}^2{d_2}^4+536\,{d_2}^2)$
$x\ f\ r$	$\frac{11}{11664}\sqrt{3}(28\,d_2+4\,d_2{}^2{d_1}^3-2\,d_3{d_1}^2+45\,d_3d_2d_1-4\,{d_3}^2{d_2}^3+9\,{d_2}^3-4\,{d_1}^2{d_2}^3-4\,{d_3}^3d_2d_1-11\,d_3{d_2}^2-4\,d_3d_2{d_1}^3+40\,d_3-14\,{d_1}^2d_2-14\,{d_3}^2d_2-2\,{d_3}^2d_1+8\,d_3{d_2}^3d_1-4\,{d_3}^2d_1{d_2}^2+8\,{d_3}^2d_2{d_1}^2-4\,d_3{d_2}^2{d_1}^2+40\,d_1-11\,d_1{d_2}^2+4\,{d_3}^3{d_2}^2)$
$x\ f\ s$	$-\frac{125}{23328}\sqrt{3}(28\,d_2+4\,d_2{}^2{d_1}^3-2\,d_3{d_1}^2+45\,d_3d_2d_1-4\,{d_3}^2{d_2}^3+9\,{d_2}^3-4\,{d_1}^2{d_2}^3-4\,{d_3}^3d_2d_1-11\,d_3{d_2}^2-4\,d_3d_2{d_1}^3+40\,d_3-14\,{d_1}^2d_2-14\,{d_3}^2d_2-2\,{d_3}^2d_1+8\,d_3{d_2}^3d_1-4\,{d_3}^2d_1{d_2}^2+8\,{d_3}^2d_2{d_1}^2-4\,d_3{d_2}^2{d_1}^2+40\,d_1-11\,d_1{d_2}^2+4\,{d_3}^3{d_2}^2)$
$x\ f\ y$	$\frac{1}{23328}\sqrt{3}(48\,d_3{d_2}^3{d_1}^3+32\,d_3d_1{d_2}^5-16\,d_3d_2{d_1}^5+16\,{d_3}^2{d_1}^4d_2+48\,{d_3}^2d_1{d_2}^4+32\,d_3{d_2}^2{d_1}^4+32\,{d_3}^4{d_2}^2d_1+48\,{d_3}^3d_2{d_1}^3+96\,{d_3}^2{d_2}^3{d_1}^2-96\,d_3{d_2}^4{d_1}^2-144\,{d_3}^2{d_2}^2{d_1}^3-144\,{d_3}^3{d_2}^3d_1-80\,{d_3}^4d_2{d_1}^2+32\,{d_3}^5d_2d_1+96\,{d_3}^3{d_2}^2{d_1}^2-320\,{d_3}^3-364\,d_3{d_2}^2{d_1}^2+844\,{d_3}^2d_2{d_1}^2+220\,{d_3}^2d_1{d_2}^2-36\,d_3{d_2}^3d_1+32\,d_3d_2{d_1}^3-1044\,{d_3}^3d_2d_1+399\,d_3d_2d_1-3258\,{d_3}^2d_2+36\,{d_2}^5-1277\,{d_2}^3+224\,{d_1}^3+935\,d_3{d_2}^2-4424\,d_1+6068\,d_2+8\,{d_3}^3{d_1}^2-592\,{d_2}^2{d_1}^3+586\,d_3{d_1}^2+856\,{d_1}^2{d_2}^3-2154\,{d_1}^2d_2+1322\,{d_3}^2d_1+3543\,d_1{d_2}^2+652\,{d_3}^3{d_2}^2-16\,{d_3}^2{d_1}^3-372\,d_1{d_2}^4-48\,{d_2}^3{d_1}^4+48\,{d_2}^4{d_1}^3+16\,{d_3}^4d_1+112\,{d_3}^4d_2+48\,{d_3}^4{d_2}^3+248\,d_3{d_2}^4-16\,{d_3}^2{d_2}^5-32\,{d_3}^5{d_2}^2-8\,d_3{d_1}^4-16\,{d_1}^2{d_2}^5+16\,{d_1}^5{d_2}^2-664\,{d_3}^2{d_2}^3-1864\,d_3+72\,{d_1}^4d_2)$
$x\ f\ z$	$\frac{1}{11664}\sqrt{3}(48\,{d_3}^2{d_1}^4d_2-324\,{d_3}^2d_1{d_2}^4+24\,d_3{d_2}^2{d_1}^4+468\,{d_3}^4{d_2}^2d_1+352\,{d_3}^3d_2{d_1}^3+840\,{d_3}^2{d_2}^3{d_1}^2-24\,d_3{d_2}^4{d_1}^2-600\,{d_3}^2{d_2}^2{d_1}^3-508\,{d_3}^3{d_2}^3d_1-408\,{d_3}^4d_2{d_1}^2+108\,{d_3}^5d_2d_1-24\,{d_3}^3{d_2}^2{d_1}^2-1080\,{d_3}^3-446\,d_3{d_2}^2{d_1}^2-932\,{d_3}^2d_2{d_1}^2+3469\,{d_3}^2d_1{d_2}^2+580\,d_3{d_2}^3d_1-380\,d_3d_2{d_1}^3-1799\,{d_3}^3d_2d_1+1242\,d_3d_2d_1+16\,{d_3}^2{d_2}^2{d_1}^5+16\,{d_3}^4{d_2}^4d_1+32\,{d_3}^3{d_2}^5d_1+32\,{d_3}^4d_2{d_1}^4-16\,{d_3}^2{d_2}^5{d_1}^2-80\,{d_3}^4{d_2}^2{d_1}^3+48\,{d_3}^2{d_2}^4{d_1}^3-16\,{d_3}^3d_2{d_1}^5-48\,{d_3}^2{d_2}^3{d_1}^4-80\,{d_3}^3{d_2}^4{d_1}^2+48\,{d_3}^4{d_2}^3{d_1}^2+48\,{d_3}^3{d_2}^3{d_1}^3+16\,{d_3}^3{d_2}^2{d_1}^4+48\,{d_3}^5{d_2}^2{d_1}^2-16\,{d_3}^5{d_2}^2{d_1}^3-48\,{d_3}^5{d_2}^3d_1+3568\,{d_3}^2d_2-198\,{d_2}^3+2362\,d_3{d_2}^2-8\,{d_3}^3{d_1}^4+16\,{d_3}^5{d_2}^4-8\,{d_3}^4{d_1}^3+188\,{d_3}^3{d_2}^4-752\,d_1-2728\,d_2+522\,{d_3}^3{d_1}^2-88\,{d_2}^2{d_1}^3+92\,d_3{d_1}^2+88\,{d_1}^2{d_2}^3+564\,{d_1}^2d_2-1756\,{d_3}^2d_1-270\,d_1{d_2}^2+221\,{d_3}^3{d_2}^2-16\,{d_3}^4{d_2}^5+212\,{d_3}^2{d_1}^3+54\,{d_3}^4d_1+378\,{d_3}^4d_2-52\,{d_3}^4{d_2}^3+54\,d_3{d_2}^4+36\,{d_3}^2{d_2}^5-108\,{d_3}^5{d_2}^2-1933\,{d_3}^2{d_2}^3-3312\,d_3)$
$x\ o\ o$	$\frac{736}{2187}\,d_2-\frac{736}{2187}\,d_3$
$x\ o\ \tilde{o}$	0
$x\ o\ p$	0
$x\ o\ q$	0
$x\ o\ r$	$-\frac{320}{2187}+\frac{80}{2187}\,{d_2}^2+\frac{80}{2187}\,d_3d_1-\frac{80}{2187}\,d_3d_2-\frac{80}{2187}\,d_1d_2$
$x\ o\ s$	0
$x\ o\ y$	0
$x\ o\ z$	0
$x\ \tilde{o}\ \tilde{o}$	$\frac{64}{2187}\,d_2-\frac{64}{2187}\,d_3$
$x\ \tilde{o}\ p$	0
$x\ \tilde{o}\ q$	0
$x\ \tilde{o}\ r$	0
$x\ \tilde{o}\ s$	0
$x\ \tilde{o}\ y$	0
$x\ \tilde{o}\ z$	0
$x\ p\ p$	$-\frac{12800}{2187}\,d_2+\frac{12800}{2187}\,d_3$
$x\ p\ q$	0
$x\ p\ r$	0
$x\ p\ s$	$\frac{1600}{2187}\,{d_2}^2-\frac{6400}{2187}+\frac{1600}{2187}\,d_3d_1-\frac{1600}{2187}\,d_3d_2-\frac{1600}{2187}\,d_1d_2$
$x\ p\ y$	0
$x\ p\ z$	0
$x\ q\ q$	$-\frac{1}{17496}\,(d_2-d_3)(-30\,d_3{d_2}^3+30\,d_1{d_2}^3-4\,{d_1}^2{d_2}^2+229\,{d_3}^2{d_2}^2+1312\,{d_2}^2-225\,d_3d_1{d_2}^2-7488\,d_3d_2-30\,{d_3}^3d_2-1152\,d_1d_2+285\,d_3d_2{d_1}^2-30\,d_2{d_1}^3-225\,{d_3}^2d_2d_1+4\,{d_1}^4+1312\,{d_3}^2-4\,{d_3}^2{d_1}^2-416\,{d_1}^2+30\,{d_3}^3d_1-4096-1152\,d_3d_1-30\,d_3{d_1}^3)$
$x\ q\ r$	$-\frac{11}{17496}\,(d_1-d_3)(2\,{d_1}^2d_2-2\,d_3{d_1}^2+32\,d_1+19\,d_3d_2d_1-17\,d_1{d_2}^2-2\,{d_3}^2d_1-96\,d_2+2\,{d_3}^2d_2+15\,{d_2}^3+32\,d_3-17\,d_3{d_2}^2)$

Table A.3: The cubic couplings for all of the fields in the action up to level 3 (continued).

$l\,m\,n$	$B_{lmn}(d_1,d_2,d_3)$
$x\ q\ s$	$\frac{125}{34992}\,(d_1-d_3)(2\,{d_1}^2d_2-2\,d_3{d_1}^2+32\,d_1+19\,d_3d_2d_1-17\,d_1{d_2}^2-2\,{d_3}^2d_1-96\,d_2+2\,{d_3}^2d_2+15\,{d_2}^3+32\,d_3-17\,d_3{d_2}^2)$
$x\ q\ y$	$\frac{76}{729}\,d_3d_1{d_2}^2+\frac{47}{1296}\,d_3d_2{d_1}^2-\frac{1319}{11664}\,{d_3}^2d_2d_1-\frac{17}{1458}\,{d_1}^2{d_2}^2{d_3}^2-\frac{1}{1458}\,{d_3}^3{d_2}^2d_1+\frac{19}{2916}\,{d_3}^3d_2{d_1}^2-\frac{23}{8748}\,d_3d_2{d_1}^4+\frac{8}{729}\,{d_3}^2{d_2}^3d_1+\frac{1}{1458}\,{d_3}^2d_2{d_1}^3+\frac{17}{2916}\,d_3{d_2}^2{d_1}^3-\frac{1}{2187}\,{d_3}^5d_2-\frac{14}{2187}\,{d_2}^4-\frac{17}{4374}\,{d_3}^4d_2d_1-\frac{5}{972}\,d_3d_1{d_2}^4-\frac{512}{729}-\frac{197}{17496}\,d_3{d_1}^3+\frac{821}{17496}\,d_2{d_1}^3-\frac{1337}{11664}\,d_3{d_2}^3-\frac{530}{2187}\,d_1d_2-\frac{229}{17496}\,{d_3}^3d_2-\frac{184}{2187}\,d_3d_1+\frac{34}{243}\,{d_1}^2-\frac{58}{243}\,d_3d_2+\frac{406}{2187}\,{d_3}^2-\frac{64}{2187}\,{d_3}^2{d_1}^2-\frac{3413}{34992}\,{d_1}^2{d_2}^2-\frac{5}{972}\,{d_3}^3{d_2}^3-\frac{16}{2187}\,{d_3}^4+\frac{3701}{34992}\,{d_3}^2{d_2}^2-\frac{4}{729}\,{d_1}^4+\frac{7}{2916}\,{d_1}^4{d_2}^2+\frac{1}{243}\,{d_3}^4{d_2}^2+\frac{1}{4374}\,d_3{d_1}^5+\frac{1}{2187}\,{d_3}^5d_1+\frac{47}{8748}\,{d_1}^2{d_2}^4-\frac{1}{4374}\,{d_3}^2{d_2}^4-\frac{1}{4374}\,d_2{d_1}^5-\frac{5}{2916}\,d_1{d_2}^5+\frac{1}{4374}\,{d_3}^2{d_1}^4+\frac{5}{2916}\,d_3{d_2}^5-\frac{1}{4374}\,{d_3}^4{d_1}^2-\frac{1}{1458}\,{d_3}^3{d_1}^3-\frac{17}{2916}\,{d_2}^3{d_1}^3+1/16\,d_1{d_2}^3+\frac{247}{5832}\,{d_3}^3d_1+\frac{1292}{2187}\,{d_2}^2$
$x\ q\ z$	$\frac{16}{81}\,d_3d_1{d_2}^2+\frac{811}{8748}\,d_3d_2{d_1}^2-\frac{7627}{8748}\,{d_3}^2d_2d_1-\frac{17}{1458}\,{d_3}^2{d_2}^3{d_1}^3-\frac{17}{1458}\,{d_3}^4{d_2}^2{d_1}^2-\frac{5}{729}\,{d_3}^3{d_2}^4d_1+\frac{17}{1458}\,{d_3}^4{d_2}^3d_1+\frac{2}{243}\,{d_3}^3{d_2}^2{d_1}^3-\frac{1}{2187}\,{d_3}^3{d_2}^3{d_1}^2+\frac{17}{4374}\,{d_3}^4d_2{d_1}^3-\frac{1}{2187}\,{d_3}^2d_2{d_1}^5+\frac{47}{4374}\,{d_3}^2{d_2}^4{d_1}^2-\frac{1}{729}\,{d_3}^5{d_2}^2d_1-\frac{7}{1458}\,{d_3}^3d_2{d_1}^4-\frac{5}{1458}\,{d_3}^2{d_2}^5d_1+\frac{7}{1458}\,{d_3}^2{d_1}^4{d_2}^2+\frac{1}{729}\,{d_3}^5d_2{d_1}^2+\frac{1}{1458}\,d_3{d_2}^3{d_1}^2-\frac{1115}{5832}\,{d_1}^2{d_2}^2{d_3}^2+\frac{56}{729}\,{d_3}^3{d_2}^2d_1+\frac{41}{1944}\,{d_3}^3d_2{d_1}^2-\frac{1}{1458}\,d_3d_2{d_1}^4+\frac{709}{5832}\,{d_3}^2{d_2}^3d_1+\frac{383}{4374}\,{d_3}^2d_2{d_1}^3+\frac{5}{972}\,d_3{d_2}^2{d_1}^3-\frac{1}{324}\,{d_3}^5d_2-\frac{409}{5832}\,{d_3}^4d_2d_1-\frac{5}{972}\,d_3d_1{d_2}^4-\frac{512}{729}-\frac{11}{4374}\,d_3{d_1}^3+\frac{11}{4374}\,d_2{d_1}^3-\frac{79}{324}\,d_3{d_2}^3+\frac{320}{2187}\,d_1d_2+\frac{13}{4374}\,{d_3}^3d_2-\frac{464}{2187}\,d_3d_1+\frac{8}{243}\,{d_1}^2-\frac{616}{2187}\,d_3d_2-\frac{136}{729}\,{d_3}^2+\frac{92}{729}\,{d_3}^2{d_1}^2-\frac{187}{8748}\,{d_1}^2{d_2}^2-\frac{1339}{17496}\,{d_3}^3{d_2}^3-\frac{4}{81}\,{d_3}^4+\frac{5083}{8748}\,{d_3}^2{d_2}^2+\frac{95}{1944}\,{d_3}^4{d_2}^2+\frac{1}{324}\,{d_3}^5d_1-\frac{67}{8748}\,{d_3}^2{d_2}^4-\frac{5}{486}\,{d_3}^2{d_1}^4+\frac{31}{1458}\,{d_3}^4{d_1}^2-\frac{187}{8748}\,{d_3}^3{d_1}^3-\frac{1}{2187}\,{d_3}^5{d_2}^3+\frac{1}{2187}\,{d_3}^3{d_1}^5+\frac{5}{1458}\,{d_3}^3{d_2}^5-\frac{17}{4374}\,{d_3}^4{d_2}^4+\frac{55}{2916}\,d_1{d_2}^3+\frac{731}{4374}\,{d_3}^3d_1+\frac{1864}{2187}\,{d_2}^2$
$x\ r\ r$	$-\frac{19}{5832}\,(d_2-d_3)(d_1-d_3)(d_1-d_2)$
$x\ r\ s$	$\frac{1375}{34992}\,(d_2-d_3)(d_1-d_3)(d_1-d_2)$
$x\ r\ y$	$-\frac{11}{34992}\,(d_1-d_2)(4\,d_2{d_1}^3-4\,d_3{d_1}^3-8\,{d_1}^2{d_2}^2+8\,d_3d_2{d_1}^2+32\,{d_1}^2+4\,d_1{d_2}^3+12\,{d_3}^3d_1-27\,d_3d_1-101\,d_1d_2-24\,{d_3}^2{d_2}d_1+8\,d_3d_1{d_2}^2-320+91\,{d_3}^2-8\,{d_3}^4-4\,d_3{d_2}^3+32\,{d_2}^2+12\,{d_3}^3d_2-27\,d_3d_2)$
$x\ r\ z$	$-\frac{11}{17496}\,(d_1-d_2)(4\,{d_3}^2d_2{d_1}^3-4\,{d_3}^3{d_1}^3+26\,{d_3}^2{d_1}^2+4\,{d_3}^4{d_1}^2+6\,d_3d_2{d_1}^2+4\,{d_3}^3d_2{d_1}^2-8\,{d_1}^2{d_2}^2{d_3}^2+4\,{d_3}^2{d_2}^3d_1-74\,d_3d_1-8\,{d_3}^4d_2d_1-103\,{d_3}^2d_2d_1-22\,d_1d_2+33\,{d_3}^3d_1+6\,d_3d_1{d_2}^2+4\,{d_3}^3{d_2}^2d_1+33\,{d_3}^3d_2+4\,{d_3}^4{d_2}^2-74\,d_3d_2-214\,{d_3}^2+64+26\,{d_3}^2{d_2}^2-27\,{d_3}^4-4\,{d_3}^3{d_2}^3)$
$x\ s\ s$	$-\frac{9475}{23328}\,(d_2-d_3)(d_1-d_3)(d_1-d_2)$
$x\ s\ y$	$\frac{125}{69984}\,(d_1-d_2)(4\,d_2{d_1}^3-4\,d_3{d_1}^3-8\,{d_1}^2{d_2}^2+8\,d_3d_2{d_1}^2+32\,{d_1}^2+4\,d_1{d_2}^3+12\,{d_3}^3d_1-27\,d_3d_1-101\,d_1d_2-24\,{d_3}^2{d_2}d_1+8\,d_3d_1{d_2}^2-320+91\,{d_3}^2-8\,{d_3}^4-4\,d_3{d_2}^3+32\,{d_2}^2+12\,{d_3}^3d_2-27\,d_3d_2)$
$x\ s\ z$	$\frac{125}{34992}\,(d_1-d_2)(4\,{d_3}^2d_2{d_1}^3-4\,{d_3}^3{d_1}^3+26\,{d_3}^2{d_1}^2+4\,{d_3}^4{d_1}^2+6\,d_3d_2{d_1}^2+4\,{d_3}^3d_2{d_1}^2-8\,{d_1}^2{d_2}^2{d_3}^2+4\,{d_3}^2{d_2}^3d_1-74\,d_3d_1-8\,{d_3}^4d_2d_1-103\,{d_3}^2d_2d_1-22\,d_1d_2+33\,{d_3}^3d_1+6\,d_3d_1{d_2}^2+4\,{d_3}^3{d_2}^2d_1+33\,{d_3}^3d_2+4\,{d_3}^4{d_2}^2-74\,d_3d_2-214\,{d_3}^2+64+26\,{d_3}^2{d_2}^2-27\,{d_3}^4-4\,{d_3}^3{d_2}^3)$
$x\ y\ y$	$-\frac{1}{69984}\,(d_2-d_3)(24000+808\,d_3d_1{d_2}^2-1400\,d_3d_2{d_1}^2+808\,{d_3}^2d_2d_1+160\,d_3d_2{d_1}^4+128\,d_3d_1{d_2}^4-160\,d_3{d_2}^2{d_1}^3-64\,d_3{d_2}^3{d_1}^2+368\,{d_1}^2{d_2}^2{d_3}^2-160\,{d_3}^3{d_2}^2d_1-64\,{d_3}^3d_2{d_1}^2-160\,{d_3}^2{d_2}^3d_1-160\,{d_3}^2d_2{d_1}^3+128\,{d_3}^4d_2d_1+3072\,{d_1}^2{d_2}^2+9543\,d_1d_2+788\,{d_3}^3d_2+9543\,d_3d_1-5639\,{d_1}^2+10809\,d_3d_2-8032\,{d_3}^2+3072\,{d_3}^2{d_1}^2-32\,{d_1}^4{d_2}^2-32\,d_3{d_1}^5+32\,{d_3}^5d_1-112\,{d_1}^2{d_2}^4-16\,{d_3}^2{d_2}^4-32\,{d_3}^5d_2-32\,d_2{d_1}^5+32\,d_1{d_2}^5-32\,{d_3}^2{d_1}^4-32\,d_3{d_2}^5+128\,{d_2}^3{d_1}^3+96\,{d_3}^3{d_2}^3+256\,{d_3}^4-2088\,{d_3}^2{d_2}^2+256\,{d_2}^4-296\,{d_1}^4+16\,{d_1}^6-964\,d_2{d_1}^3-964\,d_3{d_1}^3-2068\,d_1{d_2}^3-16\,{d_3}^4{d_2}^2-112\,{d_3}^4{d_1}^2+128\,{d_3}^3{d_1}^3-2068\,{d_3}^3d_1+788\,d_3{d_2}^3-8032\,{d_2}^2)$
$x\ y\ z$	$\frac{2}{2187}\,{d_3}^2{d_2}^2{d_1}^5+\frac{1}{486}\,d_3{d_2}^3{d_1}^3+1/6\,{d_3}^3d_2d_1+\frac{25}{243}\,d_3{d_2}^2{d_1}^2-\frac{8}{2187}\,d_3d_2d_1-\frac{1}{729}\,d_3d_1{d_2}^5-\frac{1}{1458}\,d_3d_2{d_1}^5+\frac{4}{729}\,{d_3}^4{d_2}^4d_1-\frac{4}{2187}\,{d_3}^3d_2{d_1}^5-\frac{2}{2187}\,{d_3}^2{d_2}^6d_1+\frac{2}{729}\,{d_3}^4d_2{d_1}^4+\frac{7}{2187}\,{d_3}^2{d_2}^5{d_1}^2+\frac{1}{729}\,{d_3}^4{d_2}^2{d_1}^3-\frac{1}{729}\,{d_3}^6{d_2}^2d_1-\frac{8}{2187}\,{d_3}^2{d_2}^4{d_1}^3+\frac{1}{2187}\,{d_3}^3d_2{d_1}^5+\frac{2}{2187}\,{d_3}^2{d_2}^3{d_1}^4-\frac{4}{2187}\,{d_3}^3{d_2}^4{d_1}^2-\frac{247}{1944}\,d_3d_2{d_3}^3d_1+\frac{17}{648}\,d_3d_2{d_1}^3+\frac{22}{2187}\,{d_3}^2{d_1}^4d_2-\frac{311}{11664}\,{d_3}^2d_2{d_1}^2+\frac{509}{8748}\,{d_3}^2d_1d_2{}^4-\frac{1}{1458}\,d_3d_2{}^2{d_1}^4-\frac{151}{2916}\,{d_3}^4{d_2}^2d_1-\frac{4345}{11664}\,{d_3}^2{d_1}d_2{}^2-\frac{5}{729}\,{d_3}^4{d_2}^3{d_1}^2-\frac{185}{8748}\,{d_3}^3d_2{d_1}^3-\frac{43}{486}\,{d_3}^2{d_2}^3{d_1}^2+\frac{1}{1458}\,d_3{d_2}^4{d_1}^2+\frac{223}{8748}\,{d_3}^2{d_2}^2{d_1}^3+\frac{10}{2187}\,{d_3}^3{d_2}^3d_1-\frac{23}{972}\,{d_3}^4d_2{d_1}^2+\frac{5}{729}\,{d_3}^3{d_2}^3{d_1}^3-\frac{1}{2187}\,{d_3}^2{d_2}d_1{}^6-\frac{11}{2187}\,{d_3}^3{d_2}^2{d_1}^4+\frac{1}{243}\,{d_3}^5{d_2}^2{d_1}^2+\frac{91}{2916}\,{d_3}^5d_2d_1-\frac{1}{243}\,{d_3}^5d_2{d_1}^3-\frac{1}{729}\,{d_3}^5{d_2}^3d_1+\frac{97}{1458}\,{d_3}^3{d_2}^2{d_1}^2+\frac{1}{729}\,{d_3}^6d_2{d_1}^2-\frac{32}{2187}\,{d_2}^3+\frac{527}{34992}\,{d_3}^4d_2-\frac{112}{729}\,{d_3}^3+\frac{1825}{5832}\,{d_3}^2{d_2}^3-\frac{1559}{11664}\,{d_3}^3{d_2}^2-\frac{1801}{17496}\,{d_3}^2d_2-\frac{20}{729}\,{d_1}^3+\frac{68}{729}\,d_1+\frac{100}{729}\,d_2-\frac{12199}{17496}\,d_3{d_2}^2+\frac{2}{81}\,{d_3}^5+\frac{856}{729}\,d_3+\frac{757}{3888}\,{d_3}^3{d_1}^2+\frac{7561}{17496}\,{d_3}^2d_1-\frac{5881}{17496}\,d_3{d_1}^2+\frac{989}{5832}\,d_1{d_2}^2+\frac{553}{17496}\,{d_1}^2d_2-\frac{377}{5832}\,{d_3}^2{d_1}^3-\frac{11}{1458}\,{d_1}^2{d_2}^3+\frac{11}{2187}\,d_1{d_2}^4+\frac{11}{4374}\,{d_1}^4d_2-\frac{5231}{34992}\,{d_3}^4d_1+\frac{82}{2187}\,{d_3}^4{d_1}^3-\frac{259}{8748}\,{d_3}^3{d_2}^4+\frac{83}{2187}\,{d_3}^4{d_2}^3-\frac{89}{4374}\,{d_3}^3{d_1}^4+\frac{37}{2187}\,d_3{d_2}^4-\frac{13}{2187}\,{d_3}^2{d_2}^5-\frac{5}{486}\,{d_3}^5{d_2}^2+\frac{61}{4374}\,d_3{d_1}^4+\frac{1}{1458}\,{d_3}^2{d_1}^5-\frac{61}{2916}\,{d_3}^5{d_1}^2+\frac{1}{324}\,{d_3}^6d_1-\frac{1}{324}\,{d_3}^6d_2+\frac{1}{729}\,{d_3}^5{d_1}^4-\frac{1}{729}\,{d_3}^4{d_2}^5+\frac{2}{2187}\,{d_3}^3{d_2}^6+\frac{1}{2187}\,{d_3}^6{d_2}^3-\frac{1}{729}\,{d_3}^4{d_1}^5+\frac{1}{2187}\,{d_3}^3{d_1}^6-\frac{1}{2187}\,{d_3}^6{d_1}^3$

Table A.3: The cubic couplings for all of the fields in the action up to level 3 (continued).

$l\,m\,n$	$B_{lmn}(d_1,d_2,d_3)$
$x\ z\ z$	$-\frac{1}{17496}\,(d_2-d_3)(6528+9714\,d_3d_1{d_2}^2+3744\,d_3d_2{d_1}^2+9714\,{d_3}^2d_2d_1-540\,d_3d_2{d_1}^4+162\,d_3d_1{d_2}^4-858\,d_3{d_2}^2{d_1}^3+852\,d_3{d_2}^3{d_1}^2+8877\,{d_1}^2{d_2}^2{d_3}^2-7001\,{d_3}^3{d_2}^2d_1+852\,{d_3}^3d_2{d_1}^2-7001\,{d_3}^2{d_2}^3d_1-858\,{d_3}^2d_2{d_1}^3+144\,{d_3}^3{d_2}^3{d_1}^4+48\,{d_3}^5{d_2}^3{d_1}^2-16\,{d_3}^2{d_2}^5{d_1}^3-144\,{d_3}^4{d_2}^3{d_1}^3+16\,{d_3}^2{d_2}^2{d_1}^6-48\,{d_3}^3{d_2}^2{d_1}^5+48\,{d_3}^4{d_2}^2{d_1}^4-16\,{d_3}^5{d_2}^2{d_1}^3+48\,{d_3}^3{d_2}^5{d_1}^2-48\,{d_3}^4{d_2}^5d_1+144\,{d_3}^4{d_2}^4{d_1}^2-48\,{d_3}^2{d_2}^3{d_1}^5+48\,{d_3}^2{d_2}^4{d_1}^4-48\,{d_3}^5{d_2}^4d_1-144\,{d_3}^3{d_2}^4{d_1}^3+1272\,{d_3}^2{d_2}^3{d_1}^3-660\,{d_3}^4{d_2}^2{d_1}^2-24\,d_3{d_2}^4{d_1}^3+1020\,{d_3}^3{d_2}^4d_1+1020\,{d_3}^4{d_2}^3d_1+1272\,{d_3}^3{d_2}^2{d_1}^3-2184\,{d_3}^3{d_2}^3{d_1}^2-24\,{d_3}^4d_2{d_1}^3+24\,{d_3}^2d_2{d_1}^5-660\,{d_3}^2{d_2}^4{d_1}^2+108\,{d_3}^5{d_2}^2d_1+24\,d_3{d_2}^2{d_1}^5+108\,{d_3}^2{d_2}^5d_1-744\,{d_3}^2{d_1}^4{d_2}^2+162\,{d_3}^4d_2d_1-108\,{d_3}^3{d_2}^5-336\,{d_3}^4{d_2}^4-42\,{d_1}^2{d_2}^2-11428\,d_1d_2-1998\,{d_3}^3d_2-11428\,d_3d_1-1244\,{d_1}^2+868\,d_3d_2+1728\,{d_3}^2-42\,{d_3}^2{d_1}^2-88\,{d_1}^4{d_2}^2+702\,{d_3}^2{d_2}^4-88\,{d_3}^2{d_1}^4+88\,{d_2}^3{d_1}^3-108\,{d_3}^5{d_2}^3+3949\,{d_3}^3{d_2}^3-13032\,{d_3}^2{d_2}^2+828\,d_2{d_1}^3+828\,d_3{d_1}^3-594\,d_1{d_2}^3+702\,{d_3}^4{d_2}^2+88\,{d_3}^3{d_1}^3+16\,{d_3}^5{d_2}^5-594\,{d_3}^3d_1-1998\,d_3{d_2}^3+1728\,{d_2}^2)$
$h\ h\ h$	0
$h\ h\ u$	$1/4\,\sqrt{3}$
$h\ h\ v$	$-\frac{125}{216}\,\sqrt{3}$
$h\ h\ w$	$\frac{1}{216}\,\sqrt{3}(4\,{d_1}^2-8\,d_1d_2+4\,{d_2}^2+4\,d_3d_1+4\,d_3d_2-8\,{d_3}^2-5)$
$h\ h\ f$	$\frac{1}{108}\,\sqrt{3}(2\,d_2+4\,d_3{d_1}^2-8\,d_3d_2d_1+4\,d_3{d_2}^2-9\,d_3+2\,d_1)$
$h\ h\ o$	0
$h\ h\ \tilde{o}$	0
$h\ h\ p$	0
$h\ h\ q$	$\frac{1}{162}\,(d_1-d_2)(2\,d_1-15\,d_3+2\,d_2)$
$h\ h\ r$	$1/6\,d_1-1/6\,d_2$
$h\ h\ s$	$-\frac{125}{324}\,d_1+\frac{125}{324}\,d_2$
$h\ h\ y$	$\frac{1}{324}\,(d_1-d_2)(4\,{d_1}^2+4\,d_3d_1-8\,d_1d_2-37-8\,{d_3}^2+4\,{d_2}^2+4\,d_3d_2)$
$h\ h\ z$	$\frac{1}{162}\,(d_1-d_2)(4\,{d_3}^2{d_1}^2-8\,{d_3}^2d_2d_1+6\,d_3d_1-22-27\,{d_3}^2+4\,{d_3}^2{d_2}^2+6\,d_3d_2)$
$h\ u\ u$	0
$h\ u\ v$	$-\frac{125}{324}$
$h\ u\ w$	$\frac{1}{81}\,{d_1}^2-\frac{2}{81}\,d_1d_2+\frac{1}{81}\,{d_2}^2+\frac{1}{81}\,d_3d_1+\frac{1}{81}\,d_3d_2-\frac{2}{81}\,{d_3}^2-\frac{5}{324}$
$h\ u\ f$	$\frac{1}{81}\,d_1+\frac{1}{81}\,d_2-1/18\,d_3+\frac{2}{81}\,d_3{d_1}^2-\frac{4}{81}\,d_3d_2d_1+\frac{2}{81}\,d_3{d_2}^2$
$h\ u\ o$	$-\frac{98}{729}\,\sqrt{3}$
$h\ u\ \tilde{o}$	$\frac{172}{729}\,\sqrt{3}$
$h\ u\ p$	0
$h\ u\ q$	$\frac{1}{729}\,\sqrt{3}(d_1-d_2)(2\,d_1-15\,d_3+2\,d_2)$
$h\ u\ r$	0
$h\ u\ s$	$-\frac{125}{1458}\,\sqrt{3}(d_1-d_2)$
$h\ u\ y$	$\frac{1}{1458}\,\sqrt{3}(d_1-d_2)(4\,{d_1}^2+4\,d_3d_1-8\,d_1d_2-37-8\,{d_3}^2+4\,{d_2}^2+4\,d_3d_2)$
$h\ u\ z$	$\frac{1}{729}\,\sqrt{3}(d_1-d_2)(4\,{d_3}^2{d_1}^2-8\,{d_3}^2d_2d_1+6\,d_3d_1-22-27\,{d_3}^2+4\,{d_3}^2{d_2}^2+6\,d_3d_2)$
$h\ v\ v$	0
$h\ v\ w$	0
$h\ v\ f$	0
$h\ v\ o$	$\frac{125}{243}\,\sqrt{3}$
$h\ v\ \tilde{o}$	$-\frac{250}{729}\,\sqrt{3}$
$h\ v\ p$	0
$h\ v\ q$	0
$h\ v\ r$	$\frac{125}{1458}\,\sqrt{3}(d_1-d_2)$
$h\ v\ s$	0
$h\ v\ y$	0
$h\ v\ z$	0
$h\ w\ w$	0
$h\ w\ f$	0
$h\ w\ o$	$-\frac{1}{243}\,\sqrt{3}(4\,d_1d_2-5+4\,d_3d_2-8\,{d_2}^2-8\,d_3d_1+4\,{d_1}^2+4\,{d_3}^2)$
$h\ w\ \tilde{o}$	$\frac{2}{729}\,\sqrt{3}(4\,d_1d_2-5+4\,d_3d_2-8\,{d_2}^2-8\,d_3d_1+4\,{d_1}^2+4\,{d_3}^2)$
$h\ w\ p$	0

Table A.3: The cubic couplings for all of the fields in the action up to level 3 (continued).

$l\,m\,n$	$B_{lmn}(d_1, d_2, d_3)$
$h\,w\,q$	0
$h\,w\,r$	$-\frac{1}{1458}\sqrt{3}(-8\,d_3{d_1}^2+4\,{d_1}^3-12\,d_1{d_2}^2+12\,d_3d_2d_1-37\,d_1-4\,{d_3}^2d_2+8\,{d_2}^3+32\,d_3+4\,{d_3}^2d_1-59\,d_2-4\,d_3{d_2}^2)$
$h\,w\,s$	0
$h\,w\,y$	0
$h\,w\,z$	0
$h\,f\,f$	0
$h\,f\,o$	$-\frac{2}{243}\sqrt{3}(-8\,d_3d_2d_1+4\,{d_3}^2d_2+4\,{d_1}^2d_2-9\,d_2+2\,d_3+2\,d_1)$
$h\,f\,\tilde{o}$	$\frac{4}{729}\sqrt{3}(-8\,d_3d_2d_1+4\,{d_3}^2d_2+4\,{d_1}^2d_2-9\,d_2+2\,d_3+2\,d_1)$
$h\,f\,p$	0
$h\,f\,q$	0
$h\,f\,r$	$-\frac{1}{729}\sqrt{3}(4\,d_2{d_1}^3+2\,{d_1}^2+9\,{d_2}^2+8\,d_3d_1{d_2}^2+2\,d_3d_1+30\,d_3d_2-43\,d_1d_2-4\,{d_3}^2{d_2}^2-32-4\,{d_1}^2{d_2}^2-8\,d_3d_2{d_1}^2+4\,{d_3}^2d_2d_1)$
$h\,f\,s$	0
$h\,f\,y$	0
$h\,f\,z$	0
$h\,o\,o$	0
$h\,o\,\tilde{o}$	$\frac{512}{2187}$
$h\,o\,p$	0
$h\,o\,q$	$-\frac{4}{729}\,(d_1-d_2)(2\,d_1-15\,d_3+2\,d_2)$
$h\,o\,r$	$-\frac{196}{2187}\,d_1+\frac{196}{2187}\,d_2$
$h\,o\,s$	$\frac{250}{729}\,d_1-\frac{250}{729}\,d_2$
$h\,o\,y$	$-\frac{2}{729}\,(d_1-d_2)(4\,{d_1}^2+4\,d_3d_1-8\,d_1d_2-37-8\,{d_3}^2+4\,{d_2}^2+4\,d_3d_2)$
$h\,o\,z$	$-\frac{4}{729}\,(d_1-d_2)(4\,{d_3}^2{d_1}^2-8\,{d_3}^2d_2d_1+6\,d_3d_1-22-27\,{d_3}^2+4\,{d_3}^2{d_2}^2+6\,d_3d_2)$
$h\,\tilde{o}\,\tilde{o}$	0
$h\,\tilde{o}\,p$	0
$h\,\tilde{o}\,q$	$\frac{8}{2187}\,(d_1-d_2)(2\,d_1-15\,d_3+2\,d_2)$
$h\,\tilde{o}\,r$	$\frac{344}{2187}\,d_1-\frac{344}{2187}\,d_2$
$h\,\tilde{o}\,s$	$-\frac{500}{2187}\,d_1+\frac{500}{2187}\,d_2$
$h\,\tilde{o}\,y$	$\frac{4}{2187}\,(d_1-d_2)(4\,{d_1}^2+4\,d_3d_1-8\,d_1d_2-37-8\,{d_3}^2+4\,{d_2}^2+4\,d_3d_2)$
$h\,\tilde{o}\,z$	$\frac{8}{2187}\,(d_1-d_2)(4\,{d_3}^2{d_1}^2-8\,{d_3}^2d_2d_1+6\,d_3d_1-22-27\,{d_3}^2+4\,{d_3}^2{d_2}^2+6\,d_3d_2)$
$h\,p\,p$	0
$h\,p\,q$	0
$h\,p\,r$	0
$h\,p\,s$	0
$h\,p\,y$	0
$h\,p\,z$	0
$h\,q\,q$	0
$h\,q\,r$	$\frac{4}{2187}\,{d_3}^2d_2-\frac{10}{729}\,d_3{d_2}^2+\frac{10}{729}\,d_1{d_2}^2+\frac{10}{729}\,d_3d_2d_1+\frac{56}{2187}\,d_2+\frac{4}{2187}\,{d_1}^3-\frac{34}{2187}\,{d_1}^2d_2+\frac{16}{729}\,d_3-\frac{4}{2187}\,{d_3}^2d_1-\frac{80}{2187}\,d_1$
$h\,q\,s$	0
$h\,q\,y$	0
$h\,q\,z$	0
$h\,r\,r$	0
$h\,r\,s$	$\frac{125}{2187}\,{d_1}^2-\frac{125}{2187}\,d_3d_1+\frac{125}{2187}\,d_3d_2-\frac{125}{2187}\,d_1d_2-\frac{500}{2187}$
$h\,r\,y$	$\frac{4}{729}\,d_2{d_1}^3+\frac{85}{2187}\,{d_1}^2+\frac{16}{729}\,{d_2}^2-\frac{32}{2187}\,{d_3}^2-\frac{28}{729}+\frac{8}{2187}\,{d_3}^3d_2+\frac{16}{2187}\,d_3d_1{d_2}^2+\frac{43}{2187}\,d_3d_1-\frac{11}{2187}\,d_3d_2+\frac{4}{729}\,{d_3}^2{d_1}^2-\frac{133}{2187}\,d_1d_2-\frac{4}{2187}\,{d_3}^2{d_2}^2-\frac{8}{2187}\,{d_3}^3d_1-\frac{4}{729}\,{d_1}^2{d_2}^2-\frac{4}{729}\,d_3d_2{d_1}^2-\frac{8}{2187}\,{d_3}^2d_2d_1-\frac{4}{2187}\,{d_1}^4+\frac{4}{2187}\,d_1{d_2}^3-\frac{4}{2187}\,d_3{d_2}^3$
$h\,r\,z$	$\frac{8}{2187}\,{d_3}^2{d_2}^3d_1+\frac{8}{729}\,{d_3}^2d_2{d_1}^3+\frac{44}{2187}\,{d_1}^2-\frac{8}{81}\,{d_3}^2-\frac{8}{729}\,{d_1}^2{d_2}^2{d_3}^2-\frac{8}{2187}\,{d_3}^3{d_2}^3-\frac{8}{729}\,{d_3}^3d_2{d_1}^2+\frac{2}{81}\,{d_3}^3d_2+\frac{4}{729}\,d_3d_1{d_2}^2+\frac{196}{2187}\,d_3d_1-\frac{100}{2187}\,d_3d_2+\frac{2}{27}\,{d_3}^2{d_1}^2-\frac{4}{729}\,d_3{d_1}^3-\frac{44}{2187}\,d_1d_2+\frac{28}{729}\,{d_3}^2{d_2}^2-\frac{2}{81}\,{d_3}^3d_1+\frac{8}{729}\,{d_3}^3{d_2}^2d_1+\frac{8}{2187}\,{d_3}^3{d_1}^3-\frac{82}{729}\,{d_3}^2d_2d_1-\frac{16}{729}-\frac{8}{2187}\,{d_3}^2{d_1}^4$
$h\,s\,s$	0

Table A.3: The cubic couplings for all of the fields in the action up to level 3 (continued).

$l\,m\,n$	$B_{lmn}(d_1,d_2,d_3)$
$h\ s\ y$	0
$h\ s\ z$	0
$h\ y\ y$	0
$h\ y\ z$	0
$h\ z\ z$	0
$u\ u\ u$	$\frac{1}{192}\sqrt{3}$
$u\ u\ v$	$-\frac{2375}{31104}\sqrt{3}$
$u\ u\ w$	$\frac{19}{31104}\sqrt{3}(4\,{d_1}^2-8\,d_1d_2+4\,{d_2}^2+4\,d_3d_1+4\,d_3d_2-8\,{d_3}^2-5)$
$u\ u\ f$	$\frac{19}{15552}\sqrt{3}(2\,d_2+4\,d_3{d_1}^2-8\,d_3d_2d_1+4\,d_3{d_2}^2-9\,d_3+2\,d_1)$
$u\ u\ o$	0
$u\ u\ \tilde{o}$	0
$u\ u\ p$	0
$u\ u\ q$	$\frac{19}{23328}\,(d_1-d_2)(2\,d_1-15\,d_3+2\,d_2)$
$u\ u\ r$	$\frac{1}{288}\,d_1-\frac{1}{288}\,d_2$
$u\ u\ s$	$-\frac{2375}{46656}\,d_1+\frac{2375}{46656}\,d_2$
$u\ u\ y$	$\frac{19}{46656}\,(d_1-d_2)(4\,{d_1}^2+4\,d_3d_1-8\,d_1d_2-37-8\,{d_3}^2+4\,{d_2}^2+4\,d_3d_2)$
$u\ u\ z$	$\frac{19}{23328}\,(d_1-d_2)(4\,{d_3}^2{d_1}^2-8\,{d_3}^2d_2d_1+6\,d_3d_1-22-27\,{d_3}^2+4\,{d_3}^2{d_2}^2+6\,d_3d_2)$
$u\ v\ v$	$\frac{104225}{62208}\sqrt{3}$
$u\ v\ w$	$-\frac{1375}{186624}\sqrt{3}(4\,{d_1}^2-8\,d_1d_2+4\,{d_2}^2+4\,d_3d_1+4\,d_3d_2-8\,{d_3}^2-5)$
$u\ v\ f$	$-\frac{1375}{93312}\sqrt{3}(2\,d_2+4\,d_3{d_1}^2-8\,d_3d_2d_1+4\,d_3{d_2}^2-9\,d_3+2\,d_1)$
$u\ v\ o$	$\frac{1250}{2187}$
$u\ v\ \tilde{o}$	0
$u\ v\ p$	$\frac{4400}{2187}$
$u\ v\ q$	$-\frac{1375}{139968}\,(d_1-d_2)(2\,d_1-15\,d_3+2\,d_2)$
$u\ v\ r$	$-\frac{2375}{46656}\,d_1+\frac{2375}{46656}\,d_2$
$u\ v\ s$	$\frac{104225}{93312}\,d_1-\frac{104225}{93312}\,d_2$
$u\ v\ y$	$-\frac{1375}{279936}\,(d_1-d_2)(4\,{d_1}^2+4\,d_3d_1-8\,d_1d_2-37-8\,{d_3}^2+4\,{d_2}^2+4\,d_3d_2)$
$u\ v\ z$	$-\frac{1375}{139968}\,(d_1-d_2)(4\,{d_3}^2{d_1}^2-8\,{d_3}^2d_2d_1+6\,d_3d_1-22-27\,{d_3}^2+4\,{d_3}^2{d_2}^2+6\,d_3d_2)$
$u\ w\ w$	$\frac{11}{186624}\sqrt{3}(80\,d_1{d_2}^3+537-16\,{d_3}^3d_2+80\,{d_3}^3d_1-236\,d_1d_2-80\,{d_3}^2d_2d_1-48\,{d_1}^2{d_2}^2-48\,{d_3}^2{d_1}^2-16\,d_2{d_1}^3+96\,{d_3}^2{d_2}^2+16\,{d_1}^4-16\,d_3{d_2}^3+532\,{d_3}^2-296\,{d_1}^2+532\,{d_2}^2+112\,d_3d_2{d_1}^2-32\,{d_2}^4-32\,{d_3}^4-236\,d_3d_1-3368\,d_3d_2-16\,d_3{d_1}^3-80\,d_3d_1{d_2}^2)$
$u\ w\ f$	$\frac{11}{93312}\sqrt{3}(-260\,d_3d_2d_1-32\,{d_3}^3d_2d_1-48\,d_3{d_2}^2{d_1}^2+80\,d_3{d_2}^3d_1-16\,d_3d_2{d_1}^3+80\,{d_3}^2{d_2}^2{d_1}^2-64\,{d_3}^2d_1{d_2}^2+8\,{d_1}^3-284\,{d_3}^2d_2-36\,{d_3}^3+572\,d_3{d_2}^2-328\,d_3{d_1}^2-266\,d_1-1546\,d_2+16\,{d_3}^3{d_2}^2-16\,{d_2}^3+813\,d_3+16\,{d_3}^3{d_1}^2+336\,{d_3}^2d_1-8\,d_1{d_2}^2+16\,{d_1}^2d_2+16\,{d_3}^2{d_2}^3-32\,{d_3}^2{d_1}^3-32\,d_3{d_2}^4+16\,d_3{d_1}^4)$
$u\ w\ o$	$-\frac{40}{2187}\,d_1d_2+\frac{80}{2187}\,{d_2}^2-\frac{40}{2187}\,{d_1}^2-\frac{40}{2187}\,{d_3}^2+\frac{80}{2187}\,d_3d_1-\frac{40}{2187}\,d_3d_2+\frac{50}{2187}$
$u\ w\ \tilde{o}$	0
$u\ w\ p$	0
$u\ w\ q$	$\frac{11}{17496}\,d_2{d_1}^3-\frac{605}{23328}\,{d_1}^2+\frac{7799}{69984}\,{d_2}^2-\frac{77}{4374}\,{d_3}^2+\frac{55}{11664}\,{d_3}^3d_2+\frac{539}{34992}\,d_3d_1{d_2}^2+\frac{6809}{139968}\,d_3d_1-\frac{31801}{139968}\,d_3d_2+\frac{22}{2187}\,{d_3}^2{d_1}^2-\frac{209}{34992}\,d_3{d_1}^3-\frac{253}{2187}\,d_1d_2+\frac{143}{34992}\,{d_3}^2{d_2}^2-\frac{55}{11664}\,{d_3}^3d_1-\frac{11}{5832}\,{d_1}^2{d_2}^2+\frac{11}{17496}\,d_3d_2{d_1}^2-\frac{55}{3888}\,{d_3}^2d_2d_1+\frac{11}{8748}\,{d_2}^4+\frac{11}{17496}\,{d_1}^4+\frac{176}{2187}-\frac{11}{17496}\,d_1{d_2}^3-\frac{22}{2187}\,d_3{d_2}^3$
$u\ w\ r$	$-\frac{19}{11664}\,{d_3}^2d_2+\frac{19}{3888}\,d_3d_2d_1-\frac{19}{3888}\,d_1{d_2}^2-\frac{19}{5832}\,d_3{d_1}^2-\frac{703}{46656}\,d_1-\frac{19}{11664}\,d_3{d_2}^2+\frac{19}{5832}\,{d_2}^3-\frac{1121}{46656}\,d_2+\frac{19}{11664}\,{d_1}^3+\frac{19}{1458}\,d_3+\frac{19}{11664}\,{d_3}^2d_1$
$u\ w\ s$	$\frac{50875}{279936}\,d_1+\frac{81125}{279936}\,d_2-\frac{1375}{8748}\,d_3-\frac{1375}{23328}\,d_3d_2d_1-\frac{1375}{69984}\,{d_3}^2d_1+\frac{1375}{69984}\,{d_3}^2d_2+\frac{1375}{69984}\,d_3{d_2}^2+\frac{1375}{34992}\,d_3{d_1}^2+\frac{1375}{23328}\,d_1{d_2}^2-\frac{1375}{69984}\,{d_1}^3-\frac{1375}{34992}\,{d_2}^3$
$u\ w\ y$	$-\frac{11429}{69984}\,d_3d_2d_1+\frac{55}{23328}\,{d_1}^2d_2-\frac{11}{2916}\,{d_3}^2{d_2}^3-\frac{11}{5832}\,{d_3}^2{d_1}^3+\frac{11}{2187}\,{d_1}^2{d_2}^3-\frac{77}{17496}\,d_1{d_2}^4-\frac{11}{8748}\,{d_2}^2{d_1}^3-\frac{11}{8748}\,{d_3}^4d_1+\frac{11}{8748}\,{d_3}^4d_2+\frac{11}{17496}\,d_3{d_2}^4+\frac{121}{17496}\,{d_3}^2d_1{d_2}^2-\frac{11}{2916}\,{d_3}^3d_2d_1-\frac{11}{1458}\,d_3{d_2}^2{d_1}^2+\frac{11}{4374}\,d_3{d_2}^3d_1+\frac{11}{2187}\,d_3d_2{d_1}^3-\frac{11}{8748}\,{d_3}^2d_2{d_1}^2+\frac{4631}{34992}\,d_3{d_2}^2+\frac{44}{729}\,d_1{d_2}^2+\frac{55}{69984}\,d_3{d_1}^2+\frac{2167}{69984}\,{d_3}^2d_1-\frac{253}{11664}\,{d_1}^3-\frac{319}{7776}\,{d_2}^3-\frac{11}{8748}\,{d_1}^4d_2-\frac{11}{17496}\,d_3{d_1}^4+\frac{26323}{279936}\,d_1-\frac{71731}{279936}\,d_2+\frac{11}{8748}\,{d_2}^5+\frac{11}{17496}\,{d_1}^5-\frac{22}{2187}\,{d_3}^3+\frac{649}{69984}\,{d_3}^2d_2+\frac{473}{8748}\,d_3+\frac{11}{17496}\,{d_3}^3{d_2}^2+\frac{55}{17496}\,{d_3}^3{d_1}^2$

Table A.3: The cubic couplings for all of the fields in the action up to level 3 (continued).

$l\,m\,n$	$B_{lmn}(d_1,d_2,d_3)$
$u\,w\,z$	$-\frac{715}{1944}\,d_3d_2d_1-\frac{2717}{34992}\,{d_3}^2{d_2}^3-\frac{385}{8748}\,{d_3}^2{d_1}^3-\frac{11}{1296}\,{d_3}^4d_1+\frac{11}{1296}\,{d_3}^4d_2+\frac{11}{2916}\,d_3{d_2}^4+\frac{671}{5832}\,{d_3}^2d_1{d_2}^2-\frac{1001}{11664}\,{d_3}^3d_2d_1-\frac{11}{1944}\,d_3{d_2}^2{d_1}^2-\frac{11}{5832}\,d_3{d_2}^3d_1+\frac{11}{5832}\,d_3d_2{d_1}^3+\frac{77}{11664}\,{d_3}^2d_2{d_1}^2+\frac{23881}{69984}\,d_3{d_2}^2+\frac{121}{5832}\,d_1{d_2}^2-\frac{4477}{69984}\,d_3{d_1}^2-\frac{11}{4374}\,{d_3}^2{d_1}^4d_2-\frac{77}{8748}\,{d_3}^2d_1{d_2}^4+\frac{11}{2916}\,{d_3}^4{d_2}^2d_1+\frac{77}{8748}\,{d_3}^3d_2{d_1}^3+\frac{22}{2187}\,{d_3}^2{d_2}^3{d_1}^2-\frac{11}{4374}\,{d_3}^2{d_2}^2{d_1}^3+\frac{55}{8748}\,{d_3}^3{d_2}^3d_1-\frac{11}{2916}\,{d_3}^4d_2{d_1}^2-\frac{11}{972}\,{d_3}^3{d_2}^2{d_1}^2+\frac{37477}{139968}\,{d_3}^2d_1-\frac{121}{17496}\,{d_1}^3-\frac{121}{8748}\,{d_2}^3+\frac{11}{5832}\,d_3{d_1}^4+\frac{1661}{69984}\,d_1-\frac{32285}{69984}\,d_2-\frac{11}{162}\,{d_3}^3-\frac{4741}{139968}\,{d_3}^2d_2+\frac{55}{243}\,d_3+\frac{143}{3888}\,{d_3}^3{d_2}^2+\frac{143}{2916}\,{d_3}^3{d_1}^2+\frac{11}{8748}\,{d_3}^4{d_1}^3-\frac{11}{8748}\,{d_3}^3{d_2}^4-\frac{11}{8748}\,{d_3}^4{d_2}^3-\frac{11}{4374}\,{d_3}^3{d_1}^4+\frac{11}{4374}\,{d_3}^2{d_2}^5+\frac{11}{8748}\,{d_3}^2{d_1}^5$
$u\,f\,f$	$\frac{11}{46656}\sqrt{3}(-768+320\,d_3d_1{d_2}^2-360\,d_3d_2{d_1}^2+64\,{d_1}^2{d_2}^2{d_3}^2-32\,{d_3}^2{d_2}^2d_1+16\,{d_3}^3d_2{d_1}^2+16\,d_3d_2{d_1}^4-32\,{d_3}^2{d_2}^3d_1-32\,{d_3}^2d_2{d_1}^3-32\,d_3{d_2}^2{d_1}^3+16\,d_3{d_2}^3{d_1}^2+1109\,d_3d_2-18\,{d_3}^2-270\,d_1d_2+4\,{d_1}^2-270\,d_3d_1+16\,{d_3}^3{d_2}^3+8\,{d_3}^2{d_1}^2-240\,{d_3}^2{d_2}^2+8\,{d_1}^2{d_2}^2-36\,d_3{d_2}^3+8\,d_3{d_1}^3-18\,{d_2}^2+8\,d_2{d_1}^3+320\,{d_3}^2d_2d_1-36\,{d_3}^3d_2)$
$u\,f\,o$	$-\frac{80}{2187}\,{d_3}^2d_2-\frac{40}{2187}\,d_3-\frac{80}{2187}\,{d_1}^2d_2+\frac{160}{2187}\,d_3d_2d_1-\frac{40}{2187}\,d_1+\frac{20}{243}\,d_2$
$u\,f\,\tilde{o}$	0
$u\,f\,p$	0
$u\,f\,q$	$-\frac{286}{2187}\,d_1+\frac{22}{81}\,d_2-\frac{451}{2187}\,d_3+\frac{55}{5832}\,d_3{d_2}^2{d_1}^2+\frac{7799}{69984}\,d_3d_2d_1+\frac{11}{4374}\,d_3{d_2}^3d_1-\frac{11}{8748}\,{d_3}^2{d_2}^3-\frac{11}{8748}\,{d_1}^2{d_2}^3+\frac{55}{5832}\,{d_3}^3{d_2}^2-\frac{55}{5832}\,{d_3}^3d_2d_1-\frac{209}{17496}\,d_3d_2{d_1}^3-\frac{55}{11664}\,{d_3}^2d_1-\frac{1067}{34992}\,{d_3}^2d_2-\frac{3641}{69984}\,d_3{d_2}^2-\frac{143}{34992}\,d_3{d_1}^2+\frac{517}{17496}\,d_1{d_2}^2+\frac{11}{17496}\,{d_1}^3+\frac{11}{8748}\,{d_1}^4d_2-\frac{1859}{34992}\,{d_1}^2d_2+\frac{44}{2187}\,{d_3}^2d_2{d_1}^2+\frac{11}{3888}\,{d_2}^3-\frac{55}{2916}\,{d_3}^2d_1{d_2}^2$
$u\,f\,r$	$\frac{19}{5832}\,d_2{d_1}^3-\frac{19}{5832}\,{d_3}^2{d_2}^2-\frac{19}{5832}\,{d_1}^2{d_2}^2-\frac{817}{23328}\,d_1d_2+\frac{95}{3888}\,d_3d_2+\frac{19}{5832}\,{d_3}^2d_2d_1+\frac{19}{2916}\,d_3d_1{d_2}^2-\frac{19}{729}+\frac{19}{2592}\,{d_2}^2-\frac{19}{2916}\,d_3d_2{d_1}^2+\frac{19}{11664}\,d_3d_1+\frac{19}{11664}\,{d_1}^2$
$u\,f\,s$	$-\frac{1375}{34992}\,d_2{d_1}^3-\frac{1375}{69984}\,{d_1}^2-\frac{1375}{15552}\,{d_2}^2-\frac{1375}{17496}\,d_3d_1{d_2}^2-\frac{1375}{69984}\,d_3d_1-\frac{6875}{23328}\,d_3d_2+\frac{59125}{139968}\,d_1d_2+\frac{1375}{34992}\,{d_3}^2{d_2}^2+\frac{1375}{4374}+\frac{1375}{34992}\,{d_1}^2{d_2}^2+\frac{1375}{17496}\,d_3d_2{d_1}^2-\frac{1375}{34992}\,{d_3}^2d_2d_1$
$u\,f\,y$	$-\frac{913}{17496}\,d_3d_1{d_2}^2-\frac{11}{4374}\,{d_3}^4d_2d_1+\frac{11}{4374}\,d_3d_1{d_2}^4-\frac{55}{34992}\,d_3d_2{d_1}^2-\frac{275}{1458}-\frac{11}{8748}\,{d_1}^2{d_2}^2{d_3}^2-\frac{11}{2187}\,{d_3}^3{d_2}^2d_1+\frac{55}{8748}\,{d_3}^3d_2{d_1}^2-\frac{11}{8748}\,d_3d_2{d_1}^4+\frac{55}{8748}\,{d_3}^2{d_2}^3d_1-\frac{11}{2916}\,{d_3}^2d_2{d_1}^3+\frac{11}{1458}\,d_3{d_2}^2{d_1}^3-\frac{77}{8748}\,d_3{d_2}^3{d_1}^2+\frac{15719}{69984}\,d_3d_2+\frac{44}{2187}\,{d_3}^2+\frac{37213}{139968}\,d_1d_2-\frac{2519}{69984}\,{d_1}^2-\frac{9559}{69984}\,d_3d_1-\frac{11}{8748}\,{d_3}^3{d_2}^3-\frac{11}{17496}\,{d_3}^2{d_1}^2-\frac{869}{34992}\,{d_3}^2{d_2}^2+\frac{1441}{17496}\,{d_1}^2{d_2}^2+\frac{1133}{34992}\,d_3{d_2}^3+\frac{11}{8748}\,d_3{d_1}^3-\frac{8261}{46656}\,{d_2}^2-\frac{11}{8748}\,{d_3}^3d_1-\frac{1375}{34992}\,d_1{d_2}^3-\frac{11}{2916}\,{d_1}^4{d_2}^2+\frac{11}{4374}\,{d_3}^4{d_2}^2-\frac{11}{8748}\,{d_1}^2{d_2}^4-\frac{11}{8748}\,{d_3}^2{d_2}^4+\frac{11}{8748}\,d_2{d_1}^5+\frac{11}{2916}\,{d_2}^3{d_1}^3+\frac{11}{17496}\,{d_1}^4-\frac{407}{8748}\,d_2{d_1}^3+\frac{2299}{34992}\,{d_3}^2d_2d_1-\frac{55}{2916}\,{d_3}^3d_2+\frac{11}{3888}\,{d_2}^4$
$u\,f\,z$	$\frac{1067}{17496}\,d_3d_1{d_2}^2-\frac{110}{243}-\frac{11}{648}\,{d_3}^4d_2d_1-\frac{4609}{34992}\,d_3d_2{d_1}^2+\frac{77}{486}\,{d_1}^2{d_2}^2{d_3}^2-\frac{110}{729}\,{d_3}^3{d_2}^2d_1+\frac{275}{2916}\,{d_3}^3d_2{d_1}^2+\frac{11}{2916}\,d_3d_2{d_1}^4-\frac{1243}{17496}\,{d_3}^2{d_2}^3d_1-\frac{275}{2916}\,{d_3}^2d_2{d_1}^3-\frac{11}{2916}\,d_3{d_2}^3{d_1}^2+\frac{11}{1458}\,{d_3}^2{d_2}^3{d_1}^3-\frac{11}{1458}\,{d_3}^4{d_2}^2{d_1}^2+\frac{11}{2187}\,{d_3}^3{d_2}^4d_1+\frac{11}{1458}\,{d_3}^4{d_2}^3d_1+\frac{11}{729}\,{d_3}^3{d_2}^2{d_1}^3-\frac{11}{729}\,{d_3}^3{d_2}^3{d_1}^2+\frac{11}{4374}\,{d_3}^4d_2{d_1}^3+\frac{11}{4374}\,{d_3}^2{d_2}^2{d_1}^5-\frac{11}{4374}\,{d_3}^2{d_2}^4{d_1}^2-\frac{11}{2187}\,{d_3}^3d_2{d_1}^4-\frac{11}{1458}\,{d_3}^2{d_1}^4{d_2}^2+\frac{13849}{17496}\,d_3d_2+\frac{11}{81}\,{d_3}^2+\frac{2387}{34992}\,d_1d_2-\frac{121}{17496}\,{d_1}^2-\frac{6985}{17496}\,d_3d_1+\frac{121}{2187}\,{d_3}^3{d_2}^3-\frac{781}{11664}\,{d_3}^2{d_1}^2-\frac{29293}{69984}\,{d_3}^2{d_2}^2+\frac{121}{8748}\,{d_1}^2{d_2}^2+\frac{11}{1296}\,d_3{d_2}^3+\frac{11}{5832}\,d_3{d_1}^3-\frac{121}{3888}\,{d_2}^2+\frac{11}{8748}\,{d_3}^2{d_1}^4+\frac{11}{8748}\,{d_3}^3{d_1}^3-\frac{11}{4374}\,{d_3}^4{d_2}^4-\frac{11}{1296}\,{d_3}^3d_1+\frac{11}{648}\,{d_3}^4{d_2}^2+\frac{11}{1944}\,{d_3}^2{d_2}^4-\frac{121}{8748}\,d_2{d_1}^3+\frac{47707}{69984}\,{d_3}^2d_2d_1-\frac{55}{432}\,{d_3}^3d_2$
$u\,o\,o$	$\frac{4304}{19683}\sqrt{3}$
$u\,o\,\tilde{o}$	0
$u\,o\,p$	0
$u\,o\,q$	$\frac{40}{19683}\sqrt{3}(d_1-d_2)(2\,d_1-15\,d_3+2\,d_2)$
$u\,o\,r$	0
$u\,o\,s$	$-\frac{2500}{19683}\sqrt{3}(d_1-d_2)$
$u\,o\,y$	$\frac{20}{19683}\sqrt{3}(d_1-d_2)(4\,{d_1}^2+4\,d_3d_1-8\,d_1d_2-37-8\,{d_3}^2+4\,{d_2}^2+4\,d_3d_2)$
$u\,o\,z$	$\frac{40}{19683}\sqrt{3}(d_1-d_2)(4\,{d_3}^2{d_1}^2-8\,{d_3}^2d_2d_1+6\,d_3d_1-22-27\,{d_3}^2+4\,{d_3}^2{d_2}^2+6\,d_3d_2)$
$u\,\tilde{o}\,\tilde{o}$	$\frac{6496}{19683}\sqrt{3}$
$u\,\tilde{o}\,p$	0
$u\,\tilde{o}\,q$	0
$u\,\tilde{o}\,r$	0
$u\,\tilde{o}\,s$	0
$u\,\tilde{o}\,y$	0
$u\,\tilde{o}\,z$	0
$u\,p\,p$	$-\frac{70400}{19683}\sqrt{3}$
$u\,p\,q$	0
$u\,p\,r$	0
$u\,p\,s$	$-\frac{8800}{19683}\sqrt{3}(d_1-d_2)$

Table A.3: The cubic couplings for all of the fields in the action up to level 3 (continued).

$l\,m\,n$	$B_{lmn}(d_1,d_2,d_3)$
$u\ p\ y$	0
$u\ p\ z$	0
$u\ q\ q$	$-\frac{11}{314928}\sqrt{3}(30\,d_1{d_2}^3+4096-30\,{d_3}^3d_2+30\,{d_3}^3d_1-504\,d_1d_2-225\,{d_3}^2d_2d_1-4\,{d_1}^2{d_2}^2-4\,{d_3}^2{d_1}^2-30\,d_2{d_1}^3+229\,{d_3}^2{d_2}^2+4\,{d_1}^4-30\,d_3{d_2}^3+1368\,{d_3}^2-912\,{d_1}^2+1368\,{d_2}^2+285\,d_3d_2d_1^2-504\,d_3d_1-8532\,d_3d_2-30\,d_3{d_1}^3-225\,d_3d_1{d_2}^2)$
$u\ q\ r$	$-\frac{19}{104976}\sqrt{3}(28\,d_2+15\,d_3d_2d_1+2\,{d_1}^3-15\,d_3{d_2}^2+24\,d_3-17\,{d_1}^2d_2+2\,{d_3}^2d_2-2\,{d_3}^2d_1-40\,d_1+15\,d_1{d_2}^2)$
$u\ q\ s$	$\frac{1375}{629856}\sqrt{3}(28\,d_2+15\,d_3d_2d_1+2\,{d_1}^3-15\,d_3{d_2}^2+24\,d_3-17\,{d_1}^2d_2+2\,{d_3}^2d_2-2\,{d_3}^2d_1-40\,d_1+15\,d_1{d_2}^2)$
$u\ q\ y$	$-\frac{11}{629856}\sqrt{3}(-120\,{d_3}^3d_2d_1-188\,d_3{d_2}^2{d_1}^2+240\,d_3{d_2}^3d_1+220\,{d_3}^2d_2{d_1}^2-144\,{d_3}^2d_1{d_2}^2-2139\,d_3d_2d_1-554\,{d_1}^3+336\,{d_2}^3-1610\,{d_3}^2d_2-16\,{d_3}^4d_2+8\,{d_1}^5+1925\,{d_1}^2d_2+840\,d_1-19020\,d_2+128\,{d_3}^3{d_2}^2-8\,{d_3}^3{d_1}^2-1536\,d_3{d_1}^2-52\,{d_3}^2{d_2}^3-24\,{d_3}^2{d_1}^3-188\,{d_1}^2{d_2}^3+60\,d_1{d_2}^4-84\,{d_1}^4d_2+204\,{d_2}^2{d_1}^3+16\,{d_3}^4d_1-60\,d_3{d_2}^4+8\,d_3{d_1}^4-192\,{d_3}^3+10760\,d_3+3579\,d_3{d_2}^2+1898\,{d_3}^2d_1-1707\,d_1{d_2}^2)$
$u\ q\ z$	$-\frac{11}{314928}\sqrt{3}(-981\,{d_3}^3d_2d_1-12\,d_3{d_2}^2{d_1}^2+90\,d_3{d_2}^3d_1+1845\,{d_3}^2d_2{d_1}^2-1557\,{d_3}^2d_1{d_2}^2-1842\,d_3d_2d_1-90\,d_3d_2{d_1}^3-84\,{d_3}^2{d_1}^4d_2+60\,{d_3}^2d_1{d_2}^4-24\,{d_3}^4{d_2}^2d_1+60\,{d_3}^3d_2{d_1}^3-188\,{d_3}^2{d_2}^3{d_1}^2+204\,{d_3}^2{d_2}^2{d_1}^3+180\,{d_3}^3{d_2}^3d_1+24\,{d_3}^4d_2{d_1}^2-180\,{d_3}^3{d_2}^2{d_1}^2-44\,{d_1}^3-5840\,{d_3}^2d_2-54\,{d_3}^4d_2+374\,{d_1}^2d_2-2832\,d_1-15528\,d_2+705\,{d_3}^3{d_2}^2+276\,{d_3}^3{d_1}^2-2736\,d_3{d_1}^2+246\,{d_3}^2{d_2}^3-534\,{d_3}^2{d_1}^3+54\,{d_3}^4d_1+12\,d_3{d_1}^4-8\,{d_3}^4{d_1}^3-60\,{d_3}^3{d_2}^4+8\,{d_3}^4{d_2}^3+8\,{d_3}^2{d_1}^5-648\,{d_3}^3+15216\,d_3+4434\,d_3{d_2}^2+6452\,{d_3}^2d_1-330\,d_1{d_2}^2)$
$u\ r\ r$	$-\frac{1}{1296}\sqrt{3}(-4-d_1d_2+{d_1}^2-d_3d_1+d_3d_2)$
$u\ r\ s$	$\frac{2375}{209952}\sqrt{3}(-4-d_1d_2+{d_1}^2-d_3d_1+d_3d_2)$
$u\ r\ y$	$-\frac{19}{209952}\sqrt{3}(-4\,d_1{d_2}^3+84-8\,{d_3}^3d_2+8\,{d_3}^3d_1+133\,d_1d_2+8\,{d_3}^2d_2d_1+12\,{d_1}^2{d_2}^2-12\,{d_3}^2{d_1}^2-12\,d_2{d_1}^3+4\,{d_3}^2{d_2}^2+4\,{d_1}^4+4\,d_3{d_2}^3+32\,{d_3}^2-85\,{d_1}^2-48\,{d_2}^2+12\,d_3d_2{d_1}^2-43\,d_3d_1+11\,d_3d_2-16\,d_3d_1{d_2}^2)$
$u\ r\ z$	$-\frac{19}{104976}\sqrt{3}(-4\,{d_3}^3{d_1}^3+24+12\,{d_3}^3d_2{d_1}^2-27\,{d_3}^3d_2+27\,{d_3}^3d_1+22\,d_1d_2+123\,{d_3}^2d_2d_1-81\,{d_3}^2{d_1}^2-42\,{d_3}^2{d_2}^2-4\,{d_3}^2{d_2}^3d_1+108\,{d_3}^2-22\,{d_1}^2-12\,{d_3}^3{d_2}^2d_1+4\,{d_3}^3{d_2}^3-98\,d_3d_1+50\,d_3d_2+4\,{d_3}^2{d_1}^4+6\,d_3{d_1}^3-6\,d_3d_1{d_2}^2-12\,{d_3}^2d_2{d_1}^3+12\,{d_1}^2{d_2}^2{d_3}^2)$
$u\ s\ s$	$-\frac{104225}{4199904}\sqrt{3}(-4-d_1d_2+{d_1}^2-d_3d_1+d_3d_2)$
$u\ s\ y$	$\frac{1375}{1259712}\sqrt{3}(-4\,d_1{d_2}^3+84-8\,{d_3}^3d_2+8\,{d_3}^3d_1+133\,d_1d_2+8\,{d_3}^2d_2d_1+12\,{d_1}^2{d_2}^2-12\,{d_3}^2{d_1}^2-12\,d_2{d_1}^3+4\,{d_3}^2{d_2}^2+4\,{d_1}^4+4\,d_3{d_2}^3+32\,{d_3}^2-85\,{d_1}^2-48\,{d_2}^2+12\,d_3d_2{d_1}^2-43\,d_3d_1+11\,d_3d_2-16\,d_3d_1{d_2}^2)$
$u\ s\ z$	$\frac{1375}{629856}\sqrt{3}(-4\,{d_3}^3{d_1}^3+24+12\,{d_3}^3d_2{d_1}^2-27\,{d_3}^3d_2+27\,{d_3}^3d_1+22\,d_1d_2+123\,{d_3}^2d_2d_1-81\,{d_3}^2{d_1}^2-42\,{d_3}^2{d_2}^2-4\,{d_3}^2{d_2}^3d_1+108\,{d_3}^2-22\,{d_1}^2-12\,{d_3}^3{d_2}^2d_1+4\,{d_3}^3{d_2}^3-98\,d_3d_1+50\,d_3d_2+4\,{d_3}^2{d_1}^4+6\,d_3{d_1}^3-6\,d_3d_1{d_2}^2-12\,{d_3}^2d_2{d_1}^3+12\,{d_1}^2{d_2}^2{d_3}^2)$
$u\ y\ y$	$-\frac{11}{1259712}\sqrt{3}(-38628-32\,{d_3}^2{d_1}^4+3944\,d_3d_1{d_2}^2+368\,{d_1}^2{d_2}^2{d_3}^2-160\,{d_3}^2d_2{d_1}^3-160\,{d_3}^3{d_2}^2d_1-160\,{d_3}^2{d_2}^3d_1-64\,{d_3}^3d_2{d_1}^2+128\,{d_3}^4d_2d_1+160\,d_3d_2{d_1}^4+128\,d_3d_1{d_2}^4-160\,d_3{d_2}^2{d_1}^3-64\,d_3{d_2}^3{d_1}^2-5688\,d_3d_2{d_1}^2+96\,{d_3}^3{d_2}^3+32633\,d_3d_2-5808\,{d_3}^2-6313\,d_1d_2+7993\,{d_1}^2-6313\,d_3d_1+1728\,{d_3}^2{d_1}^2-3752\,{d_3}^2{d_2}^2+384\,{d_3}^4+1728\,{d_1}^2{d_2}^2+340\,d_3{d_2}^3+384\,{d_2}^4-16\,{d_3}^4{d_2}^2+636\,d_3{d_1}^3-1876\,d_1{d_2}^3-5808\,{d_2}^2-32\,{d_1}^4{d_2}^2-32\,d_3{d_1}^5+32\,{d_3}^5d_1-112\,{d_1}^2{d_2}^4-16\,{d_3}^2{d_2}^4-32\,{d_3}^5d_2-32\,d_2{d_1}^5+32\,d_1{d_2}^5-32\,d_3{d_2}^5-112\,{d_3}^4{d_1}^2+128\,{d_2}^3{d_1}^3+128\,{d_3}^3{d_1}^3-1876\,{d_3}^3d_1+636\,d_2{d_1}^3+3944\,{d_3}^2d_2d_1+340\,{d_3}^3d_2-872\,{d_1}^4+16\,{d_1}^6)$
$u\ y\ z$	$-\frac{11}{629856}\sqrt{3}(-31224-904\,{d_3}^2{d_1}^4+5518\,d_3d_1{d_2}^2+1728\,{d_1}^2{d_2}^2{d_3}^2+636\,{d_3}^2d_2{d_1}^3+156\,{d_3}^3{d_2}^2d_1-1796\,{d_3}^2{d_2}^3d_1-2520\,{d_3}^3d_2{d_1}^2+128\,{d_3}^2{d_2}^3{d_1}^3+192\,{d_3}^4{d_2}^2{d_1}^2+96\,{d_3}^3{d_2}^4d_1-96\,{d_3}^4{d_2}^3d_1-112\,{d_3}^3{d_2}^2{d_1}^3-48\,{d_3}^3{d_2}^3{d_1}^2-160\,{d_3}^4d_2{d_1}^3-32\,{d_3}^2{d_2}^2{d_1}^5-112\,{d_3}^2{d_2}^4{d_1}^2-48\,{d_3}^5{d_2}^2d_1+144\,{d_3}^3d_2{d_1}^4+32\,{d_3}^2{d_2}^5d_1-32\,{d_3}^2{d_1}^4{d_2}^2+48\,{d_3}^5d_2{d_1}^2+1584\,{d_3}^4d_2d_1+24\,d_3d_2{d_1}^4+48\,d_3d_1{d_2}^4-72\,d_3{d_2}^2{d_1}^3-24\,d_3{d_2}^3{d_1}^2-4872\,d_3d_2{d_1}^2+668\,{d_3}^3{d_2}^3+38950\,d_3d_2-17340\,{d_3}^2-6478\,d_1d_2+1102\,{d_1}^2+1130\,d_3d_1+10749\,{d_3}^2{d_1}^2-10246\,{d_3}^2{d_2}^2+1296\,{d_3}^4-16\,{d_3}^5{d_1}^3+264\,{d_1}^2{d_2}^2-400\,d_3{d_2}^3-660\,{d_3}^4{d_2}^2-1398\,d_3{d_1}^3-176\,d_1{d_2}^3-192\,{d_2}^2+24\,d_3{d_1}^5+108\,{d_3}^5d_1+336\,{d_3}^2{d_2}^4-108\,{d_3}^5d_2-924\,{d_3}^4{d_1}^2+16\,{d_3}^5{d_2}^3-48\,{d_3}^3{d_1}^5-32\,{d_3}^3{d_2}^5+48\,{d_3}^4{d_1}^4+16\,{d_3}^2{d_1}^6+1696\,{d_3}^3{d_1}^3-9551\,{d_3}^3d_1+3817\,{d_3}^2d_2d_1+5087\,{d_3}^3d_2-88\,{d_1}^4+16\,{d_3}^4{d_2}^4)$

Table A.3: The cubic couplings for all of the fields in the action up to level 3 (continued).

$l\,m\,n$	$B_{lmn}(d_1,d_2,d_3)$
$u\ z\ z$	$-\frac{11}{314928}\sqrt{3}(-30864+24\,d_3{d_2}^2{d_1}^5-88\,{d_3}^2{d_1}^4+18186\,d_3d_1{d_2}^2+13485\,{d_1}^2{d_2}^2{d_3}^2-1338\,{d_3}^2d_2{d_1}^3-10745\,{d_3}^3{d_2}^2d_1-10745\,{d_3}^2{d_2}^3d_1+564\,{d_3}^3d_2{d_1}^2+144\,{d_3}^3{d_2}^3{d_1}^4+48\,{d_3}^5d_2{d_3}^3{d_1}^2-16\,{d_3}^2{d_2}^5{d_1}^3-144\,{d_3}^4{d_2}^3{d_1}^3+16\,{d_3}^2{d_2}^2{d_1}^6-48\,{d_3}^3{d_2}^2{d_1}^5+48\,{d_3}^4{d_2}^2{d_1}^4-16\,{d_3}^5{d_2}^2{d_1}^3+48\,{d_3}^3{d_2}^5{d_1}^2-48\,{d_3}^4{d_2}^5d_1+1656\,{d_3}^2{d_2}^3{d_1}^3-852\,{d_3}^4{d_2}^2{d_1}^2+1404\,{d_3}^3{d_2}^4d_1+1404\,{d_3}^4{d_2}^3d_1+1656\,{d_3}^3{d_2}^2{d_1}^3-2952\,{d_3}^3{d_2}^3{d_1}^2-24\,{d_3}^4d_2{d_1}^3+24\,{d_3}^2d_2{d_1}^5-852\,{d_3}^2{d_2}^4{d_1}^2+108\,{d_3}^5{d_2}^2d_1+108\,{d_3}^2{d_2}^5d_1-936\,{d_3}^2{d_1}^4{d_2}^2+144\,{d_3}^4{d_2}^4{d_1}^2-48\,{d_3}^2{d_2}^3{d_1}^5+48\,{d_3}^2{d_2}^4{d_1}^4-48\,{d_3}^5{d_2}^4d_1-144\,{d_3}^3{d_2}^4{d_1}^3-24\,d_3d_2{d_1}^4{d_1}^3+162\,{d_3}^4d_2d_1+36\,d_3d_2d_1{}^4+162\,d_3d_1{d_2}^4-1338\,d_3{d_2}^2{d_1}^3+564\,d_3{d_2}^3{d_1}^2-8208\,d_3d_2{d_1}^2+6925\,{d_3}^3{d_2}^3+54916\,d_3d_2-648\,{d_3}^2-8980\,d_1d_2+484\,{d_1}^2-8980\,d_3d_1+1014\,{d_3}^2{d_1}^2-33084\,{d_3}^2{d_2}^2+1014\,{d_1}^2{d_2}^2-1350\,d_3{d_2}^3+1134\,{d_3}^4{d_2}^2-132\,d_3{d_1}^3-594\,d_1{d_2}^3-648\,{d_2}^2-88\,{d_1}^4{d_2}^2+1134\,{d_3}^2{d_2}^4+88\,{d_2}^3{d_1}^3-108\,{d_3}^5{d_2}^3-108\,{d_3}^3{d_2}^5+88\,{d_3}^3{d_1}^3-594\,{d_3}^3d_1-132\,d_2{d_1}^3+18186\,{d_3}^2{d_2}d_1-1350\,{d_3}^3d_2+16\,{d_3}^5{d_2}^5-528\,{d_3}^4{d_2}^4)$
$v\ v\ v$	$-\frac{219775}{13824}\sqrt{3}$
$v\ v\ w$	$\frac{9475}{124416}\sqrt{3}(4\,{d_1}^2-8\,d_1d_2+4\,{d_2}^2+4\,d_3d_1+4\,d_3d_2-8\,{d_3}^2-5)$
$v\ v\ f$	$\frac{9475}{62208}\sqrt{3}(2\,d_2+4\,d_3{d_1}^2-8\,d_3d_2d_1+4\,d_3{d_2}^2-9\,d_3+2\,d_1)$
$v\ v\ o$	0
$v\ v\ \tilde{o}$	0
$v\ v\ p$	0
$v\ v\ q$	$\frac{9475}{93312}(d_1-d_2)(2\,d_1-15\,d_3+2\,d_2)$
$v\ v\ r$	$\frac{104225}{93312}\,d_1-\frac{104225}{93312}\,d_2$
$v\ v\ s$	$-\frac{219775}{20736}\,d_1+\frac{219775}{20736}\,d_2$
$v\ v\ y$	$\frac{9475}{186624}(d_1-d_2)(4\,{d_1}^2+4\,d_3d_1-8\,d_1d_2-37-8\,{d_3}^2+4\,{d_2}^2+4\,d_3d_2)$
$v\ v\ z$	$\frac{9475}{93312}(d_1-d_2)(4\,{d_3}^2{d_1}^2-8\,{d_3}^2d_2d_1+6\,d_3d_1-22-27\,{d_3}^2+4\,{d_3}^2{d_2}^2+6\,d_3d_2)$
$v\,w\,w$	$-\frac{125}{373248}\sqrt{3}(80\,d_1{d_2}^3+537-16\,{d_3}^3d_2+80\,{d_3}^3d_1-236\,d_1d_2-80\,{d_3}^2d_2d_1-48\,{d_1}^2{d_2}^2-48\,{d_3}^2{d_1}^2-16\,d_2{d_1}^3+96\,{d_3}^2{d_2}^2+16\,{d_1}^4-16\,d_3{d_2}^3+532\,{d_3}^2-296\,{d_1}^2+532\,{d_2}^2+112\,d_3d_2{d_1}^2-32\,{d_2}^4-32\,{d_3}^4-236\,d_3d_1-3368\,d_3d_2-16\,d_3{d_1}^3-80\,d_3d_1{d_2}^2)$
$v\,w\,f$	$-\frac{125}{186624}\sqrt{3}(-32\,{d_3}^3d_2d_1-48\,d_3{d_2}^2{d_1}^2-260\,d_3d_2d_1+80\,d_3{d_2}^3d_1-16\,d_3d_2{d_1}^3+80\,{d_3}^2d_2{d_1}^2-64\,{d_3}^2d_1{d_2}^2-16\,{d_2}^3-36\,{d_3}^3+572\,d_3{d_2}^2-328\,d_3{d_1}^2-8\,d_1{d_2}^2+16\,{d_1}^2d_2+16\,{d_3}^2{d_2}^3-32\,{d_3}^2{d_1}^3-32\,d_3{d_2}^4+16\,d_3{d_1}^4-284\,{d_3}^2d_2+16\,{d_3}^3{d_2}^2+16\,{d_3}^3{d_1}^2+336\,{d_3}^2d_1+8\,{d_1}^3-266\,d_1-1546\,d_2+813\,d_3)$
$v\,w\,o$	0
$v\,w\,\tilde{o}$	0
$v\,w\,p$	$-\frac{800}{2187}\,{d_1}^2+\frac{1600}{2187}\,{d_2}^2-\frac{800}{2187}\,{d_3}^2+\frac{1600}{2187}\,d_3d_1-\frac{800}{2187}\,d_3d_2-\frac{800}{2187}\,d_1d_2+\frac{1000}{2187}$
$v\,w\,q$	$-\frac{125}{34992}\,d_2{d_1}^3+\frac{6875}{46656}\,{d_1}^2-\frac{88625}{139968}\,{d_2}^2+\frac{875}{8748}\,{d_3}^2-\frac{625}{23328}\,{d_3}^3d_2-\frac{6125}{69984}\,d_3d_1{d_2}^2-\frac{77375}{279936}\,d_3d_1+\frac{361375}{279936}\,d_3d_2-\frac{125}{2187}\,{d_3}^2{d_1}^2+\frac{2375}{69984}\,d_3{d_1}^3+\frac{2875}{4374}\,d_1d_2-\frac{1625}{69984}\,{d_3}^2{d_2}^2+\frac{625}{23328}\,{d_3}^3d_1+\frac{125}{11664}\,{d_1}^2{d_2}^2-\frac{125}{34992}\,d_3d_2{d_1}^2+\frac{625}{7776}\,{d_3}^2d_2d_1-\frac{125}{17496}\,{d_2}^4-\frac{125}{34992}\,{d_1}^4+\frac{125}{34992}\,d_1{d_2}^3+\frac{125}{2187}\,d_3{d_2}^3-\frac{1000}{2187}$
$v\,w\,r$	$\frac{50875}{279936}\,d_1+\frac{81125}{279936}\,d_2-\frac{1375}{8748}\,d_3-\frac{1375}{23328}\,d_3d_2d_1-\frac{1375}{69984}\,{d_3}^2d_1+\frac{1375}{69984}\,{d_3}^2d_2+\frac{1375}{69984}\,d_3{d_2}^2+\frac{1375}{34992}\,d_3{d_1}^2+\frac{1375}{23328}\,d_1{d_2}^2-\frac{1375}{69984}\,{d_1}^3-\frac{1375}{34992}\,{d_2}^3$
$v\,w\,s$	$-\frac{350575}{186624}\,d_1-\frac{559025}{186624}\,d_2+\frac{9475}{5832}\,d_3+\frac{9475}{15552}\,d_3d_2d_1+\frac{9475}{46656}\,{d_3}^2d_1-\frac{9475}{46656}\,{d_3}^2d_2-\frac{9475}{46656}\,d_3{d_2}^2-\frac{9475}{23328}\,d_3{d_1}^2-\frac{9475}{15552}\,d_1{d_2}^2+\frac{9475}{46656}\,{d_1}^3+\frac{9475}{23328}\,{d_2}^3$
$v\,w\,y$	$\frac{125}{5832}\,{d_3}^3d_2d_1+\frac{125}{2916}\,d_3{d_2}^2{d_1}^2+\frac{129875}{139968}\,d_3d_2d_1-\frac{125}{8748}\,d_3{d_2}^3d_1-\frac{125}{4374}\,d_3d_2{d_1}^3+\frac{125}{17496}\,{d_3}^2{d_2}d_1{}^2-\frac{1375}{34992}\,{d_3}^2{d_1}{d_2}^2+\frac{3625}{15552}\,{d_2}^3+\frac{125}{2187}\,{d_3}^3-\frac{52625}{69984}\,d_3{d_2}^2-\frac{625}{139968}\,d_3{d_1}^2-\frac{250}{729}\,d_1{d_2}^2-\frac{625}{46656}\,{d_1}^2d_2+\frac{125}{5832}\,{d_3}^2{d_2}^3+\frac{125}{11664}\,{d_3}^2{d_1}^3-\frac{125}{34992}\,d_3{d_2}^4+\frac{125}{34992}\,d_3{d_1}^4-\frac{7375}{139968}\,{d_3}^2d_2-\frac{125}{34992}\,{d_3}^3{d_2}^2-\frac{625}{34992}\,{d_3}^3{d_1}^2-\frac{24625}{139968}\,{d_3}^2d_1-\frac{125}{4374}\,{d_1}^2{d_2}^3+\frac{875}{34992}\,d_1{d_2}^4+\frac{125}{17496}\,{d_1}^4d_2+\frac{125}{17496}\,{d_2}^2{d_1}^3+\frac{125}{17496}\,{d_3}^4d_1-\frac{125}{17496}\,{d_3}^4d_2+\frac{2875}{23328}\,{d_1}^3-\frac{299125}{559872}\,d_1+\frac{815125}{559872}\,d_2-\frac{125}{17496}\,{d_2}^5-\frac{125}{34992}\,{d_1}^5-\frac{5375}{17496}\,d_3$
$v\,w\,z$	$\frac{11375}{23328}\,{d_3}^3d_2d_1+\frac{125}{3888}\,d_3{d_2}^2{d_1}^2+\frac{8125}{3888}\,d_3d_2d_1+\frac{125}{11664}\,d_3{d_2}^3d_1-\frac{125}{11664}\,d_3d_2{d_1}^3-\frac{875}{23328}\,{d_3}^2d_2{d_1}^2-\frac{7625}{11664}\,{d_3}^2d_1{d_2}^2+\frac{1375}{17496}\,{d_2}^3+\frac{125}{8748}\,{d_3}^2{d_1}^4d_2+\frac{875}{17496}\,{d_3}^2d_1{d_2}^4-\frac{125}{5832}\,{d_3}^4{d_2}^2d_1-\frac{875}{17496}\,{d_3}^3d_2{d_1}^3-\frac{125}{2187}\,{d_3}^2{d_2}^3{d_1}^2+\frac{125}{8748}\,{d_3}^2{d_2}^2{d_1}^3-\frac{625}{17496}\,{d_3}^3{d_2}^3d_1+\frac{125}{5832}\,{d_3}^4d_2{d_1}^2+\frac{125}{1944}\,{d_3}^3{d_2}^2{d_1}^2+\frac{125}{324}\,{d_3}^3-\frac{271375}{139968}\,d_3{d_2}^2+\frac{50875}{139968}\,d_3{d_1}^2-\frac{1375}{11664}\,d_1{d_2}^2+\frac{30875}{69984}\,{d_3}^2{d_2}^3+\frac{4375}{17496}\,{d_3}^2{d_1}^3-\frac{125}{5832}\,d_3{d_2}^4-\frac{125}{11664}\,d_3{d_1}^4+\frac{53875}{279936}\,{d_3}^2d_2-\frac{1625}{7776}\,{d_3}^3{d_2}^2-\frac{1625}{5832}\,{d_3}^3{d_1}^2-\frac{425875}{279936}\,{d_3}^2d_1+\frac{125}{2592}\,{d_3}^4d_1-\frac{125}{2592}\,{d_3}^4d_2+\frac{1375}{34992}\,{d_1}^3-\frac{125}{17496}\,{d_3}^4{d_1}^3-\frac{18875}{139968}\,d_1+\frac{366875}{139968}\,d_2+\frac{125}{17496}\,{d_3}^3{d_2}^4+\frac{125}{17496}\,{d_3}^4{d_2}^3+\frac{125}{8748}\,{d_3}^3{d_1}^4-\frac{125}{8748}\,{d_3}^2{d_2}^5-\frac{125}{17496}\,{d_3}^2{d_1}^5-\frac{625}{486}\,d_3$

Table A.3: The cubic couplings for all of the fields in the action up to level 3 (continued).

$l\,m\,n$	$B_{lmn}(d_1,d_2,d_3)$
$v\ f\ f$	$-\frac{125}{93312}\sqrt{3}(-768+64\,{d_1}^2{d_2}^2{d_3}^2-32\,{d_3}^3{d_2}^2d_1+16\,{d_3}^3d_2{d_1}^2+16\,d_3d_2{d_1}^4-32\,{d_3}^2{d_2}^3d_1-32\,{d_3}^2d_2{d_1}^3-32\,d_3{d_2}^2{d_1}^3+16\,d_3{d_2}^3{d_1}^2+320\,d_3d_1{d_2}^2-360\,d_3d_2{d_1}^2+16\,{d_3}^3{d_2}^3+1109\,d_3d_2-18\,{d_3}^2-270\,d_1d_2+4\,{d_1}^2-270\,d_3d_1+8\,{d_3}^2{d_1}^2-240\,{d_3}^2{d_2}^2+8\,{d_1}^2{d_2}^2-36\,d_3{d_2}^3+8\,d_3{d_1}^3+320\,{d_3}^2d_2d_1-36\,{d_3}^3d_2)$
$v\ f\ o$	0
$v\ f\ \tilde{o}$	0
$v\ f\ p$	$-\frac{800}{2187}\,d_1+\frac{400}{243}\,d_2-\frac{800}{2187}\,d_3+\frac{3200}{2187}\,d_3d_2d_1-\frac{1600}{2187}\,{d_3}^2d_2-\frac{1600}{2187}\,{d_1}^2d_2$
$v\ f\ q$	$\frac{1625}{2187}\,d_1-\frac{125}{81}\,d_2+\frac{5125}{4374}\,d_3-\frac{625}{11664}\,d_3{d_2}^2{d_1}^2-\frac{88625}{139968}\,d_3d_2d_1-\frac{125}{8748}\,d_3{d_2}^3d_1+\frac{125}{17496}\,{d_3}^2{d_2}^3+\frac{125}{17496}\,{d_1}^2{d_2}^3-\frac{625}{11664}\,{d_3}^3{d_2}^2+\frac{625}{11664}\,{d_3}^3d_2d_1+\frac{2375}{34992}\,d_3d_2{d_1}^3+\frac{625}{23328}\,{d_3}^2d_1+\frac{12125}{69984}\,{d_3}^2d_2+\frac{41375}{139968}\,d_3{d_2}^2+\frac{1625}{69984}\,d_3{d_1}^2-\frac{5875}{34992}\,d_1{d_2}^2-\frac{125}{34992}\,{d_1}^3-\frac{125}{17496}\,{d_1}^4d_2+\frac{21125}{69984}\,{d_1}^2d_2-\frac{250}{2187}\,{d_3}^2d_1{d_2}^2-\frac{125}{7776}\,{d_2}^3+\frac{625}{5832}\,{d_3}^2{d_1}^2d_2$
$v\ f\ r$	$-\frac{1375}{34992}\,d_2{d_1}^3-\frac{1375}{69984}\,{d_1}^2-\frac{1375}{15552}\,{d_2}^2-\frac{1375}{17496}\,d_3d_1{d_2}^2-\frac{1375}{69984}\,d_3d_1-\frac{6875}{23328}\,d_3d_2+\frac{59125}{139968}\,d_1d_2+\frac{1375}{34992}\,{d_3}^2{d_2}^2+\frac{1375}{4374}+\frac{1375}{34992}\,{d_1}^2{d_2}^2+\frac{1375}{17496}\,d_3d_2{d_1}^2-\frac{1375}{34992}\,{d_3}^2d_2d_1$
$v\ f\ s$	$\frac{9475}{23328}\,d_2{d_1}^3+\frac{9475}{46656}\,{d_1}^2+\frac{9475}{10368}\,{d_2}^2+\frac{9475}{11664}\,d_3d_1{d_2}^2-\frac{9475}{2916}+\frac{9475}{46656}\,d_3d_1+\frac{47375}{15552}\,d_3d_2-\frac{407425}{93312}\,d_1d_2-\frac{9475}{23328}\,{d_3}^2{d_2}^2-\frac{9475}{23328}\,{d_1}^2{d_2}^2-\frac{9475}{11664}\,d_3d_2{d_1}^2+\frac{9475}{23328}\,{d_3}^2d_2d_1$
$v\ f\ y$	$-\frac{125}{17496}\,{d_1}^2{d_2}^2{d_3}^2+\frac{125}{4374}\,{d_3}^3{d_2}^2d_1-\frac{625}{17496}\,{d_3}^3d_2{d_1}^2+\frac{125}{17496}\,d_3d_2{d_1}^4-\frac{625}{17496}\,{d_3}^2{d_2}^3d_1+\frac{125}{5832}\,{d_3}^2d_2{d_1}^3-\frac{125}{2916}\,d_3{d_2}^2{d_1}^3+\frac{875}{17496}\,d_3{d_2}^3{d_1}^2+\frac{10375}{34992}\,d_3d_1{d_2}^2+\frac{625}{69984}\,d_3d_2{d_1}^2+\frac{125}{17496}\,{d_3}^3{d_2}^3+\frac{3125}{2916}-\frac{178625}{139968}\,d_3d_2-\frac{250}{2187}\,{d_3}^2-\frac{422875}{279936}\,d_1d_2+\frac{28625}{139968}\,{d_1}^2+\frac{108625}{139968}\,d_3d_1+\frac{125}{34992}\,{d_3}^2{d_1}^2-\frac{125}{8748}\,d_3d_1{d_2}^4+\frac{9875}{69984}\,{d_3}^2{d_2}^2+\frac{125}{8748}\,{d_3}^4d_2d_1-\frac{16375}{34992}\,{d_1}^2{d_2}^2-\frac{12875}{69984}\,d_3{d_2}^3-\frac{125}{7776}\,{d_2}^4-\frac{125}{17496}\,d_3{d_1}^3+\frac{15625}{69984}\,d_1{d_2}^3+\frac{93875}{93312}\,{d_2}^2-\frac{125}{8748}\,{d_3}^4{d_2}^2+\frac{125}{17496}\,{d_3}^3d_1+\frac{4625}{17496}\,d_2{d_1}^3-\frac{26125}{69984}\,{d_3}^2d_2d_1+\frac{625}{5832}\,{d_3}^3d_2+\frac{125}{5832}\,{d_1}^4{d_2}^2+\frac{125}{17496}\,{d_1}^2{d_2}^4+\frac{125}{17496}\,{d_3}^2{d_2}^4-\frac{125}{17496}\,d_2{d_1}^5-\frac{125}{5832}\,{d_2}^3{d_1}^3-\frac{125}{34992}\,{d_1}^4$
$v\ f\ z$	$-\frac{875}{972}\,{d_1}^2{d_2}^2{d_3}^2+\frac{625}{729}\,{d_3}^3{d_2}^2d_1-\frac{3125}{5832}\,{d_3}^3d_2{d_1}^2-\frac{125}{5832}\,d_3d_2{d_1}^4+\frac{14125}{34992}\,{d_3}^2{d_2}^3d_1+\frac{3125}{5832}\,{d_3}^2d_2{d_1}^3+\frac{125}{5832}\,d_3{d_2}^3{d_1}^2-\frac{12125}{34992}\,d_3d_1{d_2}^2-\frac{125}{2916}\,{d_3}^2{d_2}^3{d_1}^3+\frac{125}{2916}\,{d_3}^4{d_2}^2{d_1}^2-\frac{125}{4374}\,{d_3}^3{d_2}^4d_1-\frac{125}{2916}\,{d_3}^4{d_2}^3d_1-\frac{125}{1458}\,{d_3}^3{d_2}^2{d_1}^3+\frac{125}{1458}\,{d_3}^3{d_2}^3{d_1}^2-\frac{125}{8748}\,{d_3}^4d_2{d_1}^3-\frac{125}{8748}\,{d_3}^2d_2{d_1}^5+\frac{125}{8748}\,{d_3}^2{d_2}^4{d_1}^2+\frac{125}{4374}\,{d_3}^3d_2{d_1}^4+\frac{125}{2916}\,{d_3}^2{d_1}^4{d_2}^2+\frac{52375}{69984}\,d_3d_2{d_1}^2-\frac{1375}{4374}\,{d_3}^3{d_2}^3-\frac{157375}{34992}\,d_3d_2-\frac{125}{162}\,{d_3}^2-\frac{27125}{69984}\,d_1d_2+\frac{1375}{34992}\,{d_1}^2+\frac{79375}{34992}\,d_3d_1+\frac{625}{243}+\frac{8875}{23328}\,{d_3}^2{d_1}^2+\frac{332875}{139968}\,{d_3}^2{d_2}^2+\frac{125}{1296}\,{d_3}^4d_2d_1+\frac{125}{8748}\,{d_3}^4{d_2}^4-\frac{1375}{17496}\,{d_1}^2{d_2}^2-\frac{125}{2592}\,d_3{d_2}^3-\frac{125}{11664}\,d_3{d_1}^3+\frac{1375}{7776}\,{d_2}^2-\frac{125}{1296}\,{d_3}^4{d_2}^2+\frac{125}{2592}\,{d_3}^3d_1+\frac{1375}{17496}\,d_2{d_1}^3-\frac{542125}{139968}\,{d_3}^2d_2d_1+\frac{625}{864}\,{d_3}^3d_2-\frac{125}{3888}\,{d_3}^2{d_2}^4-\frac{125}{17496}\,{d_3}^2{d_1}^4-\frac{125}{17496}\,{d_3}^3{d_1}^3$
$v\ o\ o$	$-\frac{23000}{19683}\sqrt{3}$
$v\ o\ \tilde{o}$	0
$v\ o\ p$	0
$v\ o\ q$	0
$v\ o\ r$	$\frac{2500}{19683}\sqrt{3}(d_1-d_2)$
$v\ o\ s$	0
$v\ o\ y$	0
$v\ o\ z$	0
$v\ \tilde{o}\ \tilde{o}$	$-\frac{2000}{19683}\sqrt{3}$
$v\ \tilde{o}\ p$	0
$v\ \tilde{o}\ q$	0
$v\ \tilde{o}\ r$	0
$v\ \tilde{o}\ s$	0
$v\ \tilde{o}\ y$	0
$v\ \tilde{o}\ z$	0
$v\ p\ p$	$\frac{348800}{19683}\sqrt{3}$
$v\ p\ q$	$\frac{800}{19683}\sqrt{3}(d_1-d_2)(2\,d_1-15\,d_3+2\,d_2)$
$v\ p\ r$	$\frac{8800}{19683}\sqrt{3}(d_1-d_2)$
$v\ p\ s$	0
$v\ p\ y$	$\frac{400}{19683}\sqrt{3}(d_1-d_2)(4\,{d_1}^2+4\,d_3d_1-8\,d_1d_2-37-8\,{d_3}^2+4\,{d_2}^2+4\,d_3d_2)$
$v\ p\ z$	$\frac{800}{19683}\sqrt{3}(d_1-d_2)(4\,{d_3}^2{d_1}^2-8\,{d_3}^2d_2d_1+6\,d_3d_1-22-27\,{d_3}^2+4\,{d_3}^2{d_2}^2+6\,d_3d_2)$
$v\ q\ q$	$\frac{125}{629856}\sqrt{3}(30\,d_1{d_2}^3+4096-30\,{d_3}^3d_2+30\,{d_3}^3d_1-504\,d_1d_2-225\,{d_3}^2d_2d_1-4\,{d_1}^2{d_2}^2-4\,{d_3}^2{d_1}^2-30\,d_2{d_1}^3+229\,{d_3}^2{d_2}^2+4\,{d_1}^4-30\,d_3{d_2}^3+1368\,{d_3}^2-912\,{d_1}^2+1368\,{d_2}^2+285\,d_3d_2{d_1}^2-504\,d_3d_1-8532\,d_3d_2-30\,d_3{d_1}^3-225\,d_3d_1{d_2}^2)$
$v\ q\ r$	$\frac{1375}{629856}\sqrt{3}(28\,d_2+15\,d_3d_2d_1+2\,{d_1}^3-15\,d_3{d_2}^2+24\,d_3-17\,{d_1}^2d_2+2\,{d_3}^2d_2-2\,{d_3}^2d_1-40\,d_1+15\,d_1{d_2}^2)$

Table A.3: The cubic couplings for all of the fields in the action up to level 3 (continued).

$l\,m\,n$	$B_{lmn}(d_1,d_2,d_3)$
$v\ q\ s$	$-\frac{9475}{419904}\sqrt{3}(28\,d_2+15\,d_3d_2d_1+2\,{d_1}^3-15\,d_3{d_2}^2+24\,d_3-17\,{d_1}^2d_2+2\,{d_3}^2d_2-2\,{d_3}^2d_1-40\,d_1+15\,d_1{d_2}^2)$
$v\ q\ y$	$\frac{125}{1259712}\sqrt{3}(-2139\,d_3d_2d_1+3579\,d_3{d_2}^2-120\,{d_3}^3d_2d_1-188\,d_3{d_2}^2{d_1}^2+240\,d_3{d_2}^3d_1+336\,{d_2}^3-1610\,{d_3}^2d_2+1898\,{d_3}^2d_1-1707\,d_1{d_2}^2-554\,{d_1}^3+1925\,{d_1}^2d_2+128\,{d_3}^3{d_2}^2-8\,{d_3}^3{d_1}^2-1536\,d_3{d_1}^2-52\,{d_3}^2{d_2}^3-24\,{d_3}^2{d_1}^3-188\,{d_1}^2{d_2}^3+60\,d_1{d_2}^4-84\,{d_1}^4d_2+204\,{d_2}^2{d_1}^3+16\,{d_3}^4d_1-16\,{d_3}^4d_2+220\,{d_3}^2d_2{d_1}^2+840\,d_1-19020\,d_2-60\,d_3{d_2}^4+8\,d_3{d_1}^4-144\,{d_3}^2{d_1}{d_2}^2+8\,{d_1}^5-192\,{d_3}^3+10760\,d_3)$
$v\ q\ z$	$\frac{125}{629856}\sqrt{3}(-1842\,d_3d_2d_1-90\,d_3d_2{d_1}^3-84\,{d_3}^2{d_1}^4d_2+60\,{d_3}^2d_1{d_2}^4-24\,{d_3}^4{d_2}^2d_1+60\,{d_3}^3d_2{d_1}^3-188\,{d_3}^2{d_2}^3{d_1}^2+204\,{d_3}^2{d_2}^2{d_1}^3+180\,{d_3}^3{d_2}^3d_1+24\,{d_3}^4d_2{d_1}^2-180\,{d_3}^3{d_2}^2{d_1}^2+4434\,d_3{d_2}^2-981\,{d_3}^3d_2d_1-12\,d_3{d_2}^2{d_1}^2+90\,d_3{d_2}^3d_1-5840\,{d_3}^2d_2+6452\,{d_3}^2d_1-330\,d_1{d_2}^2-44\,{d_1}^3+374\,{d_1}^2d_2+705\,{d_3}^3{d_2}^2+276\,{d_3}^3{d_1}^2-2736\,d_3{d_1}^2+246\,{d_3}^2{d_2}^3-534\,{d_3}^2{d_1}^3+54\,{d_3}^4d_1-54\,{d_3}^4d_2+1845\,{d_3}^2d_2{d_1}^2-8\,{d_3}^4{d_1}^3-60\,{d_3}^3{d_2}^4+8\,{d_3}^4{d_2}^3+8\,{d_3}^2{d_1}^5-2832\,d_1-15528\,d_2+12\,d_3{d_1}^4-1557\,{d_3}^2{d_1}{d_2}^2-648\,{d_3}^3+15216\,d_3)$
$v\ r\ r$	$\frac{2375}{209952}\sqrt{3}(-4-d_1d_2+{d_1}^2-d_3d_1+d_3d_2)$
$v\ r\ s$	$-\frac{104225}{419904}\sqrt{3}(-4-d_1d_2+{d_1}^2-d_3d_1+d_3d_2)$
$v\ r\ y$	$\frac{1375}{1259712}\sqrt{3}(-4\,d_1{d_2}^3+84-8\,{d_3}^3d_2+8\,{d_3}^3d_1+133\,d_1d_2+8\,{d_3}^2d_2d_1+12\,{d_1}^2{d_2}^2-12\,{d_3}^2{d_1}^2-12\,d_2{d_1}^3+4\,{d_3}^2{d_2}^2+4\,{d_1}^4+4\,d_3{d_2}^3+32\,{d_3}^2-85\,{d_1}^2-48\,{d_2}^2+12\,d_3d_2{d_1}^2-43\,d_3d_1+11\,d_3d_2-16\,d_3d_1{d_2}^2)$
$v\ r\ z$	$\frac{1375}{629856}\sqrt{3}(-4\,{d_3}^3{d_1}^3+24+12\,{d_3}^3d_2{d_1}^2-27\,{d_3}^3d_2+27\,{d_3}^3d_1+22\,d_1d_2+123\,{d_3}^2d_2d_1-81\,{d_3}^2{d_1}^2-42\,{d_3}^2{d_2}^2-4\,{d_3}^2{d_2}^3d_1+108\,{d_3}^2-22\,{d_1}^2-12\,{d_3}^3{d_2}^2d_1+4\,{d_3}^3{d_2}^3-98\,d_3d_1+50\,d_3d_2+4\,{d_3}^2{d_1}^4+6\,d_3{d_1}^3-6\,d_3d_1{d_2}^2-12\,{d_3}^2d_2{d_1}^3+12\,{d_1}^2{d_2}^2{d_3}^2)$
$v\ s\ s$	$\frac{219775}{93312}\sqrt{3}(-4-d_1d_2+{d_1}^2-d_3d_1+d_3d_2)$
$v\ s\ y$	$-\frac{9475}{839808}\sqrt{3}(-4\,d_1{d_2}^3+84-8\,{d_3}^3d_2+8\,{d_3}^3d_1+133\,d_1d_2+8\,{d_3}^2d_2d_1+12\,{d_1}^2{d_2}^2-12\,{d_3}^2{d_1}^2-12\,d_2{d_1}^3+4\,{d_3}^2{d_2}^2+4\,{d_1}^4+4\,d_3{d_2}^3+32\,{d_3}^2-85\,{d_1}^2-48\,{d_2}^2+12\,d_3d_2{d_1}^2-43\,d_3d_1+11\,d_3d_2-16\,d_3d_1{d_2}^2)$
$v\ s\ z$	$-\frac{9475}{419904}\sqrt{3}(-4\,{d_3}^3{d_1}^3+24+12\,{d_3}^3d_2{d_1}^2-27\,{d_3}^3d_2+27\,{d_3}^3d_1+22\,d_1d_2+123\,{d_3}^2d_2d_1-81\,{d_3}^2{d_1}^2-42\,{d_3}^2{d_2}^2-4\,{d_3}^2{d_2}^3d_1+108\,{d_3}^2-22\,{d_1}^2-12\,{d_3}^3{d_2}^2d_1+4\,{d_3}^3{d_2}^3-98\,d_3d_1+50\,d_3d_2+4\,{d_3}^2{d_1}^4+6\,d_3{d_1}^3-6\,d_3d_1{d_2}^2-12\,{d_3}^2d_2{d_1}^3+12\,{d_1}^2{d_2}^2{d_3}^2)$
$v\ y\ y$	$\frac{125}{2519424}\sqrt{3}(-38628-5688\,d_3d_2{d_1}^2+3944\,d_3d_1{d_2}^2+128\,{d_3}^4d_2d_1+160\,d_3d_2{d_1}^4+128\,d_3d_1{d_2}^4-160\,d_3{d_2}^2{d_1}^3-64\,d_3{d_2}^3{d_1}^2+368\,{d_1}^2{d_2}^2{d_3}^2-160\,{d_3}^2d_2{d_1}^3-160\,{d_3}^3{d_2}^2d_1-160\,{d_3}^2{d_2}^3d_1-64\,{d_3}^3d_2{d_1}^2+340\,d_3{d_2}^3+32633\,d_3d_2-5808\,{d_3}^2-6313\,d_1d_2+7993\,{d_1}^2-6313\,d_3d_1-5808\,{d_2}^2+1728\,{d_3}^2{d_1}^2-3752\,{d_3}^2{d_2}^2+384\,{d_2}^4+16\,{d_1}^6+384\,{d_3}^4-32\,{d_3}^2{d_1}^4+636\,d_3{d_1}^3+128\,{d_3}^3{d_1}^3-32\,{d_1}^4{d_2}^2-16\,{d_3}^4{d_2}^2-32\,d_3{d_1}^5+32\,{d_3}^5d_1-112\,{d_1}^2{d_2}^4-16\,{d_3}^2{d_2}^4-32\,{d_3}^5d_2-32\,d_2{d_1}^5+32\,d_1{d_2}^5-32\,d_3{d_2}^5-112\,{d_3}^4{d_1}^2+1728\,{d_1}^2{d_2}^2-1876\,{d_3}^3d_1-1876\,d_1{d_2}^3+3944\,{d_3}^2d_2d_1-872\,{d_1}^4+340\,{d_3}^3d_2+128\,{d_2}^3{d_1}^3+96\,{d_3}^3{d_2}^3+636\,d_2{d_1}^3)$
$v\ y\ z$	$\frac{125}{1259712}\sqrt{3}(-31224-4872\,d_3d_2{d_1}^2+5518\,d_3d_1{d_2}^2+1584\,{d_3}^4d_2d_1+24\,d_3d_2{d_1}^4+48\,d_3d_1{d_2}^4-72\,d_3{d_2}^2{d_1}^3-24\,d_3{d_2}^3{d_1}^2+1728\,{d_1}^2{d_2}^2{d_3}^2+636\,{d_3}^2d_2{d_1}^3+156\,{d_3}^3{d_2}^2d_1-1796\,{d_3}^2{d_2}^3d_1-2520\,{d_3}^3d_2{d_1}^2+128\,{d_3}^2{d_2}^3{d_1}^3+192\,{d_3}^4{d_2}^2{d_1}^2+96\,{d_3}^3{d_2}^4d_1-96\,{d_3}^4{d_2}^3d_1-112\,{d_3}^3{d_2}^2{d_1}^3-48\,{d_3}^3{d_2}^3{d_1}^2-400\,d_3{d_2}^3-160\,{d_3}^4d_2{d_1}^3-32\,{d_3}^2d_2{d_1}^5-112\,{d_3}^2{d_2}^4{d_1}^2-48\,{d_3}^5{d_2}^2d_1+144\,{d_3}^3d_2{d_1}^4+32\,{d_3}^2{d_2}^5d_1-32\,{d_3}^2{d_1}^4{d_2}^2+48\,{d_3}^5d_2{d_1}^2+38950\,d_3d_2-17340\,{d_3}^2-6478\,d_1d_2+1102\,{d_1}^2+1130\,d_3d_1-192\,{d_2}^2+10749\,{d_3}^2{d_1}^2-10246\,{d_3}^2{d_2}^2+1296\,{d_3}^4-904\,{d_3}^2{d_1}^4-16\,{d_3}^5{d_1}^3+16\,{d_3}^5{d_2}^3-48\,{d_3}^3{d_1}^5-32\,{d_3}^3{d_2}^5-1398\,d_3{d_1}^3+1696\,{d_3}^3{d_1}^3-660\,{d_3}^4{d_2}^2+24\,d_3{d_1}^5+108\,{d_3}^5d_1+336\,{d_3}^2{d_2}^4-108\,{d_3}^5d_2-924\,{d_3}^4{d_1}^2+264\,{d_1}^2{d_2}^2-9551\,{d_3}^3d_1-176\,d_1{d_2}^3+3817\,{d_3}^2d_2d_1-88\,{d_1}^4+5087\,{d_3}^3d_2+16\,{d_3}^4{d_2}^4+48\,{d_3}^4{d_1}^4+16\,{d_3}^2{d_1}^6+668\,{d_3}^3{d_2}^3)$
$v\ z\ z$	$\frac{125}{629856}\sqrt{3}(-30864-8208\,d_3d_2{d_1}^2+144\,{d_3}^3{d_2}^3{d_1}^4+48\,{d_3}^5{d_2}^3{d_1}^2-16\,{d_3}^2{d_2}^5{d_1}^3-144\,{d_3}^4{d_2}^3{d_1}^3+16\,{d_3}^2{d_2}^2{d_1}^6-48\,{d_3}^3{d_2}^2{d_1}^5+48\,{d_3}^4{d_2}^2{d_1}^4-16\,{d_3}^5{d_2}^2{d_1}^3+48\,{d_3}^3{d_2}^5{d_1}^2-48\,{d_3}^4{d_2}^5d_1+144\,{d_3}^4{d_2}^4{d_1}^2-48\,{d_3}^2{d_2}^3{d_1}^5+48\,{d_3}^2{d_2}^4{d_1}^4-48\,{d_3}^5{d_2}^4d_1-144\,{d_3}^3{d_2}^4{d_1}^3-24\,d_3{d_2}^4{d_1}^3+18186\,d_3d_1{d_2}^2+24\,d_3{d_2}^2{d_1}^5+162\,{d_3}^4d_2d_1+36\,d_3d_2{d_1}^4+162\,d_3d_1{d_2}^4-1338\,d_3{d_2}^2{d_1}^3+564\,d_3{d_2}^3{d_1}^2+13485\,{d_1}^2{d_2}^2{d_3}^2-1338\,{d_3}^2d_2{d_1}^3-10745\,{d_3}^3{d_2}^2d_1-10745\,{d_3}^2{d_2}^3d_1+564\,{d_3}^3d_2{d_1}^2+1656\,{d_3}^2{d_2}^2{d_3}^1{}^3-852\,{d_3}^4{d_2}^2{d_1}^2+1404\,{d_3}^3{d_2}^4d_1+1404\,{d_3}^4{d_2}^3d_1+1656\,{d_3}^3{d_2}^2{d_1}^3-2952\,{d_3}^3{d_2}^3{d_1}^2-1350\,d_3{d_2}^3-24\,{d_3}^4d_2{d_1}^3+24\,{d_3}^2d_2{d_1}^5-852\,{d_3}^2{d_2}^4{d_1}^2+108\,{d_3}^5{d_2}^2d_1+108\,{d_3}^2{d_2}^5d_1-936\,{d_3}^2{d_1}^4{d_2}^2+54916\,d_3d_2-648\,{d_3}^2-8980\,d_1d_2+484\,{d_1}^2-8980\,d_3d_1-648\,{d_2}^2+1014\,{d_3}^2{d_1}^2-33084\,{d_3}^2{d_2}^2-88\,{d_3}^2{d_1}^4-108\,{d_3}^5{d_2}^3-108\,{d_3}^3{d_2}^5-132\,d_3{d_1}^3+88\,{d_3}^3{d_1}^3-88\,{d_1}^4{d_2}^2+1134\,{d_3}^4{d_2}^2+1134\,{d_3}^2{d_2}^4+1014\,{d_1}^2{d_2}^2-594\,{d_3}^3d_1-594\,d_1{d_2}^3+18186\,{d_3}^2d_2d_1-1350\,{d_3}^3d_2-528\,{d_3}^4{d_2}^4+88\,{d_2}^3{d_1}^3+16\,{d_3}^5{d_2}^5+6925\,{d_3}^3{d_2}^3-132\,d_2{d_1}^3)$

Table A.3: The cubic couplings for all of the fields in the action up to level 3 (continued).

$l\,m\,n$	$B_{lmn}(d_1,d_2,d_3)$
$w\,w\,w$	$-\frac{1}{373248}\sqrt{3}(-24963-6384\,d_3d_2{d_1}^2-6384\,d_3d_1{d_2}^2+1152\,{d_3}^4d_2d_1+1152\,d_3d_2{d_1}^4+1152\,d_3d_1{d_2}^4-960\,d_3{d_2}^2{d_1}^3-960\,d_3{d_2}^3{d_1}^2+2688\,{d_1}^2{d_2}^2{d_3}^2-960\,{d_3}^2d_2{d_1}^3-960\,{d_3}^3{d_2}^2d_1-960\,{d_3}^2{d_2}^3d_1-960\,{d_3}^3d_2{d_1}^2+15600\,d_3{d_2}^3-384\,{d_3}^4{d_1}^2-27392\,d_3d_2+44800\,{d_3}^2-27392\,d_1d_2+44800\,{d_1}^2-27392\,d_3d_1+44800\,{d_2}^2-18432\,{d_3}^2{d_1}^2-18432\,{d_3}^2{d_2}^2-6384\,{d_1}^4-6384\,{d_3}^4-384\,{d_3}^2{d_1}^4+15600\,d_3{d_1}^3+128\,{d_2}^6+128\,{d_3}^6+128\,{d_1}^6+896\,{d_3}^3{d_1}^3-192\,d_3{d_1}^5-192\,{d_3}^5d_1-384\,{d_1}^2{d_2}^4-192\,{d_3}^5d_2-192\,d_2{d_1}^5-192\,d_1{d_2}^5-192\,d_3{d_2}^5-384\,{d_1}^4{d_2}^2-384\,{d_3}^4{d_2}^2-384\,{d_3}^2{d_2}^4-18432\,{d_1}^2{d_2}^2-6384\,{d_2}^4+15600\,{d_3}^3d_1+15600\,d_1{d_2}^3-6384\,{d_3}^2d_2d_1+15600\,{d_3}^3d_2+896\,{d_2}^3{d_1}^3+896\,{d_3}^3{d_2}^3+15600\,d_2{d_1}^3)$
$w\,w\,f$	$-\frac{1}{186624}\sqrt{3}(3032\,{d_2}^3+144\,{d_3}^5-832\,{d_3}^3{d_2}^3d_1-64\,{d_3}^4{d_2}{d_1}^2+128\,{d_3}^5d_2d_1+1280\,{d_3}^3{d_2}^2{d_1}^2+896\,d_3{d_2}^3{d_1}^3+6896\,{d_3}^3d_2d_1-17728\,d_3{d_2}^2{d_1}^2-33776\,d_3d_2d_1-192\,d_3d_1{d_2}^5-192\,d_3d_2{d_1}^5+15536\,d_3{d_2}^3d_1+15536\,d_3d_2{d_1}^3+960\,{d_3}^2{d_1}^4d_2-9984\,{d_3}^2d_2{d_1}^2+960\,{d_3}^2d_1{d_2}^4-384\,d_3{d_2}^2{d_1}^4-64\,{d_3}^4{d_2}^2d_1-9984\,{d_3}^2d_1{d_2}^2-832\,{d_3}^3d_2{d_1}^3-640\,{d_3}^2{d_2}^3{d_1}^2-384\,d_3{d_2}^4{d_1}^2-640\,{d_3}^2{d_2}^2{d_1}^3+64\,{d_2}^5-616\,{d_3}^3+1576\,{d_1}^2d_2+9952\,{d_3}^2{d_1}^3-160\,{d_1}^2{d_2}^3+96\,d_1{d_2}^4+96\,{d_1}^4d_2-160\,{d_2}^2{d_1}^3-176\,{d_3}^4d_1+64\,{d_3}^4{d_1}^3+192\,{d_3}^3{d_2}^4+64\,{d_3}^4{d_2}^3+192\,{d_3}^3{d_1}^4-6672\,d_3{d_2}^4-320\,{d_3}^2{d_2}^5-64\,{d_3}^5{d_2}^2-6672\,d_3{d_1}^4-320\,{d_3}^2{d_1}^5-64\,{d_3}^5{d_1}^2+128\,d_3{d_2}^6+128\,d_3{d_1}^6+3032\,{d_1}^3-1842\,d_1-1842\,d_2-15868\,{d_3}^2d_2-3312\,{d_3}^3{d_1}^2-15868\,{d_3}^2d_1+37160\,d_3{d_1}^2+1576\,d_1{d_2}^2-3312\,{d_3}^3{d_2}^2+37160\,d_3{d_2}^2+64\,{d_1}^5-3871\,d_3+9952\,{d_3}^2{d_2}^3-176\,{d_3}^4d_2)$
$w\,w\,o$	0
$w\,w\,\tilde{o}$	0
$w\,w\,p$	0
$w\,w\,q$	$-\frac{1}{279936}(d_1-d_2)(2008\,{d_2}^3+240\,{d_3}^5+1744\,{d_3}^3d_2d_1+1760\,d_3{d_2}^2{d_1}^2-79528\,d_3d_2d_1-240\,d_3{d_2}^3d_1-240\,d_3d_2{d_1}^3-1328\,{d_3}^2d_2{d_1}^2-1328\,{d_3}^2d_1{d_2}^2+64\,{d_2}^5-15192\,{d_3}^3-2008\,{d_1}^2d_2+1296\,{d_3}^2{d_1}^3-160\,{d_1}^2{d_2}^3+96\,d_1{d_2}^4+96\,{d_1}^4d_2-160\,{d_2}^2{d_1}^3-272\,{d_3}^4d_1-640\,d_3{d_2}^4-640\,d_3{d_1}^4+2008\,{d_1}^3-15858\,d_1-15858\,d_2+21628\,{d_3}^2d_2-688\,{d_3}^3{d_1}^2+21628\,{d_3}^2d_1-8444\,d_3{d_1}^2-2008\,d_1{d_2}^2-688\,{d_3}^3{d_2}^2-8444\,d_3{d_2}^2+64\,{d_1}^5+40215\,d_3+1296\,{d_3}^2{d_2}^3-272\,{d_3}^4d_2)$
$w\,w\,r$	$-\frac{11}{279936}(d_1-d_2)(32\,{d_1}^4-80\,d_3{d_1}^3+16\,d_2{d_1}^3+80\,d_3d_2{d_1}^2-1044\,{d_1}^2+48\,{d_3}^2{d_1}^2-96\,{d_1}^2{d_2}^2+1260\,d_3d_1-112\,{d_3}^2d_2d_1+16\,{d_3}^3d_1+2088\,d_1d_2+16\,d_1{d_2}^3+80\,d_3d_1{d_2}^2-216\,{d_3}^2+32\,{d_2}^4+48\,{d_3}^2{d_2}^2-80\,d_3{d_2}^3-1044\,{d_2}^2-16\,{d_3}^4+2695+1260\,d_3d_2+16\,{d_3}^3d_2)$
$w\,w\,s$	$\frac{125}{559872}(d_1-d_2)(32\,{d_1}^4-80\,d_3{d_1}^3+16\,d_2{d_1}^3+80\,d_3d_2{d_1}^2-1044\,{d_1}^2+48\,{d_3}^2{d_1}^2-96\,{d_1}^2{d_2}^2+1260\,d_3d_1-112\,{d_3}^2d_2d_1+16\,{d_3}^3d_1+2088\,d_1d_2+16\,d_1{d_2}^3+80\,d_3d_1{d_2}^2-216\,{d_3}^2+32\,{d_2}^4+48\,{d_3}^2{d_2}^2-80\,d_3{d_2}^3-1044\,{d_2}^2-16\,{d_3}^4+2695+1260\,d_3d_2+16\,{d_3}^3d_2)$
$w\,w\,y$	$-\frac{1}{559872}(d_1-d_2)(-149379-20208\,d_3d_2{d_1}^2-20208\,d_3d_1{d_2}^2+1152\,{d_3}^4d_2d_1+1152\,d_3d_2{d_1}^4+1152\,d_3d_1{d_2}^4-960\,d_3{d_2}^2{d_1}^3-960\,d_3{d_2}^3{d_1}^2+2688\,{d_1}^2{d_2}^2{d_3}^2-960\,{d_3}^2d_2{d_1}^3-960\,{d_3}^3{d_2}^2d_1-960\,{d_3}^2{d_2}^3d_1-960\,{d_3}^3d_2{d_1}^2+20208\,d_3{d_2}^3-384\,{d_3}^4{d_1}^2-80384\,d_3d_2+44800\,{d_3}^2-158720\,d_1d_2+97792\,{d_1}^2-80384\,d_3d_1+97792\,{d_2}^2-13824\,{d_3}^2{d_1}^2-13824\,{d_3}^2{d_2}^2-9456\,{d_1}^4-1776\,{d_3}^4-384\,{d_3}^2{d_1}^4+20208\,d_3{d_1}^3+128\,{d_2}^6+128\,{d_3}^6+128\,{d_1}^6+896\,{d_3}^3{d_1}^3-192\,d_3{d_1}^5-192\,{d_3}^5d_1-384\,{d_1}^2{d_2}^4-192\,{d_3}^5d_2-192\,d_2{d_1}^5-192\,d_1{d_2}^5-192\,d_3{d_2}^5-384\,{d_1}^4{d_2}^2-384\,{d_3}^4{d_2}^2-384\,{d_3}^2{d_2}^4-9216\,{d_1}^2{d_2}^2-9456\,{d_2}^4+4848\,{d_3}^3d_1+14064\,d_1{d_2}^3+19728\,{d_3}^2d_2d_1+4848\,{d_3}^3d_2+896\,{d_2}^3{d_1}^3+896\,{d_3}^3{d_2}^3+14064\,d_2{d_1}^3)$
$w\,w\,z$	$-\frac{1}{279936}(d_1-d_2)(23142-7784\,d_3d_2{d_1}^2-7784\,d_3d_1{d_2}^2+13136\,{d_3}^4d_2d_1+288\,d_3d_2{d_1}^4+288\,d_3d_1{d_2}^4-480\,d_3{d_2}^2{d_1}^3-480\,d_3{d_2}^3{d_1}^2+128\,{d_3}^6d_2d_1+896\,{d_3}^2{d_2}^3{d_1}^3+1280\,{d_3}^4{d_2}^2{d_1}^2+960\,{d_3}^3{d_2}^4d_1-832\,{d_3}^4{d_2}^3d_1-640\,{d_3}^3{d_2}^2{d_1}^3-640\,{d_3}^3{d_2}^3{d_1}^2-832\,{d_3}^4d_2{d_1}^3-192\,{d_3}^2d_2{d_1}^5-384\,{d_3}^2{d_2}^4{d_1}^2-64\,{d_3}^5{d_2}^2d_1+960\,{d_3}^3d_2{d_1}^4-192\,{d_3}^2{d_2}^5d_1-384\,{d_3}^2{d_1}^4{d_2}^2-64\,{d_3}^5d_2{d_1}^2-9216\,{d_1}^2{d_2}^2{d_3}^2+14224\,{d_3}^2d_2{d_1}^3-15776\,{d_3}^3{d_2}^2d_1+14224\,{d_3}^2{d_2}^3d_1-15776\,{d_3}^3d_2{d_1}^2+7784\,d_3{d_2}^3-6160\,{d_3}^4{d_1}^2-9758\,d_3d_2-114605\,{d_3}^2-164720\,d_1d_2-9800\,{d_1}^2-9758\,d_3d_1-9800\,{d_2}^2+95904\,{d_3}^2{d_1}^2+95904\,{d_3}^2{d_2}^2-704\,{d_1}^4+12328\,{d_3}^4+64\,{d_3}^5{d_1}^3-9616\,{d_3}^2{d_1}^4+7784\,d_3{d_1}^3+432\,{d_3}^6+15680\,{d_3}^3{d_1}^3+192\,d_3{d_1}^5-528\,{d_3}^5d_1-528\,{d_3}^5d_2+192\,d_3{d_2}^5-6160\,{d_3}^4{d_2}^2-9616\,{d_3}^2{d_2}^4+2112\,{d_1}^2{d_2}^2-704\,{d_2}^4-78676\,{d_3}^3d_1-352\,d_1{d_2}^3+16960\,{d_3}^2d_2d_1+64\,{d_3}^5{d_2}^3+128\,{d_3}^2{d_2}^6-64\,{d_3}^6{d_2}^2-78676\,{d_3}^3d_2-320\,{d_3}^3{d_1}^5-320\,{d_3}^3{d_2}^5+192\,{d_3}^4{d_1}^4+128\,{d_3}^2{d_1}^6-64\,{d_3}^6{d_1}^2+192\,{d_3}^4{d_2}^4+15680\,{d_3}^3{d_2}^3-352\,d_2{d_1}^3)$

Table A.3: The cubic couplings for all of the fields in the action up to level 3 (continued).

$l\,m\,n$	$B_{lmn}(d_1,d_2,d_3)$
$w\,f\,f$	$-\frac{1}{93312}\sqrt{3}(4352 + 29744\,d_3d_2{d_1}^2 - 22276\,d_3d_1{d_2}^2 - 112\,{d_3}^4d_2d_1 - 6960\,d_3d_2{d_1}^4 - 112\,d_3d_1{d_2}^4 + 9984\,d_3{d_2}^2{d_1}^3 - 3056\,d_3{d_2}^3{d_1}^2 - 704\,{d_3}^2{d_2}^3{d_1}^3 - 192\,{d_3}^3{d_2}^4d_1 - 192\,{d_3}^4{d_2}^3d_1 - 704\,{d_3}^3{d_2}^2{d_1}^3 + 768\,{d_3}^3{d_2}^3{d_1}^2 + 64\,{d_3}^4d_2{d_1}^3 - 320\,{d_3}^2d_2{d_1}^5 + 128\,{d_3}^5{d_2}^2d_1 + 192\,{d_3}^3d_2{d_1}^4 + 128\,{d_3}^2{d_2}^5d_1 + 896\,{d_3}^2{d_1}^4{d_2}^2 - 64\,{d_3}^5d_2{d_1}^2 + 128\,d_3d_2{d_1}^6 + 64\,d_3{d_2}^4{d_1}^3 + 192\,d_3{d_2}^3{d_1}^4 - 320\,d_3{d_2}^2{d_1}^5 - 64\,d_3{d_2}^5{d_1}^2 - 13248\,{d_1}^2{d_2}^2{d_3}^2 + 9984\,{d_3}^2d_2{d_1}^3 + 3248\,{d_3}^3{d_2}^2d_1 + 3248\,{d_3}^2{d_2}^3d_1 - 3056\,{d_3}^3d_2{d_1}^2 - 2456\,d_3{d_2}^3 - 32\,{d_3}^4{d_1}^2 + 14249\,d_3d_2 - 9050\,{d_3}^2 - 1862\,d_1d_2 + 20\,{d_1}^2 - 1862\,d_3d_1 - 9050\,{d_2}^2 + 1472\,{d_3}^2{d_1}^2 + 7304\,{d_3}^2{d_2}^2 + 32\,{d_1}^4 + 72\,{d_3}^4 + 32\,{d_3}^2{d_1}^4 + 2984\,d_3{d_1}^3 - 64\,{d_3}^3{d_1}^3 + 64\,d_3{d_1}^5 - 32\,{d_1}^2{d_2}^4 + 144\,{d_3}^5d_2 + 64\,d_2{d_1}^5 + 144\,d_3{d_2}^5 + 32\,{d_1}^4{d_2}^2 - 352\,{d_3}^4{d_2}^2 - 352\,{d_3}^2{d_2}^4 + 1472\,{d_1}^2{d_2}^2 + 72\,{d_2}^4 + 1664\,{d_3}^3d_1 + 1664\,d_1{d_2}^3 - 22276\,{d_3}^2d_2d_1 - 64\,{d_3}^5{d_2}^3 - 2456\,{d_3}^3d_2 - 64\,{d_3}^3{d_2}^5 + 128\,{d_3}^4{d_2}^4 - 64\,{d_2}^3{d_1}^3 + 496\,{d_3}^3{d_2}^3 + 2984\,d_2{d_1}^3)$
$w\,f\,o$	0
$w\,f\,\tilde{o}$	0
$w\,f\,p$	0
$w\,f\,q$	$\frac{5}{2916}\,{d_3}^5{d_2}^2 - \frac{623}{23328}\,{d_2}^3 - \frac{7}{4374}\,d_3{d_2}^3{d_1}^3 + \frac{221}{1944}\,{d_3}^3d_2d_1 + \frac{827}{17496}\,d_3{d_2}^2{d_1}^2 - \frac{8081}{15552}\,d_3d_2d_1 + \frac{1}{2187}\,d_3d_1{d_2}^5 + \frac{10}{2187}\,d_3d_2{d_1}^5 - \frac{92}{2187}\,d_3{d_2}^3d_1 + \frac{1889}{34992}\,d_3d_2{d_1}^3 - \frac{1}{108}\,{d_3}^2{d_1}^4d_2 - \frac{5363}{34992}\,{d_3}^2d_2{d_1}^2 - \frac{10}{2187}\,{d_3}^2d_1{d_2}^4 - \frac{53}{8748}\,d_3{d_2}^2{d_1}^4 + \frac{5}{2916}\,{d_3}^4{d_2}^2d_1 - \frac{995}{34992}\,{d_3}^2{d_1}^2{d_2}^2 + \frac{43}{8748}\,{d_3}^3d_2{d_1}^3 - \frac{11}{4374}\,{d_3}^2{d_2}^3{d_1}^2 + \frac{23}{8748}\,d_3{d_2}^4{d_1}^2 + \frac{145}{8748}\,{d_3}^2{d_2}^2{d_1}^3 + \frac{31}{4374}\,{d_3}^3{d_2}^3d_1 + \frac{17}{8748}\,{d_3}^4d_2{d_1}^2 - \frac{5}{2916}\,{d_3}^5d_2d_1 - \frac{31}{2187}\,{d_3}^3{d_2}^2{d_1}^2 - \frac{1}{4374}\,{d_3}^2{d_2}^5 + \frac{1}{1944}\,{d_2}^5 - \frac{25}{729}\,{d_3}^3 + \frac{19}{8748}\,{d_3}^3{d_2}^4 + \frac{5}{5832}\,{d_3}^4d_2 + \frac{187}{34992}\,{d_1}^3 - \frac{761}{17496}\,{d_3}^3{d_2}^2 + \frac{119}{2187}\,{d_3}^2{d_2}^3 - \frac{8}{2187}\,{d_3}^4{d_2}^3 - \frac{55}{3888}\,d_3{d_2}^4 + \frac{9367}{139968}\,d_3{d_2}^2 - \frac{7}{243}\,d_1 - \frac{29}{729}\,d_2 + \frac{7}{4374}\,d_3{d_1}^4 - \frac{1}{4374}\,{d_1}^2{d_2}^5 - \frac{1}{2187}\,d_2{d_1}^6 + \frac{1}{4374}\,{d_1}^5{d_2}^2 - \frac{1}{4374}\,{d_1}^5 + \frac{143}{1458}\,d_3 + \frac{1223}{23328}\,{d_3}^2d_2 - \frac{7}{4374}\,{d_3}^3{d_1}^2 + \frac{83}{7776}\,{d_3}^2d_1 + \frac{16321}{69984}\,d_3{d_1}^2 + \frac{1349}{34992}\,d_1{d_2}^2 + \frac{2671}{23328}\,{d_1}^2d_2 + \frac{19}{17496}\,{d_3}^2{d_1}^3 - \frac{7}{2187}\,{d_1}^2{d_2}^3 + \frac{167}{17496}\,d_1{d_2}^4 + \frac{1}{1458}\,{d_2}^3{d_1}^4 - \frac{1}{4374}\,{d_2}^4{d_1}^3 - \frac{241}{17496}\,{d_1}^4d_2 + \frac{317}{17496}\,{d_2}^2{d_1}^3 - \frac{5}{5832}\,{d_3}^4d_1$
$w\,f\,r$	$-\frac{3509}{34992}\,d_3d_2{d_1}^2 + \frac{1991}{34992}\,d_3d_1{d_2}^2 + \frac{11}{8748}\,{d_3}^4d_2d_1 + \frac{55}{8748}\,d_3d_2{d_1}^4 + \frac{11}{4374}\,d_3d_1{d_2}^4 - \frac{11}{972}\,d_3{d_2}^2{d_1}^3 + \frac{11}{4374}\,d_3{d_2}^3{d_1}^2 + \frac{407}{4374} + \frac{22}{2187}\,{d_1}^2{d_2}^2{d_3}^2 - \frac{11}{2916}\,{d_3}^2d_2{d_1}^3 - \frac{11}{8748}\,{d_3}^3{d_2}^2d_1 - \frac{11}{2187}\,{d_3}^2{d_2}^3d_1 - \frac{11}{8748}\,{d_3}^3d_2{d_1}^2 - \frac{143}{8748}\,d_3{d_2}^3 + \frac{1309}{23328}\,d_3d_2 - \frac{11}{729}\,{d_3}^2 - \frac{13123}{139968}\,d_1d_2 - \frac{6391}{69984}\,{d_1}^2 - \frac{605}{23328}\,d_3d_1 - \frac{2255}{139968}\,{d_2}^2 + \frac{11}{8748}\,{d_3}^2{d_1}^2 + \frac{275}{17496}\,{d_3}^2{d_2}^2 - \frac{11}{8748}\,{d_1}^4 - \frac{11}{17496}\,d_3{d_1}^3 - \frac{11}{8748}\,{d_1}^2{d_2}^4 - \frac{11}{4374}\,d_2{d_1}^5 + \frac{11}{2916}\,{d_1}^4{d_2}^2 - \frac{11}{8748}\,{d_3}^4{d_2}^2 - \frac{11}{8748}\,{d_3}^2{d_2}^4 - \frac{1177}{17496}\,{d_1}^2{d_2}^2 + \frac{11}{3888}\,{d_2}^4 + \frac{11}{17496}\,{d_3}^3d_1 + \frac{55}{5832}\,d_1{d_2}^3 + \frac{77}{5832}\,{d_3}^2d_2d_1 - \frac{11}{17496}\,{d_3}^3d_2 + \frac{11}{4374}\,{d_3}^3{d_2}^3 + \frac{3025}{34992}\,d_2{d_1}^3$
$w\,f\,s$	$\frac{39875}{69984}\,d_3d_2{d_1}^2 - \frac{22625}{69984}\,d_3d_1{d_2}^2 - \frac{125}{17496}\,{d_3}^4d_2d_1 - \frac{625}{17496}\,d_3d_2{d_1}^4 - \frac{125}{8748}\,d_3d_1{d_2}^4 + \frac{125}{1944}\,d_3{d_2}^2{d_1}^3 - \frac{125}{8748}\,d_3{d_2}^3{d_1}^2 - \frac{125}{2187}\,{d_1}^2{d_2}^2{d_3}^2 + \frac{125}{5832}\,{d_3}^2d_2{d_1}^3 + \frac{125}{17496}\,{d_3}^3{d_2}^2d_1 + \frac{125}{4374}\,{d_3}^2{d_2}^3d_1 + \frac{125}{17496}\,{d_3}^3d_2{d_1}^2 + \frac{1625}{17496}\,d_3{d_2}^3 - \frac{14875}{46656}\,d_3d_2 + \frac{125}{1458}\,{d_3}^2 + \frac{149125}{279936}\,d_1d_2 + \frac{72625}{139968}\,{d_1}^2 + \frac{6875}{46656}\,d_3d_1 + \frac{25625}{279936}\,{d_2}^2 - \frac{4625}{8748} - \frac{125}{17496}\,{d_3}^2{d_1}^2 - \frac{3125}{34992}\,{d_3}^2{d_2}^2 + \frac{125}{17496}\,{d_1}^4 + \frac{125}{34992}\,d_3{d_1}^3 + \frac{125}{17496}\,{d_1}^2{d_2}^4 + \frac{125}{8748}\,d_2{d_1}^5 - \frac{125}{5832}\,{d_1}^4{d_2}^2 + \frac{125}{17496}\,{d_3}^4{d_2}^2 + \frac{125}{17496}\,{d_3}^2{d_2}^4 + \frac{13375}{34992}\,{d_1}^2{d_2}^2 - \frac{125}{7776}\,{d_2}^4 - \frac{125}{34992}\,{d_3}^3d_1 - \frac{625}{11664}\,d_1{d_2}^3 - \frac{875}{11664}\,{d_3}^2d_2d_1 + \frac{125}{34992}\,{d_3}^3d_2 - \frac{125}{8748}\,{d_3}^3{d_2}^3 - \frac{34375}{69984}\,d_2{d_1}^3$
$w\,f\,y$	$\frac{3809}{11664}\,d_3d_2{d_1}^2 - \frac{20989}{69984}\,d_3d_1{d_2}^2 + \frac{5}{648}\,{d_3}^4d_2d_1 - \frac{1253}{17496}\,d_3d_2{d_1}^4 + \frac{157}{8748}\,d_3d_1{d_2}^4 + \frac{2555}{17496}\,d_3{d_2}^2{d_1}^3 - \frac{1439}{17496}\,d_3{d_2}^3{d_1}^2 - \frac{5}{729}\,{d_3}^2{d_2}^3{d_1}^3 - \frac{7}{2187}\,{d_3}^3{d_2}^4d_1 + \frac{2}{729}\,{d_3}^4{d_2}^3d_1 + \frac{4}{729}\,{d_3}^3{d_2}^2{d_1}^3 + \frac{1}{1458}\,{d_3}^3{d_2}^3{d_1}^2 + \frac{1}{729}\,{d_3}^4d_2{d_1}^3 + \frac{1}{729}\,{d_3}^2d_2{d_1}^5 + \frac{1}{2187}\,{d_3}^5{d_2}^2d_1 - \frac{7}{2187}\,{d_3}^3d_2{d_1}^4 + \frac{2}{2187}\,{d_3}^2{d_1}^4{d_2}^2 + \frac{1}{1458}\,{d_3}^5d_2{d_1}^2 + \frac{1}{1458}\,d_3d_2{d_1}^6 - \frac{2}{729}\,d_3{d_2}^4{d_1}^3 + \frac{14}{2187}\,d_3{d_2}^3{d_1}^4 - \frac{1}{243}\,d_3{d_2}^2{d_1}^5 - \frac{1}{1458}\,d_3{d_2}^5{d_1}^2 - \frac{313}{4374}\,{d_1}^2{d_2}^2{d_3}^2 + \frac{5}{108}\,{d_3}^2d_2{d_1}^3 + \frac{413}{17496}\,{d_3}^3{d_2}^2d_1 + \frac{31}{17496}\,{d_3}^2{d_2}^3d_1 - \frac{103}{5832}\,{d_3}^3d_2{d_1}^2 - \frac{895}{69984}\,d_3{d_2}^3 - \frac{1}{2916}\,{d_3}^4{d_1}^2 - \frac{611}{2916} - \frac{16729}{139968}\,d_3d_2 + \frac{19}{486}\,{d_3}^2 + \frac{38765}{279936}\,d_1d_2 + \frac{27065}{139968}\,{d_1}^2 + \frac{15385}{139968}\,d_3d_1 + \frac{5387}{93312}\,{d_2}^2 - \frac{773}{34992}\,{d_3}^2{d_1}^2 + \frac{2165}{34992}\,{d_3}^2{d_2}^2 - \frac{1}{2187}\,{d_3}^6d_2d_1 - \frac{7}{1458}\,{d_3}^4{d_2}^2{d_1}^2 + \frac{7}{1458}\,{d_3}^2{d_2}^4{d_1}^2 - \frac{41}{11664}\,{d_1}^4 + \frac{1}{2187}\,d_3d_1{d_2}^6 + \frac{4}{729}\,{d_3}^4 - \frac{1}{4374}\,{d_3}^2{d_2}^6 + \frac{5}{8748}\,{d_3}^2{d_1}^4 - \frac{5}{34992}\,d_3{d_1}^3 + \frac{1}{1944}\,{d_2}^6 - \frac{1}{4374}\,{d_1}^6 + \frac{5}{8748}\,{d_3}^3{d_1}^3 - \frac{1}{2916}\,d_3{d_1}^5 - \frac{1}{4374}\,{d_3}^5d_1 - \frac{25}{4374}\,{d_1}^2{d_2}^4 + \frac{1}{4374}\,{d_3}^5d_2 + \frac{613}{17496}\,d_2{d_1}^5 - \frac{13}{4374}\,d_1{d_2}^5 + \frac{7}{5832}\,d_3{d_2}^5 - \frac{1391}{17496}\,{d_1}^4{d_2}^2 - \frac{107}{5832}\,{d_3}^4{d_2}^2 - \frac{175}{17496}\,{d_3}^2{d_2}^4 + \frac{34345}{69984}\,{d_1}^2{d_2}^2 - \frac{143}{11664}\,{d_2}^4 - \frac{443}{34992}\,{d_3}^3d_1 - \frac{5797}{69984}\,d_1{d_2}^3 - \frac{74}{729}\,{d_3}^2d_2d_1 - \frac{5}{4374}\,{d_3}^5{d_2}^3 - \frac{133}{34992}\,{d_3}^3d_2 + \frac{1}{2187}\,{d_2}^5{d_1}^3 + \frac{1}{4374}\,{d_3}^3{d_2}^5 + \frac{1}{1458}\,{d_3}^4{d_2}^4 + \frac{925}{17496}\,{d_2}^3{d_1}^3 + \frac{1}{2187}\,{d_2}^4{d_1}^4 + \frac{77}{2916}\,{d_3}^3{d_2}^3 + \frac{1}{2187}\,{d_3}^6{d_2}^2 - \frac{4}{2187}\,{d_1}^5{d_2}^3 - \frac{1}{2187}\,{d_1}^7d_2 - \frac{1}{4374}\,{d_1}^2{d_2}^6 + \frac{7}{4374}\,{d_2}^2{d_1}^6 - \frac{1943}{5832}\,d_2{d_1}^3$

Table A.3: The cubic couplings for all of the fields in the action up to level 3 (continued).

$l\,m\,n$	$B_{lmn}(d_1,d_2,d_3)$
$w\,f\,z$	$\frac{1769}{23328}\,d_3d_2{d_1}^2+\frac{577}{34992}\,d_3d_1{d_2}^2-\frac{803}{17496}\,{d_3}^4d_2d_1-\frac{943}{17496}\,d_3d_2{d_1}^4+\frac{413}{17496}\,d_3d_1{d_2}^4+\frac{449}{5832}\,d_3{d_2}^2{d_1}^3-\frac{32}{2187}\,d_3{d_2}^3{d_1}^2+\frac{883}{8748}\,{d_3}^2{d_2}^3{d_1}^3+\frac{137}{8748}\,{d_3}^3{d_2}^4d_1+\frac{110}{2187}\,{d_3}^4{d_2}^3d_1+\frac{121}{486}\,{d_3}^3{d_2}^2{d_1}^3-\frac{1339}{8748}\,{d_3}^3{d_2}^3{d_1}^2+\frac{365}{8748}\,{d_3}^4d_2{d_1}^3+\frac{623}{8748}\,{d_3}^2d_2{d_1}^5+\frac{11}{2916}\,{d_3}^5{d_2}^2d_1-\frac{245}{2187}\,{d_3}^3d_2{d_1}^4-\frac{10}{2187}\,{d_3}^2{d_2}^5d_1-\frac{1385}{8748}\,{d_3}^2{d_1}^4{d_2}^2+\frac{1}{324}\,{d_3}^5d_2{d_1}^2+\frac{2}{2187}\,{d_3}^3{d_2}^6d_1+\frac{1}{2187}\,{d_3}^6d_2{d_1}^3+\frac{25}{2187}\,{d_3}^3{d_2}^3{d_1}^4-\frac{1}{2187}\,{d_3}^5d_2{d_1}^4+\frac{1}{729}\,{d_3}^5{d_2}^3{d_1}^2-\frac{1}{729}\,d_3d_2{d_1}^6-\frac{1}{729}\,{d_3}^6{d_2}^2{d_1}^2-\frac{1}{1458}\,d_3{d_2}^4{d_1}^3+\frac{2}{2187}\,{d_3}^2{d_2}^5{d_1}^3-\frac{23}{2187}\,{d_3}^4{d_2}^3{d_1}^3+\frac{7}{2187}\,{d_3}^2{d_2}^2{d_1}^6-\frac{19}{2187}\,{d_3}^3{d_2}^2{d_1}^5+\frac{14}{2187}\,{d_3}^4{d_2}^2{d_1}^4+\frac{1}{2187}\,{d_3}^5{d_2}^2{d_1}^3+\frac{1}{486}\,d_3{d_2}^3{d_1}^4-\frac{2}{2187}\,{d_3}^3{d_2}^5{d_1}^2+\frac{1}{1458}\,d_3{d_2}^2{d_1}^5-\frac{1}{2187}\,{d_3}^2{d_2}^6{d_1}^2-\frac{1}{729}\,{d_3}^4d_2{d_1}^5-\frac{2}{2187}\,{d_3}^4{d_2}^5d_1+\frac{5}{729}\,{d_3}^4{d_2}^4{d_1}^2-\frac{8}{2187}\,{d_3}^2{d_2}^3{d_1}^5+\frac{2}{2187}\,{d_3}^2{d_2}^4{d_1}^4-\frac{5}{2187}\,{d_3}^5{d_2}^4d_1-\frac{11}{2187}\,{d_3}^3{d_2}^4{d_1}^3-\frac{1}{1458}\,d_3{d_2}^5{d_1}^2+\frac{26833}{34992}\,{d_1}^2{d_2}^2{d_3}^2-\frac{1895}{2916}\,{d_3}^2d_2{d_1}^3-\frac{17909}{34992}\,{d_3}^3{d_2}^2d_1-\frac{6931}{34992}\,{d_3}^2{d_2}^3d_1+\frac{22255}{34992}\,{d_3}^3d_2{d_1}^2+\frac{1}{729}\,{d_3}^6{d_2}^3d_1-\frac{85}{2592}\,d_3{d_2}^3+\frac{43}{729}-\frac{14}{729}\,{d_3}^4{d_1}^2-\frac{2}{2187}\,{d_3}^2d_2{d_1}^7+\frac{5}{2187}\,{d_3}^3d_2{d_1}^6-\frac{167}{34992}\,d_3d_2-\frac{19}{54}\,{d_3}^2-\frac{49085}{69984}\,d_1d_2+\frac{17143}{34992}\,{d_1}^2-\frac{1465}{34992}\,d_3d_1+\frac{325}{23328}\,{d_2}^2-\frac{9863}{69984}\,{d_3}^2{d_1}^2+\frac{32939}{139968}\,{d_3}^2{d_2}^2-\frac{1}{324}\,{d_3}^6d_2d_1-\frac{139}{1458}\,{d_3}^4{d_2}^2{d_1}^2-\frac{43}{4374}\,{d_3}^2{d_2}^4{d_1}^2+\frac{11}{4374}\,{d_1}^4+1/27\,{d_3}^4+\frac{1}{972}\,{d_3}^2{d_2}^6+\frac{1}{2187}\,{d_3}^4{d_1}^4-\frac{149}{17496}\,{d_3}^2{d_1}^4+\frac{605}{34992}\,d_3{d_1}^3-\frac{95}{8748}\,{d_3}^3{d_1}^3-\frac{1}{1458}\,d_3{d_1}^5-\frac{1}{648}\,{d_3}^5d_1+\frac{11}{4374}\,{d_1}^2{d_2}^4+\frac{1}{648}\,{d_3}^5d_2+\frac{11}{2187}\,d_2{d_1}^5+\frac{1}{648}\,d_3{d_2}^5-\frac{11}{1458}\,{d_1}^4{d_2}^2-\frac{157}{17496}\,{d_3}^4{d_2}^2-\frac{110}{2187}\,{d_3}^2{d_2}^4+\frac{1177}{8748}\,{d_1}^2{d_2}^2-\frac{11}{1944}\,{d_2}^4+\frac{13775}{69984}\,{d_3}^3d_1-\frac{293}{8748}\,d_1{d_2}^3+\frac{95075}{139968}\,{d_3}^2d_2d_1-\frac{31}{4374}\,{d_3}^5{d_2}^3-\frac{20111}{69984}\,{d_3}^3d_2+\frac{1}{1458}\,{d_3}^3{d_2}^5+\frac{25}{8748}\,{d_3}^4{d_2}^4+\frac{395}{5832}\,{d_3}^3{d_2}^3-\frac{1}{2187}\,{d_3}^6{d_2}^4-\frac{1}{2187}\,{d_3}^4{d_2}^6+\frac{1}{4374}\,{d_3}^5{d_1}^3-\frac{1}{4374}\,{d_3}^3{d_1}^5-\frac{1}{2187}\,{d_3}^2{d_1}^6+\frac{2}{2187}\,{d_3}^5{d_2}^5+\frac{1}{324}\,{d_3}^6{d_2}^2+\frac{119}{1944}\,d_2{d_1}^3$
$w\,o\,o$	$-\frac{184}{19683}\,\sqrt{3}(5-4\,d_1d_2-4\,{d_3}^2+8\,{d_1}^2-4\,{d_2}^2-4\,d_3d_1+8\,d_3d_2)$
$w\,o\,\tilde{o}$	0
$w\,o\,p$	0
$w\,o\,q$	0
$w\,o\,r$	$\frac{20}{19683}\,\sqrt{3}(-4\,d_3{d_1}^2-4\,{d_3}^2d_1-8\,d_3{d_2}^2+12\,d_3d_2d_1-12\,{d_1}^2d_2+4\,{d_3}^2d_2+4\,{d_2}^3-59\,d_1-37\,d_2+32\,d_3+8\,{d_1}^3)$
$w\,o\,s$	0
$w\,o\,y$	0
$w\,o\,z$	0
$w\,\tilde{o}\,\tilde{o}$	$-\frac{16}{19683}\,\sqrt{3}(5-4\,d_1d_2-4\,{d_3}^2+8\,{d_1}^2-4\,{d_2}^2-4\,d_3d_1+8\,d_3d_2)$
$w\,\tilde{o}\,p$	0
$w\,\tilde{o}\,q$	0
$w\,\tilde{o}\,r$	0
$w\,\tilde{o}\,s$	0
$w\,\tilde{o}\,y$	0
$w\,\tilde{o}\,z$	0
$w\,p\,p$	$\frac{3200}{19683}\,\sqrt{3}(5-4\,d_1d_2-4\,{d_3}^2+8\,{d_1}^2-4\,{d_2}^2-4\,d_3d_1+8\,d_3d_2)$
$w\,p\,q$	0
$w\,p\,r$	0
$w\,p\,s$	$\frac{400}{19683}\,\sqrt{3}(-4\,d_3{d_1}^2-4\,{d_3}^2d_1-8\,d_3{d_2}^2+12\,d_3d_2d_1-12\,{d_1}^2d_2+4\,{d_3}^2d_2+4\,{d_2}^3-59\,d_1-37\,d_2+32\,d_3+8\,{d_1}^3)$
$w\,p\,y$	0
$w\,p\,z$	0
$w\,q\,q$	$\frac{1}{629856}\,\sqrt{3}(-45056+58801\,d_3d_2{d_1}^2-40661\,d_3d_1{d_2}^2+1260\,{d_3}^4d_2d_1+2552\,d_3d_2{d_1}^4+1260\,d_3d_1{d_2}^4-3044\,d_3{d_2}^2{d_1}^3-632\,d_3{d_2}^3{d_1}^2+5944\,{d_1}^2{d_2}^2{d_3}^2-3044\,{d_3}^2d_2{d_1}^3-1816\,{d_3}^3{d_2}^2d_1-1816\,{d_3}^2{d_2}^3d_1-632\,{d_3}^3d_2{d_1}^2+35674\,d_3{d_2}^3-104\,{d_3}^4{d_1}^2-91172\,d_3d_2+44984\,{d_3}^2+82216\,d_1d_2+20528\,{d_1}^2+82216\,d_3d_1+44984\,{d_2}^2+34764\,{d_3}^2{d_1}^2-60455\,{d_3}^2{d_2}^2-1644\,{d_1}^4-5024\,{d_3}^4+72\,{d_3}^2{d_1}^4-30230\,d_3{d_1}^3+32\,{d_1}^6+376\,{d_3}^3{d_1}^3-256\,d_3{d_1}^5-120\,{d_3}^5d_1-104\,{d_1}^2{d_2}^4+120\,{d_3}^5d_2-256\,d_2{d_1}^5-120\,d_1{d_2}^5+120\,d_3{d_2}^5+72\,{d_1}^4{d_2}^2-1156\,{d_3}^4{d_2}^2-1156\,{d_3}^2{d_2}^4+34764\,{d_1}^2{d_2}^2-5024\,{d_2}^4+7126\,{d_3}^3d_1+7126\,d_1{d_2}^3-40661\,{d_3}^2d_2d_1+35674\,{d_3}^3d_2+376\,{d_2}^3{d_1}^3+2072\,{d_3}^3{d_2}^3-30230\,d_2{d_1}^3)$
$w\,q\,r$	$\frac{11}{629856}\,\sqrt{3}(123\,d_3d_2d_1-84\,{d_3}^3d_2d_1-376\,d_3{d_2}^2{d_1}^2+120\,d_3{d_2}^3d_1+204\,d_3d_2{d_1}^3+32\,{d_3}^2d_2{d_1}^2+120\,{d_3}^2d_1{d_2}^2-3029\,{d_1}^2d_2-971\,d_3{d_2}^2-138\,{d_3}^2d_1-1056\,d_3{d_1}^2+954\,{d_3}^2d_2-128\,{d_3}^2{d_2}^3+112\,{d_2}^3+8\,{d_3}^3{d_1}^2+3195\,d_1{d_2}^2-24\,{d_3}^2{d_1}^3+8\,{d_1}^2{d_2}^3-60\,d_1{d_2}^4-144\,{d_1}^4d_2+180\,{d_2}^2{d_1}^3+8\,{d_3}^4d_1+60\,d_3{d_2}^4-8\,d_3{d_1}^4+970\,{d_1}^3-4040\,d_1-1780\,d_2-160\,{d_3}^3-8\,{d_3}^4d_2+76\,{d_3}^3{d_2}^2+16\,{d_1}^5+1400\,d_3)$

Table A.3: The cubic couplings for all of the fields in the action up to level 3 (continued).

$l\,m\,n$	$B_{lmn}(d_1,d_2,d_3)$
$w\,q\,s$	$-\frac{125}{1259712}\sqrt{3}(123\,d_3d_2d_1 - 84\,{d_3}^3d_2d_1 - 376\,d_3{d_2}^2{d_1}^2 + 120\,d_3{d_2}^3d_1 + 204\,d_3d_2{d_1}^3 + 32\,{d_3}^2d_2{d_1}^2 + 120\,{d_3}^2d_1{d_2}^2 - 3029\,d_3{d_1}^2d_2 - 971\,d_3{d_2}^2 - 138\,{d_3}^2d_1 - 1056\,d_3{d_1}^2 + 954\,{d_3}^2d_2 - 128\,{d_3}^2{d_2}^3 + 112\,{d_2}^3 + 8\,{d_3}^3{d_1}^2 + 3195\,d_1{d_2}^2 - 24\,{d_3}^2{d_1}^3 + 8\,{d_1}^2{d_2}^3 - 60\,d_1{d_2}^4 - 144\,{d_1}^4d_2 + 180\,{d_2}^2{d_1}^3 + 8\,{d_3}^4d_1 + 60\,d_3{d_2}^4 - 8\,d_3{d_1}^4 + 970\,{d_1}^3 - 4040\,d_1 - 1780\,d_2 - 160\,{d_3}^3 - 8\,{d_3}^4d_2 + 76\,{d_3}^3{d_2}^2 + 16\,{d_1}^5 + 1400\,d_3)$
$w\,q\,y$	$\frac{1}{1259712}\sqrt{3}(111689\,d_3d_2d_1 - 2000\,{d_3}^2{d_2}^2{d_1}^3 + 672\,{d_3}^5d_2d_1 + 4624\,{d_3}^3{d_2}^2{d_1}^2 - 448\,{d_2}^5 + 5056\,d_3{d_2}^3{d_1}^3 - 240\,d_3d_1{d_2}^5 + 368\,d_3d_2{d_1}^5 + 2256\,{d_3}^2{d_1}^4d_2 + 2704\,{d_3}^2d_1{d_2}^4 - 3024\,d_3{d_2}^2{d_1}^4 - 896\,{d_3}^4{d_2}^2d_1 - 2000\,{d_3}^3d_2{d_1}^3 - 2432\,{d_3}^2{d_2}^3{d_1}^2 - 2432\,d_3{d_2}^4{d_1}^2 + 27404\,{d_3}^3d_2d_1 + 106348\,d_3{d_2}^2{d_1}^2 + 7960\,d_3{d_2}^3d_1 - 81468\,d_3d_2{d_1}^3 + 54572\,{d_3}^2d_2{d_1}^2 - 114280\,{d_3}^2d_1{d_2}^2 + 129817\,{d_1}^2d_2 - 2713\,d_3{d_2}^2 + 5010\,{d_3}^2d_1 + 60576\,d_3{d_1}^2 + 64\,{d_1}^7 + 1280\,{d_3}^5 + 17182\,{d_3}^2d_2 + 27708\,{d_3}^2{d_2}^3 + 76128\,{d_2}^3 + 560\,{d_3}^3{d_1}^2 - 98631\,d_1{d_2}^2 + 6784\,{d_3}^2{d_1}^3 - 36628\,{d_1}^2{d_2}^3 + 20120\,d_1{d_2}^4 + 2860\,{d_1}^4d_2 + 14392\,{d_2}^2{d_1}^3 - 4440\,{d_3}^4d_1 - 18968\,d_3{d_2}^4 - 3888\,d_3{d_1}^4 - 53650\,{d_1}^3 - 272\,{d_3}^2{d_2}^5 - 640\,{d_3}^5{d_2}^2 - 256\,{d_3}^2{d_1}^5 - 32\,{d_3}^5{d_1}^2 - 240\,d_1{d_2}^6 + 512\,{d_1}^2{d_2}^5 - 704\,d_2{d_1}^6 + 1936\,{d_1}^5{d_2}^2 - 1936\,{d_3}^3{d_2}^3d_1 + 129896\,d_1 - 278012\,d_2 - 24224\,{d_3}^3 - 3368\,{d_3}^4d_2 - 6204\,{d_3}^3{d_2}^2 - 64\,{d_3}^6d_1 + 64\,{d_3}^6d_2 + 240\,d_3{d_2}^6 + 32\,d_3{d_1}^6 - 656\,{d_3}^4d_2{d_1}^2 - 296\,{d_1}^5 + 55592\,d_3 - 1984\,{d_2}^3{d_1}^4 + 416\,{d_2}^4{d_1}^3 + 256\,{d_3}^4{d_1}^3 - 688\,{d_3}^3{d_2}^4 + 1296\,{d_3}^4{d_2}^3)$
$w\,q\,z$	$\frac{1}{629856}\sqrt{3}(144870\,d_3d_2d_1 + 15160\,{d_3}^2{d_2}^2{d_1}^3 + 6108\,{d_3}^5d_2d_1 + 33972\,{d_3}^3{d_2}^2{d_1}^2 + 1128\,d_3{d_2}^3{d_1}^3 - 360\,d_3d_1{d_2}^5 - 768\,d_3d_2{d_1}^5 + 2596\,{d_3}^2{d_1}^4d_2 + 20600\,{d_3}^2d_1{d_2}^4 + 216\,d_3{d_2}^2{d_1}^4 - 19920\,{d_3}^4{d_2}^2d_1 - 18920\,{d_3}^3d_2{d_1}^3 - 38084\,{d_3}^2{d_2}^3{d_1}^2 - 312\,d_3{d_2}^4{d_1}^2 + 1936\,{d_3}^2{d_2}^2{d_1}^5 + 1504\,{d_3}^4{d_2}^4d_1 - 240\,{d_3}^2{d_2}^6d_1 + 320\,{d_3}^4d_2{d_1}^4 + 512\,{d_3}^2{d_2}^5{d_1}^2 + 128\,{d_3}^4{d_2}^2{d_1}^3 + 96\,{d_3}^6{d_2}^2d_1 + 416\,{d_3}^2{d_2}^4{d_1}^3 + 880\,{d_3}^3d_2{d_1}^5 - 1984\,{d_3}^2{d_2}^3{d_1}^4 - 2224\,{d_3}^3{d_2}^4{d_1}^2 - 1344\,{d_3}^4{d_2}^3{d_1}^2 + 4304\,{d_3}^3{d_2}^3{d_1}^3 - 704\,{d_3}^2d_2{d_1}^6 - 3168\,{d_3}^3{d_2}^2{d_1}^4 + 1008\,{d_3}^5{d_2}^2{d_1}^2 - 400\,{d_3}^5d_2{d_1}^3 - 944\,{d_3}^5{d_2}^3d_1 - 96\,{d_3}^6d_2{d_1}^2 + 81567\,{d_3}^3d_2d_1 + 112564\,d_3{d_2}^2{d_1}^2 + 18738\,d_3{d_2}^3d_1 - 95178\,d_3d_2{d_1}^3 + 133801\,{d_3}^2d_2{d_1}^2 - 252969\,{d_3}^2d_1{d_2}^2 + 68686\,{d_1}^2d_2 + 15514\,d_3{d_2}^2 - 77820\,{d_3}^2d_1 + 128336\,d_3{d_1}^2 + 4320\,{d_3}^5 - 106416\,{d_3}^2d_2 + 43006\,{d_3}^2{d_2}^3 + 57184\,{d_2}^3 - 43244\,{d_3}^3{d_1}^2 + 11886\,d_1{d_2}^2 + 19618\,{d_3}^2{d_1}^3 - 176\,{d_1}^2{d_2}^3 + 1320\,d_1{d_2}^4 + 3168\,{d_1}^4d_2 - 3960\,{d_2}^2{d_1}^3 + 4894\,{d_3}^4d_1 - 16392\,d_3{d_2}^4 - 4756\,d_3{d_1}^4 - 65372\,{d_1}^3 - 88\,{d_3}^2{d_2}^5 - 4020\,{d_3}^5{d_2}^2 - 184\,{d_3}^2{d_1}^5 - 2088\,{d_3}^5{d_1}^2 - 5140\,{d_3}^3{d_2}^3d_1 + 189104\,d_1 - 148040\,d_2 + 6168\,{d_3}^3 - 28846\,{d_3}^4d_2 + 22877\,{d_3}^3{d_2}^2 - 824\,{d_3}^3{d_1}^4 - 216\,{d_3}^6d_1 + 216\,{d_3}^6d_2 + 96\,d_3{d_1}^6 + 5520\,{d_3}^4d_2{d_1}^2 - 352\,{d_1}^5 + 32\,{d_3}^5{d_1}^4 - 512\,{d_3}^4{d_2}^5 + 304\,{d_3}^5{d_2}^4 + 240\,{d_3}^3{d_2}^6 - 32\,{d_3}^6{d_2}^3 - 96\,{d_3}^4{d_1}^5 - 32\,{d_3}^3{d_1}^6 + 32\,{d_3}^6{d_1}^3 + 64\,{d_3}^2{d_1}^7 - 29904\,d_3 + 1680\,{d_3}^4{d_1}^3 - 9088\,{d_3}^3{d_2}^4 + 12720\,{d_3}^4{d_2}^3)$
$w\,r\,r$	$\frac{19}{209952}\sqrt{3}(4\,d_1{d_2}^3 + 108 - 4\,{d_3}^3d_2 + 4\,{d_3}^3d_1 + 75\,d_1d_2 - 8\,{d_3}^2d_2d_1 - 12\,d_2{d_1}^3 + 8\,{d_3}^2{d_2}^2 + 8\,{d_1}^4 - 4\,d_3{d_2}^3 - 16\,{d_3}^2 - 155\,{d_1}^2 - 16\,{d_2}^2 + 24\,d_3d_2{d_1}^2 + 75\,d_3d_1 + 37\,d_3d_2 - 12\,d_3{d_1}^3 - 8\,d_3d_1{d_2}^2)$
$w\,r\,s$	$-\frac{1375}{1259712}\sqrt{3}(4\,d_1{d_2}^3 + 108 - 4\,{d_3}^3d_2 + 4\,{d_3}^3d_1 + 75\,d_1d_2 - 8\,{d_3}^2d_2d_1 - 12\,d_2{d_1}^3 + 8\,{d_3}^2{d_2}^2 + 8\,{d_1}^4 - 4\,d_3{d_2}^3 - 16\,{d_3}^2 - 155\,{d_1}^2 - 16\,{d_2}^2 + 24\,d_3d_2{d_1}^2 + 75\,d_3d_1 + 37\,d_3d_2 - 12\,d_3{d_1}^3 - 8\,d_3d_1{d_2}^2)$
$w\,r\,y$	$\frac{11}{1259712}\sqrt{3}(3876 - 5244\,d_3d_2{d_1}^2 + 920\,d_3d_1{d_2}^2 + 64\,{d_3}^4d_2d_1 + 176\,d_3d_2{d_1}^4 + 16\,d_3d_1{d_2}^4 - 320\,d_3{d_2}^2{d_1}^3 + 160\,d_3{d_2}^3d_1^2 + 160\,{d_1}^2{d_2}^2{d_3}^2 + 112\,{d_3}^2d_2{d_1}^3 + 112\,{d_3}^3{d_2}^2d_1 - 176\,{d_3}^2{d_2}^3d_1 - 272\,{d_3}^3d_2{d_1}^2 - 24\,d_3{d_2}^3 + 16\,{d_3}^4{d_1}^2 + 2967\,d_3d_2 - 2576\,{d_3}^2 - 7159\,d_1d_2 + 3959\,{d_1}^2 - 4455\,d_3d_1 - 928\,{d_2}^2 - 1980\,{d_3}^2{d_1}^2 + 812\,{d_3}^2{d_2}^2 - 1684\,{d_1}^4 + 128\,{d_3}^4 - 112\,{d_3}^2{d_1}^4 + 3580\,d_3{d_1}^3 + 32\,{d_1}^6 + 112\,{d_3}^3{d_1}^3 - 16\,d_3{d_1}^5 - 32\,{d_3}^5d_1 - 32\,{d_1}^2{d_2}^4 + 32\,{d_3}^5d_2 - 112\,d_2{d_1}^5 + 16\,d_1{d_2}^5 - 16\,d_3{d_2}^5 + 128\,{d_1}^4{d_2}^2 - 80\,{d_3}^4{d_2}^2 + 16\,{d_3}^2{d_2}^4 - 1668\,{d_1}^2{d_2}^2 + 64\,{d_2}^4 - 44\,{d_3}^3d_1 - 104\,d_1{d_2}^3 + 2832\,{d_3}^2d_2d_1 - 980\,{d_3}^3d_2 - 32\,{d_2}^3{d_1}^3 + 48\,{d_3}^3{d_2}^3 + 3392\,d_2{d_1}^3)$
$w\,r\,z$	$\frac{11}{629856}\sqrt{3}(-648 - 3696\,d_3d_2{d_1}^2 - 238\,d_3d_1{d_2}^2 + 600\,{d_3}^4d_2d_1 - 24\,d_3d_2{d_1}^4 + 24\,d_3d_1{d_2}^4 - 72\,d_3{d_2}^2{d_1}^3 + 24\,d_3{d_2}^3d_1^2 - 32\,{d_3}^2{d_2}^3{d_1}^3 + 96\,{d_3}^4{d_2}^2{d_1}^2 - 96\,{d_3}^4{d_2}^3d_1 - 272\,{d_3}^3{d_2}^2{d_1}^3 + 144\,{d_3}^3{d_2}^3{d_1}^2 - 32\,{d_3}^4d_2{d_1}^3 - 112\,{d_3}^2{d_2}^2{d_1}^5 - 32\,{d_3}^2{d_2}^4{d_1}^2 + 48\,{d_3}^5{d_2}^2d_1 + 192\,{d_3}^3d_2{d_1}^4 + 16\,{d_3}^2{d_2}^5d_1 + 128\,{d_3}^2{d_1}^4{d_2}^2 - 48\,{d_3}^5d_2{d_1}^2 - 1572\,{d_1}^2{d_2}^2{d_3}^2 + 3344\,{d_3}^2d_2{d_1}^3 + 1116\,{d_3}^3{d_2}^2d_1 - 136\,{d_3}^2{d_2}^3d_1 - 2940\,{d_3}^3d_2{d_1}^2 - 392\,d_3{d_2}^3 - 168\,{d_3}^4{d_1}^2 + 3386\,d_3d_2 + 252\,{d_3}^2 - 1906\,d_1d_2 - 4270\,{d_1}^2 - 5834\,d_3d_1 + 608\,{d_2}^2 + 5547\,{d_3}^2{d_1}^2 + 238\,{d_3}^2{d_2}^2 - 176\,{d_1}^4 + 432\,{d_3}^4 - 1676\,{d_3}^2{d_1}^4 + 3174\,d_3{d_1}^3 + 1520\,{d_3}^3{d_1}^3 - 16\,{d_3}^5{d_2}^3 - 48\,{d_3}^3{d_1}^5 - 16\,{d_3}^3{d_2}^5 + 32\,{d_3}^4{d_2}^4 + 32\,{d_3}^2{d_1}^6 + 48\,d_3{d_1}^5 - 108\,{d_3}^5d_1 + 108\,{d_3}^5d_2 - 432\,{d_3}^4{d_2}^2 + 40\,{d_3}^2{d_2}^4 - 2593\,{d_3}^3d_1 - 88\,d_1{d_2}^3 - 1849\,{d_3}^2d_2d_1 - 623\,{d_3}^3d_2 + 16\,{d_3}^5{d_1}^3 + 304\,{d_3}^3{d_2}^3 + 264\,d_2{d_1}^3)$
$w\,s\,s$	$\frac{9475}{839808}\sqrt{3}(4\,d_1{d_2}^3 + 108 - 4\,{d_3}^3d_2 + 4\,{d_3}^3d_1 + 75\,d_1d_2 - 8\,{d_3}^2d_2d_1 - 12\,d_2{d_1}^3 + 8\,{d_3}^2{d_2}^2 + 8\,{d_1}^4 - 4\,d_3{d_2}^3 - 16\,{d_3}^2 - 155\,{d_1}^2 - 16\,{d_2}^2 + 24\,d_3d_2{d_1}^2 + 75\,d_3d_1 + 37\,d_3d_2 - 12\,d_3{d_1}^3 - 8\,d_3d_1{d_2}^2)$

Table A.3: The cubic couplings for all of the fields in the action up to level 3 (continued).

$l\,m\,n$	$B_{lmn}(d_1,d_2,d_3)$
$w\ s\ y$	$-\frac{125}{2519424}\sqrt{3}(3876 - 5244\,d_3d_2{d_1}^2 + 920\,d_3d_1{d_2}^2 + 64\,{d_3}^4d_2d_1 + 176\,d_3d_2{d_1}^4 + 16\,d_3d_1{d_2}^4 - 320\,d_3{d_2}^2{d_1}^3 + 160\,d_3{d_2}^3{d_1}^2 + 160\,{d_1}^2{d_2}^2{d_3}^2 + 112\,{d_3}^2d_2{d_1}^3 + 112\,{d_3}^3{d_2}^2d_1 - 176\,{d_3}^2{d_2}^3d_1 - 272\,{d_3}^3d_2{d_1}^2 - 24\,d_3{d_2}^3 + 16\,{d_3}^4{d_1}^2 + 2967\,d_3d_2 - 2576\,{d_3}^2 - 7159\,d_1d_2 + 3959\,{d_1}^2 - 4455\,d_3d_1 - 928\,{d_2}^2 - 1980\,{d_3}^2{d_1}^2 + 812\,{d_3}^2{d_2}^2 - 1684\,{d_1}^4 + 128\,{d_3}^4 - 112\,{d_3}^2{d_1}^4 + 3580\,d_3{d_1}^3 + 32\,{d_1}^6 + 112\,{d_3}^3{d_1}^3 - 16\,d_3{d_1}^5 - 32\,{d_3}^5d_1 - 32\,{d_1}^2{d_2}^4 + 32\,{d_3}^5d_2 - 112\,d_2{d_1}^5 + 16\,d_1{d_2}^5 - 16\,d_3{d_2}^5 + 128\,{d_1}^4{d_2}^2 - 80\,{d_3}^4{d_2}^2 + 16\,{d_3}^2{d_2}^4 - 1668\,{d_1}^2{d_2}^2 + 64\,{d_2}^4 - 44\,{d_3}^3d_1 - 104\,d_1{d_2}^3 + 2832\,{d_3}^2d_2d_1 - 980\,{d_3}^3d_2 - 32\,{d_2}^3{d_1}^3 + 48\,{d_3}^3{d_2}^3 + 3392\,d_2{d_1}^3)$
$w\ s\ z$	$-\frac{125}{1259712}\sqrt{3}(-648 - 3696\,d_3d_2{d_1}^2 - 238\,d_3d_1{d_2}^2 - 32\,{d_3}^2{d_2}^3{d_1}^3 + 96\,{d_3}^4{d_2}^2{d_1}^2 - 96\,{d_3}^4{d_2}^3d_1 - 272\,{d_3}^3{d_2}^2{d_1}^3 + 144\,{d_3}^3{d_2}^3{d_1}^2 - 32\,{d_3}^4d_2{d_1}^3 - 112\,{d_3}^2d_2{d_1}^5 - 32\,{d_3}^2{d_2}^4{d_1}^2 + 48\,{d_3}^5{d_2}^2d_1 + 192\,{d_3}^3d_2{d_1}^4 + 16\,{d_3}^2{d_2}^5d_1 + 128\,{d_3}^2{d_1}^4{d_2}^2 - 48\,{d_3}^5d_2{d_1}^2 + 600\,{d_3}^4d_2d_1 - 24\,d_3d_2{d_1}^4 + 24\,d_3d_1{d_2}^4 - 72\,d_3d_2{d_1}^3 + 24\,d_3{d_2}^3{d_1}^2 - 1572\,{d_1}^2{d_2}^2{d_3}^2 + 3344\,{d_3}^2d_2{d_1}^3 + 1116\,{d_3}^3{d_2}^2d_1 - 136\,{d_3}^2{d_2}^3d_1 - 2940\,{d_3}^3d_2{d_1}^2 - 392\,d_3{d_2}^3 - 168\,{d_3}^4{d_1}^2 + 3386\,d_3d_2 + 252\,{d_3}^2 - 1906\,d_1d_2 - 4270\,{d_1}^2 - 5834\,d_3d_1 + 608\,{d_2}^2 + 5547\,{d_3}^2{d_1}^2 + 238\,{d_3}^2{d_2}^2 - 176\,{d_1}^4 + 432\,{d_3}^4 - 1676\,{d_3}^2{d_1}^4 + 3174\,d_3{d_1}^3 - 48\,{d_3}^3{d_1}^5 - 16\,{d_3}^5{d_2}^3 + 1520\,{d_3}^3{d_1}^3 + 16\,{d_3}^5{d_1}^3 + 48\,d_3{d_1}^5 - 108\,{d_3}^5d_1 + 108\,{d_3}^5d_2 - 432\,{d_3}^4{d_2}^2 + 40\,{d_3}^2{d_2}^4 + 32\,{d_3}^2{d_1}^6 - 2593\,{d_3}^3d_1 - 88\,d_1{d_2}^3 - 1849\,{d_3}^2d_2d_1 + 32\,{d_3}^4{d_2}^4 - 623\,{d_3}^3d_2 + 304\,{d_3}^3{d_2}^3 - 16\,{d_3}^3{d_2}^5 + 264\,d_2{d_1}^3)$
$w\ y\ y$	$\frac{1}{2519424}\sqrt{3}(195084 + 703936\,d_3d_2{d_1}^2 - 244800\,d_3d_1{d_2}^2 - 3648\,{d_3}^2{d_2}^3{d_1}^3 - 1536\,{d_3}^4{d_2}^2{d_1}^2 - 1472\,{d_3}^4{d_2}^3d_1 - 3648\,{d_3}^3{d_2}^2{d_1}^3 + 5504\,{d_3}^3{d_2}^3{d_1}^2 + 3392\,{d_3}^4d_2{d_1}^3 - 1920\,{d_3}^2d_2{d_1}^5 - 1536\,{d_3}^2{d_2}^4{d_1}^2 + 1728\,{d_3}^5{d_2}^2d_1 - 1280\,{d_3}^3d_2{d_1}^4 + 1728\,{d_3}^2{d_2}^5d_1 + 5760\,{d_3}^2{d_1}^4{d_2}^2 - 1536\,{d_3}^5d_2{d_1}^2 - 5904\,{d_3}^4d_2d_1 - 88512\,d_3d_2{d_1}^4 - 5904\,d_3d_1{d_2}^4 + 67056\,d_3{d_2}^2{d_1}^3 - 528\,d_3{d_2}^3{d_1}^2 + 1664\,d_3d_2{d_1}^6 - 128\,{d_3}^6d_2d_1 + 3392\,d_3{d_2}^4{d_1}^3 - 1472\,{d_3}^3{d_2}^4d_1 - 1280\,d_3{d_2}^3{d_1}^4 - 1920\,d_3{d_2}^2{d_1}^5 - 128\,d_3d_1{d_2}^6 - 1536\,d_3{d_2}^5{d_1}^2 - 65808\,{d_1}^2{d_2}^2{d_3}^2 + 67056\,{d_3}^2d_2{d_1}^3 + 9504\,{d_3}^3{d_2}^2d_1 + 9504\,{d_3}^2{d_2}^3d_1 - 528\,{d_3}^3d_2{d_1}^2 - 28096\,d_3{d_2}^3 - 6624\,{d_3}^4{d_1}^2 + 157821\,d_3d_2 - 285952\,{d_3}^2 + 718979\,d_1d_2 - 860035\,{d_1}^2 + 718979\,d_3d_1 - 285952\,{d_2}^2 + 275712\,{d_3}^2{d_1}^2 + 73472\,{d_3}^2{d_2}^2 - 192\,{d_3}^6{d_2}^2 + 231616\,{d_1}^4 - 192\,{d_3}^2{d_2}^6 + 22464\,{d_3}^4 + 192\,{d_2}^5{d_1}^3 + 1280\,{d_1}^5{d_2}^3 - 1280\,{d_2}^4{d_1}^4 - 1280\,{d_3}^4{d_1}^4 + 320\,{d_1}^2{d_2}^6 - 320\,{d_1}^7d_2 + 128\,{d_3}^7d_2 - 128\,{d_3}^7d_1 - 320\,d_3{d_1}^7 - 192\,{d_2}^2{d_1}^6 - 128\,d_1{d_2}^7 + 128\,d_3{d_2}^7 + 320\,{d_3}^6{d_1}^2 - 21744\,{d_3}^2{d_1}^4 - 455616\,d_3{d_1}^3 - 512\,{d_2}^6 + 1280\,{d_3}^3{d_1}^5 + 128\,{d_1}^8 - 512\,{d_3}^6 - 13040\,{d_1}^6 - 384\,{d_3}^5{d_2}^3 + 4336\,{d_3}^3{d_1}^3 + 192\,{d_3}^5{d_1}^3 + 31968\,d_3{d_1}^5 + 5616\,{d_3}^5d_1 - 6624\,{d_1}^2{d_2}^4 - 4080\,{d_3}^5d_2 + 31968\,d_2{d_1}^5 + 5616\,d_1{d_2}^5 - 4080\,d_3{d_2}^5 - 21744\,{d_1}^4{d_2}^2 + 10992\,{d_3}^4{d_2}^2 + 10992\,{d_3}^2{d_2}^4 + 275712\,{d_1}^2{d_2}^2 + 22464\,{d_2}^4 - 192\,{d_3}^2{d_1}^6 - 74176\,{d_3}^3d_1 - 74176\,d_1{d_2}^3 - 244800\,{d_3}^2d_2d_1 + 896\,{d_3}^4{d_2}^4 - 28096\,{d_3}^3d_2 + 4336\,{d_2}^3{d_1}^3 - 12800\,{d_3}^3{d_2}^3 - 384\,{d_3}^3{d_2}^5 - 455616\,d_2{d_1}^3)$
$w\ y\ z$	$\frac{1}{1259712}\sqrt{3}(-176856 + 377992\,d_3d_2{d_1}^2 - 203946\,d_3d_1{d_2}^2 + 4496\,{d_3}^2{d_2}^3{d_1}^3 - 37728\,{d_3}^4{d_2}^2{d_1}^2 - 12240\,{d_3}^4{d_2}^3d_1 + 53648\,{d_3}^3{d_2}^2{d_1}^3 - 2736\,{d_3}^3{d_2}^3{d_1}^2 + 61760\,{d_3}^4d_2{d_1}^3 + 32192\,{d_3}^2d_2{d_1}^5 - 7712\,{d_3}^2{d_2}^4{d_1}^2 + 17520\,{d_3}^5{d_2}^2d_1 - 80128\,{d_3}^3d_2{d_1}^4 + 5872\,{d_3}^2{d_2}^5d_1 - 21136\,{d_3}^2{d_1}^4{d_2}^2 - 15456\,{d_3}^5d_2{d_1}^2 - 108136\,{d_3}^4d_2d_1 - 15536\,d_3d_2{d_1}^4 - 14728\,d_3d_1{d_2}^4 + 17888\,d_3{d_2}^2{d_1}^3 + 7664\,d_3{d_2}^3{d_1}^2 + 96\,d_3d_2{d_1}^6 - 1968\,{d_3}^6d_2d_1 + 768\,d_3{d_2}^4{d_1}^3 + 3808\,{d_3}^3{d_2}^4d_1 - 768\,d_3{d_2}^2{d_1}^5 - 192\,d_3d_1{d_2}^6 - 96\,d_3{d_2}^5{d_1}^2 + 96608\,{d_1}^2{d_2}^2{d_3}^2 - 278480\,{d_3}^2d_2{d_1}^3 - 46348\,{d_3}^3{d_2}^2d_1 - 76208\,{d_3}^2{d_2}^3d_1 + 407648\,{d_3}^3d_2{d_1}^2 - 78760\,d_3{d_2}^3 + 130748\,{d_3}^4{d_1}^2 - 192\,{d_3}^7{d_1}^2d_2 - 320\,{d_3}^2d_2{d_1}^7 + 1600\,{d_3}^3d_2{d_1}^6 - 128\,{d_3}^2{d_2}^7d_1 + 320\,{d_3}^6d_2{d_1}^3 - 1280\,{d_3}^3{d_2}^3{d_1}^4 + 896\,{d_3}^5d_2{d_1}^4 + 2240\,{d_3}^5{d_2}^3{d_1}^2 - 192\,{d_3}^6{d_2}^2{d_1}^2 + 192\,{d_3}^2{d_2}^5{d_1}^3 - 2112\,{d_3}^4{d_2}^3{d_1}^3 - 192\,{d_3}^2{d_2}^2{d_1}^6 - 1408\,{d_3}^3{d_2}^2{d_1}^5 + 3712\,{d_3}^4{d_2}^2{d_1}^4 - 2112\,{d_3}^5{d_2}^2{d_1}^3 - 1472\,{d_3}^3{d_2}^5{d_1}^2 + 320\,{d_3}^2{d_2}^6{d_1}^2 - 2304\,{d_3}^4d_2{d_1}^5 + 1088\,{d_3}^4{d_2}^5d_1 - 576\,{d_3}^4{d_2}^4{d_1}^2 + 1280\,{d_3}^2{d_2}^3{d_1}^5 - 1280\,{d_3}^2{d_2}^4{d_1}^4 - 1088\,{d_3}^5{d_2}^4d_1 + 2880\,{d_3}^3{d_2}^4{d_1}^3 + 192\,{d_3}^7{d_2}^2d_1 - 64\,{d_3}^6{d_2}^3d_1 + 168830\,d_3d_2 - 68364\,{d_3}^2 + 385754\,d_1d_2 + 62150\,{d_1}^2 + 289906\,d_3d_1 - 36256\,{d_2}^2 - 690639\,{d_3}^2{d_1}^2 - 99166\,{d_3}^2{d_2}^2 + 240\,{d_3}^6{d_2}^2 + 2232\,{d_1}^4 - 320\,{d_3}^2{d_2}^6 + 96\,{d_3}^4 - 24144\,{d_3}^4{d_1}^4 + 432\,{d_3}^7d_2 - 432\,{d_3}^7d_1 + 192\,d_3{d_1}^7 + 1728\,{d_3}^6{d_1}^2 + 231800\,{d_3}^2{d_1}^4 - 132150\,d_3{d_1}^3 + 32208\,{d_3}^3{d_1}^5 + 64\,{d_3}^6{d_2}^4 + 128\,{d_3}^3{d_2}^7 - 320\,{d_3}^4{d_2}^6 - 64\,{d_3}^7{d_2}^3 + 192\,{d_3}^5{d_2}^5 - 448\,{d_3}^3{d_1}^7 + 64\,{d_3}^7{d_1}^3 + 512\,{d_3}^4{d_1}^6 - 128\,{d_3}^6{d_1}^4 - 128\,{d_3}^5{d_1}^5 - 1728\,{d_3}^6 - 704\,{d_1}^6 - 5904\,{d_3}^5{d_2}^3 - 376436\,{d_3}^3{d_1}^3 + 3840\,{d_3}^5{d_1}^3 + 1576\,d_3{d_1}^5 - 1768\,{d_3}^5d_1 - 352\,{d_1}^2{d_2}^4 + 5992\,{d_3}^5d_2 + 352\,d_2{d_1}^5 + 704\,d_1{d_2}^5 + 3136\,d_3{d_2}^5 + 2464\,{d_1}^4{d_2}^2 - 25876\,{d_3}^4{d_2}^2 + 26280\,{d_3}^2{d_2}^4 + 135720\,{d_1}^2{d_2}^2 - 4864\,{d_2}^4 - 13392\,{d_3}^2{d_1}^6 + 446781\,{d_3}^3d_1 + 32712\,d_1{d_2}^3 + 109357\,{d_3}^2d_2d_1 + 12352\,{d_3}^4{d_2}^4 + 99\,{d_3}^3d_2 - 2464\,{d_2}^3{d_1}^3 + 128\,{d_3}^2{d_1}^8 + 15904\,{d_3}^3{d_2}^3 - 6800\,{d_3}^3{d_2}^5 - 165800\,d_2{d_1}^3)$

Table A.3: The cubic couplings for all of the fields in the action up to level 3 (continued).

$l\,m\,n$	$B_{lmn}(d_1,d_2,d_3)$
$w\,z\,z$	$\frac{1}{629856}\sqrt{3}(-149712+596880\,d_3d_2{d_1}^2-628238\,d_3d_1{d_2}^2-346172\,{d_3}^2{d_2}^3{d_1}^3+128276\,{d_3}^4{d_2}^2{d_1}^2-127212\,{d_3}^4{d_2}^3d_1-346172\,{d_3}^3{d_2}^2{d_1}^3+446544\,{d_3}^3{d_2}^3{d_1}^2+5744\,{d_3}^4d_2{d_1}^3+1912\,{d_3}^2{d_2}^2{d_1}^5+128276\,{d_3}^2{d_2}^4{d_1}^2+9560\,{d_3}^5{d_2}^2d_1-6696\,{d_3}^3d_2{d_1}^4+9560\,{d_3}^2{d_2}^5d_1+231632\,{d_3}^2{d_1}^4{d_2}^2-5208\,{d_3}^5d_2{d_1}^2-4662\,{d_3}^4d_2d_1-13740\,d_3d_2{d_1}^4-4662\,d_3d_1{d_2}^4+88710\,d_3d_2{d_2}^2{d_1}^3-71196\,d_3{d_2}^3{d_1}^2+288\,d_3d_2{d_1}^6-648\,{d_3}^6d_2d_1+5744\,d_3{d_2}^4{d_1}^3-127212\,{d_3}^3{d_2}^4d_1-6696\,d_3{d_2}^3{d_1}^4+1912\,d_3{d_2}^2{d_1}^5-648\,d_3d_1{d_2}^6-5208\,d_3{d_2}^5{d_1}^2-256\,{d_3}^5{d_2}^6d_1-448\,{d_3}^2{d_2}^3{d_1}^7+64\,{d_3}^2{d_2}^7{d_1}^3+96\,d_3{d_2}^6{d_1}^3-192\,{d_3}^3{d_2}^7{d_1}^2+192\,{d_3}^4{d_2}^7d_1-970623\,{d_1}^2{d_2}^2{d_3}^2+88710\,{d_3}^2d_2{d_1}^3+527771\,{d_3}^3{d_2}^2d_1+527771\,{d_3}^2{d_2}^3d_1-71196\,{d_3}^3d_2{d_1}^2+39890\,d_3{d_2}^3+6768\,{d_3}^4{d_1}^2-448\,{d_3}^3{d_2}^2{d_1}^7+192\,{d_3}^2d_2{d_1}^7-96\,{d_3}^3d_2{d_1}^6-432\,{d_3}^2{d_2}^7d_1+96\,{d_3}^6d_2{d_1}^3-77424\,{d_3}^3{d_2}^3{d_1}^4+96\,{d_3}^5d_2{d_1}^4-10896\,{d_3}^5{d_2}^3{d_1}^2+1440\,{d_3}^6{d_2}^2{d_1}^2+3520\,{d_3}^2{d_2}^5{d_1}^3+57024\,{d_3}^4{d_2}^3{d_1}^3-13744\,{d_3}^2{d_2}^2{d_1}^6+32208\,{d_3}^3{d_2}^2{d_1}^5-23184\,{d_3}^4{d_2}^2{d_1}^4+3520\,{d_3}^5{d_2}^2{d_1}^3-10896\,{d_3}^3{d_2}^5{d_1}^2+1440\,{d_3}^2{d_2}^6{d_1}^2-288\,{d_3}^4d_2{d_1}^5+7488\,{d_3}^4{d_2}^5d_1-40752\,{d_3}^4{d_2}^4{d_1}^2+32208\,{d_3}^2{d_2}^3{d_1}^5-23184\,{d_3}^2{d_2}^4{d_1}^4+7488\,{d_3}^5{d_2}^4d_1+57024\,{d_3}^3{d_2}^4{d_1}^3-432\,{d_3}^7{d_2}^2d_1-1248\,{d_3}^6{d_2}^3d_1-64\,{d_3}^7{d_2}^5+256\,{d_3}^3{d_2}^6{d_1}^3-128\,{d_3}^2{d_2}^6{d_1}^4+512\,{d_3}^2{d_2}^4{d_1}^6-128\,{d_3}^6{d_2}^2{d_1}^4+256\,{d_3}^6{d_2}^3{d_1}^3-2112\,{d_3}^4{d_2}^3{d_1}^5-9964\,d_3d_2-127464\,{d_3}^2+561628\,d_1d_2+8948\,{d_1}^2+561628\,d_3d_1-128\,{d_3}^5{d_2}^2{d_1}^5-288\,d_3{d_2}^4{d_1}^5-1248\,{d_3}^3{d_2}^6d_1-96\,d_3{d_2}^3{d_1}^6+1664\,{d_1}^6{d_3}^3{d_2}^3-1664\,{d_3}^5{d_2}^4{d_1}^3+96\,d_3{d_1}^4{d_2}^5-127464\,{d_2}^2+512\,{d_3}^4{d_2}^2{d_1}^6-128\,{d_3}^2{d_2}^5{d_1}^5+832\,{d_3}^5{d_2}^3{d_1}^4+832\,{d_3}^3{d_2}^5{d_1}^4-1664\,{d_3}^4{d_2}^5{d_1}^3-2112\,{d_3}^3{d_2}^4{d_1}^5+1280\,{d_1}^2{d_3}^5{d_2}^5+3072\,{d_1}^4{d_3}^4{d_2}^4+245838\,{d_3}^2{d_1}^2+128\,{d_3}^2{d_1}^8{d_2}^2+192\,d_3{d_1}^7{d_2}^2-9676\,{d_3}^2{d_2}^2+64\,{d_3}^7{d_2}^2{d_1}^3-256\,{d_3}^6{d_2}^5d_1+192\,{d_3}^7{d_2}^4d_1-192\,{d_3}^7{d_2}^3{d_1}^2-1080\,{d_3}^6{d_2}^2+3872\,{d_1}^4-1080\,{d_3}^2{d_2}^6+128\,{d_3}^6{d_2}^6-16416\,{d_3}^4-352\,{d_2}^5{d_1}^3+1056\,{d_1}^5{d_2}^3-704\,{d_2}^2{d_1}^6+2056\,{d_3}^2{d_1}^4-201924\,d_3{d_1}^3+1056\,{d_3}^3{d_1}^5-64\,{d_3}^5{d_2}^7-288\,{d_3}^6{d_2}^4+432\,{d_3}^3{d_2}^7-288\,{d_3}^4{d_2}^6+432\,{d_3}^7{d_2}^3-208\,{d_3}^5{d_2}^5-8416\,{d_3}^5{d_2}^3-32416\,{d_3}^3{d_1}^3-352\,{d_3}^5{d_1}^3-1056\,d_3{d_1}^5+2376\,{d_3}^5d_1+6768\,{d_1}^2{d_2}^4+10584\,{d_3}^5d_2-1056\,d_2{d_1}^5+2376\,d_1{d_2}^5+10584\,d_3{d_2}^5+2056\,{d_1}^4{d_2}^2-32826\,{d_3}^4{d_2}^2-32826\,{d_3}^2{d_2}^4+245838\,{d_1}^2{d_2}^2-16416\,{d_2}^4-704\,{d_3}^2{d_1}^6+59350\,{d_3}^3d_1+59350\,d_1{d_2}^3-628238\,{d_3}^2d_2d_1+21416\,{d_3}^4{d_2}^4+39890\,{d_3}^3d_2-32416\,{d_2}^3{d_1}^3-7855\,{d_3}^3{d_2}^3-8416\,{d_3}^3{d_2}^5-201924\,d_2{d_1}^3)$
$f\,f\,f$	$\frac{1}{46656}\sqrt{3}(-1576\,{d_3}^2{d_1}^3-1576\,{d_1}^2{d_2}^3+9094\,{d_1}^2d_2-1576\,{d_3}^2{d_2}^3+9094\,d_3{d_1}^2+64\,{d_3}^5{d_2}^3d_1+192\,{d_3}^3{d_2}^2{d_1}^2-128\,d_3d_1{d_2}^4+64\,{d_3}^3{d_2}^5d_1-128\,{d_3}^4d_2{d_1}^4-36\,{d_3}^3-128\,{d_3}^2{d_2}^5{d_1}^2+64\,d_3{d_2}^5{d_1}^3+128\,{d_3}^4{d_2}^2{d_1}^3+128\,{d_3}^2{d_2}^4{d_1}^3+64\,d_3{d_2}^3{d_1}^5+64\,{d_3}^3d_2{d_1}^5+128\,{d_3}^2{d_2}^3{d_1}^4+128\,{d_3}^3{d_2}^4{d_1}^2+4264\,d_3{d_2}^3d_1+4264\,d_3d_2{d_1}^3+288\,{d_3}^2{d_1}^4d_2-968\,{d_3}^2{d_2}d_1{}^2+288\,{d_3}^2d_1{d_2}^4+288\,d_3{d_2}^2{d_1}^4+288\,{d_3}^4{d_2}^2d_1-968\,{d_3}^2{d_1}d_2{}^2+128\,{d_3}^4{d_2}^3{d_1}^2-688\,{d_3}^3d_2{d_1}^3+192\,{d_3}^2{d_2}^3{d_1}^2+288\,d_3{d_2}^4{d_1}^2+192\,{d_3}^2{d_2}^2{d_1}^3-688\,{d_3}^3{d_2}^3d_1+288\,{d_3}^4d_2{d_1}^2-384\,{d_3}^3{d_2}^3{d_1}^3+128\,{d_3}^3{d_2}^2{d_1}^4-128\,{d_3}^5{d_2}^2{d_1}^2-144\,{d_3}^5d_2d_1+64\,{d_3}^5d_2{d_1}^3-36\,{d_1}^3-128\,{d_3}^4{d_2}^4d_1-36\,{d_2}^3-144\,d_3d_2{d_1}^5-72\,d_3{d_1}^4+4264\,{d_3}^3d_2d_1-968\,d_3{d_2}^2{d_1}^2-29493\,d_3d_2d_1-144\,d_3d_1{d_2}^5-72\,d_3{d_2}^4-128\,{d_3}^2{d_2}^2{d_1}^5-688\,d_3{d_2}^3{d_1}^3+32\,{d_3}^4{d_2}^3+32\,{d_3}^3{d_1}^4+32\,{d_3}^3{d_2}^4+9094\,d_1{d_2}^2+32\,{d_3}^4{d_1}^3-72\,{d_3}^4d_2+9094\,{d_3}^2d_1-72\,{d_3}^4d_1+9094\,d_3{d_2}^2-1576\,{d_3}^3{d_1}^2-1576\,{d_2}^2{d_1}^3+32\,{d_2}^3{d_1}^4+32\,{d_2}^4{d_1}^3-72\,{d_1}^4d_2-72\,d_1{d_2}^4-1576\,{d_3}^3{d_2}^2-4352\,d_1-4352\,d_2+9094\,{d_3}^2d_2-4352\,d_3)$
$f\,f\,o$	0
$f\,f\,\tilde{o}$	0
$f\,f\,p$	0
$f\,f\,q$	$\frac{1}{69984}(d_1-d_2)(16\,{d_3}^2{d_1}^3-1320\,{d_1}^2{d_2}^3+3910\,{d_1}^2d_2+16\,{d_3}^2{d_2}^3+114\,d_3{d_1}^2-1088\,{d_3}^3{d_2}^2{d_1}^2-4860\,{d_3}^3+1948\,d_3{d_2}^3d_1+1948\,d_3d_2{d_1}^3+32\,{d_3}^2{d_1}^4d_2-7424\,{d_3}^2d_2{d_1}^2+32\,{d_3}^2d_1{d_2}^4-64\,d_3{d_2}^2{d_1}^4+512\,{d_3}^4{d_2}^2d_1-7424\,{d_3}^2d_1{d_2}^2-304\,{d_3}^3d_2{d_1}^3+640\,{d_3}^2{d_2}^3{d_1}^2-64\,d_3{d_2}^4{d_1}^2+640\,{d_3}^2{d_2}^2{d_1}^3-304\,{d_3}^3{d_2}^3d_1+512\,{d_3}^4d_2{d_1}^2-240\,{d_3}^5d_2d_1-36\,{d_1}^3-36\,{d_2}^3+6584\,{d_3}^3d_2d_1+7568\,d_3{d_2}^2{d_1}^2-9555\,d_3d_2d_1-368\,d_3{d_2}^3{d_1}^3+3910\,d_1{d_2}^2-120\,{d_3}^4d_2+1562\,{d_3}^2d_1-120\,{d_3}^4d_1+114\,d_3{d_2}^2-104\,{d_3}^3{d_1}^2-1320\,{d_2}^2{d_1}^3+32\,{d_2}^3{d_1}^4+32\,{d_2}^4{d_1}^3-72\,{d_1}^4d_2-72\,d_1{d_2}^4-104\,{d_3}^3{d_2}^2-3648\,d_1-3648\,d_2+1562\,{d_3}^2d_2+30048\,d_3)$
$f\,f\,r$	$\frac{11}{69984}(d_1-d_2)(608+16\,{d_3}^4d_2d_1-232\,{d_3}^2d_2d_1+64\,{d_1}^2{d_2}^2{d_3}^2-32\,{d_3}^3{d_2}^2d_1-32\,{d_3}^3d_2{d_1}^2+16\,{d_3}^2{d_2}^3d_1+16\,{d_3}^2d_2{d_1}^3-32\,d_3{d_2}^2{d_1}^3-32\,d_3{d_2}^3{d_1}^2+192\,d_3d_2{d_1}^2-18\,{d_1}^2-188\,{d_3}^2-18\,{d_2}^2+192\,d_3d_1{d_2}^2+8\,{d_3}^3d_2-36\,d_2{d_1}^3-334\,d_3d_1+8\,{d_3}^2{d_1}^2+8\,{d_3}^3d_1-36\,d_1{d_2}^3+565\,d_1d_2-112\,{d_1}^2{d_2}^2+16\,{d_2}^3{d_1}^3+8\,{d_3}^2{d_2}^2-334\,d_3d_2)$

Table A.3: The cubic couplings for all of the fields in the action up to level 3 (continued).

$l\,m\,n$	$B_{lmn}(d_1,d_2,d_3)$
$f\ f\ s$	$-\frac{125}{139968}\,(d_1-d_2)(608+16\,{d_3}^4d_2d_1-232\,{d_3}^2d_2d_1+64\,{d_1}^2{d_2}^2{d_3}^2-32\,{d_3}^3{d_2}^2d_1-32\,{d_3}^3d_2{d_1}^2+16\,{d_3}^2{d_2}^3d_1+16\,{d_3}^2d_2{d_1}^3-32\,d_3{d_2}^2{d_1}^3-32\,d_3{d_2}^3{d_1}^2+192\,d_3d_2{d_1}^2-18\,{d_1}^2-188\,{d_3}^2-18\,{d_2}^2+192\,d_3d_1{d_2}^2+8\,{d_3}^3d_2-36\,d_2{d_1}^3-334\,d_3d_1+8\,{d_3}^2{d_1}^2+8\,{d_3}^3d_1-36\,d_1{d_2}^3+565\,d_1d_2-112\,{d_1}^2{d_2}^2+16\,{d_2}^3{d_1}^3+8\,{d_3}^2{d_2}^2-334\,d_3d_2)$
$f\ f\ y$	$\frac{1}{139968}\,(d_1-d_2)(-40416+5424\,{d_3}^4d_2d_1-7344\,{d_3}^2d_2d_1+8128\,{d_1}^2{d_2}^2{d_3}^2-7424\,{d_3}^3{d_2}^2d_1-7424\,{d_3}^3d_2{d_1}^2+2544\,{d_3}^2{d_2}^3d_1+2544\,{d_3}^2d_2{d_1}^3-1200\,d_3{d_2}^2{d_1}^3-1200\,d_3{d_2}^3{d_1}^2+12804\,d_3d_2{d_1}^2-128\,{d_3}^6d_2d_1-768\,{d_3}^2{d_2}^3{d_1}^3-896\,{d_3}^4{d_2}^2{d_1}^2+192\,d_3{d_2}^4{d_1}^3-64\,{d_3}^3{d_2}^4d_1-192\,{d_3}^4{d_2}^3d_1+704\,{d_3}^3{d_2}^2{d_1}^3+704\,{d_3}^3{d_2}^3{d_1}^2-192\,{d_3}^4d_2{d_1}^3+64\,{d_3}^2d_2{d_1}^5+192\,d_3{d_2}^3{d_1}^4+320\,{d_3}^5{d_2}^2d_1-128\,d_3{d_2}^2{d_1}^5-64\,{d_3}^3d_2{d_1}^4+64\,{d_3}^2{d_2}^5d_1+320\,{d_3}^5d_2{d_1}^2-400\,d_3d_2{d_1}^4-400\,d_3d_1{d_2}^4-128\,d_3{d_2}^5{d_1}^2+17178\,{d_1}^2+9260\,{d_3}^2+17178\,{d_2}^2+12804\,d_3d_1{d_2}^2-1920\,d_3{d_2}^3-3496\,{d_3}^3d_2+64\,{d_3}^3{d_2}^3+5528\,d_2{d_1}^3+31686\,d_3d_1-2752\,{d_3}^2{d_1}^2-3496\,{d_3}^3d_1+5528\,d_1{d_2}^3-71849\,d_1d_2-14344\,{d_1}^2{d_2}^2-2032\,{d_2}^3{d_1}^3-72\,{d_1}^4+32\,{d_3}^2{d_1}^4-64\,{d_3}^5d_2+1504\,{d_3}^4-1920\,d_3{d_1}^3+864\,{d_1}^4{d_2}^2-64\,{d_3}^5d_1-2752\,{d_3}^2{d_2}^2-32\,{d_3}^4{d_2}^2+864\,{d_1}^2{d_2}^4+32\,{d_3}^2{d_2}^4-144\,d_2{d_1}^5-144\,d_1{d_2}^5-32\,{d_3}^4{d_1}^2+64\,{d_3}^3{d_1}^3+64\,{d_2}^5{d_1}^3+64\,{d_1}^5{d_2}^3-128\,{d_2}^4{d_1}^4+31686\,d_3d_2-72\,{d_2}^4)$
$f\ f\ z$	$\frac{1}{69984}\,(d_1-d_2)(42432+128\,{d_3}^4{d_2}^2{d_1}^4+4440\,{d_3}^4d_2d_1-71247\,{d_3}^2d_2d_1-4328\,{d_1}^2{d_2}^2{d_3}^2-904\,{d_3}^3{d_2}^2d_1-904\,{d_3}^3d_2{d_1}^2+9040\,{d_3}^2{d_2}^3d_1+9040\,{d_3}^2d_2{d_1}^3-3256\,d_3{d_2}^2{d_1}^3-3256\,d_3{d_2}^3{d_1}^2+5458\,d_3d_2{d_1}^2+128\,{d_3}^5{d_2}^2{d_1}^3-128\,{d_3}^3{d_2}^5{d_1}^2+64\,{d_3}^4d_2{d_1}^5+64\,{d_3}^4{d_2}^5d_1+128\,{d_3}^4{d_2}^4{d_1}^2+64\,{d_3}^2{d_2}^3{d_1}^5-128\,{d_3}^2{d_2}^4{d_1}^4-128\,{d_3}^5{d_2}^4d_1+128\,{d_3}^3{d_2}^4{d_1}^3+672\,{d_3}^2{d_2}^4{d_1}^2+672\,{d_3}^2{d_1}^4{d_2}^2+64\,{d_3}^6{d_2}^3d_1+64\,{d_3}^6d_2{d_1}^3+128\,{d_3}^3{d_2}^3{d_1}^4-128\,{d_3}^5d_2{d_1}^4+128\,{d_3}^5{d_2}^3{d_1}^2-128\,{d_3}^6{d_2}^2{d_1}^2+64\,{d_3}^2{d_2}^5{d_1}^3-384\,{d_3}^4{d_2}^3{d_1}^3-128\,{d_3}^3{d_2}^2{d_1}^5-432\,{d_3}^6d_2d_1-2256\,{d_3}^2{d_2}^3{d_1}^3-2240\,{d_3}^4{d_2}^2{d_1}^2+96\,d_3{d_2}^4{d_1}^3-160\,{d_3}^3{d_2}^4d_1-592\,{d_3}^4{d_2}^3d_1+1600\,{d_3}^3{d_2}^2{d_1}^3+1600\,{d_3}^3{d_2}^3{d_1}^2-592\,{d_3}^4d_2{d_1}^3-144\,{d_3}^2d_2{d_1}^5+96\,d_3{d_2}^3{d_1}^4+928\,{d_3}^5{d_2}^2d_1-160\,{d_3}^3d_2{d_1}^4-144\,{d_3}^2{d_2}^5d_1+928\,{d_3}^5d_2{d_1}^2-216\,d_3d_2{d_1}^4-216\,d_3d_1{d_2}^4+396\,{d_1}^2+32\,{d_3}^5{d_1}^3+32\,{d_3}^5{d_2}^3+32\,{d_3}^4{d_1}^4-67576\,{d_3}^2+32\,{d_3}^4{d_2}^4+396\,{d_2}^2+5458\,d_3d_1{d_2}^2-108\,d_3{d_2}^3+27682\,{d_3}^3d_2-1800\,{d_3}^3{d_2}^3+792\,d_2{d_1}^3-4620\,d_3d_1+16354\,{d_3}^2{d_1}^2+27682\,{d_3}^3d_1+792\,d_1{d_2}^3-8846\,d_1d_2+4512\,{d_1}^2{d_2}^2-352\,{d_2}^3{d_1}^3-72\,{d_3}^2{d_1}^4-216\,{d_3}^5d_2+5076\,{d_3}^4-108\,d_3{d_1}^3-216\,{d_3}^5d_1+16354\,{d_3}^2{d_2}^2-2456\,{d_3}^4{d_2}^2-72\,{d_3}^2{d_2}^4-2456\,{d_3}^4{d_1}^2-1800\,{d_3}^3{d_1}^3-4620\,d_3d_2)$
$f\ o\ o$	$\frac{368}{19683}\,\sqrt{3}(4\,{d_3}^2d_1+4\,d_1{d_2}^2-8\,d_3d_2d_1-9\,d_1+2\,d_2+2\,d_3)$
$f\ o\ \tilde{o}$	0
$f\ o\ p$	0
$f\ o\ q$	0
$f\ o\ r$	$-\frac{40}{19683}\,\sqrt{3}(4\,{d_3}^2{d_1}^2-2\,d_3d_2+4\,{d_1}^2{d_2}^2-30\,d_3d_1-4\,{d_3}^2d_2d_1+8\,d_3d_1{d_2}^2-8\,d_3d_2{d_1}^2-4\,d_1{d_2}^3+32-2\,{d_2}^2+43\,d_1d_2-9\,{d_1}^2)$
$f\ o\ s$	0
$f\ o\ y$	0
$f\ o\ z$	0
$f\ \tilde{o}\ \tilde{o}$	$\frac{32}{19683}\,\sqrt{3}(4\,{d_3}^2d_1+4\,d_1{d_2}^2-8\,d_3d_2d_1-9\,d_1+2\,d_2+2\,d_3)$
$f\ \tilde{o}\ p$	0
$f\ \tilde{o}\ q$	0
$f\ \tilde{o}\ r$	0
$f\ \tilde{o}\ s$	0
$f\ \tilde{o}\ y$	0
$f\ \tilde{o}\ z$	0
$f\ p\ p$	$-\frac{6400}{19683}\,\sqrt{3}(4\,{d_3}^2d_1+4\,d_1{d_2}^2-8\,d_3d_2d_1-9\,d_1+2\,d_2+2\,d_3)$
$f\ p\ q$	0
$f\ p\ r$	0
$f\ p\ s$	$-\frac{800}{19683}\,\sqrt{3}(4\,{d_3}^2{d_1}^2-2\,d_3d_2+4\,{d_1}^2{d_2}^2-30\,d_3d_1-4\,{d_3}^2d_2d_1+8\,d_3d_1{d_2}^2-8\,d_3d_2{d_1}^2-4\,d_1{d_2}^3+32-2\,{d_2}^2+43\,d_1d_2-9\,{d_1}^2)$
$f\ p\ y$	0
$f\ p\ z$	0

Table A.3: The cubic couplings for all of the fields in the action up to level 3 (continued).

$l\,m\,n$	$B_{lmn}(d_1,d_2,d_3)$
$f\ q\ q$	$-\frac{1}{314928}\sqrt{3}(62804\,d_3d_2d_1 + 120\,d_3{d_2}^2{d_1}^4 + 1156\,{d_3}^4{d_2}^2d_1 + 58639\,{d_3}^2d_1{d_2}^2 + 1172\,{d_3}^3d_2{d_1}^3 + 1020\,{d_3}^2{d_2}^3{d_1}^2 - 1140\,d_3{d_2}^4{d_1}^2 - 2312\,{d_3}^2{d_2}^2{d_1}^3 - 2072\,{d_3}^3{d_2}^3d_1 - 1140\,{d_3}^4d_2{d_1}^2 - 120\,{d_3}^5d_2d_1 + 1020\,{d_3}^3{d_2}^2{d_1}^2 + 1172\,d_3{d_2}^3{d_1}^3 - 35944\,{d_3}^3d_2d_1 + 9787\,d_3{d_2}^2{d_1}^2 - 120\,d_3d_1{d_2}^5 - 32\,d_3d_2{d_1}^5 - 35944\,d_3{d_2}^3d_1 - 3325\,d_3d_2{d_1}^3 + 16168\,{d_3}^2d_2 + 398\,{d_3}^3{d_2}^2 - 3312\,{d_1}^3 + 120\,{d_3}^2{d_1}^4d_2 + 9787\,{d_3}^2d_2{d_1}^2 + 1156\,{d_3}^2d_1{d_2}^4 + 112\,{d_3}^3 - 36\,{d_1}^5 + 112\,{d_2}^3 + 36864\,d_1 - 51200\,d_2 + 120\,{d_1}^2{d_2}^5 + 16\,{d_1}^5{d_2}^2 - 62536\,{d_3}^2d_1 - 62536\,d_1{d_2}^2 - 60\,{d_3}^4d_2 - 51200\,d_3 - 7478\,{d_3}^3{d_1}^2 + 16168\,d_3{d_2}^2 + 35224\,d_3{d_1}^2 + 35224\,{d_1}^2d_2 + 398\,{d_3}^2{d_2}^3 + 296\,{d_3}^2{d_1}^3 - 7478\,{d_1}^2{d_2}^3 + 5084\,d_1{d_2}^4 - 120\,{d_2}^3{d_1}^4 - 16\,{d_2}^4{d_1}^3 + 278\,{d_1}^4d_2 + 296\,{d_2}^2{d_1}^3 + 5084\,{d_3}^4d_1 - 16\,{d_3}^4{d_1}^3 - 120\,{d_3}^3{d_1}^4 - 60\,d_3{d_2}^4 + 278\,d_3{d_1}^4 + 16\,{d_3}^2{d_1}^5 + 120\,{d_3}^5{d_1}^2)$
$f\ q\ r$	$-\frac{11}{314928}\sqrt{3}(2048 - 18\,{d_1}^4 + 8\,{d_3}^4d_2d_1 - 936\,{d_3}^2d_2d_1 - 68\,{d_1}^2{d_2}^2{d_3}^2 - 76\,{d_3}^3{d_2}^2d_1 + 76\,{d_3}^3d_2{d_1}^2 - 16\,d_3d_2{d_1}^4 - 60\,d_3d_1{d_2}^4 + 128\,{d_3}^2{d_2}^3d_1 - 68\,{d_3}^2d_2{d_1}^3 + 136\,d_3{d_2}^2{d_1}^3 - 60\,d_3{d_2}^3{d_1}^2 + 279\,d_3d_2{d_1}^2 + 1091\,d_3d_1{d_2}^2 - 536\,{d_1}^2 + 8\,{d_3}^2{d_1}^4 + 413\,d_2{d_1}^3 + 4\,{d_3}^3d_2 - 744\,d_3d_1 + 178\,{d_3}^2{d_1}^2 - 252\,d_3{d_1}^3 - 82\,d_1{d_2}^3 - 30\,d_3{d_2}^3 + 8\,{d_1}^4{d_2}^2 + 60\,{d_1}^2{d_2}^4 - 8\,{d_3}^4{d_1}^2 + 3124\,d_1d_2 - 777\,{d_1}^2{d_2}^2 - 68\,{d_2}^3{d_1}^3 - 248\,d_3d_2 - 1256\,{d_2}^2 + 156\,{d_3}^3d_1 - 16\,{d_3}^2 - 26\,{d_3}^2{d_2}^2)$
$f\ q\ s$	$\frac{125}{629856}\sqrt{3}(2048 - 18\,{d_1}^4 + 8\,{d_3}^4d_2d_1 - 936\,{d_3}^2d_2d_1 - 68\,{d_1}^2{d_2}^2{d_3}^2 - 76\,{d_3}^3{d_2}^2d_1 + 76\,{d_3}^3d_2{d_1}^2 - 16\,d_3d_2{d_1}^4 - 60\,d_3d_1{d_2}^4 + 128\,{d_3}^2{d_2}^3d_1 - 68\,{d_3}^2d_2{d_1}^3 + 136\,d_3{d_2}^2{d_1}^3 - 60\,d_3{d_2}^3{d_1}^2 + 279\,d_3d_2{d_1}^2 + 1091\,d_3d_1{d_2}^2 - 536\,{d_1}^2 + 8\,{d_3}^2{d_1}^4 + 413\,d_2{d_1}^3 + 4\,{d_3}^3d_2 - 744\,d_3d_1 + 178\,{d_3}^2{d_1}^2 - 252\,d_3{d_1}^3 - 82\,d_1{d_2}^3 - 30\,d_3{d_2}^3 + 8\,{d_1}^4{d_2}^2 + 60\,{d_1}^2{d_2}^4 - 8\,{d_3}^4{d_1}^2 + 3124\,d_1d_2 - 777\,{d_1}^2{d_2}^2 - 68\,{d_2}^3{d_1}^3 - 248\,d_3d_2 - 1256\,{d_2}^2 + 156\,{d_3}^3d_1 - 16\,{d_3}^2 - 26\,{d_3}^2{d_2}^2)$
$f\ q\ y$	$-\frac{1}{629856}\sqrt{3}(-43008 + 11130\,{d_1}^4 + 3224\,{d_3}^4d_2d_1 - 43096\,{d_3}^2d_2d_1 + 44324\,{d_1}^2{d_2}^2{d_3}^2 + 5164\,{d_3}^3{d_2}^2d_1 - 18268\,{d_3}^3d_2{d_1}^2 + 11704\,d_3d_2{d_1}^4 + 19808\,d_3d_1{d_2}^4 - 27308\,{d_3}^2{d_2}^3d_1 - 3672\,{d_3}^2{d_2}^2{d_1}^3 - 13812\,d_3{d_2}^2{d_1}^3 - 19700\,d_3{d_2}^3{d_1}^2 + 97021\,d_3d_2{d_1}^2 - 42975\,d_3d_1{d_2}^2 - 64\,d_3d_2{d_1}^6 - 64\,{d_3}^6d_2d_1 + 1632\,{d_3}^2{d_2}^3{d_1}^3 + 448\,{d_3}^4{d_2}^2{d_1}^2 + 752\,d_3{d_2}^4{d_1}^3 + 688\,{d_3}^3{d_2}^4d_1 - 1296\,{d_3}^4{d_2}^3d_1 - 2544\,{d_3}^3{d_2}^2{d_1}^3 + 1632\,{d_3}^3{d_2}^3{d_1}^2 + 944\,{d_3}^4d_2{d_1}^3 - 400\,{d_3}^2{d_2}^2{d_1}^5 - 2256\,{d_3}^2{d_2}^4{d_1}^2 - 1632\,d_3{d_2}^3{d_1}^4 + 640\,{d_3}^5{d_2}^2d_1 + 704\,d_3{d_2}^2{d_1}^5 + 192\,{d_3}^3d_2{d_1}^4 + 272\,{d_3}^2{d_2}^5d_1 + 720\,{d_3}^2{d_1}^4{d_2}^2 - 608\,{d_3}^5d_2{d_1}^2 - 240\,d_3d_1{d_2}^6 + 480\,d_3{d_2}^5{d_1}^2 - 4576\,{d_2}^4 + 128\,{d_3}^4 - 22536\,{d_1}^2 - 72\,{d_1}^6 - 704\,{d_3}^2{d_1}^4 + 224\,{d_3}^4{d_2}^2 - 752\,{d_2}^5{d_1}^3 - 72705\,d_2{d_1}^3 - 4116\,{d_3}^3d_2 - 92920\,d_3d_1 - 25050\,{d_3}^2{d_1}^2 + 16812\,d_3{d_1}^3 - 68086\,d_1{d_2}^3 + 5014\,d_3{d_2}^3 - 12924\,{d_1}^4{d_2}^2 - 11584\,{d_1}^2{d_2}^4 + 4104\,{d_3}^4{d_1}^2 + 248252\,d_1d_2 + 70253\,{d_1}^2{d_2}^2 + 21704\,{d_2}^3{d_1}^3 - 86952\,d_3d_2 + 13576\,{d_2}^2 + 24948\,{d_3}^3d_1 - 1592\,d_3{d_1}^5 - 224\,{d_3}^2{d_2}^4 - 32\,{d_3}^5d_2 + 2308\,d_2{d_1}^5 + 568\,d_1{d_2}^5 - 120\,d_3{d_2}^5 + 152\,{d_3}^3{d_2}^3 - 2024\,{d_3}^3{d_1}^3 - 32\,{d_3}^5{d_1}^3 + 32\,{d_3}^3{d_1}^5 - 336\,{d_1}^5{d_2}^3 - 96\,{d_3}^4{d_1}^4 + 816\,{d_2}^4{d_1}^4 + 32\,{d_3}^2{d_1}^6 + 240\,{d_1}^2{d_2}^6 + 32\,{d_2}^2{d_1}^6 + 64\,{d_3}^6{d_1}^2 - 1248\,{d_3}^5d_1 + 8528\,{d_3}^2 + 35298\,{d_3}^2{d_2}^2)$
$f\ q\ z$	$-\frac{1}{314928}\sqrt{3}(-110592 + 396\,{d_1}^4 + 28744\,{d_3}^4d_2d_1 + 68916\,{d_3}^2d_2d_1 + 114695\,{d_1}^2{d_2}^2{d_3}^2 - 32309\,{d_3}^3{d_2}^2d_1 - 23833\,{d_3}^3d_2{d_1}^2 + 1186\,d_3d_2{d_1}^4 + 16572\,d_3d_1{d_2}^4 - 34124\,{d_3}^2{d_2}^3d_1 - 61029\,{d_3}^2{d_2}^2{d_1}^3 - 2104\,d_3{d_2}^2{d_1}^3 - 21114\,d_3{d_2}^3{d_1}^2 + 136910\,d_3d_2{d_1}^2 - 70810\,d_3d_1{d_2}^2 - 64\,{d_3}^3d_2{d_1}^6 - 240\,{d_3}^3{d_2}^6d_1 + 96\,{d_3}^6d_2{d_1}^3 - 1392\,{d_3}^3{d_2}^3{d_1}^4 + 304\,{d_3}^5d_2{d_1}^4 + 912\,{d_3}^5{d_2}^3{d_1}^2 - 96\,{d_3}^6{d_2}^2{d_1}^2 - 752\,{d_3}^2{d_2}^5{d_1}^3 + 784\,{d_3}^4{d_2}^3{d_1}^3 + 32\,{d_3}^2{d_2}^2{d_1}^6 + 672\,{d_3}^3{d_2}^2{d_1}^5 + 304\,{d_3}^4{d_2}^2{d_1}^4 - 912\,{d_3}^5{d_2}^2{d_1}^3 + 240\,{d_3}^3{d_2}^5{d_1}^2 + 240\,{d_3}^2{d_2}^6{d_1}^2 - 336\,{d_3}^4d_2{d_1}^5 + 512\,{d_3}^4{d_2}^5d_1 - 1296\,{d_3}^4{d_2}^4{d_1}^2 - 336\,{d_3}^2{d_2}^3{d_1}^5 + 816\,{d_3}^2{d_2}^4{d_1}^4 - 304\,{d_3}^5{d_2}^4d_1 - 216\,{d_3}^6d_2d_1 + 21480\,{d_3}^2{d_2}^3{d_1}^3 + 18636\,{d_3}^4{d_2}^2{d_1}^2 - 48\,d_3{d_2}^4{d_1}^3 + 9808\,{d_3}^3{d_2}^4d_1 - 12440\,{d_3}^4{d_2}^3d_1 - 13860\,{d_3}^3{d_2}^2{d_1}^3 - 4984\,{d_3}^3{d_2}^3{d_1}^2 - 5308\,{d_3}^4d_2{d_1}^3 + 2212\,{d_3}^2d_2{d_1}^5 - 11704\,{d_3}^2{d_2}^4{d_1}^2 - 360\,d_3{d_2}^3{d_1}^4 + 3972\,{d_3}^5{d_2}^2d_1 + 48\,d_3{d_2}^2{d_1}^5 + 10628\,{d_3}^3d_2{d_1}^4 + 208\,{d_3}^2{d_2}^5d_1 - 12124\,{d_3}^2{d_1}^4{d_2}^2 - 5844\,{d_3}^5d_2{d_1}^2 + 360\,d_3{d_2}^5{d_1}^2 + 784\,{d_3}^3{d_2}^4{d_1}^3 + 32\,{d_3}^6{d_2}^3d_1 + 432\,{d_3}^4 + 64656\,{d_1}^2 + 10798\,{d_3}^2{d_1}^4 - 32\,{d_3}^6{d_1}^4 + 534\,{d_3}^4{d_2}^2 - 8062\,d_2{d_1}^3 - 26896\,{d_3}^3d_2 - 30352\,d_3d_1 - 97268\,{d_3}^2{d_1}^2 - 5416\,d_3{d_1}^3 - 57844\,d_1{d_2}^3 + 996\,d_3{d_2}^3 - 176\,{d_1}^4{d_2}^2 - 1320\,{d_1}^2{d_2}^4 - 6190\,{d_3}^4{d_1}^2 + 116936\,d_1d_2 - 5434\,{d_1}^2{d_2}^2 + 1496\,{d_2}^3{d_1}^3 - 117296\,d_3d_2 - 2192\,{d_2}^2 + 9520\,{d_3}^3d_1 - 108\,d_3{d_1}^5 - 4756\,{d_3}^2{d_2}^4 - 108\,{d_3}^5d_2 + 4334\,{d_3}^3{d_2}^3 + 13024\,{d_3}^3{d_1}^3 + 1856\,{d_3}^5{d_1}^3 - 1472\,{d_3}^3{d_1}^5 - 784\,{d_3}^4{d_1}^4 - 72\,{d_3}^2{d_1}^6 + 216\,{d_3}^6{d_1}^2 - 4212\,{d_3}^5d_1 - 120\,{d_3}^3{d_2}^5 - 104\,{d_3}^4{d_2}^4 + 32\,{d_3}^4{d_1}^6 + 79968\,{d_3}^2 + 68132\,{d_3}^2{d_2}^2 + 16\,{d_3}^5{d_2}^3)$
$f\ r\ r$	$-\frac{19}{104976}\sqrt{3}(-4\,{d_3}^3{d_1}^2 - 40\,d_2 + 4\,{d_2}^2{d_1}^3 + 11\,d_3{d_1}^2 - 45\,d_3d_2d_1 - 9\,{d_1}^3 - 4\,{d_1}^2{d_2}^3 + 4\,{d_3}^3d_2d_1 + 2\,d_3{d_2}^2 - 8\,d_3d_2{d_1}^3 - 40\,d_3 + 4\,{d_3}^2{d_1}^3 + 11\,{d_1}^2d_2 + 2\,{d_3}^2d_2 + 14\,{d_3}^2d_1 + 4\,d_3{d_2}^3d_1 - 8\,{d_3}^2d_1{d_2}^2 + 4\,{d_3}^2d_2{d_1}^2 + 4\,d_3{d_2}^2{d_1}^2 - 28\,d_1 + 14\,d_1{d_2}^2)$
$f\ r\ s$	$\frac{1375}{629856}\sqrt{3}(-4\,{d_3}^3{d_1}^2 - 40\,d_2 + 4\,{d_2}^2{d_1}^3 + 11\,d_3{d_1}^2 - 45\,d_3d_2d_1 - 9\,{d_1}^3 - 4\,{d_1}^2{d_2}^3 + 4\,{d_3}^3d_2d_1 + 2\,d_3{d_2}^2 - 8\,d_3d_2{d_1}^3 - 40\,d_3 + 4\,{d_3}^2{d_1}^3 + 11\,{d_1}^2d_2 + 2\,{d_3}^2d_2 + 14\,{d_3}^2d_1 + 4\,d_3{d_2}^3d_1 - 8\,{d_3}^2d_1{d_2}^2 + 4\,{d_3}^2d_2{d_1}^2 + 4\,d_3{d_2}^2{d_1}^2 - 28\,d_1 + 14\,d_1{d_2}^2)$

Table A.3: The cubic couplings for all of the fields in the action up to level 3 (continued).

$l\,m\,n$	$B_{lmn}(d_1,d_2,d_3)$
$f\ r\ y$	$-\frac{11}{629856}\sqrt{3}(-48\,d_3{d_2}^3{d_1}^3+16\,d_3d_1{d_2}^5-32\,d_3d_2{d_1}^5-48\,{d_3}^2{d_1}^4d_2-16\,{d_3}^2d_1{d_2}^4+96\,d_3{d_2}^2{d_1}^4+80\,{d_3}^4{d_2}^2d_1+144\,{d_3}^3d_2{d_1}^3+144\,{d_3}^2{d_2}^3{d_1}^2-32\,d_3{d_2}^4{d_1}^2-96\,{d_3}^2{d_2}^2{d_1}^3-48\,{d_3}^3{d_2}^3d_1-32\,{d_3}^4d_2{d_1}^2-32\,{d_3}^5d_2d_1-96\,{d_3}^3{d_2}^2{d_1}^2-399\,d_3d_2d_1-844\,{d_3}^2d_1{d_2}^2+1044\,{d_3}^3d_2d_1+364\,d_3{d_2}^2{d_1}^2-32\,d_3{d_2}^3d_1+36\,d_3d_2{d_1}^3-1322\,{d_3}^2d_2+1277\,{d_1}^3-220\,{d_3}^2d_2{d_1}^2-8\,{d_3}^3{d_2}^2+16\,{d_3}^2{d_2}^3-72\,d_1{d_2}^4-48\,{d_2}^3{d_1}^4+48\,{d_2}^4{d_1}^3+372\,{d_1}^4d_2-112\,{d_3}^4d_1-48\,{d_3}^4{d_1}^3+8\,d_3{d_2}^4-248\,d_3{d_1}^4+16\,{d_3}^2{d_1}^5+32\,{d_3}^5{d_1}^2-16\,{d_1}^2{d_2}^5+16\,{d_1}^5{d_2}^2-16\,{d_3}^4d_2-224\,{d_2}^3-6068\,d_1+4424\,d_2-36\,{d_1}^5+3258\,{d_3}^2d_1+2154\,d_1{d_2}^2+320\,{d_3}^3+1864\,d_3-652\,{d_3}^3{d_1}^2-586\,d_3{d_2}^2-935\,d_3{d_1}^2-3543\,{d_1}^2d_2+664\,{d_3}^2{d_1}^3+592\,{d_1}^2{d_2}^3-856\,{d_2}^2{d_1}^3)$
$f\ r\ z$	$-\frac{11}{314928}\sqrt{3}(324\,{d_3}^2{d_1}^4d_2-48\,{d_3}^2d_1{d_2}^4+24\,d_3{d_2}^2{d_1}^4+408\,{d_3}^4{d_2}^2d_1+508\,{d_3}^3d_2{d_1}^3+600\,{d_3}^2{d_2}^3{d_1}^2-24\,d_3{d_2}^4{d_1}^2-840\,{d_3}^2{d_2}^2{d_1}^3-352\,{d_3}^3{d_2}^3d_1-468\,{d_3}^4d_2{d_1}^2-108\,{d_3}^5d_2d_1+24\,{d_3}^3{d_2}^2{d_1}^2+16\,{d_3}^2{d_2}^2{d_1}^5-32\,{d_3}^4{d_2}^4d_1+16\,{d_3}^3{d_2}^5d_1-16\,{d_3}^4d_2{d_1}^4-16\,{d_3}^2{d_2}^5{d_1}^2-48\,{d_3}^4{d_2}^2{d_1}^3+48\,{d_3}^2{d_2}^4{d_1}^3-32\,{d_3}^3d_2{d_1}^5-48\,{d_3}^2{d_2}^3{d_1}^4-16\,{d_3}^3{d_2}^4{d_1}^2+80\,{d_3}^4{d_2}^3{d_1}^2-48\,{d_3}^3{d_2}^3{d_1}^3+80\,{d_3}^3{d_2}^2{d_1}^4-48\,{d_3}^5{d_2}^2{d_1}^2+48\,{d_3}^5d_2{d_1}^3+16\,{d_3}^5{d_2}^3d_1-1242\,d_3d_2d_1+932\,{d_3}^2{d_1}{d_2}^2+1799\,{d_3}^3d_2d_1+446\,d_3{d_2}^2{d_1}^2+380\,d_3{d_2}^3d_1-580\,d_3d_2{d_1}^3+1756\,{d_3}^2d_2+198\,{d_1}^3-3469\,{d_3}^2d_2{d_1}^2-522\,{d_3}^3{d_2}^2-212\,{d_3}^2{d_2}^3-378\,{d_3}^4d_1+52\,{d_3}^4{d_1}^3-54\,d_3{d_1}^4-36\,{d_3}^2{d_1}^5+108\,{d_3}^5{d_1}^2-54\,{d_3}^4d_2-16\,{d_3}^5{d_1}^4+8\,{d_3}^4{d_2}^3-188\,{d_3}^3{d_1}^4+2728\,d_1+752\,d_2+8\,{d_3}^3{d_2}^4+16\,{d_3}^4{d_1}^5-3568\,{d_3}^2d_1-564\,d_1{d_2}^2+1080\,{d_3}^3+3312\,d_3-221\,{d_3}^3{d_1}^2-92\,d_3{d_2}^2-2362\,d_3{d_1}^2+270\,{d_1}^2d_2+1933\,{d_3}^2{d_1}^3+88\,{d_1}^2{d_2}^3-88\,{d_2}^2{d_1}^3)$
$f\ s\ s$	$-\frac{9475}{419904}\sqrt{3}(-4\,{d_3}^3{d_1}^2-40\,d_2+4\,{d_2}^2{d_1}^3+11\,d_3{d_1}^2-45\,d_3d_2d_1-9\,{d_1}^3-4\,{d_1}^2{d_2}^3+4\,{d_3}^3d_2d_1+2\,d_3{d_2}^2-8\,d_3d_2{d_1}^3-40\,d_3+4\,{d_3}^2{d_1}^3+11\,{d_1}^2d_2+2\,{d_3}^2d_2+14\,{d_3}^2d_1+4\,d_3{d_2}^3d_1-8\,{d_3}^2d_1{d_2}^2+4\,{d_3}^2d_2{d_1}^2+4\,d_3{d_2}^2{d_1}^2-28\,d_1+14\,d_1{d_2}^2)$
$f\ s\ y$	$\frac{125}{1259712}\sqrt{3}(-48\,{d_3}^2{d_1}^4d_2-16\,{d_3}^2d_1{d_2}^4+96\,d_3{d_2}^2{d_1}^4+80\,{d_3}^4{d_2}^2d_1+144\,{d_3}^3d_2{d_1}^3+144\,{d_3}^2{d_2}^3{d_1}^2-32\,d_3{d_2}^4{d_1}^2-96\,{d_3}^2{d_2}^2{d_1}^3-48\,{d_3}^3{d_2}^3d_1-32\,{d_3}^5d_2d_1-96\,{d_3}^3{d_2}^2{d_1}^2-224\,{d_2}^3-399\,d_3d_2d_1-48\,d_3{d_2}^3{d_1}^3+16\,d_3d_1{d_2}^5-32\,d_3d_2{d_1}^5-844\,{d_3}^2d_1{d_2}^2+1044\,{d_3}^3d_2d_1+364\,d_3{d_2}^2{d_1}^2-32\,d_3{d_2}^3d_1+36\,d_3d_2{d_1}^3-1322\,{d_3}^2d_2+1277\,{d_1}^3-220\,{d_3}^2d_2{d_1}^2-8\,{d_3}^3{d_2}^2+16\,{d_3}^2{d_2}^3-112\,{d_3}^4d_1-48\,{d_3}^4{d_1}^3-248\,d_3{d_1}^4+16\,{d_3}^2{d_1}^5+32\,{d_3}^5{d_1}^2-16\,{d_3}^4d_2-6068\,d_1+4424\,d_2-36\,{d_1}^5-16\,{d_1}^2{d_2}^5+16\,{d_1}^5{d_2}^2+3258\,{d_3}^2d_1+2154\,d_1{d_2}^2+320\,{d_3}^3+1864\,d_3-72\,d_1{d_2}^4-48\,{d_2}^3{d_1}^4+48\,{d_2}^4{d_1}^3+372\,{d_1}^4d_2+8\,d_3{d_2}^4-652\,{d_3}^3{d_1}^2-586\,d_3{d_2}^2-935\,d_3{d_1}^2-3543\,{d_1}^2d_2+664\,{d_3}^2{d_1}^3+592\,{d_1}^2{d_2}^3-856\,{d_2}^2{d_1}^3)$
$f\ s\ z$	$\frac{125}{629856}\sqrt{3}(16\,{d_3}^2{d_2}^2{d_1}^5-32\,{d_3}^4{d_2}^4d_1+16\,{d_3}^3{d_2}^5d_1-16\,{d_3}^4d_2{d_1}^4-16\,{d_3}^2{d_2}^5{d_1}^2-48\,{d_3}^4{d_2}^2{d_1}^3+48\,{d_3}^2{d_2}^4{d_1}^3-32\,{d_3}^3d_2{d_1}^5-48\,{d_3}^2{d_2}^3{d_1}^4-16\,{d_3}^3{d_2}^4{d_1}^2+324\,{d_3}^2{d_1}^4d_2-48\,{d_3}^2d_1{d_2}^4+24\,d_3{d_2}^2{d_1}^4+408\,{d_3}^4{d_2}^2d_1+508\,{d_3}^3d_2{d_1}^3+600\,{d_3}^2{d_2}^3{d_1}^2-24\,d_3{d_2}^4{d_1}^2-840\,{d_3}^2{d_2}^2{d_1}^3-352\,{d_3}^3{d_2}^3d_1-468\,{d_3}^4d_2{d_1}^2-108\,{d_3}^5d_2d_1+24\,{d_3}^3{d_2}^2{d_1}^2+80\,{d_3}^4{d_2}^3{d_1}^2-48\,{d_3}^3{d_2}^3{d_1}^3+80\,{d_3}^3{d_2}^2{d_1}^4-48\,{d_3}^5{d_2}^2{d_1}^2+48\,{d_3}^5d_2{d_1}^3+16\,{d_3}^5{d_2}^3d_1-1242\,d_3d_2d_1+932\,{d_3}^2d_1{d_2}^2+1799\,{d_3}^3d_2d_1+446\,d_3{d_2}^2{d_1}^2+380\,d_3{d_2}^3d_1-580\,d_3d_2{d_1}^3+1756\,{d_3}^2d_2+198\,{d_1}^3-3469\,{d_3}^2d_2{d_1}^2+8\,{d_3}^3{d_2}^4+8\,{d_3}^4{d_2}^3-188\,{d_3}^3{d_1}^4-522\,{d_3}^3{d_2}^2-212\,{d_3}^2{d_2}^3-378\,{d_3}^4d_1+52\,{d_3}^4{d_1}^3-54\,d_3{d_1}^4-36\,{d_3}^2{d_1}^5+108\,{d_3}^5{d_1}^2-54\,{d_3}^4d_2+16\,{d_3}^4{d_1}^5-16\,{d_3}^5{d_1}^4+2728\,d_1+752\,d_2-3568\,{d_3}^2d_1-564\,d_1{d_2}^2+1080\,{d_3}^3+3312\,d_3-221\,{d_3}^3{d_1}^2-92\,d_3{d_2}^2-2362\,d_3{d_1}^2+270\,{d_1}^2d_2+1933\,{d_3}^2{d_1}^3+88\,{d_1}^2{d_2}^3-88\,{d_2}^2{d_1}^3)$
$f\ y\ y$	$-\frac{1}{1259712}\sqrt{3}(-1536\,{d_3}^2{d_2}^2{d_1}^5-896\,{d_3}^4{d_2}^4d_1+384\,{d_3}^3{d_2}^5d_1-1664\,{d_3}^4{d_2}d_1{d_1}^4-1536\,{d_3}^2{d_2}^5{d_1}^2+1536\,{d_3}^4{d_2}^2{d_1}^3+1536\,{d_3}^2{d_2}^4{d_1}^3+896\,{d_3}^3d_2{d_1}^5+1152\,{d_3}^2{d_2}^3{d_1}^4+1152\,{d_3}^3{d_2}^4{d_1}^2+11952\,{d_3}^2{d_1}^4d_2-10992\,{d_3}^2d_1{d_2}^4+11952\,d_3{d_2}^2{d_1}^4-10992\,{d_3}^4{d_2}^2d_1-23264\,{d_3}^3d_2{d_1}^3+2320\,{d_3}^2{d_2}^3{d_1}^2+7264\,d_3{d_2}^4{d_1}^2+8272\,{d_3}^2{d_2}^2{d_1}^3+11776\,{d_3}^3{d_2}^3d_1+7264\,{d_3}^4d_2{d_1}^2+4528\,{d_3}^5d_2d_1+2320\,{d_3}^3{d_2}^2{d_1}^2-6112\,{d_2}^3+1152\,{d_3}^4{d_2}^3{d_1}^2-3456\,{d_3}^3{d_2}^3{d_1}^3+1152\,{d_3}^3{d_2}^2{d_1}^4-1536\,{d_3}^5{d_2}^2{d_1}^2+640\,{d_3}^5d_2{d_1}^3+384\,{d_3}^5{d_2}^3d_1+128\,{d_3}^2d_2{d_1}^6-128\,{d_3}^7d_2d_1+256\,{d_3}^6d_2{d_1}^2-534533\,d_3d_2d_1-23264\,d_3{d_2}^3{d_1}^3+4528\,d_3d_1{d_2}^5-3808\,d_3d_2{d_1}^5-45760\,{d_3}^2d_1{d_2}^2-128\,d_3d_2{d_1}^7-128\,d_3d_1{d_2}^7-1664\,d_3{d_1}^4{d_2}^4+192\,{d_3}^2{d_2}^6d_1+640\,d_3{d_2}^5{d_1}^3+192\,{d_3}^6{d_2}^2d_1+896\,d_3{d_2}^3{d_1}^5+256\,d_3{d_2}^6{d_1}^2+128\,d_3{d_2}^2{d_1}^6+40088\,{d_3}^3d_2d_1-39540\,d_3{d_2}^2{d_1}^2+40088\,d_3{d_2}^3d_1+95264\,d_3d_2{d_1}^3+122642\,{d_3}^2d_2-56577\,{d_1}^3-39540\,{d_3}^2d_2{d_1}^2+160\,{d_3}^3{d_2}^4+160\,{d_3}^4{d_2}^3-11472\,{d_3}^3{d_1}^4-5288\,{d_3}^3{d_2}^2-5288\,{d_3}^2{d_2}^3-28264\,{d_3}^4d_1+18928\,{d_3}^4{d_1}^3+9428\,d_3{d_1}^4+1344\,{d_3}^2{d_1}^5-9552\,{d_3}^5{d_1}^2-1112\,{d_3}^4d_2-96\,{d_3}^2{d_2}^5-96\,{d_3}^5{d_2}^2+576\,d_1{d_2}^6+320\,d_2{d_1}^6+576\,{d_3}^6d_1-64\,{d_3}^6d_2-64\,d_3{d_2}^6+320\,d_3{d_1}^6-128\,{d_1}^5{d_2}^4-128\,{d_2}^3{d_1}^6-448\,{d_2}^6{d_1}^3-128\,{d_3}^3{d_1}^6-448\,{d_3}^6{d_1}^3+128\,{d_1}^2{d_2}^7+64\,{d_1}^7{d_2}^2+64\,{d_3}^2{d_1}^7+128\,{d_3}^7{d_1}^2-128\,{d_3}^4{d_1}^5-144\,{d_1}^7+512\,{d_2}^5{d_1}^4+512\,{d_3}^5{d_1}^4+205764\,d_1-286440\,d_2+1792\,{d_2}^5+4776\,{d_1}^5-9552\,{d_1}^2{d_2}^5+1344\,{d_1}^5{d_2}^2+200174\,{d_3}^2d_1+200174\,d_1{d_2}^2+1792\,{d_3}^5-6112\,{d_3}^3-286440\,d_3-28264\,d_1{d_2}^4-11472\,{d_2}^3{d_1}^4+18928\,{d_2}^4{d_1}^3+9428\,{d_1}^4d_2-1112\,d_3{d_2}^4+89680\,{d_3}^3{d_1}^2+122642\,d_3{d_2}^2+68963\,d_3{d_1}^2+68963\,{d_1}^2d_2-93924\,{d_3}^2{d_1}^3+89680\,{d_1}^2{d_2}^3-93924\,{d_2}^2{d_1}^3)$

Table A.3: The cubic couplings for all of the fields in the action up to level 3 (continued).

$l\,m\,n$	$B_{lmn}(d_1,d_2,d_3)$
$f\ y\ z$	$-\frac{1}{629856}\sqrt{3}(-192\,{d_3}^5{d_2}^5d_1+64\,{d_3}^2{d_2}^2{d_1}^7+32\,{d_3}^6{d_2}^3+704\,{d_3}^4{d_2}^4{d_1}^3-64\,{d_3}^3{d_2}^6+64\,{d_3}^5{d_2}^4-32\,{d_3}^4{d_2}^5+1024\,{d_3}^2{d_2}^2{d_1}^5-12416\,{d_3}^4{d_2}^4d_1+7184\,{d_3}^3{d_2}^5d_1-3568\,{d_3}^4d_2{d_1}^4-9616\,{d_3}^2{d_2}^5{d_1}^2-400\,{d_3}^4{d_2}^2{d_1}^3+19120\,{d_3}^2{d_2}^4{d_1}^3-272\,{d_3}^3d_2{d_1}^5-10896\,{d_3}^2{d_2}^3{d_1}^4-1360\,{d_3}^3{d_2}^4{d_1}^2+23668\,{d_3}^2{d_1}^4d_2-31632\,{d_3}^2d_1{d_2}^4-1056\,d_3{d_2}^2{d_1}^4+44284\,{d_3}^4{d_2}^2d_1+28360\,{d_3}^3d_2{d_1}^3+85608\,{d_3}^2{d_2}^3{d_1}^2+13016\,d_3{d_2}^4{d_1}^2-63748\,{d_3}^2{d_2}^2{d_1}^3-4960\,{d_3}^3{d_2}^3d_1-27388\,{d_3}^4d_2{d_1}^2+896\,{d_3}^5d_2d_1-45816\,{d_3}^3{d_2}^2{d_1}^2-6016\,{d_2}^3+192\,{d_3}^6{d_1}^5+19024\,{d_3}^4{d_2}^3{d_1}^2-64\,{d_3}^7{d_1}^4-192\,{d_3}^5{d_1}^6-18928\,{d_3}^3{d_2}^3{d_1}^3+12880\,{d_3}^3{d_2}^2{d_1}^4-10704\,{d_3}^5{d_2}^2{d_1}^2+1136\,{d_3}^5d_2{d_1}^3+5552\,{d_3}^5{d_2}^3d_1+64\,{d_3}^4{d_1}^7+128\,{d_3}^2{d_2}d_1{}^6-432\,{d_3}^7d_2d_1+2496\,{d_3}^6d_2{d_1}^2-128\,{d_3}^2{d_2}^4{d_1}^5-512\,{d_3}^6d_2{d_1}^4+768\,{d_3}^5{d_2}^2{d_1}^4+192\,{d_3}^5d_2{d_1}^5+512\,{d_3}^2{d_2}^5{d_1}^4-1024\,{d_3}^4{d_2}^5{d_1}^2+128\,{d_3}^2{d_2}^2{d_1}^7+64\,{d_3}^7{d_2}^3d_1+256\,{d_3}^4d_2{d_1}^6+128\,{d_3}^3{d_2}^6{d_1}^2+832\,{d_3}^3{d_2}^3{d_1}^5+768\,{d_3}^4{d_2}^3{d_1}^4+192\,{d_3}^7{d_1}^3d_2-1088\,{d_3}^4{d_2}^2{d_1}^5-376734\,d_3d_2d_1-9240\,d_3{d_2}^3{d_1}^3-3040\,d_3d_1{d_2}^5-4072\,d_3d_2{d_1}^5+87780\,{d_3}^2d_1{d_2}^2-192\,{d_3}^7{d_2}^2{d_1}^2+960\,{d_3}^5{d_2}^4{d_1}^2+320\,{d_3}^4{d_2}^6d_1-128\,{d_3}^3{d_2}^7d_1-64\,{d_3}^6{d_2}^4d_1+64\,{d_3}^3{d_2}^2{d_1}^6-128\,{d_3}^3d_2{d_1}^7-1536\,{d_3}^5{d_2}^3{d_1}^3-128\,{d_3}^2{d_2}^3{d_1}^6+704\,{d_3}^3{d_2}^5{d_1}^3-448\,{d_3}^2{d_2}^6{d_1}^3+384\,{d_3}^6{d_2}^2{d_1}^3-1472\,{d_3}^3{d_2}^4{d_1}^4-288\,d_3{d_1}^4{d_2}^4+384\,{d_3}^2{d_2}^6d_1-96\,d_3{d_2}^5{d_1}^3-336\,{d_3}^6{d_2}^2d_1+96\,d_3{d_2}^3{d_1}^5+192\,d_3{d_2}^6{d_1}^2+96\,d_3{d_2}^2{d_1}^6-198187\,{d_3}^3d_2d_1-678\,d_3{d_2}^2{d_1}^2+79524\,d_3{d_2}^3d_1+47596\,d_3d_2{d_1}^3+40628\,{d_3}^2{d_2}^2-31422\,{d_1}^3-71247\,{d_3}^2d_2{d_1}^2-1576\,{d_3}^3{d_2}^4-3056\,{d_3}^4{d_2}^3-24968\,{d_3}^3{d_1}^4+29618\,{d_3}^3{d_2}^2-3244\,{d_3}^2{d_2}^3-73534\,{d_3}^4d_1+29360\,{d_3}^4{d_1}^3+23158\,d_3{d_1}^4+9368\,{d_3}^2{d_1}^5-14144\,{d_3}^5{d_1}^2+53470\,{d_3}^4d_2+1696\,{d_3}^2{d_2}^5-3072\,{d_3}^5{d_2}^2+1944\,{d_3}^6d_1-216\,{d_3}^6d_2-216\,d_3{d_1}^6+560\,{d_3}^3{d_1}^6-2192\,{d_3}^6{d_1}^3-144\,{d_3}^2{d_1}^7+432\,{d_3}^7{d_1}^2-2608\,{d_3}^4{d_1}^5+3952\,{d_3}^5{d_1}^4+160824\,d_1-230832\,d_2+792\,{d_1}^5-704\,{d_1}^2{d_2}^5-352\,{d_1}^5{d_2}^2+442192\,{d_3}^2d_1-24316\,d_1{d_2}^2+6048\,{d_3}^5-234840\,{d_3}^3-103344\,d_3+4512\,d_1{d_2}^4+1056\,{d_2}^4{d_1}^3+7504\,{d_1}^4d_2+736\,d_3{d_2}^4+215465\,{d_3}^3{d_1}^2+98188\,d_3{d_2}^2-29086\,d_3{d_1}^2+154970\,{d_1}^2d_2-174233\,{d_3}^2{d_1}^3-19448\,{d_1}^2{d_2}^3-15632\,{d_2}^2{d_1}^3)$
$f\ z\ z$	$-\frac{1}{314928}\sqrt{3}(-48\,{d_3}^5{d_2}^5d_1-144\,{d_3}^2{d_2}^2{d_1}^7-216\,{d_3}^6{d_2}^3+5712\,{d_3}^4{d_2}^4{d_1}^3-216\,{d_3}^3{d_2}^6-2808\,{d_3}^5{d_2}^4-2808\,{d_3}^4{d_2}^5+13672\,{d_3}^2{d_2}^2{d_1}^5-4472\,{d_3}^4{d_2}^4d_1+14944\,{d_3}^3{d_2}^5d_1-2000\,{d_3}^4d_2{d_1}^4-24680\,{d_3}^2{d_2}^5{d_1}^2+25032\,{d_3}^4{d_2}^2{d_1}^3+25032\,{d_3}^2{d_2}^4{d_1}^3-3712\,{d_3}^3d_2{d_1}^5-10304\,{d_3}^2{d_2}^3{d_1}^4-1960\,{d_3}^3{d_2}^4{d_1}^2+23218\,{d_3}^2{d_1}^4d_2-37420\,{d_3}^2d_1{d_2}^4+23218\,d_3{d_2}^2{d_1}^4-37420\,{d_3}^4{d_2}^2d_1+27896\,{d_3}^3d_2{d_1}^3+152019\,{d_3}^2{d_2}^3{d_1}^2-2130\,d_3{d_2}^4{d_1}^2-228813\,{d_3}^2{d_2}^2{d_1}^3-191849\,{d_3}^3{d_2}^3d_1-2130\,{d_3}^4d_2{d_1}^2-10260\,{d_3}^5d_2d_1+152019\,{d_3}^3{d_2}^2{d_1}^2-20304\,{d_2}^3-1960\,{d_3}^4{d_2}^3{d_1}^2-10272\,{d_3}^3{d_2}^3{d_1}^3-10304\,{d_3}^3{d_2}^2{d_1}^4-24680\,{d_3}^5{d_2}^2{d_1}^2+4512\,{d_3}^5d_2{d_1}^3+14944\,{d_3}^5{d_2}^3d_1-216\,{d_3}^2{d_2}d_1{}^6+648\,{d_3}^6d_2{d_1}^2-2736\,{d_3}^2{d_2}^4{d_1}^5-96\,{d_3}^6d_2{d_1}^4+3984\,{d_3}^5{d_2}^2{d_1}^4+3984\,{d_3}^2{d_2}^5{d_1}^4-1296\,{d_3}^4{d_2}^5{d_1}^2+432\,{d_3}^2{d_2}^7{d_1}^2-432\,{d_3}^7{d_2}^3d_1+96\,{d_3}^4d_2{d_1}^6+1776\,{d_3}^3{d_2}^6{d_1}^2+2928\,{d_3}^3{d_2}^3{d_1}^5-1968\,{d_3}^4{d_2}^3{d_1}^4-2736\,{d_3}^4{d_2}^2{d_1}^5-281716\,d_3d_2d_1+27896\,d_3{d_2}^3{d_1}^3-10260\,d_3d_1{d_2}^5-324\,d_3d_2{d_1}^5+549796\,{d_3}^2d_1{d_2}^2+432\,{d_3}^7{d_2}^2{d_1}^2-1296\,{d_3}^5{d_2}^4{d_1}^2+192\,{d_3}^4{d_2}^6d_1-432\,{d_3}^3{d_2}^7d_1+192\,{d_3}^6{d_2}^4d_1+368\,{d_3}^3{d_2}^2{d_1}^6-2672\,{d_3}^5{d_2}^3{d_1}^3+368\,{d_3}^2{d_2}^3{d_1}^6-2672\,{d_3}^3{d_2}^5{d_1}^3-1904\,{d_3}^2{d_2}^6{d_1}^3-1904\,{d_3}^6{d_2}^2{d_1}^3-1968\,{d_3}^3{d_2}^4{d_1}^4-2000\,d_3{d_1}^4{d_2}^4+1296\,{d_3}^2{d_2}^6d_1+4512\,d_3{d_2}^5{d_1}^3+1296\,{d_3}^6{d_2}^2d_1-3712\,d_3{d_2}^3{d_1}^5+648\,d_3{d_2}^6{d_1}^2-216\,d_3{d_2}^2{d_1}^6-15626\,{d_3}^3d_2d_1-170942\,d_3{d_2}^2{d_1}^2-15626\,d_3{d_2}^3d_1-6560\,d_3d_2{d_1}^3+371384\,{d_3}^2d_2-4356\,{d_1}^3-170942\,{d_3}^2d_2{d_1}^2+51062\,{d_3}^3{d_2}^4+192\,{d_3}^3{d_2}^5{d_1}^5+64\,{d_3}^4{d_2}^2{d_1}^7+192\,{d_3}^6{d_2}^2{d_1}^5+64\,{d_3}^7{d_2}^5d_1+192\,{d_3}^6{d_2}^5{d_1}^2+64\,{d_3}^2{d_2}^4{d_1}^7+512\,{d_3}^4{d_2}^5{d_1}^4-448\,{d_3}^6{d_2}^3{d_1}^4-192\,{d_3}^7{d_2}^4{d_1}^2+192\,{d_3}^5{d_2}^6{d_1}^2+192\,{d_3}^2{d_2}^6{d_1}^5-64\,{d_3}^2{d_2}^7{d_1}^4+96\,d_3{d_2}^4{d_1}^6+512\,{d_3}^5{d_2}^4{d_1}^4+51062\,{d_3}^4{d_2}^3+192\,{d_3}^3{d_2}^7{d_1}^3+192\,{d_3}^4{d_2}^6{d_1}^3+192\,{d_3}^7{d_2}^3{d_1}^3+192\,{d_3}^3{d_2}^4{d_1}^6+6184\,{d_3}^3{d_1}^4-96\,d_3{d_2}^6{d_1}^4-64\,{d_3}^7{d_2}^2{d_1}^4-448\,{d_3}^3{d_2}^6{d_1}^4+64\,{d_3}^5{d_2}^7d_1+1776\,{d_3}^6{d_2}^3{d_1}^2-254820\,{d_3}^3{d_2}^2-254820\,{d_3}^2{d_2}^3+192\,{d_3}^4{d_2}^3{d_1}^6-192\,{d_3}^4{d_2}^7{d_1}^2+192\,{d_3}^5{d_2}^3{d_1}^5+192\,{d_3}^6{d_2}^4{d_1}^3-192\,{d_3}^2{d_2}^5{d_1}^6-192\,{d_3}^5{d_2}^2{d_1}^6-768\,{d_3}^4{d_2}^4{d_1}^5-128\,{d_3}^3{d_2}^3{d_1}^7-128\,{d_3}^6{d_2}^6d_1-768\,{d_3}^5{d_2}^5{d_1}^3+15228\,{d_3}^4d_1-4216\,{d_3}^4{d_1}^3+1188\,d_3{d_1}^4+792\,{d_3}^2{d_1}^5-2376\,{d_3}^5{d_1}^2+2484\,{d_3}^4d_2+5724\,{d_3}^2{d_2}^5+5724\,{d_3}^5{d_2}^2-352\,{d_1}^5{d_2}^4-352\,{d_3}^4{d_1}^5+352\,{d_2}^5{d_1}^4+352\,{d_3}^5{d_1}^4+146448\,d_1-330144\,d_2-2376\,{d_1}^2{d_2}^5+792\,{d_1}^5{d_2}^2+25312\,{d_3}^2d_1+25312\,d_1{d_2}^2-20304\,{d_3}^3+32\,{d_3}^5{d_2}^6+32\,{d_3}^6{d_2}^5-330144\,d_3+15228\,d_1{d_2}^4+6184\,{d_2}^3{d_1}^4-4216\,{d_2}^4{d_1}^3+1188\,{d_1}^4d_2+2484\,d_3{d_2}^4-5890\,{d_3}^3{d_1}^2+371384\,d_3{d_2}^2+199292\,d_3{d_1}^2+199292\,{d_1}^2d_2-42782\,{d_3}^2{d_1}^3-5890\,{d_1}^2{d_2}^3-42782\,{d_2}^2{d_1}^3)$
$o\ o\ o$	0
$o\ o\ \tilde{o}$	0
$o\ o\ p$	0
$o\ o\ q$	$\frac{736}{59049}\,(d_1-d_2)(2\,d_1-15\,d_3+2\,d_2)$
$o\ o\ r$	$\frac{8608}{59049}\,d_1-\frac{8608}{59049}\,d_2$
$o\ o\ s$	$-\frac{46000}{59049}\,d_1+\frac{46000}{59049}\,d_2$

Table A.3: The cubic couplings for all of the fields in the action up to level 3 (continued).

$l\,m\,n$	$B_{lmn}(d_1, d_2, d_3)$
$o\ o\ y$	$\frac{368}{59049}\,(d_1 - d_2)(4\,{d_1}^2 + 4\,d_3 d_1 - 8\,d_1 d_2 - 37 - 8\,{d_3}^2 + 4\,{d_2}^2 + 4\,d_3 d_2)$
$o\ o\ z$	$\frac{736}{59049}\,(d_1 - d_2)(4\,{d_3}^2{d_1}^2 - 8\,{d_3}^2 d_2 d_1 + 6\,d_3 d_1 - 22 - 27\,{d_3}^2 + 4\,{d_3}^2{d_2}^2 + 6\,d_3 d_2)$
$o\ \tilde{o}\ \tilde{o}$	0
$o\ \tilde{o}\ p$	0
$o\ \tilde{o}\ q$	0
$o\ \tilde{o}\ r$	0
$o\ \tilde{o}\ s$	0
$o\ \tilde{o}\ y$	0
$o\ \tilde{o}\ z$	0
$o\ p\ p$	0
$o\ p\ q$	0
$o\ p\ r$	0
$o\ p\ s$	0
$o\ p\ y$	0
$o\ p\ z$	0
$o\ q\ q$	0
$o\ q\ r$	$-\frac{400}{19683}\,d_3 d_2 d_1 + \frac{3200}{59049}\,d_1 - \frac{2240}{59049}\,d_2 - \frac{640}{19683}\,d_3 + \frac{160}{59049}\,{d_3}^2 d_1 - \frac{160}{59049}\,{d_3}^2 d_2 + \frac{400}{19683}\,d_3 {d_2}^2 - \frac{400}{19683}\,d_1 {d_2}^2 + \frac{1360}{59049}\,{d_1}^2 d_2 - \frac{160}{59049}\,{d_1}^3$
$o\ q\ s$	0
$o\ q\ y$	0
$o\ q\ z$	0
$o\ r\ r$	0
$o\ r\ s$	$\frac{5000}{59049}\,d_3 d_1 - \frac{5000}{59049}\,d_3 d_2 + \frac{20000}{59049} - \frac{5000}{59049}\,{d_1}^2 + \frac{5000}{59049}\,d_1 d_2$
$o\ r\ y$	$\frac{160}{59049}\,{d_3}^2{d_2}^2 + \frac{160}{59049}\,d_3{d_2}^3 + \frac{320}{59049}\,{d_3}^3 d_1 + \frac{160}{19683}\,{d_1}^2{d_2}^2 + \frac{320}{59049}\,{d_3}^2 d_2 d_1 - \frac{1720}{59049}\,d_3 d_1 + \frac{1120}{19683} + \frac{160}{19683}\,d_3{d_2}{d_1}^2 - \frac{160}{59049}\,d_1{d_2}^3 - \frac{160}{19683}\,{d_3}^2{d_1}^2 + \frac{160}{59049}\,{d_1}^4 + \frac{1280}{59049}\,{d_3}^2 + \frac{5320}{59049}\,d_1 d_2 + \frac{440}{59049}\,d_3 d_2 - \frac{3400}{59049}\,{d_1}^2 - \frac{320}{59049}\,{d_3}^3 d_2 - \frac{160}{19683}\,d_2{d_1}^3 - \frac{640}{19683}\,{d_2}^2 - \frac{640}{59049}\,d_3 d_1 {d_2}^2$
$o\ r\ z$	$-\frac{1760}{59049}\,{d_1}^2 - \frac{320}{59049}\,{d_3}^3{d_1}^3 + \frac{80}{2187}\,{d_3}^3 d_1 + \frac{160}{19683}\,d_3{d_1}^3 + \frac{320}{59049}\,{d_3}^2{d_1}^4 + \frac{320}{59049}\,{d_3}^3{d_2}^3 - \frac{7840}{59049}\,d_3 d_1 - \frac{80}{2187}\,{d_3}^3 d_2 - \frac{80}{729}\,{d_3}^2{d_1}^2 + \frac{1760}{59049}\,d_1 d_2 + \frac{3280}{19683}\,{d_3}^2 d_2 d_1 + \frac{4000}{59049}\,d_3 d_2 + \frac{320}{2187}\,{d_3}^2 + \frac{640}{19683} + \frac{320}{19683}\,{d_1}^2{d_2}^2{d_3}^2 - \frac{320}{59049}\,{d_3}^2{d_2}^3 d_1 + \frac{320}{19683}\,{d_3}^3 d_2{d_1}^2 - \frac{160}{19683}\,d_3 d_1{d_2}^2 - \frac{320}{19683}\,{d_3}^2 d_2{d_1}^3 - \frac{320}{19683}\,{d_3}^3{d_2}^2 d_1 - \frac{1120}{19683}\,{d_3}^2{d_2}^2$
$o\ s\ s$	0
$o\ s\ y$	0
$o\ s\ z$	0
$o\ y\ y$	0
$o\ y\ z$	0
$o\ z\ z$	0
$\tilde{o}\ \tilde{o}\ \tilde{o}$	0
$\tilde{o}\ \tilde{o}\ p$	0
$\tilde{o}\ \tilde{o}\ q$	$\frac{64}{59049}\,(d_1 - d_2)(2\,d_1 - 15\,d_3 + 2\,d_2)$
$\tilde{o}\ \tilde{o}\ r$	$\frac{12992}{59049}\,d_1 - \frac{12992}{59049}\,d_2$
$\tilde{o}\ \tilde{o}\ s$	$-\frac{4000}{59049}\,d_1 + \frac{4000}{59049}\,d_2$
$\tilde{o}\ \tilde{o}\ y$	$\frac{32}{59049}\,(d_1 - d_2)(4\,{d_1}^2 + 4\,d_3 d_1 - 8\,d_1 d_2 - 37 - 8\,{d_3}^2 + 4\,{d_2}^2 + 4\,d_3 d_2)$
$\tilde{o}\ \tilde{o}\ z$	$\frac{64}{59049}\,(d_1 - d_2)(4\,{d_3}^2{d_1}^2 - 8\,{d_3}^2 d_2 d_1 + 6\,d_3 d_1 - 22 - 27\,{d_3}^2 + 4\,{d_3}^2{d_2}^2 + 6\,d_3 d_2)$
$\tilde{o}\ p\ p$	0
$\tilde{o}\ p\ q$	0
$\tilde{o}\ p\ r$	0
$\tilde{o}\ p\ s$	0
$\tilde{o}\ p\ y$	0
$\tilde{o}\ p\ z$	0
$\tilde{o}\ q\ q$	0
$\tilde{o}\ q\ r$	0
$\tilde{o}\ q\ s$	0
$\tilde{o}\ q\ y$	0
$\tilde{o}\ q\ z$	0

Table A.3: The cubic couplings for all of the fields in the action up to level 3 (continued).

$l\,m\,n$	$B_{lmn}(d_1, d_2, d_3)$
$\tilde{o}\ r\ r$	0
$\tilde{o}\ r\ s$	0
$\tilde{o}\ r\ y$	0
$\tilde{o}\ r\ z$	0
$\tilde{o}\ s\ s$	0
$\tilde{o}\ s\ y$	0
$\tilde{o}\ s\ z$	0
$\tilde{o}\ y\ y$	0
$\tilde{o}\ y\ z$	0
$\tilde{o}\ z\ z$	0
$p\ p\ p$	0
$p\ p\ q$	$-\frac{12800}{59049}\,(d_1 - d_2)(2\,d_1 - 15\,d_3 + 2\,d_2)$
$p\ p\ r$	$-\frac{140800}{59049}\,d_1 + \frac{140800}{59049}\,d_2$
$p\ p\ s$	$\frac{697600}{59049}\,d_1 - \frac{697600}{59049}\,d_2$
$p\ p\ y$	$-\frac{6400}{59049}\,(d_1 - d_2)(4\,{d_1}^2 + 4\,d_3 d_1 - 8\,d_1 d_2 - 37 - 8\,{d_3}^2 + 4\,{d_2}^2 + 4\,d_3 d_2)$
$p\ p\ z$	$-\frac{12800}{59049}\,(d_1 - d_2)(4\,{d_3}^2{d_1}^2 - 8\,{d_3}^2 d_2 d_1 + 6\,d_3 d_1 - 22 - 27\,{d_3}^2 + 4\,{d_3}^2{d_2}^2 + 6\,d_3 d_2)$
$p\ q\ q$	0
$p\ q\ r$	0
$p\ q\ s$	$\frac{64000}{59049}\,d_1 - \frac{44800}{59049}\,d_2 - \frac{12800}{19683}\,d_3 - \frac{8000}{19683}\,d_3 d_2 d_1 + \frac{3200}{59049}\,{d_3}^2 d_1 - \frac{3200}{59049}\,{d_3}^2 d_2 + \frac{8000}{19683}\,d_3 {d_2}^2 - \frac{8000}{19683}\,d_1 {d_2}^2 - \frac{3200}{59049}\,{d_1}^3 + \frac{27200}{59049}\,{d_1}^2 d_2$
$p\ q\ y$	0
$p\ q\ z$	0
$p\ r\ r$	0
$p\ r\ s$	$-\frac{17600}{59049}\,{d_1}^2 + \frac{17600}{59049}\,d_3 d_1 - \frac{17600}{59049}\,d_3 d_2 + \frac{17600}{59049}\,d_1 d_2 + \frac{70400}{59049}$
$p\ r\ y$	0
$p\ r\ z$	0
$p\ s\ s$	0
$p\ s\ y$	$-\frac{3200}{19683}\,d_2 {d_1}^3 - \frac{68000}{59049}\,{d_1}^2 - \frac{12800}{19683}\,{d_2}^2 + \frac{25600}{59049}\,{d_3}^2 - \frac{6400}{59049}\,{d_3}^3 d_2 - \frac{12800}{59049}\,d_3 d_1 {d_2}^2 - \frac{34400}{59049}\,d_3 d_1 + \frac{8800}{59049}\,d_3 d_2 - \frac{3200}{19683}\,{d_3}^2{d_1}^2 + \frac{106400}{59049}\,d_1 d_2 + \frac{3200}{59049}\,{d_3}^2{d_2}^2 + \frac{6400}{59049}\,{d_3}^3 d_1 + \frac{3200}{19683}\,{d_1}^2{d_2}^2 + \frac{3200}{19683}\,d_3 d_2 {d_1}^2 + \frac{6400}{59049}\,{d_3}^2 d_2 d_1 + \frac{3200}{59049}\,{d_1}^4 - \frac{3200}{59049}\,d_1 {d_2}^3 + \frac{3200}{59049}\,d_3 {d_2}^3 + \frac{22400}{19683}$
$p\ s\ z$	$-\frac{6400}{59049}\,{d_3}^2 {d_2}^3 d_1 - \frac{6400}{19683}\,{d_3}^2 d_2 {d_1}^3 - \frac{35200}{59049}\,{d_1}^2 + \frac{6400}{2187}\,{d_3}^2 + \frac{6400}{19683}\,{d_1}^2{d_2}^2{d_3}^2 + \frac{6400}{59049}\,{d_3}^3{d_2}^3 + \frac{6400}{19683}\,{d_3}^3 d_2 {d_1}^2 - \frac{1600}{2187}\,{d_3}^3 d_2 - \frac{3200}{19683}\,d_3 d_1 {d_2}^2 - \frac{156800}{59049}\,d_3 d_1 + \frac{80000}{59049}\,d_3 d_2 - \frac{1600}{729}\,{d_3}^2{d_1}^2 + \frac{3200}{19683}\,d_3 {d_1}^3 + \frac{35200}{59049}\,d_1 d_2 - \frac{22400}{19683}\,{d_3}^2{d_2}^2 + \frac{1600}{2187}\,{d_3}^3 d_1 - \frac{6400}{19683}\,{d_3}^3{d_2}^2 d_1 - \frac{6400}{59049}\,{d_3}^3{d_1}^3 + \frac{65600}{19683}\,{d_3}^2 d_2 d_1 + \frac{6400}{59049}\,{d_3}^2{d_1}^4 + \frac{12800}{19683}$
$p\ y\ y$	0
$p\ y\ z$	0
$p\ z\ z$	0
$q\ q\ q$	$\frac{1}{472392}\,(d_2 - d_3)(d_1 - d_3)(d_1 - d_2)(60\,{d_1}^3 - 398\,{d_1}^2 d_2 - 398\,d_3 {d_1}^2 + 3539\,d_3 d_2 d_1 - 18144\,d_1 - 398\,{d_3}^2 d_1 - 398\,d_1 {d_2}^2 + 60\,{d_2}^3 - 398\,d_3 {d_2}^2 + 60\,{d_3}^3 - 18144\,d_3 - 18144\,d_2 - 398\,{d_3}^2 d_2)$
$q\ q\ r$	$\frac{11}{472392}\,(d_1 - d_2)(30\,d_2 {d_1}^3 - 30\,d_3 {d_1}^3 + 225\,d_3 d_2 {d_1}^2 - 1312\,{d_1}^2 - 229\,{d_1}^2{d_2}^2 + 4\,{d_3}^2{d_1}^2 + 1152\,d_3 d_1 + 30\,{d_3}^3 d_1 + 7488\,d_1 d_2 + 30\,d_1 {d_2}^3 - 285\,{d_3}^2 d_2 d_1 + 225\,d_3 d_1 {d_2}^2 + 416\,{d_3}^2 - 1312\,{d_2}^2 + 4096 - 30\,d_3 {d_2}^3 - 4\,{d_3}^4 + 4\,{d_3}^2{d_2}^2 + 1152\,d_3 d_2 + 30\,{d_3}^3 d_2)$
$q\ q\ s$	$-\frac{125}{944784}\,(d_1 - d_2)(30\,d_2 {d_1}^3 - 30\,d_3 {d_1}^3 + 225\,d_3 d_2 {d_1}^2 - 1312\,{d_1}^2 - 229\,{d_1}^2{d_2}^2 + 4\,{d_3}^2{d_1}^2 + 1152\,d_3 d_1 + 30\,{d_3}^3 d_1 + 7488\,d_1 d_2 + 30\,d_1 {d_2}^3 - 285\,{d_3}^2 d_2 d_1 + 225\,d_3 d_1 {d_2}^2 + 416\,{d_3}^2 - 1312\,{d_2}^2 + 4096 - 30\,d_3 {d_2}^3 - 4\,{d_3}^4 + 4\,{d_3}^2{d_2}^2 + 1152\,d_3 d_2 + 30\,{d_3}^3 d_2)$
$q\ q\ y$	$\frac{1}{944784}\,(d_1 - d_2)(4096 + 2552\,{d_3}^4 d_2 d_1 + 1260\,d_3 d_2 {d_1}^4 + 1260\,d_3 d_1 {d_2}^4 - 1816\,d_3 {d_2}^2 {d_1}^3 - 1816\,d_3 {d_2}^3 {d_1}^2 - 3044\,{d_3}^3{d_2}^2 d_1 - 632\,{d_3}^2 {d_2}^3 {d_1}^3 - 3044\,{d_3}^3 d_2 {d_1}^2 - 632\,{d_3}^2{d_2}^3 d_1 + 5944\,{d_1}^2{d_2}^2{d_3}^2 + 2072\,{d_2}^3{d_1}^3 - 54405\,d_3 d_2 {d_1}^2 - 71968\,{d_3}^2 + 85425\,{d_3}^2 d_2 d_1 - 4800\,{d_2}^4 - 4800\,{d_1}^4 + 376\,{d_3}^3{d_1}^3 + 10902\,d_3 {d_1}^3 - 104\,{d_3}^2{d_1}^4 + 376\,{d_3}^3{d_2}^3 - 33024\,d_3 d_1 - 160768\,d_1 d_2 - 33024\,d_3 d_2 + 30090\,d_2 {d_1}^3 - 44327\,{d_1}^2{d_2}^2 + 67616\,{d_2}^2 + 32\,{d_3}^6 + 30090\,d_1 {d_2}^3 - 1156\,{d_1}^4{d_2}^2 + 72\,{d_3}^4{d_2}^2 - 120\,d_3 {d_1}^5 - 256\,{d_3}^5 d_1 - 1156\,{d_1}^2{d_2}^4 - 104\,{d_3}^2{d_2}^4 - 256\,{d_3}^5 d_2 + 120\,d_2 {d_1}^5 + 120\,d_1 {d_2}^5 - 120\,d_3 {d_2}^5 + 72\,{d_3}^4{d_1}^2 - 54405\,d_3 d_1 {d_2}^2 + 34796\,{d_3}^2{d_1}^2 + 34796\,{d_3}^2{d_2}^2 - 38358\,{d_3}^3 d_2 + 2452\,{d_3}^4 + 10902\,d_3 {d_2}^3 + 67616\,{d_1}^2 - 38358\,{d_3}^3 d_1)$

Table A.3: The cubic couplings for all of the fields in the action up to level 3 (continued).

$l\,m\,n$	$B_{lmn}(d_1,d_2,d_3)$
$q\ q\ z$	$\frac{1}{472392}\,(d_1-d_2)(53248+12663\,{d_3}^4d_2d_1+180\,d_3d_2{d_1}^4+180\,d_3d_1{d_2}^4-1194\,d_3{d_2}^2{d_1}^3-1194\,d_3{d_2}^3{d_1}^2-17553\,{d_3}^3{d_2}^2d_1+31560\,{d_3}^2d_2{d_1}^3-17553\,{d_3}^3d_2{d_1}^2+31560\,{d_3}^2{d_2}^3d_1-43917\,{d_1}^2{d_2}^2{d_3}^2+32\,{d_3}^6d_2d_1+2072\,{d_3}^2{d_2}^3{d_1}^3+2312\,{d_3}^4{d_2}^2{d_1}^2+1140\,{d_3}^3{d_2}^4d_1-1172\,{d_3}^4{d_2}^3d_1-1020\,{d_3}^3{d_2}^2{d_1}^3-1020\,{d_3}^3{d_2}^3{d_1}^2-1172\,{d_3}^4d_2{d_1}^3+120\,{d_3}^2d_2{d_1}^5-1156\,{d_3}^2{d_2}^4{d_1}^2-120\,{d_3}^5{d_2}^2d_1+1140\,{d_3}^3d_2{d_1}^4+120\,{d_3}^2{d_2}^5d_1-1156\,{d_3}^2{d_1}^4{d_2}^2-120\,{d_3}^5d_2{d_1}^2-59382\,d_3d_2{d_1}^2-167616\,{d_3}^2-15106\,{d_3}^2d_2d_1+10626\,{d_3}^3{d_1}^3+660\,d_3{d_1}^3-4980\,{d_3}^2{d_1}^4+10626\,{d_3}^3{d_2}^3+37248\,d_3d_1-33984\,d_1d_2+37248\,d_3d_2-660\,d_2{d_1}^3+5038\,{d_1}^2{d_2}^2-960\,{d_2}^2+108\,{d_3}^6-16\,{d_3}^6{d_2}^2+120\,{d_3}^5{d_1}^3+120\,{d_3}^5{d_2}^3-120\,{d_3}^3{d_1}^5-120\,{d_3}^3{d_2}^5+16\,{d_3}^4{d_2}^4+16\,{d_3}^4{d_1}^4-16\,{d_3}^6{d_1}^2-660\,d_1{d_2}^3-2232\,{d_3}^4{d_2}^2-834\,{d_3}^5d_1-4980\,{d_3}^2{d_2}^4-834\,{d_3}^5d_2-2232\,{d_3}^4{d_1}^2-59382\,d_3d_1{d_2}^2+124360\,{d_3}^2{d_1}^2+124360\,{d_3}^2{d_2}^2-126804\,{d_3}^3d_2+23416\,{d_3}^4+660\,d_3{d_2}^3-960\,{d_1}^2-126804\,{d_3}^3d_1)$
$q\ r\ r$	$\frac{19}{157464}\,(d_2-d_3)(2\,d_1{d_2}^2-2\,d_3{d_2}^2+19\,d_3d_2d_1+32\,d_2-17\,{d_1}^2d_2-2\,{d_3}^2d_2+15\,{d_1}^3-96\,d_1+2\,{d_3}^2d_1+32\,d_3-17\,d_3{d_1}^2)$
$q\ r\ s$	$-\frac{1375}{944784}\,(d_2-d_3)(2\,d_1{d_2}^2-2\,d_3{d_2}^2+19\,d_3d_2d_1+32\,d_2-17\,{d_1}^2d_2-2\,{d_3}^2d_2+15\,{d_1}^3-96\,d_1+2\,{d_3}^2d_1+32\,d_3-17\,d_3{d_1}^2)$
$q\ r\ y$	$\frac{187}{118098}\,{d_3}^4d_2d_1+\frac{55}{26244}\,d_3d_2{d_1}^4+\frac{253}{236196}\,d_3d_1{d_2}^4-\frac{187}{78732}\,d_3{d_2}^3{d_1}^2+\frac{154}{59049}\,{d_1}^4-\frac{209}{78732}\,{d_3}^3{d_2}^2d_1-\frac{88}{19683}\,{d_3}^2d_2{d_1}^3+\frac{11}{39366}\,{d_3}^3d_2{d_1}^2-\frac{11}{39366}\,{d_3}^2{d_2}^3d_1+\frac{187}{39366}\,{d_1}^2{d_2}^2{d_3}^2+\frac{5632}{19683}-\frac{836}{19683}\,d_3d_2{d_1}^2-\frac{4466}{59049}\,{d_3}^2+\frac{14509}{314928}\,{d_3}^2d_2d_1+\frac{55}{26244}\,{d_3}^3{d_1}^3+\frac{14707}{314928}\,d_3{d_1}^3+\frac{11}{118098}\,{d_3}^2{d_1}^4+\frac{11}{39366}\,{d_3}^3{d_2}^3+\frac{187}{78732}\,{d_2}^3{d_1}^3+\frac{638}{6561}\,d_3d_1+\frac{5830}{59049}\,d_1d_2+\frac{2024}{59049}\,d_3d_2-\frac{11}{432}\,d_2{d_1}^3+\frac{37543}{944784}\,{d_1}^2{d_2}^2-\frac{374}{6561}\,{d_2}^2+\frac{44}{19683}\,{d_2}^4-\frac{517}{236196}\,{d_1}^4{d_2}^2-\frac{77}{78732}\,{d_1}^2{d_2}^4+\frac{55}{78732}\,d_2{d_1}^5+\frac{11}{118098}\,d_1{d_2}^5-\frac{11}{118098}\,d_3{d_2}^5-\frac{9031}{472392}\,d_1{d_2}^3+\frac{11}{118098}\,{d_3}^4{d_2}^2+\frac{11}{59049}\,{d_3}^5d_1-\frac{11}{118098}\,{d_3}^2{d_2}^4-\frac{11}{59049}\,{d_3}^5d_2-\frac{11}{6561}\,{d_3}^4{d_1}^2-\frac{517}{34992}\,d_3d_1{d_2}^2-\frac{40711}{944784}\,{d_3}^2{d_1}^2+\frac{704}{59049}\,{d_3}^2{d_2}^2-\frac{2717}{157464}\,{d_3}^3d_2+\frac{176}{59049}\,{d_3}^4+\frac{2167}{472392}\,d_3{d_2}^2-\frac{14212}{59049}\,{d_1}^2-\frac{55}{78732}\,d_3{d_1}^5+\frac{2519}{472392}\,{d_3}^3d_1$
$q\ r\ z$	$\frac{4499}{157464}\,{d_3}^4d_2d_1+\frac{55}{26244}\,d_3d_2{d_1}^4+\frac{11}{39366}\,d_3d_1{d_2}^4-\frac{55}{26244}\,d_3{d_2}^3{d_1}^2+\frac{187}{39366}\,{d_3}^2{d_2}^3{d_1}^3+\frac{187}{39366}\,{d_3}^4{d_2}^2{d_1}^2+\frac{77}{39366}\,{d_3}^3{d_2}^4d_1-\frac{187}{118098}\,{d_3}^4{d_2}^3d_1+\frac{11}{59049}\,{d_3}^3{d_2}^2{d_1}^3-\frac{22}{6561}\,{d_3}^3{d_2}^3{d_1}^2-\frac{187}{39366}\,{d_3}^4d_2{d_1}^3+\frac{55}{39366}\,{d_3}^2d_2{d_1}^5-\frac{77}{39366}\,{d_3}^2{d_2}^4{d_1}^2-\frac{11}{19683}\,{d_3}^5{d_2}^2d_1+\frac{55}{19683}\,{d_3}^3d_2{d_1}^4+\frac{11}{59049}\,{d_3}^2{d_2}^5d_1-\frac{517}{118098}\,{d_3}^2{d_1}^4{d_2}^2+\frac{11}{19683}\,{d_3}^5d_2{d_1}^2-\frac{11}{39366}\,d_3{d_2}^2{d_1}^3-\frac{451}{52488}\,{d_3}^3{d_2}^2d_1-\frac{7799}{157464}\,{d_3}^2d_2{d_1}^3-\frac{616}{19683}\,{d_3}^3d_2{d_1}^2-\frac{4213}{118098}\,{d_3}^2{d_2}^3d_1+\frac{12265}{157464}\,{d_1}^2{d_2}^2{d_3}^2+\frac{5632}{19683}-\frac{11}{59049}\,{d_3}^3{d_2}^5-\frac{55}{39366}\,{d_3}^3{d_1}^5+\frac{11}{59049}\,{d_3}^5{d_2}^3-\frac{11}{59049}\,{d_3}^5{d_1}^3-\frac{176}{2187}\,d_3d_2{d_1}^2+\frac{1496}{19683}\,{d_3}^2+\frac{83897}{236196}\,{d_3}^2d_2d_1+\frac{14729}{472392}\,{d_3}^3{d_1}^3+\frac{869}{8748}\,d_3{d_1}^3+\frac{737}{236196}\,{d_3}^2{d_1}^4+\frac{2057}{236196}\,{d_3}^3{d_2}^3+\frac{6776}{59049}\,d_3d_1-\frac{3520}{59049}\,d_1d_2+\frac{5104}{59049}\,d_3d_2-\frac{605}{78732}\,d_2{d_1}^3+\frac{2057}{236196}\,{d_1}^2{d_2}^2-\frac{88}{6561}\,{d_2}^2-\frac{121}{118098}\,{d_1}^2{d_2}^3-\frac{341}{39366}\,{d_3}^4{d_2}^2+\frac{11}{8748}\,{d_3}^5d_1+\frac{55}{13122}\,{d_3}^2{d_2}^4-\frac{11}{8748}\,{d_3}^5d_2-\frac{1045}{52488}\,{d_3}^4{d_1}^2+\frac{187}{118098}\,{d_3}^4{d_1}^4-\frac{8921}{236196}\,d_3d_1{d_2}^2-\frac{55913}{236196}\,{d_3}^2{d_1}^2-\frac{1012}{19683}\,{d_3}^2{d_2}^2-\frac{8041}{118098}\,{d_3}^3d_2+\frac{44}{2187}\,{d_3}^4+\frac{121}{118098}\,d_3{d_2}^3-\frac{20504}{59049}\,{d_1}^2-\frac{143}{118098}\,{d_3}^3d_1$
$q\ s\ s$	$\frac{9475}{629856}\,(d_2-d_3)(2\,d_1{d_2}^2-2\,d_3{d_2}^2+19\,d_3d_2d_1+32\,d_2-17\,{d_1}^2d_2-2\,{d_3}^2d_2+15\,{d_1}^3-96\,d_1+2\,{d_3}^2d_1+32\,d_3-17\,d_3{d_1}^2)$
$q\ s\ y$	$-\frac{2125}{236196}\,{d_3}^4d_2d_1-\frac{625}{52488}\,d_3d_2{d_1}^4-\frac{2875}{472392}\,d_3d_1{d_2}^4+\frac{2125}{157464}\,d_3{d_2}^3{d_1}^2-\frac{875}{59049}\,{d_1}^4+\frac{2375}{157464}\,{d_3}^3{d_2}^2d_1+\frac{500}{19683}\,{d_3}^2d_2{d_1}^3-\frac{125}{78732}\,{d_3}^3d_2{d_1}^2+\frac{125}{78732}\,{d_3}^2{d_2}^3d_1-\frac{2125}{78732}\,{d_1}^2{d_2}^2{d_3}^2-\frac{32000}{19683}+\frac{4750}{19683}\,d_3d_2{d_1}^2+\frac{25375}{59049}\,{d_3}^2-\frac{164875}{629856}\,{d_3}^2d_2d_1-\frac{625}{52488}\,{d_3}^3{d_1}^3-\frac{167125}{629856}\,d_3{d_1}^3-\frac{125}{236196}\,{d_3}^2{d_1}^4-\frac{125}{78732}\,{d_3}^3{d_2}^3-\frac{2125}{157464}\,{d_2}^3{d_1}^3-\frac{3625}{6561}\,d_3d_1-\frac{33125}{59049}\,d_1d_2-\frac{11500}{59049}\,d_3d_2+\frac{125}{864}\,d_2{d_1}^3-\frac{426625}{1889568}\,{d_1}^2{d_2}^2+\frac{2125}{6561}\,{d_2}^2-\frac{250}{19683}\,{d_2}^4+\frac{5875}{472392}\,{d_1}^4{d_2}^2+\frac{875}{157464}\,{d_1}^2{d_2}^4-\frac{625}{157464}\,d_2{d_1}^5-\frac{125}{236196}\,d_1{d_2}^5+\frac{125}{236196}\,d_3{d_2}^5+\frac{102625}{944784}\,d_1{d_2}^3-\frac{125}{236196}\,{d_3}^4{d_2}^2-\frac{125}{118098}\,{d_3}^5d_1+\frac{125}{236196}\,{d_3}^2{d_2}^4+\frac{125}{118098}\,{d_3}^5d_2+\frac{125}{13122}\,{d_3}^4{d_1}^2+\frac{5875}{69984}\,d_3d_1{d_2}^2+\frac{462625}{1889568}\,{d_3}^2{d_1}^2-\frac{4000}{59049}\,{d_3}^2{d_2}^2+\frac{30875}{314928}\,{d_3}^3d_2-\frac{1000}{59049}\,{d_3}^4-\frac{24625}{944784}\,d_3{d_2}^3+\frac{80750}{59049}\,{d_1}^2+\frac{625}{157464}\,d_3{d_1}^5-\frac{28625}{944784}\,{d_3}^3d_1$
$q\ s\ z$	$-\frac{2125}{78732}\,{d_3}^2{d_2}^3{d_1}^3-\frac{2125}{78732}\,{d_3}^4{d_2}^2{d_1}^2-\frac{875}{78732}\,{d_3}^3{d_2}^4d_1+\frac{2125}{236196}\,{d_3}^4{d_2}^3d_1-\frac{51125}{314928}\,{d_3}^4d_2{d_1}^3-\frac{125}{118098}\,{d_3}^3{d_2}^2{d_1}^3+\frac{125}{6561}\,{d_3}^3{d_2}^3{d_1}^2+\frac{2125}{78732}\,{d_3}^4{d_2}^2d_1{}^3-\frac{625}{78732}\,{d_3}^2{d_2}^2{d_1}^5-\frac{625}{52488}\,d_3{d_2}^2{d_1}^4-\frac{125}{78732}\,d_3d_1{d_2}^4+\frac{875}{78732}\,{d_3}^2{d_2}^4{d_1}^2+\frac{125}{39366}\,{d_3}^5{d_2}^2d_1-\frac{625}{39366}\,{d_3}^3{d_2}{d_1}^4+\frac{625}{52488}\,d_3{d_2}^3{d_1}^2-\frac{125}{118098}\,{d_3}^2{d_2}^5d_1+\frac{5875}{236196}\,{d_3}^2{d_1}^4{d_2}^2-\frac{125}{39366}\,{d_3}^5{d_2}{d_1}^2+\frac{125}{78732}\,d_3{d_2}^2{d_1}^3+\frac{5125}{104976}\,{d_3}^3{d_2}^2d_1+\frac{88625}{314928}\,{d_3}^2{d_2}{d_1}^3+\frac{3500}{19683}\,{d_3}^3{d_2}{d_1}^2+\frac{47875}{236196}\,{d_3}^2{d_2}^3d_1-\frac{139375}{314928}\,{d_1}^2{d_2}^2{d_3}^2-\frac{32000}{19683}+\frac{1000}{2187}\,d_3d_2{d_1}^2-\frac{8500}{19683}\,{d_3}^2-\frac{953375}{472392}\,{d_3}^2d_2d_1-\frac{167375}{944784}\,{d_3}^3{d_1}^3-\frac{9875}{17496}\,d_3{d_1}^3-\frac{8375}{472392}\,{d_3}^2{d_1}^4-\frac{23375}{472392}\,{d_3}^3{d_2}^3-\frac{38500}{59049}\,d_3d_1+\frac{20000}{59049}\,d_1d_2-\frac{29000}{59049}\,d_3d_2+\frac{6875}{157464}\,d_2{d_1}^3-\frac{23375}{472392}\,{d_1}^2{d_2}^2+\frac{500}{6561}\,{d_2}^2+\frac{1375}{236196}\,d_1{d_2}^3+\frac{125}{118098}\,{d_3}^3{d_2}^5+\frac{3875}{78732}\,{d_3}^4{d_2}^2-\frac{125}{17496}\,{d_3}^5d_1-\frac{625}{26244}\,{d_3}^2{d_2}^4+\frac{125}{17496}\,{d_3}^5d_2+\frac{11875}{104976}\,{d_3}^4{d_1}^2+\frac{101375}{472392}\,d_3d_1{d_2}^2+\frac{6353375}{472392}\,{d_3}^2{d_1}^2+\frac{5750}{19683}\,{d_3}^2{d_2}^2+\frac{91375}{236196}\,{d_3}^3d_2+\frac{125}{118098}\,{d_3}^5{d_1}^3-\frac{250}{2187}\,{d_3}^4-\frac{1375}{236196}\,d_3{d_2}^3+\frac{625}{78732}\,{d_3}^3{d_1}^5-\frac{125}{118098}\,{d_3}^5{d_2}^3+\frac{116500}{59049}\,{d_1}^2+\frac{1625}{236196}\,{d_3}^3d_1-\frac{2125}{236196}\,{d_3}^4{d_1}^4$

Table A.3: The cubic couplings for all of the fields in the action up to level 3 (continued).

$l\,m\,n$	$B_{lmn}(d_1,d_2,d_3)$
$q\ y\ y$	$\frac{1}{1889568}\,(d_2-d_3)(424251\,d_3d_2d_1-800\,d_3d_1{d_2}^5+2528\,d_3d_2{d_1}^5-10748\,d_3{d_2}^3d_1-182520\,d_3{d_2}^1{d_1}^3-2656\,{d_3}^2{d_1}^4d_2+135240\,{d_3}^2{d_2}^1{d_1}^2-176\,{d_3}^2d_1{d_2}^4-2656\,d_3{d_2}^2{d_1}^4-176\,{d_3}^4{d_2}^2d_1-93944\,{d_3}^2d_1{d_2}^2-896\,{d_3}^3d_2{d_1}^3-3008\,{d_3}^2{d_2}^3{d_1}^2+2272\,d_3{d_2}^4{d_1}^2+6160\,{d_3}^2{d_2}^2{d_1}^3+2080\,{d_3}^3{d_2}^3d_1+2272\,{d_3}^4d_2{d_1}^2-800\,{d_3}^5d_2d_1-3008\,{d_3}^3{d_2}^2{d_1}^2-896\,d_3{d_2}^3{d_1}^3-10748\,{d_3}^3d_2d_1+135240\,d_3{d_2}^2{d_1}^2-54066\,{d_3}^2d_2+43328\,{d_3}^3-54066\,d_3{d_2}^2+43328\,{d_2}^3-25390\,d_1{d_2}^2-25390\,{d_3}^2d_1-173897\,d_3{d_1}^2-173897\,{d_1}^2d_2+102295\,{d_1}^3-160\,{d_3}^4{d_2}^3-24408\,{d_1}^5+472\,{d_3}^4d_2+64\,{d_3}^6d_2+64\,d_3{d_2}^6-512\,d_3{d_1}^6+240\,{d_1}^7-15480\,{d_3}^2{d_1}^3-15660\,{d_1}^2{d_2}^3+9512\,d_1{d_2}^4+1984\,{d_2}^3{d_1}^4-1936\,{d_2}^4{d_1}^3+47572\,{d_1}^4d_2-15480\,{d_2}^2{d_1}^3+9512\,{d_3}^4d_1-1936\,{d_3}^4{d_1}^3+1984\,{d_3}^3{d_1}^4+472\,d_3{d_2}^4+47572\,d_3{d_1}^4+96\,{d_3}^2{d_2}^5-416\,{d_3}^2{d_1}^5+704\,{d_3}^5{d_1}^2-64\,d_1{d_2}^6+704\,{d_1}^2{d_2}^5-512\,d_2{d_1}^6-416\,{d_1}^5{d_2}^2-64\,{d_3}^6d_1+434912\,d_1-240224\,d_2-160\,{d_3}^3{d_2}^4+1064\,{d_3}^2{d_2}^3-15660\,{d_3}^3{d_1}^2+96\,{d_3}^5{d_2}^2-240224\,d_3-1536\,{d_2}^5-1536\,{d_3}^5+1064\,{d_3}^3{d_2}^2)$
$q\ y\ z$	$\frac{5}{13122}\,d_3d_2{d_1}^6+\frac{2}{19683}\,{d_3}^7{d_1}^2d_2+\frac{5}{19683}\,{d_3}^2{d_2}^1{d_1}^7-\frac{5}{19683}\,{d_3}^3d_2{d_1}^6+\frac{197}{26244}\,{d_3}^6d_2d_1-\frac{14}{19683}\,{d_3}^3{d_2}^6d_1-\frac{4}{59049}\,{d_3}^2{d_2}^7d_1-\frac{65}{59049}\,{d_3}^6d_2{d_1}^3-\frac{1}{243}\,{d_3}^3{d_2}^3{d_1}^4+\frac{17}{6561}\,{d_3}^5d_2{d_1}^4+\frac{11}{19683}\,{d_3}^5{d_2}^3{d_1}^2+\frac{23}{19683}\,{d_3}^6{d_2}^2{d_1}^2-\frac{121}{59049}\,{d_3}^2{d_2}^5{d_1}^3+\frac{29}{6561}\,{d_3}^4{d_2}^3{d_1}^3-\frac{32}{59049}\,{d_3}^2{d_2}^2{d_1}^6+\frac{19}{6561}\,{d_3}^3{d_2}^2{d_1}^5-\frac{55}{59049}\,{d_3}^4{d_2}^2{d_1}^4-\frac{49}{19683}\,{d_3}^5{d_2}^2{d_1}^3+\frac{22}{19683}\,{d_3}^3{d_2}^5{d_1}^2+\frac{44}{59049}\,{d_3}^2{d_2}^6{d_1}^2-\frac{94}{59049}\,{d_3}^4{d_2}d_1{}^5+\frac{61}{59049}\,{d_3}^4{d_2}^5d_1-\frac{218}{59049}\,{d_3}^4{d_2}^4{d_1}^2-\frac{26}{59049}\,{d_3}^2{d_2}^3{d_1}^5+\frac{124}{59049}\,{d_3}^2{d_2}^4{d_1}^4+\frac{2}{6561}\,{d_3}^5{d_2}^4d_1+\frac{74}{59049}\,{d_3}^3{d_2}^4{d_1}^3-\frac{2}{19683}\,{d_3}^7{d_2}^2d_1-\frac{35}{2187}\,{d_3}^2{d_2}^3{d_1}^3+\frac{979}{78732}\,{d_3}^4{d_2}^2{d_1}^2-\frac{1}{4374}\,d_3{d_2}^4{d_1}^3-\frac{1283}{78732}\,{d_3}^3{d_2}^4d_1-\frac{2327}{118098}\,{d_3}^4{d_2}^3d_1-\frac{12007}{118098}\,{d_3}^3{d_2}^2{d_1}^3+\frac{506}{6561}\,{d_3}^3{d_2}^3{d_1}^2+\frac{3221}{78732}\,{d_3}^4d_2{d_1}^3-\frac{526}{19683}\,{d_3}^2{d_2}d_1{}^5-\frac{1265}{78732}\,{d_3}^2{d_2}^4{d_1}^2-\frac{47}{39366}\,d_3{d_2}^3{d_1}^4+\frac{613}{39366}\,{d_3}^5{d_2}^2d_1+\frac{13}{39366}\,d_3{d_2}^2{d_1}^5+\frac{587}{26244}\,{d_3}^3d_2{d_1}^4+\frac{1079}{118098}\,{d_3}^2{d_2}^5d_1+\frac{12179}{236196}\,{d_3}^2{d_1}^4{d_2}^2-\frac{337}{8748}\,{d_3}^5d_2{d_1}^2-\frac{82351}{944784}\,{d_3}^4d_2d_1-\frac{109015}{472392}\,{d_3}^2{d_2}d_1-\frac{33271}{314928}\,{d_1}^2{d_2}^2{d_3}^2-\frac{1}{2187}\,{d_3}^6{d_2}^3d_1+\frac{124823}{314928}\,{d_3}^3{d_2}^2d_1-\frac{14659}{39366}\,{d_3}^3d_2{d_1}^2-\frac{1597}{52488}\,d_3d_2{d_1}^4-\frac{1091}{236196}\,d_3d_1{d_2}^4-\frac{5171}{26244}\,{d_3}^2{d_2}^3d_1+\frac{292651}{944784}\,{d_3}^2d_2{d_1}^3-\frac{9403}{78732}\,d_3{d_2}^2{d_1}^3+\frac{19267}{157464}\,d_3{d_2}^3{d_1}^2-\frac{2}{19683}\,d_3d_1{d_2}^6+\frac{4408}{19683}\,d_3d_2{d_1}^2+\frac{124471}{472392}\,d_3d_1{d_2}^2+\frac{16}{19683}\,d_3{d_2}^5{d_1}^2-\frac{256}{2187}-\frac{380}{6561}\,{d_1}^4+\frac{3188}{6561}\,{d_3}^2-\frac{782}{6561}\,{d_3}^4-\frac{6284}{59049}\,{d_2}^2-\frac{22}{59049}\,d_3{d_2}^5+\frac{1996}{6561}\,{d_1}^2-\frac{103}{39366}\,{d_3}^6{d_2}^2-\frac{2}{59049}\,{d_3}^4{d_2}^6+\frac{2}{59049}\,{d_3}^6{d_2}^4-\frac{10}{6561}\,{d_3}^2{d_2}^6+\frac{32}{6561}\,{d_2}^4+\frac{4}{59049}\,{d_3}^3{d_2}^7+\frac{5321}{236196}\,{d_3}^5{d_1}^3+\frac{25}{59049}\,{d_3}^5{d_2}^3+\frac{71}{4374}\,{d_3}^3{d_1}^5+\frac{265}{118098}\,{d_3}^3{d_2}^5-\frac{2}{19683}\,{d_3}^5{d_2}^5-\frac{5}{19683}\,{d_3}^3{d_1}^7+\frac{47}{59049}\,{d_3}^4{d_1}^6+\frac{7}{19683}\,{d_3}^6{d_1}^4-\frac{17}{19683}\,{d_3}^5{d_1}^5-\frac{1}{4374}\,{d_3}^7d_2+\frac{371}{157464}\,d_2{d_1}^3+\frac{49511}{236196}\,{d_3}^3d_2-\frac{9668}{19683}\,d_3d_1-\frac{760}{6561}\,d_3d_2-\frac{101657}{472392}\,{d_3}^2{d_1}^2-\frac{2593}{52488}\,d_3{d_1}^3-\frac{2858}{19683}\,{d_3}^2{d_2}^2+\frac{24289}{236196}\,{d_3}^3d_1+\frac{15575}{236196}\,d_1{d_2}^3-\frac{19031}{236196}\,d_3{d_2}^3+\frac{11}{59049}\,{d_1}^4{d_2}^2-\frac{5339}{236196}\,{d_3}^4{d_2}^2+\frac{655}{39366}\,d_3{d_1}^5-\frac{31871}{472392}\,{d_3}^5d_1-\frac{22}{6561}\,{d_1}^2{d_2}^4+\frac{9835}{236196}\,{d_3}^2{d_2}^4+\frac{13871}{472392}\,{d_3}^5d_2-\frac{55}{39366}\,d_2{d_1}^5+\frac{22}{59049}\,d_1{d_2}^5+\frac{13997}{472392}\,{d_3}^2{d_1}^4+\frac{22691}{104976}\,{d_3}^4{d_1}^2-\frac{3605}{157464}\,{d_3}^3{d_2}^3-\frac{43253}{314928}\,{d_3}^3{d_1}^3+\frac{12752}{59049}\,d_1d_2-\frac{43399}{472392}\,{d_1}^2{d_2}^2+\frac{55}{13122}\,{d_2}^3{d_1}^3+\frac{2}{59049}\,{d_3}^7{d_2}^3+\frac{1}{4374}\,{d_3}^7d_1-\frac{5}{13122}\,{d_3}^2{d_1}^6+\frac{1}{13122}\,{d_3}^4{d_2}^4-\frac{1991}{59049}\,{d_3}^4{d_1}^4+\frac{4}{729}\,{d_3}^6-\frac{385}{78732}\,{d_3}^6{d_1}^2-\frac{2}{59049}\,{d_3}^7{d_1}^3$
$q\ z\ z$	$\frac{1}{472392}\,(d_2-d_3)(256876\,d_3d_2d_1-324\,d_3d_1{d_2}^5+14940\,d_3d_2{d_1}^5-45138\,d_3{d_2}^3d_1-212496\,d_3d_2{d_1}^3-27742\,{d_3}^2{d_1}^4d_2+401154\,{d_3}^2{d_2}^2d_1{}^2+59920\,{d_3}^2d_1{d_2}^4-27742\,d_3{d_2}^2{d_1}^4+59920\,{d_3}^4{d_2}^2d_1-666816\,{d_3}^2d_1{d_2}^2+2032\,{d_3}^3d_2{d_1}^3-198201\,{d_3}^2{d_2}^3{d_1}^2+3030\,d_3{d_2}^4{d_1}^2+208779\,{d_3}^2{d_2}^2{d_1}^3+172487\,{d_3}^3{d_2}^3d_1+3030\,{d_3}^4d_2{d_1}^2-324\,{d_3}^5d_2d_1-198201\,{d_3}^3{d_2}^2{d_1}^2+2032\,d_3{d_2}^3{d_1}^3-45138\,{d_3}^3d_2d_1+401154\,d_3{d_2}^2{d_1}^2-206600\,{d_3}^2d_2+15552\,{d_3}^3-206600\,d_3{d_2}^2+15552\,{d_2}^3+184136\,d_1{d_2}^2+184136\,{d_3}^2d_1+180124\,d_3{d_1}^2+180124\,{d_1}^2d_2+4380\,{d_1}^3-31958\,{d_3}^4{d_2}^3-96\,{d_3}^6{d_2}^3{d_1}^2-96\,{d_3}^3{d_2}^6{d_1}^2+37884\,{d_3}^4{d_2}^3{d_1}^2+2352\,{d_3}^3{d_2}^3{d_1}^5-62424\,{d_3}^3{d_2}^3{d_1}^3-2544\,{d_3}^4{d_2}^3{d_1}^4+816\,{d_3}^4{d_2}^2{d_1}^5+360\,{d_3}^2{d_2}d_1{}^6+31320\,{d_3}^3{d_2}^2{d_1}^4+4476\,{d_3}^5{d_2}^2{d_1}^2+48\,{d_3}^5{d_2}d_1{}^3-6948\,{d_3}^5{d_2}^3d_1-1104\,{d_3}^4{d_2}^5{d_1}^2-752\,{d_3}^3{d_2}^2{d_1}^6-216\,{d_3}^2{d_2}^6d_1-360\,{d_3}^4{d_2}d_1{}^4+4476\,{d_3}^2{d_2}^5{d_1}^2+1040\,{d_3}^5{d_2}^3{d_1}^3+48\,d_3{d_2}^5{d_1}^3-20076\,{d_3}^4{d_2}^2{d_1}^3-216\,{d_3}^6{d_2}^2d_1-752\,{d_3}^2{d_2}^3{d_1}^6-20076\,{d_3}^2{d_2}^4{d_1}^3+1040\,{d_3}^3{d_2}^5{d_1}^3+32\,{d_3}^2{d_2}^6{d_1}^3+32\,{d_3}^6{d_2}^2{d_1}^3-48\,d_3{d_2}^3{d_1}^5-48\,{d_3}^3{d_2}d_1{}^5-2544\,{d_3}^3{d_2}^4{d_1}^4+31320\,{d_3}^2{d_2}^3{d_1}^4+37884\,{d_3}^3{d_2}^4{d_1}^2+816\,{d_3}^2{d_2}^4{d_1}^5+360\,d_3{d_2}^2{d_1}^6-336\,{d_3}^5{d_2}^2{d_1}^4-336\,{d_3}^2{d_2}^5{d_1}^4+432\,{d_3}^5{d_2}^5d_1-15864\,{d_3}^2{d_2}^2{d_1}^5+240\,{d_3}^2{d_2}^2{d_1}^7+2736\,{d_3}^4{d_2}^4{d_1}^3-19872\,{d_3}^4{d_2}^4d_1-1104\,{d_3}^5{d_2}^4{d_1}^2+96\,{d_3}^4{d_2}^6d_1-360\,d_3{d_1}^4{d_2}^4-6948\,{d_3}^3{d_2}^5d_1+96\,{d_3}^6{d_2}^4d_1-1188\,{d_3}^4d_2+3090\,{d_3}^2{d_1}^3-17274\,{d_1}^2{d_2}^3+1188\,d_1{d_2}^4+1496\,{d_2}^3{d_1}^4-176\,{d_2}^4{d_1}^3-56700\,{d_1}^4d_2+3090\,{d_2}^2{d_1}^3+1188\,{d_3}^4d_1-176\,{d_3}^4{d_1}^3+1496\,{d_3}^3{d_1}^4-1188\,d_3{d_2}^4-56700\,d_3{d_1}^4-4860\,{d_3}^2{d_2}^5-1320\,{d_3}^2{d_1}^5-1320\,{d_1}^5{d_2}^2+165120\,d_1-273024\,d_2-31958\,{d_3}^3{d_2}^4+136140\,{d_3}^2{d_2}^3-17274\,{d_3}^3d_1{}^2-4860\,{d_3}^5{d_2}^2-273024\,d_3+2424\,{d_3}^4{d_2}^5+2424\,{d_3}^5{d_2}^4+216\,{d_3}^3{d_2}^6+216\,{d_3}^6{d_2}^3-32\,{d_3}^5{d_2}^6-32\,{d_3}^6{d_2}^5+136140\,{d_3}^3{d_2}^2)$
$r\ r\ r$	$-\frac{1}{1944}\,(d_2-d_3)(d_1-d_3)(d_1-d_2)$
$r\ r\ s$	$\frac{2375}{314928}\,(d_2-d_3)(d_1-d_3)(d_1-d_2)$
$r\ r\ y$	$-\frac{19}{314928}\,(d_1-d_2)(4\,d_2{d_1}^3-4\,d_3{d_1}^3-8\,{d_1}^2{d_2}^2+8\,d_3d_2{d_1}^2+32\,{d_1}^2+4\,d_1{d_2}^3+12\,{d_3}^3d_1-27\,d_3d_1-101\,d_1d_2-24\,{d_3}^2{d_2}d_1+8\,d_3d_1{d_2}^2-320+91\,{d_3}^2-8\,{d_3}^4-4\,d_3{d_2}^3+32\,{d_2}^2+12\,{d_3}^3d_2-27\,d_3d_2)$

Table A.3: The cubic couplings for all of the fields in the action up to level 3 (continued).

$l\,m\,n$	$B_{lmn}(d_1,d_2,d_3)$
$r\ r\ z$	$-\frac{19}{157464}\,(d_1-d_2)(4\,{d_3}^2{d_2}{d_1}^3-4\,{d_3}^3{d_1}^3+26\,{d_3}^2{d_1}^2+4\,{d_3}^4{d_1}^2+6\,d_3{d_2}{d_1}^2+4\,{d_3}^3{d_2}{d_1}^2-8\,{d_1}^2{d_2}^2{d_3}^2+4\,{d_3}^2{d_2}^3d_1-74\,d_3d_1-8\,{d_3}^4{d_2}d_1-103\,{d_3}^2{d_2}d_1-22\,d_1d_2+33\,{d_3}^3d_1+6\,d_3d_1{d_2}^2+4\,{d_3}^3{d_2}^2d_1+33\,{d_3}^3d_2+4\,{d_3}^4{d_2}^2-74\,d_3d_2-214\,{d_3}^2+64+26\,{d_3}^2{d_2}^2-27\,{d_3}^4-4\,{d_3}^3{d_2}^3)$
$r\ s\ s$	$-\frac{104225}{629856}\,(d_2-d_3)(d_1-d_3)(d_1-d_2)$
$r\ s\ y$	$\frac{1375}{1889568}\,(d_1-d_2)(4\,{d_2}{d_1}^3-4\,{d_3}{d_1}^3-8\,{d_1}^2{d_2}^2+8\,{d_3}{d_2}{d_1}^2+32\,{d_1}^2+4\,{d_1}{d_2}^3+12\,{d_3}^3d_1-27\,{d_3}{d_1}-101\,{d_1}{d_2}-24\,{d_3}^2{d_2}{d_1}+8\,{d_3}{d_1}{d_2}^2-320+91\,{d_3}^2-8\,{d_3}^4-4\,{d_3}{d_2}^3+32\,{d_2}^2+12\,{d_3}^3d_2-27\,{d_3}{d_2})$
$r\ s\ z$	$\frac{1375}{944784}\,(d_1-d_2)(4\,{d_3}^2{d_2}{d_1}^3-4\,{d_3}^3{d_1}^3+26\,{d_3}^2{d_1}^2+4\,{d_3}^4{d_1}^2+6\,{d_3}{d_2}{d_1}^2+4\,{d_3}^3{d_2}{d_1}^2-8\,{d_1}^2{d_2}^2{d_3}^2+4\,{d_3}^2{d_2}^3d_1-74\,d_3d_1-8\,{d_3}^4{d_2}d_1-103\,{d_3}^2{d_2}d_1-22\,d_1d_2+33\,{d_3}^3d_1+6\,d_3d_1{d_2}^2+4\,{d_3}^3{d_2}^2d_1+33\,{d_3}^3d_2+4\,{d_3}^4{d_2}^2-74\,d_3d_2-214\,{d_3}^2+64+26\,{d_3}^2{d_2}^2-27\,{d_3}^4-4\,{d_3}^3{d_2}^3)$
$r\ y\ y$	$-\frac{11}{1889568}\,(d_2-d_3)(24000-160\,{d_3}^3{d_2}^2d_1+128\,{d_3}^4{d_2}d_1-160\,{d_3}^2{d_2}^3d_1+368\,{d_1}^2{d_2}^2{d_3}^2-64\,{d_3}^3{d_2}{d_1}^2-160\,{d_3}^2{d_2}{d_1}^3+808\,{d_3}{d_1}{d_2}^2+808\,{d_3}^2{d_2}d_1-1400\,{d_3}{d_2}{d_1}^2+160\,{d_3}{d_2}{d_1}^4+128\,{d_3}{d_1}{d_2}^4-160\,{d_3}{d_2}^2{d_1}^3-64\,{d_3}{d_2}^3{d_1}^2-32\,{d_3}^2{d_1}^4+128\,{d_2}^3{d_1}^3-32\,{d_3}{d_2}^5-964\,{d_2}{d_1}^3+3072\,{d_1}^2{d_2}^2-2068\,{d_1}{d_2}^3+9543\,{d_3}{d_1}+9543\,{d_1}{d_2}+788\,{d_3}^3d_2+10809\,{d_3}{d_2}-5639\,{d_1}^2-964\,{d_3}{d_1}^3+256\,{d_2}^4-296\,{d_1}^4+16\,{d_1}^6-2068\,{d_3}^3d_1-8032\,{d_3}^2+256\,{d_3}^4+788\,{d_3}{d_2}^3+128\,{d_3}^3{d_1}^3+3072\,{d_3}^2{d_1}^2-112\,{d_3}^4{d_1}^2-8032\,{d_2}^2-16\,{d_3}^4{d_2}^2-2088\,{d_3}^2{d_2}^2+96\,{d_3}^3{d_2}^3-32\,{d_1}^4{d_2}^2-32\,{d_3}{d_1}^5+32\,{d_3}^5d_1-112\,{d_1}^2{d_2}^4-16\,{d_3}^2{d_2}^4-32\,{d_3}^5d_2-32\,{d_2}{d_1}^5+32\,{d_1}{d_2}^5)$
$r\ y\ z$	$\frac{22}{59049}\,{d_3}^2{d_2}^2{d_1}^5+\frac{11}{13122}\,{d_3}{d_2}^3{d_1}^3+\frac{11}{162}\,{d_3}^3{d_2}{d_1}+\frac{275}{6561}\,{d_3}{d_2}^2{d_1}^2-\frac{88}{59049}\,{d_3}{d_2}{d_1}-\frac{11}{19683}\,{d_3}{d_1}{d_2}^5-\frac{11}{39366}\,{d_3}{d_2}{d_1}^5+\frac{44}{19683}\,{d_3}^4{d_2}^4{d_1}-\frac{44}{59049}\,{d_3}^3{d_2}^5{d_1}-\frac{22}{59049}\,{d_3}^2{d_2}^6{d_1}+\frac{22}{19683}\,{d_3}^4{d_2}{d_1}^4+\frac{77}{59049}\,{d_3}^2{d_2}^5{d_1}^2+\frac{11}{19683}\,{d_3}^4{d_2}^2{d_1}^3-\frac{11}{19683}\,{d_3}^6{d_2}^2{d_1}-\frac{88}{59049}\,{d_3}^2{d_2}^4{d_1}^3+\frac{11}{59049}\,{d_3}^3{d_2}{d_1}^5+\frac{22}{59049}\,{d_3}^2{d_2}^3{d_1}^4-\frac{44}{59049}\,{d_3}^3{d_2}^4{d_1}^2-\frac{2717}{52488}\,{d_3}{d_2}^3{d_1}+\frac{187}{17496}\,{d_3}{d_2}{d_1}^3+\frac{242}{59049}\,{d_3}^2{d_1}^4{d_2}-\frac{3421}{314928}\,{d_3}^2{d_2}{d_1}^2+\frac{5599}{236196}\,{d_3}^2{d_1}{d_2}^4-\frac{11}{39366}\,{d_3}{d_2}^2{d_1}^4-\frac{1661}{78732}\,{d_3}^4{d_2}^2{d_1}-\frac{47795}{314928}\,{d_3}^2{d_1}{d_2}^2-\frac{55}{19683}\,{d_3}^4{d_2}^3{d_1}^2-\frac{2035}{236196}\,{d_3}^3{d_2}{d_1}^3-\frac{473}{13122}\,{d_3}^2{d_2}^3{d_1}^2+\frac{11}{39366}\,{d_3}{d_2}^4{d_1}^2+\frac{2453}{236196}\,{d_3}^2{d_2}^2{d_1}^3+\frac{110}{59049}\,{d_3}^3{d_2}^3{d_1}-\frac{253}{26244}\,{d_3}^4{d_2}{d_1}^2+\frac{55}{19683}\,{d_3}^3{d_2}^3{d_1}^3-\frac{11}{59049}\,{d_3}^2{d_2}{d_1}^6-\frac{121}{59049}\,{d_3}^3{d_2}^2{d_1}^4+\frac{11}{6561}\,{d_3}^5{d_2}^2{d_1}^2+\frac{1001}{78732}\,{d_3}^5{d_2}{d_1}-\frac{11}{6561}\,{d_3}^5{d_2}{d_1}^3-\frac{11}{19683}\,{d_3}^5{d_2}^3{d_1}+\frac{1067}{39366}\,{d_3}^3{d_2}^2{d_1}^2+\frac{11}{19683}\,{d_3}^6{d_2}{d_1}^2-\frac{134189}{472392}\,{d_3}{d_2}^2-\frac{19811}{472392}\,{d_3}^2{d_2}-\frac{220}{19683}\,{d_1}^3-\frac{352}{59049}\,{d_2}^3+\frac{22}{2187}\,{d_3}^5-\frac{11}{59049}\,{d_3}^6{d_1}^3+\frac{11}{59049}\,{d_3}^3{d_1}^6-\frac{11}{19683}\,{d_3}^4{d_1}^5+\frac{11}{59049}\,{d_3}^6{d_2}^3-\frac{11}{19683}\,{d_3}^4{d_2}^5+\frac{748}{19683}\,{d_1}+\frac{1100}{19683}\,{d_2}-\frac{17149}{314928}\,{d_3}^3{d_2}^2+\frac{8327}{104976}\,{d_3}^3{d_1}^2+\frac{83171}{472392}\,{d_3}^2{d_1}+\frac{11}{19683}\,{d_3}^5{d_1}^4-\frac{64691}{472392}\,{d_3}{d_1}^2+\frac{10879}{157464}\,{d_1}{d_2}^2+\frac{6083}{472392}\,{d_1}^2{d_2}+\frac{20075}{157464}\,{d_3}^2{d_2}^3-\frac{4147}{157464}\,{d_3}^2{d_1}^3-\frac{121}{39366}\,{d_1}^2{d_2}^3+\frac{121}{59049}\,{d_1}{d_2}^4+\frac{121}{118098}\,{d_1}^4{d_2}-\frac{57541}{944784}\,{d_3}^4{d_1}+\frac{5797}{944784}\,{d_3}^4{d_2}+\frac{902}{59049}\,{d_3}^4{d_1}^3-\frac{2849}{236196}\,{d_3}^3{d_2}^4+\frac{913}{59049}\,{d_3}^4{d_2}^3-\frac{979}{118098}\,{d_3}^3{d_1}^4+\frac{407}{59049}\,{d_3}{d_2}^4-\frac{143}{59049}\,{d_3}^2{d_2}^5-\frac{55}{13122}\,{d_3}^5{d_2}^2+\frac{671}{118098}\,{d_3}{d_1}^4+\frac{11}{39366}\,{d_3}^2{d_1}^5-\frac{671}{78732}\,{d_3}^5{d_1}^2+\frac{11}{8748}\,{d_3}^6{d_1}-\frac{11}{8748}\,{d_3}^6{d_2}+\frac{22}{59049}\,{d_3}^3{d_2}^6-\frac{1232}{19683}\,{d_3}^3+\frac{9416}{19683}\,{d_3}$
$r\ z\ z$	$-\frac{11}{472392}\,(d_2-d_3)(6528+144\,{d_3}^3{d_2}^3{d_1}^4+48\,{d_3}^5{d_2}^3{d_1}^2-16\,{d_3}^2{d_2}^5{d_1}^3-144\,{d_3}^4{d_2}^3{d_1}^3+16\,{d_3}^2{d_2}^2{d_1}^6-48\,{d_3}^3{d_2}^2{d_1}^5+48\,{d_3}^4{d_2}^2{d_1}^4-16\,{d_3}^5{d_2}^2{d_1}^3+48\,{d_3}^3{d_2}^5{d_1}^2-48\,{d_3}^4{d_2}^5{d_1}+144\,{d_3}^4{d_2}^4{d_1}^2-48\,{d_3}^2{d_2}^3{d_1}^5+48\,{d_3}^2{d_2}^4{d_1}^4-48\,{d_3}^5{d_2}^4{d_1}-144\,{d_3}^3{d_2}^4{d_1}^3+1272\,{d_3}^2{d_2}^3{d_1}^3-660\,{d_3}^4{d_2}^2{d_1}^2-24\,{d_3}{d_2}^4{d_1}^3+1020\,{d_3}^3{d_2}^4{d_1}+1020\,{d_3}^4{d_2}^3{d_1}+1272\,{d_3}^3{d_2}^2{d_1}^3-2184\,{d_3}^3{d_2}^3{d_1}^2-24\,{d_3}^4{d_2}{d_1}^3+24\,{d_3}^2{d_2}{d_1}^5-660\,{d_3}^2{d_2}^4{d_1}^2+108\,{d_3}^5{d_2}^2{d_1}+24\,{d_3}{d_2}^2{d_1}^5+108\,{d_3}^2{d_2}^5{d_1}-744\,{d_3}^2{d_1}^4{d_2}^2-7001\,{d_3}^3{d_2}^2{d_1}+162\,{d_3}^4{d_2}{d_1}-7001\,{d_3}^2{d_2}^3{d_1}+8877\,{d_1}^2{d_2}^2{d_3}^2+852\,{d_3}^3{d_2}{d_1}^2-858\,{d_3}^2{d_2}{d_1}^3+9714\,{d_3}{d_1}{d_2}^2+9714\,{d_3}^2{d_2}{d_1}+3744\,{d_3}{d_2}{d_1}^2-540\,{d_3}{d_2}{d_1}^4+162\,{d_3}{d_1}{d_2}^4-858\,{d_3}{d_2}^2{d_1}^3+852\,{d_3}{d_2}^3{d_1}^2-88\,{d_3}^2{d_1}^4+88\,{d_2}^3{d_1}^3-108\,{d_3}^3{d_2}^5+828\,{d_2}{d_1}^3-42\,{d_1}^2{d_2}^2-594\,{d_1}{d_2}^3-11428\,{d_3}{d_1}-11428\,{d_1}{d_2}-1998\,{d_3}^3{d_2}+868\,{d_3}{d_2}-1244\,{d_1}^2+828\,{d_3}{d_1}^3-594\,{d_3}^3{d_1}+1728\,{d_3}^2-1998\,{d_3}{d_2}^3-108\,{d_3}^5{d_2}^3+88\,{d_3}^3{d_1}^3-42\,{d_3}^2{d_1}^2+1728\,{d_2}^2+702\,{d_3}^4{d_2}^2-13032\,{d_3}^2{d_2}^2+3949\,{d_3}^3{d_2}^3+16\,{d_3}^5{d_2}^5-336\,{d_3}^4{d_2}^4-88\,{d_1}^4{d_2}^2+702\,{d_3}^2{d_2}^4)$
$s\ s\ s$	$\frac{219775}{139968}\,(d_2-d_3)(d_1-d_3)(d_1-d_2)$
$s\ s\ y$	$-\frac{9475}{1259712}\,(d_1-d_2)(4\,{d_2}{d_1}^3-4\,{d_3}{d_1}^3-8\,{d_1}^2{d_2}^2+8\,{d_3}{d_2}{d_1}^2+32\,{d_1}^2+4\,{d_1}{d_2}^3+12\,{d_3}^3d_1-27\,{d_3}{d_1}-101\,{d_1}{d_2}-24\,{d_3}^2{d_2}{d_1}+8\,{d_3}{d_1}{d_2}^2-320+91\,{d_3}^2-8\,{d_3}^4-4\,{d_3}{d_2}^3+32\,{d_2}^2+12\,{d_3}^3d_2-27\,{d_3}{d_2})$
$s\ s\ z$	$-\frac{9475}{629856}\,(d_1-d_2)(4\,{d_3}^2{d_2}{d_1}^3-4\,{d_3}^3{d_1}^3+26\,{d_3}^2{d_1}^2+4\,{d_3}^4{d_1}^2+6\,{d_3}{d_2}{d_1}^2+4\,{d_3}^3{d_2}{d_1}^2-8\,{d_1}^2{d_2}^2{d_3}^2+4\,{d_3}^2{d_2}^3d_1-74\,d_3d_1-8\,{d_3}^4{d_2}d_1-103\,{d_3}^2{d_2}d_1-22\,d_1d_2+33\,{d_3}^3d_1+6\,d_3d_1{d_2}^2+4\,{d_3}^3{d_2}^2d_1+33\,{d_3}^3d_2+4\,{d_3}^4{d_2}^2-74\,d_3d_2-214\,{d_3}^2+64+26\,{d_3}^2{d_2}^2-27\,{d_3}^4-4\,{d_3}^3{d_2}^3)$
$s\ y\ y$	$\frac{125}{3779136}\,(d_2-d_3)(24000+256\,{d_2}^4-160\,{d_3}^3{d_2}^2d_1+128\,{d_3}^4{d_2}d_1-160\,{d_3}^2{d_2}^3d_1+368\,{d_1}^2{d_2}^2{d_3}^2-64\,{d_3}^3{d_2}{d_1}^2-160\,{d_3}^2{d_2}{d_1}^3+808\,{d_3}{d_1}{d_2}^2+808\,{d_3}^2{d_2}d_1-1400\,{d_3}{d_2}{d_1}^2-296\,{d_1}^4+160\,{d_3}{d_2}{d_1}^4+128\,{d_3}{d_1}{d_2}^4-160\,{d_3}{d_2}^2{d_1}^3-64\,{d_3}{d_2}^3{d_1}^2-32\,{d_3}^2{d_1}^4+128\,{d_2}^3{d_1}^3-112\,{d_3}^4{d_1}^2-964\,{d_2}{d_1}^3+3072\,{d_1}^2{d_2}^2-2068\,{d_1}{d_2}^3+9543\,{d_3}{d_1}+9543\,{d_1}{d_2}+788\,{d_3}^3d_2+10809\,{d_3}{d_2}+256\,{d_3}^4-5639\,{d_1}^2-964\,{d_3}{d_1}^3-2068\,{d_3}^3d_1-8032\,{d_3}^2+788\,{d_3}{d_2}^3+16\,{d_1}^6+128\,{d_3}^3{d_1}^3+3072\,{d_3}^2{d_1}^2-8032\,{d_2}^2-16\,{d_3}^4{d_2}^2-2088\,{d_3}^2{d_2}^2+96\,{d_3}^3{d_2}^3-32\,{d_3}{d_1}^5+32\,{d_3}^5d_1-112\,{d_1}^2{d_2}^4-32\,{d_3}^5d_2-32\,{d_2}{d_1}^5+32\,{d_1}{d_2}^5-32\,{d_3}{d_2}^5-32\,{d_1}^4{d_2}^2-16\,{d_3}^2{d_2}^4)$

Table A.3: The cubic couplings for all of the fields in the action up to level 3 (continued).

$l\,m\,n$	$B_{lmn}(d_1,d_2,d_3)$
$s\ y\ z$	$\frac{125}{78732}\,d_3d_2{d_1}^5-\frac{250}{19683}\,{d_3}^4{d_2}^4d_1+\frac{250}{59049}\,{d_3}^3{d_2}^5d_1+\frac{125}{59049}\,{d_3}^2{d_2}^6d_1-\frac{125}{19683}\,{d_3}^4d_2{d_1}^4-\frac{875}{118098}\,{d_3}^2{d_2}^5{d_1}^2-\frac{125}{39366}\,{d_3}^4{d_2}^2{d_1}^3+\frac{125}{39366}\,{d_3}^6{d_2}^2d_1+\frac{500}{59049}\,{d_3}^2{d_2}^4{d_1}^3-\frac{125}{118098}\,{d_3}^3d_2{d_1}^5-\frac{125}{59049}\,{d_3}^2{d_2}^3{d_1}^4+\frac{250}{59049}\,{d_3}^3{d_2}^4{d_1}^2+\frac{30875}{104976}\,d_3d_2{}^3d_1-\frac{2125}{34992}\,d_3d_2d_1{}^3-\frac{1375}{59049}\,{d_3}^2{d_1}^4d_2+\frac{38875}{629856}\,{d_3}^2d_2{d_1}^2-\frac{63625}{472392}\,{d_3}^2d_1d_2{}^4+\frac{125}{78732}\,d_3d_2{}^2d_1{}^4+\frac{18875}{157464}\,{d_3}^4{d_2}^2d_1+\frac{543125}{629856}\,{d_3}^2d_1d_2{}^2+\frac{625}{39366}\,{d_3}^4d_2{}^3d_1{}^2+\frac{23125}{472392}\,{d_3}^3d_2d_1{}^3+\frac{5375}{26244}\,{d_3}^2{d_2}^3{d_1}^2-\frac{125}{78732}\,d_3{d_2}^4{d_1}^2-\frac{27875}{472392}\,{d_3}^2{d_2}^2{d_1}^3-\frac{625}{59049}\,{d_3}^3{d_2}^3d_1+\frac{2875}{52488}\,{d_3}^4d_2{d_1}^2-\frac{625}{39366}\,{d_3}^3{d_2}^3{d_1}^3+\frac{125}{118098}\,{d_3}^2{d_2}^2{d_1}^6+\frac{1375}{118098}\,{d_3}^3{d_2}^2{d_1}^4-\frac{125}{13122}\,{d_3}^5{d_2}^2{d_1}^2-\frac{11375}{157464}\,{d_3}^5d_2d_1+\frac{125}{13122}\,{d_3}^5d_2{d_1}^3+\frac{125}{39366}\,{d_3}^5{d_2}^3d_1-\frac{12125}{78732}\,{d_3}^3{d_2}^2{d_1}^2-\frac{125}{39366}\,{d_3}^6d_2{d_1}^2-\frac{125}{59049}\,{d_3}^2{d_2}^2{d_1}^5-\frac{125}{26244}\,d_3{d_2}^3{d_1}^3-\frac{125}{324}\,{d_3}^3d_2d_1+\frac{2000}{59049}\,{d_2}^3-\frac{3125}{13122}\,d_3{d_2}^2{d_1}^2+\frac{500}{59049}\,d_3d_2d_1+\frac{125}{39366}\,d_3d_1{d_2}^5+\frac{225125}{944784}\,{d_3}^2d_2-\frac{94625}{209952}\,{d_3}^3{d_1}^2+\frac{735125}{944784}\,d_3{d_1}^2-\frac{123625}{314928}\,d_1{d_2}^2-\frac{69125}{944784}\,{d_1}^2d_2+\frac{47125}{314928}\,{d_3}^2{d_1}^3+\frac{1375}{78732}\,{d_1}^2{d_2}^3-\frac{1375}{118098}\,d_1{d_2}^4-\frac{1375}{236196}\,{d_1}^4d_2+\frac{653875}{1889568}\,{d_3}^4d_1-\frac{5125}{59049}\,{d_3}^4{d_1}^3+\frac{32375}{472392}\,{d_3}^3{d_2}^4-\frac{10375}{118098}\,{d_3}^4{d_2}^3+\frac{11125}{236196}\,{d_3}^3{d_1}^4-\frac{4625}{118098}\,d_3{d_2}^4+\frac{1625}{118098}\,{d_3}^2{d_2}^5+\frac{625}{26244}\,{d_3}^5{d_2}^2-\frac{7625}{236196}\,d_3{d_1}^4-\frac{125}{78732}\,{d_3}^2{d_1}^5+\frac{7625}{157464}\,{d_3}^5{d_1}^2-\frac{125}{17496}\,{d_3}^6d_1+\frac{125}{17496}\,{d_3}^6d_2-\frac{125}{39366}\,{d_3}^5{d_1}^4+\frac{125}{39366}\,{d_3}^4{d_2}^5-\frac{125}{59049}\,{d_3}^3{d_2}^6-\frac{125}{118098}\,{d_3}^6{d_2}^3+\frac{125}{39366}\,{d_3}^4{d_1}^5-\frac{125}{118098}\,{d_3}^3{d_1}^6+\frac{125}{118098}\,{d_3}^6{d_1}^3+\frac{1250}{19683}\,{d_1}^3+\frac{7000}{19683}\,{d_3}^3-\frac{65875}{1889568}\,{d_3}^4d_2-\frac{4250}{19683}\,d_1-\frac{6250}{19683}\,d_2-\frac{125}{2187}\,{d_3}^5+\frac{1524875}{944784}\,d_3{d_2}^2+\frac{194875}{629856}\,{d_3}^3{d_2}^2-\frac{945125}{944784}\,{d_3}^2d_1-\frac{228125}{314928}\,{d_3}^2{d_2}^3-\frac{53500}{19683}\,d_3$
$s\ z\ z$	$\frac{125}{944784}\,(d_2-d_3)(6528-744\,{d_3}^2{d_1}^4{d_2}^2-7001\,{d_3}^3{d_2}^2d_1+162\,{d_3}^4d_2d_1-7001\,{d_3}^2{d_2}^3d_1+8877\,{d_1}^2{d_2}^2{d_3}^2+852\,{d_3}^3d_2{d_1}^2-858\,{d_3}^2d_2{d_1}^3+9714\,d_3d_1{d_2}^2+9714\,{d_3}^2d_2d_1+3744\,d_3d_2{d_1}^2+144\,{d_3}^3{d_2}^3{d_1}^4+48\,{d_3}^5{d_2}^3{d_1}^2-16\,{d_3}^2{d_2}^5{d_1}^3-144\,{d_3}^4{d_2}^3{d_1}^3+16\,{d_3}^2{d_2}^2{d_1}^6-48\,{d_3}^3{d_2}^2{d_1}^5+48\,{d_3}^4{d_2}^2{d_1}^4-16\,{d_3}^5{d_2}^2{d_1}^3+48\,{d_3}^3{d_2}^5{d_1}^2-48\,{d_3}^4{d_2}^5d_1+144\,{d_3}^4{d_2}^4{d_1}^2-48\,{d_3}^2{d_2}^3{d_1}^5+48\,{d_3}^2{d_2}^4{d_1}^4-48\,{d_3}^5{d_2}^4d_1-144\,{d_3}^3{d_2}^4{d_1}^3+1272\,{d_3}^2{d_2}^3{d_1}^3-660\,{d_3}^4{d_2}^2{d_1}^2-24\,d_3{d_2}^4{d_1}^3+1020\,{d_3}^3{d_2}^4d_1+1020\,{d_3}^4{d_2}^3d_1+1272\,{d_3}^3{d_2}^2{d_1}^3-2184\,{d_3}^3{d_2}^3{d_1}^2-24\,{d_3}^4{d_2}^2d_1{}^3+24\,{d_3}^2{d_2}^2{d_1}^5-660\,{d_3}^2{d_2}^4{d_1}^2+108\,{d_3}^5{d_2}^2d_1+24\,d_3{d_2}^2{d_1}^5+108\,{d_3}^2{d_2}^5d_1-540\,d_3d_2{d_1}^4+162\,d_3d_1{d_2}^4-858\,d_3{d_2}^2{d_1}^3+852\,d_3{d_2}^3{d_1}^2-108\,{d_3}^5{d_2}^3-88\,{d_3}^2{d_1}^4+88\,{d_2}^3{d_1}^3-108\,{d_3}^3{d_2}^5-336\,{d_3}^4{d_2}^4+16\,{d_3}^5{d_2}^5+828\,d_2{d_1}^3-42\,{d_1}^2{d_2}^2-594\,d_1{d_2}^3-11428\,d_3d_1-11428\,d_1d_2-1998\,{d_3}^3d_2+868\,d_3d_2-1244\,{d_1}^2+828\,d_3{d_1}^3-594\,{d_3}^3d_1+1728\,{d_3}^2-1998\,d_3{d_2}^3+88\,{d_3}^3{d_1}^3-42\,{d_3}^2{d_1}^2+1728\,{d_2}^2+702\,{d_3}^4{d_2}^2-13032\,{d_3}^2{d_2}^2+3949\,{d_3}^3{d_2}^3-88\,{d_1}^4{d_2}^2+702\,{d_3}^2{d_2}^4)$
$y\ y\ y$	$\frac{1}{3779136}\,(d_2-d_3)(d_1-d_3)(d_1-d_2)(665213-960\,{d_3}^3{d_2}^2d_1+1152\,{d_3}^4d_2d_1-960\,{d_3}^2{d_2}^3d_1+2688\,{d_1}^2{d_2}^2{d_3}^2-960\,{d_3}^3d_2{d_1}^2-960\,{d_3}^2d_2{d_1}^3-7920\,d_3d_1{d_2}^2-7920\,{d_3}^2d_2d_1-7920\,d_3d_2{d_1}^2-7920\,{d_3}^4+1152\,d_3d_2{d_1}^4+1152\,d_3d_1{d_2}^4-960\,d_3{d_2}^2{d_1}^3-960\,d_3{d_2}^3{d_1}^2-7920\,{d_1}^4-384\,{d_3}^2{d_1}^4+896\,{d_2}^3{d_1}^3-192\,d_3{d_2}^5+128\,{d_2}^6+7920\,d_2{d_1}^3+7920\,d_1{d_2}^3-70144\,d_3d_1-70144\,d_1d_2+7920\,{d_3}^3d_2-70144\,d_3d_2-7920\,{d_2}^4+53504\,{d_1}^2+7920\,d_3{d_1}^3+128\,{d_3}^6+7920\,{d_3}^3d_1+128\,{d_1}^6+53504\,{d_3}^2+7920\,d_3{d_2}^3+896\,{d_3}^3{d_1}^3+53504\,{d_2}^2-384\,{d_3}^4{d_2}^2+896\,{d_3}^3{d_2}^3-192\,d_3{d_1}^5-192\,{d_3}^5d_1-384\,{d_1}^2{d_2}^4-192\,{d_3}^5d_2-192\,d_2{d_1}^5-192\,d_1{d_2}^5-384\,{d_3}^4{d_1}^2-384\,{d_1}^4{d_2}^2-384\,{d_3}^2{d_2}^4)$
$y\ y\ z$	$\frac{1}{1889568}\,(d_1-d_2)(146496+128\,d_1{d_3}^8d_2+192\,d_3d_2{d_1}^6-128\,{d_3}^7{d_1}^2d_2+128\,{d_3}^2d_2{d_1}^7-256\,{d_3}^3d_2{d_1}^6+11552\,{d_3}^6d_2d_1-256\,{d_3}^3{d_2}^6d_1+128\,{d_3}^2{d_2}^7d_1-896\,{d_3}^6d_2{d_1}^3-1152\,{d_3}^3{d_2}^3{d_1}^4+1664\,{d_3}^5d_2{d_1}^4-1152\,{d_3}^5{d_2}^3{d_1}^2+1536\,{d_3}^6{d_2}^2{d_1}^2-384\,{d_3}^2{d_2}^5{d_1}^3+3456\,{d_3}^4{d_2}^3{d_1}^3-192\,{d_3}^2{d_2}^2{d_1}^6+1536\,{d_3}^3{d_2}^2{d_1}^5-1536\,{d_3}^4{d_2}^2{d_1}^4-1152\,{d_3}^5{d_2}^2{d_1}^3+1536\,{d_3}^3{d_2}^5{d_1}^2-192\,{d_3}^2{d_2}^6{d_1}^2-640\,{d_3}^4d_2{d_1}^5-640\,{d_3}^4{d_2}^5d_1-1536\,{d_3}^4{d_2}^4{d_1}^2-384\,{d_3}^2{d_2}^3{d_1}^5+896\,{d_3}^2{d_2}^4{d_1}^4+1664\,{d_3}^5{d_2}^4d_1-1152\,{d_3}^3{d_2}^4{d_1}^3-128\,{d_3}^7{d_2}^2d_1+960\,{d_3}^2{d_2}^3{d_1}^3+23184\,{d_3}^4{d_2}^2{d_1}^2-480\,d_3{d_2}^4{d_1}^3+6752\,{d_3}^3{d_2}^4d_1+15840\,{d_3}^4{d_2}^3d_1-18192\,{d_3}^3{d_2}^2{d_1}^3-18192\,{d_3}^3{d_2}^3{d_1}^2+15840\,{d_3}^4d_2{d_1}^3-8560\,{d_3}^2d_2{d_1}^5+8272\,{d_3}^2{d_2}^4{d_1}^2-480\,d_3{d_2}^3{d_1}^4-21744\,{d_3}^5{d_2}^2d_1+288\,d_3{d_2}^2{d_1}^5+6752\,{d_3}^3d_2{d_1}^4-8560\,{d_3}^2{d_2}^5d_1+8272\,{d_3}^2{d_1}^4{d_2}^2-21744\,{d_3}^5d_2{d_1}^2-896\,{d_3}^6{d_2}^3d_1+192\,d_3d_1{d_2}^6+288\,d_3{d_2}^5{d_1}^2-128\,{d_3}^3{d_2}^7+448\,{d_3}^4{d_2}^6-143132\,{d_3}^3{d_2}^2d_1+128\,{d_3}^7{d_2}^3+51984\,{d_3}^4d_2d_1+55872\,{d_3}^2{d_2}^3d_1+83280\,{d_1}^2{d_2}^2{d_3}^2-143132\,{d_3}^3d_2{d_1}^2+55872\,{d_3}^2d_2{d_1}^3+77786\,d_3d_1{d_2}^2+318879\,{d_3}^2d_2d_1+77786\,d_3d_2{d_1}^2-103469\,{d_3}^4-4096\,{d_3}^6{d_2}^2+128\,{d_3}^6{d_2}^4-192\,{d_3}^2{d_2}^6+20304\,{d_3}^5{d_2}^3-960\,{d_3}^7d_2-512\,{d_3}^5{d_2}^5-128\,{d_3}^3{d_1}^7+448\,{d_3}^4{d_1}^6+128\,{d_3}^6{d_1}^4+4232\,d_3d_2{d_1}^4+4232\,d_3d_1{d_2}^4-328\,d_3d_2{d_1}^3-328\,d_3{d_2}^3{d_1}^2+7680\,{d_1}^4+128\,{d_3}^7{d_1}^3-4096\,{d_3}^6{d_1}^2-192\,{d_3}^2{d_1}^6-26832\,{d_3}^4{d_1}^4-960\,{d_3}^7d_1-26832\,{d_3}^4{d_2}^4-170864\,{d_1}^2{d_2}^2+20304\,{d_3}^5{d_1}^3+11344\,{d_3}^3{d_1}^5+11344\,{d_3}^3{d_2}^5-512\,{d_3}^5{d_1}^5-64\,{d_3}^8{d_1}^2+432\,{d_3}^8-64\,{d_3}^8{d_2}^2+6872\,{d_3}^2{d_1}^4+2112\,{d_2}^3{d_1}^3-3904\,d_3{d_2}^5-14408\,d_2{d_1}^3-14408\,d_1{d_2}^3-967174\,d_3d_1+519398\,d_1d_2-12081\,{d_3}^3d_2-967174\,d_3d_2+7680\,{d_2}^4+30912\,{d_1}^2+112136\,d_3{d_1}^3+1576\,{d_3}^6-12081\,{d_3}^3d_1+1063270\,{d_3}^2+112136\,d_3{d_2}^3-181098\,{d_3}^2{d_2}^2-139704\,{d_3}^3{d_1}^3+30912\,{d_2}^2-181098\,{d_3}^2{d_1}^2+227316\,{d_3}^4{d_2}^2-139704\,{d_3}^3{d_2}^3-3904\,d_3{d_1}^5-75644\,{d_3}^5d_1-352\,{d_1}^2{d_2}^4-75644\,{d_3}^5d_2-704\,d_2{d_1}^5-704\,d_1{d_2}^5+227316\,{d_3}^4{d_1}^2-352\,{d_1}^4{d_2}^2+6872\,{d_3}^2{d_2}^4)$

Table A.3: The cubic couplings for all of the fields in the action up to level 3 (continued).

$l\,m\,n$	$B_{lmn}(d_1,d_2,d_3)$
$y\ z\ z$	$\frac{1}{944784}\,(d_2-d_3)(-109440-4320\,d_3d_2{d_1}^6+192\,{d_3}^2d_2{d_1}^7-96\,{d_3}^3d_2{d_1}^6-648\,{d_3}^6d_2d_1+288\,{d_3}^3{d_2}^6d_1-432\,{d_3}^2{d_2}^7d_1+96\,{d_3}^6d_2{d_1}^3-62064\,{d_3}^3{d_2}^3{d_1}^4+96\,{d_3}^5d_2{d_1}^4-9360\,{d_3}^5{d_2}^3{d_1}^2+672\,{d_3}^6{d_2}^2{d_1}^2+3776\,{d_3}^2{d_2}^5{d_1}^3+43968\,{d_3}^4{d_2}^3{d_1}^3-11696\,{d_3}^2{d_2}^2{d_1}^6+26832\,{d_3}^3{d_2}^2{d_1}^5-19344\,{d_3}^4{d_2}^2{d_1}^4+3776\,{d_3}^5{d_2}^2{d_1}^3-9360\,{d_3}^3{d_2}^5{d_1}^2+672\,{d_3}^2{d_2}^6{d_1}^2-288\,{d_3}^4d_2{d_1}^5+3648\,{d_3}^4{d_2}^5d_1-26928\,{d_3}^4{d_2}^4{d_1}^2+26832\,{d_3}^2{d_2}^3{d_1}^5-19344\,{d_3}^2{d_2}^4{d_1}^4+3648\,{d_3}^5{d_2}^4d_1+43968\,{d_3}^3{d_2}^4{d_1}^3-432\,{d_3}^7{d_2}^2d_1-202940\,{d_3}^2{d_2}^3{d_1}^3+82772\,{d_3}^4{d_2}^2{d_1}^2+1904\,d_3{d_2}^4{d_1}^3-74028\,{d_3}^3{d_2}^4d_1-74028\,{d_3}^4{d_2}^3d_1-202940\,{d_3}^3{d_2}^2{d_1}^3+250704\,{d_3}^3{d_2}^3{d_1}^2+1904\,{d_3}^4d_2{d_1}^3+8824\,{d_3}^2d_2{d_1}^5+82772\,{d_3}^2{d_2}^4{d_1}^2-4008\,d_3{d_2}^3{d_1}^4+12056\,{d_3}^5{d_2}^2d_1+8824\,d_3{d_2}^2{d_1}^5-4008\,{d_3}^3d_2{d_1}^4+12056\,{d_3}^2{d_2}^5d_1+123536\,{d_3}^2{d_1}^4{d_2}^2-6360\,{d_3}^5d_2{d_1}^2+288\,{d_3}^6{d_2}^3d_1-648\,d_3d_1{d_2}^6-6360\,d_3{d_2}^5{d_1}^2+432\,{d_3}^3{d_2}^7-1056\,{d_3}^4{d_2}^6+9739\,{d_3}^3{d_2}^2d_1+432\,{d_3}^7{d_2}^3+55434\,{d_3}^4d_2d_1+9739\,{d_3}^2{d_2}^3d_1-229887\,{d_1}^2{d_2}^2{d_3}^2-19356\,{d_3}^3d_2{d_1}^2+9894\,{d_3}^2d_2{d_1}^3+4954\,d_3d_1{d_2}^2+4954\,{d_3}^2d_2d_1-197760\,d_3d_2{d_1}^2+1280\,{d_1}^2{d_3}^5{d_2}^5-25920\,{d_3}^4+3072\,{d_1}^4{d_3}^4{d_2}^4+256\,{d_3}^3{d_2}^6{d_1}^3-128\,{d_3}^2{d_2}^6{d_1}^4+512\,{d_3}^2{d_2}^4{d_1}^6-128\,{d_3}^6{d_2}^2{d_1}^4+648\,{d_3}^6{d_2}^2+256\,{d_3}^6{d_2}^3{d_1}^3-2112\,{d_3}^4{d_2}^3{d_1}^5-128\,{d_3}^5{d_2}^2{d_1}^5-288\,d_3{d_2}^4{d_1}^5-448\,{d_3}^3{d_2}^2{d_1}^7-256\,{d_3}^5{d_2}^6d_1-448\,{d_3}^2{d_2}^3{d_1}^7+64\,{d_3}^2{d_2}^7{d_1}^3+96\,d_3{d_2}^6{d_1}^3-1056\,{d_3}^6{d_2}^4-192\,{d_3}^3{d_2}^7{d_1}^2+648\,{d_3}^2{d_2}^6+192\,{d_3}^4{d_2}^7d_1-96\,d_3{d_2}^3{d_1}^6+1664\,{d_1}^6{d_3}^3{d_2}^3-1664\,{d_3}^5{d_2}^4{d_1}^3+96\,d_3{d_1}^4{d_2}^5+512\,{d_3}^4{d_2}^2{d_1}^6-128\,{d_3}^2{d_2}^5{d_1}^5+832\,{d_3}^5{d_2}^3{d_1}^4+832\,{d_3}^3{d_2}^5{d_1}^4-1664\,{d_3}^4{d_2}^5{d_1}^3-2112\,{d_3}^3{d_2}^4{d_1}^5+128\,{d_3}^2{d_1}^8{d_2}^2+192\,d_3{d_1}^7{d_2}^2+64\,{d_3}^7{d_2}^2{d_1}^3-256\,{d_3}^6{d_2}^5d_1+192\,{d_3}^7{d_2}^4d_1-192\,{d_3}^7{d_2}^3{d_1}^2-15712\,{d_3}^5{d_2}^3+1840\,{d_3}^5{d_2}^5+87828\,d_3d_2{d_1}^4+55434\,d_3d_1{d_2}^4+9894\,d_3{d_2}^2{d_1}^3-19356\,d_3{d_2}^3{d_1}^2-9952\,{d_1}^4-704\,{d_3}^2{d_1}^6+25064\,{d_3}^4{d_2}^4+476142\,{d_1}^2{d_2}^2-352\,{d_3}^5{d_1}^3+1056\,{d_3}^3{d_1}^5-15712\,{d_3}^3{d_2}^5-13048\,{d_3}^2{d_1}^4-29216\,{d_2}^3{d_1}^3+13176\,d_3{d_2}^5-64\,{d_3}^5{d_2}^7-64\,{d_3}^7{d_2}^5-161796\,d_2{d_1}^3-26954\,d_1{d_2}^3-488884\,d_3d_1-488884\,d_1d_2-216406\,{d_3}^3d_2+1286260\,d_3d_2-25920\,{d_2}^4+330292\,{d_1}^2-161796\,d_3{d_1}^3-26954\,{d_3}^3d_1-9792\,{d_3}^2-216406\,d_3{d_2}^3-2728\,{d_3}^2{d_2}^2-29216\,{d_3}^3{d_1}^3-9792\,{d_2}^2+476142\,{d_3}^2{d_1}^2-94074\,{d_3}^4{d_2}^2+236977\,{d_3}^3{d_2}^3-352\,{d_2}^5{d_1}^3+1056\,{d_1}^5{d_2}^3-704\,{d_2}^2{d_1}^6+128\,{d_3}^6{d_2}^6+6624\,d_3{d_1}^5+2376\,{d_3}^5d_1+10992\,{d_1}^2{d_2}^4+13176\,{d_3}^5d_2+6624\,d_2{d_1}^5+2376\,d_1{d_2}^5+10992\,{d_3}^4{d_1}^2-13048\,{d_1}^4{d_2}^2-94074\,{d_3}^2{d_2}^4)$
$z\ z\ z$	$-\frac{1}{472392}\,(d_2-d_3)(d_1-d_2)(d_1-d_3)(-404632+576\,{d_3}^3{d_2}^3{d_1}^4+96\,{d_3}^5d_2{d_1}^4+864\,{d_3}^5{d_2}^3{d_1}^2-432\,{d_3}^6{d_2}^2{d_1}^2+864\,{d_3}^2{d_2}^5{d_1}^3+576\,{d_3}^4{d_2}^3{d_1}^3-432\,{d_3}^2{d_2}^2{d_1}^6+864\,{d_3}^3{d_2}^2{d_1}^5-2064\,{d_3}^4{d_2}^2{d_1}^4+864\,{d_3}^5{d_2}^2{d_1}^3+864\,{d_3}^3{d_2}^5{d_1}^2-432\,{d_3}^2{d_2}^6{d_1}^2+96\,{d_3}^4d_2{d_1}^5+96\,{d_3}^4{d_2}^5d_1-2064\,{d_3}^4{d_2}^4{d_1}^2+864\,{d_3}^2{d_2}^3{d_1}^5-2064\,{d_3}^2{d_2}^4{d_1}^4+96\,{d_3}^5{d_2}^4d_1+576\,{d_3}^3{d_2}^4{d_1}^3-7560\,{d_3}^2{d_2}^3{d_1}^3+22344\,{d_3}^4{d_2}^2{d_1}^2-6568\,d_3{d_2}^4{d_1}^3-6568\,{d_3}^3{d_2}^4d_1-6568\,{d_3}^4{d_2}^3d_1-7560\,{d_3}^3{d_2}^2{d_1}^3-7560\,{d_3}^3{d_2}^3{d_1}^2-6568\,{d_3}^4d_2{d_1}^3-648\,{d_3}^2d_2{d_1}^5+22344\,{d_3}^2{d_2}^4{d_1}^2-6568\,d_3{d_2}^3{d_1}^4-648\,{d_3}^5{d_2}^2d_1-648\,d_3{d_2}^2{d_1}^5-6568\,{d_3}^3d_2{d_1}^4-648\,{d_3}^2{d_2}^5d_1+22344\,{d_3}^2{d_1}^4{d_2}^2-648\,{d_3}^5d_2{d_1}^2-648\,d_3{d_2}^5{d_1}^2+80130\,{d_3}^3{d_2}^2d_1+14580\,{d_3}^4d_2d_1+80130\,{d_3}^2{d_2}^3d_1-300231\,{d_1}^2{d_2}^2{d_3}^2+80130\,{d_3}^3d_2{d_1}^2+80130\,{d_3}^2d_2{d_1}^3-351344\,d_3d_1{d_2}^2-351344\,{d_3}^2d_2d_1-351344\,d_3d_2{d_1}^2-128\,{d_1}^2{d_3}^5{d_2}^5-384\,{d_1}^4{d_3}^4{d_2}^4-128\,{d_3}^3{d_2}^6{d_1}^3+64\,{d_3}^2{d_2}^6{d_1}^4+64\,{d_3}^2{d_2}^4{d_1}^6+64\,{d_3}^6{d_2}^2{d_1}^4-128\,{d_3}^6{d_2}^3{d_1}^3+128\,{d_3}^4{d_2}^3{d_1}^5-128\,{d_3}^5{d_2}^2{d_1}^5+96\,d_3{d_2}^4{d_1}^5-352\,{d_3}^4{d_1}^4-352\,{d_2}^4{d_1}^4-128\,{d_1}^6{d_3}^3{d_2}^3+128\,{d_3}^5{d_2}^4{d_1}^3+96\,d_3{d_1}^4{d_2}^5+64\,{d_3}^4{d_2}^2{d_1}^6-128\,{d_3}^2{d_2}^5{d_1}^5+128\,{d_3}^5{d_2}^3{d_1}^4+128\,{d_3}^3{d_2}^5{d_1}^4+128\,{d_3}^4{d_2}^5{d_1}^3+128\,{d_3}^3{d_2}^4{d_1}^5+14580\,d_3d_2{d_1}^4+14580\,d_3d_1{d_2}^4+80130\,d_3{d_2}^2{d_1}^3+80130\,d_3{d_2}^3{d_1}^2+64\,{d_3}^4{d_2}^6{d_1}^2-352\,{d_3}^4{d_2}^4-97630\,{d_1}^2{d_2}^2+64\,{d_3}^6{d_2}^4{d_1}^2+2376\,{d_3}^2{d_1}^4+10464\,{d_2}^3{d_1}^3-22356\,d_2{d_1}^3-22356\,d_1{d_2}^3+592176\,d_3d_1+592176\,d_1d_2-22356\,{d_3}^3d_2+592176\,d_3d_2+33588\,{d_1}^2-22356\,d_3{d_1}^3-22356\,{d_3}^3d_1+33588\,{d_3}^2-22356\,d_3{d_2}^3-97630\,{d_3}^2{d_2}^2+10464\,{d_3}^3{d_1}^3+33588\,{d_2}^2-97630\,{d_3}^2{d_1}^2+2376\,{d_3}^4{d_2}^2+10464\,{d_3}^3{d_2}^3+2376\,{d_1}^2{d_2}^4+2376\,{d_3}^4{d_1}^2+2376\,{d_1}^4{d_2}^2+2376\,{d_3}^2{d_2}^4)$

Table A.3: The cubic couplings for all of the fields in the action up to level 3 (continued).

Appendix B

Rolling Tachyon Code

In section 5.3 I described what was necessary in order to programmatically construct the marginal solution of [36] and then compute some simple quantities based on that solution. This appendix contains the code that was used to actually perform these tasks.

B.1 Maple Code

The Maple portion of the program does all of the algebraic work necessary to build the solution and compute expectation values. This is not designed to do the significant amount of numerical work in actually evaluating the quantities found here; that is done in C++.

For those not familiar with the Maple language, it is the built-in language of the computer algebra system Maple. As such it has built-in functions for many common tasks such as summing terms, finding taylor coefficients, or integrating functions. Most of these should be relatively straightforward, but I will try to explain a few of the less intuitive commands.

Functions are defined using the arrow operator, so $f(x) = x^2$ would be written as `f:=x->x^2;`. While standard operators such as addition, multiplication, and the exponentiation just used are often written infix, they are interpreted as functions so `1+2+3` is the same thing as `‘+‘(1,2,3)`, at least for associative operators. A comma separated list is known as a sequence and can be generated with the `seq` function, so that the previous example is also equivalent to `‘+‘(seq(n,n=1..3))`. The function `op` is quite powerful and nuanced and since I will use it quite often it deserves some explanation. The command `op(i,expr)` returns the i-th operand of the expression in its second argument. This is useful for parsing the arguments of an unevaluated function, and can even return the function itself as the 0th operand. `op` also works with constructs which are not really functions, such as lists and sets. If `i` is omitted, `op` returns a sequence of all operands (except the 0th), and if a range is specified instead then that subsequence of operands is returned. Negative indices are interpreted as counting backwards from the last operand (or element in a list).

Due to the program being written before we finalized our conventions for renormalization schemes, there are a few notational differences. The renormalization constants C_0 and C_1 are referred to in the code as `RC2` and `RCk` respectively. The constant C^L not appearing in the solution is `RCL`. Despite the fact that the counterterms are defined using the little g scheme, as in sections 4.2.1 and 4.3.2, the notation uses capital `G`. In describing functions such as `V_r` I have occasionally used the useful shorthand notation $\left[V^{(n)}(a,b)\right]_r \stackrel{\text{def}}{=} \frac{1}{n!}\left[V(a,b)^n\right]_r$ which is standard in [36]. We should now be ready to see the Maple portion of the program. Comments are prefixed with # and will appear in green.

Program B.1: These Maple procedures define wedge states with insertions and the operations used on them. Correlation functions of wedge states with known insertions can also be calculated and simplified. A description of this program appears in section 5.3.

```
# -*-mapl-*- (nowrap)
restart:

#a wedge is [width, {variable=range or point}, V(1)*V(t1)*...] leave out integrals, as those will be implied by specifying ranges for variables
`type/wedge`:=[algebraic,set(name={nonnegint..posint,algebraic}),algebraic]:
#a wpoly is the same as a wedge, but with the operator content replaced by a list representing taylor coefficients in λ
`type/wpoly`:=[algebraic,set(name={nonnegint..posint,algebraic}),list(algebraic)]:

`type/wsing`:={wedge,wpoly}: #one wedge state
`type/wsum`:=specfunc({wsing,wsum},`&+`): #a sum of wedge states
`type/wtype`:={wsing,wsum}:

#some constants
wId:=[0,{},1]:
wzero:=[0,{},0]:
wpId:=[0,{},[1]]:
wpzero:=[0,{},[0]]:

#define the marginal operator, assumed to have 1/z^2 self-OPE
#V_bare:=t->dX(t)/sqrt(alphaprime): #use this version for the translation operator
V_bare:=t->(E(1,t)+E(-1,t))/sqrt(2): #use this version of the rolling tachyon

#convert a wpoly to a wedge
##A the wedge state (or sum) to convert
to_wedge:=proc(A::wtype)::wtype:
   if type(A,wsum) then
      return map(to_wedge,A);
   elif type(A,wedge) then
      return A;
   else
      return [A[1],A[2],add(lambda^(n-1)*A[3][n],n=1..nops(A[3]))]:
   fi:
end proc:

#convert a wedge to a wpoly, truncating to O(λ^n)
##A the wedge state (or sum) to convert
##n the truncation order
to_wpoly:=proc(A::wtype,n::nonnegint)::wtype:
   if type(A,wsum) then
      return map(to_wpoly,A,n);
   elif type(A,wpoly) then #might want to truncate to n here, currently left as is
      return A;
   else
```

```
44          return [A[1],A[2],[seq(coeftayl(A[3],lambda=0,k),k=0..n)]]:
45      fi:
46  end proc:

48  #the star product, takes arbitrarily many operands which should be of type wtype
49  ##the name parameter LAMBDA_MAX truncates the result to O(λ^LAMBDA_MAX) to avoid excess computation
50  star:=proc(A,B,{LAMBDA_MAX::nonnegative:=infinity})
51      local ret, i, C, vars, bdom, bins, bsrt, cins, nm, lm, subslist:
52      if type(A,wsum) then
53          ret:=map(star,A,B,':-LAMBDA_MAX'=LAMBDA_MAX);
54      elif type(B,wsum) then
55          ret:=map2(star,A,B,':-LAMBDA_MAX'=LAMBDA_MAX);
56      elif type(A,wpoly) and type(B,wpoly) then
57          if A[3]=[seq(0,n=1..nops(A[3]))] or B[3]=[seq(0,n=1..nops(B[3]))]
                then
58              return wpzero;
59          fi:
60          vars:=map(lhs,A[2]):
61          bdom:={}:
62          bins:=B[3]:
63          subslist:=[]:
64          bsrt:=sort([op(B[2])],((a,b)->lexorder(lhs(a),lhs(b)))): #ensure
                lexicographical ordering of coordinates is preserved
65          for i from 1 to nops(bsrt) do
66              nm:=newvar(vars,lhs(bsrt[i])): #ensure variable names are unique
67              bdom:=bdom union {nm=map((x->x+A[1]),rhs(bsrt[i]))}: #shift
                    insertion locations in B
68              subslist:=[op(subslist),lhs(bsrt[i])=nm]: #add to the list of variables
                    to rename
69              vars:=vars union {nm}:
70          od:
71          bins:=eval(bins,subslist): #perform the change of variables in the operators
72          lm:=min(LAMBDA_MAX,nops(A[3])+nops(B[3])-2):
73          cins:=[seq(add(piecewise(k>=nops(A[3]),0,A[3][k+1])*piecewise(n-k
                >=nops(bins),0,bins[n-k+1]),k=0..n),n=0..lm)]: #multiply
                operators
74          C:=[A[1]+B[1],A[2] union bdom,cins]:
75          ret:=C;
76      elif type(A,wedge) and type(B,wedge) then
77          if A[3]=0 or B[3]=0 then
78              return wzero;
79          fi:
80          vars:=map(lhs,A[2]):
81          bdom:={}:
82          bins:=B[3]:
83          subslist:=[]:
84          bsrt:=sort([op(B[2])],((a,b)->lexorder(lhs(a),lhs(b)))): #ensure
                lexicographical ordering of coordinates is preserved
85          for i from 1 to nops(bsrt) do
86              nm:=newvar(vars,lhs(bsrt[i])): #ensure variable names are unique
87              bdom:=bdom union {nm=map((x->x+A[1]),rhs(bsrt[i]))}: #shift
```

```
                insertion locations in B
88          subslist:=[op(subslist),lhs(bsrt[i])=nm]: #add to the list of variables
                to rename
89          vars:=vars union {nm}:
90       od:
91       cins:=A[3]*eval(bins,subslist): #perform changes of variables and multiply the
             operators for both wedge states
92       if LAMBDA_MAX < infinity then #for efficiency, truncate to fixed power of λ
93          cins:=convert(taylor(cins,lambda,trunc(LAMBDA_MAX)+1),polynom)
                :
94       fi:
95       C:=[A[1]+B[1],A[2] union bdom,cins]:
96       ret:=C;
97    elif type(A,wsing) and type(B,wsing) then
98       ret:=star(to_wedge(A),to_wedge(B),':-LAMBDA_MAX'=LAMBDA_MAX);
99    else
100      ret:=A &* B;
101   fi:
102   if _nrest=0 then #if there are no more operands
103      return ret;
104   else
105      #A ∗ B ∗ C ∗ D = ((A ∗ B) ∗ C) ∗ D etc.
106      return star(ret,_rest,':-LAMBDA_MAX'=LAMBDA_MAX);
107   fi:
108end proc:

110#adjust variable names to avoid conflict when using star
111##used is a set of names already taken
112##oldvar should be an indexed symbol which will have its index adjusted for uniqueness
113newvar:=proc(used::set(name),oldvar::name)
114   local i:
115   if type(oldvar,indexed) and nops(oldvar)=1 then
116      i:=op(oldvar):
117      while op(0,oldvar)[i] in used do
118         i:=i+1:
119      od:
120      return op(0,oldvar)[i];
121   elif type(oldvar,symbol) then
122      print("support for renaming simple symbols has been removed",
          oldvar);
123      return oldvar;
124      i:=1:
125      while oldvar||i in used do
126         i:=i+1:
127      od:
128      #return oldvar||i;
129   else
130      print("variable of unknown type, not handled",oldvar);
131      return oldvar;
132   fi:
133end proc:
```

```
#multiply a wedge B by a scalar a
ctimesw:=proc(a::algebraic,B)
   local acol, ins, i, j, d:
   if type(B,wedge) then
      return [B[1],B[2],a*B[3]];
   elif type(B,wpoly) and type(a,polynom(anything,lambda)) then #wpoly
      types cannot be multiplied by non-polynomial λ
      acol:=collect(a,lambda):
      ins:=[seq(0,n=1..nops(B[3])+degree(acol,lambda))]:
      if type(acol,`+`) then
         acol:=[op(acol)]:
      else
         acol:=[acol]:
      fi:
      for i from 1 to nops(acol) do
         d:=degree(acol[i],lambda):
         for j from 1 to nops(B[3]) do
            ins[j+d]:=ins[j+d]+B[3][j]*acol[i]/lambda^d:
         od:
      od:
      return [B[1],B[2],ins];
   elif type(B,wsum) then
      return map2(ctimesw,a,B);
   else
      print("Warning: ctimesw called with wrong type.",a,B);
      return a*B;
   fi:
end proc:

#takes a wsum and removes wedge states with 0 amplitude
#this also flattens sums by removing parentheses: (A+B)+C → A+B+C
plus0:=proc(expr)
   local newexpr, term, i:
   if type(expr,wsum) then
      newexpr:=[]:
      for i from 1 to nops(expr) do
         term:=plus0(op(i,expr)):
         if type(term,wsum) then #A+(B+C)=A+B+C
            if nops(term) <> 1 or op(1,term) <> wzero then
               newexpr:=[op(newexpr),op(term)]:
            fi:
         elif type(term,wedge) then
            if term[3]<>0 then
               newexpr:=[op(newexpr),term]:
            fi:
         elif type(term,wpoly) then
            if term[3]<>[seq(0,n=1..nops(term[3]))] then
               newexpr:=[op(newexpr),term]:
            fi:
         else
```

```
184             newexpr:=[op(newexpr),term]:
185          fi:
186       od:
187       if nops(newexpr) = 0 then
188          newexpr:=[wzero]:
189       fi:
190       return &+(op(newexpr));
191    else
192       return expr;
193    fi:
194 end proc:

196 #act on the operator content of a wedge (or wpoly) with expand
197 #return a separate wedge (wpoly) for each term in the result
198 ##expr is the wedge, wpoly, or wsum to expand
199 wexpand:=proc(expr)
200    local ins, outw, i:
201    if type(expr,wsum) then
202       return map(wexpand,expr);
203    elif type(expr,wedge) then
204       ins:=expand(expr[3]):
205       if type(ins,`+`) then
206          ins:=&+(op(ins)):
207          return map((x->[expr[1],expr[2],x]),ins);
208       else
209          return [expr[1],expr[2],ins];
210       fi:
211    elif type(expr,wpoly) then
212       outw:=[]:
213       for i from 1 to nops(expr[3]) do
214          ins:=expand(expr[3][i]):
215          if type(ins,`+`) then
216             ins:=[op(ins)]:
217          else
218             ins:=[ins]:
219          fi:
220          if ins<>[0] then
221             outw:=[op(outw),seq([expr[1],expr[2],[seq(0,k=1..i-1),ins[j
                  ]]],j=1..nops(ins))]:
222          fi:
223       od:
224       if nops(outw)=0 then
225          return wpzero;
226       elif nops(outw)=1 then
227          return op(outw);
228       else
229          return `&+`(op(outw));
230       fi:
231    else
232       print("Warning: wexpand on unhandled type.");
233       return expr;
```

```
234     fi:
235 end proc:

237 #merges wedges with the same circumference and operator insertion locations
238 #operator content is added for matching wedges in a wsum
239 ##expr should be a sum of wedges. wpolys may work (untested), but mixing the two will likely fail
240 wcombine:=proc(expr)
241     local i, j, tosort, sorted, res, term:
242     if type(expr,wsum) then
243         tosort:=plus0(varsort(expr)):
244         if type(tosort,wsum) then
245             tosort:=[op(tosort)]:
246             sorted:={}:
247             res:=wzero:
248             for i from 1 to nops(tosort) do
249                 if not i in sorted then
250                     term:=tosort[i]:
251                     sorted:=sorted union {i}:
252                     for j from i+1 to nops(tosort) do
253                         if not j in sorted then
254                             if tosort[i][1]=tosort[j][1] and tosort[i][2]=
                                    tosort[j][2] then
255                                 term:=subsop(3=term[3]+tosort[j][3],term):
256                                 sorted:=sorted union {j}:
257                             fi:
258                         fi:
259                     od:
260                     res:=res&+term:
261                 fi:
262             od:
263             return plus0(res);
264         else
265             return tosort;
266         fi:
267     else
268         return expr;
269     fi:
270 end proc:

272 #renames the dummy variables appearing in the second element of wedges
273 #variable names are sorted so that if i < j then t[i] is to the left of t[j]
274 #variables which are at fixed location (unintegrated) but do not appear anywhere in the operator
        content are removed
275 varsort:=proc(expr)
276     local i, j, splitdom, found, orderproc, sublist, varoot, remlist,
            inw:
277     if type(expr,wsum) then
278         return map(varsort,expr);
279     elif type(expr,wsing) then
280         remlist:={}:
281         for i from 1 to nops(expr[2]) do
```

```
282             if type(rhs(op(i,expr[2])),numeric) and not has(expr[3],lhs(op
                    (i,expr[2]))) then
283                 remlist:=remlist union {op(i,expr[2])}:
284             fi:
285         od:
286         inw:=subsop(2=expr[2] minus remlist,expr):
287         splitdom:={}:
288         #the local function orderproc contains rules for breaking ties
289         #our convention is to preserve order of indices when two insertions are coincident
290         #orderproc currently assumes that all insertions are at (or integrated between) integer
                locations
291         orderproc:=(x,y)->piecewise(type(rhs(x),range),op(1,rhs(x))+1/2,
                rhs(x))
292             +piecewise(type(lhs(x),indexed),op(1,lhs(x))/1000,0) <
293             +piecewise(type(rhs(y),range),op(1,rhs(y))+1/2,rhs(y))
294             +piecewise(type(lhs(y),indexed),op(1,lhs(y))/1000,0):
295         for i from 1 to nops(inw[2]) do
296             found:=false:
297             for j from 1 to nops(splitdom) while not found do
298                 if op(0,lhs(op(i,inw[2])))=op(0,lhs(op(j,splitdom)[1]))
                        then
299                     found:=true:
300                     splitdom:=subsop(j=[op(op(j,splitdom)),op(i,inw[2])],
                            splitdom):
301                 fi:
302             od:
303             if not found then
304                 splitdom:=splitdom union {[op(i,inw[2])]}:
305             fi:
306         od:
307         splitdom:=map(sort,splitdom,orderproc):
308         sublist:=[]:
309         for i from 1 to nops(splitdom) do
310             varoot:=op(0,lhs(op(i,splitdom)[1])):
311             for j from 1 to nops(op(i,splitdom)) do
312                 sublist:=[op(sublist),lhs(op(i,splitdom)[j])=varoot[j]]:
313             od:
314         od:
315         return eval(inw,sublist);
316     else
317         print("calling varsort on non-wedge");
318         return expr;
319     fi:
320 end proc:

322 #find the wedge state taylor coefficient of λ^n
323 ##A the wedge state or sum
324 ##lambda should normally be 'lambda' for our purposes (must be for wpoly types)
325 ##n the truncation order
326 pickoff:=proc(A,lambda::name,n::nonnegint)
327     local ins:
```

```
328     if type(A,function) and op(0,A)=`&+` then
329        return plus0(map(pickoff,A,lambda,n));
330     elif type(A,wpoly) then
331        if lambda<>'lambda' then
332           print("don't use pickoff on polynomial wedges without lambda")
                ;
333        fi:
334        if n+1>nops(A[3]) then
335           return [A[1],A[2],0];
336        else
337           return [A[1],A[2],A[3][n+1]];
338        fi:
339     elif type(A,wedge) then
340        ins:=coeftayl(A[3],lambda=0,n):
341        return [A[1],A[2],ins];
342     else #unhandled type
343        return PICKOFF(A,lambda,n);
344     fi:
345  end proc:

347  #star product removing a unit width from the left edge to make the first argument act as a bra state
348  starip:=proc()
349     local interws:
350     interws:=star([-1,{},1],args):
351     return interws;
352  end proc:

354  #the integrated b ghosts, B, can be inserted anywhere and will only change the wedge state if they
         cross a c ghost
355  #move all B insertions to the right end of the wedge
356  #b ghosts are not needed for the solution of [36]
357  #this function is a schematic for how b ghost functionality could be added, but it is not presently used
358  sortB:=proc(expr)
359     local grand, dom, i, j, m, n, opins, orderproc;
360     if not hasfun(expr,B) then
361        return expr;
362     fi:
363     if type(expr,wsum) then
364        return map(sortB,expr);
365     elif type(expr,wsing) then
366        grand:=expr[3]:
367        dom:=expr[2]:
368        if type(grand,`+`) then
369           return sortB(plus0(wexpand(expr)));
370        elif type(grand,`*`) then
371           opins:=[]:
372           for i from 1 to nops(grand) do
373              if type(op(i,grand),function) and op(0,op(i,grand)) in {B,c
                     ,dc} then
374                 opins:=[op(opins),[op(0,op(i,grand)),op(1,op(i,grand)),'
                        unknown']]:
```

```
375                 for j from 1 to nops(dom) do
376                     if lhs(op(j,dom))=opins[-1][2] then
377                         opins[-1][3]:=rhs(op(j,dom)):
378                         break:
379                     fi:
380                 od:
381             fi:
382         od:
383         orderproc:=(x,y)->x[3]+piecewise(has(x[1],dc),1/100,0) < y[3]+
                piecewise(has(y[1],dc),1/100,0):
384         opins:=sort(opins,orderproc):
385         for i from 1 to nops(opins) do
386             if opins[i][1]=B then
387                 break;
388             fi:
389         od:
390         if i = nops(opins) then
391             return expr;
392         elif opins[i+1][1] = B then
393             return wzero;
394         elif opins[i+1][1] in {c,dc} then
395             for m from 1 to nops(grand) do
396                 if op(m,grand)=B(opins[i][2]) then
397                     break;
398                 fi:
399             od:
400             for n from 1 to nops(grand) do
401                 if op(n,grand)=opins[i+1][1](opins[i+1][2]) then
402                     break;
403                 fi:
404             od:
405             for j from 1 to nops(dom) do
406                 if lhs(op(j,dom))=opins[i][2] then
407                     break;
408                 fi:
409             od:
410             return sortB(ctimesw(-1,[expr[1],subsop(j=(opins[i][2]=
                    opins[i+1][3]+piecewise(has(opins[i+1][1],dc)
                    ,1/50,1/200)),dom),grand])) &+
411                 sortB([expr[1],dom,subsop(m=1,n=1,grand)]);
412         fi:
413     fi:
414 fi:
415 end proc:

417 #define the renormalization used for V(a,b)^2
418 #g^D_ab(t1,t2) is G_r(t1,t2,wdth,a,b)
419 ##t1,t2 the variables which will be integrated
420 ##wdth an inert placeholder for the wedge width
421 ##a,b the endpoints of the integration
422 #not all of these parameters will be needed depending on the renormalizing function
```

```
#renormalization function from (4.22) and (4.39) of [36], normally overwritten
G_r:=(t1,t2,wdth,a,b)->-Pi^2/(wdth+1)^2/sin(Pi*(t2-t1)/(wdth+1))^2+ln(
    Pi^2/(wdth+1)^2/sin(Pi*(b-a)/(wdth+1))^2)/(b-a)^2:
#my version satisfying assumptions (4.5)
G_r:=(t1,t2,wdth,a,b)->-1/(t2-t1)^2-2*(1+ln(b-a)+RC2+RCk*(b-a))/(b-a)
    ^2:
#RC2:=0:  RCk:=0: #if we wish to choose the simplest values we can uncomment this line

#the operator [V^(n)(a,b)]_r is first represented by the inert function V_ren(n,a,b,vars,wdth)
#this is later replaced by V_r(n,a,b,vars,wdth) which evaluates to the appropriate operators and
    renormalizing subtractions
#V_ren should not be evaluated too soon, as Q_B will not act correctly on V_r

##n the number of integrated operators to use
##a,b the limits of integration
##vars a list of symbols (normally indexed) to use as the locations of the insertions
##wdth an inert name representing the width of the final wedge
#note that n should match nops(vars)
V_r:=proc(n::nonnegint,a,b,vars::list(name),wdth)
   local pairs, removals, usedvars, keeppair, i, j, k, res, term:
   if nops(vars) <> n then
      print("Warning: in V_r n is barely used, make sure number of vars
          is correct instead",n,vars);
   fi:
   if n = 0 then
      return 1;
   elif n < 0 then
      return 0;
   fi:
   pairs:=combinat[choose](vars,2):
   removals:=combinat[choose](pairs):
   pairs:=[]:
   for i from 1 to nops(removals) do
      usedvars:={}: keeppair:=true:
      for j from 1 to nops(removals[i]) while keeppair do
         for k from 1 to nops(removals[i][j]) do
            if removals[i][j][k] in usedvars then
               keeppair:=false:
            else
               usedvars:=usedvars union {removals[i][j][k]}:
            fi:
         od:
      od:
      if keeppair then
         pairs:=[op(pairs),removals[i]]:
      fi:
   od:
   res:=0:
   for i from 1 to nops(pairs) do
      term:=1/n!: usedvars:={}:
```

```
      for j from 1 to nops(pairs[i]) do
         term:=term*G_r(pairs[i][j][1],pairs[i][j][2],wdth,a,b):
         usedvars:=usedvars union {pairs[i][j][1],pairs[i][j][2]}:
      od:
      for j from 1 to nops(vars) do
         if not vars[j] in usedvars then
            term:=term*V_bare(vars[j]):
            usedvars:=usedvars union {vars[j]}:
         fi:
      od:
      res:=res+term:
   od:
   return res;
end proc:

#g^L_ab(t) is G_Left(t,wdth,a,b)
#renormalization function from (4.22) and (4.31) of [36], normally overwritten
G_Left:=(t,wdth,a,b)->-Pi^2/(wdth+1)^2/sin(Pi*(t-a)/(wdth+1))^2-Pi/(
   wdth+1)*cot(Pi*(b-a)/(wdth+1))/(b-a):
#my version satisfying assumptions (4.5)
G_Left:=(t,wdth,a,b)->-1/(t-a)^2-1/(b-a)^2-RCL/(b-a):
#RCL:=0: #simplest value chosen, commented out

#[V(a)V^(n-1)(a,b)]_r is represented by the inert function V_L_ren(n,a,b,vars,wdth)
#it is evaluated by the function V_Left(n,a,b,vars,wdth)
#the first variable, vars[1], is the insertion held fixed
#n should match nops(vars)
V_Left:=proc(n::nonnegint,a,b,vars::list(name),wdth)
   local pairs, removals, usedvars, keeppair, i, j, k, res, term:
   if nops(vars) <> n then
      print("Warning: in V_Left n is barely used, make sure number of
         vars is correct instead",n,vars);
   fi:
   if n < 1 then
      return 0;
   fi:
   pairs:=combinat[choose](vars,2):
   removals:=combinat[choose](pairs):
   pairs:=[]:
   for i from 1 to nops(removals) do
      usedvars:={}: keeppair:=true:
      for j from 1 to nops(removals[i]) while keeppair do
         for k from 1 to nops(removals[i][j]) do
            if removals[i][j][k] in usedvars then
               keeppair:=false:
            else
               usedvars:=usedvars union {removals[i][j][k]}:
            fi:
         od:
      od:
      if keeppair then
```

```
519            pairs:=[op(pairs),removals[i]]:
520         fi:
521      od:
522      res:=0:
523      for i from 1 to nops(pairs) do
524         term:=1/(n-1)!: usedvars:={}:
525         for j from 1 to nops(pairs[i]) do
526            if pairs[i][j][1] = vars[1] then
527               term:=term*G_Left(pairs[i][j][2],wdth,a,b):
528            elif pairs[i][j][2] = vars[1] then
529               term:=term*G_Left(pairs[i][j][1],wdth,a,b):
530            else
531               term:=term*G_r(pairs[i][j][1],pairs[i][j][2],wdth,a,b):
532            fi:
533            usedvars:=usedvars union {pairs[i][j][1],pairs[i][j][2]}:
534         od:
535         for j from 1 to nops(vars) do
536            if not vars[j] in usedvars then
537               term:=term*V_bare(vars[j]):
538               usedvars:=usedvars union {vars[j]}:
539            fi:
540         od:
541         res:=res+term:
542      od:
543      return res;
544   end proc:

546   #these are equivalent to the left-handed versions above, but with the rightmost insertion held fixed
547   G_Right:=(t,wdth,a,b)->-Pi^2/(wdth+1)^2/sin(Pi*(b-t)/(wdth+1))^2-Pi/(
         wdth+1)*cot(Pi*(b-a)/(wdth+1))/(b-a): #(4.22) and
         (4.37)
548   G_Right:=(t,wdth,a,b)->-1/(t-b)^2-1/(b-a)^2-RCR/(b-a):
549   RCR:=RCL: #seems like a very safe assumption
550   #[V^(n-1)(a,b)V(b)]_r is V_Right(n,a,b,vars,wdth), inert form is V_R_ren
551   #last variable, vars[n], is held fixed
552   V_Right:=proc(n::nonnegint,a,b,vars::list(name),wdth)
553      local pairs, removals, usedvars, keeppair, i, j, k, res, term:
554      if nops(vars) <> n then
555         print("Warning: in V_Right n is barely used, make sure number of
               vars is correct instead",n,vars);
556      fi:
557      if n < 1 then
558         return 0;
559      fi:
560      pairs:=combinat[choose](vars,2):
561      removals:=combinat[choose](pairs):
562      pairs:=[]:
563      for i from 1 to nops(removals) do
564         usedvars:={}: keeppair:=true:
565         for j from 1 to nops(removals[i]) while keeppair do
566            for k from 1 to nops(removals[i][j]) do
```

```
567             if removals[i][j][k] in usedvars then
568                keeppair:=false:
569             else
570                usedvars:=usedvars union {removals[i][j][k]}:
571             fi:
572          od:
573       od:
574       if keeppair then
575          pairs:=[op(pairs),removals[i]]:
576       fi:
577    od:
578    res:=0:
579    for i from 1 to nops(pairs) do
580       term:=1/(n-1)!: usedvars:={}:
581       for j from 1 to nops(pairs[i]) do
582          if pairs[i][j][1] = vars[n] then
583             term:=term*G_Right(pairs[i][j][2],wdth,a,b):
584          elif pairs[i][j][2] = vars[n] then
585             term:=term*G_Right(pairs[i][j][1],wdth,a,b):
586          else
587             term:=term*G_r(pairs[i][j][1],pairs[i][j][2],wdth,a,b):
588          fi:
589          usedvars:=usedvars union {pairs[i][j][1],pairs[i][j][2]}:
590       od:
591       for j from 1 to nops(vars) do
592          if not vars[j] in usedvars then
593             term:=term*V_bare(vars[j]):
594             usedvars:=usedvars union {vars[j]}:
595          fi:
596       od:
597       res:=res+term:
598    od:
599    return res;
600 end proc:

602 #[V(a)V^(n-2)(a,b)V(b)]_r
603 #the first and last elements of vars are held fixed at the left and right respectively
604 V_LR:=proc(n::nonnegint,a,b,vars::list(name),wdth)
605    local pairs, removals, usedvars, keeppair, i, j, k, res, term:
606    if nops(vars) <> n then
607       print("Warning: in V_LR n is barely used, make sure number of
              vars is correct instead",n,vars);
608    fi:
609    if n < 2 then
610       return 0;
611    fi:
612    pairs:=combinat[choose](vars,2):
613    removals:=combinat[choose](pairs):
614    pairs:=[]:
615    for i from 1 to nops(removals) do
616       usedvars:={}: keeppair:=true:
```

```
617       for j from 1 to nops(removals[i]) while keeppair do
618          for k from 1 to nops(removals[i][j]) do
619             if removals[i][j][k] in usedvars then
620                keeppair:=false:
621             else
622                usedvars:=usedvars union {removals[i][j][k]}:
623             fi:
624          od:
625       od:
626       if keeppair then
627          pairs:=[op(pairs),removals[i]]:
628       fi:
629    od:
630    res:=0:
631    for i from 1 to nops(pairs) do
632       term:=1/(n-2)!: usedvars:={}:
633       for j from 1 to nops(pairs[i]) do
634          if {pairs[i][j][1],pairs[i][j][2]}={vars[1],vars[n]} then
635             term:=0:
636          elif pairs[i][j][1] = vars[1] then
637             term:=term*G_Left(pairs[i][j][2],wdth,a,b):
638          elif pairs[i][j][2] = vars[1] then
639             term:=term*G_Left(pairs[i][j][1],wdth,a,b):
640          elif pairs[i][j][1] = vars[n] then
641             term:=term*G_Right(pairs[i][j][2],wdth,a,b):
642          elif pairs[i][j][2] = vars[n] then
643             term:=term*G_Right(pairs[i][j][1],wdth,a,b):
644          else
645             term:=term*G_r(pairs[i][j][1],pairs[i][j][2],wdth,a,b):
646          fi:
647          usedvars:=usedvars union {pairs[i][j][1],pairs[i][j][2]}:
648       od:
649       for j from 1 to nops(vars) do
650          if not vars[j] in usedvars then
651             term:=term*V_bare(vars[j]):
652             usedvars:=usedvars union {vars[j]}:
653          fi:
654       od:
655       res:=res+term:
656    od:
657    return res;
658 end proc:

660 #find the wedge state U^(n) defined in (2.47) of [36]
661 #this is only the state U^(n), it is 0-th order in λ by definition
662 Ucoeff:=proc(n::nonnegint)
663    local i, vars, ins:
664    global wedgewidth:
665    if n=0 then
666       return wId;
667    elif n=1 then
```

```
668         return wzero;
669     else
670         vars:=[]:
671         for i from 1 to n do
672             vars:=[op(vars),t[i]=1..n]:
673         od:
674         ins:=V_ren(n,a[1],b[1],map(lhs,vars),wedgewidth):
675         return [n,{a[1]=1,b[1]=n,op(vars)},[ins]];
676     fi:
677 end proc:

679 #all of U = \sum_n \lambda^n U^(n)
680 #"option system, remember" allows Maple to store the result for faster reexecution
681 ##cutoff is the order in \lambda to stop the taylor series
682 U:=proc(cutoff) option system, remember:
683     return &+(seq(ctimesw(lambda^n,Ucoeff(n)),n=0..cutoff));
684 end proc:

686 #like U above but excluding the term U^(0)
687 #since U = 1 + x, we expand f(U) about U = 1 using this
688 Utail:=proc(cutoff) option system, remember:
689     return &+(seq(ctimesw(lambda^n,Ucoeff(n)),n=1..cutoff));
690 end proc:

692 #\frac{1}{U} defined by its taylor series for small lambda, see [36] equation (2.58)
693 Uinv:=proc(cutoff) option system, remember:
694     return plus0(&+(wpId,seq(star(wpId,seq(ctimesw(-1,Utail(cutoff)),i
        =1..n),LAMBDA_MAX=cutoff),n=1..cutoff)));
695 end proc:

697 #\sqrt{U} defined by its taylor series for small lambda, see [36] equation (2.58)
698 Usqrt:=proc(cutoff) option system, remember:
699     return plus0(&+(wpId,seq(ctimesw(coeftayl(sqrt(1+x),x=0,n),star(wpId
        ,seq(Utail(cutoff),i=1..n),LAMBDA_MAX=cutoff)),n=1..cutoff)));
700 end proc:

702 #\frac{1}{\sqrt{U}} defined by its taylor series for small lambda, see [36] equation (2.58)
703 Uinvsqrt:=proc(cutoff) option system, remember:
704     return plus0(&+(wpId,seq(ctimesw(coeftayl(1/sqrt(1+x),x=0,n),star(
        wpId,seq(Utail(cutoff),i=1..n),LAMBDA_MAX=cutoff)),n=1..cutoff)))
        ;
705 end proc:

707 #the wedge state A_L defined in (3.22) and (4.57) of [36]
708 ##cutoff is the order in \lambda to stop the taylor series
709 A_L:=proc(cutoff)
710     local n, vars, ret:
711     global wedgewidth:
712     ret:=wpzero:
713     for n from 1 to cutoff do
```

```
714         vars:=[t[1]=1,seq(t[i]=1..n,i=2..n)]:
715         ret:=ret &+ [n,{a[1]=1,b[1]=n,op(vars)},[seq(0,i=1..n),c(t[1])*
                V_L_ren(n,a[1],b[1],map(lhs,vars),wedgewidth)]]:
716         if n>1 then
717            vars:=[t[1]=1,seq(t[i]=1..n,i=2..n-1)]:
718            ret:=ret &+ [n,{a[1]=1,b[1]=n,op(vars)},[seq(0,i=1..n),(RCL*c(
                  t[1])-(1/2)*dc(t[1]))*V_ren(n-2,a[1],b[1],map(lhs,vars[2..n
                  -1]),wedgewidth)]]:
719         fi:
720      od:
721      return ret;
722   end proc:

724   #the wedge state A_R defined in (3.22) and (4.57) of [36]
725   A_R:=proc(cutoff)
726      local n, vars, ret:
727      global wedgewidth:
728      ret:=wpzero:
729      for n from 1 to cutoff do
730         vars:=[seq(t[i]=1..n,i=1..n-1),t[n]=n]:
731         ret:=ret &+ [n,{a[1]=1,b[1]=n,op(vars)},[seq(0,i=1..n),c(t[n])*
                V_R_ren(n,a[1],b[1],map(lhs,vars),wedgewidth)]]:
732         if n>1 then
733            vars:=[seq(t[i]=1..n,i=1..n-2),t[n-1]=n]:
734            ret:=ret &+ [n,{a[1]=1,b[1]=n,op(vars)},[seq(0,i=1..n),(RCL*c(
                  t[n-1])+(1/2)*dc(t[n-1]))*V_ren(n-2,a[1],b[1],map(lhs,vars
                  [1..n-2]),wedgewidth)]]:
735         fi:
736      od:
737      return ret;
738   end proc:

740   #a simple tachyonic conformal patch, or future
741   #used to find the inner product of a wedge with the state generated by the operator e^{kX}
742   #ghost number here is 2 in order to saturate ghosts with a string field of ghost number 1
743   confpatch:=proc(k::integer)
744      return [0,{tL[0]=0,tL[1]=0},[(2/Pi)^(k^2-1)*dc(tL[0])*c(tL[1])*E(-k,
          tL[1])]];
745   end proc:

747   #the "left" solution defined in [36] equation (3.45)
748   ##n is the order in λ at which the solution should be calculated
749   ##if keep is specified then the solution is calculated for all orders in λ up to and including n
750   ##if keep is not specified (the default) then only the n-th order is calculated
751   Psi_L:=proc(n,{keep::boolean:=false})
752      local PSI:
753      PSI:=star(A_L(n),Uinv(n),LAMBDA_MAX=n):
754      if not keep then
755         return pickoff(PSI,lambda,n);
756      else
757         return plus0(PSI);
```

```
758     fi:
759 end proc:

761 #the "right" solution defined in [36] equation (3.48)
762 Psi_R:=proc(n,{keep::boolean:=false})
763     local PSI:
764     PSI:=star(Uinv(n),A_R(n),LAMBDA_MAX=n):
765     if not keep then
766         return pickoff(PSI,lambda,n);
767     else
768         return plus0(PSI);
769     fi:
770 end proc:

772 #the solution satisfying the reality condition
773 #as defined on line 1 of [36] equation (3.51)
774 Psi_L_real:=proc(n,{keep::boolean:=false}) option system, remember:
775     local PSI:
776     PSI:=star(Uinvsqrt(n),A_L(n),Uinvsqrt(n),LAMBDA_MAX=n) &+ star(
            Uinvsqrt(n),Q_B(Usqrt(n)),LAMBDA_MAX=n):
777     if not keep then
778         return pickoff(PSI,lambda,n);
779     else
780         return plus0(PSI);
781     fi:
782 end proc:

784 #same as above, but this time as defined on line 2 of [36] equation (3.51)
785 Psi_R_real:=proc(n,{keep::boolean:=false}) option system, remember:
786     local PSI:
787     PSI:=star(Uinvsqrt(n),A_R(n),Uinvsqrt(n),LAMBDA_MAX=n) &+ star(Usqrt
            (n),Q_B(Uinvsqrt(n)),LAMBDA_MAX=n):
788     if not keep then
789         return pickoff(PSI,lambda,n);
790     else
791         return plus0(PSI);
792     fi:
793 end proc:

795 #the BRST operator, acts on wedge states or their sums
796 #this is described in section 5.3.4
797 Q_B:=proc(inexpr)
798     local expr, i, j, k, grandlist, grand, dom, remainv, removev,
            grandterm, outw, orderproc, grassign, OL2, OR2:
799     expr:=wexpand(inexpr):
800     if type(expr,wsum) then
801         return map(Q_B,expr);
802     elif type(expr,wpoly) then #wpoly not handled separately, convert to wedge
803         return to_wpoly(Q_B(to_wedge(expr)),nops(expr[3])-1);
804     elif type(expr,wedge) then
805         OL2:=t->RCL*c(t)-dc(t)/2:
```

```
806         OR2:=t->RCL*c(t)+dc(t)/2:
807         expr:=varsort(expr):
808         grand:=expr[3]:
809         dom:=expr[2]:
810         outw:=wzero:
811         if type(grand,`*`) then
812            grand:=[op(grand)]:
813            #sort operators according to position on the boundary
814            #ghosts shifted right slightly to prevent early sign factors
815            #ghost shift must be smaller than minimum separation between operators from different
                   wedges, assumes a non-zero minimum
816            #this is a bit of a hack
817            orderproc:=(x,y)->piecewise(type(x,function),min(op(eval(map(
                   lhs,dom) intersect indets(x),map((z->piecewise(type(rhs(z),
                   range),lhs(z)=(op(1,rhs(z))+op(2,rhs(z)))/2,z)),dom))))+
                   piecewise(evalb(op(0,x) in {c,dc}),1/100,0),0)
818               < piecewise(type(y,function),min(op(eval(map(lhs,dom)
                      intersect indets(y),map((z->piecewise(type(rhs(z),range)
                      ,lhs(z)=(op(1,rhs(z))+op(2,rhs(z)))/2,z)),dom))))+
                      piecewise(evalb(op(0,y) in {c,dc}),1/100,0),0):
819            grand:=sort(grand,orderproc):
820            grassign:=1:
821            for i from 1 to nops(grand) do #find the integrated wedge insertion to
                   replace with a fixed insertion
822               if type(grand[i],function) and op(0,grand[i])=V_ren and op
                      (1,grand[i])>0 then
823                  grandterm:=grand:
824                  remainv:=dom: removev:={}:
825                  #we could always choose t[1] as the insertion to fix, but for clarity we will use
                         t[n] when it is fixed at the right
826                  for j from 1 to nops(dom) do
827                     if lhs(op(j,dom))=op(4,grand[i])[op(1,grand[i])] then
828                        remainv:=remainv minus {op(j,dom)}:
829                        removev:=removev union {op(j,dom)}:
830                     fi:
831                  od:
832                  grandterm[i]:=grassign*c(op(4,grand[i])[op(1,grand[i])])
                         *V_R_ren(op(grand[i])): #the subsop puts the first variable name
                         last (on the right)
833                  outw:=outw &+ [expr[1],remainv union map((x->lhs(x)=op
                         (2,rhs(x))),removev),`*`(op(grandterm))]:
834                  if op(1,grand[i])>1 then #repeat the process with cV endpoint
                         replaced by ∂c
835                     for j from 1 to nops(remainv) do
836                        if lhs(op(j,remainv))=op(4,grand[i])[1] then
837                           removev:=removev union {op(j,remainv)}:
838                        fi:
839                     od:
840                     remainv:=remainv minus removev:
841                     grandterm[i]:=grassign*OR2(op(4,grand[i])[op(1,grand[
                            i])])*subsop(1=op(1,grand[i])-2,4=[op(2..op(1,
```

```
                grand[i])-1,op(4,grand[i]))],V_ren(op(grand[i]))):
842             outw:=outw &+ [expr[1],remainv union map((x->lhs(x)=
                    op(2,rhs(x))),removev),`*`(op(grandterm))]:
843          fi:
844          remainv:=dom: removev:={}:
845          for j from 1 to nops(dom) do
846             if lhs(op(j,dom))=op(4,grand[i])[1] then
847                remainv:=remainv minus {op(j,dom)}:
848                removev:=removev union {op(j,dom)}:
849             fi:
850          od:
851          grandterm[i]:=grassign*c(op(4,grand[i])[1])*V_L_ren(op(
                grand[i])):
852          outw:=outw &+ [expr[1],remainv union map((x->lhs(x)=op
                (1,rhs(x))),removev),`*`(-1,op(grandterm))]:
853          if op(1,grand[i])>1 then #repeat the process with cV endpoints
                replaced by ∂c
854             for j from 1 to nops(remainv) do
855                if lhs(op(j,remainv))=op(4,grand[i])[2] then
856                   removev:=removev union {op(j,remainv)}:
857                fi:
858             od:
859             remainv:=remainv minus removev:
860             grandterm[i]:=grassign*OL2(op(4,grand[i])[1])*subsop
                   (1=op(1,grand[i])-2,4=[op(3..op(1,grand[i]),op(4,
                   grand[i]))],V_ren(op(grand[i]))):
861             outw:=outw &+ [expr[1],remainv union map((x->lhs(x)=
                   op(1,rhs(x))),removev),`*`(-1,op(grandterm))]:
862          fi:
863       elif type(grand[i],function) and op(0,grand[i])=V_L_ren and
           op(1,grand[i])>1 then
864          grandterm:=grand:
865          remainv:=dom: removev:={}:
866          for j from 1 to nops(dom) do #find the integrated wedge insertion to
                replace with a fixed insertion
867             if lhs(op(j,dom))=op(4,grand[i])[2] then #first insertion
                   already fixed, use [2] instead
868                remainv:=remainv minus {op(j,dom)}:
869                removev:=removev union {op(j,dom)}:
870             fi:
871          od:
872          #term 1 in (5.14)
873          grandterm[i]:=grassign*subsop(4=[op(4,grand[i])[1],op
                (3..op(1,grand[i]),op(4,grand[i])),op(4,grand[i])
                [2]],V_LR_ren(op(grand[i]))):
874          outw:=outw &+ [expr[1],remainv union map((x->lhs(x)=op
                (2,rhs(x))),removev),`*`(-1,c(op(4,grand[i])[2]),op(
                grandterm))]:
875          if op(1,grand[i]) >= 3 then #a cV at one end and a ∂c at the other
876             #terms 3 and 5 in (5.14)
877             grandterm[i]:=grassign*subsop(1=op(1,grand[i])-2,4=[
```

```
                op(3..op(1,grand[i])-1,op(4,grand[i])),op(4,grand[
                i])[2]],V_R_ren(op(grand[i]))):
878             outw:=outw &+ [expr[1],remove(has,remainv,op(4,grand[
                i])[op(1,grand[i])]) union map((x->lhs(x)=op(2,rhs
                (x))),removev),`*`(-2,OL2(op(4,grand[i])[1]),c(op
                (4,grand[i])[2]),op(remove(has,grandterm,c(op(4,
                grand[i])[1])))):]:
879             #term 2 in (5.14)
880             grandterm[i]:=grassign*subsop(1=op(1,grand[i])-2,4=[
                op(4,grand[i])[1],op(3..op(1,grand[i])-1,op(4,
                grand[i]))],V_L_ren(op(grand[i]))):
881             outw:=outw &+ [expr[1],remove(has,remainv,op(4,grand[
                i])[op(1,grand[i])]) union map((x->lhs(x)=op(2,rhs
                (x))),removev),`*`(-1,OR2(op(4,grand[i])[2]),op(
                grandterm))]:
882             if op(1,grand[i]) >= 4 then #∂c at both ends
883                #terms 4 and 6 in (5.14)
884                grandterm[i]:=grassign*subsop(1=op(1,grand[i])
                   -4,4=[op(3..op(1,grand[i])-2,op(4,grand[i]))],
                   V_ren(op(grand[i]))):
885                outw:=outw &+ [expr[1],remove(has,remainv,{op(4,
                   grand[i])[op(1,grand[i])],op(4,grand[i])[op(1,
                   grand[i])-1]}) union map((x->lhs(x)=op(2,rhs(x)
                   )),removev),`*`(-2,OL2(op(4,grand[i])[1]),OR2(
                   op(4,grand[i])[2]),op(remove(has,grandterm,c(op
                   (4,grand[i])[1])))):]:
886                #term 8 in (5.14)
887                outw:=outw &+ [expr[1],remove(has,remainv,{op(4,
                   grand[i])[op(1,grand[i])],op(4,grand[i])[op(1,
                   grand[i])-1]}) union map((x->lhs(x)=op(1,rhs(x)
                   )),removev),`*`(1,OL2(op(4,grand[i])[1]),OL2(op
                   (4,grand[i])[2]),op(remove(has,grandterm,c(op
                   (4,grand[i])[1])))):]:
888             fi:
889             #term 7 in (5.14)
890             grandterm[i]:=grassign*subsop(1=op(1,grand[i])-2,4=[
                op(4,grand[i])[2],op(3..op(1,grand[i])-1,op(4,
                grand[i]))],V_L_ren(op(grand[i]))):
891             outw:=outw &+ [expr[1],remove(has,remainv,op(4,grand[
                i])[op(1,grand[i])]) union map((x->lhs(x)=op(1,rhs
                (x))),removev),`*`(1,OL2(op(4,grand[i])[1]),c(op
                (4,grand[i])[2]),op(remove(has,grandterm,c(op(4,
                grand[i])[1])))):]:
892          fi:
893       elif type(grand[i],function) and op(0,grand[i])=V_R_ren and
           op(1,grand[i])>1 then #this section behaves very similarly to
          V_L_ren
894          grandterm:=grand:
895          remainv:=dom: removev:={}:
896          for j from 1 to nops(dom) do
897             if lhs(op(j,dom))=op(4,grand[i])[1] then
```

```
898                     remainv:=remainv minus {op(j,dom)}:
899                     removev:=removev union {op(j,dom)}:
900                  fi:
901               od:
902               #term 1 in (5.15)
903               grandterm[i]:=grassign*V_LR_ren(op(grand[i])):
904               outw:=outw &+ [expr[1],remainv union map((x->lhs(x)=op
                     (1,rhs(x))),removev),`*`(-1,c(op(4,grand[i])[1]),op(
                     grandterm))]:
905               if op(1,grand[i]) >= 3 then
906                  #term 2 in (5.15)
907                  grandterm[i]:=grassign*subsop(1=op(1,grand[i])-2,4=[
                        op(2..op(1,grand[i])-2,op(4,grand[i])),op(4,grand[
                        i])[op(1,grand[i])]],V_R_ren(op(grand[i]))):
908                  outw:=outw &+ [expr[1],remove(has,remainv,op(4,grand[
                        i])[op(1,grand[i])-1]) union map((x->lhs(x)=op(1,
                        rhs(x))),removev),`*`(-1,OL2(op(4,grand[i])[1]),op
                        (grandterm))]:
909                  if op(1,grand[i]) >= 4 then
910                     #term 3 in (5.15)
911                     grandterm[i]:=grassign*subsop(1=op(1,grand[i])
                           -4,4=[op(2..op(1,grand[i])-3,op(4,grand[i]))],
                           V_ren(op(grand[i]))):
912                     outw:=outw &+ [expr[1],remove(has,remainv,{op(4,
                           grand[i])[op(1,grand[i])-1],op(4,grand[i])[op
                           (1,grand[i])-2]}) union map((x->lhs(x)=op(2,rhs
                           (x))),removev),`*`(-1,OR2(op(4,grand[i])[1]),
                           OR2(op(4,grand[i])[op(1,grand[i])]),op(remove(
                           has,grandterm,c(op(4,grand[i])[op(1,grand[i])])
                           )))]:
913                  fi:
914                  #term 4 in (5.15)
915                  grandterm[i]:=grassign*subsop(1=op(1,grand[i])-2,4=[
                        op(2..op(1,grand[i])-2,op(4,grand[i])),op(4,grand[
                        i])[op(1,grand[i])]],V_R_ren(op(grand[i]))):
916                  outw:=outw &+ [expr[1],remove(has,remainv,op(4,grand[
                        i])[op(1,grand[i])-1]) union map((x->lhs(x)=op(2,
                        rhs(x))),removev),`*`(-1,c(op(4,grand[i])[1]),OR2(
                        op(4,grand[i])[op(1,grand[i])]),op(remove(has,
                        grandterm,c(op(4,grand[i])[op(1,grand[i])])))))]:
917               fi:
918            elif type(grand[i],function) and op(0,grand[i]) in {c,dc}
                  then
919               #introduce a sign factor for $Q_B(A*B)$
920               grassign:=-grassign:
921            elif type(grand[i],function) and not type(grand[i],trig)
                  then
922               userinfo(1,Q_B,"Warning: Q may be called on an unhandled
                     function. Assume ",Q(grand[i])=0);
923            fi:
924         od:
```

```
925             return outw;
926          elif type(grand,`+`) then
927             userinfo(1,Q_B,"Warning, `+` integrand shouldn't happen at
                    this point.");
928             return wexpand(expr);
929          elif type(grand,numeric) then
930             return wzero;
931          else
932             userinfo(1,Q_B,"Warning, operator insertions not handled by
                    Q_B:",grand);
933             return Q(expr);
934          fi:
935       else
936          print("Warning, Q_B only acts on wedges:",expr);
937          return Q(inexpr);
938       fi:
939    end proc:

941    corr:=proc(expr,{ww:=wedgewidth},{domout:=false})
942       local i, j, k, grand, uhp, Ematter, otherfacts, Cghosts, Cdiff, conf
              , Xmatter, Xpairs, Xdoubles, Corder,
943          used, keep, Xcorr, netE, netC, pow, var, Mcorr, Gcorr, dom,
                fixedpts, outgrand, dfcts, indfcts, tempgrand, wdth:
944       if type(expr,wsum) then #if domout then change + to &+, not yet implemented
945          return `+`(op(map(corr,plus0(wexpand(eval(expr,[V_ren=V_r,V_L_ren
                =V_Left,V_R_ren=V_Right,V_LL_ren=V_LL,V_RR_ren=V_RR,V_LR_ren=
                V_LR])))),':-ww'=ww,':-domout'=domout)));
946       elif type(expr,wpoly) then
947          return corr(to_wedge(expr),':-ww'=ww,':-domout'=domout);
948       elif type(expr,wedge) then
949          #finally substitute in the operators' renormalizations
950          grand:=eval(expr[3],[V_ren=V_r,V_L_ren=V_Left,V_R_ren=V_Right,
                V_LL_ren=V_LL,V_RR_ren=V_RR,V_LR_ren=V_LR]):
951          wdth:=expr[1]:
952          uhp:=unapply(tan(Pi*x/(wdth+1))/2,x): #transform coordinates to UHP
953          Ematter:=[]: Cghosts:=[]: Cdiff:=[]: Xmatter:=[]: otherfacts:=1:
954          netE:=0: netC:=0:
955          conf:=1:
956          if type(grand,`+`) or type(expand(grand),`+`) then
957             return corr(plus0(wexpand(eval(expr,[V_ren=V_r,V_L_ren=V_Left,
                   V_R_ren=V_Right,V_LL_ren=V_LL,V_RR_ren=V_RR,V_LR_ren=V_LR])
                   )),':-ww'=ww,':-domout'=domout);
958          elif type(grand,`*`) then #we have a single product of operators, so we can
                compute this term
959             for i from 1 to nops(grand) do
960                if type(op(i,grand),function) and op(0,op(i,grand)) = E
                      then #e^(pow*X(var))
961                   pow:=op(1,op(i,grand)):
962                   var:=op(2,op(i,grand)):
963                   netE:=netE+pow:
964                   #transform to UHP with weight pow^2
```

```
965                 conf:=conf*(Pi/2/(wdth+1))^(pow^2)*sec(Pi*var/(wdth+1))
                        ^(2*pow^2):
966                 Ematter:=[op(Ematter),[pow,var]]:
967             elif type(op(i,grand),function) and op(0,op(i,grand)) = c
                    then #c(var)
968                 netC:=netC+1:
969                 var:=op(op(i,grand)):
970                 #transform to schnabl frame with weight -1
971                 conf:=conf*(wdth+1)/Pi:
972                 Cghosts:=[op(Cghosts),var]:
973             elif type(op(i,grand),function) and op(0,op(i,grand)) = dc
                    then #∂c(var)
974                 netC:=netC+1:
975                 #no conformal factor, weight 0
976                 Cghosts:=[op(Cghosts),op(op(i,grand))]:
977                 Cdiff:=[op(Cdiff),op(op(i,grand))]:
978             elif type(op(i,grand),function) and op(0,op(i,grand)) = dX
                    then #∂X(var)
979                 var:=op(op(i,grand)):
980                 #transform to UHP with weight 1
981                 conf:=conf*(Pi/2/(wdth+1))*sec(Pi*var/(wdth+1))^2:
982                 Xmatter:=[op(Xmatter),var]:
983             #additional operators to be handled can go here
984             elif type(op(i,grand),function) and op(0,op(i,grand)) = b
                    then
985                 print("Warning: b-ghosts not handled yet, this will be
                        wrong.");
986             else #functions and numerical factors, not operators
987                 otherfacts:=otherfacts*op(i,grand):
988             fi:
989         od:
990         #must conserve momentum and saturate ghosts
991         if netE <> 0 or netC <> 3 then
992             Mcorr:=0:
993             return 0;
994         else
995             Mcorr:=1:
996             Corder:=proc(a,b)::boolean:
997                 local sep:
998                 sep:=eval(b-a,expr[2]):
999                 if sep>0 then return true;
1000                elif sep<0 then return false;
1001                else return lexorder(a,b);
1002                fi:
1003            end proc:
1004            #put the ghost insertions in order so the sign is consistent
1005            Cghosts:=sort(Cghosts,Corder):
1006            for i from 1 to nops(Cghosts) do
1007                Cdiff:=eval(Cdiff,Cghosts[i]=i);
1008            od:
1009        fi:
```

```
#construct matter correlator on UHP, this part only handles exponentials, equation (6.2.35) of [6]
for i from 1 to nops(Ematter) do
   for j from i+1 to nops(Ematter) do
      Mcorr:=Mcorr*(uhp(Ematter[i][2])-uhp(Ematter[j][2]))^(2*Ematter[i][1]*Ematter[j][1]):
   od:
od:
#∂X part of matter correlator
#first make a list of pairs of ∂X operators to contract with each other
Xpairs:=combinat[choose](Xmatter,2):
Xdoubles:=combinat[choose](Xpairs):
Xpairs:=[]:
for i from 1 to nops(Xdoubles) do
   used:={}: keep:=true:
   for j from 1 to nops(Xdoubles[i]) while keep do
      for k from 1 to nops(Xdoubles[i][j]) while keep do
         if Xdoubles[i][j][k] in used then
            keep:=false:
         else
            used:=used union {Xdoubles[i][j][k]}:
         fi:
      od:
   od:
   if keep then
      Xpairs:=[op(Xpairs),Xdoubles[i]]:
   fi:
od:
Xcorr:=[]:
for i from 1 to nops(Xpairs) do
   Xcorr:=[op(Xcorr),1]:
   #purely ∂X part of mater correlator
   for j from 1 to nops(Xpairs[i]) do
      Xcorr[i]:=Xcorr[i]*2*alphaprime/(uhp(Xpairs[i][j][1])-uhp(Xpairs[i][j][2]))^2:
   od:
   #cross terms for e^{kX} and ∂X
   for j from 1 to nops(Xmatter) do
      keep:=true:
      for k from 1 to nops(Xpairs[i]) while keep do
         if Xmatter[j]=Xpairs[i][k][1] or Xmatter[j]=Xpairs[i][k][2] then
            keep:=false:
         fi:
      od: k:='k':
      if keep then
         Xcorr[i]:=Xcorr[i]*add(2*Ematter[k][1]*sqrt(alphaprime)/(uhp(Xmatter[j])-uhp(Ematter[k][2])),k=1..nops(Ematter)):
      fi:
   od:
```

```
1055            od:
1056            Xcorr:=`+`(op(Xcorr)):
1057            #construct the ghost correlator in Schnabl frame, no b ghosts
1058            #use equation (D.11) of [25]
1059            Gcorr:=D[op(Cdiff)]((x,y,z)->sin(x-y)*sin(x-z)*sin(y-z))(op(
                    map((x->Pi*x/(wdth+1)),Cghosts))):
1060            outgrand:=otherfacts*conf*Mcorr*Xcorr*Gcorr:
1061            outgrand:=eval(outgrand,ww=wdth):
1062        elif type(grand,numeric) then #wedge contains no operators
1063            outgrand:=grand:
1064        else
1065            print("some other kind of integrand... not handled",op(0,grand
                    ),grand);
1066            outgrand:=grand:
1067        fi:
1068        #determine which variables are fixed and which are integrated
1069        dom:=[]: fixedpts:=[]:
1070        for i from 1 to nops(expr[2]) do
1071            if type(op(i,expr[2]),name=range) then
1072                dom:=[op(dom),op(i,expr[2])]:
1073            else
1074                fixedpts:=[op(fixedpts),op(i,expr[2])]:
1075            fi:
1076        od:
1077        fixedpts:=eval(fixedpts,ww=wdth): #in case insertion locations are given in
                terms of the wedge circumference
1078        dom:=eval(dom,ww=wdth):
1079        if nops(dom) > 0 then #there are integrated insertions
1080            try
1081                #always use inert integrals, since they usually can't be done exactly
1082                return Int(eval(outgrand,fixedpts),dom);
1083            catch: #if fixed insertions alone give rise to singularities
1084                #fix the insertions one at a time to single out the problem ones
1085                for i from 1 to nops(fixedpts) do
1086                    try
1087                        outgrand:=eval(outgrand,fixedpts[i]):
1088                    catch:
1089                        if type(outgrand,`*`) then
1090                            #separate out the factors that depend on the variable
1091                            dfcts:=1: indfcts:=1:
1092                            for j from 1 to nops(outgrand) do
1093                                if depends(op(j,outgrand),lhs(fixedpts[i]))
                                        then
1094                                    dfcts:=dfcts*op(j,outgrand):
1095                                else
1096                                    indfcts:=indfcts*op(j,outgrand):
1097                                fi:
1098                            od:
1099                        else
1100                            indfcts:=1:
1101                            dfcts:=outgrand:
```

```
1102                    fi:
1103                    #indfcts:=simplify(indfcts,trig): #not worth the execution time
1104                    #dfcts:=simplify(dfcts,trig):
1105                    #try a limit, if that still fails use Limit instead
1106                    userinfo(2,corr,"switching from eval to limit",dfcts,
                            fixedpts[i]);
1107                    tempgrand:=indfcts*limit(dfcts,fixedpts[i]):
1108                    if has(tempgrand,{undefined,infinity}) then
1109                       outgrand:=indfcts*Limit(dfcts,fixedpts[i]):
1110                    else
1111                       outgrand:=tempgrand:
1112                    fi:
1113                    userinfo(2,corr,"done limit");
1114                 end try:
1115              od:
1116              return Int(outgrand,dom);
1117           end try:
1118        else #same as above but without any integrals required
1119           try
1120              return eval(outgrand,fixedpts);
1121           catch:
1122              for i from 1 to nops(fixedpts) do
1123                 try
1124                    outgrand:=eval(outgrand,fixedpts[i]):
1125                 catch:
1126                    #if no integration then this is usually a simple function, so don't bother
                          separating the factors
1127                    userinfo(2,corr,"switching from eval to limit",
                          outgrand,fixedpts[i]);
1128                    tempgrand:=limit(outgrand,fixedpts[i]):
1129                    if has(tempgrand,{undefined,infinity}) then
1130                       outgrand:=Limit(outgrand,fixedpts[i]):
1131                    else
1132                       outgrand:=tempgrand:
1133                    fi:
1134                    userinfo(2,corr,"done limit");
1135                 end try:
1136              od:
1137              return outgrand;
1138           end try:
1139        fi:
1140     else
1141        print("some other kind of expr... not handled",op(0,expr),expr);
1142        return expr;
1143     fi:
1144  end proc:

1146  #rescale variables to put all integrals over the unit hypercube
1147  #also combines integrals with the same dimension so that singularities can cancel between terms
1148  to_cube:=proc(expr)
1149     local i, j, k, grand, dom, newdom, ab, nm, csum, othterms, lims,
```

```
    limnm, limvars, newlim, limterms, nonlimterms:
if type(expr,constant) then
    return expr;
elif type(expr,`+`) then
    grand:=[]: dom:=[]: othterms:=0:
    csum:=map(to_cube,[op(expr)]): #first rescale each integral separately
    #now join integrals with same dimension
    for i from 1 to nops(csum) do
        if type(csum[i],function) and op(0,csum[i])=Int then
            if op(2,csum[i]) in dom then
                for j from 1 to nops(dom) do
                    if dom[j]=op(2,csum[i]) then
                        grand:=subsop(j=grand[j]+op(1,csum[i]),grand):
                    fi:
                od:
            else
                grand:=[op(grand),op(1,csum[i])]:
                dom:=[op(dom),op(2,csum[i])]:
            fi:
        else
            othterms:=othterms+csum[i]:
        fi:
    od:
    #now similarly merge any inert limits in the integrand
    #for our purposes this shouldn't be needed
    for i from 1 to nops(grand) do
        lims:=selectfun(grand[i],Limit):
        limvars:={}:
        for j from 1 to nops(lims) do
            if type(op(2,op(j,lims)),equation) then
                limvars:=limvars union {op(2,op(j,lims))}:
            else
                limvars:=limvars union {op(op(2,op(j,lims)))}:
            fi:
            grand[i]:=subs(op(j,lims)=op(1,op(j,lims)),grand[i]):
        od:
        for j from 1 to nops(limvars) do
            if type(grand[i],`+`) then
                limterms:=0:
                nonlimterms:=0:
                for k from 1 to nops(grand[i]) do
                    if has(op(k,grand[i]),lhs(op(j,limvars))) then
                        limterms:=limterms+op(k,grand[i]):
                    else
                        nonlimterms:=nonlimterms+op(k,grand[i]):
                    fi:
                od:
                grand[i]:=nonlimterms+limit(limterms,op(j,limvars)):
            else
                grand[i]:=limit(grand[i],op(j,limvars)):
            fi:
```

```
1200            od:
1201        od:
1202        return `+`(seq(Int(grand[x],dom[x],param3),x=1..nops(dom)),
                othterms);
1203    elif type(expr,`*`) then #typically a constant times an integral
1204        if type(op(1,expr),function) or nops(expr) > 2 then
1205            print("warning, could be mixing up integrals... but probably
                    not:",expr);
1206        fi:
1207        csum:=map(to_cube,[op(expr)]):
1208        othterms:=1: grand:=[]: dom:=[]:
1209        for i from 1 to nops(csum) do
1210            if type(op(i,csum),constant) then
1211                othterms:=othterms*op(i,csum):
1212            elif type(op(i,csum),function) and op(0,op(i,csum))=Int then
1213                grand:=[op(grand),op(1,op(i,csum))]:
1214                dom:=[op(dom),op(2,op(i,csum))]:
1215            else
1216                print("Warning: `*` has a non-constant, non-Int factor.");
1217                othterms:=othterms*op(i,csum):
1218            fi:
1219        od:
1220        if nops(grand)=0 then
1221            return othterms;
1222        else
1223            grand[1]:=grand[1]*othterms:
1224            return `*`(seq(Int(grand[x],dom[x],param3),x=1..nops(grand)));
1225        fi:
1226    elif type(expr,function) and op(0,expr)=Int then #rescale a single integral to
        the unit hypercube
1227        grand:=op(1,expr):
1228        dom:=op(2,expr):
1229        newdom:=[]:
1230        for i from 1 to nops(dom) do
1231            ab:=[op(1,rhs(dom[i])),op(2,rhs(dom[i]))]:
1232            nm:=newvar(map(lhs,{op(newdom)}),s[1]):
1233            grand:=subs(lhs(dom[i])=ab[1]+(ab[2]-ab[1])*nm,grand*(ab[2]-ab
                    [1])):
1234            newdom:=[op(newdom),nm=0..1]:
1235        od:
1236        if hasfun(grand,{limit,Limit}) then #shift any remaining limits to 0
1237            lims:=selectfun(grand,{limit,Limit}):
1238            limvars:={}:
1239            for i from 1 to nops(lims) do
1240                nm,ab:=lhs(op(2,op(i,lims))),rhs(op(2,op(i,lims))):
1241                limnm:=newvar(limvars union map(lhs,{op(newdom)}),s[1]):
1242                limvars:=limvars union {limnm}:
1243                newlim:=subs(nm=limnm-ab,op(1,op(i,lims))):
1244                grand:=subs(op(i,lims)=Limit(newlim,limnm=0),grand):
1245            od:
1246        fi:
```

```
1247        if type(grand,numeric) then
1248           return grand;
1249        else
1250           return Int(grand,newdom,param3); #param3 is any extra parameters for
                   numerical evaluation, normally set to NULL
1251        fi:
1252     else
1253        print("Warning: not handled by to_cube");
1254        return expr;
1255     fi:
1256  end proc:

1258  #create a function or sum of functions representing the integrals
1259  #these functions are suitable for exporting to C
1260  to_funcs:=proc(expr)
1261     local i, grand, dom:
1262     global Fnms:
1263     if type(expr,constant) then
1264        if expr=0 then
1265           return 0;
1266        fi:
1267        i:=1:
1268        while type(`F`||i,procedure) do #skip to an unused name
1269           i:=i+1:
1270        od:
1271        `F`||i:=unapply(subs(Pi=PI,expr),x):
1272        Fnms:=[op(Fnms),evaln(`F`||i)]:
1273        return (`F`||i);
1274     elif type(expr,`+`) or type(expr,`*`) then
1275        return map(to_funcs,expr);
1276     elif type(expr,function) and op(0,expr)=Int then
1277        grand:=op(1,expr):
1278        #grand:=simplify(grand): #this could help with rounding errors, but at a large
               performance cost
1279        grand:=subs(Pi=PI,grand):
1280        if grand=0 then
1281           return 0;
1282        fi:
1283        dom:=op(2,expr):
1284        i:=1:
1285        while type(`F`||i,procedure) do #skip to an unused name
1286           i:=i+1:
1287        od:
1288        `F`||i:=unapply(grand,op(map(lhs,dom))):
1289        Fnms:=[op(Fnms),evaln(`F`||i)]:
1290        #the C++ syntax to integrate over the unit hypercube will be
               CubeInt(dimension,function,result,standard_deviation,chi_squared);
1291        return CubeInt(nops(dom),(`F`||i),res[i],sig[i],chi[i]);
1292     else #if unsure what type, just treat it similarly to a constant
1293        i:=1:
1294        while type(`F`||i,procedure) do
```

```
1295            i:=i+1:
1296        od:
1297        `F`||i:=unapply(subs(Pi=PI,expr),x):
1298        Fnms:=[op(Fnms),evaln(`F`||i)]:
1299        return (`F`||i);
1300    fi:
1301 end proc:

1303 #converts the inert integrals to a form which can be evaluated symbolically
1304 #useful for low dimension only
1305 #resulting integrals can be evaluated with the value command
1306 vints:=proc(expr)
1307    local i, dom, grand:
1308    if type(expr,`+`) or type(expr,`*`) then
1309        return map(vints,expr);
1310    elif type(expr,function) and op(0,expr)=Int and type(op(2,expr),list
        ) then
1311        dom:=op(2,expr):
1312        grand:=op(1,expr):
1313        for i from 1 to nops(dom) do
1314            grand:=Int(grand,dom[i]):
1315        od:
1316        return grand;
1317    else
1318        return expr;
1319    fi:
1320 end proc:

1322 #take the derivative of an inert integral which should not have the differentiation variable as an
       integration variable
1323 #this is for constructing taylor series with respect to the renormalization constants
1324 #the builtin function diff is supposed to handle this, but can fail for the special inert
       multidimensional integration syntax
1325 ##x can be a list, in which case a derivative is taken with respect to each element
1326 diffint:=proc(f,x)
1327    if type(x,list) then
1328        if x=[] then
1329            return f;
1330        else
1331            return diffint(diffint(f,x[1]),x[2..-1]);
1332        fi:
1333    else
1334        if type(f,`+`) or type(f,wsum) then
1335            return map(diffint,f,x);
1336        elif type(f,function) and op(0,f)=`Int` and not x in op(2,f) then
1337            return Int(diff(op(1,f),x),op(2..-1,f));
1338        elif type(f,`*`) then
1339            return add(subsop(i=diffint(op(i,f),x),f),i=1..nops(f)):
1340        else
1341            return diff(f,x);
1342        fi:
```

```
1343     fi:
1344 end proc:

1346 #the main function to construct the solution at order λ^n and find tachyon modes
1347 #this is done for Nmin < n < Nmax
1348 #finds a taylor series in the renormalization constants RCk, RC2, and RCL
1349 ##out is the filename the C++ output is written to
1350 ##eom and action, if set, will also produce the necesary integrands to test the equation of motion and
     the action
1351 tacconst:=proc(Nmax,{out:=terminal},{Nmin:=2},{eom:=false},{action:=
     false})
1352     local n, k, i, j, m, nkpart, csum, rsget, sgget, RCstrget, oR2, oRk,
          oRL, outf, eomnkpart, ceomsum, eomnPsiLkpart, ceomPsiLsum,
         eomnPsirkpart, ceomPsirsum, kineticparts, cubicparts, ckineticsum
         , ccubicsum;
1353     global Fnms, RC2, RCk, RCL:
1354     Fnms:=[]:
1355     oR2:=RC2: oRk:=RCk: oRL:=RCL:
1356     RC2:='RC2': RCk:='RCk': RCL:='RCL':
1357     #functions to get the variables holding the result and standard deviation for an integral
1358     rsget:=(fn)->piecewise(type(fn,`+`),map(rsget,fn),type(fn,function)
         and op(0,fn)=CubeInt,subsop(1=op(1,op(3,fn))-1,op(3,fn)),evalf(fn
         )):
1359     sgget:=(fn)->piecewise(type(fn,`+`),map(sgget,fn),type(fn,function)
         and op(0,fn)=CubeInt,subsop(1=op(1,op(4,fn))-1,op(4,fn)),evalf(0)
         ):
1360     #function to get a string for C0^i * C1^j * CL^m
1361     RCstrget:=(i,j,m)->cat("(%%G+/-%%G)",piecewise(i=0,"","C0^"||i),
         piecewise(j=0,"","C1^"||j),piecewise(m=0,"","CL^"||m));
1362     #construct the solution
1363     for n from Nmin to Nmax do
1364        print("Building ",Psi[n]);
1365        (psi||n):=Psi_L_real(n):
1366        save psi||n, "reCpsi"||n||".txt"; #save the solution to a file for reference
1367        if eom then
1368           print("Building ",EOM[n]);
1369           #construct the equation of motion with ghost number 2
1370           (eom||n):=`&+`(seq(star(Psi_L_real(l),Psi_L_real(n-l)),l=0..n)
                ,Q_B(Psi_L_real(n))):
1371           #find the tachyon component with k units of momentum
1372           for k from n mod 2 to n by 2 do
1373              print("Building functions for ",EOM[n],exp(k*X));
1374              eomnkpart[n,k]:=corr(star([0,{tL[0]=0},[(2/Pi)^(k^2-1)*c(tL
                   [0])*E(-k,tL[0])]],(eom||n))):
1375              for i from 0 to floor(n/2) do
1376                 for j from 0 to floor(n/2)-i do
1377                    for m from 0 to floor(n/2)-i-j do #taylor expand in
                         renormalization constants
1378                       ceomsum[n,k,i,j,m]:=to_funcs(to_cube(eval(diffint(
                            eomnkpart[n,k],[RC2$i,RCk$j,RCL$m]),[RC2=0,RCk
                            =0,RCL=0]))):
```

```
1379                od:
1380             od:
1381          od:
1382       od:
1383       #find the overlap of the equation of motion with the solution for two gauge choices
1384       for k from 1 to Nmax-n+1 do
1385          print("Building functions for ",EOM[n],Psi_L[k]);
1386          eomnPsiLkpart[n,k]:=corr(starip(Psi_L(k),(eom||n))):
1387          for i from 0 to floor((n+k)/2) do
1388             for j from 0 to floor((n+k)/2)-i do
1389                for m from 0 to floor((n+k)/2)-i-j do
1390                   ceomPsiLsum[n,k,i,j,m]:=to_funcs(to_cube(eval(
                          diffint(eomnPsiLkpart[n,k],[RC2$i,RCk$j,RCL$m])
                          ,[RC2=0,RCk=0,RCL=0]))):
1391                od:
1392             od:
1393          od:
1394          print("Building functions for ",EOM[n],Psi[k]);
1395          eomnPsirkpart[n,k]:=corr(starip(Psi_L_real(k),(eom||n))):
1396          for i from 0 to floor((n+k)/2) do
1397             for j from 0 to floor((n+k)/2)-i do
1398                for m from 0 to floor((n+k)/2)-i-j do
1399                   ceomPsirsum[n,k,i,j,m]:=to_funcs(to_cube(eval(
                          diffint(eomnPsirkpart[n,k],[RC2$i,RCk$j,RCL$m])
                          ,[RC2=0,RCk=0,RCL=0]))):
1400                od:
1401             od:
1402          od:
1403       od:
1404    fi:
1405    if action then
1406       #find the kinetic and cubic terms of the action separately
1407       print("Building ",kinetic[n]);
1408       (kineticact||n):=`&+`(seq(starip(Psi_L_real(l),Q_B(Psi_L_real(
             n-l))),l=0..n));
1409       print("Building ",cubic[n]);
1410       (cubicact||n):=pickoff(starip(Psi_L_real(n-2),Psi_L_real(n-2),
             Psi_L_real(n-2),LAMBDA_MAX=n),lambda,n):
1411       print("Building functions for ",kinetic[n]);
1412       kineticparts[n]:=corr(kineticact||n): #the kinetic term's expectation
             value
1413       for i from 0 to floor(n/2) do
1414          for j from 0 to floor(n/2)-i do
1415             for m from 0 to floor(n/2)-i-j do
1416                ckineticsum[n,i,j,m]:=to_funcs(to_cube(eval(diffint(
                      kineticparts[n],[RC2$i,RCk$j,RCL$m]),[RC2=0,RCk=0,
                      RCL=0]))):
1417             od:
1418          od:
1419       od:
1420       print("Building functions for ",cubic[n]);
```

```
1421            cubicparts[n]:=corr(cubicact||n): #the cubic term's expectation value
1422            for i from 0 to floor(n/2) do
1423               for j from 0 to floor(n/2)-i do
1424                  for m from 0 to floor(n/2)-i-j do
1425                     ccubicsum[n,i,j,m]:=to_funcs(to_cube(eval(diffint(
                           cubicparts[n],[RC2$i,RCk$j,RCL$m]),[RC2=0,RCk=0,
                           RCL=0]))):
1426                  od:
1427               od:
1428            od:
1429         fi:
1430      od:
1431      for n from Nmin to Nmax do
1432         for k from n mod 2 to n by 2 do
1433            #find the tachyon profile itself
1434            print("Building functions for "||beta[n,k]);
1435            nkpart[n,k]:=corr(star(confpatch(k),(psi||n))):
1436            for i from 0 to floor(n/2) do
1437               for j from 0 to floor(n/2)-i do
1438                  for m from 0 to floor(n/2)-i-j do
1439                     csum[n,k,i,j,m]:=to_funcs(to_cube(eval(diffint(nkpart
                           [n,k],[RC2$i,RCk$j,RCL$m]),[RC2=0,RCk=0,RCL=0]))):
1440                  od:
1441               od:
1442            od:
1443         od:
1444      od:
1445      if out <> terminal then
1446         print("Writing C code to file.");
1447      fi:
1448      #write lines of C++ code to compute each of the necessary integrals
1449      #each line has all integrals which should be added together as a single number
1450      #resultname is only for clarity, as the true output is stored in the arrays res and sig
1451      for n from Nmin to Nmax do
1452         if eom then
1453            for k from n mod 2 to n by 2 do
1454               for i from 0 to floor(n/2) do
1455                  for j from 0 to floor(n/2)-i do
1456                     for m from 0 to floor(n/2)-i-j do
1457                        if ceomsum[n,k,i,j,m] <> 0 then
1458                           CodeGeneration[C](ceomsum[n,k,i,j,m],resultname
                                 =eomtac,output=out);
1459                        fi:
1460                     od:
1461                  od:
1462               od:
1463            od:
1464            for k from 1 to Nmax-n+1 do
1465               for i from 0 to floor((n+k)/2) do
1466                  for j from 0 to floor((n+k)/2)-i do
1467                     for m from 0 to floor((n+k)/2)-i-j do
```

```
1468                    if ceomPsiLsum[n,k,i,j,m] <> 0 then
1469                       CodeGeneration[C](ceomPsiLsum[n,k,i,j,m],
                              resultname=eomPsiL,output=out);
1470                    fi:
1471                    if ceomPsirsum[n,k,i,j,m] <> 0 then
1472                       CodeGeneration[C](ceomPsirsum[n,k,i,j,m],
                              resultname=eomPsir,output=out);
1473                    fi:
1474                 od:
1475              od:
1476           od:
1477        od:
1478     fi:
1479     if action then
1480        for i from 0 to floor(n/2) do
1481           for j from 0 to floor(n/2)-i do
1482              for m from 0 to floor(n/2)-i-j do
1483                 if ckineticsum[n,i,j,m] <> 0 then
1484                    CodeGeneration[C](ckineticsum[n,i,j,m],resultname=
                           kineticaction,output=out);
1485                 fi:
1486                 if ccubicsum[n,i,j,m] <> 0 then
1487                    CodeGeneration[C](ccubicsum[n,i,j,m],resultname=
                           cubicaction,output=out);
1488                 fi:
1489              od:
1490           od:
1491        od:
1492     fi:
1493     for k from n mod 2 to n by 2 do
1494        for i from 0 to floor(n/2) do
1495           for j from 0 to floor(n/2)-i do
1496              for m from 0 to floor(n/2)-i-j do
1497                 if csum[n,k,i,j,m] <> 0 then
1498                    CodeGeneration[C](csum[n,k,i,j,m],resultname=
                           tacprofile,output=out);
1499                 fi:
1500              od:
1501           od:
1502        od:
1503     od:
1504  od:
1505  if out <> terminal then #CodeGeneration won't share its file handle, have to close and
       reopen
1506     fclose(out):
1507     outf:=fopen(out,APPEND):
1508  else
1509     outf:=out:
1510  fi:
1511  #write C++ code to output a summary of all results
1512  if eom then
```

```
1513        for n from Nmin to Nmax do
1514           for k from n mod 2 to n by 2 do
1515              fprintf(outf,cat("printf(""e^",k," EOM(",n,") = ",op
                     (2..-1,[seq(seq(seq(op([" + ",RCstrget(i,j,m)]),m=0..
                     floor(n/2)-i-j),j=0..floor(n/2)-i),i=0..floor(n/2))]),"
                     \\n""
1516              ,seq(seq(seq(cat(",",convert(rsget(ceomsum[n,k,i,j,m]),
                     string),",",convert(sgget(ceomsum[n,k,i,j,m]),string)),m
                     =0..floor(n/2)-i-j),j=0..floor(n/2)-i),i=0..floor(n/2)),
                     ");\n"));
1517           od:
1518        od:
1519        for n from Nmin to Nmax do
1520           for k from 1 to Nmax-n+1 do
1521              fprintf(outf,cat("printf(""Psi_L[",k,"]EOM(",n,") = ",op
                     (2..-1,[seq(seq(seq(op([" + ",RCstrget(i,j,m)]),m=0..
                     floor((n+k)/2)-i-j),j=0..floor((n+k)/2)-i),i=0..floor((n
                     +k)/2))]),"\\n""
1522              ,seq(seq(seq(cat(",",convert(rsget(ceomPsiLsum[n,k,i,j,m]),
                     string),",",convert(sgget(ceomPsiLsum[n,k,i,j,m]),string
                     )),m=0..floor((n+k)/2)-i-j),j=0..floor((n+k)/2)-i),i=0..
                     floor((n+k)/2)),");\n"));
1523              fprintf(outf,cat("printf(""Psi_real[",k,"]EOM(",n,") = ",op
                     (2..-1,[seq(seq(seq(op([" + ",RCstrget(i,j,m)]),m=0..
                     floor((n+k)/2)-i-j),j=0..floor((n+k)/2)-i),i=0..floor((n
                     +k)/2))]),"\\n""
1524              ,seq(seq(seq(cat(",",convert(rsget(ceomPsirsum[n,k,i,j,m]),
                     string),",",convert(sgget(ceomPsirsum[n,k,i,j,m]),string
                     )),m=0..floor((n+k)/2)-i-j),j=0..floor((n+k)/2)-i),i=0..
                     floor((n+k)/2)),");\n"));
1525           od:
1526        od:
1527     fi:
1528     if action then
1529        for n from Nmin to Nmax do
1530           fprintf(outf,cat("printf(""kinetic(",n,") = ",op(2..-1,[seq(
                  seq(seq(op([" + ",RCstrget(i,j,m)]),m=0..floor(n/2)-i-j),j
                  =0..floor(n/2)-i),i=0..floor(n/2))]),"\\n""
1531           ,seq(seq(seq(cat(",",convert(rsget(ckineticsum[n,i,j,m]),
                  string),",",convert(sgget(ckineticsum[n,i,j,m]),string)),m
                  =0..floor(n/2)-i-j),j=0..floor(n/2)-i),i=0..floor(n/2)),")
                  ;\n"));
1532           fprintf(outf,cat("printf(""cubic(",n,") = ",op(2..-1,[seq(seq(
                  seq(op([" + ",RCstrget(i,j,m)]),m=0..floor(n/2)-i-j),j=0..
                  floor(n/2)-i),i=0..floor(n/2))]),"\\n""
1533           ,seq(seq(seq(cat(",",convert(rsget(ccubicsum[n,i,j,m]),string)
                  ,",",convert(sgget(ccubicsum[n,i,j,m]),string)),m=0..floor(
                  n/2)-i-j),j=0..floor(n/2)-i),i=0..floor(n/2)),");\n"));
1534        od:
1535     fi:
1536     for n from Nmin to Nmax do
```

```
1537        for k from n mod 2 to n by 2 do
1538           fprintf(outf,cat("printf(""beta[",n,",",k,"] = ",op(2..-1,[seq
                  (seq(seq(op([" + ",RCstrget(i,j,m)]),m=0..floor(n/2)-i-j),j
                  =0..floor(n/2)-i),i=0..floor(n/2))]),"\\n"""
1539           ,seq(seq(seq(cat(",",convert(rsget(csum[n,k,i,j,m]),string),",
                  ",convert(sgget(csum[n,k,i,j,m]),string)),m=0..floor(n/2)-i
                  -j),j=0..floor(n/2)-i),i=0..floor(n/2)),");\n"));
1540        od:
1541     od:
1542     if out <> terminal then #give CodeGeneration back its file handle
1543        fclose(out):
1544     fi:
1545     #write out all of the integrands to the file
1546     map(CodeGeneration[C],Fnms,digits=round(evalhf(16)),output=out,
           deducetypes=false);
1547     RC2:=oR2: RCk:=oRk: RCL:=oRL:
1548     print("Done.");
1549  end proc:

1551  #interface(prettyprint=0):
1552  #tacconst(6,out="all-RC.mapleout.txt",eom,action);
```

B.2 Sample C++ Program

Once the contents of section B.1 have been loaded into Maple, the simplest quantity to calculate with it is the solution satisfying the reality condition at order λ^2. To do this we run the command `tacconst(2,out="tacRC-brief.txt");` which will produce two files as output. The first is `reCpsi2.txt` meaning the solution Ψ satisfying the *re*ality condition, with the renormalization constants C, at order λ^2. The wedge states are stored as plain text and can be read back into Maple for future use to avoid extra calculations. The second file, `tacRC-brief.txt`, was named in the command and contains the correlation functions to be integrated along with commands to do so. The first few lines of the file should be copied and pasted into the C++ file being used. Constant functions which are not integrated will need to have parentheses added manually in order to comply with C syntax, so `F2` below will become `F2()`. In addition, in order to provide clearer output I have added an additional parameter to the `CubeInt` function which repeats the function number. This can be seen near the end of program B.6. There is one more notational difference here. In the output, the coefficients are listed as β_n^k instead of the $\beta_n^{(j)}$ notation we used in chapter 5. This makes it more convenient to write $T(t) = \sum_{n=1}^{\infty}\sum_{k=-n}^{n}\lambda^n\beta_n^k e^{kt}$, but less obvious which coefficients naturally form the "rows" we studied. The two are simply related by $\beta_n^{(j)} = \beta_n^{n-2j}$ and $\beta_n^{-k} = \beta_n^k$.

Program B.2: Sample C++ command lines as output by Maple

```
1 tacprofile = CubeInt(1, F1, res[0], sig[0], chi[0]) + F2;
2 tacprofile = CubeInt(1, F3, res[2], sig[2], chi[2]) + F4;
3 tacprofile = CubeInt(1, F5, res[4], sig[4], chi[4]);
4 printf("beta[2,0] = (%G+/-%G) + (%G+/-%G)CL^1 + (%G+/-%G)C1^1 + (%G+/-%
     G)C0^1\n",res[0]+F2,sig[0],res[2]+F4,sig[2],0.,0.,0.,0.);
```

```
5  printf("beta[2,2] = (%G+/-%G) + (%G+/-%G)CL^1 + (%G+/-%G)C1^1 + (%G+/-%
       G)C0^1\n",res[4],sig[4],0.,0.,0.,0.,0.,0.);
```

The rest of the file `tacRC-brief.txt` contains the function definitions that will be integrated. For the case of $\Psi^{(2)}$ in our example, this is fairly short.

Program B.3: Sample C++ functions before they are edited in preparation for use. These are to be integrated in order to find the tachyon profile of $\Psi^{(2)}$. The constant functions have parameter `x` because Maple does not consider functions without parameters to be functions at all.

```
6  #include <math.h>

8  double F1 (double s_1)
9  {
10   return(-0.27e2 / 0.16e2 / PI * pow(s_1 - 0.1e1, -0.2e1) - 0.27e2 /
         0.16e2 / PI * pow(s_1, -0.2e1) - 0.27e2 / 0.8e1 / PI + 0.3e1 /
         0.16e2 * PI * pow(0.1e1 / cos(PI * (0.1e1 + s_1) / 0.3e1), 0.2e1)
         * pow(sqrt(0.3e1) / 0.2e1 - tan(PI * (0.1e1 + s_1) / 0.3e1) / 0.2
         e1, -0.2e1) + 0.3e1 / 0.16e2 * PI * pow(0.1e1 / cos(PI * (0.1e1 +
         s_1) / 0.3e1), 0.2e1) * pow(tan(PI * (0.1e1 + s_1) / 0.3e1) / 0.2
         e1 + sqrt(0.3e1) / 0.2e1, -0.2e1));
11 }
12 #include <math.h>

14 double F2 (double x)
15 {
16   return(-0.3e1 / 0.8e1 * sqrt(0.3e1));
17 }
18 double F3 (double s_1)
19 {
20   return(-0.27e2 / 0.8e1 / PI);
21 }
22 double F4 (double x)
23 {
24   return(0.27e2 / 0.8e1 / PI);
25 }
26 #include <math.h>

28 double F5 (double s_1)
29 {
30   return(0.8e1 / 0.243e3 * PI * pow(0.1e1 / cos(PI * (0.1e1 + s_1) /
         0.3e1), 0.2e1) * pow(tan(PI * (0.1e1 + s_1) / 0.3e1), -0.4e1) *
         pow(sqrt(0.3e1) / 0.2e1 - tan(PI * (0.1e1 + s_1) / 0.3e1) / 0.2e1,
          0.2e1) + 0.8e1 / 0.243e3 * PI * pow(0.1e1 / cos(PI * (0.1e1 + s_1
         ) / 0.3e1), 0.2e1) * pow(tan(PI * (0.1e1 + s_1) / 0.3e1), -0.4e1)
         * pow(tan(PI * (0.1e1 + s_1) / 0.3e1) / 0.2e1 + sqrt(0.3e1) / 0.2
         e1, 0.2e1));
31 }
```

As shown here, this is not really usable so a series of simple replacements must be performed. The `include` statements which Maple insists on putting before each integrand need to be

removed, and numerical integration routines typically expect their integrands to take a single array rather than individual components of a coordinate. For a few short functions like these it is simplest to do this by hand, but when the functions become much longer at higher orders the Unix command `sed` is useful for quickly performing several find and replace operations. When we are done, the example above should look like program B.4.

Program B.4: Sample C++ header file with function definitions to be integrated by C++ in order to find the tachyon profile of $\Psi^{(2)}$.

```
1  double F1 (double s[]) { double s_1 = s[0];
2    return(-0.27e2 / 0.16e2 / PI * pow(s_1 - 0.1e1, -0.2e1) - 0.27e2 /
         0.16e2 / PI * pow(s_1, -0.2e1) - 0.27e2 / 0.8e1 / PI + 0.3e1 /
         0.16e2 * PI * pow(0.1e1 / cos(PI * (0.1e1 + s_1) / 0.3e1), 0.2e1)
         * pow(sqrt(0.3e1) / 0.2e1 - tan(PI * (0.1e1 + s_1) / 0.3e1) / 0.2
         e1, -0.2e1) + 0.3e1 / 0.16e2 * PI * pow(0.1e1 / cos(PI * (0.1e1 +
         s_1) / 0.3e1), 0.2e1) * pow(tan(PI * (0.1e1 + s_1) / 0.3e1) / 0.2
         e1 + sqrt(0.3e1) / 0.2e1, -0.2e1));
3  }

5  double F2 () {
6    return(-0.3e1 / 0.8e1 * sqrt(0.3e1));
7  }
8  double F3 (double s[]) { double s_1 = s[0];
9    return(-0.27e2 / 0.8e1 / PI);
10 }
11 double F4 () {
12   return(0.27e2 / 0.8e1 / PI);
13 }

15 double F5 (double s[]) { double s_1 = s[0];
16   return(0.8e1 / 0.243e3 * PI * pow(0.1e1 / cos(PI * (0.1e1 + s_1) /
         0.3e1), 0.2e1) * pow(tan(PI * (0.1e1 + s_1) / 0.3e1), -0.4e1) *
         pow(sqrt(0.3e1) / 0.2e1 - tan(PI * (0.1e1 + s_1) / 0.3e1) / 0.2e1,
          0.2e1) + 0.8e1 / 0.243e3 * PI * pow(0.1e1 / cos(PI * (0.1e1 + s_1
         ) / 0.3e1), 0.2e1) * pow(tan(PI * (0.1e1 + s_1) / 0.3e1), -0.4e1)
         * pow(tan(PI * (0.1e1 + s_1) / 0.3e1) / 0.2e1 + sqrt(0.3e1) / 0.2
         e1, 0.2e1));
17 }
```

This header file, which we will call `tacRC-brief.h`, can be included in a main C++ program to provide the integrands. The file can contain many more integrands, describing the solution at higher orders in λ, and only the portion produced by Maple and described in program B.2 will need to be changed. To see how quickly the size of the integrand functions increases, in program B.5 we look at a function representing $\beta_3^{(0)}$. This is the third order analogue of `F5` in the above code fragment, and it is already much larger. By 6th order, individual integrands can involve several megabytes of text.

Program B.5: The C++ function to be integrated in order to find the $\beta_3^{(0)}$ component of the tachyon profile.

```
double F160 (double s[]) { double s_1 = s[0]; double s_2 = s[1];
  return(-PI * PI * sqrt(0.2e1) * pow(0.1e1 / cos(PI * (0.2e1 + s_1) /
     0.4e1), 0.2e1) * pow(0.1e1 / cos(PI * (0.2e1 + s_2) / 0.4e1), 0.2
     e1) * pow(tan(PI * (0.2e1 + s_1) / 0.4e1), -0.6e1) * pow(tan(PI *
     (0.2e1 + s_2) / 0.4e1), -0.6e1) * pow(0.1e1 / 0.2e1 - tan(PI *
     (0.2e1 + s_1) / 0.4e1) / 0.2e1, 0.2e1) * pow(0.1e1 / 0.2e1 - tan(
     PI * (0.2e1 + s_2) / 0.4e1) / 0.2e1, 0.2e1) * pow(tan(PI * (0.2e1
     + s_1) / 0.4e1) / 0.2e1 - tan(PI * (0.2e1 + s_2) / 0.4e1) / 0.2e1,
      0.2e1) / 0.1024e4 + PI * PI * sqrt(0.2e1) * pow(0.1e1 / cos(PI *
     (0.1e1 + 0.2e1 * s_1) / 0.4e1), 0.2e1) * pow(0.1e1 / cos(PI * (0.1
     e1 + 0.2e1 * s_2) / 0.4e1), 0.2e1) * pow(tan(PI * (0.1e1 + 0.2e1 *
      s_1) / 0.4e1), -0.6e1) * pow(tan(PI * (0.1e1 + 0.2e1 * s_2) / 0.4
     e1), -0.6e1) * pow(tan(PI * (0.1e1 + 0.2e1 * s_1) / 0.4e1) / 0.2e1
      - tan(PI * (0.1e1 + 0.2e1 * s_2) / 0.4e1) / 0.2e1, 0.2e1) * pow(
     tan(PI * (0.1e1 + 0.2e1 * s_1) / 0.4e1) / 0.2e1 + 0.1e1 / 0.2e1,
     0.2e1) * pow(tan(PI * (0.1e1 + 0.2e1 * s_2) / 0.4e1) / 0.2e1 + 0.1
     e1 / 0.2e1, 0.2e1) / 0.256e3 + PI * PI * sqrt(0.2e1) * pow(0.1e1 /
      cos(PI * (0.1e1 + 0.2e1 * s_1) / 0.4e1), 0.2e1) * pow(0.1e1 / cos
     (PI * (0.1e1 + 0.2e1 * s_2) / 0.4e1), 0.2e1) * pow(tan(PI * (0.1e1
      + 0.2e1 * s_1) / 0.4e1), -0.6e1) * pow(tan(PI * (0.1e1 + 0.2e1 *
     s_2) / 0.4e1), -0.6e1) * pow(0.1e1 / 0.2e1 - tan(PI * (0.1e1 + 0.2
     e1 * s_1) / 0.4e1) / 0.2e1, 0.2e1) * pow(0.1e1 / 0.2e1 - tan(PI *
     (0.1e1 + 0.2e1 * s_2) / 0.4e1) / 0.2e1, 0.2e1) * pow(tan(PI * (0.1
     e1 + 0.2e1 * s_1) / 0.4e1) / 0.2e1 - tan(PI * (0.1e1 + 0.2e1 * s_2
     ) / 0.4e1) / 0.2e1, 0.2e1) / 0.256e3 - PI * PI * sqrt(0.2e1) * pow
     (0.1e1 / cos(PI * (s_1 + 0.1e1) / 0.4e1), 0.2e1) * pow(0.1e1 / cos
     (PI * (s_2 + 0.1e1) / 0.4e1), 0.2e1) * pow(tan(PI * (s_1 + 0.1e1)
     / 0.4e1), -0.6e1) * pow(tan(PI * (s_2 + 0.1e1) / 0.4e1), -0.6e1) *
      pow(tan(PI * (s_1 + 0.1e1) / 0.4e1) / 0.2e1 - tan(PI * (s_2 + 0.1
     e1) / 0.4e1) / 0.2e1, 0.2e1) * pow(tan(PI * (s_1 + 0.1e1) / 0.4e1)
      / 0.2e1 + 0.1e1 / 0.2e1, 0.2e1) * pow(tan(PI * (s_2 + 0.1e1) /
     0.4e1) / 0.2e1 + 0.1e1 / 0.2e1, 0.2e1) / 0.1024e4);
}
```

Returning to the second order example, we now look at the body of the C++ program to perform the numerical integration. The three functions worth noting are `safety_shifter`, `CubeInt`, and of course `main`. The `main` function simply contains the statements to evaluate each integral, store the results, and then print them in a formatted list. It evaluates the integrals by repeatedly calling the `CubeInt` function. It sets all of the various parameters of integration, such as the maximum number of samples to use, and then calls library routines to perform the integrals. In between the library routines and the integrands is the `safety_shifter` function, which prevents the integrands from being evaluated at points where some of the terms might be divergent. The reason for this regularization is discussed in section 5.3.7. Compiling this sample program requires linking the GSL and CUBA libraries with the `-lgsl` and `-lcuba` command line options. If the libraries are not part of the standard search path then the locations of them and their header files must also be specified with the `-L` and `-I` options respectively.

Program B.6: Sample C++ program for the numerical evaluation of integrals representing the tachyon profile at order λ^2.

```
#include <stdlib.h>
#include <stdio.h>
#include <time.h>
#include <cmath>
#include "cuba.h"
#include <gsl/gsl_integration.h>
#include <gsl/gsl_errno.h>

#define PI 3.1415926535897932385
#include "tacRC-brief.h"

//we introduce a small regulator (eps) to keep test points away from the boundary of the integration
    region and diagonals
//this process reduces roundoff errors from adding divergent terms
int safety_shifter(const int *ndim, const double xx[],
                   const int *ncomp, double ff[], void* fnName) {
    double feval, startstack, eps = 0.0003;
    double x[*ndim];
    double (*fxn)(double[]) = (double (*)(double[]))fnName;
    int i, j, k, samepoints, adjusted = 1, nAdjusted = 0;
    for (i=0; i<*ndim; i++) {x[i] = xx[i];}
    while (adjusted) {
        adjusted = 0;
        //check for coordinates on the boundary
        samepoints = 0;
        for (i=0; i<*ndim; i++) {
            if (x[i] < .99*eps) {
                samepoints += 1;
            }
        }
        if (samepoints > 0) {
            k = 0;
            for (i=0; i<*ndim; i++) {
                if (x[i] < .99*eps) {
                    k+=1;
                    x[i] = eps*k;
                    adjusted = 1;
                }
            }
        }
        samepoints = 0;
        for (i=0; i<*ndim; i++) {
            if (x[i] > 1 - .99*eps) {
                samepoints += 1;
            }
        }
        if (samepoints > 0) {
            k = 0;
```

```
48              for (i=0; i<*ndim; i++) {
49                  if (x[i] > 1 - .99*eps) {
50                      k+=1;
51                      x[i] = 1 - eps*k;
52                      adjusted = 1;
53                  }
54              }
55          }
56          for (i=0; i<*ndim; i++) {
57              //check for coordinates which have hit x[i]
58              samepoints = 0;
59              for (j=i+1; j<*ndim; j++) {
60                  if (fabs(x[i]-x[j]) < (.99 * eps * (samepoints+1))) {
61                      samepoints +=1;
62                  }
63              }
64              if (samepoints > 0) {
65                  startstack = x[i] - eps*(samepoints/2.);
66                  x[i] = startstack;
67                  adjusted = 1;
68                  k = 1;
69                  for (j=i+1; j<*ndim; j++) {
70                      if (fabs(x[i]-x[j]) < (.99 * eps * (samepoints))) {
71                          x[j] = startstack + k*eps;
72                          k++;
73                      }
74                  }
75              }
76          }
77          if (!adjusted) {
78              break;
79          }
80          nAdjusted += 1;
81          if (nAdjusted > 15) {
82              break;
83          }
84      }
85      feval = fxn(x);
86      ff[0] = feval;
87      return 0;
88  }

90  double gslevaluator(double x, void* fnName) {
91      double s[1];
92      double r[1];
93      const int one = 1;
94      s[0] = x;
95      safety_shifter(&one,s,&one,r,fnName);
96      return r[0];
97  }
```

```
100 void gsl_error_printer (const char * reason, const char * file, int
       line, int gsl_errno) {
101     printf ("GSL ERROR: ERROR NO ", gsl_errno, file, line, reason);

103     fflush (stdout);

105     return;
106 }

108 double CubeInt(int dim, double fxn(double[]), int fNum, double &res,
       double &sdev, double &chi) {
109     double integral[dim], error[dim], prob[dim];
110     int nregions, neval, fail;
111     int ncomp = 1; //dimension of evaluated f (1 because f is a scalar function)
112     int nvec = 1; //number of inputs function can take at once
113     double epsrel = 1E-2; //relative error goal is 1%
114     double epsabs = 0.; //absolute error goal
115     int flags = 0; //flags: verbose=0, combine all passes
116     int seed = time(NULL); //random seed
117     int MCminevals = 0, MCmaxevals = 50000*pow(2,dim); //minimum and
          maximum number of function calls for monte carlo algorithms
118     int CUminevals = 0, CUmaxevals = 4000*pow(2,dim); //minimum and
          maximum number of function calls for Cuhre
119     int key = 0; //cubature rule for Cuhre, use default
120     int nstart = 1000, nincrease = 500, nbatch = 1000, gridno = 0; //
          some Vegas-specific arguments, defaults
          used
121     int nnew = 1000, flatness = 25; //some Suave-specific arguments, defaults used
122     char *statefile = NULL; //file to save intermediate calculations
123     gsl_integration_workspace *gslw; //"workspace" for QAG
124     gsl_function gslF; //"function" for QAG to call
125     int QAGkey = 3; //integration rule for QAG, 3 is 31 point Gauss-Kronrod
126     res = 0; sdev = 0; chi = 0;

128     if (0) { //set to 1 to try Vegas
129         printf("VEGAS algorithm used in %d dimensions to evaluate F%d\n
              ",dim,fNum);
130         Vegas(dim, //number of dimensions
131               ncomp,
132               safety_shifter, //function for Vegas to call
133               (void*) fxn, //function for safety_shifter to call
134               nvec, epsrel, epsabs, flags, seed, MCminevals, MCmaxevals
                  , nstart, nincrease, nbatch, gridno, statefile,
135               &neval, //OUTPUT number of function calls that were actually used
136               &fail, //OUTPUT 0 if target accuracy was reached
137               integral, //OUTPUT result of the integral
138               error, //OUTPUT error estimate for integral
139               prob); //OUTPUT probability that error is inaccurate
140         res = integral[0];
141         sdev = error[0];
```

```
142         chi = prob[0];
143         printf("VEGAS used %d function calls with fail=%d\n",neval,fail
                );
144         printf("VEGAS returned (%G +/- %G) with p=%.3f\n", res, sdev,
                chi);
145         printf("\n");
146     }
147     if (0) { //set to 1 to try Suave
148         printf("SUAVE algorithm used in %d dimensions to evaluate F%d\n
                ",dim,fNum);
149         Suave(dim, //number of dimensions
150               ncomp,
151               safety_shifter, //function for Suave to call
152               (void*) fxn, //function for safety_shifter to call
153               nvec, epsrel, epsabs, flags, seed, MCminevals, MCmaxevals
                    , nnew, flatness, statefile,
154               &nregions, //OUTPUT number of subregions used
155               &neval, //OUTPUT number of function calls that were actually used
156               &fail, //OUTPUT 0 if target accuracy was reached
157               integral, //OUTPUT result of the integral
158               error, //OUTPUT error estimate for integral
159               prob); //OUTPUT probability that error is inaccurate
160         res = integral[0];
161         sdev = error[0];
162         chi = prob[0];
163         printf("SUAVE used %d function calls in %d regions with fail=%d
                \n",neval,nregions,fail);
164         printf("SUAVE returned (%G +/- %G) with p=%.3f\n", res, sdev,
                chi);
165         printf("\n");
166     }
167     if (dim > 1 && 1) { //set to 1 to try Cuhre
168         printf("CUHRE algorithm used in %d dimensions to evaluate F%d\n
                ",dim,fNum);
169         Cuhre(dim, //number of dimensions
170               ncomp,
171               safety_shifter, //function for Cuhre to call
172               (void*) fxn, //function for safety_shifter to call
173               nvec, epsrel, epsabs, flags, CUminevals, CUmaxevals, key,
                     statefile,
174               &nregions, //OUTPUT number of subregions used
175               &neval, //OUTPUT number of function calls that were actually used
176               &fail, //OUTPUT 0 if target accuracy was reached
177               integral, //OUTPUT result of the integral
178               error, //OUTPUT error estimate for integral
179               prob); //OUTPUT probability that error is inaccurate
180         if (std::isfinite(integral[0])) {
181             res = integral[0];
182             sdev = error[0];
183             chi = prob[0];
184         }
```

```
185         printf("CUHRE used %d function calls in %d regions with fail=%d
                \n",neval,nregions,fail);
186         if (fail > -1) {
187             printf("CUHRE returned (%G +/- %G) with p=%.3f\n", integral
                    [0], error[0], prob[0]);
188         }
189         if (!std::isfinite(integral[0])) {
190             printf("CUHRE is being ignored\n");
191         }
192         printf("\n");
193     }
194     if (dim == 1 && 1) { //set to 1 to try QAG
195         printf("QAG algorithm used in %d dimension to evaluate F%d\n",
                dim,fNum);
196         gslw = gsl_integration_workspace_alloc(CUmaxevals); //this should
                limit the runtime of QAG
197         gslF.function = &gslevaluator;
198         gslF.params = (void*) fxn;
199         gsl_integration_qag(&gslF, //function to call
200                             0, 1, //limits of integration
201                             1E-6, //epsabs replaced because QAG doesn't like failure
202                             epsrel,
203                             CUmaxevals, QAGkey, gslw,
204                             &integral[0], //OUTPUT result of the integral
205                             &error[0]); //OUTPUT error estimate for integral
206         res = integral[0];
207         sdev = error[0];
208         chi = 0; //hopefully QAG is "never wrong"
209         printf("QAG used ?? function calls in %d regions\n",0,(int)(
                gslw->size));
210         gsl_integration_workspace_free(gslw);
211         printf("QAG returned (%G +/- %G)\n", res, sdev);
212         printf("\n");
213     }
214     return res;
215 }

217 int main() {
218     int n;
219     double res[242], sig[242], chi[242];
220     double tacprofile, eomtac, eomPsiL, eomPsir, kineticaction,
            cubicaction;

222     gsl_set_error_handler(&gsl_error_printer);

224     tacprofile = CubeInt(1, F1, 1, res[0], sig[0], chi[0]) + F2();
225     tacprofile = CubeInt(1, F3, 3, res[2], sig[2], chi[2]) + F4();
226     tacprofile = CubeInt(1, F5, 5, res[4], sig[4], chi[4]);
227     printf("beta[2,0] = (%G+/-%G) + (%G+/-%G)CL^1 + (%G+/-%G)C1^1 + (%G
            +/-%G)C0^1\n",res[0]+F2(),sig[0],res[2]+F4(),sig[2],0.,0.,0.,0.)
            ;
```

```
228     printf("beta[2,2] = (%G+/-%G) + (%G+/-%G)CL^1 + (%G+/-%G)C1^1 + (%G
            +/-%G)C0^1\n",res[4],sig[4],0.,0.,0.,0.,0.,0.);

230     printf("\n------------------------------\n");
231     return 0;
232 }
```